RADAR

Research Archive and Digital Asset Repository

OXFORD
BROOKES
UNIVERSITY

Determination of the main parameters affecting the performance of bridge falsework systems

João Pereira Cabanas Gonçalves André (2014)

https://radar.brookes.ac.uk/radar/items/732cbb02-e327-4b09-a46c-c5dbb3a7065c/1/

When referring to this work, the full bibliographic details must be given as follows:

André, J P C G (2014) *Determination of the main parameters affecting the performance of bridge falsework systems* PhD, Oxford Brookes University

WWW.BROOKES.AC.UK/GO/RADAR

Determination of the main parameters affecting the performance of bridge falsework systems

João Pereira Cabanas Gonçalves André

**Submitted in partial fulfilment of the requirements
for the degree of Doctor of Philosophy**

December 2014

Faculty of Technology, Design and Environment

Oxford Brookes University

OXFORD
BROOKES
UNIVERSITY

ABSTRACT

Bridge falsework systems are one of the most common temporary structures used in the construction industry, namely to support the formwork during the construction, rehabilitation or retrofit works of concrete bridges and viaducts.

This Thesis presents new results and research that improve the available knowledge about the structural behaviour, reliability, robustness and risk of these structures. The main, internal and external, hazards are identified and detailed, including the procedural, enabling and triggering hazards. The use of reduction factors to determine the values of the applied loads to design bridge falsework, and other temporary structures, is critically analysed and it is recommended not to use them, unless supported by specific site data. The importance of implementing effective quality control, inspection and communication measures to manage human errors during planning, designing and operation is highlighted.

From the 192 tests carried out during the experimental campaign, consisting of five different tests using three different joint types, new results are obtained concerning bridge falsework components, namely the bending behaviour and resistance of spigot joints and forkhead joints (falsework to formwork interface) from which no published research was found. Existing joint models are evaluated and improved alternative models are developed.

The results of numerical studies of a selected structural system are presented using a novel joint finite element and information gathered from the experimental tests. This new finite element has features that the available elements in *ABAQUS®* program do not have, specifically the capability of simulating an analytical modelling of the cyclic behaviour of joints with allowance for stiffness and resistance degradation and joint failure. The accuracy and precision of the developed numerical models improves the existing numerical results of full-scale tests of bridge falsework systems, in respect to structural behaviour and resistance. It is recommended that formwork should be explicitly modelled and modelling of spigot joints should follow the model presented in this Thesis. From a sensitivity analysis of the bridge falsework systems to modelling hypothesis, it is found that the most important joints are the beam-to-column joint, followed by the forkhead joint and the spigot joint, with variations of up to 70% between the resistance of the system when the joints are modelled as continuous or as pinned.

A key contribution of the Thesis is to introduce a novel risk management methodology based on newly developed robustness and fragility indices. This new methodology is applicable, in principle, to all structural analyses not only those concerning bridge falsework systems. Based on advanced deterministic studies, the main parameters affecting the performance of bridge falsework are identified, analysed and discussed. These studies involved a comprehensive set of external and internal hazards: (i) applied external actions of different nature and (ii) structural configurations to design bridge falsework. It is found that differential ground settlements are a critical action and that stiffer systems are more sensitive. Also, it is highlighted by use of plenty examples that bracing is an essential design requirement.

Advanced stochastic investigations are also carried out, in which the key random variables that control the stochastic behaviour of bridge falsework systems are identified, namely joint looseness and initial stiffness after looseness. Possible strategies to increase robustness and decrease fragility are discussed and based on an application example the cost-benefit of alternative solutions is investigated. It is concluded that implementing quality control and quality assurance procedures to bridge falsework elements is an extremely effective and efficient way of reducing existing risks.

The information gathered in this Thesis can be used to develop more rational and reliable bridge falsework structures thus safer and more design efficient.

DECLARATION

This Thesis contains no material which has been accepted for the award of any other degree or diploma in any university or other institution and affirms that to the best of my knowledge, the Thesis contains no material previously published or written by another person, except where due reference is made in the text of Thesis.

ACKNOWLEDGEMENTS

The development of this Thesis would have not been possible without the guidance, support and incentive of my supervisors.

I'm deeply thankful to Dr. Rob Beale for having accepted me at Oxford Brookes University, to have shared with me his extensive knowledge about temporary structures in general and to have the patience of listening to me for long hours in his office to debate about the questions I had during the development of the Thesis. I also thank him for the endless support he showed to me which I'm truly and forever grateful. I finally want to express my gratefulness for his friendship.

The same applies to Dr. António Baptista, which over my ten years working at "Laboratório Nacional de Engenharia Civil" (LNEC), Lisbon, has been teaching me, mentoring me and sharing with me all his large knowledge about a wide range of civil engineering related problems. I'm truthfully grateful for all he has done in my favour, for the way he always pushed me to go that little bit extra mile in order to obtain a better understanding of things. I have very fond memories about our discussions concerning temporary structures and how could complex problems be addressed, which in the end I hope are found in the present Thesis. I finally want to express my gratefulness for his friendship.

A special thanks to Dr. Leroy Gardner and Dr. Anand Thite for accepting being the Thesis examiners and for providing excellent suggestions to increase the readability and potential applicability of the Thesis methods and contents.

I also have to thank Dr. Carlos Pina, President of LNEC, Dr. Almeida Fernandes and Dr. José Catarino, past and current Head of Structures Department and Dr. Manuel Pipa and Dr. Helena Cruz, past and current responsible for LNEC's division where I have been working, for giving me all necessary conditions that I needed to finish this Thesis.

I also thank LNEC and "Fundação para a Ciência e a Tecnologia" for having funded this investigation, and to Harsco Corporation for their cooperation in providing test specimens.

Many others have helped me finish this marathon. In particular Mike Godley, Javier Rodriguez, Pablo Antolin Sanchez, Raymond Salter, Kieron Tew, Michael Hartman, Bruno Sudret, Luisa Giulliani, members of Stackoverflow forum (https://stackoverflow.com/), members of other online groups that helped me solve the problems I encountered along the way.

I also would like to thank my friends Pedro, Francisco, Luís, Marco, David, Ramos, Ana Sofia, José Luís and others for giving me the incentive to finish this work.

I also wish to express my gratitude to Ana for supporting me throughout this enduring challenge.

Finally, but foremost, I'd like to thank my parents, Mariana and José, for being the best parents in every moment of my life.

LABORATÓRIO NACIONAL
DE ENGENHARIA CIVIL

FCT
Fundação para a Ciência e a Tecnologia
MINISTÉRIO DA CIÊNCIA, TECNOLOGIA E ENSINO SUPERIOR

TABLE OF CONTENTS

LIST OF FIGURES

CHAPTER 4

CHAPTER 5

CHAPTER 6

LIST OF TABLES

CHAPTER 4

CHAPTER 5

CHAPTER 6

LIST OF SYMBOLS

$\mathbf{E}^{ID}$, matrix with additional label *ID*

Q^{ID}, vector with additional label *ID*

ϕ, finite rotation vector

x_n, scalar, the *n*th element of the vector *X*

A or S, action

B, benefit

C, cost

D, damage

F_R, fragility index

G, performance function

I_R, robustness index

P, probability of an event

P_f, probability of failure

R, resistance

E, energy

D, damage energy

H, hazard

P, *F*, *G* or *Q*, load

W, wind load

f( ) or pdf, probability density function

F( ) or cdf, cumulative distribution function

COV, coefficient of variation

μ and σ, the mean and the standard deviation of a probabilistic distribution

β, the Hasofer-Lind reliability index

Φ, normal cumulative distribution function

R, return period

n, design working life or exposure period

γ, partial factor to be applied to the characteristic value of load

ψ, load combination factor

g, gravitational constant

L, *h* or *z*, length or dimension

M, bending moment

N, axial force

θ, bending rotation

k, stiffness

δ, displacement

e and ε, deformation and strain of material, respectively

1

INTRODUCTION

1.1 Problem statement and motivation

The present Thesis concerns bridge falsework systems. There are various types of structural systems available in the market: from towered systems made of steel built-up members, frame systems of steel beams and columns with structural profiled sections, to proprietary modular 3-D frame systems of metallic elements connected by special couplers. In civil engineering there are many applications of these structural systems ranging from the construction, rehabilitation to the retrofit of bridge structures. Figure 1.1 illustrates some examples of bridge falsework systems.

There are several stakeholders directly or indirectly concerned with bridge falsework systems: researchers, designers, producers, clients, consultants, insurers, contractors, sub-contractors and workers. In this context, the assemblage, use and dismantling of bridge falsework systems is usually done by a specialised sub-contractor, in accordance with a standard project or with a special developed project depending on the work complexity.

Since the industrial revolution, the construction industry and in particular bridge falsework projects have been experiencing new challenges and some fundamental changes. Through time the role of bridge falsework in the cost, construction rate, safety, quality, durability, efficiency, utility and aesthetics of any bridge project has increased in a consistent fashion (fib, 2009). Therefore, it is not surprising that a correct choice, good planning, design and operation of bridge falsework are keys for the success of every bridge project. In particular, it is vital that synchronised planning and continuous knowledge exchange exists between the bridge designer, the bridge contractor, the bridge falsework designer, the bridge falsework contractor and others.

Unfortunately this is not always a reality. As pointed out in (fib, 2009) the framework of bridge construction consists of complex interactions between all the above mentioned stakeholders who have different backgrounds and can have different priorities, perceptions and goals, some of which can even be contradictory. Despite the construction phase being the most critical stage of a structures' lifetime – most failures occur during construction rather than after projects have been completed, see (Ratay, 2009 ; Scheer, 2010) for examples – some stakeholders still do not recognise the importance of these systems: they are "temporary" and, therefore, their role is considered to be minor compared to that of the permanent structures. Consequently, the design and use of bridge falsework systems are not usually treated as carefully as in the case of permanent structures and do not receive the same level of research attention and research funding.

Figure A

Figure B

Figure C

Figure D

Figure 1.1: Examples of bridge falsework. Top row – *Left*: **©Grupo FCM www.grupofcm.com,** *Right*: **©CONSTRUGOMES www.fiomental.com/construgomes, Bottom row –** *Left*: **©CONSTRUGOMES,** *Right*: **©RMD Kwikform www.rmdkwikform.com.**

This is clearly evidenced by the number and the state-of-the-art level of existing standards and guidance documents concerning permanent structures as opposed to those relating to temporary structures. Until recently, national and international design codes/standards and/or guidance documents concerning temporary structures were based on simple design procedures, for example: the columns' effective lengths of bridge falsework were only governed by the vertical spacing of horizontal members, not considering the system's overall stability. The use of the effective length concept as a design procedure, although simple, is not accurate since it is based on an element level safety check and it assumes that the element's deformed shape is very similar to its first global elastic buckling mode. Therefore, the use of full second-order non-linear analysis and design procedures is recommended.

Traditionally, bridge falsework structures are usually designed using safe load tables developed by the producers of the proprietary equipment in general based on existing standards or on in-house developed design methods. Often, these tables do not provide information regarding (i) quality requirements (*e.g.* the specification of design tolerances), or (ii) risk assessment for specific applications (*e.g.* special loading and foundation conditions). Additionally, the design rules applied to bridge falsework structures are not uniform and therefore the actual reliability levels are usually smaller and exhibit a greater variation than the corresponding reliability levels of permanent structures.

To counter this well rooted reality, and under an increasing pressure from public opinion, there has been an effort in some countries like UK, beginning with the Bragg report following the River Loddon accident (Bragg, 1975), and continuing with other documents (BSI, 2008a), and more lately at a European level (BSI, 2011) to publish standards and guidance documents prepared by special technical commissions. Still, reference is missing to the design working life of these structural components: *"(...) structures or parts of structures that can be dismantled with a view to being re-used should not be considered as temporary"* (BSI, 2002a). Despite the recent research investigations, the

design of bridge falsework structures is still frequently associated with high uncertainty levels, due to insufficient information about their real behaviour at the construction site – in particular, little information is available about the actual geometric imperfections and load eccentricities values or the influence of foundation settlements on their resistance, reliability and robustness.

It must be acknowledged that most of the problems not dealt with during the planning and design phases will have to be handled on the site. However, the lack of expertise in the field and tight project deadlines have a tendency to make construction workers behave unsafely, take unnecessary chances, and endanger both themselves and the structures (temporary and permanent). Long sub-contractor chains lead inevitably to loss of communication between the various agents and to loss of responsibility for the supervision, inspection and dismounting procedures.

It should be stressed that the design and use of bridge falsework structures places very complex and different challenges from the ones associated with permanent structures, such as:

- Generally, the design of bridge falsework structures is controlled by construction loads, *i.e.* the self-weight of the permanent structure. As a result, these temporary structures are subject to load values close to, and sometimes even above, the assumed design values during almost their entire service period, whereas the design of permanent structures is often controlled by load cases that will only occur for a brief period of time, or that have a small probability of occurring, during their design working lifetime.

- Bridge falsework structures are used for short periods of time, although due to multiple re-use cycles their design working life can sum up to 15 years or more. Based on the temporary nature of the use of these structures, some design philosophies specify smaller design values for the actions than the ones used in the design of permanent structures, which may lead to unsafe structures. Furthermore, since the ratio between their cost and the cost associated with their collapse is much lower than for permanent structures, this methodology needs to be reconsidered using a risk informed approach;

- Bridge falsework structures are assembled, (re)used for short periods and dismantled several times in repetitive cycles. As a result, flaws in erection, inspection and maintenance procedures are likely to occur, leading to construction errors with potential severe consequences. Additionally, as stated previously, the cooperation between the various stakeholders involved in their design and operation is not always the appropriate one. These facts can multiply by several orders of magnitude the risk associated with these structures, since their design often does not account for human errors in assembly and operation. All of the above represent possible critical hazard scenarios, and their number is far greater than any permanent structure needs to be designed against. Furthermore, permanent structures are generally assembled only once and are used for large periods of time and exhibit a much higher degree of inherent robustness against human errors;

- Finally, bridge falsework structures due to their purpose are generally constituted by slender elements, and therefore their performance is more sensitive than permanent structures to errors during their erection and operation, and to the use of damaged elements due to inadequate maintenance and quality control. Site control is essential and the appointment of Temporary Works Coordinators as suggested in (BSI, 2008a) should be implemented.

The biased framework outlined above contributes strongly to the high number of incidents and accidents involving the use of bridge falsework systems, which frequently cause human casualties and severe injuries, work inefficiency and partial (or total) structural damage of the infrastructure. Since 1970, several falsework collapses have been reported worldwide, with a growing trend in the developing world like China, India and Dubai where a boom in construction works has taken place. According to (Xie, Wang, 2009) in China, 27 collapses of bridge falsework systems occurred during 2005-2009 period, killing 100 workers and causing a higher, although unspecified, number of injuries. The 2010 collapse of a viaduct near Amarante, north of Portugal, together with other major

accidents involving these structures in the last decade, show that Portugal is not an exception concerning this problem. Another relevant example is the collapse of a viaduct in Andorra in 2009, leading to five fatalities and six injured workers, most of them Portuguese.

(Matousek, Schneider, 1976) analysed 800 cases of damage to structures, looking for their causes. They found that most types of damages occurred during the execution phase, with temporary structures being responsible for 9% of the collapse cases, 11% of the resulting economic costs and 22% of all casualties. The principal cause was human errors (errors, lapses or omissions) related to deficient planning, design and execution. (Hadipriono, Wang, 1987) studied the causes of falsework collapses during construction and concluded that almost all triggering and enabling events stemmed from procedural causes like inadequate review of falsework design/erection and inadequate falsework/formwork inspection during concreting operations. Additionally, they found that 74% of falsework collapses occurred during concrete pouring operations. (Eldukair, Ayyub, 1991) studied 604 structural and construction failures in the United States during the period of 1975-1986. They observed that temporary structures were responsible for about 10% of the total number of failures.

In 1978, (Billings, Routley, 1978) reviewed the available literature about falsework collapses and have found recurrent deficiencies about (i) foundations, see also (Carvalho et al., 2004), (ii) lateral stability, (iii) design errors, (iv) details and (v) materials, to which can be added planning errors (*e.g.* insufficient inspection plans). A study developed in 2004 by the UK's Health and Safety Executive (HSE) (Bennett, 2004) found that approximately in one out of six accidents with temporary structures the original designer could have done something to prevent it from happening, but failed to take that opportunity. This can be justified by the findings of a survey (Pallett et al., 2001) commissioned by the HSE where a sample of persons directly related to falsework design and procurement were interviewed to assess the level of awareness of the structural behaviour of falsework. The findings show that there is:

- *"A lack of understanding of the fundamentals of stability of falsework and the basic principles involved. This shortfall occurs at all levels;*
- *Wind load is rarely considered;*
- *There is a lack of clarity in terms of design brief and coverage of key aspects such as ground conditions;*
- *The lateral restraint assumptions made by designers were often ignored/misunderstood by those on site;*
- *There is a lack of adequate checking and a worrying lack of design expertise;*
- *Erection accuracy leaves much to be desired".*

Recently, the HSE conducted an extensive study on what are major hazard events in construction (HSE, 2011). They found out that failure to recognise hazardous scenarios and influencing factors, poor teamwork and lack of experience and competence were the main causal factors to accidents. Particularly, regarding the design of temporary structures the highlighted causal factors consisted of inadequate design or (late) design changes, underlying lack of robustness and incorrect as-built drawings and information.

Beyond human losses and injuries, these accidents may cause considerable economic, financial, environmental and political costs as well as damage to reputations and increased insurance premiums. Yet, despite their importance and extensive practical use, the existing research concerning bridge falsework systems is very limited, see (Beale, 2014). From the bibliographic review only a few number of papers were found related to bridge falsework systems (Sexsmith, 1998 ; Sexsmith, Reid, 2003 ; Zhang et al., 2009 ; Xie, Wang, 2009 ; Zeng, Hu, 2010), but even a fewer number of papers were found concerning their robustness and risk. In this context, there is a need for research of these systems, namely to contribute for a better understanding of their reliability, robustness and risk during their design working life.

However, research on steel access scaffold structures, similar but not as complex as those used on bridge falsework has been increasing in the last years. The main contributions have been made by researchers in UK, China and more recently Australia. Several authors have endeavour research to characterise the behaviour of joints between access scaffold elements. Here, works by (Godley, Beale, 1997) and (Chandrangsu, Rasmussen, 2008) should be highlighted. However, some results are contradictory and there is still lack of data concerning the complete behaviour of some couplers.

Regarding the evaluation of loads applied to falsework, this is still an ongoing topic as can be seen in the papers of (Rosowsky, 1995) and (Hill, 2004).

Finally, design rules have been developed by Peng's team in China for modular access scaffolds (Peng et al., 2009), and in Europe by Beale and Godley for proprietary access scaffolds (Beale, Godley, 2006). However, a unified analysis scheme which can take into account the various types of non-linearities and complexities existing in bridge falsework systems is still missing.

1.2 Objectives

The present Thesis contributes to a better knowledge about the structural behaviour, reliability, robustness and risk of bridge falsework systems. In particular:

- Identifies relevant hazard scenarios and their procedural causes, enabling and triggering events.

- Increases the available database of results regarding the behaviour of different types of joints of a selected structural solution, some of which have not yet been studied. Also, the existing disagreements between past researches are analysed.

- Performs advanced deterministic and stochastic analysis of selected structural systems to (i) identify critical components to the system's structural behaviour, reliability, robustness and risk, and (ii) evaluate its sensitivity to factors, such as: geometrical imperfections of the members (vertical, horizontal and top and base jacks), as a result of less than effective inspection, and actions of different nature.

- Suggests solutions to enhance the reliability, the robustness and reduce risk of these structures. Select one simple solution and analyse it under a risk informed decision-making process. This involves the development of a new risk methodology based on novel robustness and fragility measures.

1.3 Significance of the study

The present Thesis concerns bridge falsework systems made of slender (prone to buckling) vertical and horizontal steel tubes connected by special couplers. Failures involving these structures are one of the most common types of accidents in civil engineering leading to disproportionate consequences. This reality calls for a paradigm change regarding the design and use of bridge falsework systems.

Researchers and designers must realise that uncertainty is always present despite the significant evolution in structural engineering knowledge brought (i) by the use of ever-increasing computational capacity and (ii) by advances in experimental investigation. The natural consequence of uncertainty is risk. A risk free structure is a naive, uneconomical objective: risk cannot be eliminated; rather it must be managed rationally through a risk informed decision-making process. It is therefore essential that those who research or design structures realise the importance of considering the design working life risks to structural safety and the benefits that will come by doing so. These design principles are even more important in the field of temporary structures, and in particular bridge falsework systems.

In practice the design of bridge falsework is usually an oversimplified process, based on a comparison of the design forces with reference resistance values given by falsework system producers, without knowing their fundamentals, which may lead to their misuse (Baptista, Silva, 2002). This is particularly common in the process of selecting the system bracing configuration, which often suffers from lack of appropriate studies and thus constitute an enabling event of collapses. Recent analysis done by (Rodrigues, 2010), show that commonly used configurations of bracing elements could be insufficient to assure appropriate stability of the structure.

Various factors that have a decisive influence on the behaviour, resistance and performance of falsework, such as (i) foundation settlements, (ii) load redistributions due to asymmetrical concreting, (iii) system stiffness variations (combining traditional falsework with steel girders for example), (iv) system imperfections, (v) joint deformation capacity, (vi) use of damaged components such as couplers and (vii) other factors that originate from the interaction between the evolutive permanent structure under construction and the temporary structure, are not usually directly accounted for in the design. They are often expected to be covered by the safety margins adopted by the falsework system producers, but these may be insufficient to withstand the global coupled effect of the abovementioned factors, for example.

The severe consequences of all the accidents involving bridge falsework clearly justify the research needs for a holistic approach of bridge falsework systems risk management. The present research contributes for a better understanding of the structural behaviour, robustness and risk of these structures, so that adequate margins against failure may be maintained throughout the whole design/construction/operation process.

Robustness has been present in a more direct or indirect way in several structural codes throughout the last thirty years. Robustness is defined in ISO 2394 (ISO, 1998) as the "*ability of a structure not to be damaged by events like fire, explosions, impact or consequences of human errors, to an extent disproportionate to the original cause*". In this way robustness can be seen as a measure of the sensitivity of a given structure to disproportionate collapse. However, to date there is not one document that specifies a general purpose design method for robustness in a consistent manner. Moreover, there is a complete absence in codes about rules, design requirements or procedures to evaluate robustness of temporary structures, and in particular of bridge falsework systems.

Bridge falsework systems typically exhibit low robustness because (i) they are made of elements with a similar resistance distributed in a uniform mesh and (ii) the critical load case is usually linked with the weight of the permanent structure and the system is designed such as to reach a uniform safety margin of each element. Therefore, a significant number of elements are critical to the global stability of the system, and if one fails it is likely others will also fail leading to an unexpected, sudden and extensive disproportionate collapse of the system (thus low robust). Additionally, factors such as lack of competence in design, absence of rigorous quality control, poor site supervision will also contribute to decrease the robustness of the system because the number of critical elements can be expected to increase. These factors will also have a negative effect on the reliability of the system and on the levels of uncertainty associated to the risks of collapse of these structures.

In the present Thesis, the structural behaviour, robustness and risk of falsework systems are analysed. After a thorough bibliographic review, a series of experimental tests of a specific type of connections used in bridge falsework systems are carried out, aimed to increase the available data, and clarify some existing disagreements concerning their behaviour. This task benefited from cooperation with an industry partner.

These results together with the already available information constitute the basis for validation and verification of advanced numerical models. The latter take into consideration several sources of non-linearity including the possible occurrence of separation between elements due to failure of components. The aim of these numerical models is to establish a solid basis for the next goal of this research: the robustness and risk assessment of bridge falsework systems.

In this Thesis, a new robustness index is presented with advantages over existing methods. Additionally, a fragility index, which is a measure of the structural damages for a given load value is also presented. This fragility index constitutes the backbone of the risk framework methodology that is presented, detailed and illustrated in this research.

To perform risk analysis, advanced stochastic methods involving Design of Experiments (DoE), predictive modelling (Data Mining) and Monte Carlo methods are used and the results discussed.

This research provides a number of contributions to knowledge; one of the key contributions being the study of the structural behaviour of bridge falsework systems to a variety of hazard scenarios, and the analysis of the influence of certain decisive factors on the risk of these structures, such as the nature of the applied actions or the choice of the structural system. Also, the proposed methodology forms a rational method to evaluate the risk of bridge falsework systems taking into account the whole life cycle of these structures. Another key contribution is the discussion of a possible simple solution for the reduction of risks involving bridge falsework systems.

1.4 Methodology

The tasks developed in the frame of this research are divided in three work packages. Its execution required a link with a leading industry partner, Harsco Corporation (www.harsco.com), which shared their practical experience and initial guidance on research focus, and finally cooperated in the supply of experimental test materials.

Work package one is dedicated to a bibliographic review, namely about (i) characterizing existing structural solutions of bridge falsework systems, (ii) identifying of the main causes for their collapses, (iii) the state-of-the-art of experimental and numerical investigations about the behaviour of bridge falsework systems.

Work package two defines experimental procedures and characterises experimentally several types of joints between members of bridge falsework Cuplok® systems. This package also contains the development, validation and verification of the numerical modelling of bridge falsework systems. More specifically, a new joint finite element will be presented. Additionally, the influence of several numerical modelling hypotheses is discussed.

In Work package three, a methodology of structural design in the context of risk informed decision-making is presented using the definition and advantages of new robustness and fragility measures. This methodology is then applied to studies intended to:

- Identify critical scenarios to the system's structural behaviour, reliability, robustness and risk;
- Evaluate its sensitivity to factors, such as: (i) material properties, (ii) geometrical imperfections of the members, (iii) bracing configurations, (iv) actions of different nature (construction loads, wind, differential ground settlements) (vi) efficiency of the inspection and quality assurance plans (vii) structural system configurations (namely using steel girder beams to span over roads or other obstacles).

Finally, a possible simple solution for the reduction of risks involving bridge falsework systems is also presented, analysed and discussed.

1.4.1 Experimental tests

1.4.1.1 Characterization of the connections

The most commonly used bridge falsework systems are proprietary structures developed and designed by specialised companies. The structural system of these structures is constituted by vertical elements, called standards, made of circular hollow section (CHS) tubes which are connected at certain locations to horizontal elements, called ledgers, which usually have the same cross-section of the

standards. Connections between standards and ledgers can be of different types depending on the system developed by the producers: (i) Cuplok® systems; (ii) Wedge systems or (iii) other similar systems. Additionally, there are the traditional tube and fitting scaffold systems which use right angle and putlog couplers to connect the various elements – the use of these systems as bridge falsework is nowadays uncommon due to their low productivity and will not be addressed further.

In all systems, when multiple standards are needed to achieve the desired height, adjoining standards are united by spigot joints. Additionally, jacks are positioned at the bottom and at the top of the lower and upper standards, respectively, that allow a fine adjustment of the system's height.

Concerning the connections between standards and brace elements (used to increase the systems' lateral stiffness) the range varies from hook couplers, swivel couplers and welded connections. Finally, regarding the support conditions: at the top a forkhead is usually used while a baseplate is positioned at the bottom.

1.4.1.2 Past research

Several studies, see Table 1.1 have been carried out in the past to characterise the behaviour and resistance of some of these joints. Emphasis should be made to work of Beale and Godley at Oxford Brookes University, of Voelkel in Germany and of Chandrangsu *et al* in Australia.

Table 1.1: Summary of the available results of access scaffolds joints.

Reference	System type	Joint type	Type of test	Stiffness (average values)	Resistance (average values)
(Voelkel, 1990)	Cuplok®	Ledger-to-standard	Joint bending tests (Cyclic)	78 kN.m/rad* (strong axis, initial stiffness without looseness)	2,9 kN.m (strong axis)
			Frame tests (Cyclic)	5,6 kN.m/rad (weak axis, initial stiffness)	0,2 kN.m (weak axis)
		Ledger-to-standard	Joint axial tests (Monotonic)	N/A	73 kN
		Brace-to-standard (swivel joint)	Joint axial tests (Cyclic)	1360 kN/m	28 kN
(Godley, Beale, 1997)	Cuplok®	Ledger-to-standard	Joint bending tests (Cyclic)	65 kN.m/rad* (strong axis, initial stiffness without looseness)	N/A
(Godley, Beale, 2001)	Wedge type	Ledger-to-standard	Joint bending test	77 kN.m/rad (strong axis, initial stiffness without looseness, clockwise rotation)	1,7 kN.m (strong axis, clockwise rotation)
				27 kN.m/rad (strong axis, initial stiffness without looseness, anti-clockwise rotation)	1,3 kN.m (strong axis, anti-clockwise rotation)
(Chandrangsu, Rasmussen, 2008), see Table 1.2.	Cuplok®	Ledger-to-standard	Joint bending tests (Monotonic)	See Table 1.2	3,5 kN.m (strong axis)
					0,4 kN.m (weak axis)
* In tests performed by Voelkel and Beale, the initial stiffness with looseness was 10% of the initial stiffness value without looseness.					

Comparing the results, it can be seen that there are differences between the values of the initial rotational stiffness of Cuplok® ledger-to-standard joints reported by Voelkel and Godley *et al* compared to the ones presented by Chandrangsu *et al*. Regarding the ultimate bending moments the results are limited. The same applies to the joint axial tests results. Additionally, no tests results

are available to evaluate the stiffness and resistance of the spigot joints as well as of the top connections between the falsework and the formwork.

Table 1.2: Results obtained by (Chandrangsu, Rasmussen, 2008).

Joint configuration	Bending about strong axis				Bending about weak axis		
	Stiffness (kN.m/rad)						
	k_1		k_2	k_3	k_1	k_2	k_3
	Looseness alone	All tests					
4-way	39	80	102	5,3	15,0	7,5	0,8
3-way	36	75	87	5,1	14,0	7,0	1,0
2-way	41	70	77	4,6	7,5	5,0	1,5
Joint configuration	Rotation (rad)						
	β_1		β_2	β_3	β_1	β_2	β_3
4-way	0,014		0,036	0,16	0,02	0,04	0,10
3-way	0,012						
2-way	0,007						

1.4.1.3 Proposed methodology

Joint tests are justified by the importance that stiffness and resistance of the various types of connections have in the structural behaviour of bridge falsework systems. This can be seen for example in the results obtained by (Rodrigues, 2010).

In the present Thesis, testing of Cuplok® joints is performed aiming to clarify the issues referred previously and to contribute to increase the available knowledge. The test setup of ledger-to-standard Cuplok® joints follows closely the ones used in the former studies to allow comparison of results and to avoid the introduction of additional variables. However, the testing procedure is different: at start of the tests three hysteretic cycles with small amplitudes are applied whereas in the existing studies monotonic or fully hysteretic tests were carried out. This aims to assess the influence of initial low amplitude rotation cycles, that occur for instance due to wind action, have in the behaviour of ledger-to-standard Cuplok® joints.

In cases where tests have not yet been performed, proper testing procedures and tests setups are developed based on testing standards already available (BSI, 2001, 2005a ; CEN, 2006 ; BSI, 2009a), for example.

Specifically, axial and bending tests on ledger-to-standard Cuplok® joints are carried out aiming to expand the existing results database and thus increasing the accuracy of the subsequent choice of a statistical distribution for the joints behaviour and resistance. Bending tests of spigot joints and forkhead joints are also carried out.

1.4.2   Bridge falsework performance evaluation

1.4.2.1 Development of numerical models

Nowadays, numerical models are the most efficient and economical ways of analysing the structural behaviour of civil engineering structures. The increased computational capacity makes it possible to perform highly complex studies and to satisfactorily capture the real behaviour of structures.

In the present Thesis, the *Abaqus*® software is used. This is a general purpose finite element analysis software that makes possible to conduct comprehensive and complex analysis of bridge falsework systems.

In particular, ABAQUS® offers many solutions to model the materials behaviour including damage initiation and evolution. ABAQUS® offers another interesting option as it provides both explicit and implicit (static and dynamic) solvers. This is particularly important when performing progressive collapse analysis where instability phenomena are expected to control the structural behaviour.

However, ABAQUS® does not provide a sufficiently general joint finite element capable of simulating the actual behaviour of the type of joints found in bridge falsework systems. Therefore, a joint finite element is developed and integrated in ABAQUS® framework.

1.4.2.2 Robustness evaluation

Robustness of structures has been recognised as a desirable structural property following some severe failures, such as the Ronan Point Building in 1968, where the consequences due to a local and limited failure were deemed unacceptable and disproportionate to the initiating damage. The collapse of the World Trade Centre is another and recent example of the importance of structural robustness.

Since then, there has been a significant effort to develop methods to assess robustness and to quantify aspects of robustness. Approaches to define a robustness index can be divided in the following levels with decreasing complexity (Sorensen et al., 2009):

1. A risk-based robustness index based on a complete risk analysis where the consequences are divided in direct and indirect risks (Baker et al., 2008).

2. A probabilistic robustness index based on probabilities of failure of the structural system for an undamaged structure and a damaged structure (Frangopol, Curley, 1987 ; Fu, Frangopol, 1990).

3. A deterministic robustness index based on structural measures, *e.g.* advanced non-linear analysis of the structural resistance of an undamaged structure and a damaged structure. Concerning this approach there are a number of proposed indexes, such as (Starossek, 2009).

Nevertheless, both the existing definition of robustness and methods to measure robustness still have some limitations. As a result, a new definition and robustness index is presented.

1.4.2.3 Proposed methodology

In the present Thesis the resistance, robustness, fragility and risk of bridge falsework systems are studied using advanced deterministic and stochastic methods, and newly developed robustness and fragility indices that constitute the basis of a risk informed decision-making process. The following objectives have been achieved:

- To identify critical components or elements that govern the structural behaviour, robustness and structural risk of bridge falsework systems;

- To evaluate the influence on these measures of different factors, such as: (i) material properties, (ii) geometrical imperfections of the members, (iii) bracing configurations, (iv) actions of different nature (construction loads, wind, differential ground settlements) (vi) efficiency of the inspection and quality assurance plans (vii) structural system configurations (namely using steel girder beams to span over roads or other obstacles);

- To study different strategies to enhance robustness and decrease structural risk: (i) resistance, (ii) structural integrity, (iii) ductility. Select a case study to apply a full risk informed decision making concerning bridge falsework structures.

1.5 Thesis organization

The present Thesis is organised in six main Chapters:

Chapter 2. Background

In this Chapter the context, motivation, objectives and contributions of the study are presented together with a thorough bibliographic review of each of the subject areas: characterization of bridge falsework systems; current research status both considering experimental and numerical results of bridge falsework systems; identification of critical hazard scenarios including design and operation related activities.

Chapter 3. Experimental investigation

In this Chapter the complete set of tests performed in the present research is presented, along with their results and corresponding discussion.

Chapter 4. Numerical investigation

In this Chapter the formulation of a new joint finite element is presented, along with the constitutive laws of each type of joint found in Cuplok® bridge falsework systems. The process of validation and verification of the numerical models is also detailed. Finally, the influence of several modelling hypothesis is assessed and discussed.

Chapter 5. Structural design in the context of risk informed decision-making

The key theoretical contributions of the Thesis are presented in this Chapter. In particular, a holistic methodology integrating structural design in the context of risk informed decision-making is detailed, using newly developed robustness and fragility measures.

Chapter 6. Application of the proposed structural design methodology to bridge falsework systems

The key practical contributions of the Thesis are presented in this Chapter. The resistance, robustness, fragility and risk of bridge falsework systems are studied using advanced deterministic and stochastic methods.

Chapter 7. Findings and conclusion

The main conclusions of each preceding Chapters are presented together with some proposals for future works.

2

BACKGROUND

2.1 Introduction to temporary structures

As a *fib* (fib, 2009) documents states: *"The realization process of civil engineering structures is complicated: a wide variety of disciplines is involved, each with a specific contribution, and each involved somewhere between initial concept and completion. It is a challenge to structure the process in such a way that a balanced and optimized participation of the many disciplines involved is achieved. One of the critical success factors is knowledge management: each discipline should bring professional knowledge, but disciplines should interact effectively at interfaces as well. And that is where the gap in practice often appears. Temporary structures for civil engineering projects are an example of this phenomenon; they are right in the middle of a complex system of interactions: between structural engineering, site engineering, work preparation, procurement, and execution. They have a significant impact on cost, construction time, construction methodology and through-life performance of the actual, permanent structure"*.

According to McGraw-Hill Encyclopaedia of Science and Technology (McGraw-Hill, 2007): *"Temporary structures are those structures that are erected and used to aid in the construction of a permanent project. They are used to facilitate the construction of buildings, bridges, tunnels, and other above and below-ground facilities by providing access, support, and protection for the facility under construction, as well as to assure the safety of the workers and the public. Temporary structures are either dismantled and removed when the permanent works become self supporting or completed, or they are incorporated into the finished work. In addition to new construction, some temporary structures are also used in inspection, repair and maintenance work. The long list of temporary structures includes: cofferdams; earth-retaining structures; tunnelling supports; underpinning; diaphragm/slurry walls; roadway decking; construction ramps, runways and platforms; scaffolding; shoring; falsework; concrete formwork; bracing and guying; site protection structures such as sidewalk bridges, fall protection boards and nets, barricades and fences, and signs; and all sorts of unique structures that are specially conceived, designed, and erected to aid in a construction operation"*.

According to R.T. Ratay (Ratay, 1996) *"Any element used in construction which will be removed or will not be used as a part of the finished structure is considered to be of temporary nature (...)"*. Ratay also divides temporary structures in two categories relating their end use: *"The first, (...), includes temporary structures providing support for the permanent structure or other construction. (...) The second category includes temporary structures used to perform the construction or as work platforms for construction workers"* (Ratay, 1996). Therefore, a temporary structure can be characterised (i) by having a predetermined usage timeframe much shorter than of the permanent structure, and (ii) by the extended life span of its elements which can be continuously reused in new temporary structures designs.

Important problems can be immediately raised:

- If the vast majority of elements, and more often than not entire temporary structures, can be reused, should the structure be designed for small exposure periods, one to two years for example, corresponding to each usage cycle, or for larger exposure periods similar to the ones used for permanent structures, corresponding to the design working life span of the elements?

- Since temporary structures can be reused in sites with completely different wind exposure conditions and soil bearing resistances for example, which should be the design criteria if the designer decides to account for the entire life span of the structure?

- Since temporary structures are comprised by large number of elements which have to be assembled on site there is a large chance for human errors. How can they be managed?

- How can the reusage of elements be accounted for in the design process? And what is its influence on the performance of the system?

In the present Chapter answers to these important questions will be given, see in particular section 2.5. Some hints to solve this problems can be found in works of (Rosowsky, 1995), (Hill, 2004), (Mohammadi, Heydari, 2008) and in (ASCE, 2002), (fib, 2009), but general guidance is needed.

From the two categories defined by Ratay and presented above only the temporary structures used during the construction process of civil engineering structures will be further discussed, in particular: (i) bridge temporary structures and (ii) scaffold systems.

2.1.1 Bridge temporary structures

There are two types of bridge temporary structures: (i) bridge falsework (the topic of the present Thesis) and (ii) bridge construction equipment (BCE).

BS 5975:2008 (BSI, 2008a) defines falsework as: *"Any temporary structure used to support a permanent structure while it is not self-supporting"*. In the present Thesis, the term falsework will only be applied to temporary structures used in bridge construction.

The main role of bridge falsework is to provide structural safety and safety to the workers during the construction of a structure. Bridge falsework consists in temporary structures providing a stable platform upon which the formwork may be built, and giving support for the bridge superstructure until the members being constructed have attained sufficient strength to support themselves and sufficient stiffness to satisfy performance requirements.

Although, bridge falsework elements could be used in the erection of steel bridges, their use is generally associated with the construction of cast-in-place concrete bridges. The temporary structures used in building construction are referred to as "shores", or "props", and the support system as "shoring" (Ratay, 1996).

Bridge falsework systems are stationary temporary structures, *i.e.* which do not have integrated a mechanical system allowing them to move without having to be dismantled and reassembled in the new location. They were the first type of bridge temporary structures to be developed, and are simultaneously the more basic and most versatile bridge temporary structure. Detailed information about this system is presented in the next section.

Bridge falsework systems can consist on 3-D metal frame structures where "beams" and "columns" are connected to each other by special couplers, or they can be ready-to-use heavy-duty towers.

Bridge falsework systems are mostly used during the construction of concrete bridges using span-by-span *in situ* casting or span-by-span precast segmental methods. However, they can also be used in the construction of other types of bridges as support to the main BCE system.

On the other hand, BCE consists in more complex structures such as those used in the cantilever form-traveller construction method, where the formwork is incorporated in the equipment, or

bridge launching equipment which was developed to facilitate precast construction. Another significant difference between bridge falsework and BCE systems is that the later have a mechanic hydraulic system which enables the automatic controlled movement of the system without the need for dismantling and reassembling procedures. Figure 2.1 and Figure 2.2 illustrate different types of BCE. See also (André et al., 2012a).

Therefore, there are several types of bridge temporary structures, each one targeting a special application under certain engineering and economical constraints. Cardwell (Cardwell, 2010) presented a possible range of application of bridge temporary structures based on the material of bridge decks: steel, composite and concrete, see Figure 2.3.

The criteria for choosing the construction method of a bridge are manifold: from the geometrical characteristics of the superstructure, namely the layout of the bridge (plan and elevations), deck type and its material but also the height of the piers, the length of the bridge and of each span and the spans uniformity, the ground properties, the bridge context (deep valleys, crossing a waterway or a road, open field or urban area, ease of access, size of space available, etc), the labour costs and logistic issues such as availability of materials and equipment, the designer and contractor expertise, etc. In (fib, 2000 ; The Concrete Centre, 2008) pre-design aids for concrete bridges are available and in (Ayaho et al., 1997) a system for selecting the erection method for steel bridges is proposed.

Figure A   Figure B

Figure 2.1: *Left*, **Self-launching gantry systems (Rosignoli, 2002);**
Right, **Movable scaffolding systems (Lee, Daebritz, 2010).**

Figure A   Figure B

Figure 2.2: *Left*: **Incremental launching systems (Rosignoli, 2010);**
Right: **Form-traveller systems for balanced cantilever construction (Nitschke, 2010).**

Figure

Figure 2.3: Range of application of bridge temporary structures (Cardwell, 2010).

2.1.2 Scaffolds

BS 5975:2008 (BSI, 2008a) defines scaffolds as: *"A temporary structure which provides access, or on or from which persons work, or that is used to support materials, plant or equipment"*. Therefore, there is a fundamental difference between scaffold structures and bridge falsework structures scaffolds: while the former does not have a structural role, it is solely used to give access to various levels during construction, the later is designed to assure the strength, stability and stiffness of the permanent structure during its construction. Therefore, the load range applied to each system is completely different with direct implications in their design and safety requirements.

Different types of scaffolds exist, including of different materials such as steel, aluminium or even bamboo. Scaffolds are generally light structures, and each scaffold is unique, because their design varies with the site where they will be used, and with their role in the building process.

As for falsework structures, steel and aluminium scaffolds are based on vertical (standards) and horizontal (ledgers and transoms) tubular elements linked together with couplers to form a three-dimensional structure.

Scaffolds systems can range from proprietary modular ready-to-use structures to structures which can be assembled arbitrarily. Scaffolds are generally composed of several bays on which work platform units are placed at different levels, with brace and tie elements arranged in a specific configuration to achieve a better structural integrity and lateral resistance.

2.2 Introduction to bridge falsework systems

The present Thesis deals with bridge falsework systems. The type of system most commonly used corresponds to proprietary modular units consisting in an assembly of metal (steel or aluminium) tubes, generally displayed in a uniform mesh of vertical and horizontal elements (in both directions of the horizontal plane), connected to each other by special couplers, braced by diagonal members and placed under the entire formwork of a bridge section (which for short bridges could represent the entire bridge). Additionally, to the 3-D frame structures defined above, there are also available in the market other bridge falsework solutions such as heavy-duty towers made of built-up elements. Sometimes, these two different systems are used together in the same construction, see Figure 2.4.

These 3-D structural systems are often also called birdcage metal structures, tube and coupler falsework, steel frames or bridge scaffolding. The later term can be misleading, and will not be used hereafter, in the sense that scaffold structures as mentioned before are not meant to receive high construction loads; their main role is providing access to workers to different height levels.

The use of bridge falsework structural systems in bridge construction dates to the beginning of the modern bridge engineering. Thus, they had a key role on the construction of major infrastructures around the world. Nowadays with the advances of bridge engineering, novel design and construction techniques have been introduced. Cable stayed bridges, post-tensioned box-girders, composite bridges and precast construction propelled the industry to invent new ways to construct bridges, which led to the development of the bridge construction equipment (BCE) which couples civil, mechanical and electrotechnical engineering.

Nevertheless, bridge falsework systems are still widely used to build low height (9 m to 12 m; 30 m maximum) concrete bridges with small span lengths (up to 60 m (Crémer, 2003)) and not too long (500 m in general, although it is referred in (Masumoto et al., 1994) that a 725 m continuous bridge was built using this construction method), in wide valleys with good ground conditions, easy access and no major land use. This is the most flexible construction method to the designer: (i) it does not influence the bridge geometry – the bridge deck geometry can vary from span to span and exhibit complex configurations both in plan and in elevation; and (ii) it does not control the design of the structure.

Where the bridge crosses waterways or roads, or the soil properties are weak, steel trusses or steel girders can be used to sustain the formwork, transmitting the loads to heavy-duty towers placed at the ends of the span in order to avoid the obstacles. This system can also be used if the height of the bridge piers is high. Additionally, heavy-duty towers can be used as temporary supports in bridge launching or in the construction of arch bridges. Heavy-duty towers can consist in ready-to-use structures made of built-up elements or in an assembly of elements of the 3-D structural systems described previously.

The construction cycle of a cast *in situ* concrete bridge using this method of construction consists in the following stages: (i) first, the temporary structure is placed underneath the bridge section to be cast; (ii) secondly the formwork is assembled; (iii) next the concrete is cast and when it has hardened and has achieved sufficient strength the prestressing cables, if they exist, are at least partially tensioned; (iv) falsework is removed and moved to another section. In multiple span bridges, it is common practice to consider construction joints distancing one fifth of the span length of the bridge piers. In terms of construction rate, a 20 m/week cycle is normally achieved (Crémer, 2003). These systems are usually

used in each construction site for only a few weeks, although sometimes they can be continuously used for six months or more. To maximise economic benefits, bridge falsework elements are reused several times in different projects at different locations. Their broad availability, low investment needed together with cheap labour work (less specialised), also contributes to make them a strong competitor to other alternative construction methods such as prefabrication or use of MSS systems.

Complete information on the history and evolution of falsework in UK can be found in (Burrows, 1989).

Figure

Figure 2.4: Bridge falsework example (©RMD, www.rmdkwikform.com).

2.2.1 Materials

Different natural materials such as timber and bamboo have been used in the past and are still being used in Asia to construct bridge falsework systems. In the western countries, steel is the primary material option for elements of these systems due to their high strength and reusability. Typically, bridge falsework elements consist in cold-formed or hot-rolled circular hollow steel sections. Recently, following the trend of maximising the efficiency in construction, aluminium is becoming increasingly utilised as the material of elements in bridge falsework construction because of its lighter weight and ease of handling.

Hot-rolled and cold-formed hollow sections must satisfy the requirements specified in BS EN 10210-1 (BSI, 2006a) and BS EN 10219-1 (BSI, 2006b), respectively. However, since many falsework structures have been designed and produced many years ago the grade of the steel used does not follow the existing standards. Nevertheless, it is possible to correlate the old steel grades to the new ones. For example, Table 2.1 presents a comparison between the current steel grades with the ones specified in BS 4360 (BSI, 1990).

Table 2.1: Comparison between BS 4360 steel grade and current grades.

BS 4360	Current grade (BSI, 2006a, 2006b)
40B	S235JR
40C	S235J0
40D	S235J2
43B	S275JR
43C	S275J0
43D	S275J2
50B	S355JR
50C	S355J0
50D	S355J2
50DD	S355K2

2.2.2   Main elements of bridge falsework systems

Bridge falsework systems should be designed to be rapidly assembled, adaptable to particular projects, safely dismantled and envisaging their re-usage. Various types of bridge falsework systems exist, each one with different characteristics, therefore complying with the abovementioned requirements at different levels.

For instance, ready-to-use heavy-duty towers made of built-up elements consist in four main vertical members (chords) braced by batten or laced elements welded to the chords, see Figure 2.5, allow higher construction rates but their handling requires the use of cranes and their application range is limited.

Figure A   Figure B

Figure 2.5: Ready-to-use heavy-duty towers, ©RMD Kwikform, www.rmdkwikform.com.

On the other hand, 3-D steel framed structures are an assemblage of vertical and horizontal individual elements braced by diagonal members, see Figure 2.6.

Therefore, these systems require intensive labour work in assembling and dismantling operations, but since their availability is widespread these systems are still the prime bridge falsework solution. The present Thesis will be mainly devoted to the investigation of the performance of this type of bridge falsework system.

To increase their adaptability and efficiency, vertical (standards), horizontal (ledgers) and brace elements are available in different lengths and threaded universal jacks can be assembled at the bottom and at the top plates (baseplates, headplates or forkheads, respectively) to fine adjust the height of the system and allow for an easier striking of the formwork. Standard, ledger, and brace elements have a circular hollow cross-section, in general uniform along the length and also with a constant wall thickness. For brace elements there are two possible solutions: one, which is commonly used as face bracing, where the length of the element is fixed and a second, which is often used as internal adjustable bracing, consisting of two tubes with different outside diameters so that the inner tube can telescopically slide inside the outer tube to adjust the brace length. With the later solution, a single brace element can be used in different configurations: its length is defined by inserting a pin through one of the holes uniformly spaced along the length of the internal tube, and by locking the pin against a nut which is positioned in the top threaded part of the external tube.

Tubes used in bridge falsework elements often follow the requirements set in BS EN 39:2001 (BSI, 2001). Hence, tubes have a 48,3 mm outside diameter and 3,2 mm (type 3 tube) or 4,0 mm (type 4 tube) wall thickness – additionally non-standard sizes exist such as 60,3×3,2 mm or 48,3×6,0 mm. Tubes can be supplied seamless or welded, and usually have a hot-dip galvanised coating. In Table 2.2 it is presented the characteristics of the elements of a typical bridge falsework solution. Figure 2.7 illustrates a schematic representation of a bridge falsework Cuplok® solution.

Figure A   Figure B

Figure C   Figure D

Figure 2.6: Examples of bridge falsework. *Top left*: **©RMD Kwikform www.rmdkwikform.com,** *Top right*: **(Carvalho et al., 2004),** *Bottom left*: **(Rosignoli, 2010),** *Bottom right*: **(Rosignoli, Daebritz, 2010).**

2.2.3 Joints and foundations

Various types of joints can be found in bridge falsework systems, with emphasis for the 3-D framed systems. Table 2.3 presents the most common types of joints between elements of these systems.

Joints between two consecutive standards are made by means of a spigot coupler. The spigot has a smaller outside diameter than the one of the standards and can be an individual element or it can be welded to the top section of the lower standard. The length of the spigot should be equal or greater than 150 mm. The spigot can be connected to the upper (and lower) standard(s) by pins, by bolts inserted through centred holes or by locking the upper standard to a special connector welded to the spigot wall.

Several types of couplers can be used to connect ledgers to standards: from the classical right angle and putlog couplers to the proprietary solutions such as Cuplok® and wedge couplers. The last two types of couplers were developed to overcome the limitations of using the first two types, by allowing several ledger elements to connect to one standard element at a single node. For example, in the case of the Cuplok® systems, the standards have steel elements uniformly distributed along its length (in general spaced by 500 mm) consisting in bottom and upper cups – only the former is welded to the standard wall. The ledgers have two steel blades at each end which are introduced within the cups. Finally, the joint is locked by striking with two to three hammer blows the upper cup. Each Cuplok® joint can accommodate up to four elements – combination of ledgers and brace elements.

A brace element can be connected to a ledger element by a hook coupler or by a type of wedge coupler. It is recommended that the brace is fitted within 150mm of Cuplok® node (SGB, 2009). In the case of the connections between a brace element and a standard element these consist in swivel couplers.

Some of the abovementioned couplers are controlled by specific European standards. For instance, BS EN 74-1 (BSI, 2005a) defines design requirements, strength classes (A and B) and testing procedures for right angle and swivel couplers used with tube elements of 48,3 mm external diameter. Classes A and B differ in transmissible internal forces and moments and in values of load bearing capacity and stiffness. For example a class A swivel coupler has a minimum design axial failure load of 14 kN whereas a class B coupler has a minimum design axial failure load of 20 kN.
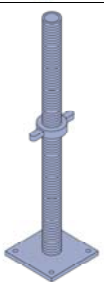
Table 2.2: Characteristics of the elements of a typical bridge falsework system.

Element	Length	Cross-section	Typical material	Illustration
Standard	0,4 m (SL), 0,8 m (SL), 1,0 m (S), 1,3 m (SL), 1,8 m (SL), 2,0 m (S), 2,3 m (SL), 3,0 m (S)	Tube with circular hollow section. Outside diameter×wall thickness: 48,3×3,2 mm	Steel: Grade 50C to BS 4360 (BSI, 1990), equivalent to S355J0 according to BS 10210-1 (BSI, 2006a) or BS 10219-1 (BSI, 2006b)	
Ledger	0,6 m, 0,9 m, 1,0 m, 1,2 m, 1,3 m, 1,6 m, 1,8 m, 2,5 m			
Face bracing	(X × Y): 1,8×1,5 m 1,8×2,0 m 2,5×1,5 m 2,5×2,0 m 3,0×2,0 m	Tube with circular hollow section. Outside diameter×wall thickness: 48,3×3,2 mm	Steel: S275 according BS 10210-1 (BSI, 2006a) or BS 10219-1 (BSI, 2006b)	
Internal adjustable bracing	(Bay×Lift): 1,0×1,2 m 1,0×1,3 m 1,0×1,6 m 1,0×1,8 m 1,0×2,5 m 1,5×1,2 m 1,5×1,3 m 1,5×1,6 m 1,5×1,8 m 1,5×2,5 m 2,0×1,3 m 2,0×1,6 m 2,0×1,8 m 2,0×2,5 m	Tubes with circular hollow sections. Outside diameter×wall thickness: Inner tube 38,0×3,2 mm Outer tube 48,3×2,9 mm		

S – Spigoted standards; SL – Spigotless standards
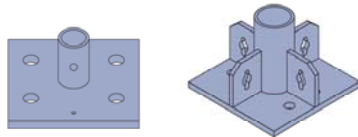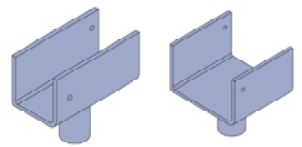
(continues)

Table 2.2: Characteristics of the elements of a typical bridge falsework system.

Element	Length	Cross-section	Typical material	Illustration
Universal jack	0,40 m (maximum extension: 0,25 m) 0,86 m (maximum extension: 0,65 m)	Tube with circular hollow section. Outside diameter×wall thickness: 38,0×5,0 mm Also available in solid steel rods	Steel: S275 according BS 10210-1 (BSI, 2006a) or BS 10219-1 (BSI, 2006b)	
Combined jack and baseplate	0,87 m	Tube with circular hollow section. Outside diameter×wall thickness: 38,1×4,0 mm		

(continues)

Table 2.2: Characteristics of the elements of a typical bridge falsework system.

Element	Dimensions (mm)	Typical material	Illustration
Baseplate and Headplate	Side length×thickness: 152×6 152×10	S275 according BS 10210-1 (BSI, 2006a) or BS 10219-1 (BSI, 2006b)	
Forkhead	Side length×thickness: 200×102×8 150×188×8 200×202×8	S275 according BS 10210-1 (BSI, 2006a) or BS 10219-1 (BSI, 2006b)	

(ends)
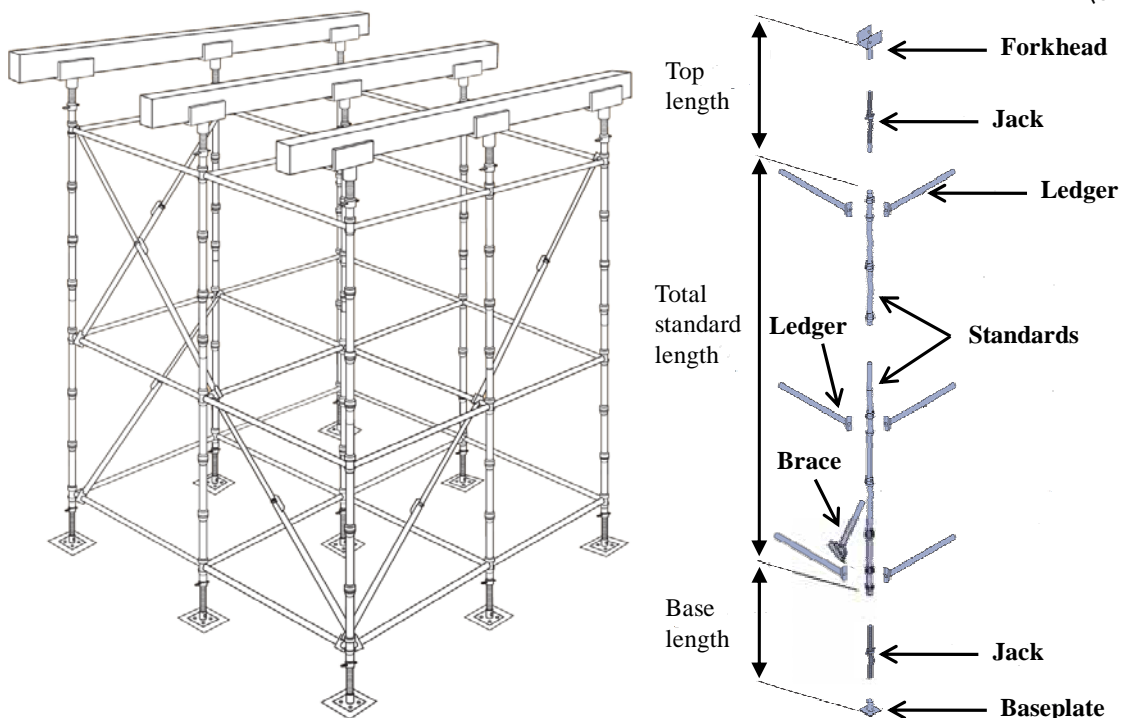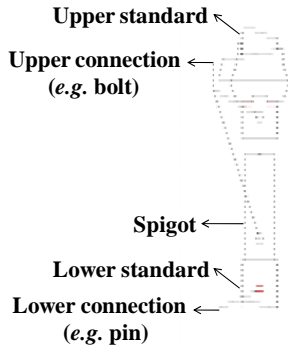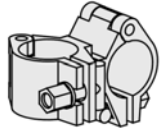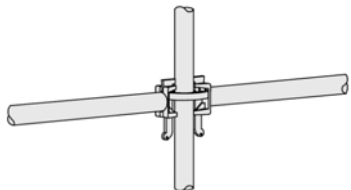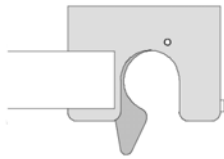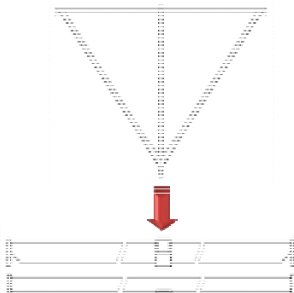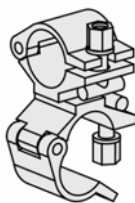
Figure 2.7: Schematic representation of bridge falsework Cuplok® solution (©HARSCO, www.harsco-i.co.uk).

Table 2.3: Types of connections between elements of a bridge falsework system.

Connection	Type	Illustration	
Standard-to-standard	Spigot joint	**Type A):** Upper standard Upper connection (*e.g.* bolt) Spigot Lower standard Lower connection (*e.g.* pin)	**Type B):**
Ledger-to-standard	Special couplers	Right-angle coupler	Putlog coupler
Ledger-to-standard		Cuplok® joint	Wedge joint
Ledger-to-brace	Hook joint or wedge joint	Hook joint:	Wedge joint:
Standard-to-brace	Swivel joint	Type A):	Type B):
Standard-to-jack Jack-to-baseplate Jack-to-headplate Jack-to-forkhead	Jack joint		

BS EN 74-3 (BSI, 2010b) specifies structural requirements for baseplates and geometrical characteristics for spigot couplers. Baseplates made of steel of a minimum grade S235 and with a

minimum thickness of 5 mm are deemed to satisfy the structural requirements. Finally, BS 1139-2.2 (BSI, 2009b) specifies requirements and test methods for putlog couplers.

Regarding bridge falsework foundations, different types of foundations exist for transmitting falsework loads to the supporting ground, see Figure 2.8.

Due to the high concentrated loads and small dimensions of the baseplates high stresses need to be transferred to the ground. Considering that the ground over which the bridge falsework foundations rest is often characterised by being soft and weak there is the need to improve the ground stiffness and resistance and/or to adopt structural solutions more complex than the ones typically used in scaffolds. If the ground is made of soil the top layers of the ground must be removed and *in situ* testing should be performed in order to characterise the type, depth, lateral and vertical variations of the soil underlying and adjacent to a falsework site. If the slope of the ground exceeds a certain value, BS EN 12812 (BSI, 2011) suggests 8%, it is recommended that the foundation should be design accounting for this factor.

Figure A   Figure B

Figure 2.8: *Left*: **Timber sole plates,** *Right*: **concrete footings**
(©RMD Kwikform, www.rmdkwikform.com).

2.2.4 Assembly

Different types of bridge falsework systems necessarily have distinct assembly procedures. However, procedures of some systems share common steps. For instance the Cuplok® and the Bosta systems (both ©HARSCO, www.harsco-i.co.uk) although having different solutions for connecting ledgers to standards share many features and the assembly procedures follow the same principles.

However, the apparent simplicity of assembling a group of light steel bridge falsework elements hides many critical details. In fact, the success of any bridge falsework system is controlled by how well the design, planning, monitoring and control procedures accounted for these details: (i) adequacy and validity of the design principles and design hypothesis used when compared to the actual conditions and actual structure, (ii) competence of the site investigation, assembly and operation sequence, (iii) proficiency and responsibility of the stakeholders and (iv) efficient communication and information management (drawings, method statement, etc.) from the design office to site workers. An example of a recommended assembly sequence, based on information given by a bridge falsework supplier, is given in the document entitled "Safety Guide: Cuplok® Falsework Erection Procedure" elaborated by SGB (now HARSCO) (SGB, 2001). It is assumed that aspects dealing with all the other details listed above are correctly assured, see BS 5975 (BSI, 2008a) for guidance.

It is often recommended to layout the structure with continuous lines of ledgers in both directions as this automatically gives accurate setting out of the standards, and to place ledgers in the lowest and highest cup of every standard row (SGB, 2006). Every row of standards must always have a spigotless standard at the top so that a jack can be inserted. To ease erection in slopes it is recommended to start assembling components at the highest elevation first and then moving to

lower heights. In order to avoid the build-up of adverse tolerances when very long structures are to be assembled, it is recommended to consider dividing the structure into several parts (SGB, 2009).

In this section a particular assembly concern will be discussed: lateral restraint provisions. These can be achieved in top-restrained falsework structures by the plate action of the formwork and the stiffness of the permanent structure or in free-standing falsework structures by proper bracing or by a combination of bracing, tying of the structure to the piers or abutments and also plan bracing. Since the design of bridge falsework is often defined by design load tables developed by the supplier, see (SGB, 2009) for instance, bracing configurations follow what is prescribed in the supporting documents of the design load tables. For example: *"In general, jack bracing should be avoided wherever possible, by designing the structure so that only the smallest jack extensions are required at top and bottom. The extension of the jack at the top, and the bottom, should be balanced, to give equal load carrying capacity"* (SGB, 2009). Cuplok® towers need to have diagonal braces in all faces from the forkhead to the baseplate. Additionally, consecutive rows of ledgers should be spaced by no more than four times the minimum plan dimension (SGB, 2009). 3-D systems with a more complex layout need a more refined analysis and assembly of elements.

Furthermore, *"Diagonal braces should be fixed to the ledgers as close to the node point as possible: the maximum gap between the side of the brace and the node point should be 50mm. The bracing should be installed immediately after the erection of each lift to ensure that all bays are properly squared up. The quantity of bracing should be calculated, but a minimum amount must always be used. This requires one complete brace from the top to the bottom ledger level in a continuous diagonal line, on each row of standards, one in seven bays in each direction"*, see Figure 2.9. *"This is preferable to the zig-zag or parallel bracing in one bay (...) as it reduces the additional load in a leg due to the horizontal loading. It is preferable that braces in adjacent panels should also be alternated in direction, as shown by the dashed lines"* in Figure 2.9 (SGB, 2009). It is however common to find bridge falsework structures with bracing only at the extreme faces, in both directions.

"On tall falsework structures consideration needs to be given to the provision of plan bracing to prevent the vertical load bearing members distorting, by lozenging in plan. Generally for falsework up to about 7 metres high, the stiffness of the formwork will provide suitable restraint and plan bracing would not be required" (BSI, 2008a).

Finally, a remark concerning the assembly of the formwork beams on the forkheads. The recommended method is illustrated in Figure 2.10 and consists in tightening the formwork beam to the forkhead sideplates by wood wedges, the forkhead must be slightly rotated to guarantee the proper alignment of the formwork beam.

Figure

Figure 2.9: Recommended bracing layout (©HARSCO, www.harsco-i.co.uk).

Figure

Figure 2.10: Fastening of the formwork beams on the forkheads (©HARSCO, www.harsco-i.co.uk).

2.3 State-of-the-art of bridge falsework systems research

2.3.1 Current design standards

Temporary structures must provide structural safety and safety to workers. Furthermore, the interaction between the temporary and the permanent structures must guarantee the specified geometry, durability, quality and, ultimately, the safety of the permanent structure. However, temporary structures do not receive the same research attention as do permanent structures, and as a result this sector of civil engineering lacks the existence of strong regulation and standardization.

Until recently, the available guidance summed up in just some few general statements in permanent structures design codes such as *"proper provisions shall be made"* and *"adequate temporary bracing shall be provided"* (Ratay, 2009). Therefore, the majority of temporary structures were designed at the discretion of the sub-contractor usually based on in-house developed design procedures prepared by the producers of the proprietary equipment and generally without supervision or in some cases with an inadequate one. As a result, the design rules applied to these temporary structures were not uniform and therefore the actual reliability levels are often smaller and exhibit a greater variation than the corresponding reliability levels of permanent structures.

In recent years there has been an effort in Europe, USA and other developed countries to diminish the uncertainty and risk involved with the use of these structures. Nowadays, the importance of bridge falsework structures increased to the point where their design, assembly and maintenance are ruled by specifically made standards and codes of practice. As expected, existing temporary structures codes profited from the available knowledge accumulated over the years, in its majority of empirical nature. Certainly lessons from past mistakes lead to changes in all phases of temporary structures, from design to use, maintenance to inspection. This was further enriched with added value from recent research studies, most of them numerical investigations. However, the improvement of design and construction codes concerning temporary structures was made at a much slower pace than for permanent structures. Until recently, existing standards were based on the allowable stress design concept – which was replaced in the 1980s in permanent structures' design codes. Nonetheless, at present most of the codes adopt the Limit State Design (LSD) philosophy.

However, since much of these codes were developed based on the existing permanent structures codes more often than not guidance is missing: *"Is this structure as safe, as wind-resistant, and as cost-effective as we can make it?"* (Gorlin, 2009). Additionally, some deep rooted axioms shared by designers and other relevant stakeholders were transmitted to the existing temporary structures codes. The majority of these codes allow that in the design of temporary works lower design loads may be used than for completed permanent structures. This is partly based on the idea that short-term loads are more closely predictable and can be more effectively controlled than the long-term live loads during the decades of use of permanent structures. Additionally, because their importance and use is considered to be not as relevant as of permanent structures, the specified partial factors applied on the resistance side are sometimes smaller than the ones specified for permanent structures.

One must always have in mind that *"codes codify safety; good designs provide it"* (fib, 2000). Structural safety comes from a coherent and comprehensive global structural concept, *i.e.* proportionate structural forms with logically defined load paths together with simple construction procedures, not from the fulfilment of code requirements which by themselves cannot assure the required safety (fib, 2000).

According to (Ratay, 2009) there are several factors inherently involved in the establishment of design loads, resistance models and partial factors that are used in the design of any structure. These include the following:

- *"Intended function of the structure*
- *Nature of loads*
- *Predictability of occurrence of loads*
- *Certainty in the magnitudes of loads*
- *Possibility of simultaneous occurrence of loads*
- *Possible secondary stresses, redundancy, and instability.*
- *Condition of the member and its material (new, used, damaged, deformed)*
- *Acceptable behaviour of the structure (such as tolerable deflections, and vibrations)*
- *Allowable degree of unacceptable behaviour*
- *Acceptable probability of total failure*
- *Consequences of failure*
- *Construction tolerances*
- *Workmanship in the construction*
- *Inspection standards*
- *Protection of the structure against damage, deterioration, and extremities of weather*
- *Intended life-span of the structure with increasing probability of occurrence of maximum loads, abnormal loads, damage, and deterioration with time".*

As it can be observed there are many topics that separate apart the design of temporary structures from the design of permanent structures. However, because of the constraints previously pointed out, research is still needed to improve design codes of temporary structures in order to properly address important aspects such as evaluation of loads for reduced exposure periods, consideration in the design process of multiple usage cycles, structural performance requirements (including robustness), acceptable and unacceptable risk levels.

Next, a brief summary of the principles of USA, European and Australian standards related to the design of bridge falsework systems will be presented.

In the USA, the most complete and up-to-date standard outlining a design philosophy and specifying minimum design loads and load combinations for temporary works is the ASCE/SEI 37-02 (ASCE, 2002). Since the scope of this document concerns mainly the load requirements during construction of buildings, other standards exist for example the AASHTO standard GSBTW-1-M (AASHTO, 2008) which covers the design of bridge falsework systems and the ACI standard 347-04 (ACI, 2004) which covers the design of formwork for concrete construction. Design guidance about bridge falsework can also be found in the State of California Falsework Manual (Department of Transportation, Division of Structures, 2001).

In Europe reference should be made to BS EN 12812 (BSI, 2011) for bridge falsework, and to BS EN 12811 (BSI, 2002b, 2003, 2004b) for scaffolds. BS EN 12812 gives performance requirements for specifying and using falsework and gives methods to design falsework to meet those requirements. The information on structural design is supplementary to the relevant Eurocodes. The standard also describes different design classes A and B.

Class A falsework is one where the structural performance can be individually evaluated and where simplified and traditional (determined by experience and established good practice) design methods can be safely used. Examples of class A falsework are adjustable telescopic steel props and formwork. The standard does not provide guidance for this class of falsework.

Class B falsework is one where simplified design methods cannot be applied and more comprehensive approaches are needed, for instance bridge falsework. Therefore, the general design philosophy of the Eurocodes is followed. BS EN 12812 gives the falsework designer two options: classes B1 and B2. The former fully adopts the Eurocodes with some additional requirements concerning information that must be included in the drawings, inspection and method statements. In the later class, BS EN 12812 specifies an alternative design procedure which differs from the one given in the Eurocodes on the amplitude of the initial geometrical imperfections (global and local), the construction loads values, the load combinations and the partial factors to be used. Nevertheless, it is expected that design methods for both classes result in equivalent reliability levels.

Still in Europe, the British Standard BS 5975 (BSI, 2008a) establishes a design framework based on the Allowable Stress Design (ASD) method for falsework, namely class A falsework according to BS EN 12812. BS 5975 also gives recommendations and guidance on the procedural controls to be applied to specification, construction, use and dismantling of falsework.

Reference will also be made to the Australian standard AS 3610 (SAA, 1995). The Canadian standard CSA 269.1 (CSA, 1975) is a very outdated document and will not be included in the following discussion.

2.3.1.1 Design philosophies

Almost all existing structural codes for the design and analysis of civil engineering infrastructures have abandoned the Permissible Stress Design philosophy (PSD), also called the Allowable Stress Design (ASD) in USA, and are now based on the Limit State Design (LSD) principles, which in USA is termed Load and Resistance Factor Design (LRFD). Nevertheless, in the USA the codes still allow the use of ASD.

The LSD principles are semi-probabilistic. In this methodology the format for structural design verification is expressed by a simple comparison between factored resistances and factored loads (or load effects) without explicitly assessing the reliability or the risks.

Due to the fact that resistances and actions are subject to uncertainties, probabilistic analyses were performed to derive statistically relevant values (characteristic values) taking into account the design working life of the structure and the uncertainty of different physical properties and conditions.

To ensure that the basis for design provides an appropriate level of structural reliability (or probability of failure), partial factors are introduced to take into account the effects of aleatory and epistemic uncertainties in the methods used to assess the characteristic values but also in the specified analysis and verification procedures. Therefore, design values for resistances are determined by dividing the characteristic values by a partial factor (larger or equal to 1) and design values for load effects are obtained by multiplying the characteristic values by a partial factor (typically larger than 1).

LSD specifies the verification of the structural reliability for several limit states, *i.e.* states beyond which the structure no longer fulfils the relevant design criteria: Ultimate Limit States (ULS) in which all possible failure modes must be evaluated, Serviceability Limit States (SLS) in which it is verified that specified service requirements are met, and other limit states such as fatigue resistance.

Finally, several load combinations must be checked to guarantee that all reasonable possible sets of physical conditions that can occur during a certain time interval, also known as design situations, are taken into account. This time interval is dependent on the design working life of the structure and is associated with a limit value for the annual probability of exceedance of the loads.

In general, three different design situations are defined each one representing a certain time interval with associated hazards, conditions and relevant structural limit states: persistent, transient and

accidental situations which refer to normal, temporary and exceptional situations. Each load combination is formed by the permanent loads, a leading variable action and the relevant accompanying variable actions which are multiplied by combination factors (smaller than one) in order to obtain concomitant actions values taking into consideration the unlikely event of simultaneous occurrence of the different actions at their maximum design values (Turkstra, Madsen, [sans date]).

LSD has been established in the Australian standard series AS 5400 (SAA, 2007), in Canadian standard S6 (CSA, 2006), in the European Structural Eurocodes, namely EN 1990 (BSI, 2002a), EN 1991 (BSI, [sans date]) and EN 1993 (BSI, [sans date]), and in USA standards ASCE/SEI 37-02 (ASCE, 2002) and AASHTO LRFD (AASHTO, 2010), for example. In the present Thesis only the bridge design codes will be discussed since bridge falsework structures are used in bridge construction and therefore to achieve a coherent design a common design framework must be used.

It should not be forgotten that the Eurocodes are only valid if used together with the corresponding National Annexes published by every European Union member state which contain the national choices for the Nationally Determined Parameters (NDPs). In the present Thesis the UK National Annexes will be used as an example.

It should be noted, that most codes allow the designer to use alternative design rules different from the ones specified if it can be demonstrated analytically or experimentally that the structural safety, serviceability and durability achieved will be at least equal to the ones expected when using the codes.

In both the AASTHO bridge code (AASHTO, 2010) and in EN 1990 it is possible for the stakeholders to manage the target reliability level of the structure. In the former code this is dependent of the structural characteristics (ductility, redundancy for example) and in the later of the consequences of failure, types of quality control and inspection procedures implemented. Bridge falsework structures can be considered as common structures based on the AASTHO criteria, but using EN 1990 an increased reliability level, achieved by considering an additional actions partial factor of 1,1, could be considered, justified by the low relative cost of safety measures compared to the large consequences of their collapse (ISO, 1998 ; JCSS, 2001), even when for the bridge a medium consequence class is considered (BSI, 2002a, 2004a). In this context, the target reliability index (see (BSI, 2002a) for definition) used in the AASHTO code calibration is equal to 3,5 (unfortunately there is no indication of the reference period associated) whereas in EN 1990 (BSI, 2002a) for a high consequence class an annual target reliability index equal to 5,2 is specified.

Considering that the AASHTO code specifies 75 years as the expected design working life, and assuming that the reference period associated with the reliability index previously indicated is equal to the expected design working life, a target reliability index of 4,5 is obtained for a one year reference period, which is lower than the one used in EN 1990 even for the medium consequences class (4,7) or than the target reliability index suggested in ASCE/SEI 7-10 (ASCE, 2010), of 4,8 for structures whose failure is sudden and results in wide spread progression of damage and for which 5 to 500 persons are exposed (Risk Category II).

No information is given in the USA standards regarding the design working life of bridge falsework structures. In EN 1990 a five years design working life for temporary structures is generally mentioned. However, since these structures can be dismantled with a view to being re-used this code demands they should not be considered as temporary. It is thought to be acceptable to consider a design working life between 15 to 30 years for bridge falsework structures (BSI, 2002a, 2004a), whereas in the Australian standard AS 1170.0 (SAA, 2002a) the minimum design working life for ultimate limit state consideration of any structure shall be 25 years.

In EN 1991-1-6 (BSI, 2005b, 2008b) a table (reproduced in Table 2.4) gives the recommended return periods, (see (BSI, 2002a) for definition), for the determination of the characteristic values of climatic actions depending on the nominal duration of the relevant design situation. It can be seen that return periods with very small values can be used which may be unconservative in some cases, see section 2.5.

On the contrary, AS 1170.0 specifies that for construction equipment structures, a 100 years return period should be considered for non-cyclonic wind actions and also for the snow action.

**Table 2.4: Recommended return periods for the determination
of the characteristic values of climatic actions (taken from EN 1991-1-6).**

Work duration	Return period (years)
≤ 3 days	2
≤ 3 months (but > 3 days)	5
≤ 1 year (but > 3 months)	10
> 1 year	50

2.3.1.2 Actions, partial factors and load combinations

With the information given in the AASHTO bridge code it is not possible to update the actions characteristic values and partial factors to account for a reduced design working life. On the contrary, this is possible using ASCE/SEI 7-10, the Eurocodes and the Australian standards. For instance using ASCE/SEI 7-10, EN 1991-1-4 (BSI, 2005c, 2008c) and AS 1170.2 (SAA, 2002b) which concern wind actions, the basic wind velocity can be derived for different return periods. To this end the first two standards specify the following formulae:

ASCE/SEI 7-10:
$$v_{b,t} = c_p \times v_{b,50} = \left[0,36 + 0,1 \times \ln(12 \times t) \right] \times v_{b,50} \qquad (2.1)$$

EN 1991-1-4:
$$v_{b,t} = c_p \times v_{b,50} = \left(\frac{1 - 0,2 \times \ln(-\ln(1-P))}{1 - 0,2 \times \ln(-\ln(0,98))} \right)^{0,5} \times v_{b,50} \qquad (2.2)$$

where $v_{b,t}$ is the basic wind velocity associated with a return period of t years, c_p is a probability factor and P is the probability of annual exceedance.

AS 1170.2 specifies several formulae for different zones and wind regimes. As can be observed in Figure 2.11 the minimum value of the probability factor to be considered in the calculation of the wind velocity for bridge falsework structures according to the EN 1991-1-4 is 0,78, and its values are always larger than the ones obtained using ASCE/SEI 7-10, which returns a minimum value of 0,68, and AS 1170.2 for which a minimum value of 0,73 is obtained for a non-cyclonic wind regime (region A). Similar analysis can be done for other actions such as snow, thermal and seismic actions.
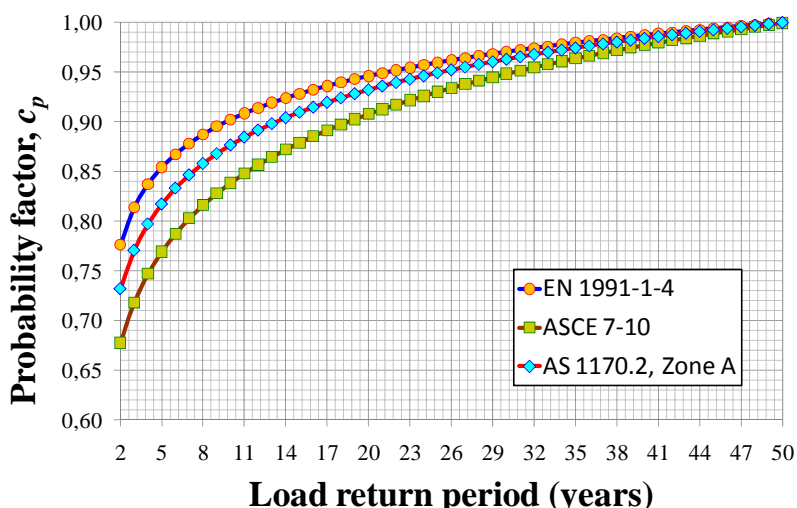
**Figure 2.11: Probability factor for wind velocity
as function of the return period, according to EN 1991-1-4, ASCE 7-10 and AS 3610.**

Still, the wind velocity to be considered for return periods smaller than 50 years depends not only on the probability factor but also on the 50 years wind velocity (including the gust factor). Considering the later, (Nieto et al., 2010) compared the AASHTO bridge code provisions with those

in EN 1991-1-4 for small span bridges, with box-girder or truss decks. They found that the results obtained using the two codes were very close to each other, with differences between -1 and +3% for the wind force.

Another study on wind loads (Bashor, Kareem, 2009) compared the ASCE/SEI 7-05 and EN 1991-1-4 provisions for tall buildings. It was found that slight (around 10%) but consistent discrepancies between the results were obtained using the two codes, in particular for urban and open exposures, with smaller characteristic forces due to wind action being attained using ASCE/SEI 7-05. Similar results are reported in (Pierre et al., 2005) for low buildings.

Regarding seismic actions, using the procedure indicated in EN 1998-2 (BSI, 2005d) it is possible to determine the probability factor to be applied to the reference peak ground acceleration in order to get the seismic action for reduced work durations. The results are presented in Figure 2.12. Note that the seismic action during the construction phase needs not be considered in the UK (BSI, 2009c).
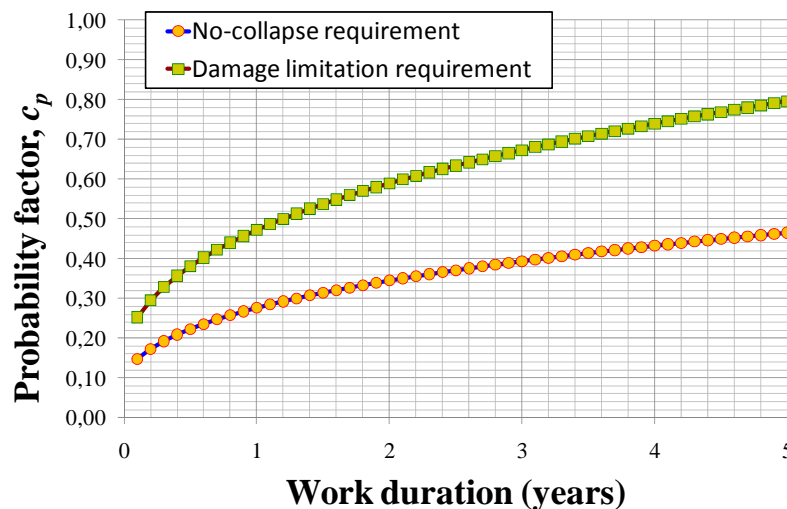
Figure 2.12: Probability factor for the peak ground acceleration as function of the work duration, according to EN 1998-2.

The AASHTO bridge code does not provide a general framework to determine the loads to be used in the design of bridge falsework structures, but only for bridges. Therefore, in the USA assistance must be sought elsewhere. For instance, ASCE/SEI 37-02 (ASCE, 2002) might be used to determine the design loads and load combinations for bridge falsework, although it has been developed with emphasis on temporary structures used in building construction. Also, it may be profitable to consider the recommendations contained in the AASHTO design guide for bridge falsework (AASHTO, 2008), but this standard is based on the ASD concept and furthermore the design verifications specified are only of a general nature. Therefore, one should be careful, perform the necessary analysis and take appropriate precautions before attempting to directly incorporate the loads specified in these standards into the rules of the AASHTO bridge code for bridge falsework structures design. Nevertheless, in the present Thesis ASCE/SEI 37-02 will be used as the reference USA standard for determining loads for bridge falsework structures design.

The ASCE/SEI 37-02 provides the design loads and load combinations for temporary structures used during construction, as well as for partially completed structures during their construction phases. This standard addresses not only imposed and dead loads due to the construction but also environmental loads, the minimum values of the partial factors and the relevant load combinations to be considered, in accordance with the limit states design concept.

The twin European standard is EN 1991-1-6 (BSI, 2005b, 2008b) which describes the principles and application rules for the determination of actions to be considered during execution of buildings and civil engineering works. Table 2.5, Table 2.6 and Table 2.7 present the loads specified in the two US standards, in the two European standards and in the Australian standard, respectively.

The construction loads presented in the abovementioned tables should always be interpreted as preliminary values. It is crucial that a proper assessment is carried out for each project to determine their values as accurately as possible. Nevertheless, comparing the values presented in the abovementioned tables it can be concluded that a link can be established between the loads specified in the various codes, although the rules given in the European codes are more structured and complete. The construction load values, in particular the concrete casting loads and material loads, specified in the AS 3610 exceed the values given in all the other standards.

Table 2.5: Loads for bridge falsework design (USA standards).

Load type	AASHTO GSBTW-1-M		Load type	ASCE/SEI 37-02	
	ID	Value		ID	Value
Permanent loads	Steel: sections, wires, cables, etc.	Min: 25,1 kN/m^3 for normal concrete	Permanent loads	Steel (CD): sections, wires, cables, etc.	Ex: ASCE/SEI 7-10
	Wood: formwork		Construction loads	Fixed (CFML), *e.g.* formwork	Ex: ASCE/SEI 7-10
	Concrete: Concrete casting loads			Variable (CVML), *e.g.* concrete casting loads, materials	Analysis dependent ASCE/SEI 7-10
	Lateral pressure of concrete (CC)	ACI 347		Lateral pressure of concrete (CC)	ACI 347
Construction loads		Equipments + 0,96 kN/m^2 + 1,1 kN/m at the outside edges of deck overhangs		Personnel and equipment (CP)	Min: 1,1 kN/worker
				Equipment reactions (CR)	See supplier documents for rated equipment
				Erection and lifting (CF)	Analysis dependent
Horizontal load		Min: 2% of vertical load		Horizontal (CH)	Max(2% of vertical load; 0,22 kN/person)
Wind load		Chapter 23, Part II of the Uniform Building Code The basic wind pressure shall be increased by 240 N/m^2 for falsework members over or adjacent to traffic openings	Variable loads	Wind (W)	ASCE/SEI 7-10 applying reduction factor, see Table 2.8
				Thermal (T)	Analysis dependent
				Snow (S)	ASCE/SEI 7-10 applying reduction factor of 0,8 if construction period is ≤ 5 years
				Earthquake (E)	ASCE/SEI 7-10, Category II, using a reduction factor ≥ 0,2 and a behaviour factor ≤ 2,5
Other loads	Loads caused by prestressing or other actions	Analysis dependent Foundation settlements should not exceed 25 mm	Other loads	Loads caused by prestressing or other actions (O)	Analysis dependent
Accidental loads	Loads caused by impact, local failure	Analysis dependent	Accidental loads	Loads caused by impact, local failure	Analysis dependent

In ASCE/SEI 37-02 the wind load applied to a structure under construction is a percentage of that applied to a permanent structure, and varies according to the exposure period, see Table 2.8. Based on the information given, the return period of the wind load considered in ASCE/SEI 37-02 can be calculated. This is presented in the right column of Table 2.8. Comparing Table 2.4 with Table 2.8 it can be observed that the return periods considered in ASCE/SEI 37-02 are larger than the ones considered in EN 1991-1-6 for short exposures but smaller for long exposures.

Table 2.6: Loads for bridge falsework design (European standards).

Load type	BS EN 12812		Load type	Eurocodes	
	ID	Value		ID	Value
Permanent loads (Q_1)	Steel: sections, wires, cables, etc.	EN 1991-1-1 + NA	Permanent loads	Steel (G): sections, wires, cables, etc.	EN 1991-1-1 + NA
	Wood: formwork			Formwork system (Qcc)	Min: 0,5 kN/m^2
Construction loads	Fresh concrete weight, precast units weight (Q_2)	25 kN/m^3 for normal reinforced fresh concrete	Construction loads (Qc)	Concrete casting loads, precast units weight (Qcf)	EN 1991-1-1 + NA 26 kN/m^3 for normal reinforced fresh concrete Additional load for *in situ* casting (working area 3 m × 3 m): 10 % concrete self-weight but ≤0,75 kN/m^2
	Concrete casting loads (Q_4)	Additional load for *in situ* casting (working area 3 m × 3 m): 10 % concrete self-weight but ≥0,75 kN/m^2 and ≤1,75 kN/m^2 Concrete pressures from CIRIA Report n° 108			
	Construction loads due to working personnel (Q_2)	Min: 0,75 kN/m^2		Construction loads due to working personnel (Qca)	Min: 0,75 kN/m^2
	Horizontal (Q_3)	1% of the Q_2 vertical load		Construction loads due to moveable heavy machinery and equipment, lifting, hoisting (Qcd)	EN 1991-3 + NA
	Construction loads due to storage of materials (Q_2)	Min: 1,5 kN/m^2		Construction loads due to storage of moveable items (Qcb)	Min distributed load: 0,2 kN/m^2 Min. concentrated load:100 kN
Variable loads	Wind actions (Q_5)	EN 1991-1-4 + NA	Variable loads	Wind actions (W)	EN 1991-1-4 + NA
	Thermal (Q_8)	If L_{bridge} ≥ 60 m then ±10 k (concrete bridge)		Thermal (T)	EN 1991-1-5 + NA
	Snow (Q_2)	Consider only if ≥ 0,75 kN/m^2		Snow (S)	EN 1991-1-3 + NA
	Earthquake (Q_7)	EN 1998-2 + NA		Earthquake (E)	EN 1998-2 + NA
Other loads	Loads caused by prestressing or other actions (Q_9)	EN 1990, EN 1992, EN 1997 + NAs	Other loads	Loads caused by prestressing or other actions (O)	EN 1990, EN 1992, EN 1997 + NAs
Accidental loads	Loads caused by impact, local failure	EN 1990, EN 1991, EN 1993 + NAs	Accidental loads	Loads caused by impact, local failure	EN 1990, EN 1991, EN 1993 + NAs

In EN 1991-1-6, a minimum wind velocity of 20 m/s is recommended for work durations of up to 3 months. In ASCE/SEI 37-02 no limit is defined, but the AASHTO bridge code contains a rule for segmental bridges built using the balanced cantilever method in which minimum value of 55 mph (25 m/s) for the wind velocity is specified for erection stability analyses. Both codes recommend however the determination of a better estimate by analysis of meteorological records for the area considered. Finally, BS EN 12812 specifies a wind pressure of 200 N/m^2 for the working wind.

The AASTHO Guide Design Specifications for Bridge Temporary Works (AASHTO, 2008) specifies a minimum design vertical load (excluding dynamic considerations) of 4,8 kN/m^2.

Table 2.7: Loads for bridge falsework design (Australian standards).

Load type	AS 3610	
	ID	Value
Permanent loads (G)	Steel: sections, wires, cables, etc.	AS 1170.1
	Wood: formwork	24 kN/m^3 for normal concrete +
	Concrete weight	$60 \times \dfrac{\text{volume of reinforcement}}{\text{total volume}}$ kN/m^3
Construction loads	Concrete casting loads (Q_c)	Additional load for *in situ* casting (working area 1,6 m × 1,6 m): 3 kN/m^2
	Personnel and equipment (Q_{uv})	1 kN/m^2
	Lateral pressure of concrete (P)	Section 4.4.5.1 AS 3610
	Load from stacked materials (M)	4 kN/m^2
	Horizontal (Q_{uh})	Min(1 kN/m; 5 kN)
Variable loads	Wind (W_u)	AS 1170.2
	Thermal (T)	Analysis dependent
	Earthquake (E_u)	AS 1170.4 if construction period > 6 months
Other loads	Loads caused by prestressing or other actions (X_m)	Analysis dependent
Accidental loads	Loads caused by impact, local failure	Analysis dependent

Table 2.8: Reduction factor specified in ASCE/SEI 37-02
to determine the wind velocity to be used during construction of structures.

Construction period	Factor	Calculated wind load return period (years)
less than 6 weeks	0,75	5
6 weeks to 1 year	0,80	7
1 to 2 years	0,85	12
2 to 5 years	0,90	20

Very limited guidance is given in both codes regarding accidental load definitions. Typical cases are those involving impact from materials or equipments, or from local failure of temporary supports and bracing elements. However, it is specified that if a static analysis is performed, the design value of the accidental action should be multiplied by an appropriate dynamic amplification factor. In EN 1991-1-6 a value equal to 2,0 is recommended, subject to better assessment, whereas in (AASHTO, 2008 ; ASCE, 2002) and in (AASHTO, 2010) a recommended minimum value equal to 1,3 and 1,5 is specified, respectively.

The general format for load combinations specified in the various codes for ULS verification (applicable both to persistent and transient design situations; not applicable to accidental and seismic design situations) can be expressed by equation (2.3) (BSI, 2002a).

$$\left.\begin{array}{c}\gamma_{G,max}\\\gamma_{G,min}\end{array}\right| \times \sum G_{k,j} + \gamma_{Q,1} \times Q_{k,1} + \sum \left.\begin{array}{c}1,0\\0\end{array}\right| \times \gamma_{Q,i} \times \psi_{0,i} \times Q_{k,i} \qquad (2.3)$$

where $\gamma_{G,max}$ and $\gamma_{G,min}$ represent the maximum and minimum partial factors to be applied to the characteristic value of permanent (dead) loads $G_{k,j}$, respectively; $\gamma_{Q,1}$ represents the partial factor to be applied to the characteristic value of the leading variable (live) action $Q_{k,1}$; $\gamma_{Q,i}$ represents the partial factors to be applied to the characteristic value of accompanying variable loads $Q_{k,i}$ and $\psi_{0,i}$ represents the combination factors of each $Q_{k,i}$.

Specific load combinations can be found in ASCE/SEI 37-02 and in AS 3610. EN 1991-1-6 does not specify load combinations, leaving this duty to the bridge falsework designer which increases his responsibilities but also allows him to optimise the design in view of performance requirements and limitations specific to each project. However, the envisaged load combinations must in all cases follow the philosophy defined in EN 1990. Due allowance should be made not to consider load combinations that will not occur. For instance, often a maximum working wind velocity is set and therefore it is not

necessary to consider simultaneously the design wind load and all construction loads, for example personnel and concrete casting loads should not be considered.

A comparison of the load partial factors specified in the AS 3610 and in the ASCE/SEI 37-02 is given in Table 2.9 and in the European standards is given in Table 2.10.

Table 2.9: Loads partial factors for bridge falsework design (Australian and USA standards).

Load type	AS 3610		Load type	ASCE/SEI 37-02		
	ID	Load partial factor γ_i		ID	Load partial factor γ_i	$\psi_{0,i} \times \gamma_i$
Permanent loads (Q_1)	Steel: sections, wires, cables, etc.	γ_{max} = 1,25 γ_{min} =1,00 or γ_i = 0,80 for limit sates involving global equilibrium (EQU)	Permanent loads	Steel (CD)	γ_{max} = 0,9; 1,2 or 1,4 γ_{min} =0,85	N/A
	Wood: formwork					
	Concrete weight					
Construction loads	Concrete casting loads (Q_c)	1,0	Construction loads	Fixed (CFML)	1,2	0
	Load from stacked materials (M)	1,5		Variable (CVML)	1,4	Analysis dependent
	Lateral pressure of concrete (P)	1,5		Lateral pressure of concrete (CC)	1,3 or 1,5	0
	Personnel and equipment (Q_{uv})	1,5		Personnel and equipment (CP)	1,6	0,5
				Erection and fitting (CF)	2,0	Analysis dependent
				Equipment reactions (CR)	1,6 or 2,0 (Rated or Unrated)	0
Variable loads	Horizontal (Q_{uh})	1,5		Horizontal (CH)	1,6	0,5
	Wind (W_u)	1,0	Variable loads	Wind (W)	1,3	0,5
	Thermal (T)	1,5		Thermal (T)	1,4	0
				Snow (S)	1,6	0,5
	Earthquake (E_u)	1,0		Earthquake (E)	1,0	0
Other loads	Loads caused by prestressing or other actions (X_m)	1,5	Other loads	Loads caused by prestressing or other actions (O)	2,0	Analysis dependent
Basic combinations	Unloaded falsework (before pouring): $\gamma_G \times G + \gamma_{Quv} \times Q_{uv} + \gamma_{Quh} \times Q_{uh} + \gamma_M \times M$ EQU: $\gamma_G \times G + \gamma_{Wu} \times W_u$		Examples (Basic combinations)	$1,4 \times D + 1,4 \times CD + 1,2 \times CFML + 1,4 \times CVML$		
	Falsework during loading (pouring): $\gamma_G \times G + \gamma_{Qc} \times Q_c$			$1,2 \times D + 1,2 \times CD + 1,2 \times CFML + 1,4 \times CVML + 1,6 \times CP + 1,6 \times CH + 0,5 \times L$		
	Loaded falsework (after pouring): $\gamma_G \times G + \gamma_{Quv} \times Q_{uv} + \gamma_{Quh} \times Q_{uh} + \gamma_M \times M + \gamma_{Xm} \times X_m$ $\gamma_G \times G + \gamma_M \times M + \gamma_{Xm} \times X_m + \gamma_{Wu} \times W_u$			$1,2 \times D + 1,2 \times CD + 1,2 \times CFML + 1,4 \times CVML + 1,3 \times W + 0,5 \times CP + 0,5 \times L$ $1,2 \times D + 1,2 \times CD + 1,2 \times CFML + 1,4 \times CVML + 1,0 \times E + 0,5 \times CP + 0,5 \times L$		
	Loaded falsework (after pouring), seismic action: $G + E_u$			$0,9 \times D + 0,9 \times CD + (1,3 \times W \text{ or } 1,0 \times E)$		

Regarding accidental design situations, such as vehicle or crane impact, the ULS load combinations format can be expressed by (BSI, 2002a):

$$\sum G_{k,j} + A_d + \sum {}^{1,0}_{0} \Big| \times \psi_i \times Q_{k,i} \tag{2.4}$$

where A_d represents the design value of the accidental action and ψ_i represents the combination factor for live load $Q_{k,i}$. The values of the combination factors ψ_i are project specific but can be

considered smaller than the values of the combination factors used in the persistent and transient design situations.

Table 2.10: Loads partial factors for bridge falsework design (European standards).

Load type	BS EN 12812		Load type	Eurocodes (Medium consequence class)		
	ID	Load partial factor γ_i		ID	Load partial factor γ_i (STR/GEO)	$\psi_{0,i}$ (Road bridges)
Permanent loads (Q_1)	Steel: sections, wires, cables, etc.	γ_{max} = 1,35 γ_{min} =1,00	Permanent loads	Steel (G)	γ_{max} = 1,35 γ_{min} =1,00	N/A
	Wood: formwork			Formwork system (Qcc)	1,5	1,0
Construction loads	Fresh concrete weight, precast units weight (Q_2)	1,5	Construction loads (Qc)	Concrete casting loads, precast units weight (Qcf)	1,5	1,0
	Concrete casting loads (Q_4)	1,5				
	Construction loads due to working personnel (Q_2)	1,5		Construction loads due to working personnel (Qca)	1,5	1,0
	Horizontal (Q_3)	1,5		Construction loads due to moveable heavy machinery and equipment, lifting, hoisting (Qcd)	1,5	1,0
	Construction loads due to storage of materials (Q_2)	1,5		Construction loads due to storage of moveable items (Qcb)	1,5	1,0
Variable loads	Wind actions (Q_5)	1,5	Variable loads	Wind actions (W)	1,5	0,8
	Thermal (Q_8)	1,5		Thermal (T)	1,5	0,6
	Snow (Q_2)	1,5		Snow (S)	1,5	0,8
	Earthquake (Q_7)	1,0		Earthquake (E)	EN 1998-2 + NA	0,0
Other loads	Loads caused by prestressing or other actions (Q_9)	1,5	Other loads	Loads caused by prestressing or other actions (O)	EN 1990, EN 1992, EN 1993 + NAs	EN 1990 Annex A2
Basic combinations	Unloaded falsework (before pouring): $\gamma_1 \times Q_1 + \gamma_5 \times Q_5$		Analysis dependent, refer to EN 1990			
	Falsework during loading (pouring): $\gamma_1 \times Q_1 + \gamma_2 \times Q_2 + \gamma_3 \times Q_3 + \gamma_4 \times Q_4 + \gamma_5 \times Q_5 + \gamma_8 \times Q_8$					
	Loaded falsework (after pouring): $\gamma_1 \times Q_1 + \gamma_2 \times Q_2 + \gamma_3 \times Q_3 + \gamma_5 \times Q_5 + \gamma_8 \times Q_8 + \gamma_9 \times Q_9$					
	Loaded falsework (after pouring, seismic action): $Q_1 + Q_2 + Q_4 + Q_7 + Q_8 + Q_9$					

STR/GEO: Limit states where the resistance is governed by the failure or excessive deformation of structural elements or of the ground.

Interpreting the values, it can be observed that in general the partial factors to be applied to the leading variable action specified in ASCE/SEI 37-02 are slightly higher than the corresponding values given in the Eurocodes and higher than the Australian ones. However, the combination factors specified in the USA code are much lower than the ones recommended in the Eurocodes and in the AS 3610, in particular for construction loads.

The fact that partial factors for loads are smaller in one code in comparison with others, does not necessarily imply that the design loads determined using that code will also be smaller. Design loads are

obtained in various codes by different methods and using different initial representative values, all of which can be more or less conservative. Additionally, during code calibration different target reliabilities can be selected by the code committees. Therefore, code comparison has to be carried out carefully and not by simple comparison of partial factor values. However, few studies have been published about code comparison exercises. See previous discussion concerning wind action for examples.

Finally, regarding resistance partial factors there are no major differences between the values specified in the AASHTO bridge code for the verification of SLS and ULS and the corresponding values given in the Eurocodes. For SLS, they are set to 1,0 and for ULS (persistent and transient design situations) they vary but are larger than 1,0 and in general not greater than 1,25. However, for ULS verification of seismic and accidental design situations whereas the AASHTO code specifies unit partial factors the Eurocodes require the use of the same values as for the other design situations. Additionally, in the Eurocodes resistance partial factors can alternatively be derived by testing, updated using new information by Bayesian methods and can be reduced depending on the efficiency of the control and inspection measures implemented.

2.3.2 Research on bridge falsework systems

Research concerning specifically bridge falsework systems is very limited. However, research on access steel scaffold systems, similar structures to bridge falsework systems, has been increasing in the last years. The main contributions have been made by researchers in Germany, UK, USA, China and more recently Australia. See (Beale, 2014) for a complete review of available research.

Research has been focused on trying to assess the vertical loads values during concrete casting and on developing simple design procedures for scaffolding based on numerical models which attempt to simulate as accurately as possible the behaviour of scaffolds obtained in tests. Only quite recently, attention has been driven to research the reliability of scaffolds (and falsework). This was possible due to society awareness of the still high level of accidents related to scaffolds (and falsework) and to society demand for safer structures, to the increase of public and private investment in temporary structures research as a response to the media pressure, which allowed to carry out more full-scale tests or connections tests for example, and to the development of new computational techniques which allowed for more complex and accurate analysis and thus more rational, safer and cost-effective use of falsework.

2.3.2.1 Experimental investigations

Experimental investigations are an essential tool for any pioneer research. Nowadays they provide the benchmarks for verifying the results of numerical models, but not so far ago experimental tests were the only available method to develop design rules for structural systems.

Past experimental investigations on bridge falsework systems consist predominantly on joint testing, although some full-scale tests of representative parts of structural systems were also performed.

As stated previously, joints play a key role on the performance of bridge falsework systems, due to their contribution to the stiffness and resistance of these structures. The interest in studying joints is to characterise their behaviour and strength to enable their proper modelling.

The majority of the existing experimental research has been focused in the joints between vertical elements (standards) and horizontal members (ledgers). Some limited experimental research has also been performed on swivel joints and on baseplates.

In 1990, Voelkel (Voelkel, 1990) carried out an assessment of Cuplok® scaffold systems developed by SGB (now part of Harsco Group). Several types of tests were performed to determine values of looseness, stiffness and resistance especially for the joint couplers.

In particular, ten ledger-to-standard joint tests were performed, using a 1000 mm lever arm length measured from the standard centre line, to derive the maximum rotational stiffness of the joint (joint's strong bending axis). The force was applied via a hydraulic jack equipped with a load cell to obtain the

force value. The load was applied in hysteresis loops (in clockwise and in anti-clockwise directions) on three different loading levels: ±1 kN.m, ±2 kN.m and ±3 kN.m bending moments at the joint. Finally the load was increased in the upward direction until failure of the test piece was reached. The tests results showed that looseness in the joints affects the initial stiffness of the connection which is much lower than the one determined after the ledger locks-in at the joint. After contact has been fully established the stiffness increases before plasticity sets in. An average rotational stiffness of 78 kN.m/rad after looseness was determined. In UK, (Godley, Beale, 1997) carried out similar tests (with a 300 mm lever arm) and suggested a smaller value of 65 kN.m/rad for the rotational stiffness. In line with these findings, (Peng, 2002) suggested a value equal to 74 kN.m/rad for the rotational stiffness.

Concerning the bending moment resistance of the joint the information that can be extracted from the tests is very limited since complete failure of the joint was observed in only one test (fracture located in the top cup) at a maximum bending moment of 2,9 kN.m – for the other tests no complete failure could be attained because the maximum jack stroke was reached before failure.

Regarding the bending stiffness and resistance about the joint's weak bending axis a special test was devised consisting on a 3-D frame as shown in Figure 2.13, where only the central bay was free to move laterally in the direction of the applied displacements. The tests results showed that the connections provide a very low stiffness in this direction with an average value, after looseness, of 7,2 kN/m or 5,6 kN.m/rad (Godley, Beale, 1997). Also, the connections exhibit looseness, up to 0,010 rad (whereas looseness about the joint's strong bending axis was observed to be less than 0,005 rad) with an estimated initial rotational stiffness of about 10% of the value after looseness. It was also observed that cyclic loading has detrimental effects on these parameters. The average maximum load was determined equal to 2,84 kN, or an ultimate bending moment equal to 0,18 kN.m, corresponding to the fracture of the top cup of the Cuplok® coupler.
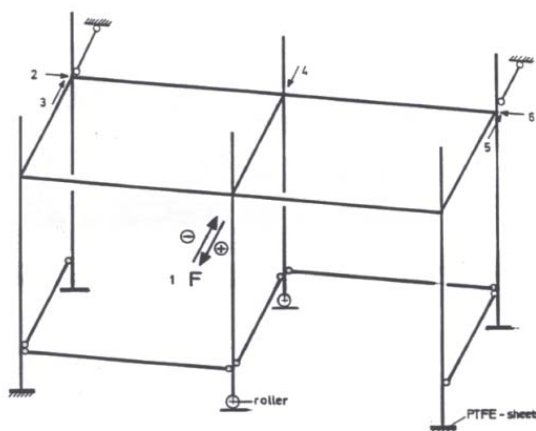
**Figure 2.13: 3-D frame to evaluate the behaviour of
ledger-to-standard joints about the vertical axis (Voelkel, 1990).**

Recently, results from a research carried out at the Sydney University have been published concerning Cuplok® joint tests (Chandrangsu, Rasmussen, 2009b) and full-scale tests (Chandrangsu, Rasmussen, 2009a). For convenience the results of the Australian experiments are summarised in Chapter 3.

Regarding the joint experiments, the adopted test setup and test method was similar to the ones already mentioned. However, a lever arm of 500 mm was used and the load was only applied monotonically in one direction for each group of tests. The objectives of these experiments were to investigate the bending stiffness and bending strength of Cuplok® joints about the vertical axis (weak bending axis, parallel to standard longitudinal axis), and about the horizontal axis (strong bending axis, perpendicular to standard longitudinal axis). Additionally, the influence of the number of elements joined by the coupler (two, three or four) was evaluated, together with the effect of the number of

hammer blows applied to the connection (three, five or seven – in practice most producers prescribe two hammer blows). Specimens used in the tests were sampled from second-handed batches.

The average ultimate bending moment values about the weak bending axis was determined to be 0,4 kN.m whereas for about the strong bending axis was determined to be 3,5 kN.m. The failure mode was usually ductile with the resistance being determined by the plastic deformation of the elements of the joint (not of the tubes). However, in some cases, brittle failures of the end weld of the ledgers were observed. It was also possible to conclude that the rotational stiffness of 4-way joints is larger, in average 30% about the strong bending axis and 50% about the weak bending axis, than the one determined for 2-way joints, and that the effect of the number of hammer blows is insignificant.

Comparing these results with the ones obtained by other researchers, and mentioned earlier, it can be seen that the major differences are the values of the rotational stiffnesses. Experiments in UK and Germany revealed that Cuplok® joints exhibited initial looseness and thus a small initial stiffness, of about 7 kN.m/rad and 0,6 kN.m/rad (10% of the rotational stiffness after looseness) about the strong and weak bending axis, respectively. On the contrary, in the Australian results (Chandrangsu, Rasmussen, 2008), the existence of looseness was much less pronounced, especially about the weak bending axis where no looseness seems to have been observed. A possible explanation for this discrepancy could be the tightness of the connection before testing. However, the UK and Germany reports refer that *"several blows of a hammer"* were applied prior to testing so this factor cannot justify by itself the differences. Finally, regarding the ultimate bending moments the average values reported by Rasmussen are between 20% to 100% higher than the ones obtained by Voelkel – it should be mentioned that the in the later tests only one complete joint failure was attained.

An important difference between the tests procedures used by Voelkel and Godley *et al* and the one used by Chandrangsu *et al* is the type of load application. In the former studies the load was applied in upward and downward consecutive cycles, whereas in the later study the load was only applied monotonically in one direction (for each test group). Therefore, the Chandrangsu *et al*'s results can only represent a possible envelope of the results obtained by the other authors. Furthermore, it may be difficult to determine looseness with monotonic tests. Monotonic tests are more suited to determine maximum resistance of the joints than to characterise their behaviour.

Another important difference between these studies concerns the test setup used to determine the behaviour of these joints under bending about the joint's weak bending axis. The test setup used by Voelkel and Godley *et al* consisted in a frame structure thus simulating the real behaviour of the connections. However, in this test an average joints' behaviour is determined, derived from three different types of joints (*i.e.* with different number of concurring elements at one node) instead of an individual type of joint.

Chandrangsu *et al* test setup is identical to the one used in the bending tests about the strong bending axis. Therefore, they could obtain the behaviour for each type of joint. However, results of Voelkel and Godley *et al* have shown that in this direction the joints exhibit a very low initial stiffness and significant looseness. This behaviour is in severe contradiction with the recent findings made by Chandrangsu *et al* which found that the there is no significant looseness present in the joint and thus the initial stiffness is high. A possible justification for these two different results can be related with the test setups used, although it is thought that the major contribution comes from the different load application methods used.

In reality, connections can exhibit cyclic behaviour under wind loads. Additionally, buckling of some elements or foundation settlements can also induce changes in the deformed configurations and variations of joint rotations, see (Rodrigues, 2010). Thus cyclic tests must be performed.

Voelkel (Voelkel, 1990) also performed axial tests of ledger-to-standard joints to determine the joint tensile resistance. In all tests, top cup facture was observed at an average axial force of 73 kN.

Finally, Voelkel (Voelkel, 1990) carried out axial tests on swivel connections between brace elements and standards. Hysteretic loops were applied to the joint at different load levels: ±5 kN, ±10 kN and ±15 kN. It was observed that during the final hysteretic loops movements of the blade ends of the swivel connection occurred within the standard cups. These deformations of about 10 mm to 20 mm caused additional bending moments in the brace tube to those resulting from the eccentric load axis, which led to failure of the swivel connection, either on the top or bottom cup or at the weld of the swivel connection. An average axial stiffness of 1360 kN/m was obtained and an average ultimate force of 28 kN was registered.

In 2001, (Godley, Beale, 2001) analysed another type of couplers typically used in scaffolding: wedge-type couplers. They concluded that this type of couplers often display substantial looseness from the beginning of the test and exhibited a different response under clockwise and anti-clockwise rotations. The results show a different average stiffness value (after initial looseness) of the joint under clockwise rotations or under anti-clockwise rotations, 77 kN.m/rad and 27 kN.m/rad, respectively, about the strong bending axis. The average rotational stiffness decreased to 16 kN.m/rad and 5 kN.m/rad, respectively, until the maximum bending moment was reached. The average maximum bending moments of the connection were equal to 1,7 kN.m and 1,3 kN.m, respectively.

More recently (Abdel-Jaber et al., 2009) studied the rotational strength and stiffness of a third and fourth type of couplers, namely the putlog couplers and right angle couplers since the existing European Standard EN 74 (BSI, 2005a, BSI, 2010a, CEN, 2006) does not give thorough recommendations. A total of 30 tests of each coupler were carried out. The putlog couplers are used to connect horizontal members (ledgers-to-ledgers), whereas the right angle couplers are used to connect horizontal to vertical members (ledgers-to-standards).

The test configuration was very similar to the one used by Vogel, although a 400 mm free length was adopted for the loaded ledger. To determine the service bending moment of the joint, a limited number of monotonic tests were carried out until failure, at a rate of 1 mm per minute of the jack stroke in only one direction per test (clockwise or anti-clockwise). Following, cyclic tests were performed in the other specimens. Three hysteretic cycles at 0,1 kN.m bending moment were applied after which the specimens were taken to collapse. Some of the specimens were new couplers where others were used. The results showed that there was little difference in performance between used and unused couplers of the same type.

The looseness, stiffness and resistance of the couplers were determined according to BS EN 12811-3 (BSI, 2002b). Results showed that putlog couplers are less stiff and resistant than the right angle couplers, but exhibit less looseness. It was also found that the two types of couplers exhibited similar behaviour under both clockwise and anti-clockwise rotations. The results obtained with right angle couplers were later published in (Beale, Godley, 2009). In April 2010, (Liu et al., 2010) tested three right angle couplers in order to obtain rotational stiffness of ledger-to-standard connections. The results returned a 16 kN.m/rad rotational stiffness very close to Beale's results.

The bibliographic review shows that research concerning baseplates used in scaffolding (and falsework) is very limited since the past research has focused on baseplates bolted to the foundation. Nevertheless, Peng (Peng, 1994) evaluated the jack base rotational stiffness to be between 4,0 and 6,8 kN.m/rad, respectively. Later, Peng (Peng, 2002) based on experimental tests proposes a rotational stiffness for the metal baseplates equal to 7 kN.m/rad.

In 1998, (Godley et al., 1998) presented a test procedure to determine the rotational stiffnesses and moment-curvature relationships of semi-rigid baseplates of cold-formed structures, *e.g.* rack storage structures. These authors studied the effects of the stiffness of the support material on the behaviour of the baseplates. Although this study does not focus on bridge falsework systems their conclusions are useful to understand the influence of certain variables. In this study, Godley *et al* carried out tests on baseplates for three values of axial compression: 20 kN, 40 kN and 80 kN. They observed that the initial stiffness was almost the same for all tests, however increasing the axial load

lead to the increase of the ultimate bending moment capacity. Furthermore, they observed from the tests using different support materials (concrete and timber, with Young's modulus of about 21,47 GPa and 0,18 GPa, respectively) that the effect of a stiffer support material translated to a higher initial stiffness but not necessarily to a higher bending resistance of the baseplate.

Regarding sleeve connections, Peng (Peng, 1994) determined the rotational and axial stiffness of this connection to be correctly modelled as rigid by comparing experimental results of full-scale tests with the results of numerical models.

Finally, in 2003 (Gorst et al., 2003) published results of a research on coefficients of static friction in temporary works. They carried out 260 combinations of different material faces used in temporary works, including both "dry" and saturated timber. For material combinations for which codified data exist, the static friction coefficient values obtained in the current research tended to lie between the maximum and minimum bound code values, but closer to the minimum values.

2.3.2.2 Numerical investigations

Research of scaffolds by numerical methods has been increasing, following the developments of computational capacity and availability, as they are a cost-effective alternative to experimental tests. However, some of the numerical studies use results obtained in experimental investigations, joints behaviour for instance.

From the bibliographic review, two groups of numerical investigations with different goals can be distinguished: (i) those focused on developing design rules for scaffolds and (ii) those focused in checking the influence of various types of hazards on the safety of scaffolds.

Regarding the first group, it was in the UK that (Harung et al., 1975) published in 1975 the first work where computers were used to predict the overall elastic instability of scaffold towers and to determine safe effective lengths for the design of scaffold columns. Their research seemed to lead to the idea that assuming full continuity at scaffold member joints was in agreement with the real behaviour of the structure.

Later in USA, (Yen et al., 1995) suggested that in order to have safe scaffolds the top should be prevented to move sideways, and bracing elements should be provided, in particular X shaped bracings in at least the inner and outer faces of the scaffold.

In 2009, (Peng et al., 2009) used results obtained in past investigations to conduct parametric analysis of scaffold critical loads. They assumed in their studies that both top and bottom joints were hinged, the same for brace-to-standard joints, while the ledger-to-standard joints were assumed rigid and spigot joints between standards were simulated by a elastic spring with a stiffness coefficient equal to 7,85 kN.m/rad. This research showed that the critical load changes with different brace configurations: they concluded that an anti-symmetric N shaped configuration is more favourable than a V configuration or a symmetric N configuration. These authors also found that the critical load decreases as the quantity of extended vertical jacks increases. By adding three and four extended vertical jacks to the bottom, the critical load decreased by 50%, for example. They also observed that when spigot joints between vertical elements are located near the story-to-story joints, the critical load is reduced.

In China, (Peng et al., 1996) developed and presented a numerical model for the analysis of two-story door-type tubular steel scaffolds. (Chu et al., 1996) also developed a non-linear numerical program which can be used directly to design steel scaffold structures thus avoiding the use of codified member checks which needs the determination of the effective length – a major source of uncertainty. Regarding, effective lengths in 2006, (Beale, Godley, 2006) showed that contrary to the current practice of considering the buckling length of the elements in compression of putlog scaffolds equal to the lift height, it depended on the tie configuration and is frequently much greater than usually assumed.

In UK, (Godley, Beale, 1997) described the analysis of large scaffold structures by 2- and 3-dimensional models, accounting for the semi-rigid behaviour of the Cuplok® joints between scaffold members. The modelling of the connections was derived from the measurements registered during an extensive testing campaign performed by Voelkel in Germany and by Godley at Oxford Brookes University. Comparing the 2-D and 3-D results there were some negligible differences. However, when comparing the results of these two models with the experimental tests (carried out by Voelkel) important differences were reported. This was justified by not having modelled the initial looseness of the joints.

Other researchers focused in the study of rack structures baseplates, using numerical models to analyse the influence of column base behaviour on slender multi-bay portal frames (Lau et al., 2005). They showed that correctly modelling the baseplate as fixed or as pinned depends on the ratio between the lateral load and the axial load, the larger this ratio is the more flexible is the baseplate.

In Australia, researchers at University of Sydney developed numerical models to study falsework structures, see (Chandrangsu, Rasmussen, 2009c) for example. Based on calibrations with experimental results they suggest a rotational stiffness of 40 kN.m/rad to simulate the top rotational restraint provided by the formwork, whereas at the bottom, rotational springs with an elastic constant equal to 100 kN.m/rad were introduced to model the baseplate rotational stiffness. Regarding translational stiffness, all degrees-of-freedom were considered as fixed at the bottom as well as at the top except for the vertical displacements at the top which were considered to be free. Ledger-to-standard joints were modelled using the results obtained in the experimental tests. The brace-to-ledger connections were assumed to be hinged, 60 mm eccentric from the ledger-to-standard joints and modelled with an axial stiffness of 1800 kN/m. The spigot joints were modelled according to model presented in the paper of (Enright et al., 2000). Regarding initial imperfections, the survey results published in (Chandrangsu, Rasmussen, 2009b) were used. Excellent agreement was obtained when comparing experimental and numerical results with an average value of the ratio between these two results equal to 1,01 and a coefficient of variation of 0,10.

Concerning the second group, (Beale et al., 1996) performed one of the first studies about the safety of scaffold structures. The analysis consisted on assessing the influence of structural faults in the partial factor value. The faults could either be a consequence of mistakes made at design, supply, storage and erection stage, or due to poor site control during the scaffold use. Numerical models were developed for both perfect and damaged structures to derive the decay of the safety of the structure. Lateral loads, to simulate the wind action, and vertical loads were accounted for. The failure event was considered to be the collapse of the first element. Hazard events included foundation settlements, geometrical imperfections, joint defects and brace eccentricities. It was determined that the second and third faults were the most severe.

Available UK data on scaffold collapses from 1986-1993 was reviewed by (Beale, Godley, 2003). The most common failures were usually caused by inadequate tying arrangements or by structural overload. Additionally, numerical simulations on a typical scaffold used in UK were carried out introducing various types of faults, isolated or combined. The greatest reduction in load carrying capacity occurred for cases of gross settlement of the foundation, out of tolerance initial geometrical imperfections of the standards, the use of putlog couplers instead of right angle couplers and inadequate tying arrangements. The results of the analysis also showed that poor site control is more detrimental to scaffold safety than poor design.

In China (Xie, Wang, 2009) after having observed that bridge falsework systems always contain some kind of hidden defects, analysed the influence of the improper erection of a vertical element (standard) on the load distribution between standards and on the probability of failure of a particular system. They performed non-linear analysis of a 3 m×3 m falsework system 8 m high supporting the weight of a concrete ribbed slab. Comparing the results obtained with and without the considered imperfection in a single element (under the central rib) they concluded that this type of imperfection leads to an increase on the surrounding standards axial load of about 50%.

Additionally, based on the results obtained by *in situ* measurements of standards out-of-plumb, they carried out a simple reliability analysis. Assuming a sine shaped pre-flexure with an amplitude following a normal distribution with a mean value of $2,4 \times L/1000$ and a standard deviation of $1,5 \times L/1000$ (where L represents the length of the standard), which are much larger than the corresponding values presented by (Chandrangsu, Rasmussen, 2009b) see section 2.5.2.5, they concluded that the presence of this type of imperfection increases the probability of failure of the system from 1% to 9%.

In 2010, (Zeng, Hu, 2010) carried out non-linear analysis of bridge falsework systems and analysed the influence of some type of common errors. They found that the stiffness of the baseplate was the most important parameter with possible resistance increases of 50%, followed by the vertical member imperfections, simulated by horizontal loads at member nodes, with a reduction of almost 20% when the horizontal loads increased from 1,0% to 2,5% of the vertical loads value. On the contrary, couplers stiffness was found to have insignificant influence. This last conclusion is in clear contrast with the findings of (Rodrigues, 2010).

Finally, (Zhang et al., 2009) based on Rasmussen's team investigations, published the first comprehensive study on the reliability of scaffolds using the First-Order Reliability-Method (FORM). The materials' mean yield stress was assumed to be 1,05 times the nominal value with a COV of 0,10. In general, variables were modelled with normal or lognormal distributions. The jack extension at the bottom and top of the frames were assumed to be equal. Three values of jack extensions are considered, *i.e.* 100 mm, 300 mm and 600 mm, covering the possible range encountered in construction practice.

Three thousand Monte Carlo simulations were conducted to generate sample distributions of the basic variables: joint stiffness, initial geometric imperfections, yield stress and load eccentricity. It was assumed that no correlation exists between basic variables. The load eccentricity was assumed to be randomly positioned towards either side of each standard. The direction and magnitude of load eccentricities of all columns are assumed uncorrelated.

The probability distribution of the construction dead load (D), *i.e.* concrete weight, was assumed to be similar to that of occupancy dead load, *i.e.* normally distributed, with a mean-to-nominal (D_m/D_n) value of 1,05 and a COV of 0,10. Concerning construction live loads (L), *i.e.* weight of workers, equipment, and stacked material, a Type I extreme distribution was used with a mean-to-nominal (L_m/L_n) value of 0,9 and a COV of 0,6.

Figure

Figure 2.14: Results from the reliability analysis of access scaffolds (Zhang et al., 2009).

An example of the results obtained is shown in Figure 2.14, where $\varphi = E_d/R_n$, E_d is the design load and R_n is the nominal resistance. It was found that the jack extension has a substantial influence on the system strength: using a higher jack extension results in lower system strength. This is mainly due to different modes of failure. While the failure of the systems with high jack extensions (600 mm) is characterised by large overall sway of the frame, the mode of failure of systems with

short jack (100 mm) exhibits S-shape flexural buckling in the column members. It was also found that β (reliability index) has a maximum value for L_n / D_n equal to 0,12.

2.4 Importance of bridge falsework systems investigation

With the industrial revolution came new challenges for civil engineers: to keep up with industrial development, new bridges, in larger scales, carrying heavier loads, had to be built at a fast pace. Bridge falsework also experienced this new complexity. However, little attention was drawn to this subject and as a result a series of falsework collapses of major significance occurred in the industrialised countries throughout the 20th century.

In 1970, as a response to the public outcry following a collapse with severe consequences, the UK construction industry established a committee under the chairmanship of S.L. Bragg to investigate the use of falsework. The result was the Bragg report (Bragg, 1975), a pioneer document which established the basis for the subsequent publication of the first UK standards concerning falsework (BSI, 1982).

Since the Bragg report, there have been a number of fundamental changes to the construction industry which had a profound effect upon the manner falsework is dealt with by all stakeholders (SCOSS, 2002):

- *"Falsework design is no longer a task of the main contractor but the responsibility is passed to a sub contractor or a specialized supplier;*
- *The structural concept of the falsework is no longer arbitrary; proprietary systems and more often modular ones are widely used nowadays in order to optimise costs and operational efficiency. Additionally the number of usage cycles of falsework components has increased dramatically;*
- *The paradigm of the construction industry has changed: intense competition in a profit orientated environment has produced a reduction of technical competence and responsibility at the design, construction and quality assurance stages of a construction project".*

Several authors have concluded that the construction period of bridges is the most vulnerable one during the bridges' lifetime. (Sexsmith, 1998) states that *"Human error, such as mistakes in the design concept or the calculations, especially for falsework and its supporting system, is a primary cause of many failures"*.

Accidents involving bridge falsework often have vast and various negative impacts: on the project profitability, on the credibility and competence of the involved companies, on the increase of the insurance premiums, on economical, financial and political costs due to postponed benefits. Additionally, when human victims occur many of the abovementioned effects are scaled-up by the media and public attention.

In 2005, (Wong et al., 2005) studied the possible failure consequences of bridges in service by a cost-evaluation method. The major costs involved, of a total of more than 25 million pounds (2009 prices) for the studied cases, sorted in a descending order, are the ones related to rebuilding costs, traffic delay costs, access and traffic management costs, casualty costs, repair costs and finally some other indirect costs. These results can easily be extrapolated to the failure of bridges during construction, by reclassifying traffic delay and traffic management costs as postponed benefits (loss of service and associated loss of revenue) due to the delayed bridge opening date.

Failures of bridge falsework systems, contrary to permanent structures, often occur due to a combination of "low strengths" and "high loads". These are usually originated by departure from commonly accepted competent professional practice, *i.e.* human errors. "Low strengths" can arise from multiple human error sources: (i) design, construction and quality control errors, (ii) current knowledge gap concerning the real structural behaviour of bridge falsework systems, namely the influence of the mentioned human errors. Regarding the definition of "high loads", two different situations must be distinguished: (i) action values, or actions effects, considered in the design phase but which become

higher than their design values, or design action effects, due to construction and quality control errors; and (ii) actions, or action effects, not considered, partially or entirely, in the design phase due to ignorance or oversight, such as foundation settlements, load redistribution or second-order effects, for example. In the definition of "high loads" it is not included catastrophic unexpected events such as floods, earthquakes, terrorism acts, vehicle impacts or other extraordinary actions.

The collapse of bridge falsework systems caused by an unaccounted or under-evaluated event cannot be acceptable. According to (Steven, 2010), the *"mind set within the construction industry over the decades from the 1900s has changed from accepting (...) 13 deaths for the construction of the major viaduct, to a mindset unacceptable of any level of injury"*. The various concerns outlined in the above paragraphs illustrate the need for a holistic approach applied to bridge falsework, *e.g.* a risk management framework, and adequate competency to undertake the task. It is essential that those involved with bridge falsework realise the importance of this change, the relevant statutory need to consider whole working life risks to structural safety, and the commercial benefits that will accrue by doing so (SCOSS, 2005).

It is clear that there is a need for scientific progress in the field of bridge falsework. A measure of the accomplishment of this task is given by our ability to reduce the uncertainties associated with bridge falsework. This is precisely the aim of the present Thesis. However, it must be realised that there will always exist a certain level of uncertainty that cannot be eliminated completely.

2.4.1 Learning from failures

As emphasised previously failures of bridge falsework are not uncommon events. Studying the most common causes of accidents is one of the available tools to assist in identifying significant risks in the construction industry (Steven, 2010), so there is a need to understand the conditions giving rise to past failures and ways to avoid such failures so that loss of life and property can be minimised.

The term failure can be associated to two conditions, collapse and distress (Wardhana, Hadipriono, 2003). Failure can be defined as the incapacity of a constructed facility or its components to perform as specified in the design and construction requirements. Distress is the unserviceability of a structure or its components, representing the loss of ability of the structure to function as planned. Collapse of a structure happens when all or a substantial part of the structure loses its structural integration and comes down.

According to (Bragg, 1975): *"Failures arise from many different causes. Each one has two elements: the technical cause which led to the collapse; and procedural errors which allowed the faults to occur and go undetected and uncorrected"*.

According to (Ratay, 2009) *"construction failures caused by defective performance or complete absence of components of temporary structures in construction is an almost daily occurrence. Just about every step along the design-construction process includes hidden risks and has been shown to be prone to errors or omissions that result in subsequent construction failure. Failures of excavation supports, scaffolding, falsework, formwork, and temporary shoring, bracing, and guying (in approximately this order) are the most frequent occurrences of temporary structure failures"*.

However, with very few exceptions that involve a considerable number of fatalities, failures of bridge falsework structures do not fill the media headlines as a collapse of a building or a bridge does. They usually happen away from the public eye, at an isolated construction site and the knowledge of their occurrence is often kept limited to very few people. One should note that even when a disaster of a bridge during its construction is covered by the media, reported in ENR (Engineering News-Record, http://enr.ecnext.com/), in books, or in other technical publications, it is nearly always the permanent structure that is described, with little or no discussion of the details of the temporary structure even if it was the cause of the collapse (Ratay, 2009). In fact, in past decades several bridge disasters were catalogued as "bridge collapses" when actually, in various accidents, only the falsework collapsed resulting in injuries and fatalities, construction delays and cumulative economic costs.

According to (Hadipriono et al., 1986), many researchers have discussed and evaluated failures of falsework structures. However, it is often difficult or impossible to determine the precise cause of a falsework failure. Typically, the main members of a falsework structure are slender elements which are used and re-used several times, being subject to rough usage and poor maintenance. A usual ground zero scenario of a falsework collapse comprises a pile of wreckage of bent tubes, in which the initial failure is probably obscured. Additionally, when studying reports of past accidents it must be taken into account that many failure investigations are carried out by private companies generally recruited by a party involved in a legal action related to the failure, and therefore could be biased. Furthermore, the reports of accident investigations are generally sealed by court order as part of the resolution of the case and become unavailable to those not directly involved, but who wish to understand causes in order to avoid repetitions.

However difficult it may be, it is extremely important to carry out failure investigations so as to ascertain the likely causes of the falsework collapse, and to be able to develop a failure database from which risk analysis of bridge falsework structures can be developed. In more detail, the importance of failure investigations has both technical and public dimensions.

Technically, it is important to understand the physical causes of a failure in order to have an overview of the safety and reliability of the studied structure, and determine whether existing standards are adequate to prevent such failures or whether the design and construction standards require revision to be improved, and disseminate these findings to the profession to avoid repetitions of the failure. It is never too much the need to emphasise the importance of trying to identify and characterise the hazard scenarios, *i.e.* the actual load combinations leading to collapse and the failure mechanisms involved in the collapse. In parallel, public and media attention are part of the aftermath of major failures, as the media, political leaders, concerned groups such as construction labour unions, and the general public become concerned about the safety of the class of structures involved in the failure.

Recently, (CIRIA, 2011 ; HSE, 2011) conducted an extensive study on what are major hazard events in construction. They found out that failures in planning, design and management of temporary works was a significant factor in about half of the case studies examined. Additionally, the main causal factors to accidents were identified: failure to recognise hazardous scenarios and influencing factors, poor teamwork and lack of experience and competence. Particularly, regarding the design of temporary structures inadequate design or (late) design changes of permanent, underlying lack of robustness and incorrect as-built drawings and information were highlighted as causal factors.

2.4.2 Bridge falsework systems accidents since 1970

The reality shows that more accidents involving scaffold structures are reported than concerning bridge falsework systems. This is easy to understand, since the number of buildings under construction, repair or retrofit works is significantly higher than those of bridges. However, the consequences of a collapse of a bridge falsework structure are far more severe than the ones due to a scaffold collapse, since the former ones are generally associated with loss of human lives, loss of considerable equipment and partial or total collapse of the permanent structure being built. Additionally, the forensic work carried out to investigate why has the falsework collapsed, not only but mainly to account for responsibilities, involves a considerably larger time span, human and technical resources. All in all, a failure of a bridge falsework structure represents a heavy burden in social and economical terms.

Various cases of bridge falsework failures have been reported in the last 20 years, including accidents in European countries, USA and more recently in China, India and in the United Arab Emirates (UAE). (Wardhana, Hadipriono, 2003) revealed that in the period between 1989 and 2000 more than 500 bridge failures were reported in USA. According to these authors less than 2% of the failures occurred during bridge construction. However, this finding can be attributed to lack of official reports describing bridge collapses during construction. (Scheer, 2010) in his book reports 440 bridge failures, of which 125 (28%) occurred during construction and 74 (17%) were related to bridge falsework. Similar

results can be obtained using the data made available in the website www.bridgeforum.org developed and maintained by the "Bridge Research Group" at Cambridge University, UK.

As part of the works carried out in the present Thesis, an extensive research over the available literature and media information has been performed concerning the numbers and causes of bridge falsework incidents and accidents. The framework of the survey was based on (Bragg, 1975) and was divided into three major components, following (Hadipriono, Wang, 1987): (i) information on the occurrences of failure, (ii) details on the enabling and triggering causes of failure, and (iii) information on the consequences of failure.

It was found that since 1970, up to 2012, 73 major accidents have occurred involving the collapse of bridge falsework structures in 19 countries.

The results showed that most often collapses are partial (47%), see Figure 2.15. It was considered that partial collapses are all cases where none, or only one, of the permanent and temporary structures collapsed completely. Therefore, in general, complete collapses were only registered in small length bridges.
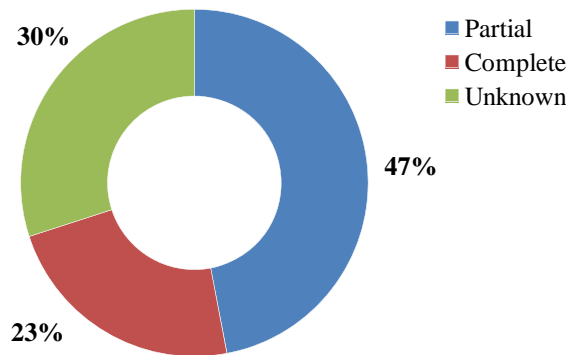
Figure 2.15: Typology of bridge falsework collapses since 1970.

No reported collapse happened because of accepted risks related to deficiencies in structural codes, or related to extraordinary severe external hazards like earthquakes, floods, landslides and hurricanes or tornados. All the collapses resulted from human errors, and the main cause of failure were design errors (28%), see Figure 2.16. However, in 49% of the accidents the causes were unknown.
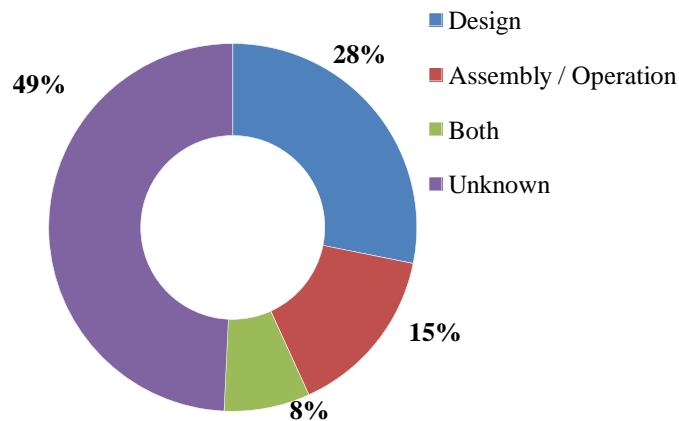
Figure 2.16: Origins of errors leading to bridge falsework collapses since 1970.

Figure 2.17 presents the evolution with time of the total number of collapses in the countries where three or more collapses have been registered. It can be observed that in most of the 19 countries considered in the survey, the total number of registered collapses is smaller than or equal to two, which could mean that the risk of using bridge falsework systems is low (although not acceptable). For example in the UK this can be justified due to established good practices and legal duties, whereas in some other countries it could mean that there are a number of unreported

collapses as suggested by (Burrows, 1989 ; Melchers et al., 1983 ; Sikkel, 1982). Therefore, the figures shown below may in some cases only represent a lower bound estimate.
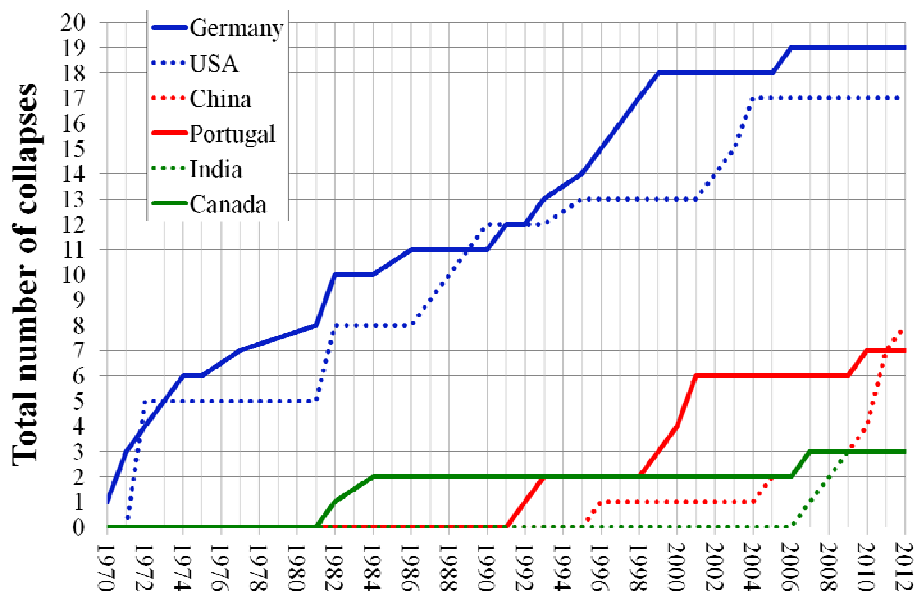
**Figure 2.17: Evolution with time of the
registered bridge falsework collapses since 1970 (countries with three or more collapses).**

Looking in detail into the available information, it was possible to distinguish between procedural causes, enabling events and triggering events. The procedural causes are related to management issues and the interrelationship between parties involved in a project. The enabling events are related to the internal condition or performance of the bridge or its components that contribute to failure. The triggering events are external events that could initiate failure of a structure. It is considered that every collapse occurs due to a series of events that involve deficiencies in management framework, errors in design, assembly and operation and a hazard which triggers the collapse.

The insight achieved by this deeper investigation is considered to be extremely valuable information for the identification of the major hazards and of the critical paths of events which could lead to the collapse of a bridge falsework structure. Also, it makes it easier to setup effective and efficient barriers to reduce and control the existing risk levels.

It should be mentioned that in a high percentage of reported accidents no detailed information was found, especially until the year 2000 (in 60% of the cases). Nonetheless, it is assumed that the results presented below are representative.

Procedural causes are related to human behaviour, organizational, planning and supervision issues. They are important in all project life management phases: from conceptual design to information, site and asset management. These areas can be further sub-divided. In the present Thesis, eight possible areas were considered, see also Figure 2.18:

- Inadequate and/or insufficient communication and collaboration between parties;
- Inadequate and/or insufficient inspection and checking of falsework/formwork;
- Inadequate and/or insufficient QC/QA practices;
- Inadequate and/or insufficient review of falsework design / assembly / operation methods;
- Inadequate and/or insufficient site supervision, monitoring and control of construction methods;
- Inadequate documentation;
- Assembly/Operation did not follow design specifications;
- Other or unknown causes.
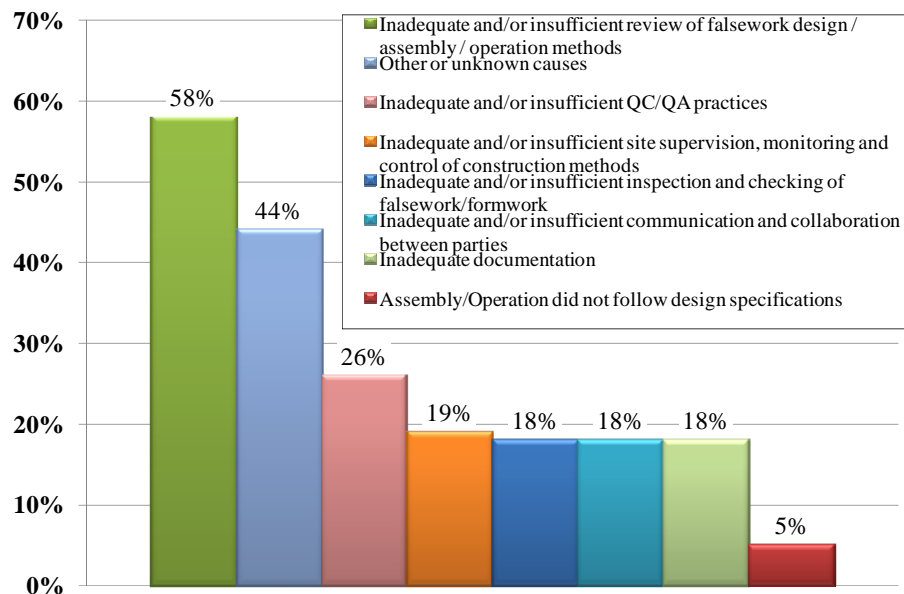
Figure 2.18: Procedural causes of bridge falsework collapses since 1970.

It was found that the main contributors to procedural causes are inadequate and/or insufficient (i) review of falsework design/assembly/operation methods, including falsework dismantling, (58%), (ii) QC/QA practices, including design and site procedures, (26%), (iii) and four more specific procedural causes which occurred in more than 15% of the collapses. However, in 44% of the accidents the procedural causes were still unknown. It can also be concluded that in general several procedural causes coincide in a given accident, meaning that accidents are caused by the occurrence of multiple errors in the various phases of the project.

Six different enabling events were considered, see also Figure 2.19:

- Inadequate and/or insufficient falsework bracing;
- Inadequate falsework foundation;
- Inadequate falsework main element;
- Improper assembly procedure;
- Other or unknown design related causes;
- Other or unknown causes.

It was found that the most important ones are (i) inadequate falsework bracing (19%), (ii) inadequate falsework main element (15%) and (iii) inadequate falsework foundation (11%). The survey showed that the primary enabling event associated with bridge falsework collapses is insufficient or missing bracing elements. This can be justified by the lack of awareness in the design and in the construction stage of the stability requirements of each bridge falsework solution. The second most important enabling event was found to be under-designed components such as jacks, couplers, standards or ledgers, but also support steel girders used to span open traffic areas. This in turn can in part be justified due to the reuse of falsework elements which are subjected to heavy loads and improper maintenance and thus can accumulate damage leading to a reduced load bearing capacity. Incorrect assembly procedures of the falsework system were reported to have been involved in only 3% of the collapses. However small this percentage is, it must be noted that before or after the collapse of the system, it is not very easy to determine if it was erected has planned, so this number should be read taken this into account. Finally, in a great number of accidents (45%) the enabling events are still unknown. Additionally, 26% of the accidents were caused by unknown design related errors.
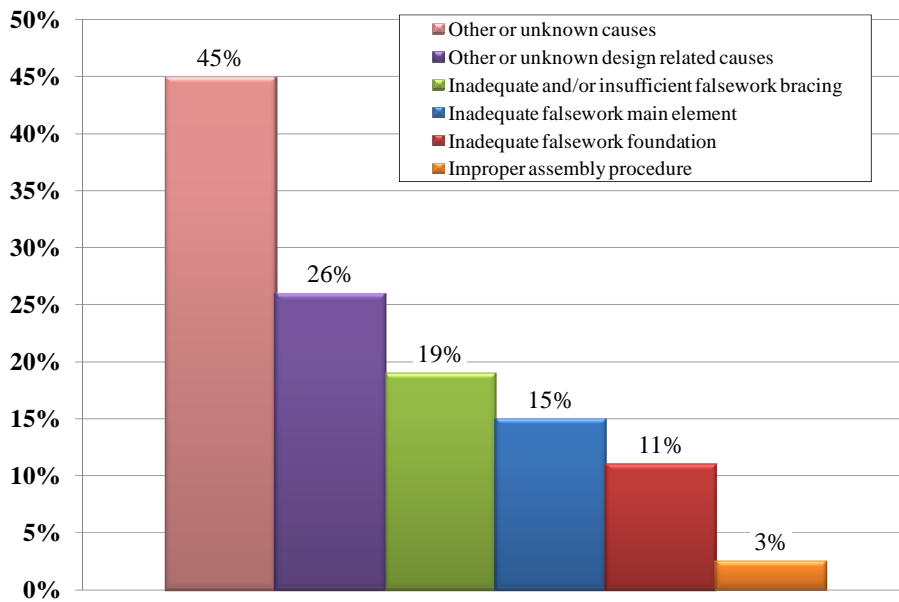
Figure 2.19: Enabling events of bridge falsework collapses since 1970.

Finally, six triggering events were analysed, see also Figure 2.20:

- Heavy rain;
- Strong winds;
- Construction material loads;
- Improper/premature falsework or formwork assembly/removal;
- Other loads;
- Unknown causes.
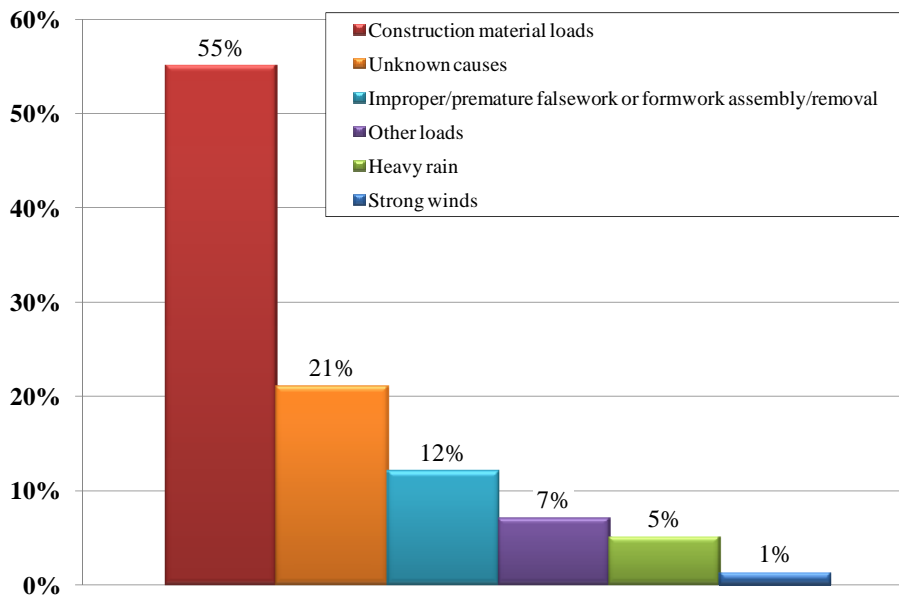
Figure 2.20: Triggering events of bridge falsework collapses since 1970.

Three events emerged as the most critical ones: (i) construction material loads (55%), (ii) unknown events (21%) and (iii) effects of improper/premature falsework or formwork assembly/removal (12%). It can be seen that expected loads during design of the falsework are responsible for 55% of collapses by triggering a local failure which then generally develops as a progressive and disproportionate collapse of part of the bridge falsework structure. These loads are mainly due to concreting operations.

Looking at the data it could be concluded that until the year 2000, the reported accidents occurred mainly in developed countries like Germany and USA, and that after the year 2000 there are an increasing number of reported bridge falsework failures in the developing world such as China, India and Dubai. The numbers also indicate a growing trend in the number of reported collapses, injuries and fatalities since 2000, see Figure 2.21 and Figure 2.22.
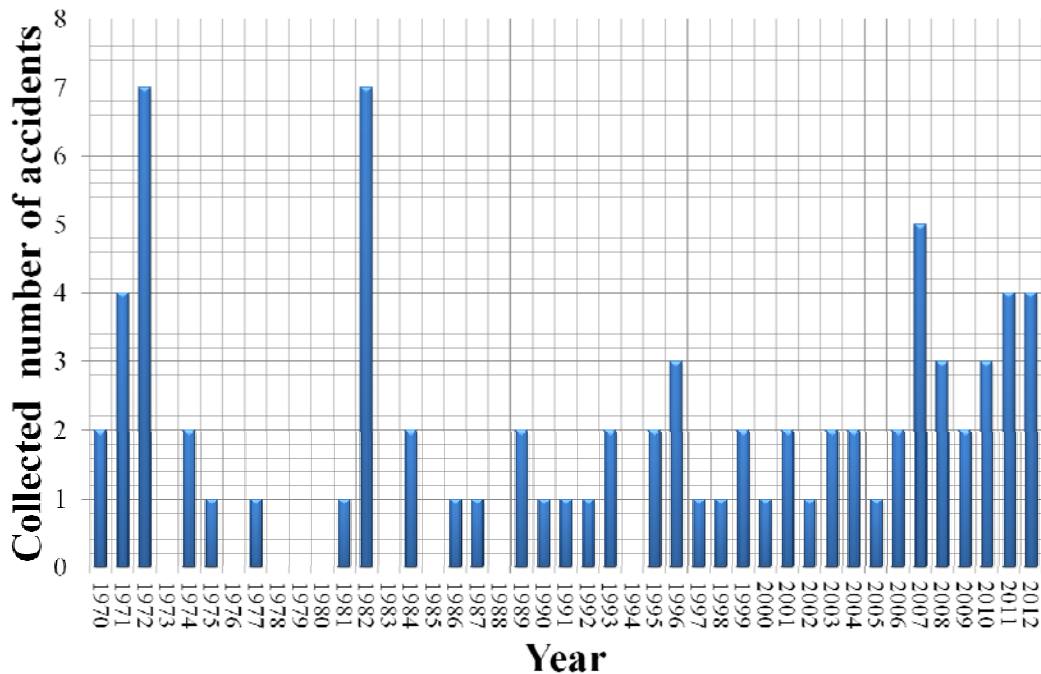
Figure 2.21: Number of bridge falsework collapses since 1970.
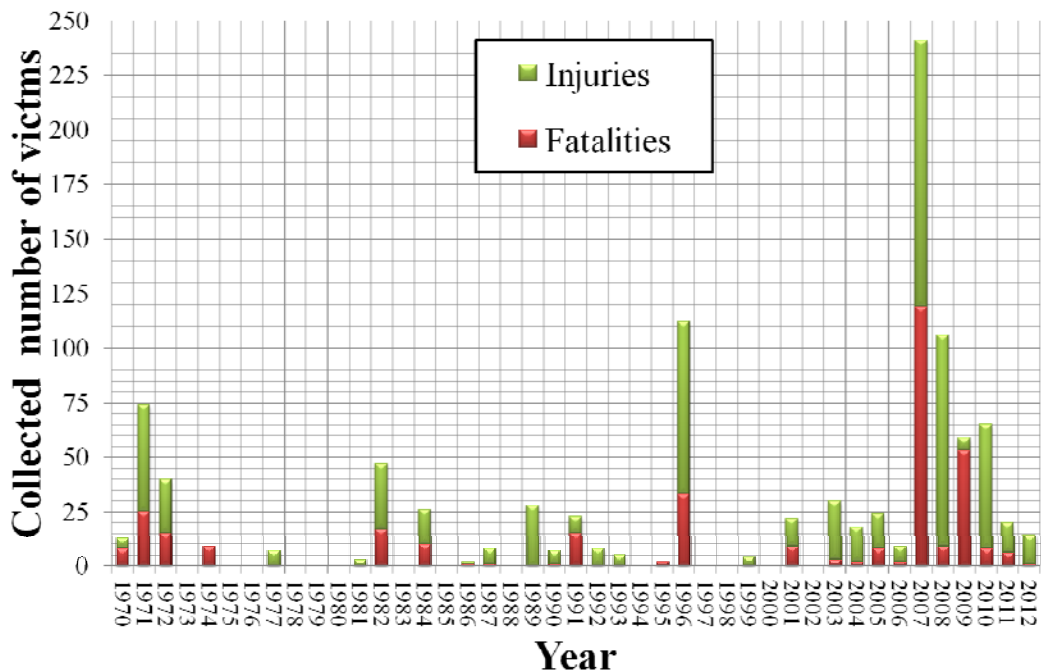
Figure 2.22: Number of victims due to bridge falsework collapses since 1970.

One should note that failures involving bridge falsework structures are much more frequent but are often not reported, because attention is set towards major accidents which result in severe consequences rather than small accidents. As Burrows states (Burrows, 1989): *"The number of failures that occur daily where no reportable accident occurs but result in economic loss for the contractor or sub-contractor in the form of remedial works or re-construction works can only be surmised"*. Melchers *et al* (Melchers et al., 1983) adds: *"(...) serviceability-type problems are extremely under-represented in formal enquiries, in "in-house" reports and newspaper reports, and even in technical papers, but constitute a*

considerable proportion, if not the major part, of negative experiences in structural engineering, as assessed by individual and generally unreported observations". Also, Sikkel (Sikkel, 1982) emphasises an important point which is the health and safety statistics reported each year with the number of accidents and fatalities represent just a very small part of all unsafe situations: only those unsafe situations which brought us an accident in some way or another. It is the tip of the iceberg. The total number of unsafe situations, including all the near-accidents could maybe ten times more (Sikkel, 1982).

2.4.3 Typology of bridge falsework systems collapses

Bridge falsework systems usually fail in a disproportionate collapse fashion, where initially one or more critical elements (vertical, lacing and brace elements or connections) fail leading to a redistribution of forces carried by these elements to the remaining structure. As a consequence, equilibrium with the external forces can no longer be achieved and the system becomes unstable which is expressed by the consecutive failure of other critical elements in a domino-type collapse mode, see Figure 2.23.Generally, the collapse of these systems is only partial since they are constituted by several sub-systems sparsely connected to each other by lacing elements (ledgers). Thus, the existing continuity conditions usually do not offer redundancy between sub-systems: usually the joints break before a total transfer of dynamic forces caused by the collapse of a sub-system to adjacent sub-systems takes place (otherwise the collapse could propagate and the affected area would increase). Furthermore, these later sub-systems may still have not been subject to the concrete weight and therefore they might be able to resist the partial transfer of dynamic forces.

Figure A   Figure B

Figure 2.23: Typical scenario after a bridge falsework collapse (©Diana Pérez/Lusa, http://expresso.sapo.pt/andorra-tres-portugueses-morrem-em-queda-de-viaduto=f546231, 22-09-14).

This type of disproportionate collapse was already studied in detail by (Starossek, 2009): The domino-type collapse is characterised by a failure of one or more elements which are connected to other similar elements in a repetitive display, and because of the force redistribution, dynamic and static horizontal pushing forces develop causing overturning movements of the structure increasing the second-order effects (for which the structure was not designed – lack of bracing) in the adjacent vertical elements which then become unstable bringing the structure to onset of collapse.

In bridge falsework systems the initiating failure usually occurs either by (i) the buckling of a standard or brace element, (ii) the exhaust of resistance of a top or base jack, or (iii) the failure of a connection. (Chandrangsu, Rasmussen, 2009c) reported several results of full-scale falsework tests properly designed so that buckling of brace elements would not occur. Vertical loads were applied uniformly distributed at the top section by hydraulic jacks and increased throughout the test. Additionally, lateral loads were introduced at the beginning of the tests and maintained constant throughout each test.

The tests results suggest that the failure modes are controlled by the jack extension length: when 600 mm top and bottom extensions are used the failure mode is sway on one direction with final failure at the jacks; on the contrary, when 300 mm extensions are used, failure occurs mainly in the

standards and spigots with only small sway displacements. Furthermore, the ultimate load decreases as the jack extension increases. The test results also showed that the bracing arrangement significantly influences the ultimate load of the system. Also, higher lift heights reduce the ultimate load. Moreover, the standards tend to fail at the top lift and around the perimeter region, especially at the corner where there is no bracing and only two ledgers are connected. In the majority of tests, maximum resistance was attained when failure occurred in spigots or jacks, as shown in Figure 2.24.

Figure

Figure 2.24: Typical failed elements on a falsework test (Chandrangsu, Rasmussen, 2009a).

In 1989, an inquiry research team assembled in the USA to study the causes of the collapse of Route 198 Baltimore-Washington Parkway Bridge, performed several tests of bridge falsework systems (Surdahl et al., 2010). The tests focused on establishing the failure modes of the bridge falsework systems. Vertical loads were uniformly distributed at the top sections of the system to simulate the loading conditions on the bridge falsework systems during construction. For the towers that failed, researchers found that the cross-bracing members between bridge falsework tower legs bowed out of plane, making them incapable of providing the bracing needed to restrain the lateral displacements of the bridge falsework tower legs. This loss of lateral stiffness resulted in the buckling and fracture of the bridge falsework tower legs.

Finally, the author of the present Thesis had the opportunity to actively participate in an accident investigation of a viaduct falsework system. The bridge geometry was complex with a circular curvature in plan and inclination angles both in the longitudinal and transversal elevations. Furthermore, an existing two-way road underneath the falsework system needed to remain open during the construction. Steel girders had to be assembled in order to span the road lanes with an intermediate support at the middle of the road. The supports consisted of bridge falsework towers.

The collapse happened while workers were pouring concrete into the bridge formwork. The failure was sudden, without warning, leading to the complete collapse of the two spans over the road. After an exhaustive numerical investigation four main enabling events were identified which could have contributed to the collapse:

(i) Instability of standards of the intermediate support (tower) of the falsework system – no bracing was installed to prevent the buckling of these elements in the longitudinal direction;

(ii) Failure of some standards and top jacks of the most loaded longitudinal frames of the falsework system assembled on top of the girder system: the connections between the ledgers and the standards did not provide the sufficient restraint necessary to avoid high second-order effects;

(iii) Flexural-torsional buckling of the most loaded steel girders – there were evidence that standards were placed eccentrically to the web axis of the girder elements;

(iv) Failure of the base jacks of the falsework system assembled on top of the girder system by excessive rotation of the girders which buckled.

Therefore, the collapse of a bridge falsework is most likely characterised by the following the sequence of events: a trigger event takes place, often the weight of the concrete being poured on the formwork, causing a local failure (one of the enabling events) which then activates other enabling events (multiple local failures) leading to the rapid and (partial) disproportionate collapse of the system along with an important part of the already concreted bridge structure. Various procedural causes are associated with the collapse, mainly design errors, for example: the designer of the falsework system may not have considered properly the influence of the flexibility of the steel girders and the discrete supports in the force distribution between elements of the falsework system.

2.5 Critical hazards in bridge falsework systems

In the following it is presented a thorough description of the key types of procedural causes, enabling and triggering events involved in bridge falsework failures.

As seen in the previous sections, failures are rarely caused by one reason only, but rather by the accumulation of the detrimental effects caused by a series of small events, each of which might be considered not critical, but the total effect exceeds the falsework safety margin. This reasoning is clearly expressed by the "Swiss cheese" model of (Reason, 1990), see Figure 2.25. In this model various protective barriers exist that keep a system from failing, such as: following good practice design recommendations; self-checking, internal and external reviews; adequate quality control, inspection and maintenance procedures, etc. However, holes exist in these safety barriers, originated by uncertainties, human errors and accepted risks. Failures will happen when these holes are aligned and the errors are not detected or properly corrected. The willingness and capacity to search for these errors is a characteristic of an organisation with a good safety culture (Blockley, 2011).

Uncertainties and human errors (errors, lapses or omissions) will always exist. These influence factors are present top to bottom in the decision-making process: from the limited knowledge of known risks and the existence of unknown risks, proper consideration of the known risks, to the competence in technical, organisational and management matters. It is a naive believe that errors can be avoided. What is important is to reduce as reasonably as possible the size, in particular the size of its effects, and the lifetime of errors to avoid serious consequences.

In the case of bridge falsework structures a failure of one critical element can determine the collapse of a significant part of the system. This is justified because the robustness of these systems is generally low, therefore they have a predisposition to disproportionate collapse. The failure of one critical element is intrinsically linked with its reliability, *i.e.* the susceptibility of that element to fail given its exposure to several hazard scenarios. The occurrence of hazard scenarios, their intensity and breadth of consequences are predetermined by the *zeitgeist* in which a particular structural system is integrated. This context is defined by human (societal and individual), cultural, economic, political and environmental factors: from the existing economic, trade and monetary system, to the different organizational levels of society and companies, type of human interactions, psychological aspects, and unpredictability of earth's behaviour.

Figure

Figure 2.25: Swiss-cheese model of Reason (Reason, 1990).

A structural failure is connected to inappropriate stiffness and/or insufficient resistance of the structure. These two variables are always linked and control the structural behaviour of bridge falsework systems.

Low stiffness can lead to (i) instability phenomena of the slender elements, to (ii) damages in the permanent structure (*e.g.* cracks in concrete) or geometrical deviations outside the allowed tolerances, and to unexpected changes of load paths and force distributions. On the other hand, resistance controls the strength of elements (connections, brace elements, etc.) exposed to external events. Depending on the type of external event, together with the change of stiffness of the system, different resistance models can be activated. To estimate the likelihood of attaining a desired failure mode the variation of resistance models and stiffness distributions along the entire structure must be properly considered.

2.5.1 Procedural causes

In this section, the most relevant procedural causes found to be associated with bridge falsework failures will be presented and discussed. Finally, a brief overview of possible measures to improve the management procedures in bridge falsework projects will be presented. In a further Chapter of the present Thesis, a risk management framework for the design of bridge falsework systems will be presented.

Procedural causes are related to the context, and to organisational and management deficiencies. These can be expressed by improper and unclear attribution of responsibilities and work priorities, inadequate communication channels, incorrect information management and presentation, appointment of inexperienced (unqualified) or incompetent staff, insufficient internal (including self-checking) and external review and quality control policies. In terms of context, the construction industry has been increasingly suffering from over-optimistic programmes and deadlines coupled with shrinking budgets and de-leveraging of responsibilities by multiple subcontracts. Bridge falsework projects are highly sensitive to these procedural causes.

The design and use of bridge falsework systems involves reaching structural equilibrium by technical expertise and achieving the required levels of performance by management expertise. These two approaches, the technical and the managerial, the "hard" and the "soft" systems, although intimately linked are very different and their coexistence is not always straightforward and peaceful, especially at their interfaces (Blockley, 2011).

Bridge falsework projects are most of the times performed without interaction, consultation and planning with other relevant stakeholders such as the permanent structures' designer, the principal contractor and the supervision team. Frequently, changes in the permanent structures' design or in the construction sequence, which often occur, with a direct impact on the performance of the bridge falsework are not properly addressed. Furthermore, specific bridge falsework activities, related to the determination of the foundation ground properties for example, are not given the correct priority. Additionally, decision criteria regarding approval of bridge falsework prior to loading, elements tolerances and quality requirements are sometimes set without consultation with the designer.

It is not uncommon for bridge falsework projects to be made of "standard" solutions taken from the system' developers guide without ensuring that they are appropriate and consistent with the project specific design requirements. The same can be said regarding the design specifications or method statements which often are a copy of the system' developers guide. Often lack of information is found in the design brief regarding site investigation, foundation testing, assembly tolerances, material requirements (important because there are various material grades available), load cases considered, loading sequence, maintenance and inspection procedures and priorities.

It must not be forgotten that bridge falsework structures are by-large one of the most common elements of some bridge construction projects. They are reused many times, including during the construction of a given bridge, requiring multiple assembly, operation and dismantling cycles. These

repetitive and routine activities can cause loss of attention and contribute to accidents. Additionally, some construction workers are chance makers, *i.e.* accident makers. One should not forget that the primary responsibility for ensuring health and safety should lie with those who create risks but also with those who work with them. Finally, due to being reused several times, deterioration processes such as corrosion, local damages or accumulation of geometrical imperfections will occur and limit the behaviour and strength of the system.

The implemented design and operation procedures should guarantee that good practice is followed in standard cases and that in special cases particular considerations, which could involve testing verification, should be used to assure that the structural safety and the safety of the workers meets the legal requirements. An important tool is self-checking (especially when doubts arise), which can be supplemented by internal and sometimes external reviews. The teams involved in the planning, design, operation and inspection should be competent in the area of bridge falsework, with sufficient experience and appropriate knowledge, and should establish direct communication channels between them, together with clear and well defined requirements and responsibility of each task, and a list of the most relevant hazards and a specification of the appropriate measures to control them.

In Great Britain every construction project which requires a construction phase likely to involve more than 30 days or 500 person days of construction work is legally bound to fulfil the requirements set in The Construction (Design and Management) Regulations 2007 (CDM2007) (HSE, 2007b). Bridge falsework fits in this definition of construction project. The CDM2007 Regulations specifies the duties of all stakeholders involved in a construction project with respect to planning, management and monitoring of health, safety and welfare in construction projects and of the coordination of the performance of these duties by duty-holders. In particular, the client shall appoint a CDM coordinator as his key adviser who will assist him with his duties during the construction project. Additionally, the construction phase cannot start until the principal contractor has prepared a construction phase plan (document recording the health and safety arrangements, site rules and any special measures for construction work) (HSE, 2007b). A temporary structure must be of such design and so installed and maintained as to withstand any foreseeable loads which may be imposed on it, and must only be used for the purposes for which it is so designed, installed and maintained (HSE, 2007b).

BS 5975:2008 (BSI, 2008a), recommends the appointment of a Temporary Works Coordinator (TWC) to coordinate and supervise the activities of all concerned, to ensure the works are brought to a safe conclusion. Additionally, Temporary Works Supervisors (TWSs) can be appointed to assist the TWC with his duties. Checking and inspection by competent TWSs should be a continuous process, starting with the materials to be used, the foundations, and progressive inspection and checks as the structure is erected. Leaving such checks until the falsework is complete is useless. Errors in the materials used, in the foundations and in the assembly procedure will be impossible to correct without dismantling. Possible checklists are presented in (CIP, 2011).

Furthermore, in section two of BS 5975:2008 (BSI, 2008a) general guidance can be found regarding the control of temporary works and general requirements, the control of procedures, the roles and responsibilities of organisations, organisational aspects, the site related aspects and organisational interfaces. Additional references are (CIRIA, 2007 ; HSE, 2007a, 2010). Figure 2.26 illustrates an example of the activities and the responsibilities in falsework design and construction for standard and special projects.

Every project should start with a clear definition of the objectives and the requirements needed to achieve them. Relevant stakeholders should bring to the table their expertise and together decide the methods needed to meet the project objectives. These are then presented to the client which has to decide if he agrees or not with them. This project management philosophy has been already codified. The Swiss standard SIA 260 (SIA, 2003) defines that the start of every project should consist in the development of three documents: (i) the Service Criteria Agreement, (ii) the Safety Plan and (iii) the List of Accepted Risks. Further information about these three documents is given in (Schneider, 2006).

The design brief should be a well structured document, containing an overview of the structure and how the structure was designed to be assembled and used, along with other design related assumptions and limitations, a Chapter containing detailed design calculations starting from the design codes used, the structural system definition, loads and load cases considered, reactions and internal forces obtained, design methods used and proofs evidence. The appendices should contain general and detailed drawings, the method statement which should include the erection procedure not forgetting the geometrical tolerances and site works needed (foundation testing for example).

Finally, the safety culture should be present at strategic, programme and operational. In this way the strategy of the organisation will be led from the top and embedded in the normal working routines and activities of the organisation. All staff should be aware of the relevance of their work to the achievement of the project objectives and training to support staff should be available.

Figure

Figure 2.26: Activities and responsibilities in falsework design and construction for standard (top) and special (bottom) projects recommended by (CIP, 2011).

2.5.2 Enabling events

Enabling events of bridge falsework failures are related to design and operation issues, most often, both of them. Take for example a partial bridge collapse that occurred in 2001 in Portugal (report is not publicly available). The collapse happened when concreting operations of the deck were being carried out. According to the failure investigation report, the accident was caused by the collapse of the bridge falsework which was found to be under-designed but also the material quality used failed to meet the design requirements and the structure was not assembled correctly – in particular some bracing elements were missing and the way the formwork beams were positioned in the system forkhead plates lead to high load eccentricities.

According to the results of the failure survey performed for this Thesis, design errors were found to be one of the most common enabling events in bridge falsework failures. No matter what bullet proof construction controls are put in place the structure will be likely to fail if it is not properly designed for the actions it will be subjected to. Design errors stem from errors in judgment, wrong assumptions, and lack of knowledge.

Reference must be made to designs based on "safe load values" taken from a design load table developed by the system's producer. In these cases, care should be taken to fully understand the hypothesis, requirements and limitations of the methods behind the design rules. This frequently involves considerations regarding the system configuration, load cases considered, length of the standards and of the ledgers, the location of the standards (face or inner elements), lateral restraints requirements (bracing configurations and top restraint provided by the plate and membrane action of the formwork), type and values of member imperfections (sway, bow and load eccentricities) and material grade of the elements. Some are included, clearly highlighted and easy to understand. However, others are not obvious or are not given. For standard cases these shortcomings can be compensated by the large partial factor included, but for more complex structures with particular load requirements or complex system configurations it may not be enough and lead to under-designed structures.

Errors during operation are also quite common. One should not forget that members of bridge falsework structures are slender and when overloaded may buckle suddenly. Therefore, controls (training, inspections and quality assurance plans) should be designed and enforced during assembly and at regular intervals during the operation to ensure that the system is built and used as it was designed. Any damaged bracing member must be reinforced or replaced and also the connections must be inspected frequently. Other important issues are the interfaces of the falsework system with the formwork and the foundation ground. On the top, it is critical to not over-extend the jacks and to minimise the load eccentricities. On the bottom the foundation adequacy to the ground properties must be assured, in particular when the ground is made of soil and there is a possibility for heavy rain during the construction of the bridge.

In the following, the most important enabling events will be presented.

2.5.2.1 System stiffness considerations

A very common enabling event is related with the failure to properly consider in the structural analysis the stiffness of the falsework system and the interaction of the falsework system with the permanent structure. Stiffness is an important characteristic of any structure because it not only controls its deformation but also the forces distribution, in the case of in continuous structures. Interaction between adjacent structures must be assessed correctly in order to get an unbiased estimate of the values of the forces and the loads path from the formwork to the foundations. Therefore, in special projects where the general design hypothesis of the design load tables developed by the falsework producer are not valid, the designer must always strive to develop as accurately as possible the structural model of the falsework system including the permanent structure. This is especially critical in complex systems such as bridge falsework systems used to span a river or a road, where steel girders or trusses are used as

flexible supports to a 3-D falsework steel structure, when large prestress forces must be applied with the bridge still supported on the falsework structure, or when soil settlements are important, see Figure 2.36.

In the former case, see Figure 2.27, the load distributions between the standards over the steel girders will not be uniform, with the outer standards receiving larger axial forces due to the higher system stiffness over the supports. The same is applicable to the standards of the support towers where the outer elements will be more stressed than the inner ones.

These effects cannot be determined by the usual analysis hypothesis and methods of calculation of the load distribution between standards, such as the tributary area method and assuming the formwork and the standards as rigid elements. In general, the design load tables provided by the falsework producers take into account these effects only indirectly by applying a large partial factor (equal or greater than two). However, this may not be enough to compensate the cumulative effects of the hazard scenarios not explicitly accounted for. Therefore, in special projects these effects should be considered explicitly in the design analysis as they will control the design of the main elements of the falsework and the bracing and lacing configurations.
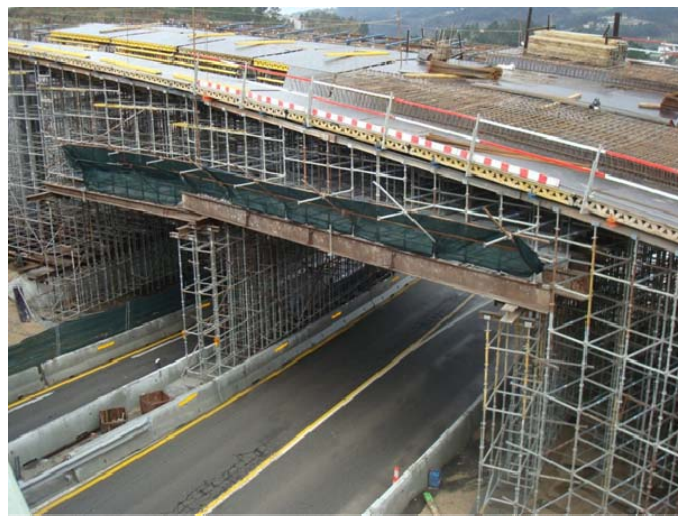
Figure 2.27: Example of a bridge falsework over an open roadway.

2.5.2.2 Vertical and horizontal Elements

The safety of falsework steel members should be verified by design rules specified in structural codes or by testing. However, what is not commonly taken into account in both solutions is the fact that these elements are reused many times and therefore their resistance will be reduced overtime (fib, 2009).

One should also mention that existing code rules focus on local safety verification and assume that when applied to all elements of the system the global safety is achieved. However, there are several examples that demonstrate otherwise. The global safety of a bridge falsework system depends on the safety of members against local failure and on the system response to local failure. Buckling of a primary load-carrying member or a critical brace element in the support towers, with no alternate load paths, could trigger a chain reaction of failures causing progressive and disproportionate collapse of the entire system. Such design considerations are however not usual.

2.5.2.3 Bracing

Bracing is one of the most important aspects in a bridge falsework structure, since their performance depends greatly on the stiffness against lateral movements provided by the bracing elements.

Bracing configuration should be determined by proper structural analysis. However, producers of bridge falsework systems often specify, in their design guidance documents, standard bracing requirements; yet, these are not always fulfilled. For example, in some projects only the exterior bays are braced, leaving the stability of internal bays resting with the (low) lateral stiffness provided

by the lacing elements and by the formwork (which might be discontinuous or not designed to resist the resulting bending and membrane forces). An additional error sometimes found in support towers, is to not include sufficient bracing elements in both directions.

Finally, the critical bracing elements – *i.e.* those that are vital for the structural integrity, and which failure would lead to the failure of a part or the entire structure – are not always identified in the analysis and in the drawings.

2.5.2.4   Joints and details

Joints are another very important element. As seen above in some systems the lateral restraint is solely provided by the lacing elements and their connections to the standards. However, the bending stiffness of these joints is usually quite low and can be even lower if they are not correctly fixed (by hammer blows) or if the joint elements show signs of damage or corrosion. Joints between brace elements and standards, or ledgers, must be checked during erection of the system to verify if the joint eccentricities are within the tolerance limits taken into account during the design of the system.

Joints between the falsework system and the bridge formwork system also need careful consideration during design and assembly. Examples of typical errors are illustrated in Figure 2.28.

Another important example are the gaps that may exist between vertical members of support towers, see Figure 2.29, which may lead to overloaded members.

Figure A

Figure B

Figure 2.28: Typical errors found in the formwork to falsework interface (CIP, 2011).

Figure

Figure 2.29: Example of gaps between support vertical members (fib, 2009).

2.5.2.5 Geometrical imperfections

There are two types of geometrical imperfections: (i) global at system level and (ii) local at member and joints level. The former type is usually called P-Δ (sway) imperfections and the later includes the P-δ (bow) imperfections, joints and load eccentricities.

Bridge falsework systems are subject to heavy vertical loads meaning that second-order effects due to geometrical imperfections and lateral loads cannot be ignored as they significantly affect the behaviour and resistance of the system.

Global imperfections can arise due to (i) deviations from the longitudinal axis of the elements caused by imperfections of the baseplates or by inappropriate foundation solutions on sloped terrain, or due to (ii) the existing looseness in the spigot joints connecting two consecutive standard elements, and in the spigot joints connecting a standard to the top (or base) jack and between jacks and forkheads (or baseplates).

Local imperfections can arise from the manufacturing processes, from design options (in particular referring to foundation solutions and joint configurations), inaccurate erection procedures or from damages introduced during the design working life of the structure.

There are several factors that can severely influence the geometrical imperfections of bridge falsework, such as:

- Erection procedure, influenced by the type of structural system (both of the falsework and of the permanent structure), site conditions, workers expertise, adequacy of quality assurance schemes and competence of people doing it;
- Tolerances at joints of the various elements especially at base and top jacks as well as intermediate joints such as spigot joints;
- Careful use and storage, and quality of maintenance of the various elements to correct defects such as corrosion, local damages due to impacts or out of tolerance geometrical imperfections.

For design purposes of falsework it is usual to use the concept of "equivalent geometric imperfections" with values which reflect the possible effects of all type of imperfections unless these effects are included in the resistance formulae for member design (BSI, 2005e). Guidance can be found in EN 12812 (BSI, 2011).

A recent survey of Cuplok® scaffold systems site imperfections measurements was carried out in 2009 by researchers of the Sydney University. The results were later published in a paper where they presented the major findings (Chandrangsu, Rasmussen, 2009b). A total of 302 on-site measurements of out-of-straightness of the standard were taken and 80 measurements of storey out-of-plumb were performed. In addition, 74 measurements of loading eccentricity, between the timber bearer and the standards top forkhead, were obtained from four different construction sites. The measurements were taken before the pouring of concrete, representing actual initial imperfections and loading eccentricities encountered in practice. It is worth mentioning that none of sites corresponded to bridge construction site, the majority corresponding to building construction sites.

From data observation, it was found that the directions (axes) of these geometric imperfections were random. Also the directions of the loading eccentricity were shown to be random and occurred on either side perpendicular to the timber bearer. The results of out-of-straightness of the standards were normalised with the lift height (L_h) and the results of storey out-of-plumb were normalised with the storey height (H) of the scaffold systems measuring from the baseplate up to the forkhead U-head.

The mean normalised out-of-straightness of the standards including standards with and without spigot joints was $L_h/2080$ with standard deviation of 0,00042; for a mean normalised out-of-straightness of the standards with spigot joints equal to $L_h/770$ with a standard deviation of 0,0008 and a mean normalised out-of-straightness of the standards without spigot joints equal to $L_h/2500$ with a standard

deviation of 0,0003. The mean normalised storey out-of-plumb was $H/625$ with standard deviation of 0,0005 whereas the mean loading eccentricity was 18,1 mm with standard deviation of 10,7 mm.

These imperfection values are quite low when compared with their design values, see EN 12812 (BSI, 2011), except for the loading eccentricities which are very large when compared with the specified minimum design value. This observation can explain why so many under-designed bridge falsework systems do not collapse, but highlights the importance of good inspection and maintenance schemes. However, results published by (Xie, Wang, 2009) show that imperfections considerably larger than the ones reported above can also be observed in bridge falsework systems. This reality is also backed up by studies developed in the UK concerning the correct erection procedures of falsework, see (Pallett et al., 2001) and (Burrows, 1989).

2.5.2.6 Foundations

Foundations are critical elements to the safety and performance of bridge falsework systems. The foundation elements are usually concrete footings (although sole plates are also used), of reduced width, thus only mobilizing the upper layers of soil near the surface. This not only reduces the ultimate resistance of the foundation but also its stiffness: the former property is directly related with the foundation smaller size, being given by the soil layers within a depth approximately between one to two times the foundation smaller size (Carvalho et al., 2004).

Bridges are located in places often associated with soils with low geo-mechanical characteristics. Therefore, the design of a bridge demands that tests should be carried out to determine the resistance and stiffness of the soil. Typically, testing includes boreholes and SPTs. However, these tests do not give any relevant information about the soil layers near the surface and are usually made prior the beginning of the construction, so often no useful information can be used in the design of the falsework structures foundations.

Additionally, in several projects of falsework structures, the design of foundation elements and the safety verification of the foundation soil are often treated lightly, for example by just using the heel of a boot of an experienced inspector or engineer. Design details, control and inspection guidelines usually do not appear explicitly. Usually, it is only made reference to a permissible stress required during the construction phase, verified later against a "safe value" obtained through some simple soil testing. However, in some cases, see below and section 2.5.3.2.3 for examples, performing a detailed soil investigation is justified. Not doing so can result in tragic accidents due to inappropriate foundations (Carvalho et al., 2004).

Problems with foundations can occur due to the substructure deficiencies or due to weak ground properties: resistance and stiffness. Substructure deficiencies are found when concrete weaker than specified is used in footings, when weak or damaged wood footings are (re)utilised, when inclined footings are used and resistance against the resulting horizontal forces is relied solely on friction, when gross baseplate imperfections exist which increase the instability proneness of the standards, when baseplates are severely eccentric relative to the centre of the footing or when insufficient foundation protection measures are implemented against the effects of weather such as flash rains.

Weak ground properties can result from uncompacted soils, presence of water or global instability of the soil due to footings near the edge of a slope (Billings, Routley, 1978).

2.5.3 Triggering events

Triggering events are related to hazards due to permanent or variable loads applied to the structure. Permanent loads include the self-weight and the superimposed dead load. Variable loads include construction loads such as the weight of the fresh concrete, the reinforcement and other materials stored in the deck, and the equipment used, the load redistribution due to the application of

prestress, and environmental loads such as the actions of snow and wind, ground settlements, thermal variations and seismic actions.

Existing design philosophy requires that during the design of any structure different design situations need to be considered: persistent, transient and accidental situations. When applied to bridge falsework systems, persistent situations can be defined as the load conditions occurring during normal operations: the dead load, the service load including the effects of prestress, and the effects of wind, snow, temperature and ground movements actions. Transient situations typically correspond to the stages of assembling and dismantling of the falsework structure. Finally, accidental situations refer to exceptional scenarios such as very strong wind gusts, impacts by equipment or by vehicles and local failures for example.

In general, the most important loads that bridge falsework structures are subjected to are the weight and pressure from concrete (the later just while concrete is still fresh), followed by other types of construction actions. In contrary to permanent structures which only receive their full design load in rare cases (*e.g.* the design traffic loads on bridges are rarely reached), usually falsework structures are normally subjected for a long period of their design working life to loads whose values are close to their design values. Thus the actual safety margin of falsework structures is lower than in permanent structures, *i.e.* the probability of failure of temporary structures is higher than that of permanent structures (fib, 2009).

Furthermore, there is no consensus regarding the load modelling during construction, taking into account formwork/falsework interaction. Many researchers have tried to improve the available models by monitoring the construction loads during concrete pouring. The falsework-formwork interaction is extremely important, since the load distribution between standards depends on (i) the stiffness of the formwork, *i.e.* the isotropic, orthotropic or anisotropic behaviour of the formwork material, (ii) the resistance of the formwork granted by the plate action and (iii) the stability of the formwork and of the formwork/falsework connection.

Additionally, there are no general guidance documents or standards addressing the issue of choosing the loads or partial factors to be used in falsework design. This is still a hot topic with two different philosophies currently under discussion:

- Code based approaches.
- Probabilistic-based risk management approaches.

Included in the code based approaches are design strategies where falsework is designed for both serviceability limit states (SLS) and ultimate limit states (ULS) using reduced return periods for environmental loads, such as the 10 or the 15 year return period for ULS wind action. It can be argued that this methodology is justified due to the smaller exposure period of temporary structures to hazards such as extreme wind gusts. However, the choice of the return periods to be considered is often quite arbitrary and tries to balance empirically the optimal use of resources at an acceptable safety level. One should not forget that return period is just an alternative statement of annual risk of exceedance, *e.g.* a 50 year return period is equivalent to say a probability of exceedance of 0,02 in one year and a 10 year return period is equivalent to say a probability of exceedance of 0,1 in one year. Therefore, using lower return periods in the design of temporary structures is equivalent to accepting a higher risk of annual load exceedance than the one considered for permanent structures. For example, assuming that the maximum wind velocities recorded in each year are discrete, identically distributed and statistically independent events, the risk of exceedance, over 10 years, of the 10 years and 50 years return periods wind velocities is given by equation (2.5), and is equal to 0,65 and 0,18, respectively. By other words, the probability that the 10 years return period wind velocity will be exceeded at least once during 10 years is greater (65%) than the one estimated to the 50 years return period wind velocity (18%), see also Figure 2.30.

$$P_n = 1 - \left(1 - P_1\right)^n \tag{2.5}$$

Rosowsky (Rosowsky, 1995) argues that the use of design loads as specified in structural codes, which can in most cases correspond to maximum lifetime loads, to temporary structures may be excessively conservative. Rosowsky then proposes a method based on the concept of maintaining comparable load exceedance probabilities to modify the partial factors of loads to take into account reduced reference periods. This concept is based on the philosophy that the probability of exceedance of a given nominal load (for a given reference period) should be the same for every reference period considered. Accordingly, for an exposure time of less than one year a reduction factor of 0,85 is suggested to be applied to the 50 years return period wind velocity. A somewhat similar analysis is presented by (Boggs, Peterka, 1992 ; Willford, Allsop, 1990). In the later document, it is proposed that the wind velocity to be considered during the construction of buildings, including the design of temporary structures, could just represent between 77% to as low as 55% of the design value specified in the design code for the permanent structure (for an exposure of less than two years). According to (Mohammadi, Heydari, 2008) the method of the reduced load level has become popular among designers of temporary structures, such as bridge falsework systems.

In the following, it is presented a simple exercise to analyse the adequacy of the use of reduction factors to derive the design wind load for temporary structures, including bridge falsework systems. It should be mentioned that wind loads have been chosen to illustrate existing relations between exposure time, return period and reliability. However, it is not necessarily the most important action for the design of bridge falsework systems as other actions such as the impact of fresh concrete, system imperfections or QA errors may be more important.
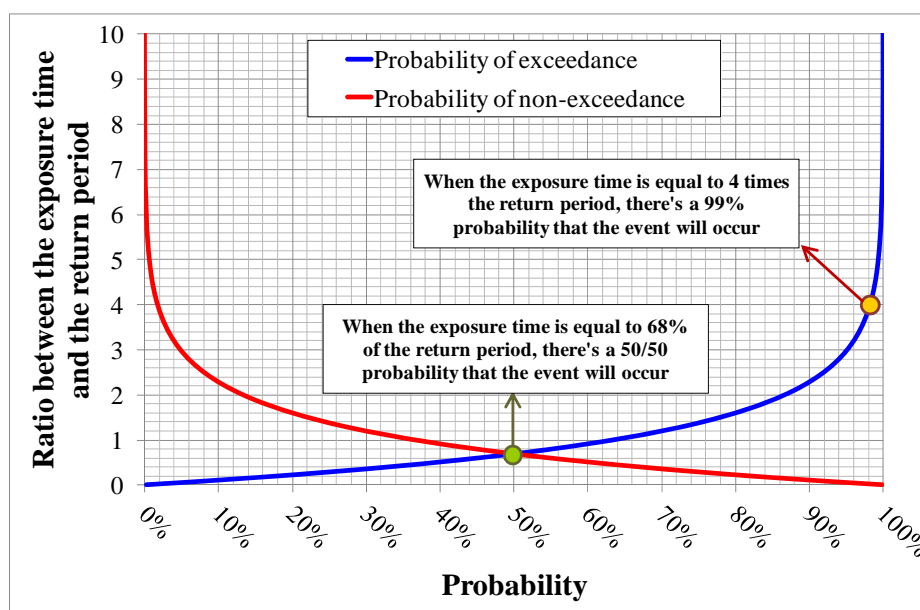
Figure 2.30: Relation between the exposure time, the return period and the risk of occurrence.

2.5.3.1   Probabilistic models of wind velocity

One crucial point when analysing the use of reduction factors relates to the accuracy of the probabilistic models used to derive the design loads of climatic actions, for instance wind. In Europe, the existing design codes use the Gumbel distribution (one of the three Generalised Extreme Value (GEV) distributions) to obtain extreme value predictions of the maximum wind velocities for high values of return periods. This distribution predicts unlimited values of the wind velocity has the return period increases, which can overestimate the actual maximum wind velocity physically possible that can be generated in the atmosphere. However, this might be counterbalanced by the uncertainty that will always exist by using a finite size sample of the data to determine the distribution parameters, see (Coles, 2001 ; Leadbetter et al., 1983). According to (Holmes, 2007), *"the approach of extracting a single maximum value of wind velocity from each year of historical data obviously has limitations in that there may be many storms during any year and only one value from all*

these storms is being used", but also only data values that are statistically independent are used, meaning that only the maximum wind velocity value per storm is used. If there are multiple similar events in each year the GEV approach might underestimate the load values for small return periods.

Additionally, (Fawcett, 2005) by analysing recorded wind velocities and including the seasonal variations in each year, showed that results obtained with the cluster peaks approach were less accurate and less precise than the results obtained when all data, above a properly chosen wind velocity threshold, are used, according to the Peaks Over Threshold approach (POT). The study revealed that, *"at levels of temporal dependence often encountered in real–life data, the cluster peaks analyses were constantly under–estimating return levels relative to the analyses making use of all threshold excesses. This suggests that designing to the maximum likelihood estimates which use cluster peak excesses – an approach currently employed by most practitioners – would result in considerable underprotection. However, further investigation has also revealed that this under–estimation becomes even more pronounced as the strength of temporal dependence is increased, but for low temporal dependence the cluster peaks analyses actually over–estimate return levels"* (Fawcett, 2005).

Figure 2.31 illustrates an example where the GEV approach has been used to determine the wind gust velocity for 2, 10 and 50 years return periods based on 46 years records of maximum yearly wind gust velocities.
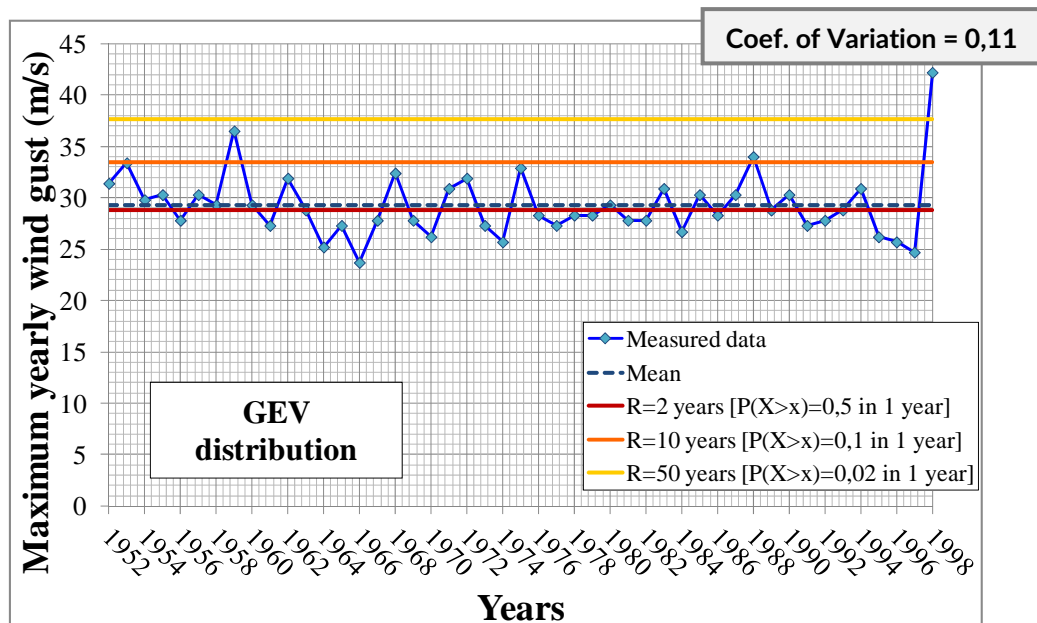
Figure 2.31: Application of the GEV approach to wind data measured in East Sale, Victoria, Australia (Holmes, 2007).

It can be seen that because of the finite sample of records the 2 years return period wind gust velocity is below the sample mean value, but the estimated exceedance probabilities associated with the three return periods fit quite well with the measured data. However, there is also the question of by how much is a given return period wind gust velocity exceeded. It is found that the 2 and 10 years return periods wind gust velocities are exceeded at maximum by 47% and 27%, respectively, and on average by 9% and 10%, respectively. Owing to the squared relationship between wind velocity and pressure, these values may be higher than the existing safety margin and taking into account the statistical uncertainties presented in the previous two paragraphs, together with the design uncertainties related to wind load effects on structures and to the structural response, the risk to the structure might be considered unacceptable. This observation gains further emphasis as the coefficient of variation of the data increases, see Figure 2.32.
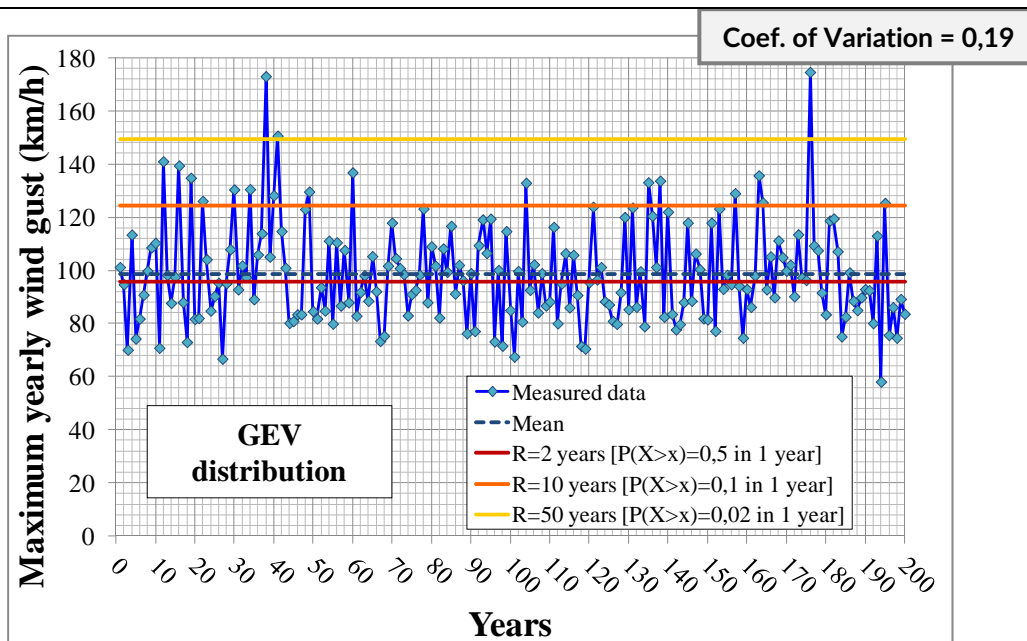
**Figure 2.32: Illustrative example of the insufficiencies of the GEV approach
for determining wind velocities for short return periods, adapted from (Castillo et al., 2004).**

2.5.3.2 Partial factors for wind loads

Therefore, it is important to check whether the usual wind load partial factor specified by the most recent structural codes, *e.g.* BS EN 1991-1-4, accounts for the variability observed in the wind measurements and for the size of exceedance over a given wind velocity threshold. In general, the wind load partial factor, γ_W, is separated into two factors: γ_f that covers the uncertainty on the value of the action itself and γ_{Sd} that covers the uncertainty in modelling the effects of actions.

The conventional values of these two factors are 1,35 and 1,10 (Gulvanessian et al., 2002). If the later value has been derived from comparison studies between results obtained by design models and measurements of wind effects on structures, the former *"has no scientific justification, and results from engineering judgement"* (Gulvanessian et al., 2002). Nevertheless, it is understood that this value leads in general to safe design load values.

However, the value of 1,35 may not suffice. For example, from the results illustrated in Figure 2.32, it is found that the 2 and 10 years return periods wind gust velocities (wind pressure) are exceeded at maximum by 82% (233%) and 42% (101%), respectively, and on average by 18% (40%) and 10% (22%), respectively.

It is also important to verify if the notional reliability indexes associated with using the specified partial factor to be applied to the wind actions satisfy the specified target reliability indexes.

The wind load partial factor can be determined by $\gamma_W = \gamma_f \times \gamma_{Sd}$. Knowing that γ_f is given by:

$$\gamma_f = \frac{W_d}{W_k} \tag{2.6}$$

where W_d and W_k represent the design and characteristic values of the wind velocity, respectively.

Using the Gumbel distribution to model the maximum wind velocities, the cumulative distribution function (cdf) of the maximum wind velocities is given by equation (2.7), assuming that wind is an ergodic random process.

$$F_{W[\tau]}(W) = \exp\left[-\exp\left(\frac{\lambda_{[\tau]} - W}{\delta_{[\tau]}}\right)\right] \text{ with } F_{W[t]}(W) = \left[F_{W[\tau]}(W)\right]^{\frac{t}{\tau}} \tag{2.7}$$

where:

$F_{W[\tau]}(W)$ represents the cdf of the maximum wind velocities related to a time period τ;

$F_{W[t]}(W)$ represents the cdf of the maximum wind velocities related to a time period $t \geq \tau$;

τ represents the unit observation time for which the action maxima values are determined and can be considered to be statistically independent of other maxima action values. For wind loads τ is usually taken as one year;

t represents a given reference period. The reference period t is dependent on the available data. In order to obtain a reliable estimate of the action value associated with a low probability of exceedance, it is, in general necessary to have an observational data set several times larger than the reference period t. Therefore, for the wind action it is common to assume a reference period of one year;

λ and δ are the distribution parameters.

The value W corresponding to a given probability of non-exceedance is given by:

$$\ln\left(-\ln\left(F_W(W)\right)\right) = \frac{\lambda - W}{\delta} \Rightarrow W = \lambda - \delta \times \ln\left(-\ln\left(F_W(W)\right)\right) \tag{2.8}$$

Estimates of the distribution parameters, the location and scale parameters, λ and δ respectively, can be obtained using the method of moments (MoM):

$$\mu = \lambda + 0,577 \times \delta \text{ and } \sigma^2 = \frac{\pi^2}{6} \times \delta^2 \tag{2.9}$$

where μ and σ are the mean and the standard deviation of the distribution.

The characteristic value of the wind velocity is obtained by fixing a maximum probability of exceedance, $P_{[t]}$, for a given reference period t, i.e. $1 - F_{W[t]}(W)$. This probability is related with a chosen return period, R, by equation (2.10).

$$R = \frac{\tau}{1 - F_{W[\tau]}(W_k)} = \frac{\tau}{1 - \left(1 - P_{[t]}\right)^{\tau/t}} \cong \frac{t}{\ln\left(\frac{1}{1 - P_{[t]}}\right)} \approx \frac{t}{P_{[t]}} \text{ for small values of } P_{[t]} \tag{2.10}$$

Then, the characteristic value of the wind velocity is obtained by introducing equation (2.10) in equation (2.8):

$$W_k = \mu_{W[1]} + \left\{-0,45 - 0,78 \times \ln\left[-\ln\left(1 - P_{[1]}\right)\right]\right\} \times \sigma_{W[1]} \tag{2.11}$$

Or if a reference period of n years is used:

$$W_k = \mu_{W[n]} + \left\{-0,45 - 0,78 \times \ln\left[-\ln\left(1 - P_{[n]}\right)\right]\right\} \times \sigma_{W[n]} \tag{2.12}$$

with:

$$F_{W[n]}(W) = \left[F_{W[1]}(W)\right]^n \Rightarrow \mu_{W[n]} = \mu_{W[1]} + 0,78 \times \ln(n) \times \sigma_{W[1]} \text{ and } \sigma_{W[n]} = \sigma_{W[1]} \tag{2.13}$$

According to (BSI, 2002a), the design value of the actions, for instance wind, may be determined by the FORM (First Order Reliability Method). Assuming that the performance function (G), see equation (2.14), is normally distributed, then the marginals are also normal distributions.

$$G = R - S \tag{2.14}$$

where R and S represent the resistance and action effects, respectively.

The probability that the design wind velocity is not exceeded is given by equation (2.15).

$$P(W \leq W_d) = \Phi(-\alpha_S \times \beta_1)$$ (2.15)

where β_1 represent the Hasofer-Lind (notional) reliability index for a reference period of one year determined from the target reliability index for the design working life (n), see equation (2.16), *i.e.* the distance from the origin (in the space of normalised variables) to the most likely failure point (design point) or in other words the minimum distance between the origin and the limit state function (failure function), see Figure 2.33, and α_S the FORM (First Order Reliability Method) sensitivity factor for effects of actions.

$$\Phi(\beta_1) = \left[\Phi(\beta_n)\right]^{\frac{1}{n}} \quad \text{and} \quad \Phi(\beta_n) = \left[\Phi(\beta_1)\right]^n$$ (2.16)
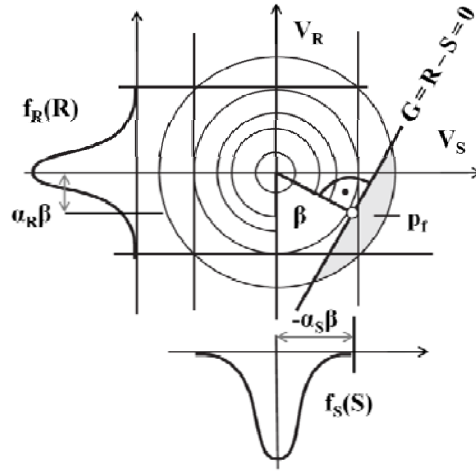
Figure 2.33: Design point, adapted from (Schneider, 2006).

If $0,16 < \alpha_S / \alpha_R < 7,6$, then α_S can be taken equal to -0,7 (BSI, 2002a). This condition is usually met in the majority of civil engineering structures and therefore the value -0,7 will be considered. The EN 1990 does not clarify if the value of -0,7 specified for the sensitivity factor for effects of actions (α_S) relates to a one year reference period or a 50 year period. In this Thesis, it was assumed that $\alpha_{S[1]}$ = -0,7. Therefore, $\alpha_{S[50]} \approx$ -0,5 for example (considering β_1 = 4,7).

Introducing equation (2.15) in equation (2.8):

$$W_d = \mu_{W[1]} + \left\{-0,45 - 0,78 \times \ln\left[-\ln\left[\Phi\left(0,7 \times \beta_1\right)\right]\right]\right\} \times \sigma_{W[1]}$$ (2.17)

Or if a reference period of n years is used:

$$W_d = \mu_{W[n]} + \left\{-0,45 - 0,78 \times \ln\left[-\ln\left[\Phi\left(\alpha_{E[n]} \times \beta_n\right)\right]\right]\right\} \times \sigma_{W[n]}$$ (2.18)

The partial factor to be applied to the wind action effects can then be obtained by equation (2.19).

$$\gamma_{W[1]} = 1,10 \times \frac{1 + \left\{-0,45 - 0,78 \times \ln\left[-\ln\left[\Phi\left(0,7 \times \beta_1\right)\right]\right]\right\} \times V_{W[1]}}{1 + \left\{-0,45 - 0,78 \times \ln\left[-\ln\left(1 - P_{[1]}\right)\right]\right\} \times V_{W[1]}}$$ (2.19)

Or by equation (2.20) if a reference period of n years is used.

$$\gamma_{W[n]} = 1,10 \times \frac{1 + \left\{-0,45 - 0,78 \times \ln\left[-\ln\left[\Phi\left(\alpha_{E[n]} \times \beta_n\right)\right]\right]\right\} \times V_{W[n]}}{1 + \left\{-0,45 - 0,78 \times \ln\left[-\ln\left(1 - P_{[n]}\right)\right]\right\} \times V_{W[n]}}$$ (2.20)

According to (JCSS, 2001), the value of the coefficient of variation of the annual maximum wind velocity gusts depends on the climate and usually assumes values between 0,10 and 0,35. Here a value of 0,26 will be considered, the same value considered in EN 1991-1-4 (BSI, 2005c). The results of varying the exposure time (n: 2, 10, 20 and 50 years), the return period (R: 2 to 100 years) and the reliability index (β: 1 to 5) are illustrated in the Figure 2.34.

A reference period of one year was used, as specified in (BSI, 2005c). If a reference period of 50 years was used instead then for the same β_1 the design wind velocity would be the same, and as a consequence, for the same annual probability of exceedance (*i.e.* same characteristic wind velocity) the partial factors needed to achieve the same β_1 are the identical. However, if the probability of exceedance is determined with reference to 50 years, then for $P_{[50]} = P_{[1]}$ the partial factors needed to achieve the same β_1 would decrease.
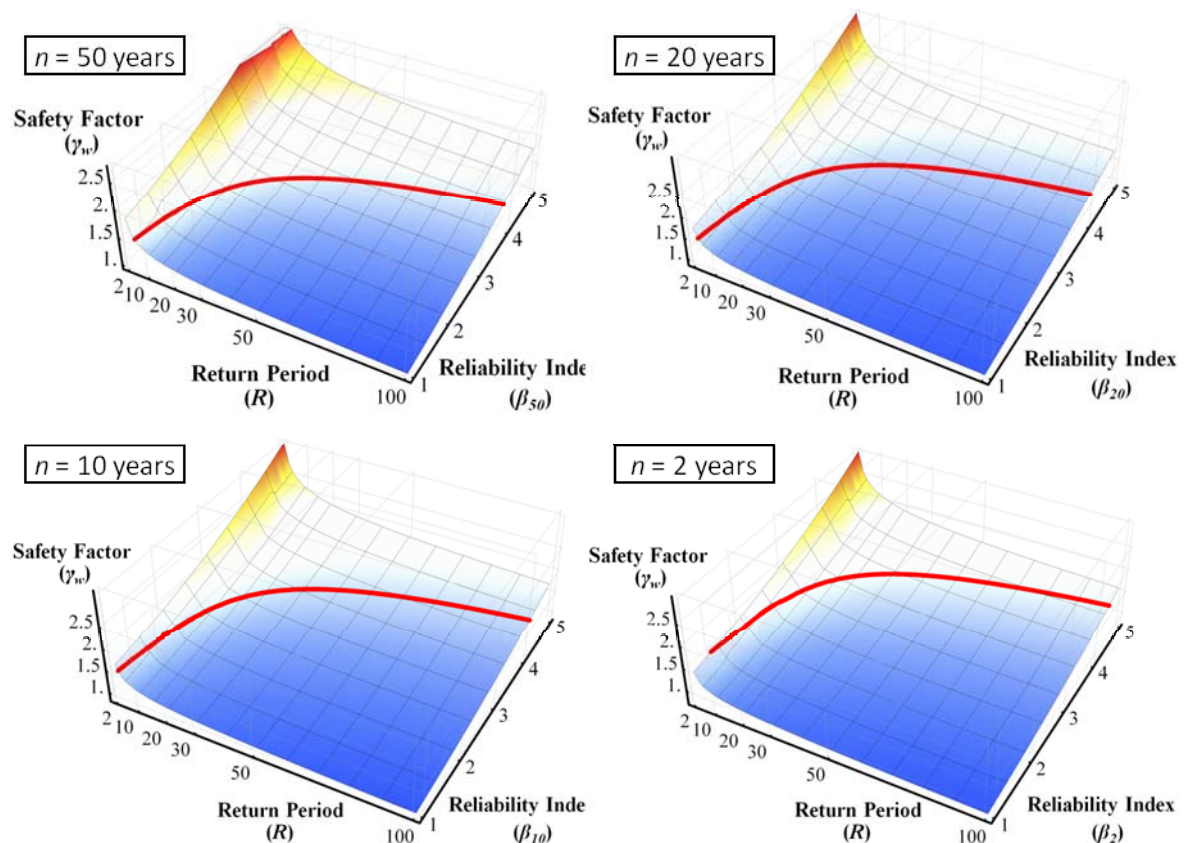
Figure 2.34: Wind load partial factor (red curve represents values for γ_W = const. = 1,5).

It may be observed that for the same return period, the reliability index achieved with γ_W = 1,5 does not change with the exposure time, as expected. For instance for R = 50 year return period $\beta_{50} \approx 3,5$ (*i.e.* $\beta_1 \approx 4,4$) for n = 50 years, and $\beta_2 \approx 4,3$ (*i.e.* $\beta_1 \approx 4,4$) for n = 2 years. An important observation is that the notional structural risk level for the wind action achieved following the existing structural codes can be higher than the target probability of failure. For instance, the notional annual probability of failure($P_{f,1}$) achieved for R = 50, γ_W = 1,5 and n = 50 is larger than the specified annual probability of failure for a structure whose collapse would have high or medium consequences in terms of human life, economy, society or environment (Consequence Class CC3 or CC2 in (BSI, 2002a), 1×10^{-7} and 1×10^{-6}, respectively), although smaller than the specified annual probability of failure (1×10^{-5}) for a structure whose collapse would have low consequences (Consequence Class CC1).

If in the case of the design of a permanent structure against wind loads, a lower target reliability than Consequence Class CC2 (β_1 = 4,7) could be accepted since the relative cost of safety measures is high; in the case of a bridge falsework structure an annual target reliability at

least equal to 4,7 may be used due to the low relative cost of safety measures. Additionally, if it had been fixed that $\alpha_{S[50]}$ = -0,7 rather than $\alpha_{S[1]}$ = -0,7, the $P_{f,1}$ achieved for R = 50, γ_W = 1,5 and n = 50 would even be larger than the target value for Consequence Class CC1.

It may also be observed that for reduced exposure times, for example 10 years, a structure designed considering a load return period of 10 years and a partial factor equal to 1,5, has an annual probability of failure of $4,0\times10^{-4}$ ($\beta_1 \approx 3,4$) which is even higher than the Consequence Class CC1 target reliability value (β_1 = 4,2). In this case, in order to achieve the CC2 annual target reliability it would be necessary to adopt a partial factor equal to 2,0 (instead of 1,5), or a return period of 80 years (instead of 10 years). Therefore, the standard use of reduction factor for short exposure times is further placed in question.

The high number of collapses of temporary structures resulting from the January and February 1990 wind storms in the UK, see (Buller, 1993), along with the severe storms of 1987, 2002, 2004, 2010 and 2011, and the trend for an increase of their frequency in the future due to the global warming (Fawcett, 2005), can be used as evidence to support the use of an improved approach to analyse the wind data and to determine more accurate reduction factors to determine design wind loads for short return periods. An improved methodology should take into account not only the definition of the exceedance probability percentile, *i.e.* from which return periods (R) of loads are obtained, but all wind velocity values higher than a certain threshold should also be included in the assessment of design wind velocities.

This approach can be further enhanced if the assumption of independence between successive extremes within seasons is broken and the short-term temporal dependence between consecutive extremes is taken into account. To model the likelihood function it might be useful to use, for instance, Markov chains of first or higher order (if greater precision is necessary) using a bivariate or multivariate logistic model for the transitions probability function, constructed such that the marginals have a Generalised Pareto Distribution (GPD), see (Fawcett, 2005) for details and an example. This approach has several advantages over the classical GEV approach, one of them being that the magnitude (size) of the exceedances over a certain threshold follow a GPD, thus this approach may solve the drawback explained before concerning the size of the exceedance. To solve this complex problem, simulation techniques such as the Markov Chain Monte Carlo (MCMC) method can be used, see (Fawcett, 2005). Additionally, the MLE method could be complemented by Bayes' Theory by updating the probability functions of the distribution parameters to properly account the model uncertainties in the results. Furthermore, Bayes' Theory can be used to explicitly estimate the wind loads for a given return period, based on the posterior distribution, thus avoiding the issues involved when using the MLE method to obtain estimates of the distribution parameters (Coles, 2001).

Another challenge is connected with updating the probability of occurrence of the 15, 50 or 100 years mean time interval of recurrence load with *in situ* measured data. For instance, if the 50 years return period load does not occur for more than 75 years it is plausible to think that the probability that it will occur in the next 5, 15 years might be considered higher than 50 years ago. If indeed this rationale is valid, it must be considered during the design of bridge falsework structures since it has direct safety implications. This type of analysis would necessarily mean the use of more refined and accurate models to estimate the wind characteristics and behaviour, both short and long term. The usual hypothesis of using a exponential distribution to model the recurrence of an event (50-year wind storm, for example) does not provide a complete solution because of its memoryless property, see equation (2.21). In order to solve the problem at hand, the validity of the assumption of independence between yearly wind extreme velocities would need to be reviewed. Bayes' Theory could be used but a careful analysis should be performed to not overestimate or underestimate the loads due to updating the *a priori* information with biased measurements or subjective data. To be efficient the use of this analysis methodology needs the measurement of wind velocity for large time periods, which often do not exist and can be difficult to obtain.

$$P\left(X > x_2 \mid X > x_1\right) = P\left(X > x_2 - x_1\right),\ x_2 > x_1 \geq 0 \tag{2.21}$$

A further and important issue related to the design of bridge falsework is the multiple reuse cycles during their design working life. For example, (Rosignoli, 2007) argues that because these structures are reused many times the meteorological loads should therefore be determined without reductions in relation to the work duration.

This problem is clearly explained in an excellent paper by (Hill, 2004). Hill gives an example of two cities, Constantown and Fickleville, where the first city maintains public buildings in service for 100 years while the second demolishes and rebuilds public buildings with more than five years (which therefore are designed for five year service life). Hill questions: which buildings are safer, Constantown's or Fickleville's? The answer is simple: it is likely that Constantown's buildings will stay in service for more than 100 years, therefore the probability that one building of Constantown is damaged after 100 years in service is greater than the probability of each one of Fickleville's buildings over the same period. However, for the same exposure time, the Fickleville's population is more likely to suffer injuries than Constantown's. Therefore Hill concludes that establishing design loads on the basis of service-life assumptions may result in significant safety inequities.

However, if the code calibration is accurate, this analysis problem may be solved by considering equal probabilities of failure for both structures. In order to obtain the same probabilities of failure the partial factors to be applied to actions during the design of the buildings with five years' design working life need to be larger than the ones applied to actions during the design of the buildings with 100 years' service life.

In fact, if the probability of failure of each building rebuild every five years in Fickleville can be assumed independent from each other and equal, *i.e.* the initial conditions of each building are the same, then the probability of failure over the 100 years in each city can be calculated by equation (2.22).

$$P_{f,100}\left(\text{Constantown}\right) = 1 - \left[1 - P_{f,1}\left(\text{Constantown}\right)\right]^{100}$$
$$P_{f,100}\left(\text{Fickleville}\right) = 20 \times P_{f,5}\left(\text{Fickleville}\right) = 20 \times \left\{1 - \left[1 - P_{f,1}\left(\text{Fickleville}\right)\right]^{5}\right\}$$

(2.22)

Therefore, in order for the buildings at the two cities have the same probability of failure:

$$P_{f,100}\left(\text{Constantown}\right) = P_{f,100}\left(\text{Fickleville}\right) \Rightarrow$$
$$\Rightarrow P_{f,1}\left(\text{Fickleville}\right) = 1 - \sqrt[5]{1 - \frac{1 - \left[1 - P_{f,1}\left(\text{Constantown}\right)\right]^{100}}{20}}$$

(2.23)

For example, if β_1(Constantown) = 4,27, Consequence Class CC2, *i.e.* $P_{f,1}$(Constantown) = 9,77×10⁻⁶, a value of $P_{f,1}$(Fickleville) = 9,76×10⁻⁶ is obtained. These values are almost equal, and therefore the partial factors might, in practice, be the same. The difference between partial factor values will increase for smaller values of the reliability index, for instance: if β_1(Constantown) = 3,00 one gets $P_{f,1}$(Constantown) = 1,35×10⁻³ and $P_{f,1}$(Fickleville) = 1,27×10⁻³, and the reliability index to be used in the design of Fickleville buildings increases to 3,02 - which still represents a fairly small difference.

A similar analysis can also be applied to problems of life extension of structures. Here, if it can be considered that the initial conditions still hold after the initially planned design working life has been reached, *i.e.* the resistance of the structure is not negatively affected by the damage accumulation due to usage, then the probability of failure before and after the analysis can be assumed independent (and equal if the design actions' models are unchanged). In this case, the total probability of failure of the structure is given by the sum of the two probabilities of failure.

The information presented in the previous paragraphs has an immediate application to bridge falsework structures. For example, it may be decided that a given bridge falsework structure should have the same probability of failure at the end of its design working life, 20 years for instance, than a building at the end of the usually considered design working life, 50 years, for a Consequence Class CC2 ($\beta_{20,\text{falsework}} = \beta_{50,\text{building}} = 3,8$). Knowing that the reliability index to be considered during

the design of the bridge falsework is given by equation (2.16) (valid for actions that have statistically independent maxima in each year) the partial factor to be applied to the wind action is plotted in Figure 2.35. It may be observed that considering return periods less than the design working life for the bridge falsework, for instance 10 years, would imply the use of a higher partial factor, 11% in this example. However, this is only true if the yearly probability of failure of the bridge falsework system is constant in all the reusage cycles during their design working life. This may not be the case: bridge falsework elements can be reused several times in various bridge projects with their own design particularities (design teams, ground characteristics, workers skills, maintenance plans, etc.) in different places with different types of weather.
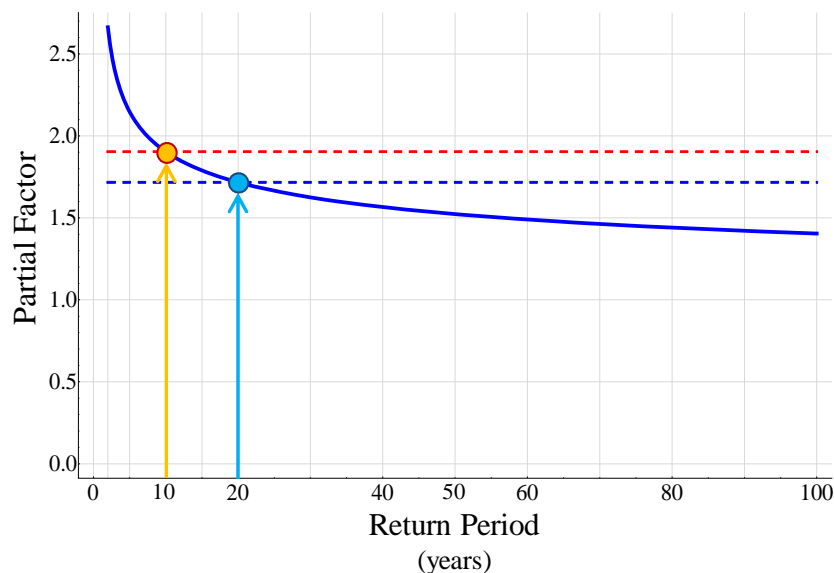
Figure 2.35: Wind load partial factor, considering a consequence class CC2 ($\beta_{20,falsework}$ = 3,8).

It may be concluded that the choice of the appropriate reduction factors to determine the design wind velocities for short return periods is influenced by many uncertainties: from the validity of the assumptions regarding the stationarity and the temporal independence of the measured data, to the methods used to fit probabilistic distributions to the wind velocity data records and to obtain the distribution parameters and moments, ending in considerations about the design working life of bridge falsework systems. Furthermore, it was demonstrated that if load values are derived from return periods less than the design working life of bridge falsework structures than in order to achieve an acceptable risk at the end of this period it is necessary to use larger partial factors applied to the loads, which is often not the case.

Therefore, it appears reasonable to recommend not using any reduction factor and adopt return periods equal to the design working life when designing bridge falsework systems. At least, for cases where meteorological data and site specific information is not available that can be used to reduce the uncertainty levels, in particular for short term usage periods of bridge falsework systems. However, this recommendation needs proper justification in terms of the proportion of the benefits achieved by reducing the risk of collapse of bridge falsework systems against the possible additional costs incurred due to the higher design wind loads. A framework to perform this kind of analysis will be presented in a future Chapter of the Thesis.

The second approach fits in the abovementioned risk management framework. For example, Sexsmith introduces a method where a design criterion is established based on minimizing the expected value of the sum of failure consequences and initial costs (Sexsmith, 1998). It was found that a higher safety margin was required when the construction cost was small compared to the cost of consequences. This is usually the case of falsework. It was also concluded that in some cases the use of reduced load return periods, such as a ten year wind load, can be seriously irrational (Sexsmith, Reid, 2003). For example, if the cost of a falsework failure is 500 times the cost of providing additional

safety, the load factor to be applied to the ten year wind load in the Vancouver region, in Canada, would be higher than 2,5 in order to minimise the total expected costs (Sexsmith, Reid, 2003).

However, in practice the design of bridge falsework is usually a simple verification of the unfactored vertical loads acting during concreting of the bridge against safe load table values developed by the falsework system manufactures. Additionally, in this design methodology various effects that have a decisive influence on the behaviour, resistance and performance of the falsework are not accounted for directly, *i.e.* they are often estimated to be included in the partial factor which was used by the falsework system manufactures when developing the load tables.

2.5.3.2.1 Vertical loads

The sequence of loading of a bridge falsework structure can have a major effect on the stresses in individual members of the structure. Important aspects that need proper consideration during planning and design phases include (i) type of equipments to be used, weight and volume of storage materials, (ii) method and sequence of pouring and (iii) method and sequence of post-tensioning (Billings, Routley, 1978).

For the design of the falsework system, the most critical stage of construction is usually during pouring of concrete. In the survey presented in section 2.4.2 and also in the data reported by (Hadipriono, Wang, 1987), it can be found that over 50% of the falsework collapses occurred during concrete pouring operations.

The design value of the vertical loads includes the system's dead load and various construction loads. The construction dead load on a particular falsework member is the weight of fresh concrete plus the weight of the formwork, reinforcing steel and prestressing steel. The weight of concrete (except lightweight concrete) is usually assumed at $2400 \, kg/m^3$. Most specifications assume an additional $100 \, kg/m^3$ of concrete to account for the weight of embedded steel, rather than requiring a calculation for those items. Regardless of the actual vertical load imposed, a minimum vertical load is included in most specifications. Typically, the minimum vertical load is $4,8 \, kN/m^2$ distributed uniformly (Ratay, 1996). The construction live load mainly includes the weight of stacked material, equipments and workers together with an allowance for localised mounding during concrete placing (Zhang et al., 2009). In general, the construction live load is considerably smaller than the construction dead load.

There are not many studies regarding the adequacy of live loads specified in structural codes simulating the action of concrete pouring during construction of bridges. However, research has been focused mainly on building construction. (Rosowsky et al., 1994) concluded that a load factor of two or greater must be applied to the then specified vertical loads (US standards) to account for load-structure interaction in the design of formwork (falsework). (Yen et al., 1995) suggested the use of an amplification factor of up to 3,5 to account for dynamic effects during concrete pouring. (Peng et al., 1997) concluded that the standards maximum axial forces are not influenced by the load pattern and load paths – designer can safely assume uniform loads –, but its values are greater than the values specified in the structural codes. Ikäheimonen in his PhD Thesis (Ikäheimonen, 1997) analysed all available data on shore loads during concreting and concluded that applying a partial factor of 1,25 to the concrete self weight plus considering a design load equal to $2,5 \, kN/m^2$ is enough to get a safe estimate of the design axial load in each standard.

Furthermore, (Billings, Routley, 1978) measured loads in standards during the construction of a prestressed concrete bridge in New Zealand. They found important observations:

(i)   considerable variation in standards axial loads in the order of ±25% of the concrete dead load occurred during concreting. These variations are caused by a number of factors: (i.1) errors in positioning the standards; (i.2) out of plumb of some of the standards; (i.3) stiffness and redundancy of the falsework;

(ii)   the design of falsework supporting major concrete bridges during construction must include allowance for loads caused by prestress and temperature gradients – where large pours are expected the loads induced by the heat of hydration of the concrete may require special investigation;

(iii)   for ground-supported falsework, the base and top jacks should be firmed up as early as possible. Finally, they suggested that for vertical loadings, a minimum factor of safety of 2,0 should be adopted for bridge falsework systems.

Quinion also reports data from monitoring falsework elements during concreting (Quinion, 1984). It was observed that as concrete construction progressed the loads in the falsework increased and approached the design values. However, as the concrete matured and particularly after a span was completed, the loads dropped in the falsework as some 20% was transferred to the piers. During post tensioning of the third and last span its extremity rose by 76 mm and the adjacent span, already built, moved 14 mm downwards. Consequently, the loads on the measured members of the second span rose by 25% from their previous values. Subsequently, during removal of the falsework the loads in some of the members which were the last to be fully relieved of load increased by a further 25%.

2.5.3.2.2   Horizontal loads

Horizontal forces arise from different sources such as (i) wind, (ii) concrete pouring method, (iii) system imperfections, (iv) insufficient system lateral stiffness and (v) foundation settlements.

All falsework design specifications include a requirement that the falsework must be capable of resisting a horizontal design load. However, this is sometimes neglected in design. This requirement is included to provide a criterion for bracing design and thus ensure the stability of the falsework system. Typically the horizontal design load will be either an assumed minimum load or the calculated wind load, whichever is greater. In most cases, the minimum horizontal load is assumed as 2% of the total supported dead load at the location under consideration although some specifications may use a higher value.

As said previously, the vertical loads generally dominate the design of bridge falsework systems. This is because the weight of the permanent structure is very high and after hardening the bridge deck acts as a top restraint of lateral movements of the falsework system. However, before the casting of the concrete the wind load needs to be considered since the formwork may not yet exist or the formwork in-plane stiffness may not be sufficient.

An anemometer (wind gauge), for example, should be required onsite and monitored continuously, and weather forecasts should be reviewed routinely. Generally, on most falsework projects, casting of concrete will not be allowed when the wind velocity exceeds the operating limits. These are usually at a Beaufort Scale 6, corresponding to a wind velocity of 14 m/s (Newman, Choo, 2003). This is known as the working wind velocity.

It is common practice to design the falsework against wind and earthquake separately and to insure the system regarding the unlikely event of a simultaneous action of the wind and the earthquake.

Additionally, lateral loads could derive from non-balanced, *i.e.* not auto-equilibrated, concrete pressures applied to the formwork (The Concrete Society, 2012). The modelling of the intensity and depth variation of these concrete pressures is still under development since no unified criteria (not too much conservative) have been achieved. Additionally, new concrete types have been introduced and regarding these little research has been made, (Proske, Graubner, 2008 ; Graubner, Proske, 2005, 2010) are the exceptions.

2.5.3.2.3   Settlements

Settlements should be assessed correctly to avoid unwanted and unusual load distributions within the elements of the bridge falsework system, and problems related to the geometry control of the

permanent structure. Settlements are most often related to movements in the foundations, but elastic deformations and initial gaps between elements and within the connections can also produce settlements.

Differential settlements can occur in situations where some supports bear on bridge footings and the rest on natural ground, when different foundation types are used (concrete and timber footings for example), see Figure 2.36, or due to variations in the properties of the soil. Differential settlements translate to unbalanced loads and consequently to overloaded standards and footings. Furthermore, the occurrence of these settlements may result in the overturning of part of the structure, causing secondary stresses for which the falsework structure was not designed for. This behaviour, if neglected in the design phase may lead to the collapse of the structure.

Figure

Figure 2.36: Example of differential foundation settlements (fib, 2009).

Structures where the vertical elements are not tied up to adjacent members, *i.e.* without bracing elements, or with joints that do not allow the redistribution of the forces between adjacent elements, are more sensitive to the effects of differential settlements. However, elements of very stiff structures, with many bracing elements, can as well be very sensitive to differential settlements as these introduce additional compression/tension loads to neighbour elements.

An example of a bridge falsework system failure caused by settlements occurred on 15th April 1982, when two spans of a partially completed post-tensioned concrete bridge, being constructed at the Riley Road interchange in East Chicago, collapsed during the casting of the deck, killing 13 workers (Sikkel, 1982). This example is different than the one mentioned in section 2.4.3.

At the time of failure virtually all the loads were supported by the falsework (isolated high-capacity towers located close to the bridge piers). The failure occurred during the casting of the deck slab of the fourth span when about 100 m length of the partially finished bridge and its supporting falsework collapsed. The ensuing investigation found that the falsework as built was substantially different in several vital details from that envisaged in the design. The collapse was probably triggered by the excessive settlement of one of the temporary foundation footings of one of the falsework towers. This caused an increase in the reactions provided by the other footings which were under-designed and thus cracked. The differential settlement of the foundations caused an estimated increase in the loads in the diagonal bracing members of the tower to about 40 kN which was grossly in excess of the average value of about 28 kN for the buckling strength of the tubes, determined from later tests. This partial tower failure induced a slight sway at the top of the tower causing the main cross-members supporting the bridge to be eccentrically loaded. The welds holding these in place fractured and one cross-beam fell away imposing an eccentric load on the tower which then buckled and collapsed, precipitating collapse of the partially-completed span.

On subsequent investigation it was found that:

- The foundations footings of the towers had been constructed on top of about 3 m of compacted fill, but this overlay 300-600 mm deep pockets of highly compressible black organic silt.

- The foundation footings were only 300 mm thick, whereas the existing code required a thickness of at least 530 mm.

- Some cracks in the foundation footings had been noted by the site surveyor a few days before the collapse, but their significance had not been appreciated.

2.6 Research needs

From what was described in the present Chapter of the Thesis, several research needs can be identified regarding bridge falsework systems:

- It is clear that a consistent methodology focused on risk informed decision-making in bridge falsework is necessary, minimizing the risks and maximizing the benefits in a cost effective way. There is a need for research aiming to promote the early consideration in the design of bridge falsework systems, and also to increase the awareness at construction sites, of the specific exposure of these structures, of the identification of the main hazard scenarios, of the importance of performing the risk analysis of the structure to each of these hazards, pin pointing the most critical failure modes and the associated enabling and triggering events. Additionally, recommendations are needed to increase the robustness of these systems. In this way the design, the assembly and use of these systems may be more rational, cost efficient and safe, optimizing the use of the limited resources available while increasing health and safety at work as well as the productivity and quality of the construction. In this Chapter the main procedural causes, enabling and triggering events of bridge falsework collapses have been identified and discussed, including methodologies to manage and control them, in particular human related errors.

- In terms of design it is evident from what was mentioned in the previous sections that the design based on the recently published Eurocodes does not guarantee many of the principles enunciated in the preceding paragraph. Particular aspects which can have a significant effect on the structural performance of bridge falsework systems are not entirely considered in these documents, such as:

  (i)   The use of reduction factors to calculate the design values of actions. It has been demonstrated that using reduction factors can result in risk levels higher than the ones specified in structural design codes. It is therefore recommended not to use any reduction factor and adopt return periods equal to the design working life when designing bridge falsework systems. At least, for cases where meteorological data and site specific information is not available that can be used to reduce the uncertainty levels, in particular for short term usage periods of bridge falsework systems;

  (ii) Considerations about the safety and cost of the structure; the partial factors applied to the loads are not calibrated for optimizing cost and safety of temporary structures;

  (iii) Analysis of the global behaviour and resistance of the system, essential to study its robustness and risk. In this regard, it should not be forgotten that existing codes are element reliability calibrated and thus can only provide quantifiable levels of reliability to the element level: the system overall reliability is not directly addressed. To achieve minimum levels of robustness, rules concerning tying resistance of the connections were introduced. However, a direct verification of the modes of failure is still not required and the "what if" scenario is still not implemented. Thus, structural systems designed according to the most up-to-date code can still be prone to disproportionate collapses, in particular bridge falsework systems;

  (iv) Modelling of the joints between elements of the system and of its boundary conditions. In this regard, for systems with Cuplok® joints no design model is

available in the existing European standards. Furthermore, the existing tests results published by researchers in UK and Australia are not completely in agreement, and there are still large opportunities for improving joint modelling specifically regarding spigot joints and forkhead joints;

(v)   Behaviour of the system under dynamic loads, for instance of temporary columns during the launching of a bridge;

(vi)   The existing codes do not specify a method for analysing the consequences arising from multiple usage cycles of the system during its design working lifetime, and for the early planning of maintenance actions that may be needed. In this regard, this Chapter introduced solutions to this problem, in particular the requirement to implement effective quality control, maintenance and inspection procedures. BS 5975 gives detailed procedural controls for temporary works which can be used to manage human errors and the reusage of elements;

(vii)   Besides the risks mentioned above, there are other hidden or not considered risks in the design philosophy specified in the existing codes. The simple fulfilment of a predetermined set of design rules developed for general use may not assure by itself the safety, the quality and cost efficiency of a specific structure. In some cases the existing rules are not suitable, sufficient and proportionate to the consequences of failure of a given structure. What is the reliability achieved? Is the level of risk acceptable, unacceptable, intolerable or tolerable? Answers to these questions cannot be found in the existing codes;

(viii) The current methodology can blind the designers, and other relevant actors, by not making clearly evident the need to thoroughly assess the impact of residual risks, of unusual risks due to specificities of the project or of risks unaccounted for in the design process.

- Not to mention that an important number of designs of bridge falsework systems are based on design load tables developed by the producers of the systems. The appeal of using these tables in the design of bridge falsework systems is their apparent simplicity and general use, thus leading to a straightforward and fast design, though sacrificing the economy of the system by using smaller resistance values (*i.e.* larger partial factors, usually in the order of two) than the ones obtained using the Eurocodes or other applicable European standards (such as the EN 12812:2008). However, more often than not these tables do not take into account the particularities of a specific system, for instance differences in stiffness between various parts of the system, ground settlements, lack of bracing in one direction, etc. Therefore, the risk associated with the use and misuse of some of these tables in the design of complex systems may be unacceptable but not fully understood by the various stakeholders involved.

- Uncertainties arising from the design are often multiplied in the field. The safety procedures specified at the construction site rely on professional judgment by competent people but are based on available historic information regarding foreseeable risks associated with work activities certain to occur during construction. As the design process is not directly focused on assessing the risks of a given structure to be used in a specific context, some uncertainties will always be propagated to the construction site. These uncertainties can escape the control net provided by the safety procedures enforced on site and the coupled effect of multiple uncertainties can lead to incidents and accidents.

The present Thesis will contribute for improving the safety of bridge falsework systems by increasing the available knowledge about the importance of some uncertainties in the performance of these systems. Various hazard scenarios will be tested to evaluate the reliability, robustness and risk of these systems. Comparisons of the results obtained will provide important insight that can be used by

the designers, contractors and workers making them aware to particular risks that can have a decisive influence on the health and safety in construction of bridges. At the same time, recommendations will be suggested in order to improve the safety, quality and cost-effectiveness of these structures when exposed to the identified critical hazards.

3

EXPERIMENTAL INVESTIGATION

3.1 Introduction

The structural behaviour of bridge falsework structures can be assessed by experimental tests and/or by numerical models. This Chapter concerns experimental tests of specific features (joints) of bridge falsework structures. The justification for performing these experimental tests resides in the important influence of joint behaviour on the overall performance of bridge falsework structures, see (Rodrigues, 2010), and in the large computer resources needed for characterising accurately the joint's behaviour within affordable runtimes together with the associated numerical modelling difficulties. Comparatively to numerical analysis, experimental tests, if properly planned and executed, are a rather easy mean to understand the joint's behaviour by identifying the main influence variables and by characterizing the joint's stiffness and resistance for the selected testing conditions.

Full-scale tests are not part of the planned experimental tests because of the limited material resources and due to laboratorial facilities restrictions, in particular the inexistence of a load frame capable of applying loads to a structure with a considerable plan area and height.

The experimental campaign performed in this Thesis included tests of three different joints: (i) ledger-to-standard joints, (ii) standard-to-standard joints and (iii) joints between the forkhead plates and the formwork beams. The objective of the first set of tests is to clarify the differences between existing results, see section 1.4.1.2, and to increase the available database of results which will be later used in the reliability and robustness analysis. The other two types of tests have never been done before (no bibliographic reference was found) and thus represent an excellent opportunity to reduce the uncertainties related to the behaviour of bridge falsework structures. A total of 192 tests were carried out.

The experimental campaign profited from the collaboration with HARSCO Infrastructure, http://www.harsco-i.co.uk/. The type of bridge falsework selected as an application example throughout the present Thesis is the Cuplok® system. The steel grade of the materials is grade 50 according to (BSI 1990), with a nominal yield stress of 355 MPa (355 N/mm^2).

No tensile tests were performed on steel coupons taken from selected samples of each different element used in the tests. However, information regarding the mechanical properties of various elements, namely ledgers and standards, given in factory production control certificates was made available by HARSCO and is presented in Annex B. Geometrical characteristics of the various elements of the Cuplok® system provided by HARSCO were measured and the results presented in Annex C. Both material properties and geometrical characteristics are relevant variables but findings

published in (Chandrangsu, 2010) suggest that they do not explain the variability of bridge falsework system's resistance.

3.2 Ledger-to-standard joint tests

As existing tests results are not consistent, in particular with regard to the ledger-to-standard joint's initial bending stiffness, a series of cantilever bending tests was performed. The proposed tests investigated the possible difference in joint behaviour between "as new" and "used" elements (elements nearing the end of their service lives), as to date no study has been found addressing this possibility. To this end, half of the tests corresponded to used elements whilst the other half corresponded to "as new" elements. However, the already used materials delivered by HARSCO were, in its great majority, in excellent conservation condition with only minor damages observed in just a few elements. In some ledgers, near the blades, there were indentations or the tubes were deformed in oval shape, perhaps due to hammer blows applied to lock the joint. Also, in some forkheads, the U plates were bent outwards.

In addition to bending tests, about both strong and weak bending axis, tensile axial tests were performed to characterise the behaviour and resistance of ledger-to-standard joints under axial forces. Note that the axial resistance of the joints is extremely important because a common failure mode of bridge falsework structures is the domino-type where large tensile forces arise on lacing members due to the failure of one or more standards.

The nominal dimensions of the CHS and nominal yield stress of the standards and ledgers were 48,3 mm × 3,2 mm and 355 MPa, respectively.

3.2.1 Joint bending tests

Bending tests were performed in two directions, about the joint strong axis (rotations resulting from displacements along local y axis) and about the joint weak bending axis (rotations resulting from displacements along local z axis), see Figure 3.1. For each direction, tests were carried out with two, three or four ledgers at the joint to incorporate all possible types of joint configurations and to analyse the influence in the joint's behaviour of the number of elements connected.
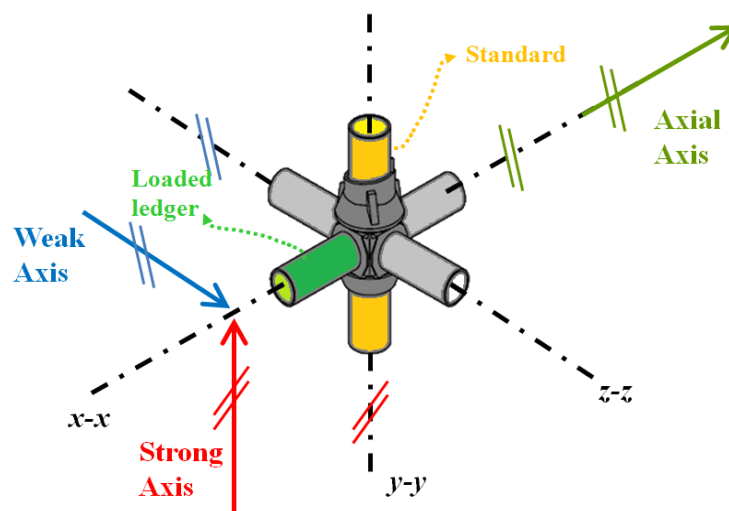
Figure 3.1: Illustration of Cuplok® joint bending axis.

All of these tests were performed at the Oxford Brookes University Technology Laboratory in an already existing rig and using newly designed accessories to clamp the standard element top and bottom ends to a rigid frame, see Figure 3.2 for an illustration of the joint bending test about the strong axis.

The test setup consisted of a 500 mm standard element clamped at the top and bottom ends to a rigid frame by bolted connections to speed up test assembly and dismantling. The Cuplok® joint

was positioned at the centre of the middle free length of the standard (equal to 300 mm) and a 600 mm ledger (termed hereafter as the loaded ledger) plus one to three other ledger elements with 50 mm length were connected at the joint depending on the tested joint configuration. The lengths of the standard and of the loaded ledger were chosen to be as small as possible to reduce their deformation by bending but not as small as to induce important distortion deformations.

Only bending moments were applied to the joint. The effect of the axial force in the ledger was therefore ignored. This option is justified based on the fact that the axial forces in the ledgers are usually just a fraction of the axial forces in the standards, due to the semi-rigid connections between the various elements, and thus the interaction between the bending moment and the axial force is not significant.

3.2.1.1   Strong axis bending tests

The test procedure consisted in applying a vertical displacement at the loaded ledger element using a lever arm equal to 300 mm in order to ensure always the attainment of joint failure, see Figure 3.2. During the tests, the load (registered by a ±50 kN load cell), the jack displacement (registered by LVDT 01, ±75 mm travel) and the joint rotation (calculated through LVDTs N1 and N2 readings, both ±50 mm travel) were measured and recorded every second. Prior to tests, all devices were verified against standards traceable within the UK national metrological quality system, and the errors thus determined represented less than 1% of the readings.
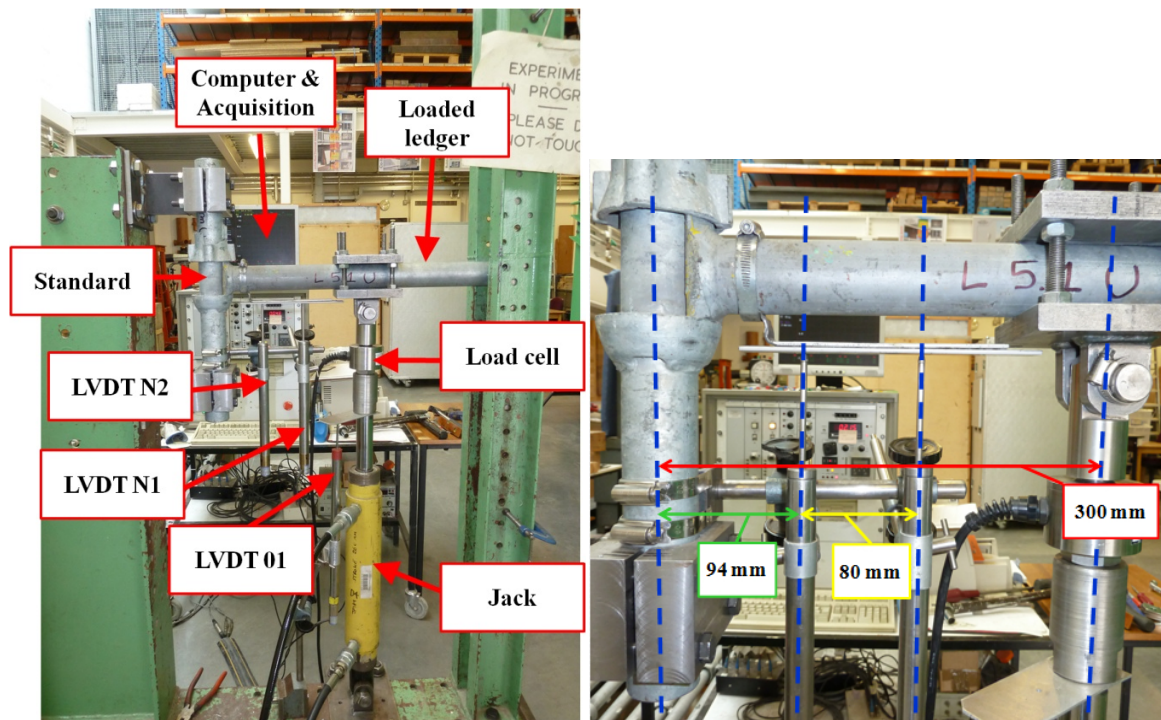
Figure 3.2: Testing setup (strong axis) - *Left*: overview and *Right*: positioning of the LVDTs.

The N1 and N2 LVDTs measured relative vertical displacements between a cross-section of the loaded ledger and a cross-section of the standard. The reference cross-section at the loaded ledger was chosen to be as close as possible to the Cuplok® joint to reduce the contribution of the bending of the ledger to the joint rotation values. This solution is more accurate than reading the vertical displacements directly on two cross-sections of the loaded ledger. The reference cross-section at the standard was chosen so to reduce the contribution of the (small) standard rotation in the determination of the joint's rotation; however this objective was not always attained directly as will be discussed later.

Reducing even more the contribution of the bending of the ledger to the joint rotation values would involve having to measure the vertical displacements at two different, but close, cross-sections along the loaded ledger length relative to the same reference section where the N1 and N2 LVDTs were clamped. With these relative displacements the relative rotations at each cross-section would be determined and

the rotation of the loaded ledger would be given by the difference of the two relative rotations. Since there is always an uncertainty present, a conservative choice was made of ignoring this correction. Therefore, the obtained joint rotation values (stiffness values) are higher (lower) than the true values.

All tests were performed under displacement control. In the majority of the tests a low displacement rate equal to 0,1 mm/s was chosen. In a limited number of tests this loading rate was increased ten times, to 1 mm/s, in order to simulate the dynamic effect of a sudden failure of a member within the bridge falsework system.

At the beginning of each test the loaded ledger was levelled horizontally and both the position and the verticality of the displacement transducers were checked.

A set of three types of tests were performed: (i) a set of preliminary tests, (ii) a set of initial tests and (iii) a set of final tests.

The objective of the preliminary tests was to evaluate the influence of several variables that can contribute for the possible observed scattering in the joint's initial behaviour. In particular, it was analysed the influence of the position of the loaded ledger in the node (this ledger was positioned at four different positions, see Figure 3.3, and at an additional position obtained by twisting the element 180º), the position of a second ledger in the joint (this ledger was positioned at three different positions while the loaded ledger remained at position P1) and the repeatability of the test (the loaded ledger was tested again at position P1 after tests at positions P2 to P4). Position P1 was defined by making the top locking element in the standard, identified with a red circle in Figure 3.3, aligned and facing the loaded ledger element. Positions P2 to P4 were obtained by rotating the standard 90º counterclockwise from the previous position.

The test procedure consisted in applying three cycles of ±2 mm and an additional three cycles of ±3 mm (the load was not allowed to exceed 1,5 kN, *i.e.* 15% of the expected maximum load). These cycles were intended to simulate the behaviour of the joints under the wind action. The displacement values were selected based on the results of a set of runs of numerical models of different configurations of bridge falsework structures under normal working wind velocity (considered to be equal to 18 m/s).

Figure 3.3: Four different ledger positions considered during the preliminary tests - *Left to right:* position P1, position P2, position P3 and position P4.

In the initial tests the specimens were loaded up to failure with no significant load reversals. Their aim was to obtain an estimate of the maximum load and an envelope for the final tests. Also, it was important to assess if the results obtained by past investigations, in particular (Chandrangsu, Rasmussen, 2011), could be reproduced in order to be able to compare their results with the ones obtained in this project. However, only a limited number of tests completely emulated the Australian tests. In the majority of tests, three displacement cycles corresponding to small rotation amplitudes were applied at the beginning of each test to erase possible friction contributions for the initial stiffness of the joint, contrary

to the Australian procedure in which the load was ramped up straight to failure. Tests with two, three and four ledgers present in the joint were performed, see Table 3.1 for details.

The final tests comprised the application of displacements in one initial direction (upwards or downwards) up to the point where the load *vs.* displacements diagram began to deviate from linearity (which occurred around 2/3 of the maximum load value, but not for loads higher than 10 kN). Past this point, the load was gradually removed after which loading was reapplied in the opposite direction (reloading phase) until the specimen failed (start of an unstable load path, *i.e.* negative slope). The results of this type of test procedure have not been published before. This behaviour can be observed after a local failure has taken place within a bridge falsework system or when an action, other than the dominant action due to the weight of the fresh concrete, occurs, for example by ground settlement. Also, as part of the final tests, the effect of locking the joint by hand rather than by hammer was studied, as well as the effect of increasing ten times the loading rate after the application of the initial cycles, see Table 3.2.

Table 3.1: Summary of initial tests.

Condition	Loading	Position	Initial cycles	Number of tests
New / Used	UP	P14	Yes	3
	DOWN	P14		3
	UP	P34		3
	UP	P14	No	3
	UP	P124	Yes	3
	UP	P1234	Yes	3

Table 3.2: Summary of final tests.

Condition	Loading / Reloading	ID	Initial cycles	Number of tests
New / Used	UP / DOWN	P14	Yes	5
	DOWN / UP	P14		5
	DOWN / UP	P14, HAND		5
	DOWN / UP	P14, HAND, FAST		5
	DOWN / UP	P124		5
	DOWN / UP	P1234		5

A total of 96 tests divided in 36 initial tests and 60 final tests were carried out in the present investigation. In all tests, the bending moment (M) and the joint rotation (θ) for the time instant $t = i$ were determined by:

$$M\big|_{t=i} = P\big|_{t=i} \times L \text{ and } \theta\big|_{t=i} = \arctan\left(\frac{d_{N1}\big|_{t=i} - d_{N2}\big|_{t=i}}{L_d}\right) \tag{3.1}$$

where L represents the lever arm length and was equal to 300 mm and L_d represents the distance between the LVDTs and was in general equal to 80 mm.

3.2.1.1.1 Results of the preliminary tests

The tests diagrams illustrated in the figures presented below have been identified with the following notation (PT)+(1L or 2L)+(P1 or P14)+(U1 or N1), meaning:

- The first part of the notation identifies the type of test: preliminary tests (PT);
- The second part identifies the number of ledgers connected at the joint: one (1L) or two (2L);
- The third part identifies the position of the ledgers: loaded ledger at position 1 (P1) for a joint with one ledger, or a loaded ledger at position 1 and an unloaded ledger at position 4 (P14) for a joint with two ledgers;
- Finally the last part identifies the condition of the tested elements and the number of the test, for example: first test using used elements (U1) or first test using new elements (N1).

From the preliminary tests it was possible to observe that (see Figure 3.4):

- When locking the joint, the top cup, which is not connected to the standard's tube wall, can move slightly upwards or downwards and this affects the joint's looseness (see section 3.2.1.2.1 for a definition) and the stiffness of the joint after looseness.

- The ledger blades are not geometrically identical (width, thickness, etc.) and additional gaps can be introduced by adding more ledgers in the joint. These gaps can however be partially compensated if the joint is correctly locked. If the joint is not hammered hard enough to be correctly locked the joint looseness can increase.

- At the start of each test, the loaded ledger was made upright before locking the joint. As the loaded ledger and/or the blades can exhibit geometrical imperfections, the loaded ledger may not be completely horizontal after the joint is locked; or this can also result from the application of the hammer blows required to lock the joint. If, in order to level again horizontally the loaded ledger, an initial negative (downward) load must be applied, then the joint downward stiffness after looseness is in general higher than the upward stiffness.

- The application of the initial cycles could lead to an increase in the looseness and to a decrease of the stiffness after looseness, or to the opposite, although in average the first case was more frequent. The joint may be initially loose but by applying initial cycles the fittings between the different parts can improve; or the initial cycles may erode the initially high friction values between surfaces in contact in the joint. This behaviour justifies the need for applying initial cycles of rotation.

- The introduction of a second ledger in the joint leads in general to a decrease of looseness and to an increase of the stiffness after looseness. This can be explained due to the additional tightness (less flexibility) of the joint provided by the extra ledger if the joint is correctly locked.

- With just one ledger at the node, the results obtained for the ledger at position P1 exhibited less looseness and higher stiffness after looseness. This may be justified by the position of the loaded ledger relative to the steel knurl positioned above the top cup to prevent it to slide freely through the standard, identified by a red circle in Figure 3.3. This feature restrains the upward displacements of the top cup.
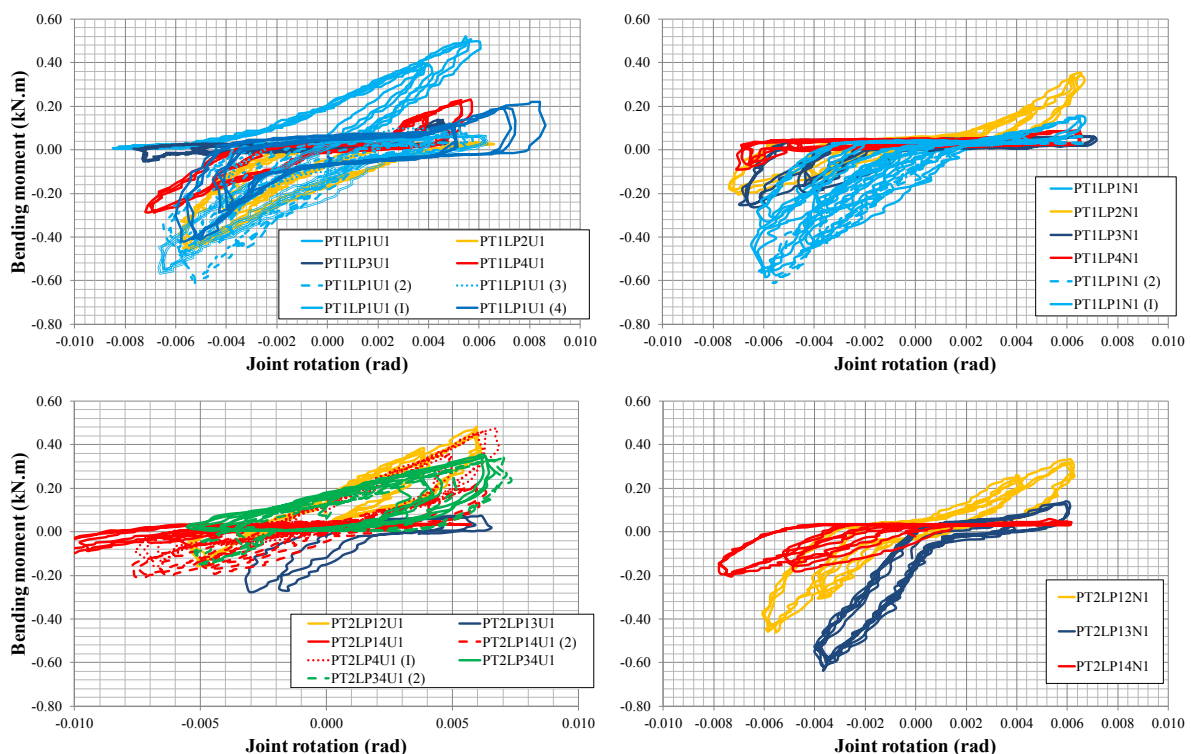
Figure 3.4: Preliminary tests results. *Top row*: One ledger; *Top left,* used elements and *Top right*: new elements; *Bottom row*: Two ledgers; *Bottom left,* used elements and *Bottom right,* new elements.

- With two ledgers at the node, the results obtained for the smaller ledger at positions P2 and P3 exhibited less looseness and higher stiffness after looseness than at position P4. It is noted that joint configuration P13 is very uncommon in actual construction. It is possible that the joint behaviour in the strong axis under wind velocities up to 18 m/s exhibits very low stiffness values, meaning that the looseness in the joint may still have not been exceeded.

From the preliminary tests it was possible to conclude that the initial bending stiffness is characterized by a high variability and that this is due to the irregular geometric characteristics of the joint elements. Also, in order to reduce the number of testing variables in the subsequent tests, a reference position was selected for the loaded ledger and for the unloaded ledgers in the case of joint configurations with two or three ledgers. The positions P1, P14 and P124 were selected, respectively, although a limited number of tests in other positions were also carried out.

3.2.1.1.2 Results of the initial tests

The results obtained for tests with two ledgers at the joint are illustrated in Figure 3.5 and Figure 3.6, with three ledgers in Figure 3.7 and with four ledgers in Figure 3.8.
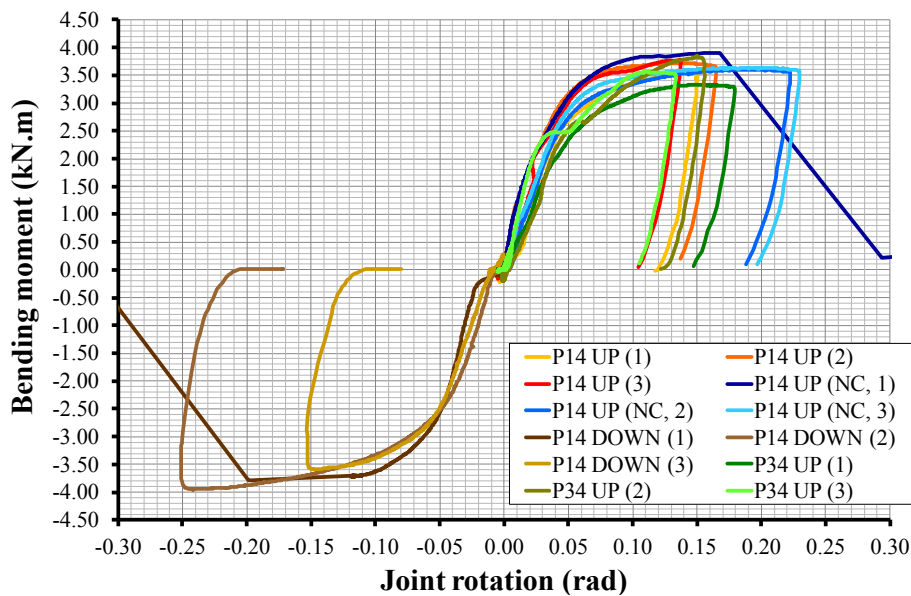
Figure 3.5: Initial tests. Results obtained with two ledgers, used elements.
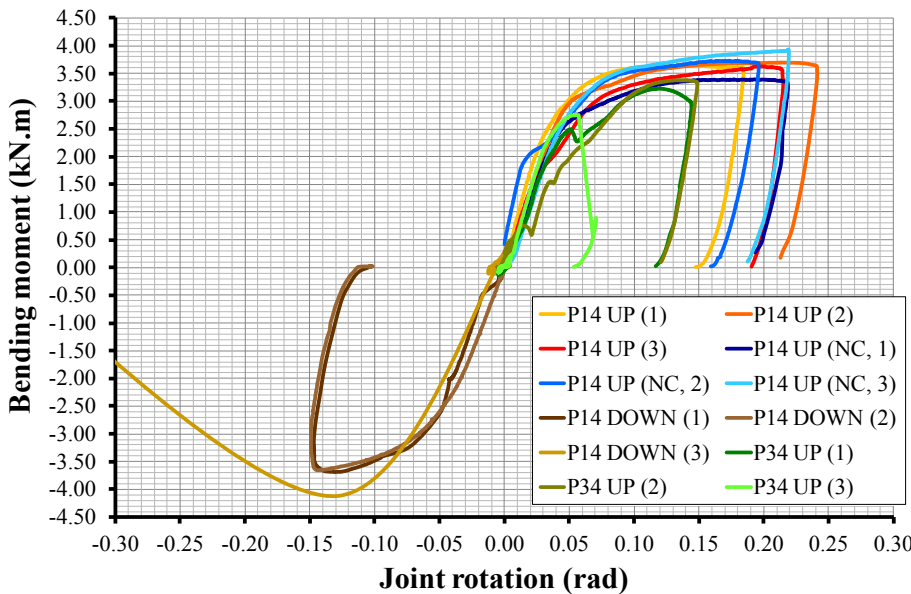
Figure 3.6: Initial tests. Results obtained with two ledgers, new elements.

From Figure 3.6 it can be observed that the most unfavourable position tested (smaller stiffness, resistance and ductility) corresponds to P34 (tests illustrated in green tones). For this position the behaviour is influenced by the slippage of one of the blades of the loaded ledger from the bottom cup due to the top cup rotation. This is a consequence of the position of the steel knurl placed at the exterior wall of the tube of the standard, diametrically opposite to the loaded ledger, to prevent the top cup from sliding freely out of the tube (see Figure 3.3). Therefore, the restraint against sliding at position P34 is smaller than, for example, the one mobilised at position P14. It is the first time this behaviour is reported.
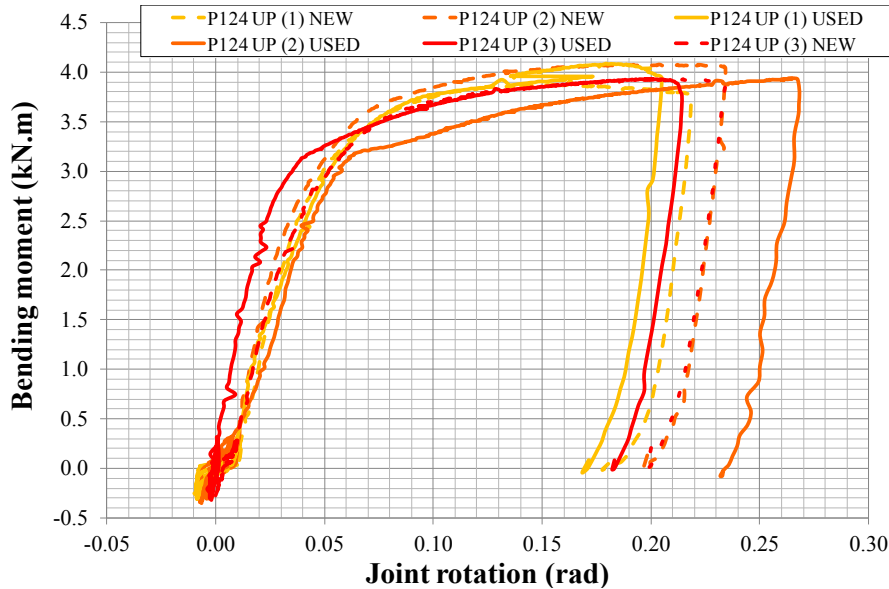
Figure 3.7: Initial tests. Results obtained with three ledgers.
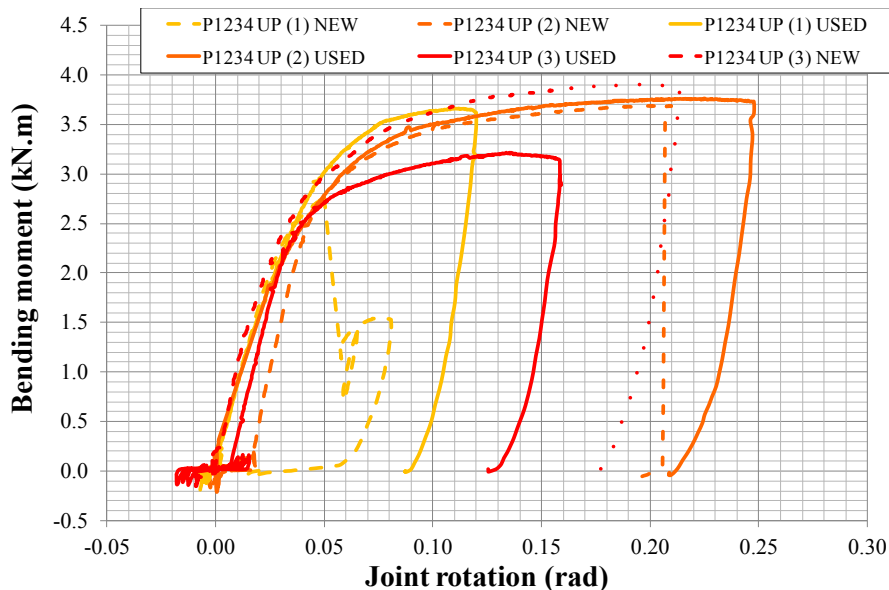
Figure 3.8: Initial tests. Results obtained with four ledgers.

It can also be observed that the results obtained with used elements exhibit, in general, a smaller ductility when compared with the results obtained with new elements. This evidence, added to a slightly higher average ultimate bending moment obtained with the used elements, may be a sign that the steel of the tested used elements has experienced work hardening, although this behaviour can also be explained by different material properties.

Brittle failures of the joints were observed with emphasis to tests using used elements. These can happen by the failure of the top cup or by shear-off of the lower blade, see Figure 3.9 (a) and (b). However, in the large majority of tests, failure was ductile with significant plastic deformations at one of the loaded ledger blades (the one bent against the bottom or top cups), at the wall of the bottom cup and at the weld connection between the bottom cup and the standard.

Comparing the results obtained with two, three or four ledgers, it is possible to observe that there is no evidence that increasing the number of ledgers in the joint leads to an increase in the ultimate bending moment resistance of the joint.

Figure 3.9: Modes of failure. *Left:* Failure of the top cup, *Centre left:* failure of the lower blade, *Centre right and Right:* typical failure mode with cracks at the bottom cup and blade welds.

3.2.1.1.3   Results of the final tests

The results obtained for tests with two ledgers at the joint are illustrated in Figure 3.10 and Figure 3.11, with three ledgers in Figure 3.12 and with four ledgers in Figure 3.13.

It can be observed that contrary to the initial tests' results, the final tests with new elements have, in general, a lower ductility (but again a lower resistance) than the final tests with used elements. Since the elements used in the final tests may correspond to a different batch than the one used in the initial tests, these results may indicate that the material characteristics of the various joint components play an important role in the behaviour of the joint in the ultimate limit states range. Brittle failures were also observed in some tests using new elements which might indicate that the production quality of certain joint components may not be sufficient. A thorough discussion of the results obtained in the final tests is presented in the following section.
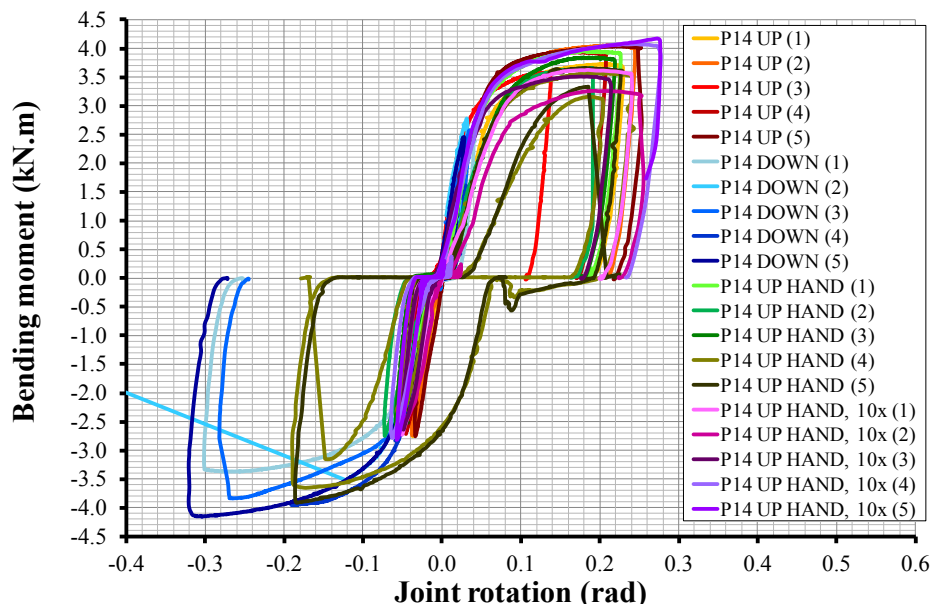
Figure 3.10: Final tests. Results obtained with two ledgers, used elements.
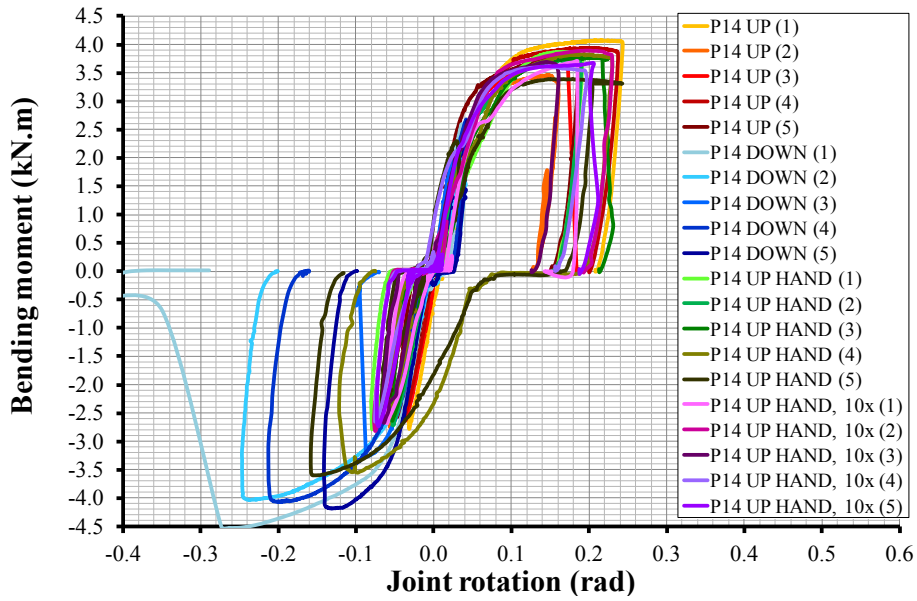
Figure 3.11: Final tests. Results obtained with two ledgers, new elements.
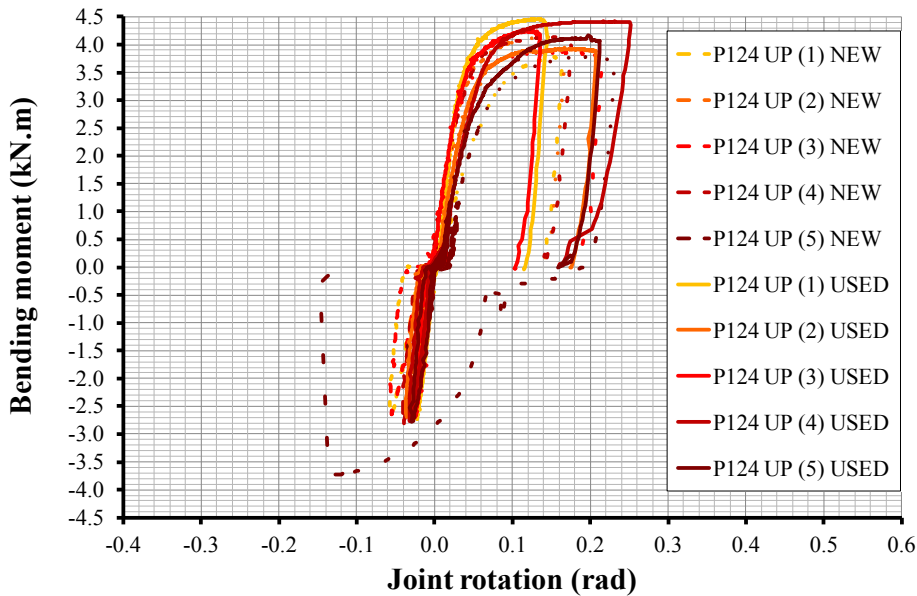
Figure 3.12: Final tests. Results obtained with three ledgers.
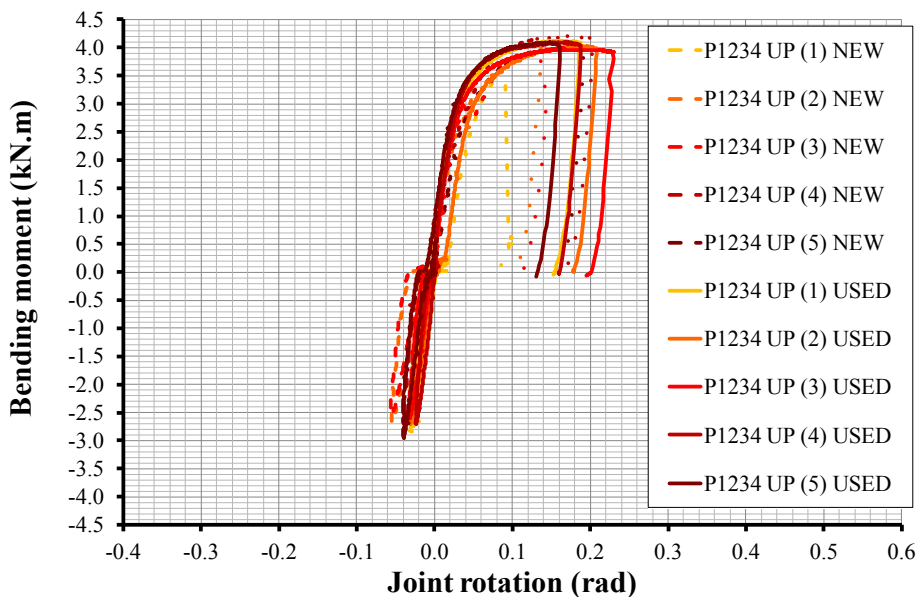
Figure 3.13: Final tests. Results obtained with four ledgers.

3.2.1.2 Statistical analysis of strong axis bending tests results

In order to be able to fully interpret the results obtained in the various types of tests performed in the experimental campaign and in order to be able to compare the results obtained for different groups of tests, carrying out a statistical analysis is critical. One of the methods which return a more comprehensive insight into the results in a graphical form is the box plot analysis. Box plots describe the results through five key parameters: the minimum value, the lower quartile (Q_1), the median (Q_2), the upper quartile (Q_3), and the maximum value. Additionally, the sample average (mean value) will also be presented (♦ or O).

In all of the following analysis, the results obtained using "as new" and used elements have been joined. This option increases the number of tests considered for each group of results. It is considered that the representativity of the findings will not be severely affected since no significant differences can be observed between the two sets of results. This observation derives greatly from the fact, already mentioned, that the used elements sent by HARSCO were all in excellent conditions. Since in actual construction, used and new elements are often used simultaneously it is important to emphasize that the results presented hereafter are not representative of materials with imperfections or other damages or exhibiting durability problems such as corrosion with a magnitude and/or extension that could affect their performance when compared to "as new" materials.

3.2.1.2.1 Looseness

Looseness is defined as the initial play between components of the joint. It is characterised here by an initial stiffness which is smaller or equal to half the value of the stiffness after looseness. The looseness present in the joint depends on the initial value of the applied forces. For the same joint, the higher the values of these initial forces, the higher the joint looseness can be. Looseness should be measured in the (re)loading parts of the joint moment *vs.* rotation diagrams, *i.e.* relative to the same referential. In general, the values of the initial forces are small and the amount of total joint looseness, the sum of the looseness for upward loads with the looseness for downward loads, is constant. However, looseness can be asymmetrically distributed in the joint, *i.e.* looseness values can differ when the joint is loaded upwards or loaded downwards.

The method presented in (BSI, 2002b) to determine the looseness in the joint depends on the stiffness of the joint after looseness, and therefore may not provide a correct estimate of the value of the joint looseness. Furthermore, in tests where the joint behaviour after looseness is non-linear, this method can return inaccurate values since it is highly sensitive to the value considered for the stiffness after looseness.

The joint's looseness was determined for each test using the procedure described in the first paragraph. The results are shown in Figure 3.14. Looseness was estimated for the first initial cycle and for the last (third) initial cycle. All tests with the same initial characteristics (*e.g.* joint configuration and test characteristics) were used in the statistical analysis, including preliminary, initial and final tests. Only tests where the joint was locked by hammer were considered. The number of considered tests is also shown in a text box.

It can be observed that there is a slight trend for a reduction of the median value of looseness from the first to the last initial cycle. This result contradicts what was stated when analysing the preliminary tests results. However, the bulk of preliminary tests correspond to tests with only one ledger at the joint (the loaded ledger), a more flexible case which was not considered in the present analysis. Additionally, if all tests are considered, including the ones where the joints have been locked by hand, there is a slight trend for an increase of the median value of looseness at the end of the application of the initial cycles. Therefore, looseness appears negatively correlated with the joint flexibility.

It is also possible to observe that the variability and the magnitude of looseness values tend to increase with the number of ledgers at the joint. However, it must be mentioned that the number of

tests with looseness decreases with the increase of the number of ledgers at the joint, from 83% for the tests with two ledgers to 75% for the tests with four ledgers.
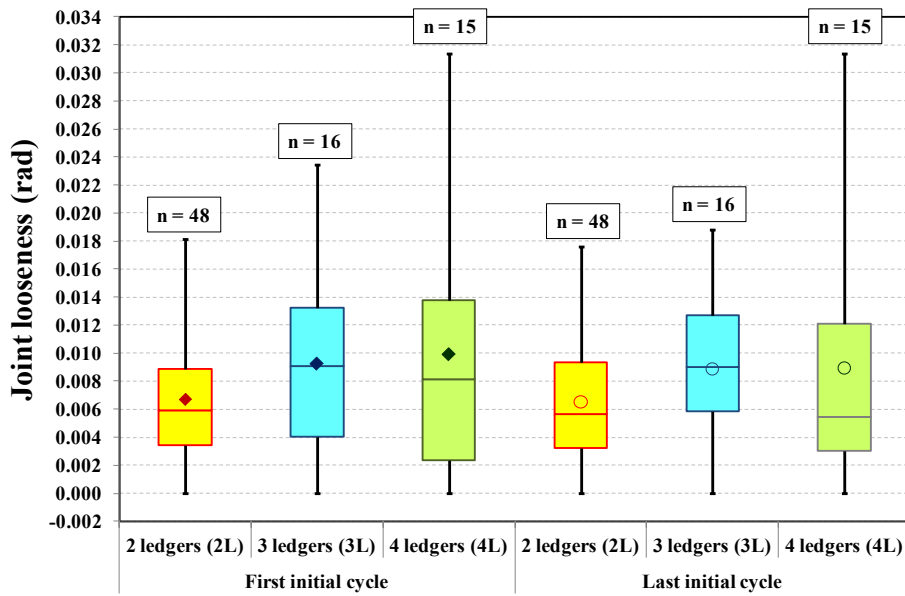
Figure 3.14: Box plots for looseness values.

Figure 3.15 shows the box plots for the initial stiffness for the case of upward displacements. It can be observed that there is a trend for a slight reduction of the median value of joint's initial stiffness at the end of the initial cycles application. It must be mentioned that for the tests where no looseness was observed upwards, the values of stiffness used to obtain the box plots presented in Figure 3.15 are not representative of the joint's initial stiffness since they were obtained for a very small series of data points. The results for downward displacements are very similar to the ones discussed above and therefore will not be presented. However, it was observed that when looseness was present, the downward's initial stiffness was smaller than the upward's initial stiffness. This can be justified due to the larger initial flexibility provided by the upper cup, which is not welded to the standard wall, when compared with the one provided by the bottom cup, which is welded to the standard wall.
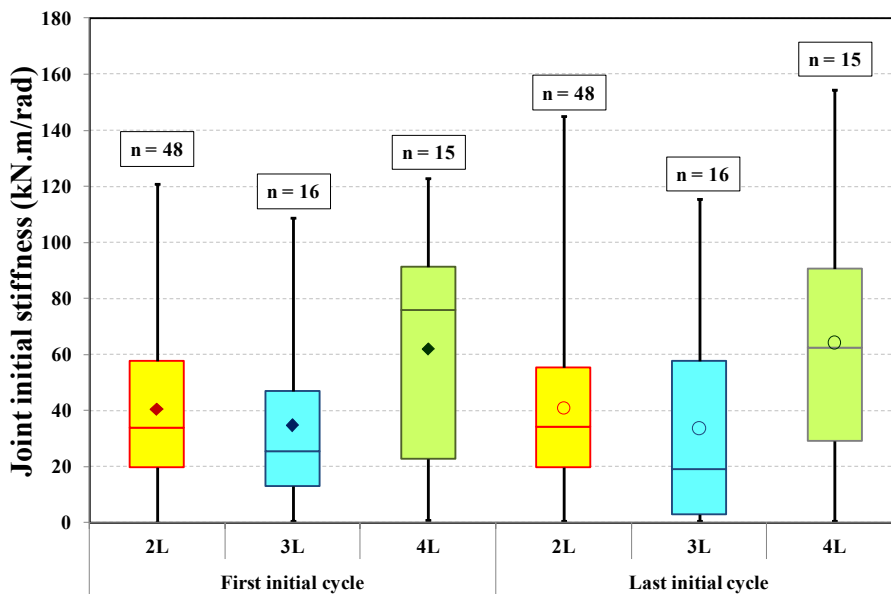
Figure 3.15: Box plots for initial stiffness values (upward loading).

Averaging all results the effect of the application of the initial cycles may not be perceptible. However, for each particular test, the application of the initial cycles could lead to an important increase in the looseness or to a significant decrease of the initial stiffness; and the opposite cases can also occur. For example, it was observed that after the last initial cycle looseness can increase

by 0,006 rad or decrease by 0,009 rad, whilst the stiffness can more than double or can decrease to just a fraction of the initial value. This effect could be important in the serviceability limit states range and justifies the need for carrying out cyclic tests. Finally, the average value of the joint looseness is equal to 0,0075 rad (≈0,43°).

3.2.1.2.2   Joint behaviour

In the present Thesis the bending moment *vs.* joint rotation (M *vs.* θ) diagrams, in each loading quadrant, were fitted a multilinear model with three (for tests without looseness) or four (for tests showing looseness) linear segments, see Figure 3.16.
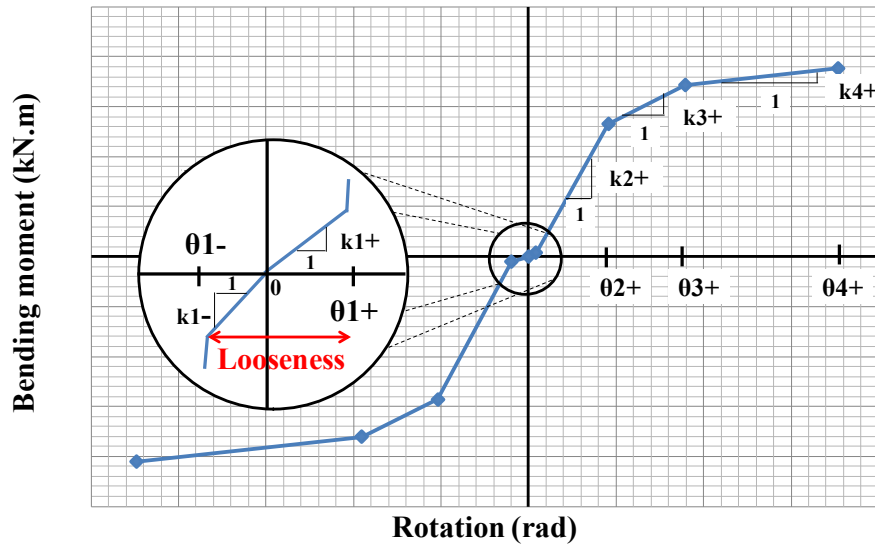
Figure 3.16: Approximation of the M *vs.* θ curves.

Notwithstanding, alternative, more accurate but more complex, models to the multilinear model chosen to fit the diagrams could have been favoured. For example, using the online curve fitting engine *zunzun* (accessible thought the website http://zunzun.com/) from a set of more than 1000 different equations, possible models could be the following:

$$M(\theta) = d + \left[\frac{a-d}{1+(\theta/c)^b} \right] \tag{3.2}$$

$$M(\theta) = \frac{a \times \theta^b}{c^b + \theta^b} \tag{3.3}$$

where *a*, *b* and *c* are model coefficients.

Another curve fitting engine is the Eureqa software (accessible through the website http://www.nutonian.com/products) which uses a machine learning technique called Symbolic Regression to predict the best fitting model to input data. The best fit models given by Eureqa belong to the following family of equations:

$$M(\theta) = a \times 10^6 \times tanh \left[b \times \theta - c \times \theta^2 \times tanh(d \times \theta - e) \right] \tag{3.4}$$

where *a*, *b*, *c*, *d* and *e* are model coefficients.

The reason why in this Thesis the simple multilinear model was selected is because the parameters of the multilinear model are easily read, they directly represent characteristics of the behaviour of the joints (a one to one representation), and by using the multilinear model it is easy to analyse the influence of each characteristic of the joint, as the stiffness after looseness for example. On the contrary, if the more complex models were selected it would be more difficult to understand what the model parameters represent and how they influence each characteristic of the joint: stiffness

evolution, maximum bending moment and ductility. Also, some of the more complex models do not respect the condition that the diagrams should start at zero bending moments for zero joint rotations.

Past investigations, see (Chandrangsu, Rasmussen, 2011), approximated the bending moment *vs.* joint rotation diagrams using a three-linear model. In the present work, a four-linear model is preferred since it allows a better accuracy to the "true" behaviour of the joint. Further elucidations will be given in the following sections.

By adopting a three-linear or a four-linear model in favour of the simpler linear and bilinear models a compatibility issue arises concerning the modelling features offered by the majority of the standard finite element analysis softwares available in the market. This is however a limitation of the current analysis suites and not of the present work.

The stiffness value of each linear segment was determined by the method described in the following.

Due to the variability in the displacements and load readings, a minimum number of points were considered for each segment. This number varied from test to test. After having selected this initial number of data points, subsequent points were additionally considered one by one. In general, the end point of each segment was given by the point after which a change of at least 10% was obtained in the value of the segment slope given by the best fitting line determined with the linear regression method. The exception to this rule happened in the last segment (corresponding to large force values) where the end point is given by the maximum absolute value of the bending moment resisted by the joint. To assure that, at maximum, only four segments were used, the final end points of each linear segment were selected by visual inspection. However, as a quality control measure, the values of the coefficient of determination (R^2) obtained by the linear regression method for each segment were always larger than 0,9. Only the results obtained from the initial and final tests were considered.

Figures 3.15 to 3.18 show the box plots determined for the stiffness values of the four linear segments (k1 to k4) for upward or downward displacements corresponding to the loading segments or to the reloading segments of tests with or without looseness. It should be mentioned that as looseness can be unevenly distributed in the joint and the joint behaviour was analysed for upward and downward displacements, it was considered that the results obtained in the upward (downward) direction, in a test where no looseness was observed for upward (downward) displacements, would be counted as results of a test of a joint without looseness. This choice was made in order to assess if looseness, even if only observed in one direction, affects the stiffness of the joint by comparing the results obtained for directions where looseness was observed with the results obtained for directions where no looseness was observed, under the same initial conditions (here for tests where joints were locked by a hammer).
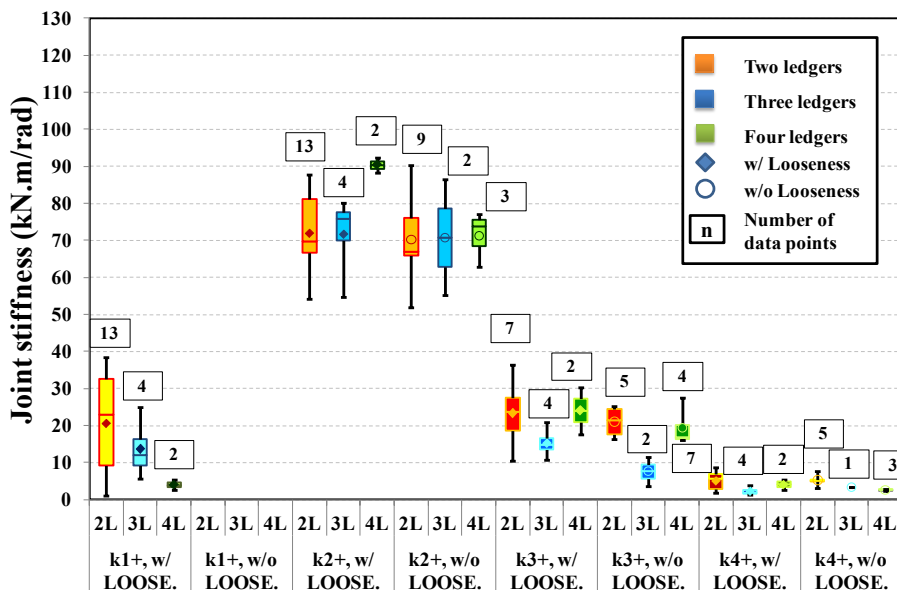
Figure 3.17: Box plots for stiffness values (upward displacements, load results).
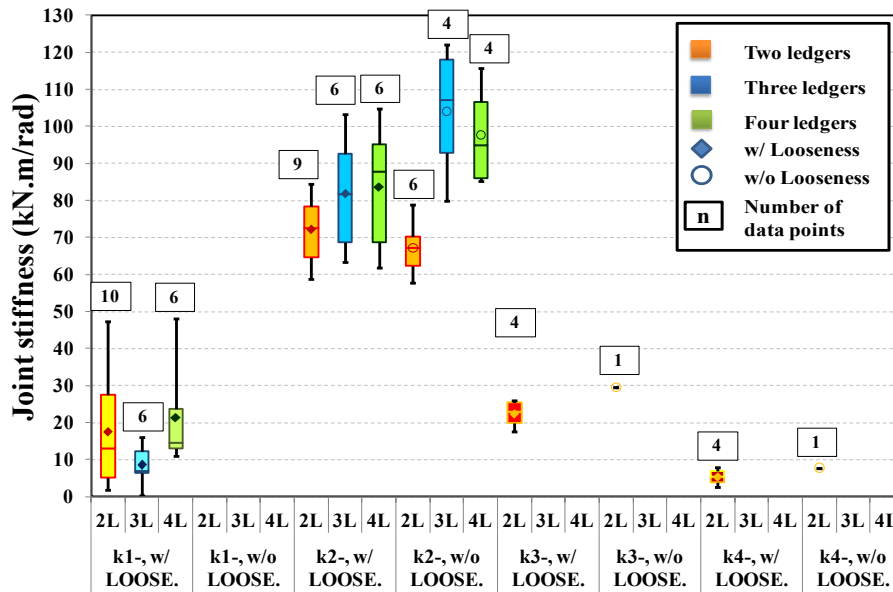
Figure 3.18: Box plots for stiffness values (downward displacements, load results).
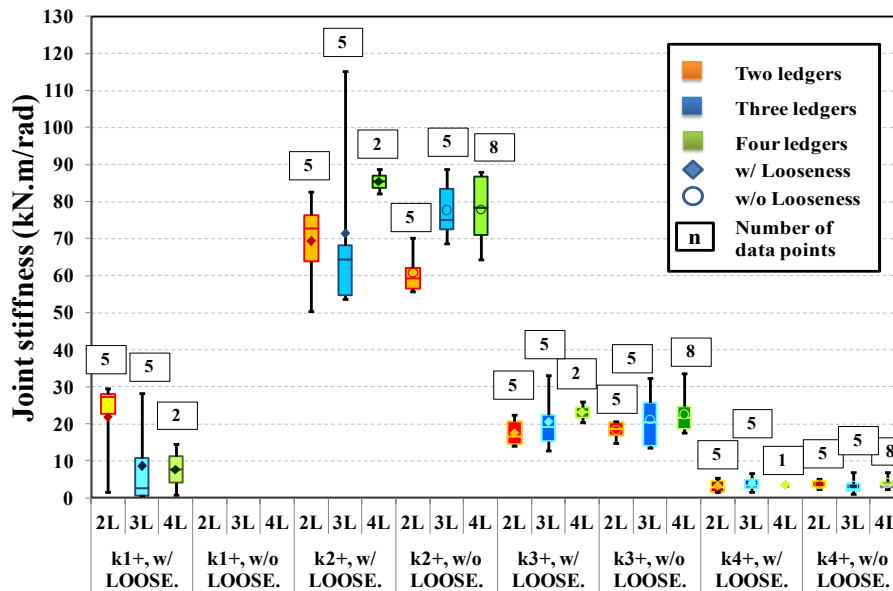
Figure 3.19: Box plots for stiffness values (upward displacements, reload results).
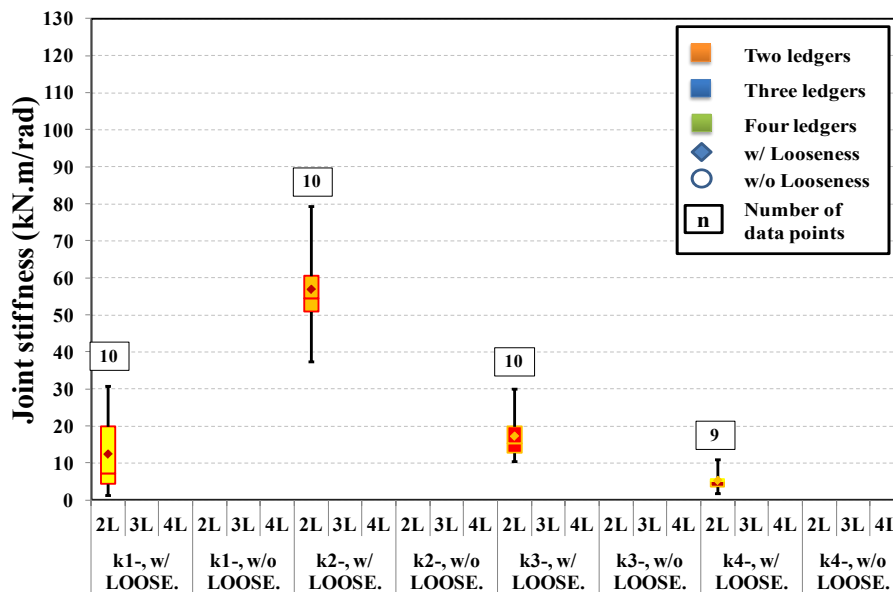
Figure 3.20: Box plots for stiffness values (downward displacements, reload results).

It can be observed that for the tests series with two ledgers at the joint, the one with a larger number of tests (data points), in average the various stiffness values obtained for upward and downward displacements are comparable. This observation can be justified by the mechanics of the joint, since if properly locked the upper cup can ensure similar restraint as the bottom cup. It will be assumed hereafter that these results belong to the same distribution and therefore can be grouped together. This hypothesis will be used in the results obtained for the load and reload segments.

The same hypothesis is applied to tests series with and without looseness since there is no statistical support to differentiate the results obtained for each series. Therefore, for joints correctly locked with a hammer, no evidence was found to support the hypothesis that looseness significantly affects the stiffness after looseness of the joint. However, statistical support may exist, as shown in the following section, if two series corresponding to two markedly different tests conditions, such as locking the joints by hand or with a hammer, are compared.

The joined results are presented in Figure 3.21 in the case of the stiffness values of each linear segment and in Figure 3.22 in the case of the joint rotation increment of each segment.
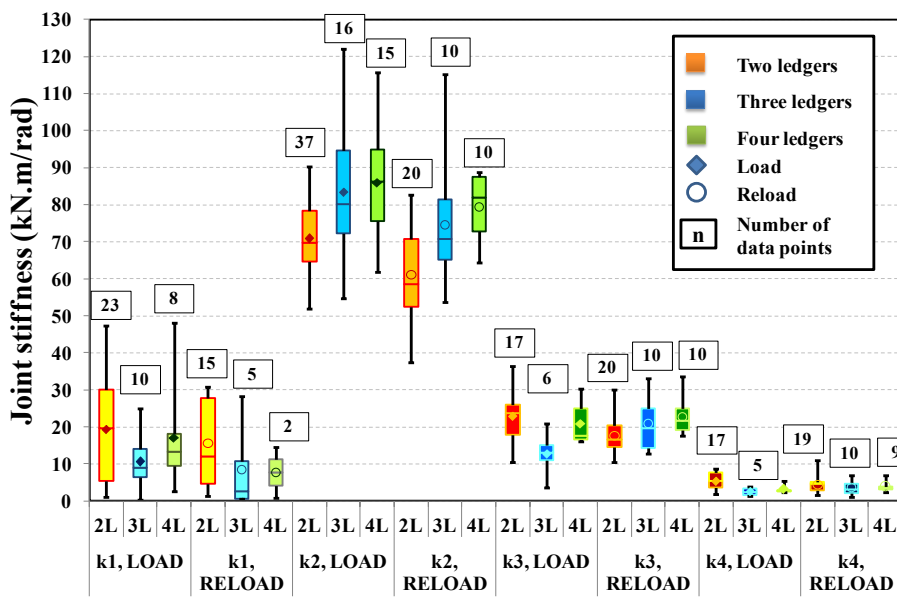
Figure 3.21: Box plots for stiffness values (load *vs*. reload results).
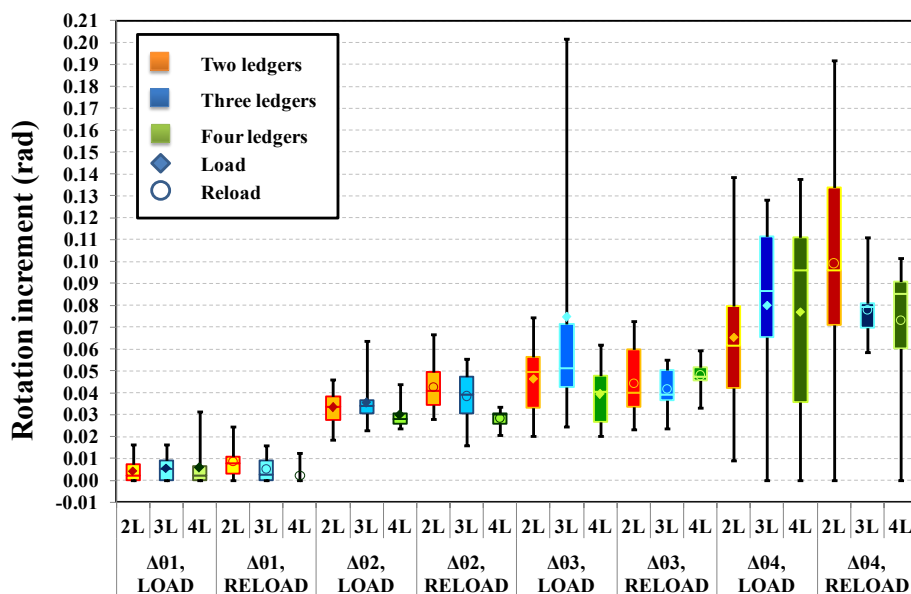
Figure 3.22: Box plots for joint rotation increment values (load *vs*. reload results).

It can be observed that the joint stiffness tends to be lower in reloading segments when compared to loading segments. This can be justified by the fact that the unloading (end of loading phase) was performed when the bending moment *vs.* displacement diagrams started to deviate from linearity (around 2/3 of the ultimate bending moment resistance) which meant that plastic deformations occurred at the joint.

By performing a *t-test* hypothesis testing analysis, using a *p-value* equal to 5%, it is possible to verify that the mean values of the two samples of k2 stiffness for tests with two ledgers may not belong to the same population. Also, it was possible to determine that the mentioned plastic deformations, although small, are sufficient to generate a reduction of 20% in the k2 stiffness for tests with two ledgers. This value corresponds to the upper bound of the 90% confidence interval of the difference between the mean values of the two samples.

Although, Minitab® Statistical Software (Minitab Inc, 2010) informs that the *t-test* method used does not assume or require that the two samples have equal variances, to support the above results it is important to determine if the variances of both samples are very different, since if they are then they may also be substantially different in shape making the median and not the mean a better indicator to analyse the differences between samples. In the case of the two samples being analysed, the median and the mean values are very close: 70,8 kN.m/rad – 69,7 kN.m/rad and 61,0 kN.m/rad – 58,4 kN.m/rad, respectively for the load and reload k2 stiffness samples. Also, by performing a *F-test* hypothesis testing analysis, using a *p-value* equal to 5%, there is not enough evidence to conclude that the standard deviations differ at this level of significance. Since sample sizes are large (at least 20 values) these statistical tests are valid even for any distribution. Therefore, there are both mechanical and statistical supports for concluding that the k2 reload stiffness is different, and smaller, than the k2 load stiffness. As a simplification (on the safe side), it will be assumed that the reduction of 20% obtained for the k2 stiffness for tests with two ledgers is extensible to the stiffness of the first (if applicable), third and fourth (if applicable) linear segments of tests with two, three and four ledgers joint configurations.

Comparing the results obtained with two, three or four ledgers, it is possible to observe that there is evidence that increasing the number of ledgers in the joint leads to an increase in the stiffness of the joint, with the median value of the k2 stiffness of joints with three and four ledgers being 15% and 25% larger than the median value of the k2 stiffness of joints with two ledgers.

In terms of joint rotation there is no clear trend and therefore the load and reload results will be joined. As a remark, it appears that the plastic deformation capacity of the joint is not significantly influenced by the number of ledgers connected at the joint.

Figure 3.23 illustrates the box plots obtained for the ultimate bending moment resistance (Mu) for load and reload results. It can be observed a trend for an increase in resistance for the tests with reloading segments. However, since the deformation capacity of the joint appears to be not significantly affected by the loading-unloading-reloading cycle the reason for this behaviour must reside in the variability of the material characteristics, namely the yield and the tensile strength of the steel of the various joint components, and not in a possible work hardening of the steel throughout the loading-unloading-reloading cycle.

In Tables 3.3 to 3.5, the average values of the loading stiffness, reloading stiffness, rotation increments, unloading stiffness and ultimate bending moment resistance are given for each of the joint configurations tested. The unloading stiffness (kU) was determined using the values of the unloading curve within the 90% and 10% range of the ultimate bending moment resistance. The value of the unloading stiffness is significantly higher than the initial stiffness after looseness (k2), due to the significant friction that is developed with the joint rotation between the surfaces in contact.

In Tables 3.6 and 3.7, the COV values of the loading stiffness, rotation increments, unloading stiffness and ultimate bending moment resistance are given for each of the joint configurations tested. It can be

observed that the parameters which characterise the joint behaviour exhibit, in general, a large variability, in particular the parameters associated with the looseness segment (k1 and Δθ1).
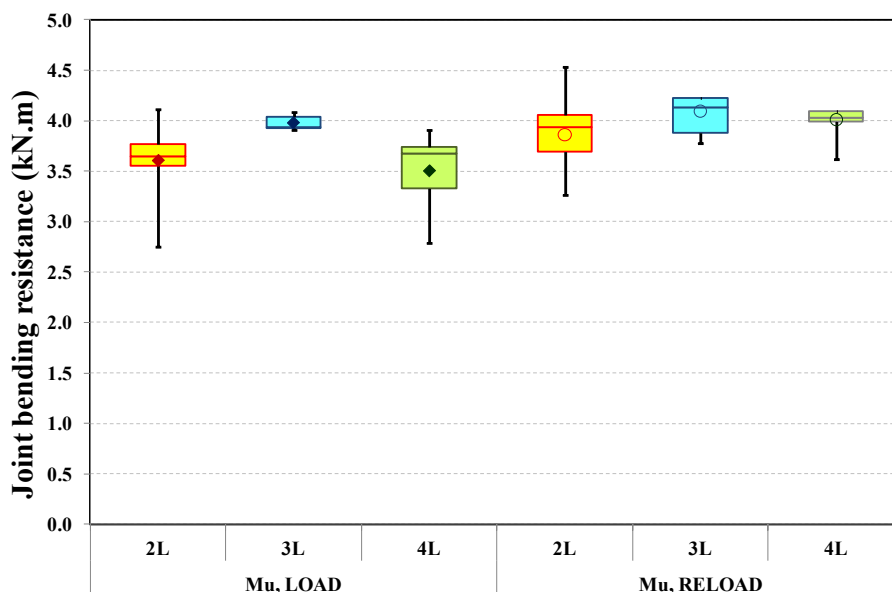
Figure 3.23: Box plots for ultimate bending moment values (load *vs.* reload results).

Table 3.3: Average values of the stiffness of the four segments (load segments).

Joint configuration	Parameter	k1 (kN.m/rad)	k2 (kN.m/rad)	k3 (kN.m/rad)	k4 (kN.m/rad)
Two ledgers		19,30	70,82	22,79	5,38
Three ledgers	Average value	10,56	83,44	12,76	2,52
Four ledgers		16,96	85,85	20,91	3,18

Table 3.4: Average values of the stiffness of the four segments
(reload segments, unload when M = 2/3 × Mu).

Joint configuration	Parameter	k1 (kN.m/rad)	k2 (kN.m/rad)	k3 (kN.m/rad)	k4 (kN.m/rad)
Two ledgers		15,44 (a)	56,65 (a)	18,24 (a)	4,31 (a)
Three ledgers	Average value	8,45 (a)	66,75 (a)	10,21 (a)	2,02 (a)
Four ledgers		13,57 (a)	68,68 (a)	16,73 (a)	2,54 (a)
(a) Considered to be 80% of the average value determined for the loading segments.					

Table 3.5: Average values of other parameters of the four segments (load and reload segments).

Joint configuration	Parameter	Δθ1 (rad)	Δθ2 (rad)	Δθ3 (rad)	Δθ4 (rad)	kU (kN.m/rad)	Mu (kN.m)
All types	Average value	0,0055	0,0357	0,0472	0,0797	132,82	3,86

Table 3.6: COV values of the stiffness of the four segments (load segments).

Joint configuration	Parameter	k1	k2	k3	k4
Two ledgers		0,74	0,14	0,27	0,57
Three ledgers	COV	0,65	0,24	0,44	0,44
Four ledgers		0,86	0,19	0,30	0,42

Table 3.7: COV values of other parameters of the four segments (load and reload segments).

Joint configuration	Parameter	Δθ1	Δθ2	Δθ3	Δθ4	kU	Mu
All types	COV	1,20	0,29	0,48	0,50	0,15	0,08

Regarding modes of failure, after gathering all the available information it was possible to distinguish between modes of failure of joints loaded upwards and downwards. In the former tests,

failure was characterised by significant plastic deformations at the wall of the bottom cup, ledger lower blade and bottom cup weld, see Figure 3.24 (*Left*), for both "as new" and used elements; while in the latter, failure was characterised by cracks at the top cup for "as new" elements, see Figure 3.24 (*Centre*), and by cracks at the upper blade for used elements, see Figure 3.24 (*Right*). No significant difference was observed regarding failure modes between two, three or four ledgers joint configurations. All failures occurred due to joint fractures and not due to tube plastic collapse.

In five final tests instead of stopping the test when load started to drop, the load direction was reversed multiple times, at the point where the load started to drop, until complete failure of the joint. The objective of these tests was to analyse the energy dissipation capacity of the Cuplok® joints. The results, illustrated in terms of bending moment *vs.* joint rotation diagrams are presented in Figure 3.25.

It is possible to observe that for such a deformation demanding loading, the joints cannot endure more than three load/reload cycles in the elastoplastic range. Also, it was possible to observe a degradation of the joints' stiffness and ductility with the cyclic loading.

Figure 3.24: Modes of failure. *Left:* **Upward loads, "as new" and used elements,** *Centre:* **downward loads and "as new" elements,** *Right:* **downward loads and used elements.**
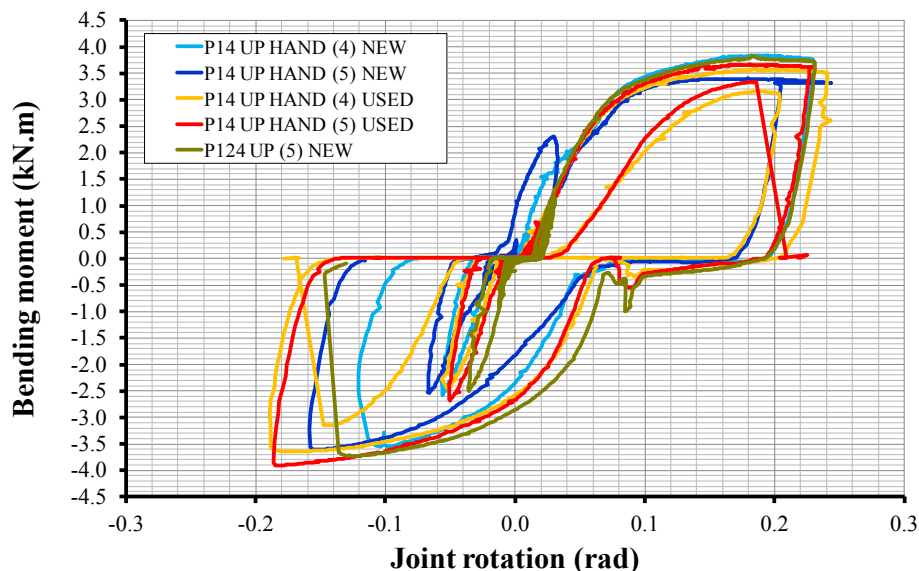
Figure 3.25: Final tests. Results obtained with multiple load/reload cycles.

3.2.1.2.3   Influence of the joint tightening method

The choice of tightening the joint by hand or with a hammer has a great influence in the joint looseness values. Tightening by hand means that the joint will always be loose and its average value can be more than the double of the average value if it was tightened by hammer: 0,017 rad against 0,007 rad, respectively.

Does this large looseness translate in a reduction of the joint stiffness after looseness? It was already observed that under the same conditions, small values of looseness seem to not change significantly the joint stiffness. Comparing the results obtained for joints locked with a hammer and by hand, it was possible to observe that tightening by hand can decrease the stiffness of the joint, see Figure 3.26 for a comparison of the stiffness for the reload segments and upward displacements. Similar conclusions can be drawn from the results for the load segments and for the downward displacements. As a safe estimate, a 30% reduction can be used to derive the k2 stiffness for joints locked by hand from the k2 stiffness for joints locked by hammer.

This statistically supported reduction in stiffness can also be justified mechanically, because large looseness values obtained by locking the joint by hand mean that the restraints imposed on the joint components are not as large as when the joint is locked by hammer. Therefore, this smaller joint fixity translates into lesser joint stiffness. However, the joint ultimate bending moment resistance appears to be not significantly affected by the joint tightening method.
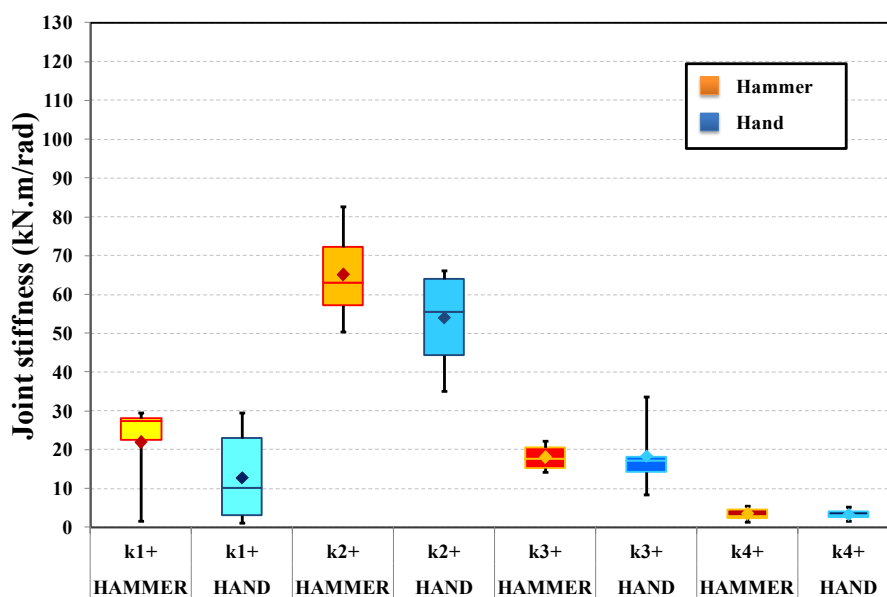
Figure 3.26: Influence of tightening method.
Box plots for stiffness values (upward displacements, reload segments).

3.2.1.2.4 Influence of the loading rate

It was also observed that increasing the loading rate ten times after the end of the initial cycles seems to reduce significantly only the initial stiffness of the joint when there is looseness, see Figure 3.27. The joint ultimate bending moment resistance appears to be not significantly affected by this increase of the loading rate.

3.2.1.2.5 Selection of probabilistic models

The problem of selecting the probabilistic model is discussed later in section 5.4.6.3. In the following it is presented the methodology used for selecting the appropriate model for the most important variables that characterize the joints behaviour under bending loads over the strong axis. These variables are the looseness, the k1 and k2 stiffnesses for load segments, the rotation associated with the last linear segment (Δθ4) and the ultimate bending moment resistance (Mu). All the models were obtained from tests where the joint was locked using a hammer and determined for the loading segments.

The probability distributions considered in the analysis were: the Normal distribution, the Lognormal distribution, the Gamma distribution, the Logistic distribution, the Weibull distribution and the Gumbel distribution. Additionally, truncated versions of these distributions were also considered.

Results from past investigations, *e.g.* (Voelkel, 1990 ; Chandrangsu, Rasmussen, 2011), could not be included because the testing procedure used by Voelkel was very different from the one considered in this project, and the expression of the tests results used by both past investigations are different from the one considered in this project (for example Voelkel approximated the bending moment *vs*. joint rotation diagrams with a single line and Chandrangsu used a trilinear approximation) and the individual tests results obtained by Chandrangsu were not available.
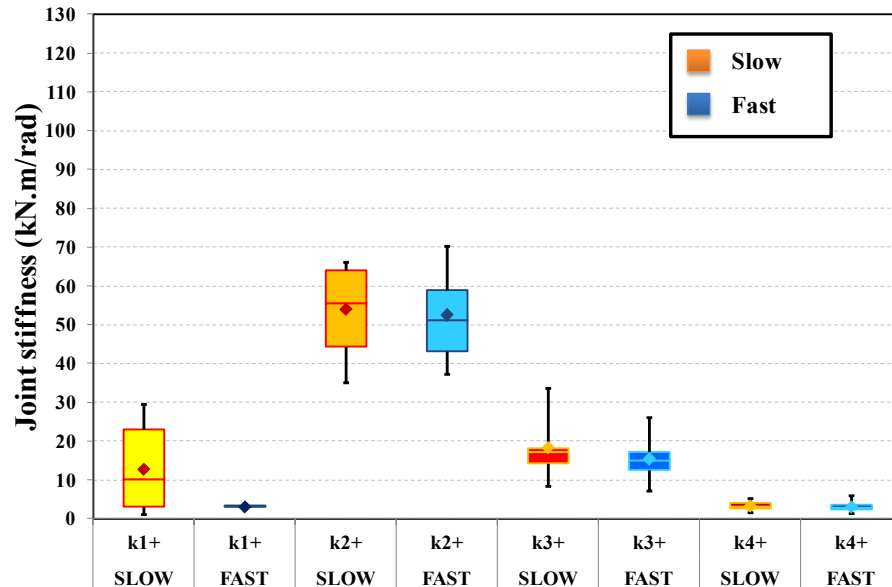
Figure 3.27: Influence of loading rate.
Box plots for stiffness values (upward displacements, reload segments).

As illustrative examples, the main analysis steps followed to derive the pdfs for the looseness and for the k2 load stiffness of joints with two ledgers (k2 2L stiffness) will be presented.

First, for a graphical analysis, the different distributions pdfs against the data histogram and of the distributions cdfs against empirical cdf are presented in Figure 3.28 and in Figure 3.29 for the looseness and k2 2L stiffness. Q-Q plots for selected distributions are also presented (see Figure 3.30); Q-Q plots are preferred to P-P plots because they allow a better visual analysis at the tails of the distribution.

The R (R Core Team, 2012) program was used to perform the various analyses. The parameters of the distributions were determined by the Maximum Likelihood method using the R package *fitdistrplus* (Delignette-Muller et al., 2012).

From Figures 3.26 and 3.27 it is possible to observe that for the looseness data the fit of the distributions is irregular but for the k2 2L stiffness the variability of the fit of the distributions is reduced. For the former variable, the results for the Log-normal, Gamma and Weibull distributions are markedly different from the other distributions. This happens because these three distributions are asymptotically left bounded to zero (they are only defined for positive values) which makes them strongly right skewed for the looseness data fit. Thus, they produce a better fit at the lower range of looseness values but an inferior fit at the higher range of looseness values than for instance the Normal distribution which allow negative values but is more densely distributed around the mean value, see also Figure 3.30.

Next, the results of classical hypothesis testing methods, considering a statistical significance value equal to 0,05 and a *null* hypothesis of accepting the distribution, are presented in Table 3.8 for the looseness and k2 2L stiffness. The *p*-values shown on the Table are associated with the observed Kolmogorov-Smirnov (KS) and Anderson-Darling (AD) statistics. If the values are larger than 0,05 it means that the test cannot reject the *null* hypothesis at this significance level (it does not mean the *null* hypothesis is true). Therefore, these tests give an indication and not an absolute answer. It can be observed that the visual information described in the previous paragraph is confirmed.
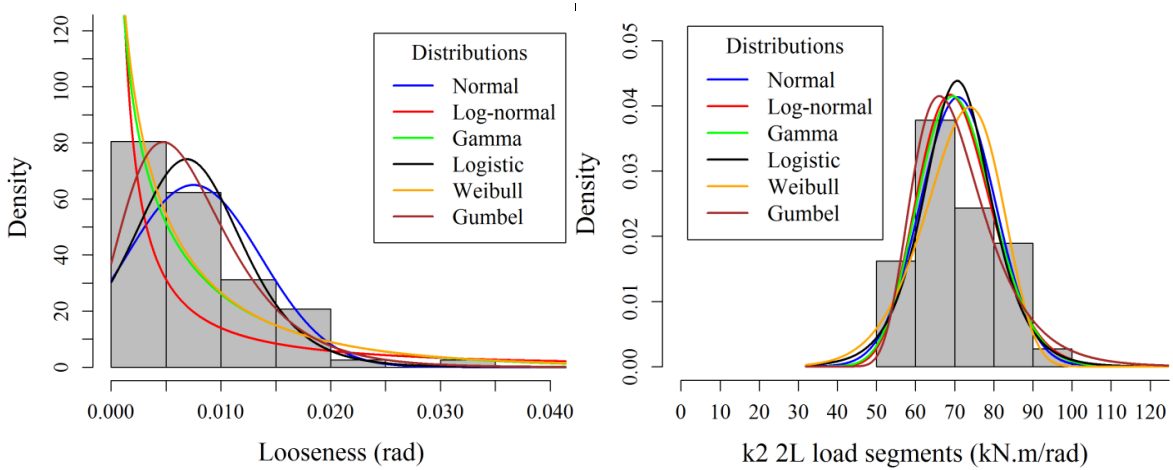
Figure 3.28: Distributions pdfs against data histogram. *Left*: **looseness,**
Right: **k2 2L stiffness for load segments.**
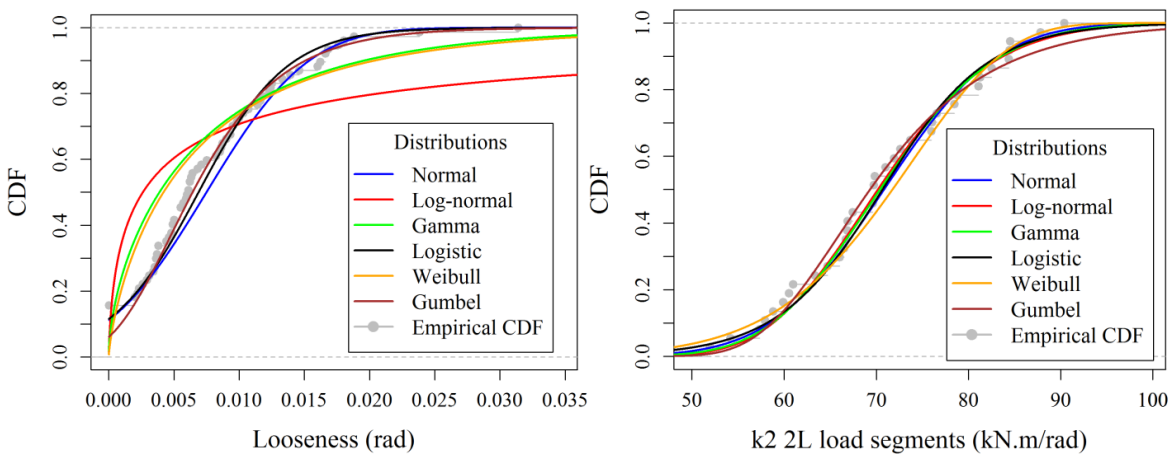
Figure 3.29: Distributions cdfs against empirical cdf. *Left*: **looseness,** *Right*: **k2 2L stiffness for load segments.**
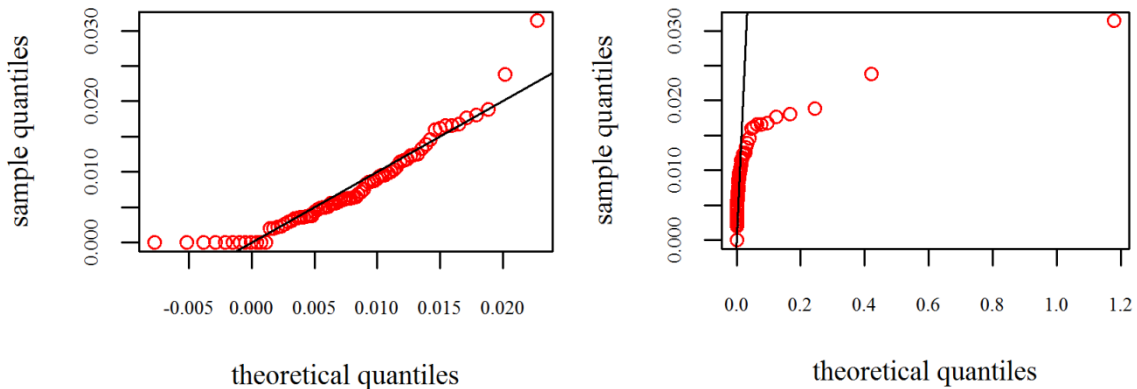
Figure 3.30: Q-Q plots for looseness. *Left*: **Normal distribution,** *Right*: **Log-normal distribution.**

Table 3.8: Goodness of fit results. Kolmogorov-Smirnov and Anderson-Darling tests: *p*-**values.**

Variable	Test	Normal	Log-normal	Gamma	Logistic	Weibull	Gumbel
Looseness	KS	0,16	0,00	0,00	0,26	0,00	0,49
	AD	0,17	0,00	0,00	0,27	0,00	-
k2 2L Stiffness	KS	0,97	0,99	0,99	0,98	0,74	0,88
	AD	0,60	0,61	0,61	0,59	0,54	-

It should be noted that because the KS test is seeded with distribution parameters determined using the input data its value must be interpreted carefully since it is harder to reject the *null* hypothesis. Also, the *p*-values obtained for AD test correspond to first quartile values of 1000

Monte Carlo simulations using input distributions with 1000 samples. The R functions *ks.test* and *adk.test* were used in this analysis.

In addition to the classical goodness of fit tests presented above, other types of analysis were also carried out: the Log-Likelihood (loglike) and the Akaike information criterion (AIC). The distribution with the highest loglike and lowest AIC values corresponds to the best fit model to the data. Since all models have the same number of parameters (two) the conclusions obtained from these two measures always agree. The results are presented in Table 3.9.

Table 3.9: Goodness of fit results. Log-Likelihood and AIC values.

Variable	Measure	Normal	Log-normal	Gamma	Logistic	Weibull	Gumbel
Looseness	loglike	282,86	279,54	**308,96**	284,41	304,00	291,55
	AIC	-561,72	-555,08	**-613,91**	-564,83	-604,01	-579,09
k2 2L Stiffness	loglike	-136,39	-136,43	**-136,33**	-137,51	-137,26	-137,65
	AIC	276,79	276,86	**276,66**	279,01	278,53	279,30

It is possible to observe that the results for the looseness obtained in this analysis differ from the results given in the previous analysis. This happens because approximately 15% of the looseness values are equal and close to zero. Thus, at the left tail there are a lot of terms contributing to the likelihood function. Since the Log-normal, Gamma and Weibull distributions fit this data better they have a larger likelihood.

It is also important to recognise that mechanical variables are physically truncated, *i.e.* they have minimum and maximum possible values. For example, looseness cannot be smaller than zero and the joint stiffness cannot be infinite. Acknowledging the reality, educated guesses of the lower and upper bounds have been performed for each of the variables being analysed. The values are presented in Table 3.10.

Table 3.10: Lower and upper bounds of joint variables.

Bound	Looseness (rad)	k1 (kN.m/rad)	k2 2L (kN.m/rad)	k2 3L (kN.m/rad)	k2 4L (kN.m/rad)	Δθ4 (rad)	Mu (kN.m)
Lower bound	0	0	5	5	5	0	1,5
Upper bound	0,04	60	100	130	150	0,25	5

Using these values, truncated versions of the distributions were tested. The results, again for the looseness and k2 2L load stiffness, are presented in Figure 3.31 and Figure 3.32 and in Table 3.11 and Table 3.12.
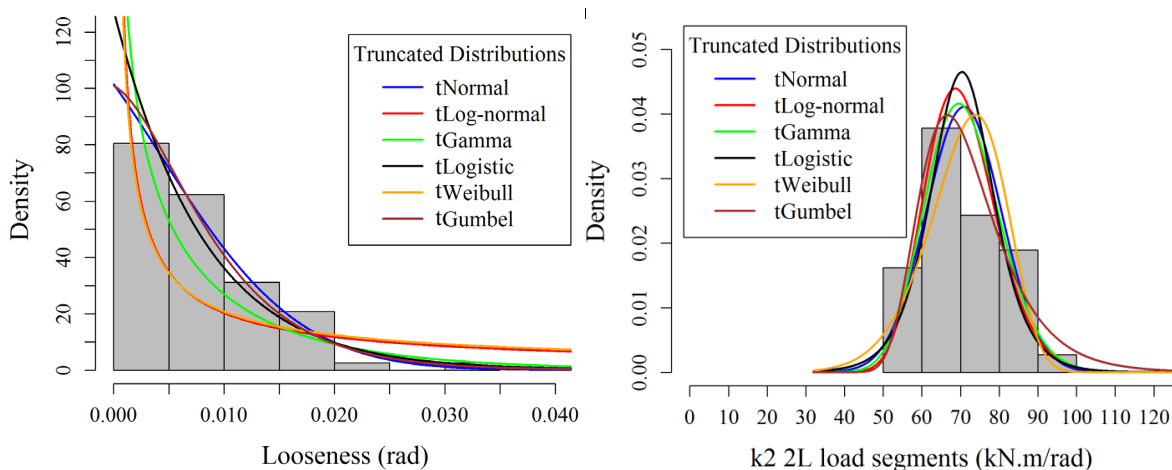
Figure 3.31: Truncated distributions pdfs against data histogram. *Left*: looseness, *Right*: k2 2L stiffness for load segments.
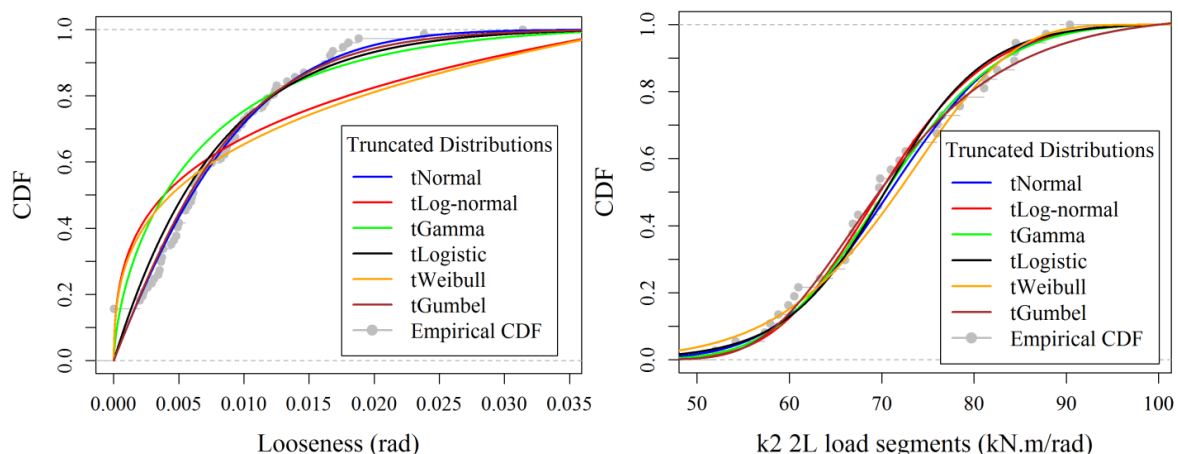
Figure 3.32: Truncated distributions cdfs against empirical cdf. *Left*: looseness,
Right: k2 2L stiffness for load segments.

Table 3.11: Goodness of fit results. Kolmogorov-Smirnov and Anderson-Darling tests: *p*-values.

Variable	Test	tNormal	tLog-normal	tGamma	tLogistic	tWeibull	tGumbel
Looseness	KS	0,16	0,24	0,20	0,16	0,23	0,16
k2 2L Stiffness		0,97	0,91	0,95	0,86	0,74	0,95

Table 3.12: Goodness of fit results. Log-Likelihood and AIC values.

Variable	Measure	tNormal	tLog-normal	tGamma	tLogistic	tWeibull	tGumbel
Looseness	loglike	301,79	1552,07	1508,96	1404,35	**1570,92**	301,14
	AIC	-599,58	-3100,13	-3013,92	-2804,70	**-3137,83**	-598,28
k2 2L stiffness	loglike	**-136,35**	-136,97	-136,43	-138,17	-137,27	-136,72
	AIC	**276,69**	277,94	276,86	280,35	278,54	277,43

It is possible to observe that the truncated distributions are closer to each other than the original distributions. The most obvious example of this is the looseness results, where the Normal, Logistic and Gumbel distributions are now similar to the other distributions. Also, for the looseness, the KS test now does not reject the *null* hypothesis for any distribution.

The Gamma distribution is no longer the best model according to the loglike method, but instead it is the Weibull for the looseness and the Normal for the k2 2L load stiffness.

The decision concerning selecting a probabilistic model must primarily consider the mechanical behaviour of the components being studied. As will be shown later in section 5.4.7.3 there is no best model but useful models. In the end, the probabilistic model was selected based on a conservative criterion. For example, it is more severe to the bridge falsework system to have larger looseness, so models that have a better fit in the range of high values of looseness were preferred. The selected truncated distributions are presented in Table 3.13.

Table 3.13: Probabilistic models for selected variables, for joints locked using a hammer.

Joint configuration	Looseness (a)	k1 (a)	k2 (a)	Δθ4 (b)	Mu (b)
Two ledgers			tWeibull		
Three ledgers	tNormal	tNormal	tWeibull	tLogistic	tWeibull
Four ledgers			tWeibull		
(a) Using loading segments values.					
(b) Using loading and reloading values.					

The values of the distributions parameters and the 95% confidence intervals are given in Table 3.14, and were determined using the ML method. Therefore, it is assumed that the probabilistic models for the distributions parameters are Gaussian.

Table 3.14: Parameters of probabilistic models.

Joint	Looseness Parameters		k1 Parameters		k2 Parameters		Δθ4 Parameters		Mu Parameters	
2L	Mean	-0,0084 (-0,0301; 0,0132)	Mean	-13,844 (-98,800; 71,112)	Shape	8,071 (6,071; 10,071)	Location	0,0232 (0,0002; 0,0461)	Shape	14,795 (12,140; 17,451)
					Scale	75,061 (71,829; 78,293)				
3L					Shape	4,878 (3,254; 6,502)				
					Scale	90,292 (80,869; 99,716)				
4L	Sd	0,0125 (0,0060; 0,0191)	Sd	27,043 (5,632; 57,837)	Shape	6,189 (3,735; 8,642)	Scale	0,0527 (0,0413; 0,0642)	Scale	3,989 (3,921; 4,058)
					Scale	92,321 (84,176; 100,466)				

By carrying out a similar analysis it was found that the looseness, k1 and k2 stiffnesses for the reloading segments can also be modelled by the same distribution families selected for the loading segments. The same conclusion was found for the results of tests where joints were locked by hand.

It is possible to obtain the Spearman (rank-order) correlation coefficients (matrix) between looseness, k2 stiffness, the k4 rotation increment (Δθ4) and the ultimate bending moment resistance (Mu). The results are presented in Table 3.15.

Table 3.15: Spearman correlation matrix for selected parameters, for joints locked using a hammer.

Variables	Looseness	k2 load	k2 reload	Δθ4	Mu
Looseness	1	0,01 (-0,24; 0,25)	-0,21 (-0,49; 0,12)	0,01 (-0,24; 0,25)	-0,15 (-0,38; 0,10)
k2 load		1	0,41 (0,11; 0,64)	0,19 (-0,06; 0,42)	0,29 (0,05; 0,50)
k2 reload			1	-0,21 (-0,49; 0,12)	0,35 (0,04; 0,60)
Δθ4		Symmetric		1	0,35 (0,11; 0,55)
Mu					1

By analysing also the scatter plots it was possible to conclude that there is a large variability in the results. Significance tests were performed in order to distinguish between a spurious correlation present in the sample and a correlation with statistical support that can be expanded to the population. These tests return probability values, and the lower the values the less the chance that the correlation derives from sampling error and therefore there is a strong indication of a true correlation. The results are presented in Table 3.16.

Additionally, the 95% confidence intervals (*CI*) of the correlation coefficients were obtained by using the Fisher transformation (Fisher, 1921):

$$95\% \ CI = \tanh\left(\operatorname{arctanh} \rho \pm 2 / \sqrt{N-3}\right) \tag{3.5}$$

where ρ is the estimate of the correlation and N is the sample size. The results are shown in Table 3.15. In general, when *CI* includes zero the correlation coefficient is considered to be zero.

Therefore, it can be observed that it is likely that the values of k2 stiffness for the load and reload segments are positively correlated. The same conclusion can be drawn for the values of the Mu with the values of k2 stiffness for the load and reload segments; and for the values of Δθ4 and Mu.

Table 3.16: Significance values of the correlation matrix for selected parameters, for joints locked using a hammer.

Variables	Looseness	k2 load	k2 reload	Δθ4	Mu
Looseness		0,97	0,18	0,91	0,23
k2 load			0,01	0,12	0,02
k2 reload				0,19	0,03
Δθ4	Symmetric				0,00
Mu					

Finally, it should be noted that the values given in the above tables are only valid and should only be used for falsework elements (ledgers and standards) made of steel with a nominal yield strength equal to or higher than 355 MPa and mean values of mechanical properties similar to the ones given in Annex B.

3.2.1.2.6 Uncertainty evaluation

It is a matter of good practices to express the results with their uncertainty estimates to assess the quality of the testing setup used and of the results obtained.

As a demonstration consider the example of the determination of the stiffness of the second segment (k2) of the moment *vs.* rotation approximation diagram. The stiffness, equal to 87,84 kN.m/rad, was determined by the linear regression method using all data points $(M;\theta)$ between the time instant t_1 and t_2 $(t_2 > t_1)$. In order to include in the uncertainty calculation the uncertainty components of the measurement devices (load cell and LVDTs), it will be considered, as a simplification, that the stiffness was determined based only on the end data points of the interval $[t_1;t_2]$. The results for each time instant are given in Table 3.17.

The expression for determining k2 is:

$$k2 = \frac{\Delta M}{\Delta \theta} = \frac{M|_{t2} - M|_{t1}}{\theta|_{t2} - \theta|_{t1}} \tag{3.6}$$

The combined uncertainty of k2, *u(k2)*, is given by equation (3.7).

$$u(k2) = \sqrt{\left(\frac{\partial k2}{\partial M}\right)^2 \times u^2(M) + \left(\frac{\partial k2}{\partial \theta}\right)^2 \times u^2(\theta) + u^2(m_{k2})} \text{ with}$$

$$u(M) = \sqrt{\left(\frac{\partial M}{\partial P}\right)^2 \times u^2(P) + \left(\frac{\partial M}{\partial L}\right)^2 \times u^2(L)} \tag{3.7}$$

$$u(\theta) = \sqrt{\left(\frac{\partial \theta}{\partial d_N}\right)^2 \times u^2(d_N) + \left(\frac{\partial \theta}{\partial L_d}\right)^2 \times u^2(L_d) + u^2(\text{correction})}$$

where *u(P)*, $u(d_N)$ represent the standard uncertainties of the load cell and of the LVDTs, respectively, considered both to be equal to the maximum error obtained in the verified scale: 1% and 0,5% of readings, respectively. Additionally, *u(L)*, $u(L_d)$ represent the combined uncertainties of the distances *L* and L_d, respectively, which are given by the standard uncertainty of the ruler used to measure the distances, determined considering a rectangular probability distribution for the mean value with a ±0,5 mm range, combined with the uncertainty associated with the accuracy of the positioning of the ruler and the accuracy of determining the lever arm (due to the existence of gaps in the joint), which are considered to be equal to ±5 mm and ±1 mm, respectively. Finally, $u(m_{k2})$ is the uncertainty of the value of the linear regression slope, considered equal to its standard deviation, S_m, which is related to the coefficient of determination (R^2) by:

$$S_m = \sqrt{\frac{\left(1-R^2\right)\times S_M^2}{\left(n-2\right)\times S_\theta^2}}$$

(3.8)

where S_M and S_θ represent the standard deviations of the bending moment and joint rotation data points between time instant t_1 and t_2, respectively.

The term u(correction) appeared in the equation of the rotation standard uncertainty because the method used to obtain the joint rotation for upward displacements is not correct. This happens because for upward displacements, the sign of the rotation of the lower section of the standard, to which the N1 and N2 LVDTs are attached, is opposite to the sign of the rotation of the ledger. The value of the error introduced was estimated by registering the rotation of the lower section of the standard through two additional LVDTs in three joint bending tests. The value obtained for this rotation represented less than 1% of the value of the rotation obtained using the LVDTs measurements. Following, the joint rotation values for upward displacements were corrected being multiplied by 0,98. Nevertheless, it was considered that this correction did not remove all uncertainty and therefore it was considered u(correction) equal to 0,5% of the joint rotation.

Using the minimum accepted value for R^2, *i.e.* 0,9, the results are presented in Table 3.18. It can be observed that the combined uncertainty is relatively small, less than 5%, in proportion to the calculated value of the k2 (87,84 kN.m/rad). Using a coverage factor equal to 2, the expanded uncertainty associated with a 95% confidence interval is equal to 8,1% of the average value of k2, which is considered to be satisfactory.

Table 3.17: Example of uncertainty estimation. Results for each time instant t_1 and t_2.

Time	d_{N1} (mm)	d_{N2} (mm)	θ (rad)	P (kN)	M (kN.m)
t_1	-0,15	-0,12	-0,0005	1,38	0,41
t_2	4,10	2,04	0,0250	9,06	2,72

Table 3.18: Example of uncertainty estimation. Determination of the combined uncertainty of k2 .

$u(\theta\vert_{t1})$ (rad)	$u(\theta\vert_{t2})$ (rad)	$u(M\vert_{t1})$ (kN.m)	$u(M\vert_{t2})$ (kN.m)	S_M (kN.m)	S_θ (rad)	S_m (kN.m/rad)	$u(k2)$ (kN.m/rad)
1,23E-05	3,13E-04	5,77E-03	3,78E-02	0,67	0,0075	3,01	3,54

3.2.1.3 Comparison of results with past investigations

Comparing the results shown above with the results reported by (Chandrangsu, Rasmussen, 2011) it is possible to observe some important differences, see Table 3.19.

In terms of looseness, it was reported by (Chandrangsu, Rasmussen, 2011) that looseness only occurred in 30% of the tests, while in the present work looseness was observed in more than 70% of the tests. This difference can be explained by the different testing procedures since in (Chandrangsu, Rasmussen, 2011) all tests were monotonic from beginning to end. Using this test procedure it is not possible to determine the looseness of the joint since as was shown in the present investigation, looseness is unevenly distributed in the upward and downward loading direction and may, in some cases, only occur after the joint is submitted to initial rotation cycles which partially erode the joint initial stiffness due to friction between surfaces generated when locking the joint.

Nevertheless, in (Chandrangsu, Rasmussen, 2011) a larger looseness average value was obtained, as well as a larger average value for the stiffness associated with looseness than the one determined in the present work. Again, these differences can, at least in part, be justified by the different test procedures adopted. It was shown that testing monotonically to failure could lead, in some tests, to artificially high initial stiffness values. In fact, the results of 46 comparable tests (with two ledgers at the joint) in the loading direction (upwards or downwards) show that in over 26% of the tests the application of initial rotation cycles decreases the stiffness of the looseness segment (in 55% of the tests this value does not change). Regarding looseness, again in the loading direction, the application

of initial cycles increases its average value by 3% but only in 15% of the tests the value of looseness increases (in 75% of the tests this value does not change).

Table 3.19: Comparison of results with past investigations.

Joint configuration	Stiffness of loading segments (kN.m/rad)							
	(Chandrangsu. K. Rasmussen 2011)				Present work			
	k1		k2	k3	k1	k2	k3	k4
	Looseness alone	All tests						
Four ledgers	39	80	102	5,3	17	86	21	3,2
Three ledgers	36	75	87	5,1	11	83	13	2,5
Two ledgers	41	70	77	4,6	19	71	23	5,4
Joint configuration	Rotation (rad)							
	(Chandrangsu, K, Rasmussen 2011)			Present work[a]				
	θ1	θ2	θ3	θ1	θ2	θ3	θ4	
Four ledgers	0,014							
Three ledgers	0,012	0,036	0,16	0,005	0,041	0,09	0,17	
Two ledgers	0,007							
Joint configuration	Ultimate bending moment resistance (kN.m)							
	(Chandrangsu, K, Rasmussen 2011)				Present work			
All	3,5				3,9			
(a) Values represent the rotation at the end of each linear segment, averaged for the loading and reloading cycles, considering upward and downward directions. Therefore, θ1 does not represent the value of looseness.								

Also, there is a difference between the stiffness values determined for k2 stiffness, in particular for the joint configuration with four ledgers. Regarding deformation capacity and ultimate bending moment resistance, it is possible to observe that (Chandrangsu, Rasmussen, 2011) report a larger deformation capacity but a lower resistance than the ones obtained in the present study. These discrepancies can be attributed to differences in the material mechanical properties and cross-section geometric characteristics between the samples of elements considered in the two studies. For example, the wall thickness of the standard elements used in the Australian study had a nominal value of 4 mm whereas in the present study this value was equal to 3,2 mm. Also, the nominal yield stress of the steel of the standard elements used in the two studies is different: 450 MPa in the Australian study and 355 MPa in the present study. Additionally, differences between actual material and geometric properties with the same nominal values are certain to have played a role in the mentioned results discrepancies.

Comparing the joint models adopted in the present work and by past studies, namely the recent Australian research, with the entire set of tests results, see Figure 3.33, it is possible to observe that the model adopted in this work exhibits a much better fit to the tests results with little added complexity.

Finally, in (Chandrangsu, Rasmussen, 2011) the probabilistic distribution functions (pdfs) selected for the different joint stiffnesses are Gaussian whereas in the present study the selected pdfs deviate from normality for some random variables.

3.2.2 Weak axis bending tests

The test setup and test procedure adopted were essentially the same described for the bending tests about the strong axis. The test procedure consisted in applying a vertical displacement at the loaded ledger element using a lever arm equal to 300 mm in order to ensure always the attainment of joint failure, see Figure 3.34. The equipment and instruments used during the tests were the same ones and in the same number as described for the strong axis tests; their positioning was also the same.

All tests were performed under displacement control setting a low displacement rate equal to 0,1 mm/s. At the beginning of each test the loaded ledger was levelled horizontally and both the position and the verticality of the displacement transducers were checked.
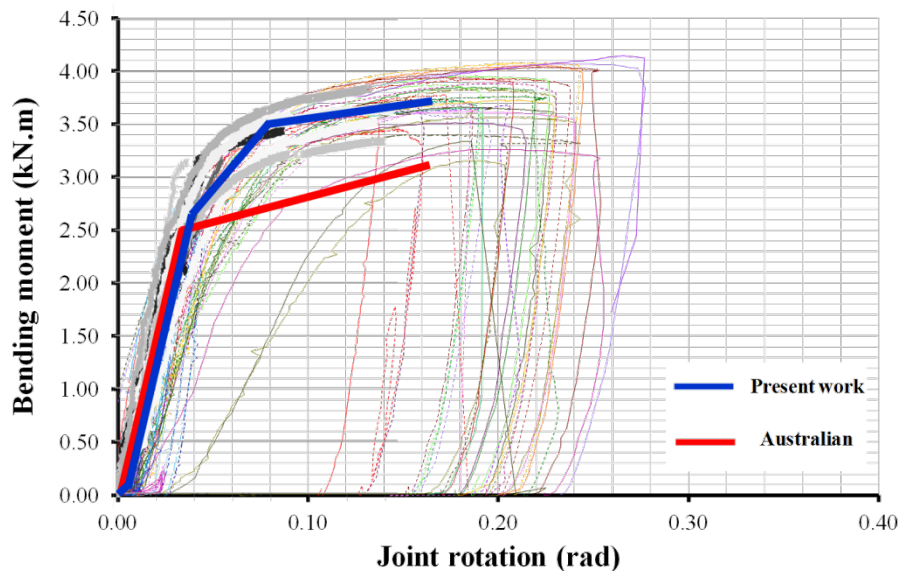
Figure 3.33: Comparison of the fit of the joint models adopted in the present work and in the Australian research to the entire set of joint tests results (present and past studies).

Figure 3.34: An overview of testing setup of the bending tests about the weak bending axis.

In contrary to the bending tests about the strong axis, for the weak bending axis a set of only two types of tests were performed: (i) a set of initial tests and (ii) a set of final tests. No preliminary tests were performed since the conclusions from the first tests, as described in the following, allowed to reduce the number of tests needed.

In all tests, three initial cycles of small displacement amplitude were applied to the joint to simulate the behaviour of the joint under wind loads.

The procedures and objectives of the initial tests and of the final tests were the same as for the strong axis tests. However, since the joint behaves very differently the test procedures had to be modified as described in the following.

As the test consisted in applying rotation on a single ledger, the joint stiffness, in this direction, comes mainly from the friction between surfaces in contact of the ledgers with surfaces of the standard and of the cups. No other significant form of restraint is mobilised. Thus, the joint stiffness strongly depends on the effectiveness of the joint locking method.

In a real scenario, it is possible that ledgers can rotate against each other thus increasing the joint stiffness by bearing action. It is also possible that ledgers could rotate in the same direction thus

reducing the contact area and possibly the joint stiffness. It is assumed that the adopted test conditions represent an average case.

After the force value became larger than the restraint provided by static friction coefficient, for upward rotations the only restraint left came from the kinetic friction coefficient resulting in a very low stiffness value. For downward rotations, the joint stiffness also diminishes but to a higher value than the one for upward rotations. This occurs because for downward rotations the joint rotation coincided with the torsion rotation applied to the upper cup to lock the joint, so the additional contact pressure generated provides some stiffness to the joint.

However, for these test conditions no real failure of the joint was attained, none of the joint components' was damaged beyond repair, no cracks or significant plastic deformations were observed. The tests were stopped for large rotation values of the loaded ledger or when the load value determined from the jack load cell consistently dropped.

Initial tests were performed with two and four ledgers connected at the joint, see Table 3.20 for details, whereas the final tests comprised tests with two, three and four ledgers connected at the joint, see Table 3.21 for details. In the final tests, the joint was unloaded when the joint rotation was approximately 0,2 rad.

A total of 48 tests divided into 18 initial tests and 30 final tests were carried out in the present investigation.

Table 3.20: Summary of initial tests.

Condition	Loading	Position	Initial cycles	Number of tests
New / Used	UP	P14	Yes	3
	DOWN	P14		3
	UP	P1234	Yes	3

Table 3.21: Summary of final tests.

Condition	Loading / Reloading	ID	Initial cycles	Number of tests
New / Used	UP / DOWN	P14	Yes	3
	DOWN / UP	P14		3
	DOWN / UP	P14, HAND		3
	DOWN / UP	P124		3
	DOWN / UP	P1234		3

The results of the initial and final tests are presented in Figure 3.35 to Figure 3.39.
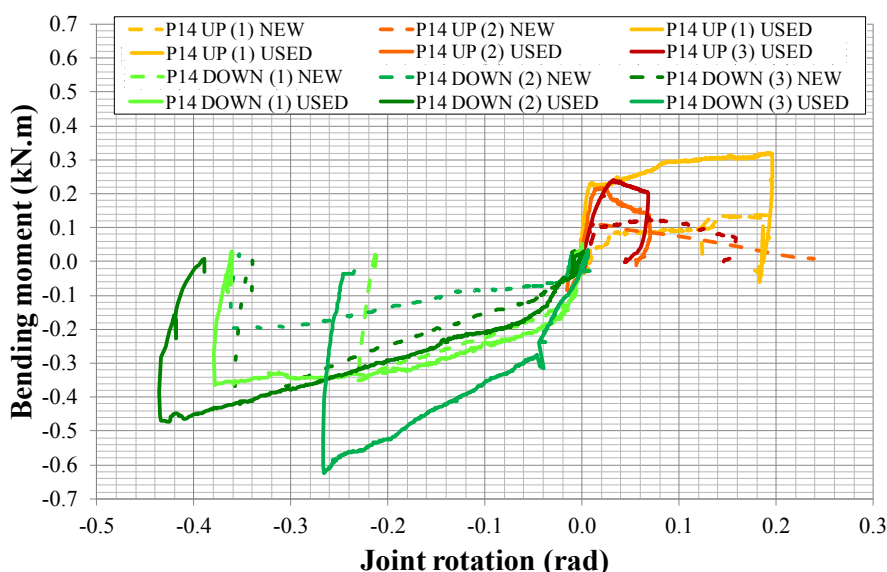
Figure 3.35: Initial tests. Results obtained with two ledgers.
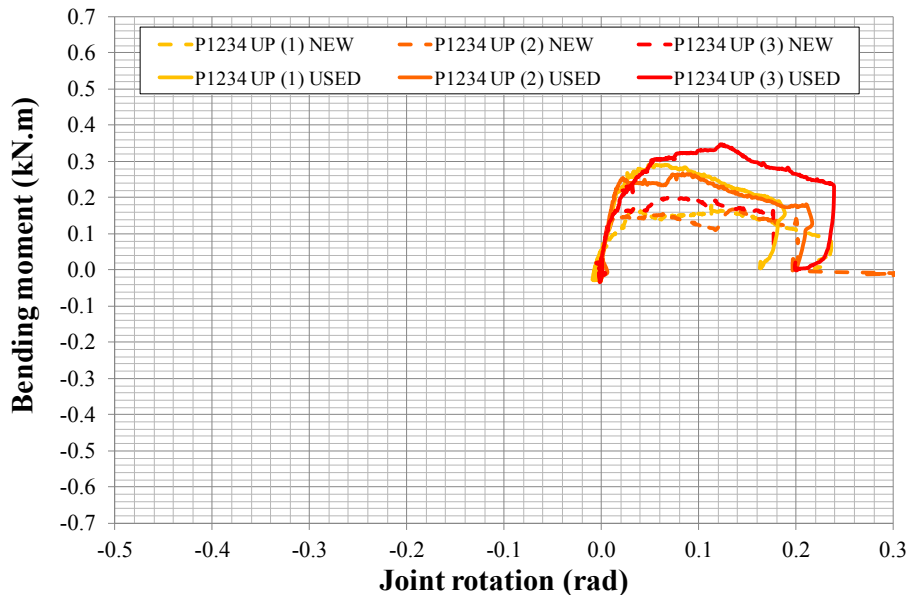
Figure 3.36: Initial tests. Results obtained with four ledgers.
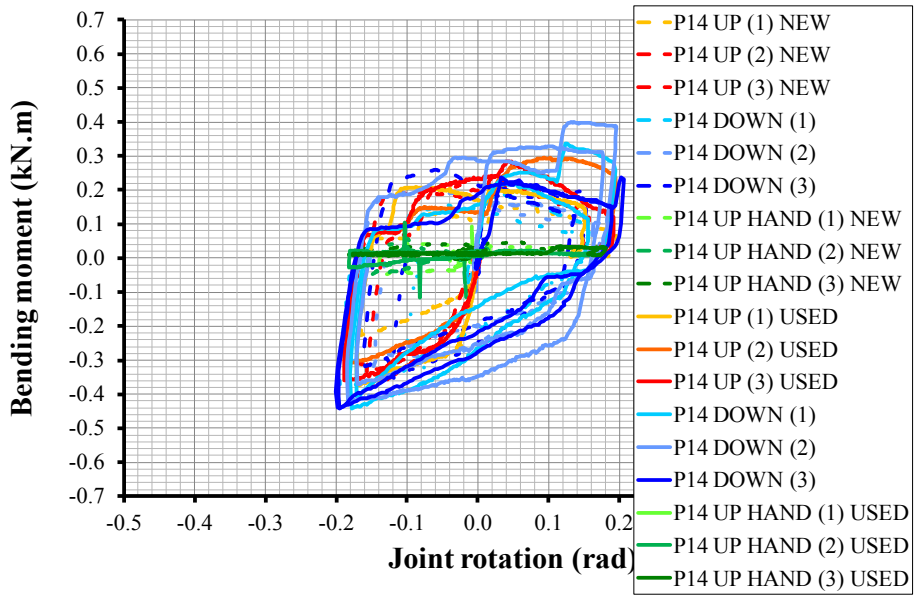
Figure 3.37: Final tests. Results obtained with two ledgers.
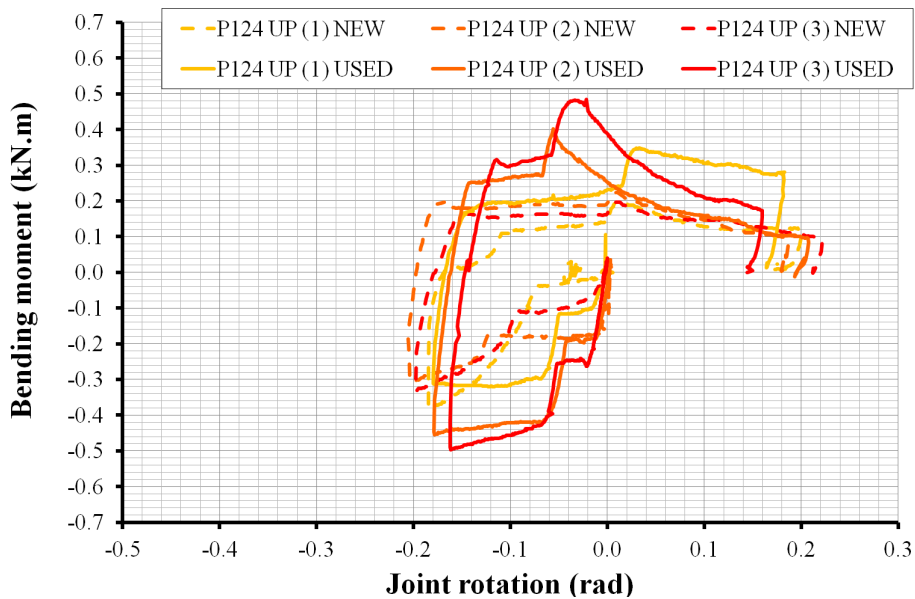
Figure 3.38: Final tests. Results obtained with three ledgers.
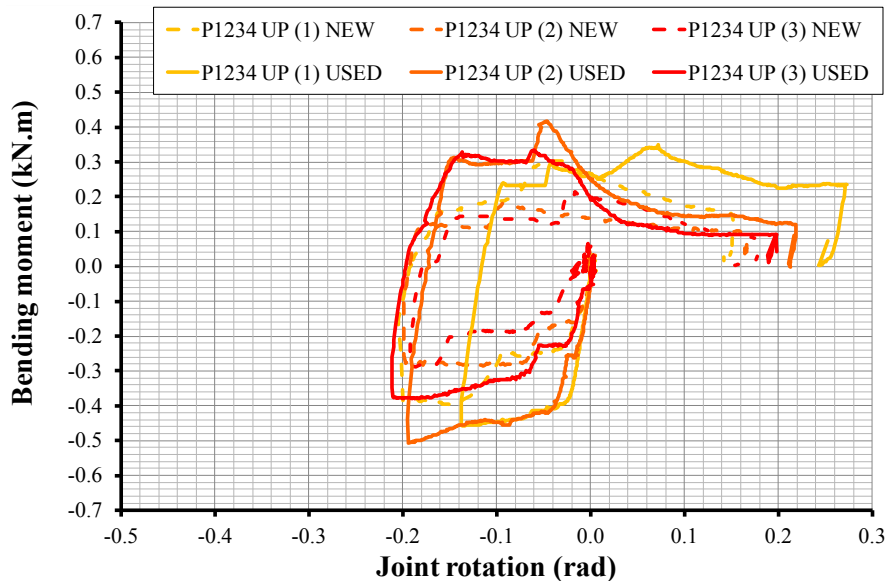
Figure 3.39: Final tests. Results obtained with four ledgers.

It could be observed that in this direction ledger-to-standard joints did not exhibit looseness, which is in agreement with the findings of (Chandrangsu, Rasmussen, 2011) and that the application of initial cycles did not seem to affect considerably the initial behaviour of the joint. Also, the joint behaviour is characterised by a larger variability than for bending about the strong axis.

Different stiffnesses were obtained for upward (+) and downward (-) rotations, but with no statistical relevance. Also, if the joint is locked by hand then the joint stiffness was negligible and the joint could be considered to be pinned for this degree of freedom. This finding highlights again the importance of a correct locking of the joints.

Although tests with "as new" elements appear to be more flexible than with used elements, there is no strong support for this behaviour in mechanical and statistical terms. Therefore, the different results will be joined. Also, the joint behaviour for all configurations tested is very similar and the tests results from all joint configurations will be joined.

Contrary to bending tests about the strong axis, the joint reloading behaviour (after unload) does not display looseness and the reload stiffness is similar to the one obtained for the load segments. Additionally, for force values larger than the restraint provided by static friction coefficient the joint no longer unloads to near zero bending moments and near zero rotations and the cyclic behaviour of the joint changes from a low energy dissipation behaviour to high energy dissipation behaviour.

The joint behaviour can be approximately simulated by the model illustrated in Figure 3.40.
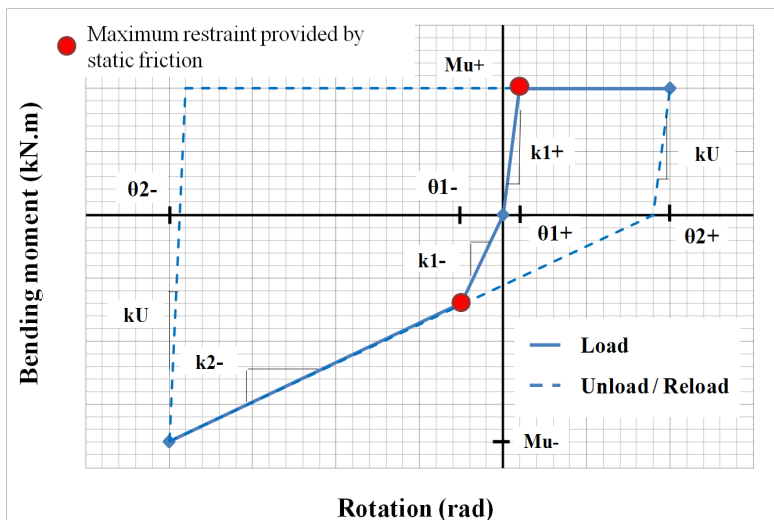
Figure 3.40: Approximation of the M *vs.* θ curves.

The average values for the different joint parameters are given in Table 3.22 and Table 3.23.

Table 3.22: Average values of the stiffness of the linear segments (load and reload segments).

Joint configuration	Parameter	k1+ (kN.m/rad)	k1- (kN.m/rad)	k2- (kN.m/rad)	kU (kN.m/rad)
All types	Average value	10,88	8,19	2,56	19,00

Table 3.23: Average values of other parameters of the linear segments (load and reload segments).

Joint configuration	Parameter	Δθ1+ (rad)	Δθ2+ (rad)	Δθ1- (rad)	Δθ2- (rad)	Mu+ (kN.m)	Mu- (kN.m)
All types	Average value	0,02	0,18	-0,02	-0,18	0,1	-0,4

Comparing these results with the ones obtained for the bending tests about the strong axis, it is possible to conclude that the joint in this direction is several times less stiff and also less resistant.

When compared with the results reported by (Chandrangsu, Rasmussen, 2011), see Tables below, it is possible to observe some differences. As before, Chandrangsu *et al* study only considered monotonic tests.

Table 3.24: Average values of the stiffness of the linear segments (load segments) in (Chandrangsu, Rasmussen, 2011).

Joint configuration	Parameter	k1 (kN.m/rad)	k2 (kN.m/rad)	k3 (kN.m/rad)
Two ledgers		7,5	5	1,5
Three ledgers	Average value	14	7	1
Four ledgers		15	7,5	0,8

Table 3.25: Average values of other parameters of the linear segments (load segments) in (Chandrangsu, Rasmussen, 2011).

Joint configuration	Parameter	Δθ1 (rad)	Δθ2 (rad)	Δθ3 (rad)	Mu (kN.m)
All types	Average value	0,02	0,04	0,10	0,4

First, (Chandrangsu, Rasmussen, 2011) obtained as a best fit model a trilinear model to simulate the joint behaviour for both upward and downward rotations, which have the same characteristics. In contrary, the present study uses bilinear model with different characteristics for upward rotations than for downward rotations. Therefore, the different behaviour registered in the present work for these two rotation directions may have been observed for the first time. In terms of stiffness, smaller values were obtained in the present study and (Chandrangsu, Rasmussen, 2011) obtained different results for different joint configurations (one, three or four ledgers at the joint) which was not observed in the tests performed in the present study. Finally, in terms of resistance, there is an agreement between the bending moment values for downward rotations but the ultimate bending moment obtained by Chandrangsu *et al* for upward rotations is four times larger than the one obtained in the present study.

3.2.3 Joint tensile axial tests

As there is only limited information (ten results showing a large variability, see (Voelkel, 1990)) about the tensile axial strength of ledger-to-standard joints and no information regarding its stiffness was available, 12 tensile axial tests of ledger-to-standard joints were performed. These tests are important since the post-failure behaviour of bridge falsework systems may be influenced by the strength and stiffness of these joints due to the development of large pull forces.

The test setup adopted is illustrated in Figure 3.41. Two 400 mm ledgers were connected to a Cuplok® joint at diametrically opposed positions and the end extremities clamped to the test machine grips. The test machine used could apply forces up to 100 kN and presented an uncertainty less than 1% of the load readings.

The load was introduced by moving the bottom grip downwards, pulling the ledgers apart. The load was applied monotonically at a rate of 0,2 mm/min only producing tension strains in the specimen. This test required the design of special grips. These consisted in two sets (top and bottom grips) of two S275 steel pieces joined by eight preloaded M12 10.9 bolts. The preload force was determined as to avoid slippage at the grips of the loaded specimen for a maximum axial load of 100 kN, without shear failure of the specimen. Each grip was then connected by a pin connection (consisting of a M24 10.9 bolt) to the testing machine.

The test setup adopted can be seen as conservative since large tension stresses will develop at each ledger, thus weakening the joint stiffness and resistance. In reality, the joint lateral restraint introduced by the system will be smaller than the one simulated and therefore asymmetrical pull forces will appear and the joint will be less stressed.
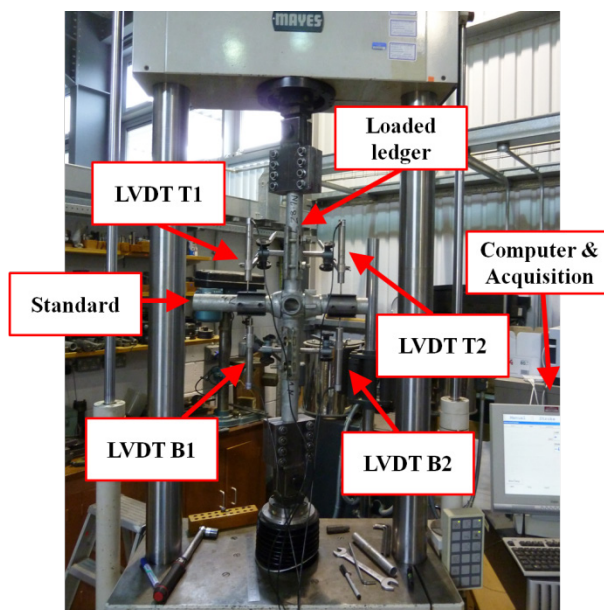
Figure 3.41: Setup for the tensile axial test of the ledger-to-standard joints.

The majority of tests were done with two ledgers, with two tests being performed with four ledgers at the joint. These two additional ledgers, with 50 mm length, were not pulled. The details of the tests are presented in Table 3.26. The different positions of the loaded ledger are illustrated in Figure 3.3.

As the bottom part of the joint is subjected to higher strains than the top part, it was expected that failure would occur in this area, either on the cups or on the ledger blades. However, since the material properties and geometrical characteristics vary from ledger to ledger (and also within the standard cups) failures were also observed at the top part of the joint, see Figure 3.42. All failures occurred due to joint fractures and not due to tube plastic collapse.

In order to calculate the stiffness of the joint, the vertical relative displacements between the ledgers (top and bottom) and the standard were recorded by four LVDTs, two positioned at each side (left and right) of the standard relative to the joint. These positionings allowed the vertical displacement of the each ledger at the joint to be estimated and removed any contribution from the rotation of the joint due to the asymmetrical stiffness and geometry of the cups (as a reminder, one of the cups, the bottom, is welded to the external wall of the standard, whereas the other, the top, is free and is used to lock the joint).

In all tests, the joint axial displacements (δ) for the time instant $t = i$ were determined by:

$$\delta_{t=i} = \frac{d_{LVDT,left}\big|_{t=i} + d_{LVDT,right}\big|_{t=i}}{L_d} \times L_{d,l} + d_{LVDT,left}\big|_{t=i} \tag{3.9}$$

where L_d represents the distance between the left and right LVDTs and $L_{d,l}$ represents the distance between the left LVDT and the centre of the ledger.

Table 3.26: Summary of tests.

Condition	Number of ledgers	Position of the loaded ledgers	Initial cycles	Number of tests
New / Used	2	P13	No	3
		P24		2
	4	P13		1

Figure 3.42: Failure at the top part of the joint.

The tests results are presented in Figure 3.43. The test label includes the ledger (bottom or top) used to represent the test. The criterion was to select the ledger involved in the failure.

It can be seen that there is an important variability in the results, which may be justified by the geometric imperfections and by the variability of the material mechanical properties of the various joint elements.

Analysing the results it is possible to observe that looseness was present in half the tests. Also, the results using "as new" elements and used elements are similar and will be joined. However, the tests using "as new" elements exhibited a smaller deformation capacity than the test with used elements. This finding again highlights the importance of proper manufacturing of the joint components to avoid structural defects.

Increasing the number of ledgers at the joint seems only to increase the maximum resistance of the joint, not affecting the joint stiffness. However, the values are within the range of results reported by (Voelkel, 1990) for axial tests using two ledgers, and therefore will be joined with the rest of the values.
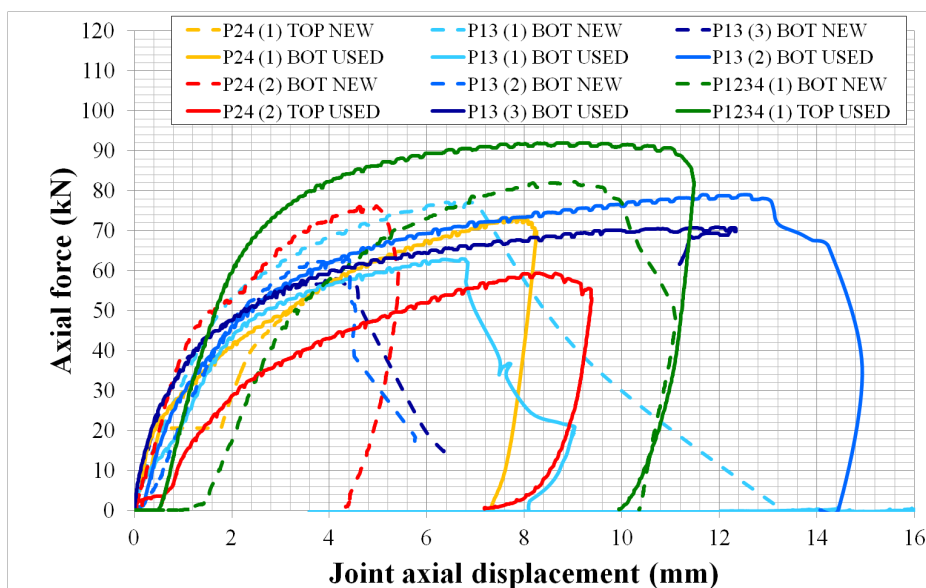
Figure 3.43: Tests results.

The joint behaviour can be simulated using the model already used for the bending tests about the strong axis, see Figure 3.16.

Table 3.27 and Table 3.28 contain the average values of the joint parameters. It is possible to observe that the average values of the axial stiffness of the ledger-to-standard joints are three orders of magnitude (×1000) higher than the bending stiffness.

Table 3.27: Average values of the stiffness of the linear segments.

Joint configuration	Parameter	k1 (kN/mm)	k2 (kN/mm)	k3 (kN/mm)	k4 (kN/mm)
All types	Average value	3,57	33,37	7,76	2,77

Table 3.28: Average values of other parameters of the linear segments.

Joint configuration	Parameter	Δδ1 (mm)	Δδ2 (mm)	Δδ3 (mm)	Δδ4 (mm)	kU (kN/mm)	Pmax (kN)
All types	Average value	0,23	1,39	3,20	2,33	127,85	70,71

Concerning the failure modes, the maximum resistance of the joint was determined by failure of the top cup (most of the times) or the bottom cup, or by slippage of the ledger blade from the top cup, see Figure 3.44.

Figure 3.44: Modes of failure. *Left,* **Bottom cup,** *Centre,* **top cup,** *Right,* **slippage of the ledger.**

A statistical analysis equal to the one presented in section 3.2.1.2.5 was carried out. The lower and upper bounds for the selected joint parameters are presented in Table 3.29. The results reported in (Voelkel, 1990) have been incorporated.

Table 3.29: Lower and upper bounds of joint variables.

Bound	k2 (kN/mm)	Pmax (kN)
Lower bound	10	30
Upper bound	80	130

The selected truncated distributions are presented in Table 3.30.

Table 3.30: Probabilistic models for selected variables.

Joint configuration	k2 (kN/mm)	Pmax (kN)
All types	tNormal	tWeibull

The values of the distributions parameters and the 95% confidence intervals are presented in Table 3.31, and were determined using the ML method.

Finally, it is possible to obtain the Spearman correlation coefficients. The results are presented in Table 3.32.

Significance tests were also performed in order to distinguish between a spurious correlation present in the sample and a correlation with statistical support that can be expanded to the population. The results are presented in Table 3.33. Additionally, the 95% confidence intervals (*CI*) of

the correlation coefficients were obtained by using the Fisher transformation (Fisher, 1921). The results are shown in Table 3.32.

Therefore, it is likely that the values of k2 stiffness and the values of Pmax are not correlated.

Finally, it should be noted that the values given in the above tables are only valid and should only be used for falsework elements (ledgers and standards) made of steel with a nominal yield strength equal to or higher than 355 MPa and mean values of mechanical properties similar to the ones given in Annex B.

Table 3.31: Parameters of probabilistic models.

Joint	k2 (kN/mm)		Pmax (kN)	
	Parameters		Parameters	
All types	Mean	32,47 (24,52; 40,43)	Shape	7,35 (5,07; 9,63)
	Sd	12,13 (5,81; 18,44)	Scale	76,37 (71,67; 81,07)

Table 3.32: Spearman correlation matrix for selected parameters, for joints locked using a hammer.

Variables	k2 (kN/mm)	Pmax (kN)
k2 (kN/mm)	1	0,01 (-0,67; 0,68)
Pmax (kN)		1

Table 3.33: Significance values of the correlation matrix for selected parameters, for joints locked using a hammer.

Variables	k2 (kN/mm)	Pmax (kN)
k2 (kN/mm)		0,97
Pmax (kN)		

3.3 Spigot joint tests

There are various types of spigot joints: (i) the spigot can be shop welded to the lower standard or (ii) it can be an independent element, for example. In the latter solution a fastener must be inserted through the hole located at the lower standard to join the two standards. Additionally, a fastener can be used in the hole located at the upper standard.

The external dimensions of the spigot (usually a SHS or a CHS cross-section) are smaller than the internal diameter of the standards' cross-section. Therefore, initially a play exists. When the standard is subject to bending this gap will introduce initial geometrical imperfections.

The resistance of this joint under combined compression and bending loading is determined by the resistance of all the joint components: (i) spigot, (ii) upper and lower standard and (iii) welded connection between the spigot and the inner wall of the lower standard and/or fasteners, if applicable.

As the full-scale tests carried out by (Chandrangsu, Rasmussen, 2008) demonstrate, the maximum resistance of bridge falsework systems is often limited by the strength of the spigot joints, see Figure 3.45. Also the existing analytical models are limited (Enright et al., 2000) and need additional verification.

In the present investigation several spigot bending joint tests, with or without axial load, were performed in order to assess the behaviour and resistance of this type of joint. The test setup is illustrated in Figure 3.46. The length of each specimen (between the supports) was 340 mm, small enough to avoid global buckling of the standard elements and large enough to avoid local buckling of the standard elements.

The selected type of spigot joint was the most commonly used, namely the welded spigot configuration. No fastener was used and the spigot was bent in the weak bending axis of the tubes (in alignment with the holes) so to obtain lower bound results. The spigots had a square hollow section (SHS) cross-section with a 32 mm nominal side length, 3,2 mm nominal wall thickness and 150 mm nominal free length measured from the top section of the lower standard. The material grade was steel grade 50 according to BS 4360 (BSI, 1990) with a nominal yield stress of 355 MPa.

Figure

Figure 3.45: Failure of a spigot joint (Chandrangsu, K. Rasmussen, 2009a).
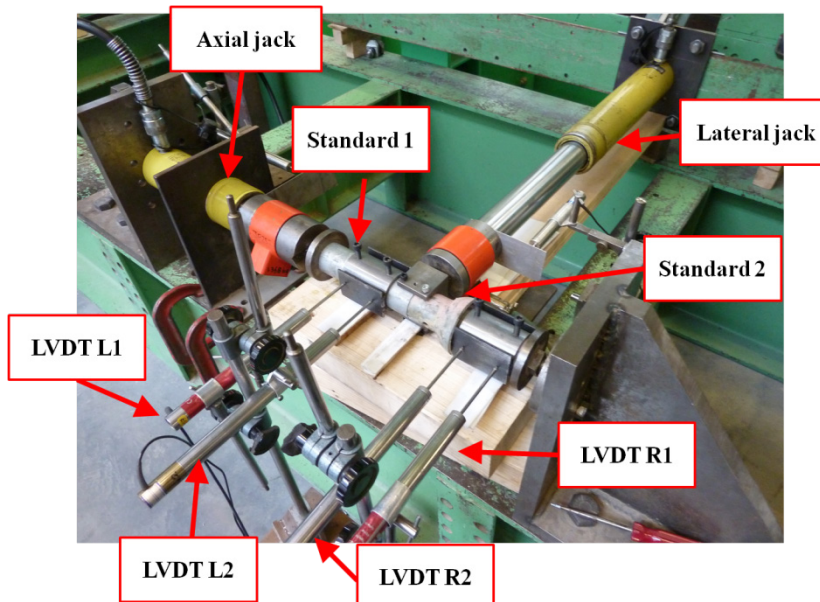
Figure 3.46: Setup of spigot joint tests.

The test method presented in BS EN 15512 (BSI, 2009a) specifies that the axial load is first applied and kept constant while the lateral load is increased until failure of the joint is attained. Three different axial load levels should be tested corresponding to 25%, 50% and 75% of the expected design axial force. This test method tries to simulate the cases where the standard suffers rotational displacements at top and bottom joints due to global buckling of the standard, global

buckling of the system or simply rotation of ledgers while the axial load remains constant. However, in cases where there is an axial load variation the test cannot reproduce the expected behaviour.

An alternative method is to derive the joint stiffness (K) and joint resistance (R) as a function of the applied axial load (P) and of the top and bottom rotation (or to simplify the mid-span lateral displacement, Δ, or rotation θ). This can be approximately achieved by a test method where both the axial force and the lateral loads are increased simultaneously, using a ratio between the horizontal and axial force, *e.g.* 10% of the axial force. Performing this method for different ratios it is possible to obtain a close approximation of the $K,R(\theta,P)$ relationship.

The test method presented in the European standard does not always return conservative values of the resistance and bending stiffness of the spigot joint. In fact, as the spigot joint involves also a contact problem, the most conservative test method can correspond to apply a high lateral load to axial load ratio and not to the opposite case, as far as the second order effects produced by the axial load do not dominate over the bending induced by the lateral load. High load ratios (horizontal load divided by axial load) imply that bending due to lateral load is dominant, meaning that the contact area between the upper and lower standards, which depends on the contact pressure at the interface section, is smaller than the one for lower load ratios. As the joint stiffness varies proportionally with the contact area, high load ratios imply lower values of the resistance and bending stiffness of the spigot joint. In practice, the dominant action can be the one induced by the rotation at the upper and lower ledger-to-standard joints or the second order effects due to the axial load and the initial geometric imperfections.

In order to make a good decision regarding the ratios between the applied lateral load and the axial load, a limited number of initial tests were carried out. Afterwards, the 20% and 50% ratios were selected as well as the case of only applying lateral load.

For each ratio at least three tests using "as new" and used specimens were performed. A total of 27 tests were performed, 6 initial tests and 21 finals tests, see Table 3.34 for details.

Table 3.34: Summary of tests.

Condition	Ratio (Lateral / Axial load)	Tests	Number of tests (New / Used)
New / Used	10%	Initial	1 / 1
	20%		1 / 1
	40%		1 / 1
	20%	Final	3 / 4
	50%		3 / 3
	Only lateral load		4 / 4

The test setup adopted for the pure bending tests is illustrated in Figure 3.47. The total free length (between supports) of each specimen was 1770 mm.
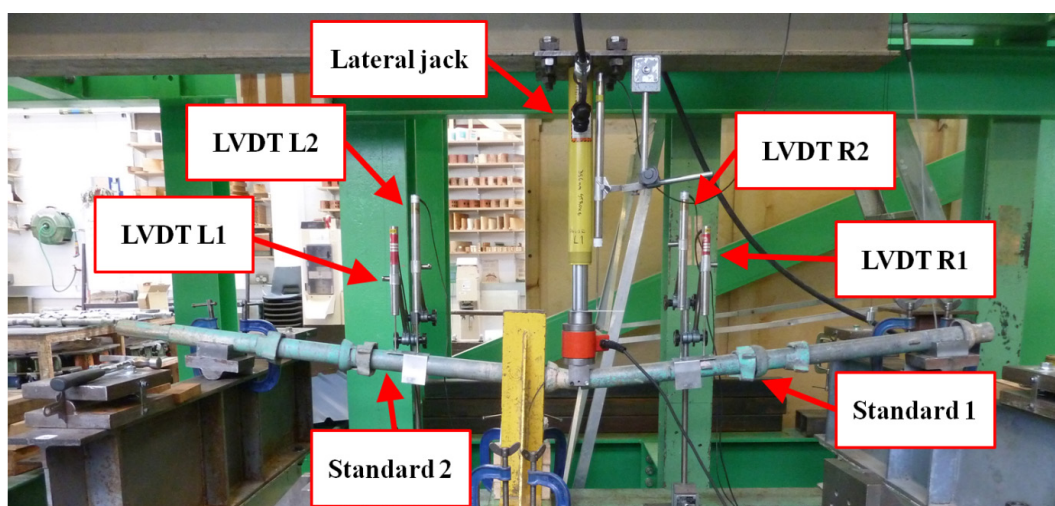
Figure 3.47: Setup of spigot joint pure bending tests.

The lateral and the axial load (when applicable) were applied at a low displacement rate (0,01 mm/s). The lateral load was applied at the interface of the two standard elements. In all the tests where axial load was applied, this load was applied first in order to develop friction enough between the ball bearings that materialised the end supports, the jack surface and a steel piece fitted within the end cross-section of each standard. After, the lateral load was introduced. The loads were applied throughout the test using this method and increased in steps of less than 5 kN.

The rotation of the spigot was determined by the rotation of each standard, which was obtained by the measurements of the horizontal displacements at two close cross-sections located in a region near the interface of the two standard elements. To apply the loads, two hydraulic jacks were used. The loads were recorded by two load cells: the axial load by a 200 kN load cell and the lateral load by a 40 kN load cell both of which with an uncertainty of less than 1% of the readings. It was not possible to apply axial loads higher than 100 kN due to a limitation of the maximum pressure of the pump connected to the jack which applied the axial load, which could not be resolved during the available testing period. The end supports at the extremities of each standard element were pinned by introducing ball bearings.

In all tests, the joint rotation (θ) for the time instant $t = i$ were determined by:

$$\theta_{t=i} = \theta_{left,t=i} + \theta_{right,t=i} \text{ with } \theta_{position,t=i} = \frac{d_{LVDT,2}\big|_{t=i} - d_{LVDT,1}\big|_{t=i}}{L_d} \tag{3.10}$$

where θ_{left} and θ_{right} represents the rotation of the left and right standard elements, respectively, and L_d represents the distance between the two LVDTs at each standard element.

The results of the final tests are presented in Figure 3.48 to Figure 3.50. The test label includes the lateral to axial load ratio, *e.g.* TA20LN1 represents a test where this ratio was equal to 20%.

For the tests using a ratio equal to 20% no failure was attained because the axial load reached values close to the maximum pressure limit of the pump. This is the reason why the ultimate bending moments for this ratio appear to be lower than the corresponding values for a ratio equal to 50%.

It can be seen that the initial behaviour of the joint is not represented. This happens because the readings of the axial and of the lateral load had to be made independently. In the beginning of the application of the loads it was observed a large scattering and it was difficult to coordinate the application of the lateral and axial loads. For this reason the initial records are not shown.

The joint behaviour can be simulated using the model already used for the bending tests about the strong axis, see Figure 3.16. Table 3.35 to Table 3.37 contain the average values of the joint parameters.

Table 3.35: Average values of the stiffness of the linear segments (used *vs.* new elements).

Ratio	Parameter	k1 (kN.m/rad)		k2 (kN.m/rad)		k3 (kN.m/rad)		k4 (kN.m/rad)		Mu (kN.m)	
		Used	New	Used	New	Used	New	Used	New	Used	New
20%	Average value	51,15	57,00	137,37	181,18	46,61	69,08	–	–	–	–
50%		–	–	108,40	147,45	36,17	42,09	8,05	6,51	3,39	3,67
Pure bending		–	–	23,10	32,74	6,52	12,48	0,65	3,54	1,52	2,07

Table 3.36: Average values of the stiffness of the linear segments (used *and* new elements).

Ratio	Parameter	k1 (kN.m/rad)	k2 (kN.m/rad)	k3 (kN.m/rad)	k4 (kN.m/rad)
20%	Average value	55,05	162,40	55,60	–
50%		–	127,92	39,13	7,28
Pure bending		–	27,92	9,50	2,09

Table 3.37: Average values of other parameters of the linear segments (used *and* new elements).

Ratio	Parameter	Δθ1 (rad)	Δθ2 (rad)	Δθ3 (rad)	Δθ4 (rad)	kU (kN.m/rad)	Mu (kN.m)
20%	Average value	0,0052	0,0136	0,0192	0,0000	–	–
50%		0,0000	0,0173	0,0160	0,0320	73,93	3,53
Pure bending		0,0000	0,0537	0,0442	0,1513	24,32	1,79
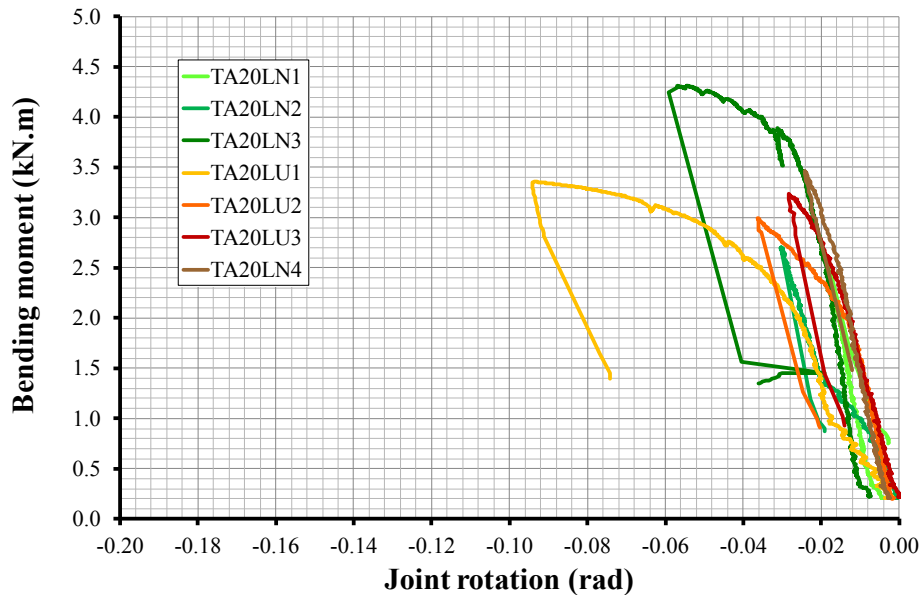
Figure 3.48: Test results for a lateral to axial load ratio equal to 20%.
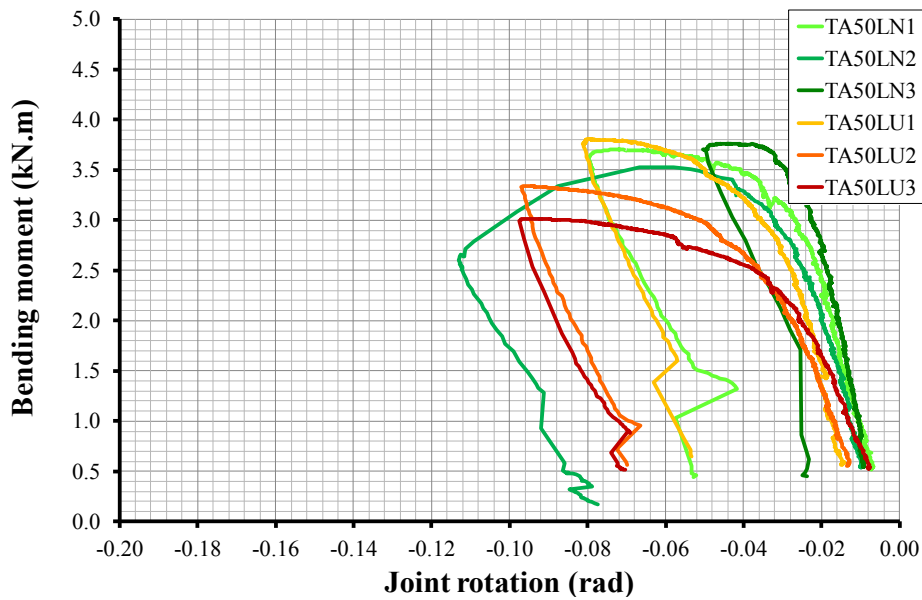
Figure 3.49: Test results for a lateral to axial load ratio equal to 50%.
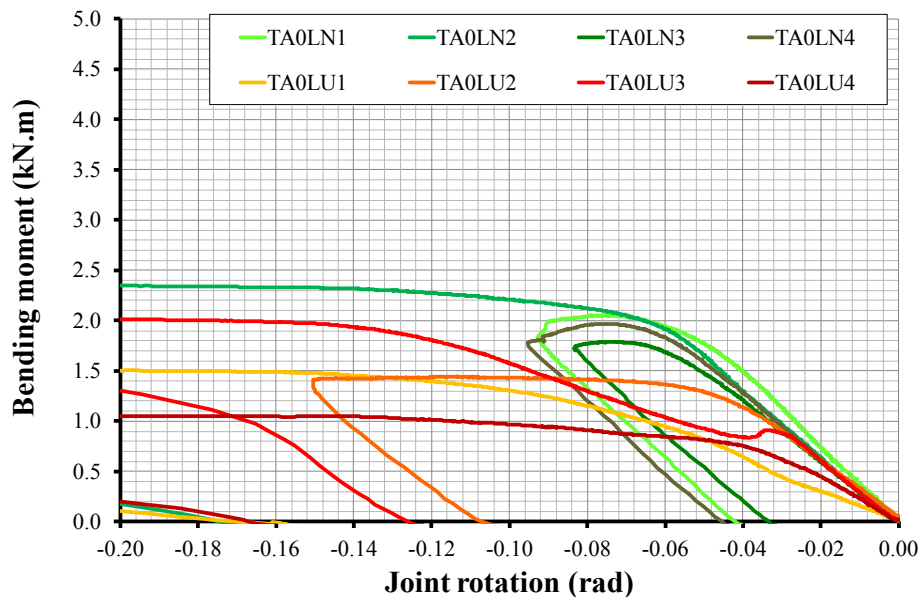
Figure 3.50: Pure bending test results.

It is possible to observe that the diagrams obtained using used elements are, in general, less stiff and less resistant that the ones obtained using "as new" elements, see Table 3.35. This observation is justified by the presence of structural defects on the welds between the spigot and the inner wall of the lower standard (some spigots could be displaced by hand before the start of the test).

It is also possible to observe that the average values of the bending stiffness, as well as of the resistance, diminish with increasing lateral to axial load ratios, as expected. In some tests no looseness was observed, but this could be due to the test setup adopted, in particular for the pure bending tests.

Most often the failure modes involved significant plastic deformations in the region subjected to tensile bending stresses around the hole on the spigot element (highlighted by the presence of extensive cracking), ovalisation of the hole on the region subjected to compressive bending stresses and deformation of the spigot, see Figure 3.51(*Left*). In some cases, it was also observed cracks on the welds joining the spigot element to the lower standard (Figure 3.51(*Centre*)) which could even result in axial displacements of the spigot (Figure 3.51(*Right*)). All failures occurred due to spigot fractures and not due to tube plastic collapse.

Figure 3.51: Modes of failure. *Left*: **Plastic deformations around spigot holes,**
Centre: **cracks in welds,** *Right*: **slippage of the spigot.**

For design purposes it is convenient to analyse the ratio between the axial load and the bending moment at the spigot (*N/M*). By doing such an analysis it is possible to develop graphs relating *N/M* with the joint stiffness, as illustrated in Figure 3.52 for the k2 stiffness.
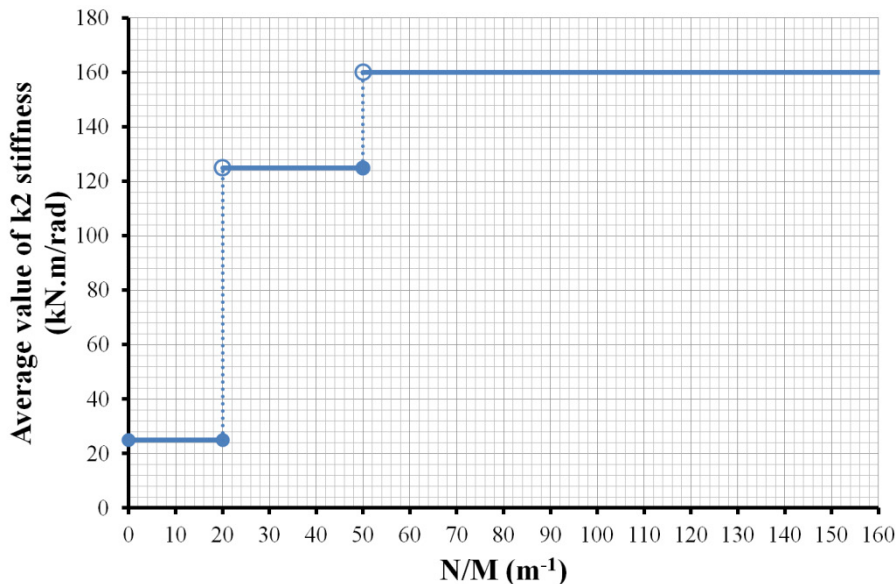
Figure 3.52: k2 stiffness as a function of N/M.

Table 3.38 and Table 3.39 define a possible structural model to analyse spigot joints where different model parameters are given which are valid for specific ranges of N/M ratio values. The values were based on *apriori* conservative simplifications with respect to the results obtained in the experimental tests.

Table 3.38: Structural model. Average values of the stiffness of the linear segments.

N/M ratio (m^{-1})	Parameter	k1 (kN.m/rad)	k2 (kN.m/rad)	k3 (kN.m/rad)	k4 (kN.m/rad)
[0;20]	Average value	55	160	55	5
]20;50]		10	125	40	5
]50;+∞]		2	25	10	2

Table 3.39: Structural model. Average values of other parameters of the linear segments.

N/M ratio (m^{-1})	Parameter	Δθ1 (rad)	Δθ2 (rad)	Δθ3 (rad)	Δθ4 (rad)	kU (kN.m/rad)	Mu (kN.m)
[0;20]	Average value	0,020	0,014	0,019	0,000	70	3,5
]20;50]		0,020	0,017	0,016	0,032	70	3,5
]50;+∞]		0,020	0,054	0,044	0,151	20	1,8

It should be noted that the values given in the above tables are only valid and should only be used for falsework elements (spigots and standards) made of steel with a nominal yield strength equal to or higher than 355 MPa and mean values of mechanical properties similar to the ones given in Annex B.

With the results obtained it is also possible to validate, or not, the analytical model proposed in (Enright et al., 2000). It was assumed that the material of the spigot was the same as of the standard with a yield stress of 400 MPa and a tensile resistance of 500 MPa (for an extension equal to 20%). Analysing Figure 3.53 it is possible to observe that the effect of the axial load on the stiffness and resistance of the spigot joint cannot be captured by the analytical model, returning unsafe values bending stiffness for low lateral to axial load ratios and possibly conservative values for high ratios.

Therefore, it is suggested to replace the analytical model by the phenomenological structural model presented above. However the phenomenological model does not allow for an explicit consideration of material characteristics different from the one of the test specimens from which it was developed, a feature that the analytical model allows.

Due to the small size of the sample of results it is not possible to estimate appropriate probabilistic models for the main variables that govern the behaviour and resistance of the spigot joints.

3.4 Forkhead joint tests

The joint between the top of the falsework system and the formwork system is in general a grey area. It is obvious that it can give an important contribution to increase the system's stiffness and resistance, however because its structural assessment involves a large uncertainty it is often modelled as a pinned joint.

The stiffness and resistance of the joint between the falsework and the formwork depends on the type of top plate (forkhead or baseplate) and on the geometrical, material and stiffness characteristics of the formwork beams and formwork system as a whole.

If the formwork beams are narrow enough so to allow the forkhead side plates to rotate without restraint and insufficient lateral confinement is enforced by means of the introduction of wood wedges between the beam and the forkhead side plates, the joint between the falsework and the formwork is indeed a pin connection. However, if, for small rotation values, there is interaction between the forkhead and the formwork beams then the joint is semi-rigid and can play an important role in stabilising the system against lateral loads.

The same comments can also be made when discussing the influence of the behaviour of the formwork system on the behaviour of the joint between the falsework and the formwork. If the formwork experiences severe stiffness degradation at early stages due to the interaction with the forkhead plate, then the joint, which could initially have a high stiffness value, will tend to a pinned joint.

Despite the large uncertainties associated with this joint, it is important to conduct a structural assessment which can be valid for cases where general good practices are followed during planning, design and operation.
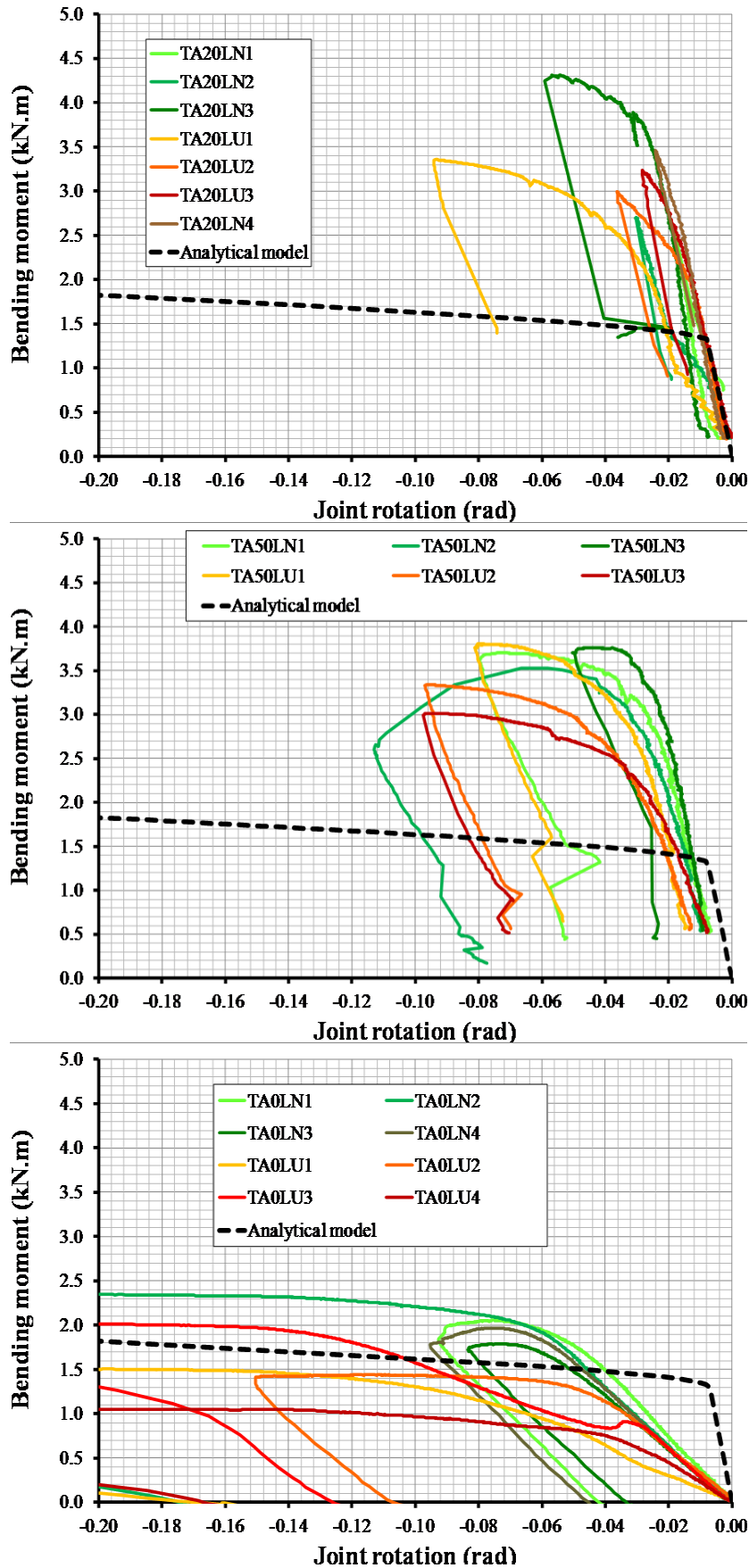
Figure 3.53: Comparison of the analytical model with the experimental results.

Therefore, ten bending tests of the joint between the forkhead plate and the formwork beam were carried out, distributed in half to each bending axis of the forkhead plate (see Figure 3.54). The

nominal dimensions of the forkheads are indicated in Figure 3.55. The nominal yield stress of the forkhead steel was equal to 355 MPa.
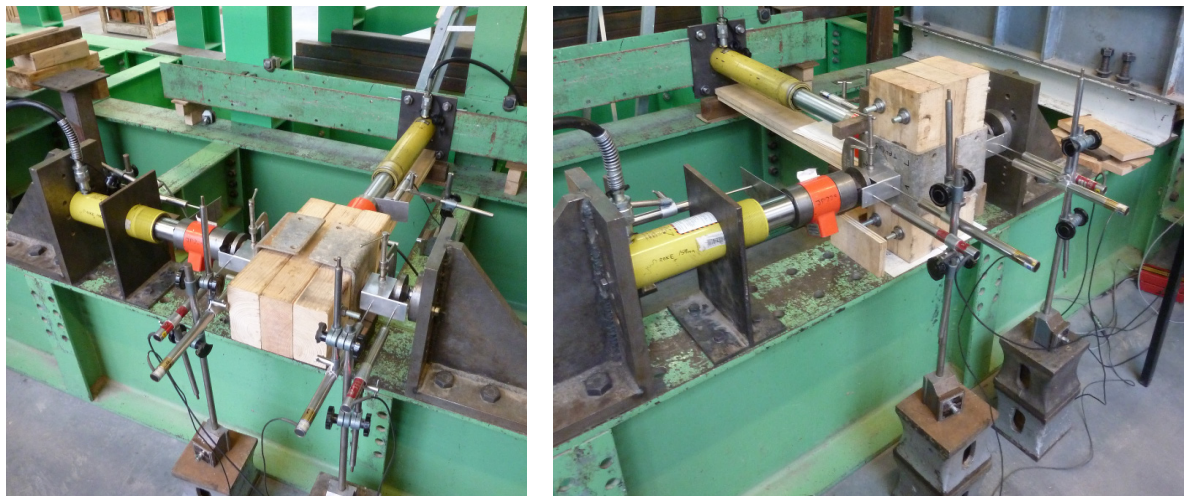
Figure 3.54: Test setup: Bending about axis 1 (*Left*), bending about axis 2 (*Right*).
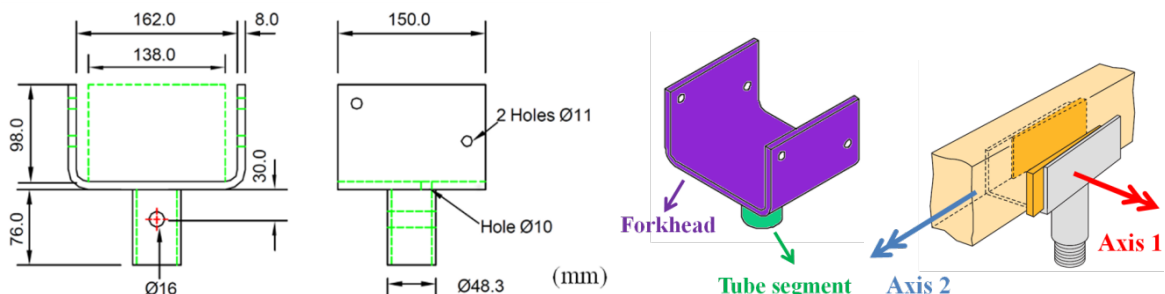
Figure 3.55: Nominal dimensions of the forkhead and illustration of the bending axis (SGB, 2009).

The formwork beam was simulated by a 300 × 500 × 130 mm (L × H × W) timber (pine) block made up of three smaller timber blocks connected to each other by steel threaded rods tightened by steel washers and nuts.

Initially, the forkhead, the top jack and a segment of a standard element were included in the joint. The former connection being ensured by a pin and the later by a collar nut. However, as initial play exist in all of these connections, it was difficult to interpret the test results and also the representativity of the results was not clear. Therefore, it was decided only to include in the test the forkhead element.

The connection of the forkhead to the rigid frame or the jack, which was used to apply the axial load, was made pinned. A rigid steel block was placed between the formwork timber elements and the other jack, through which the lateral load was applied, to minimize the chances of loading eccentricitically the timber elements. At the start of each test the positions of all elements connected were checked and aligned.

By virtue of the dimensions of both the timber block and of the forkhead there was a gap close to 10 mm between the inner side of the forkhead side plates and the timber block. No additional elements were used to close it. The gap was made equally distributed in both sides of the timber block before each bending test about axis 1. In the bending tests about axis 2 the gap was unequally distributed to a single side (the lateral load jack side) so as to test the joint in the most unfavourable configuration. The value of this load eccentricity, equal to 20 mm, corresponded to the average value obtained in the construction sites survey carried out by (Chandrangsu, K.J.R. Rasmussen, 2009b).

The forkhead rotation was determined in the same way as the rotation of each standard element in the spigot joint tests. The lateral displacements were measured at the tube segment of the forkhead element. Provided that the tube segment does not deform, i.e. behaves like a rigid segment, the rotation (θ) calculated based on the measured displacements corresponds to the joint

rotation at the forkhead, see Figure 3.56. However, because the tube segment is not a rigid element it will deform, thus the corresponding joint rotation overestimates the true value of the forkhead rotation (nevertheless an error on the safe side).
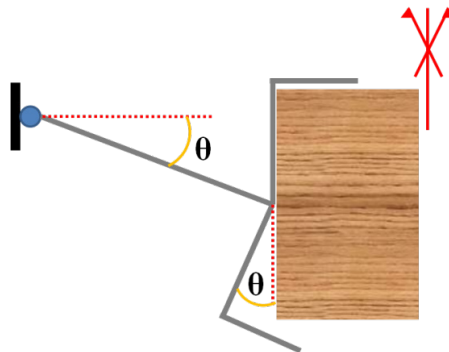
Figure 3.56: Forkhead joint rotation.

In order to estimate if the tube segment deformed plastically (thus contributing significantly to the calculated joint rotation value), measurements were made, before and after each test, of the length of the tube. In addition, measurements were also made, before and after each test, of the distance between forkhead side plates.

The loading method was the same as for the spigot joint tests. For this reason, the initial behaviour of the joints could not be accurately determined and will not be presented. The tests results are illustrated in Figure 3.57 and Figure 3.58.

Only one lateral to axial load ratio was chosen (50%). The higher the ratio is the more generally conservative will the results be. However, the choice of this ratio was made taking into consideration that the lateral stability of the ball bearings used to materialize the pinned joints was almost dependent of friction forces.

In one of the bending tests (without jacks) about axis 2 a sudden failure was attained at the beginning of the test for axial loads lower than 5 kN. The failure was due to a small vertical misalignment between the forkheads resulting in an eccentric application of the axial load which introduced a bending moment to the elements. The second-order stresses caused by this bending moment lead to premature buckling around the hole region at the weaker of the tube segments, see Figure 3.59. This failure clearly illustrates the sensitivity of this element to local effects (actions).
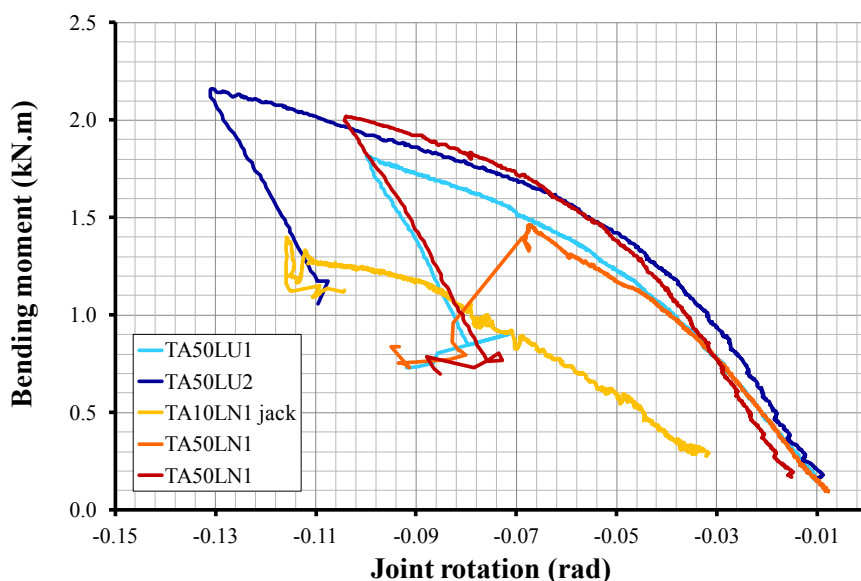
Figure 3.57: Results for the bending tests about axis 1.
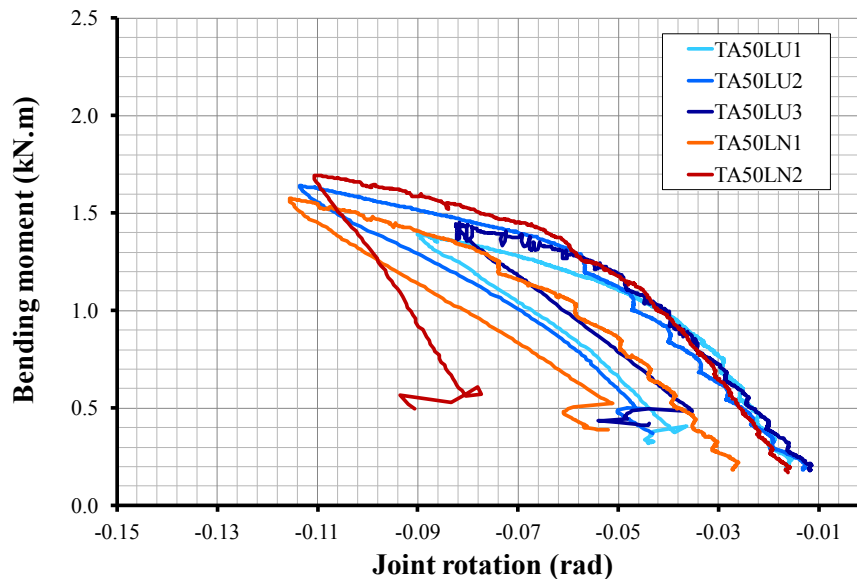
Figure 3.58: Results for the bending tests about axis 2.

Figure 3.59: Failure at the hole region due to load eccentricity - bending test about axis 2.

As for the other types of tests, the diagrams can be analysed using the model presented in Figure 3.16. Table 3.40 and Table 3.41 contain the average values of the joint parameters. It is possible to observe that the average values of the bending stiffness obtained for bending about axis 1 and axis 2 are very similar. The results of the test TA10LN1 (bending about axis 1) were not included.

Table 3.40: Average values of the stiffness of the linear segments (used *and* new elements).

Axis	Parameter	k1 (kN.m/rad)	k2 (kN.m/rad)	k3 (kN.m/rad)	k4 (kN.m/rad)
1 a)	Average value	–	32,54	13,25	8,46
2 b)		–	29,33	11,30	6,68
a: Failure at tube segment; b: Failure at forkhead.					

Table 3.41: Average values of other parameters of the linear segments (used *and* new elements).

Axis	Parameter	Δθ1 (rad)	Δθ2 (rad)	Δθ3 (rad)	Δθ4 (rad)	kU (kN.m/rad)
1 a)	Average value	0,0000	0,0353	0,0468	0,0305	45,88
2 b)		0,0000	0,0323	0,0363	0,0418	21,51
a: Failure at tube segment; b: Failure at forkhead.						

For bending tests about axis 1, the rotation occurred only at the tube segment and no rotation of the forkhead was observed, see Figure 3.60. Therefore, the forkhead rotational stiffness about axis 1 can be considered as rigid. In this axis, failure was attained when buckling around the hole region at the weaker of the tube segments occurred.

Figure 3.60: Failure mode for bending tests about axis 1: deformations at the tube segment.

For bending tests about axis 2, the rotation occurred mainly at the forkhead while the tube segment deformed elastically (confirmed by the measurements made before and after each test), see Figure 3.61. For this axis, the forkhead suffered plastic deformations resulting in an increase of the distance between side plates in the range of 2 to 7 mm. In this axis, all tests were stopped when the rotation of the element was clearly visible. Therefore, from these tests it was not possible to determine the maximum resistance of the forkhead element.
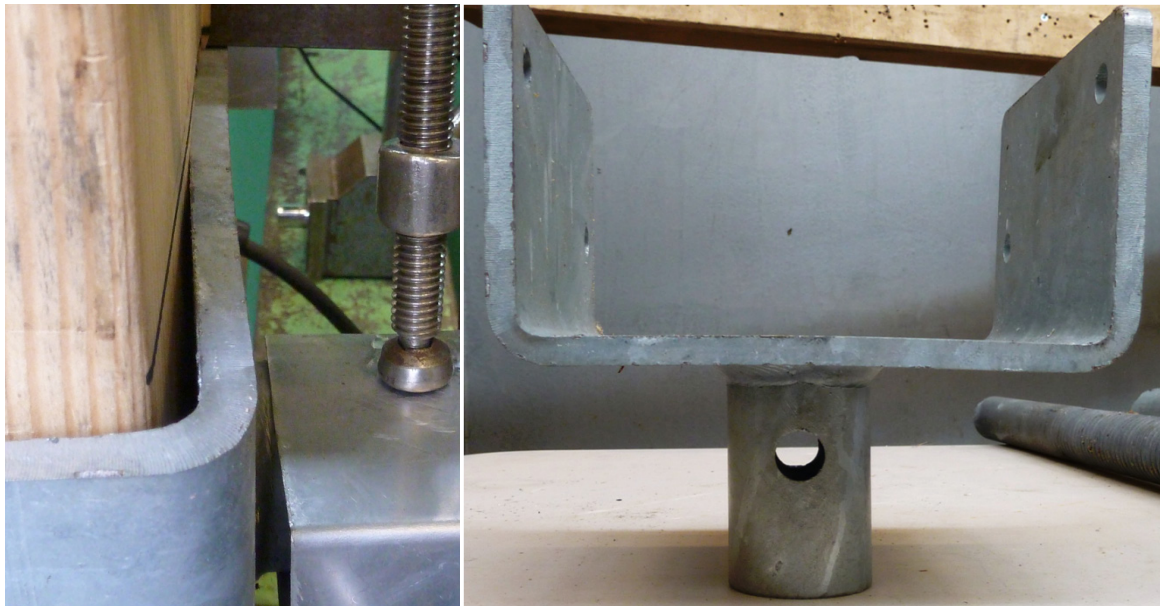
Figure 3.61: Failure mode for bending tests about axis 2: deformations at the forkhead.

As mentioned before, the joint rotation was calculated based on relative displacements measured in the tube segment. As the tube segment deformed, although elastically, the bending stiffness values obtained for the forkhead element in the bending tests about axis 2 are smaller than the actual ones. This error is on the safe side and thus it is accepted.

It must be again stressed that the bending stiffness at the interface between the falsework and the formwork also depends on the characteristics of the formwork system, including the geometrical dimensions of the formwork beams. In the tests carried out, the width of the timber blocks selected to represent the formwork beam was equal to 130 mm which is relatively large compared with the most common values, typically smaller than 80 mm. Larger width beams mean larger contact surfaces which can result in higher bending stiffness than when a smaller width beam is used. This difference may be reduced considerably if wedge elements are used to bind the formwork beam to the forkhead side plates as good construction practices recommends but sometimes are not followed.

The test results show that it is possible to mobilise an important bending stiffness at the interface between the falsework and the formwork if it is correctly designed and assembled, and these conditions remain throughout their use.

In all tests performed none exhibited looseness. This was expected since the top jack was not considered in the tests and the timber blocks were made tight to the forkhead. However, in practice gaps may exist between the formwork elements and the forkhead.

Due to the small size of the sample of results it is not possible to estimate good probabilistic models for the main variables that govern the behaviour and resistance of the tested forkhead joints.

Finally, it should be noted that the values given in the above tables are only valid and should only be used for falsework elements (forkheads) made of steel with a nominal yield strength equal to or higher than 355 MPa and mean values of mechanical properties similar to the ones given in Annex B.

3.5 Conclusions

In the present work five types of tests were performed to characterise the mechanical properties of three different types of joint: (i) Cuplok® joint between a standard element and one or more ledger elements, (ii) Spigot joint between two standard elements, and (iii) Forkhead joint between the falsework system and the formwork system. A total of 192 tests were performed. Regarding the latter two types of tests, it should be highlighted that prior to this study no results have been reported and the available models lacked verification.

The main conclusions are:

Cuplok® joint

Strong bending axis

- Averaging all results the effect of the application of the initial cycles may not be perceptible. However, for each particular test, the application of the initial cycles could lead to an important increase in the looseness or to a significant decrease of the initial stiffness; and the opposite cases can also occur. For example, it was observed that after the last initial cycle looseness can increase by 0,006 rad or decrease by 0,009 rad, whilst the stiffness can more than double or can decrease to just a fraction of the initial value. This effect could be important in the serviceability limit states range and justifies the need for carrying out cyclic tests. The average value of the joint looseness is equal to 0,007 rad (≈0,40°). Therefore, testing monotonically to failure could lead to artificially high initial stiffness values. This effect could be important in the serviceability limit states range and justifies the need for carrying out cyclic tests.

- In the present study the bending moment vs. joint rotation (M vs. θ) diagrams, in each loading quadrant, were fitted with three (for tests without looseness) or four (for tests showing looseness) linear segments. The stiffness value of each linear segment was determined by a best fit method. It can be observed that in average the various stiffness values obtained for upward and downward displacements are comparable;

- For joints correctly locked with a hammer, no evidence was found to support the hypothesis that looseness significantly affects the stiffness after looseness of the joint. However, tightening the joint by hand doubles the joint looseness values. This increased looseness contributes to an average 30% decrease in the stiffness of the joint;

- It could be observed that the joint stiffness tends to be lower (20% less) in reloading segments when compared to loading segments. This can be justified by the fact that the unloading (end of loading phase) was performed when the bending moment vs.

displacement diagrams started to deviate from linearity (around 2/3 of the ultimate bending moment resistance) which meant that plastic deformations occurred at the joint;

- Regarding modes of failure, gathering all the available information it was possible to distinguish between modes of failure of joints loaded upwards and downwards. In the former tests, failure was characterised by significant plastic deformations at the wall of the bottom cup, ledger lower blade and bottom cup weld, for both "as new" and used elements; while in the latter, failure was characterised by cracks at the top cup for "as new" elements and by cracks at the upper blade for used elements;

- It is possible to observe that the joints could not endure more than two load/reload cycles. Also, it was possible to observe a degradation of the stiffness and of the resistance with the cyclic loading.

<ins>Weak bending axis</ins>

- Different stiffnesses were obtained for upward and downward rotations, the latter being larger, due to higher friction resistance. However, the stiffness in this axis was considerably smaller (approximately five times) than that in the strong axis;

- Furthermore, if the joint was locked by hand then the joint stiffness in this direction was negligible and the joint could be considered to be pinned. This finding highlights again the importance of a correct locking of the joints.

<ins>Axial axis</ins>

- It was possible to observe that the average values of the axial stiffness of the ledger-to-standard joints are three orders of magnitude (×1000) higher than the bending stiffness.

<ins>Spigot joint</ins>

- It was possible to observe that the joint behaviour depended on the ratio between the axial force and the bending moment at the joint. The higher this ratio is, the stiffer the joint becomes;

- With the results obtained it was also possible to validate, or not, the analytical model proposed by (Enright et al., 2000). It was possible to observe that the effect of the axial load on the stiffness and resistance of the spigot joint cannot be captured by the analytical model, returning unsafe values bending stiffness for low lateral to axial load ratios and possibly conservative values for high ratios.

<ins>Forkhead joint</ins>

- The test results showed, that it is possible to mobilise an important bending stiffness at the interface between the falsework and the formwork if it is correctly designed, assembled and these conditions remain throughout the operation.

Finally, as an example, the results for the ledger-to-standard joint were analysed statistically. The selection of the probabilistic distribution for each parameter was based on classic goodness of fit tests but also on more advanced analysis. The results show that in some parameters the most suited distributions deviate greatly from normality.

4

NUMERICAL INVESTIGATION

4.1 Introduction

The structural behaviour of bridge falsework systems can be assessed by experimental tests and/or by numerical models. This Chapter concerns the development, validation and verification of numerical models of bridge falsework systems. The justification for performing these numerical tests resides in the important advantage brought by computer science into civil engineering which makes it possible nowadays to simulate with increasing accuracy and decreasing effort complex structural systems subject to various constraints of different nature: topologic, types of loading, economic, reliability and robustness for example. This ability represents a giant leap in the capability and efficiency of understanding the behaviour of structural systems with respect to risk optimisation when compared to the limited options offered by experimental tests.

To study the behaviour, resistance, robustness and reliability of bridge falsework systems the finite element analysis program *ABAQUS®* was used. Since the joint elements available in *ABAQUS®* are unable to model the non-linear analytical model derived from the joints' tests results, in particular the stiffness and resistance degradation with loading cycles, a new joint element was developed to simulate the behaviour, resistance and failure of several types of joints present in bridge falsework systems. Therefore, this Chapter starts with the details of joint modelling and the formulation of the new joint element.

Afterwards, the validation and verification procedure will be presented and discussed. Different algorithms and numerical options were tested in order to validate the numerical models. The models were then verified by comparing their results with full-scale tests results and also with numerical results obtained by other studies. Finally, it is presented in the end of this Chapter the results of a study which analysed the influence of different modelling options, including design rules given in normative documents, in the numerical behaviour of these systems.

4.2 Joint modelling

Several types of joints exist in bridge falsework systems, the most common being: (i) standard-to-ledger joints, (ii) spigot joints, (iii) brace-to-ledger joints, (iv) top and bottom boundary joints. For each type of joint different possible solutions exist, for example, Cuplok® or wedge type standard-to-ledger joints; hook or swivel brace-to-ledger joints.

Different numerical modelling techniques are available to simulate these types of joints: from the more complete 3D joint modelling using solid elements to the simple spring-like joint modelling.

Each modelling option offers relative advantages and disadvantages:

- Solid and shell models allow explicit consideration of the different parts of the joint and therefore the geometrical, material and boundary nonlinearities can be accounted for explicitly. This advantage is however countered by possible difficulties in achieving numerical convergence, plus discretisation challenges and long hours needed to develop, debug and validate each model;

- Spring-like models are easy to assemble, debug and validate. They can be based on mechanical models or on phenomenological models of the joint, which have to be determined and validated against available and reliable data. An example of a mechanical model is the components method presented in the Eurocodes for designing joints in steel structures. Phenomenological models are analytical representations of results of joints tests. Typically, one model can represent only the joint it was derived from, although it is possible to develop general analytical models which are valid for a range of geometries, material types and types of loading.

In the present Thesis the phenomenological models are preferred. The analytical models used for Cuplok® joints, spigot joints and forkhead joints have been derived from the experimental tests presented in Chapter 3. The analytical model consists in a multilinear fit to the experimental tests results. The advantages which justify why this model was chosen over more complex models have been given in Chapter 3. However, the multilinear model has slope discontinuity which is an important numerical disadvantage over fully continuous models.

Additionally, other special joints have been developed to the contact between the baseplate element and the supporting ground, and to simulate gap elements (which behave as continuous elements for compressive forces and allow free displacements and rotations if the tensile force value exceeds a certain threshold value).

4.2.1 Modelling of Cuplok® joints

From the available six degrees of freedom of the joint, three were included in the analytical models: (i) the rotations about the joint strong bending axis (rotations resulting from displacements along local *y* axis), (ii) the rotations about the joint weak bending axis (rotations resulting from displacements along local *z* axis), and (iii) axial displacements (displacements along local *x* axis), see Figure 4.1.
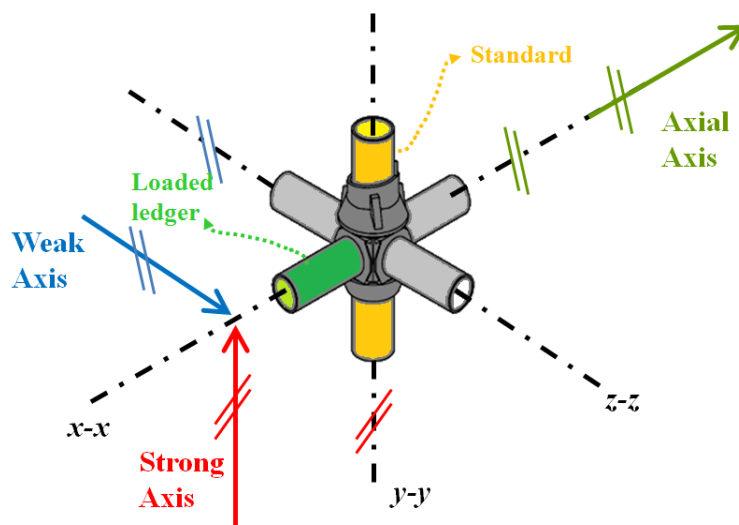
Figure 4.1: Illustration of Cuplok® degrees of freedom included in the analytical model.

4.2.1.1 Strong bending axis

The analytical model for rotations about the joint strong bending axis is as follows:

Monotonic loading (see Figure 4.2)

$$\theta \in \left[\theta_{max}^{-}, \theta_{max}^{+}\right] \Rightarrow M^i = M^{i-1} + \left(\theta^i - \theta^{i-1}\right) \times k$$

$$\theta \in \left]-\infty, \theta_{max}^{-}\right[\, , \left]\theta_{max}^{+}, +\infty\right[\Rightarrow M^i = \theta^i \times k$$

$$\theta \in \left[\theta_1^{-}, \theta_1^{+}\right] \Rightarrow k = k_1^{+} = k_1^{-} = k_1$$

$$\theta \in \left[\theta_2^{-}, \theta_1^{-}\right[\, , \left]\theta_1^{+}, \theta_2^{+}\right] \Rightarrow k = k_2^{+} = k_2^{-} = k_2$$

$$\theta \in \left[\theta_3^{-}, \theta_2^{-}\right[\, , \left]\theta_2^{+}, \theta_3^{+}\right] \Rightarrow k = k_3^{+} = k_3^{-} = k_3$$

$$\theta \in \left[\theta_4^{-}, \theta_3^{-}\right[\, , \left]\theta_3^{+}, \theta_4^{+}\right] \Rightarrow k = k_4^{+} = k_4^{-} = k_4$$

$$\theta \in \left]-\infty, \theta_4^{-}\right[\, , \left]\theta_4^{+}, +\infty\right[\Rightarrow k = k_{res}^{+} = k_{res}^{-} = k_{res}$$

$$k_2 > k_3 > k_4 > k_{res}, \; k_2 > 0,5 \times k_1$$

$$k_{res} = \text{residual stiffness} = 0,0001 \text{ N.mm/rad}$$

with

$$\theta_1^{+} \neq \theta_1^{-}$$

$$\theta_2^{+} = \left|\theta_2^{-}\right| = \theta_2$$

$$\theta_3^{+} = \left|\theta_3^{-}\right| = \theta_3$$

$$\theta_4^{+} = \left|\theta_4^{-}\right| = \theta_4$$

$$\theta_{max}^{+} = \left|\theta_{max}^{-}\right| = \theta_{max}$$

$$\theta_1^{+}, \left|\theta_1^{-}\right| < \theta_2 < \theta_3 < \theta_4 < \theta_{max}$$
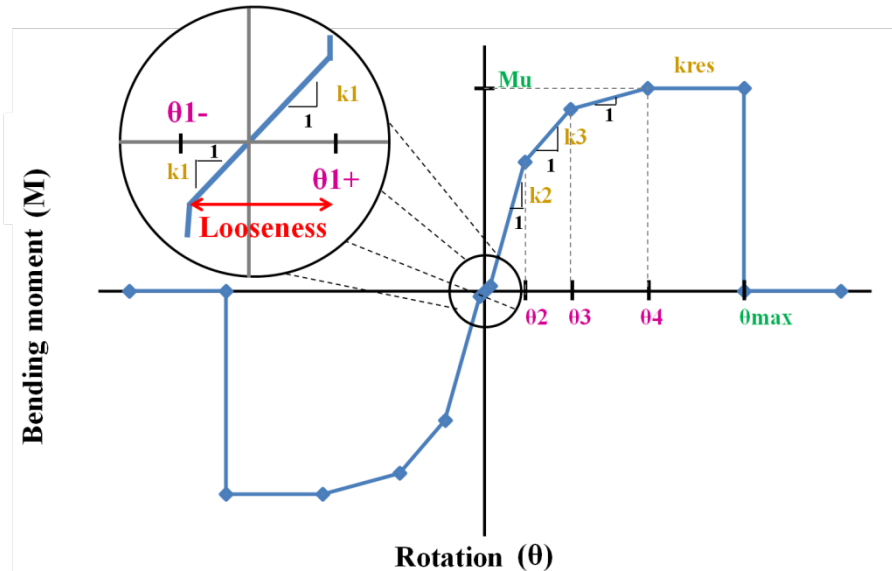
Figure 4.2: Analytical model for monotonic loading about the Cuplok® joint strong bending axis.

It is made of four loading linear segments, numbered one to four, followed by a fifth linear segment with residual stiffness, k_{res}, for bending moment values higher than the ultimate bending moment of the joint, M_U. If, eventually the imposed joint rotation, θ, exceeds the available joint rotation capacity, θ_{max}, failure of the joint occurs which is incorporated in the analytical model by transforming the joint into a linear elastic spring with residual stiffness.

Additionally, based on the results presented in Chapter 3, for rotations larger than the looseness of the joint the model assumes the same behaviour for positive and negative rotations. However, looseness may be asymmetrically distributed.

The model also makes allowance for the number of ledgers (one, three or four) present in a single Cuplok® joint by adopting different values for the stiffness of the second linear segment, k_2. Additionally, the possibility of locking the Cuplok® joint by hand rather than by a hammer is also incorporated in the model by changing the k_2 values.

In order to use consistent values of M_U and the maximum moment, $M_{maxk\theta}$, derived from the stiffness and rotation increments of the four linear segments, a compatibility check is performed at

the beginning of every increment so that the value of M_U equals $M_{max k\theta}$. This is achieved by changing the rotation increment of the linear segments, starting at segment 4.

The input parameters of the analytical model are the rotations θ_1, θ_2, θ_2, θ_4, the stiffnesses k_1, k_2, k_3, k_4, k_U and the ultimate bending moment resistance M_U.

For cyclic loading, *i.e.* when unloading occurs with possible load reversals, the behaviour of the joint changes from the one described for monotonic loading.

It was observed that the unloading stiffness, k_U, is higher than the maximum loading stiffness, $\max(k_L)$. However, for small values of the bending moment the unloading stiffness decreases to a fraction of its initial value, k_{ZERO}. Therefore, a bilinear model was adopted for the unloading phase. The model also assumes that if the joint is fully unloaded, *i.e.* rotation equal to zero, the bending moment is also zero. This is a small simplification, on the safe side, to the actual behaviour of the joint.

The loading path in the negative direction matches the unloading path until the monotonic loading path is reached, after which the monotonic loading path is followed until new unloading occurs.

Cyclic loading (see Figure 4.3)

Unloading (bilinear model):

$$\text{If } M^i < k_{ZERO} \times \theta^i \Rightarrow k = k_{ZERO} = \max\left[\frac{1}{100} \times \max(k_L), k_{res}\right], \ M^i = k_{ZERO} \times \theta^i$$

$$\text{Else } k = k_U > \max(k_L), \ M^i = M^{i-1} + \left(\theta^i - \theta^{i-1}\right) \times k$$

Load reversal:

$$\text{If } M_{max} = \max\left(M^{i-j}\right) > M_{rev}^{i-j} = \frac{2}{3} \times M_{max k\theta} \text{ and } \text{sign}\left(\theta^j\right) \neq \text{sign}\left(\theta^{j+1}\right): \quad \text{with} \quad i < j < m$$

$$k_2^{j-m} = RF \times k_2^{i-j}, \ \text{Reduction Factor } (RF) = 0,8$$

$$n_{rev} = n_{rev} + 1$$

$$\text{If } n_{rev} = 0 \Rightarrow \theta_{max} = 1,6 \times \theta_4$$

$$\text{If } n_{rev} = 1 \Rightarrow \theta_{max} = 1,4 \times \theta_4$$

$$\text{If } n_{rev} = 2 \Rightarrow \theta_{max} = 1,2 \times \theta_4$$

$$\text{If } n_{rev} = 3 \Rightarrow \theta_{max} = 0,8 \times \theta_4$$

$$\text{If } n_{rev} \geq 4 \Rightarrow \theta_{max} = 0,4 \times \theta_4$$
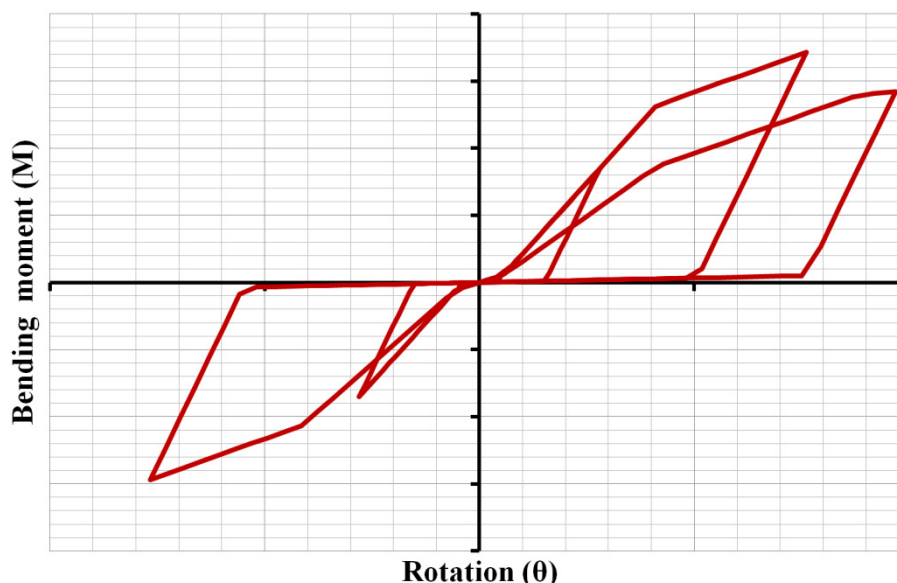
Figure 4.3: Example of the analytical model for cyclic loading about the Cuplok® joint strong bending axis.

If load reversal occurs and the maximum bending moment, M_{max}, that was applied to the joint in the previous load quadrant does not exceed a certain limit value, M_{rev}, the behaviour of the joint in the current load quadrant matches the monotonic loading behaviour. However, if $M_{max} > M_{rev}$ stiffness degradation occurs. It is assumed that only the stiffness of the second linear segment, k_2, is reduced, to 80% of the previous value. Under such conditions there is also a ductility degradation expressed by reducing the value of the available joint rotation capacity, θ_{max}.

Figure 4.4 illustrates a comparison between the experimental behaviour and the one obtained using the proposed analytical model. It may be observed that there is a reasonable agreement between the actual and the predicted joint behaviour.
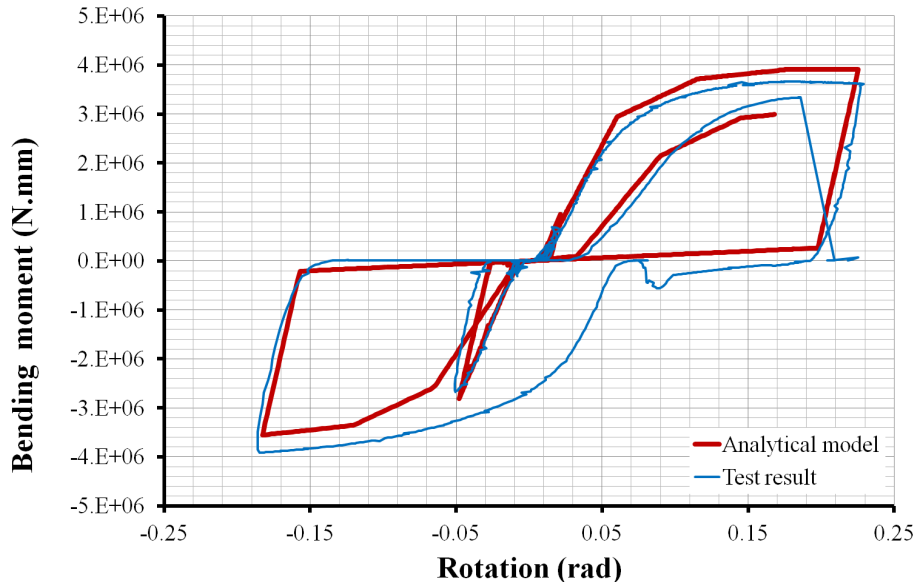
Figure 4.4: Comparison between the experimental behaviour and the one obtained using the proposed analytical model.

4.2.1.2 Weak bending axis

When the joint is locked by a hammer the analytical model for rotations about the joint weak bending axis is as follows, see Figure 4.5:
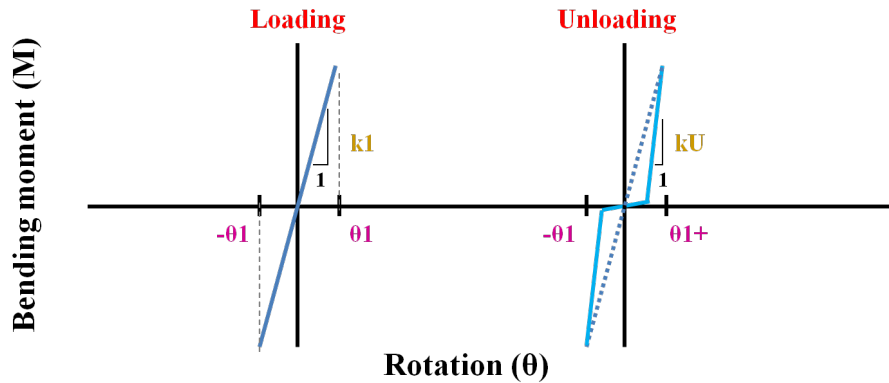
Figure 4.5: Analytical model for monotonic loading about the Cuplok® joint weak bending axis.

Force values **smaller** than the restraint provided by static friction:

$\theta \in \left[-\theta_1, \theta_1 \right]$

$M^i = M^{i-1} + \left(\theta^i - \theta^{i-1} \right) \times k$

Loading: $k_L = k_1$

Unloading: *If $M^i < k_{ZERO} \times \theta^i \Rightarrow k = k_{ZERO} = \max\left[\dfrac{1}{100} \times \max\left(k_L \right), k_{res} \right]$, $M^i = k_{ZERO} \times \theta^i$*

Else $k = k_U > \max\left(k_L \right)$

The analytical loading model adopts a linear segment with equal stiffness, k_1, for positive and negative rotations. The unloading model is the same as the one described for the strong bending axis.

Force values **larger** than the restraint provided by static friction:

$$M^i = M^{i-1} + \left(\theta^i - \theta^{i-1}\right) \times k$$

Loading: $-\theta_2 < \theta \le -\theta_1 \Rightarrow k = k_2 < k_1$

$\qquad \theta \le -\theta_2 \Rightarrow k = k_{res}$

$\qquad \theta \ge \theta_1 \Rightarrow k = k_{res}$ $\qquad\qquad$ $k_{res} = $ residual stiffness $= 0,0001$ N.mm/rad

Unloading: $k = k_U > \max\left(k_L\right)$

For a higher level of forces the analytical loading model, see Figure 4.6, for positive rotations is different than the one for negative rotations. For the former a residual stiffness is specified whereas for the latter a bilinear model is adopted, with a first linear segment with stiffness, k_2, smaller than k_1, followed by a second linear segment with residual stiffness. It is assumed that the direction of positive rotations is opposite to the joint locking direction. The unloading model is different than the one described for the strong bending axis, with just one linear segment of k_U stiffness whose value is greater than k_1.
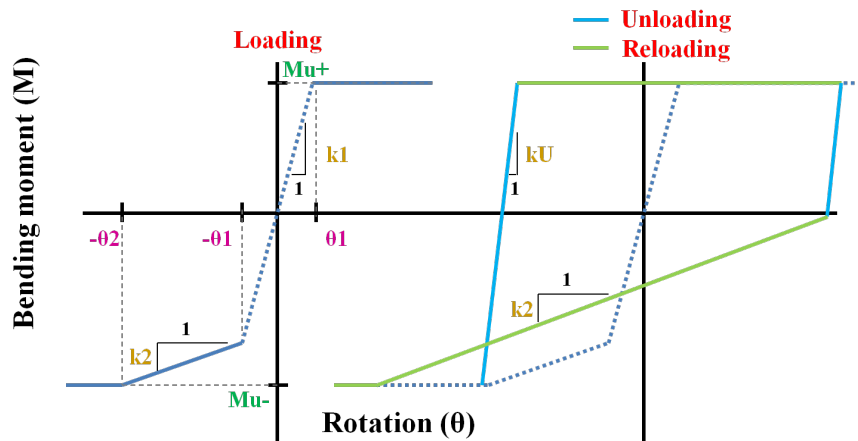
Figure 4.6: Analytical model for cyclic loading about the Cuplok® joint weak bending axis.

In both cases, the loading path in the negative direction matches the unloading path until the monotonic loading path is reached after which is followed until new unloading occurs. Figure 4.7 illustrates a comparison between the experimental behaviour and the one obtained using the proposed analytical model. It may be observed that there is a reasonable agreement between the actual and the predicted behaviour.
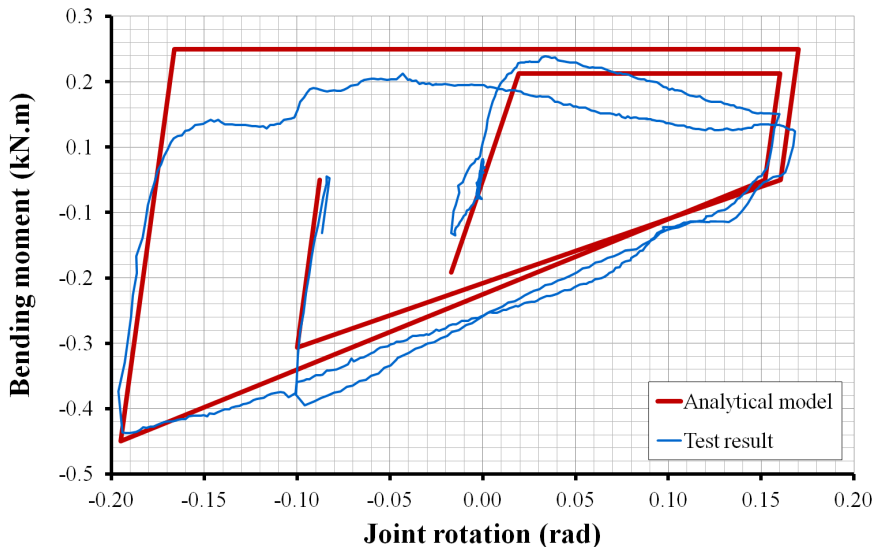
Figure 4.7: Comparison between the experimental behaviour and the one obtained using the proposed analytical model.

The input parameters of the analytical model are the rotations θ_1, θ_2, the stiffnesses k_1, k_2, k_U and the ultimate bending moment resistance for positive rotations, M_U+, and for negative rotations, M_U-.

When the joint is locked by hand it is assumed that the joint is pinned for this degree of freedom.

4.2.1.3   Axial axis

The analytical model for the axial axis is as follows, see Figure 4.8:

Compressive forces:

$$F^i = F^{i-1} + \left(\delta^i - \delta^{i-1}\right) \times k$$

$k = 1E6$ N/mm

Tensile forces:

$$\delta \in \left[0, \delta_{max}^+\right] \Rightarrow F^i = F^{i-1} + \left(\delta^i - \delta^{i-1}\right) \times k$$

$$\delta \in \left]\delta_{max}^+, +\infty\right[\Rightarrow F^i = \delta^i \times k$$

$$\delta \in \left[0, \delta_1^+\right] \Rightarrow k = k_1^+ = k_1^- = k_1 \qquad \text{with} \quad \delta_1^+ < \delta_2^+ < \delta_3^+ < \delta_4^+ < \delta_{max}^+ = 1{,}2 \times \delta_4^+$$

$$\delta \in \left]\delta_1^+, \delta_2^+\right] \Rightarrow k = k_2^+ = k_2^- = k_2$$

$$\delta \in \left]\delta_2^+, \delta_3^+\right] \Rightarrow k = k_3^+ = k_3^- = k_3$$

$$\delta \in \left]\delta_3^+, \delta_4^+\right] \Rightarrow k = k_4^+ = k_4^- = k_4$$

$$\delta \in \left]\delta_4^+, +\infty\right[\Rightarrow k = k_{res}^+ = k_{res}^- = k_{res}$$

$k_2 > k_3 > k_4 > k_{res}$, $k_2 > 0{,}5 \times k_1$

$k_{res} = $ residual stiffness $= 0{,}001$ N/mm

Unloading (bilinear model):

$$\text{If } F^i < k_{ZERO} \times \delta^i \Rightarrow k = k_{ZERO} = \max\left[\frac{1}{100} \times \max\left(k_L\right), k_{res}\right], F^i = k_{ZERO} \times \delta^i$$

$$\text{Else } k = k_U > \max\left(k_L\right), F^i = F^{i-1} + \left(\delta^i - \delta^{i-1}\right) \times k$$
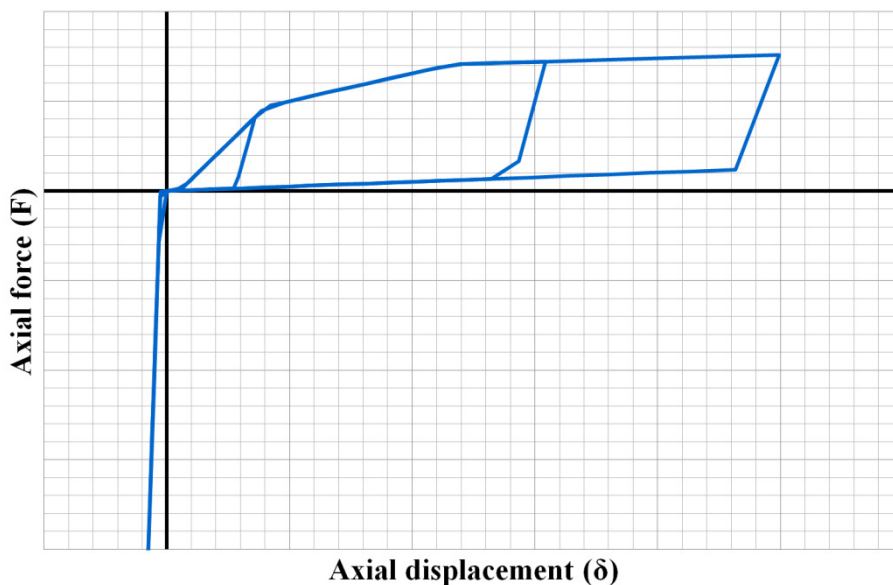
Figure 4.8: Analytical model for cyclic loading about the Cuplok® joint axial axis.

For compressive forces the analytical model considers a linear elastic behaviour with a very high stiffness, k, equal to 1×10^6 N/mm. For tensile forces a model equal as the one described for loading

about the strong bending axis is used, without considering stiffness and resistance degradation with increasing number of load reversals.

The input parameters of the analytical model are the tensile displacements δ_1, δ_2, δ_3, δ_4, the tensile stiffnesses k_1, k_2, k_3, k_4, k_U and the maximum tensile axial force F_{max}.

Figure 4.9 illustrates a comparison between the experimental behaviour and the one obtained using the proposed analytical model. It may be observed that there is a reasonable agreement between the actual and the predicted behaviour.
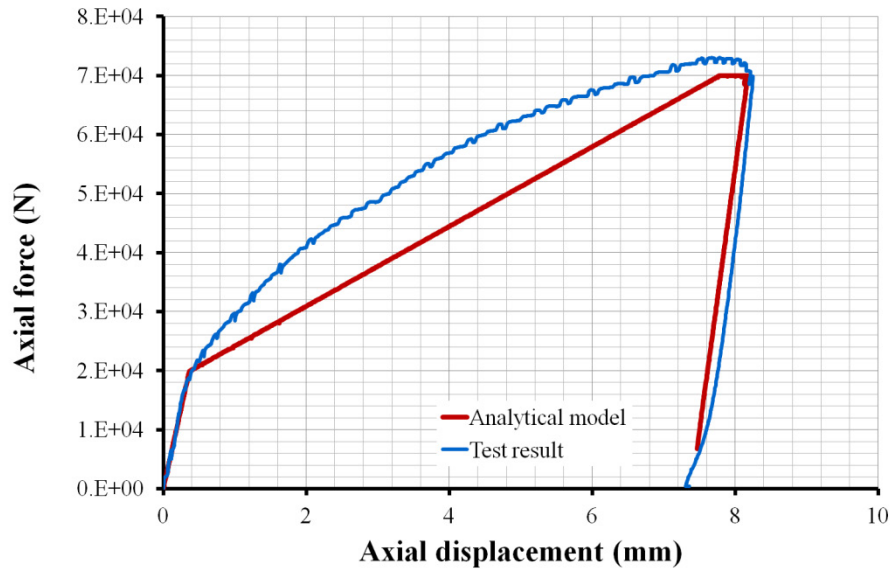
Figure 4.9: Comparison between the experimental behaviour and the one obtained using the proposed analytical model.

4.2.1.4 Other degrees of freedom

All degrees of freedom were considered to work in isolation. Therefore, no interaction between degrees of freedom was considered in the analytical model.

The degrees of freedom associated with shear displacements and torsion rotations were considered to be linear elastic and to work as rigid, with stiffness, k, equal to 1×10^6 N/mm, in the case of the degrees of freedom associated with shear displacements and as flexible in the case of the degree of freedom associated with the torsion rotations with a stiffness given as an input parameter of the analytical model. In general, a value equal to 100 kN.m/rad was adopted for the torsional axis.

4.2.2 Modelling of spigot joints

From the six degrees of freedom available at the spigot joint only the two degrees of freedom associated with the relative bending rotations between the upper and lower elements that are part of the spigot joint were included explicitly in the analytical model. The two orthogonal bending directions are initially defined by local axis y and local axis z, see Figure 4.10.
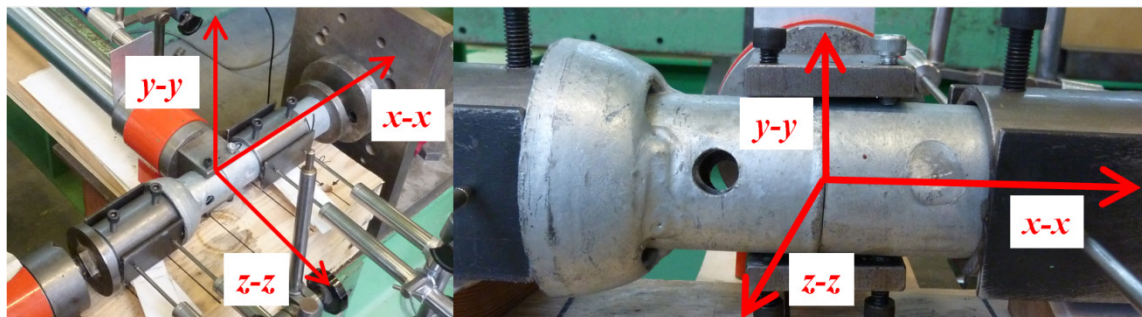
Figure 4.10: Local axis directions of spigot joint.

These directions were chosen so that one of the bending axes would coincide with the minor bending axis of the spigot element which is aligned with the two holes of the spigot tube wall.

4.2.2.1 Bending axis

The analytical model for bending rotations is as follows:

Monotonic loading

$$\theta \in \left[\theta_{max}^-, \theta_{max}^+\right] \Rightarrow M^i = M^{i-1} + \left(\theta^i - \theta^{i-1}\right) \times k$$

$$\theta \in \left]-\infty, \theta_{max}^-\right[\, , \left]\theta_{max}^+, +\infty\right[\Rightarrow M^i = \theta^i \times k$$

$$\theta \in \left[\theta_1^-, \theta_1^+\right] \Rightarrow k = k_1^+ = k_1^- = k_1$$

$$\theta \in \left[\theta_2^-, \theta_1^-\right[\, , \left]\theta_1^+, \theta_2^+\right] \Rightarrow k = k_2^+ = k_2^- = k_2$$

$$\theta \in \left[\theta_3^-, \theta_2^-\right[\, , \left]\theta_2^+, \theta_3^+\right] \Rightarrow k = k_3^+ = k_3^- = k_3 \qquad \text{with}$$

$$\theta \in \left[\theta_4^-, \theta_3^-\right[\, , \left]\theta_3^+, \theta_4^+\right] \Rightarrow k = k_4^+ = k_4^- = k_4$$

$$\theta \in \left]-\infty, \theta_4^-\right[\, , \left]\theta_4^+, +\infty\right[\Rightarrow k = k_{res}^+ = k_{res}^- = k_{res}$$

$$k_2 > k_3 > k_4 > k_{res}, \ k_2 > 0,5 \times k_1$$

$$k_{res} = \text{residual stiffness} = 0,0001 \text{ N.mm/rad}$$

$$\theta_1^+ \neq \theta_1^-$$
$$\theta_2^+ = \left|\theta_2^-\right| = \theta_2$$
$$\theta_3^+ = \left|\theta_3^-\right| = \theta_3$$
$$\theta_4^+ = \left|\theta_4^-\right| = \theta_4$$
$$\theta_{max}^+ = \left|\theta_{max}^-\right| = \theta_{max} = 1,4 \times \theta_4$$
$$\theta_1^+, \left|\theta_1^-\right| < \theta_2 < \theta_3 < \theta_4 < \theta_{max}$$

Cyclic loading

Unloading (bilinear model):

$$\textit{If } M^i < k_{ZERO} \times \theta^i \Rightarrow k = k_{ZERO} = \max\left[\frac{1}{100} \times \max(k_L), k_{res}\right], \ M^i = k_{ZERO} \times \theta^i$$

$$\textit{Else } k = k_U > \max(k_L), \ M^i = M^{i-1} + \left(\theta^i - \theta^{i-1}\right) \times k$$

As the bending failure of the spigot can occur for any arbitrary bending direction, the bending resistance of the spigot was also verified taking into account the resultant of the bending moment values about the two initially defined orthogonal bending directions.

The analytical model is equal to the one described for loading about the Cuplok® strong bending axis, without considering stiffness and resistance degradation with increasing number of load reversals.

The input parameters of the analytical model are the rotations θ_1, θ_2, θ_2, θ_4, the stiffnesses k_1, k_2, k_3, k_4, k_U and the ultimate bending moment resistance M_U. The value of these parameters change for each one of three axial force to bending moment ratios considered. Figure 4.11 illustrates an example.

Figure 4.12 illustrates a comparison between the experimental behaviour and the one obtained using the proposed analytical model. It may be observed that there is a reasonable agreement between the actual and the predicted behaviour.

As the constitutive model for bending rotations of the spigot joint depends on the ratio between the axial force and the bending moment, it was necessary to implement the following iteration process:

- Establish three ranges of N/M:
  - number 1, from $0 \leq |N/M| \leq 20 \text{ m}^{-1}$;
  - number 2, from $20 \text{ m}^{-1} < |N/M| \leq 50 \text{ m}^{-1}$;
  - number 3, from $50 \text{ m}^{-1} < |N/M| < +\infty$.
- Determine the number of N/M range, R^i, based on the last converged bending moment, M^0, and the current axial force value (N). Obtain the updated bending stiffness, k^i, and the corresponding new bending moment, M^i;
- Determine the number of N/M range, R, based on M^i, and the current axial force value (N). Obtain the updated bending stiffness, k, and the corresponding new bending moment, M;
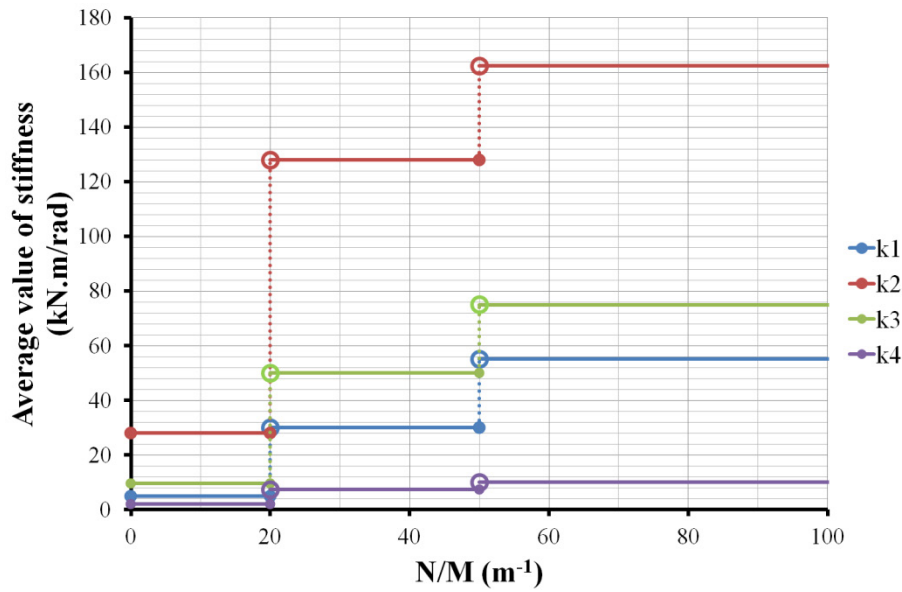
Figure 4.11: Example of the variation of joint stiffness with axial force to bending moment ratio.
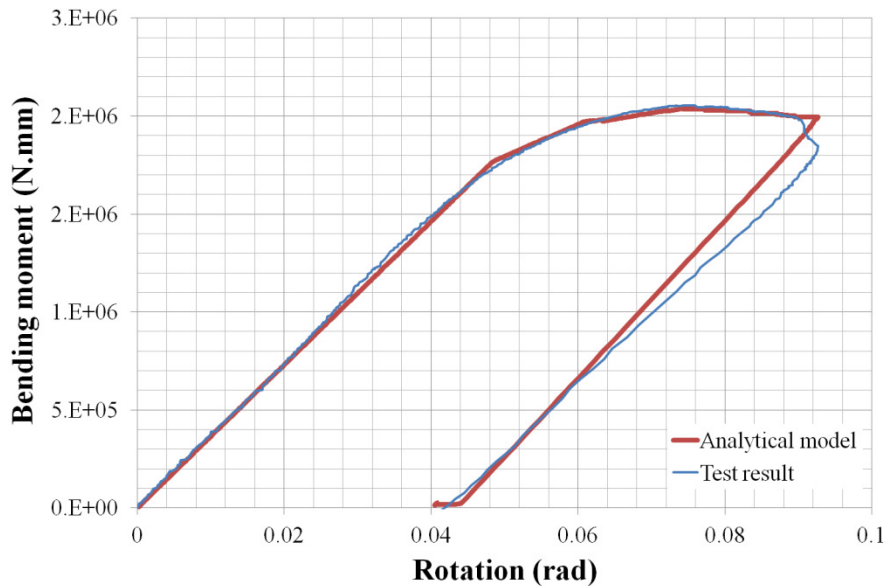
Figure 4.12: Comparison between the experimental behaviour and the one obtained using the proposed analytical model.

- Determine the number of N/M range, R^j, based on M, and the current axial force value (N). Obtain the updated bending stiffness, k^j, and the corresponding new bending moment, M^j;

- If $R^i = R = R^j$ then the bending moment for the current iteration is M and the current bending stiffness is k;

- If $R^i \neq R = R^j$ but $|R^i - R| \leq 1$ then if $|M - M^i| / M \leq \beta$ the bending moment for the current iteration is M and the current bending stiffness is k. If $|M - M^i| / M > \beta$ then a cutback is enforced;

- If $R^i = R \neq R^j$ but $|R^j - R| \leq 1$ then if $|M - M^j| / M \leq \beta$ the bending moment for the current iteration is M and the current bending stiffness is k. If $|M - M^j| / M > \beta$ then a cutback is enforced;

- If $|R^i - R| > 1$ or $|R^j - R| > 1$ or $|R^j - R^i| > 1$ a cutback is enforced.

The results obtained using $\beta = 0{,}1\%$ and $\beta = 10\%$ were almost coincident but the former value required a greater number of increments for the solver to finish the analysis. Therefore, the value of β was set to 10%.

4.2.2.2 Other degrees of freedom

All degrees of freedom were considered to work in isolation. Therefore, no interaction between degrees of freedom was considered in the analytical model.

The degrees of freedom associated with displacements were considered to be linear elastic and to work as rigid (stiffness, k, equal to 1×10^6 N/mm). In the case of the degree of freedom associated with torsion rotations a flexible joint with a stiffness given as an input parameter of the analytical model was used. In general, a value equal to 10 kN.m/rad was adopted for the torsional axis.

Besides the maximum bending rotation failure criterion it was also introduced a failure criteria associated with the maximum resistance that the spigot joint can resist if a pin is used. If a steel pin exists its strength was determined from (BSI, 1999, 2005f).

4.2.3 Modelling of forkhead joints

From the six degrees of freedom available at the forkhead joint only the degree of freedom associated with the relative bending rotation between the upper section of the top standard element or top jack element and the forkhead about the weak bending axis was included explicitly in the analytical model, defined by local axis x in Figure 4.13.
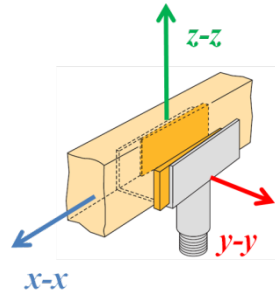
Figure 4.13: Local axis directions of forkhead joint.

4.2.3.1 Weak bending axis

The analytical model is equal to the one described for loading about the Cuplok® strong bending axis, without considering stiffness and resistance degradation with increasing number of load reversals.

The input parameters of the analytical model are the rotations θ_1, θ_2, θ_2, θ_4, the stiffnesses k_1, k_2, k_3, k_4, k_U and the ultimate bending moment resistance M_U.

Monotonic loading

$$\theta \in \left[\theta_{max}^-, \theta_{max}^+ \right] \Rightarrow M^i = M^{i-1} + \left(\theta^i - \theta^{i-1} \right) \times k$$

$$\theta \in \left]-\infty, \theta_{max}^- \right[\, , \left]\theta_{max}^+, +\infty \right[\Rightarrow M^i = \theta^i \times k$$

$$\theta \in \left[\theta_1^-, \theta_1^+ \right] \Rightarrow k = k_1^+ = k_1^- = k_1$$

$$\theta \in \left[\theta_2^-, \theta_1^- \right[\, , \left]\theta_1^+, \theta_2^+ \right] \Rightarrow k = k_2^+ = k_2^- = k_2$$

$$\theta \in \left[\theta_3^-, \theta_2^- \right[\, , \left]\theta_2^+, \theta_3^+ \right] \Rightarrow k = k_3^+ = k_3^- = k_3 \qquad \text{with}$$

$$\theta \in \left[\theta_4^-, \theta_3^- \right[\, , \left]\theta_3^+, \theta_4^+ \right] \Rightarrow k = k_4^+ = k_4^- = k_4$$

$$\theta \in \left]-\infty, \theta_4^- \right[\, , \left]\theta_4^+, +\infty \right[\Rightarrow k = k_{res}^+ = k_{res}^- = k_{res}$$

$$k_2 > k_3 > k_4 > k_{res}, \ k_2 > 0,5 \times k_1$$

$$k_{res} = \text{residual stiffness} = 0,0001 \text{ N.mm/rad}$$

$$\theta_1^+ \neq \theta_1^-$$
$$\theta_2^+ = \left|\theta_2^-\right| = \theta_2$$
$$\theta_3^+ = \left|\theta_3^-\right| = \theta_3$$
$$\theta_4^+ = \left|\theta_4^-\right| = \theta_4$$
$$\theta_{max}^+ = \left|\theta_{max}^-\right| = \theta_{max} = 1,4 \times \theta_4$$
$$\theta_1^+, \left|\theta_1^-\right| < \theta_2 < \theta_3 < \theta_4 < \theta_{max}$$

Cyclic loading

Unloading (bilinear model):

$$\textit{If } M^i < k_{ZERO} \times \theta^i \Rightarrow k = k_{ZERO} = \max\left[\frac{1}{100} \times \max(k_L), k_{res}\right], \; M^i = k_{ZERO} \times \theta^i$$

$$\textit{Else } k = k_U > \max(k_L), \; M^i = M^{i-1} + \left(\theta^i - \theta^{i-1}\right) \times k$$

Figure 4.14 illustrates a comparison between the experimental behaviour and the one obtained using the proposed analytical model. It may be observed that there is a reasonable agreement between the actual and the predicted behaviour.
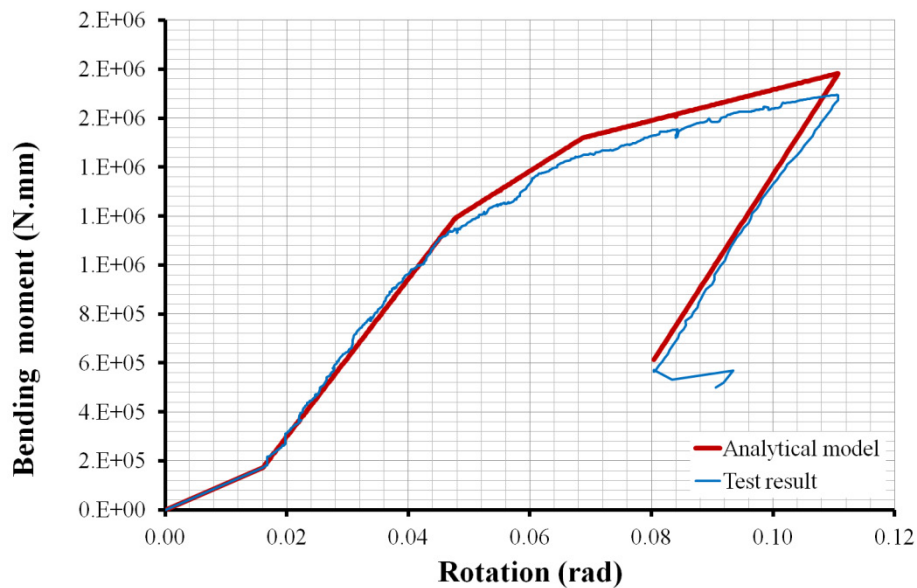
Figure 4.14: Comparison between the experimental behaviour and the one obtained using the proposed analytical model.

Due to absence of experimental results and as a simplification on the safe side, it was decided not to increase the rotational stiffness of the forkhead joint when forkheads which incorporate locating lugs to accept jack braces are used, or when jack braces are included.

4.2.3.2 Other degrees of freedom

All degrees of freedom were considered to work in isolation. Therefore, no interaction between degrees of freedom was considered in the analytical model.

The degrees of freedom associated with displacements were considered to be linear elastic and to work as rigid (stiffness, k, equal to 1×10^6 N/mm). In the case of the degree of freedom associated with torsion rotations a flexible joint with a linear elastic stiffness given as an input parameter of the analytical model was used, and finally for bending rotations about the strong bending axis (local y axis in Figure 4.13) a rigid joint with a linear elastic stiffness equal to 1×10^9 N.mm/rad was specified. In general, a value equal to 100 kN.m/rad was adopted for the torsional axis.

4.2.4 Modelling of brace joints

From the six degrees of freedom available at the brace joint, *i.e.* between a brace element and its supporting element (either a standard or a ledger element), only the degree of freedom associated with the displacements along the longitudinal (axial) axis of the brace element was included explicitly in the analytical model.

4.2.4.1 Axial axis

The analytical model for the axial axis is as follows, see Figure 4.15:

Compressive and Tensile forces:

$$\delta \in \left[-\delta_4, \delta_4 \right] \Rightarrow F^i = F^{i-1} + \left(\delta^i - \delta^{i-1} \right) \times k$$

$$\delta \in \left] -\infty, -\delta_4 \right[, \left] \delta_4, +\infty \right[\Rightarrow F^i = \delta^i \times k$$

$$\delta \in \left[\delta_1^-, \delta_1^+ \right] \Rightarrow k = k_1^+ = k_1^- = k_1$$

$$\delta \in \left[-\delta_2, \delta_1^- \right[, \left] \delta_1^+, \delta_2 \right] \Rightarrow k = k_2^+ = k_2^- = k_2$$

$$\delta \in \left[-\delta_3, -\delta_2 \right[, \left] \delta_2, \delta_3 \right] \Rightarrow k = k_3^+ = k_3^- = k_3 \quad \text{with} \quad \delta_1^+ < \delta_2^+ < \delta_3^+ < \delta_4^+$$

$$\delta \in \left[-\delta_4, -\delta_3 \right[, \left] \delta_3, \delta_4 \right] \Rightarrow k = k_4^+ = k_4^- = k_4$$

$$k_2 > k_3 > k_4, \ k_2 > 0,5 \times k_1$$

Unloading (bilinear model):

$$\textit{If } F^i < k_{ZERO} \times \delta^i \Rightarrow k = k_{ZERO} = \max \left[\frac{1}{100} \times \max \left(k_L \right), k_{res} \right], \ F^i = k_{ZERO} \times \delta^i$$

$$\textit{Else } k = k_U > \max \left(k_L \right), \ F^i = F^{i-1} + \left(\delta^i - \delta^{i-1} \right) \times k$$

The analytical model is similar to the one described for loading about the Cuplok® strong bending axis, without considering stiffness and resistance degradation with increasing number of load reversals. Also, based on the brace joint tests results reported in (Voelkel, 1990) it is assumed that these joints are brittle without significant deformation capacity for loads higher than the maximum load (associated with maximum displacement θ_4). As demonstrated in (Godley, Beale, 1997, 2001) it is necessary to properly evaluate the brace joints mechanical characteristics since for example the joint's axial stiffness is substantially different that the tube's axial stiffness. In the present work, the behaviour of the brace joints is derived from the brace joint tests results reported in (Voelkel, 1990).

The input parameters of the analytical model are the tensile displacements δ_1, δ_2, δ_3, δ_4, the tensile stiffnesses k_1, k_2, k_3, k_4, k_U and the maximum tensile axial force F_{max}.

Since the test procedure used in the tests reported in (Voelkel, 1990) is not available it is not possible to replicate the test using the proposed analytical model.
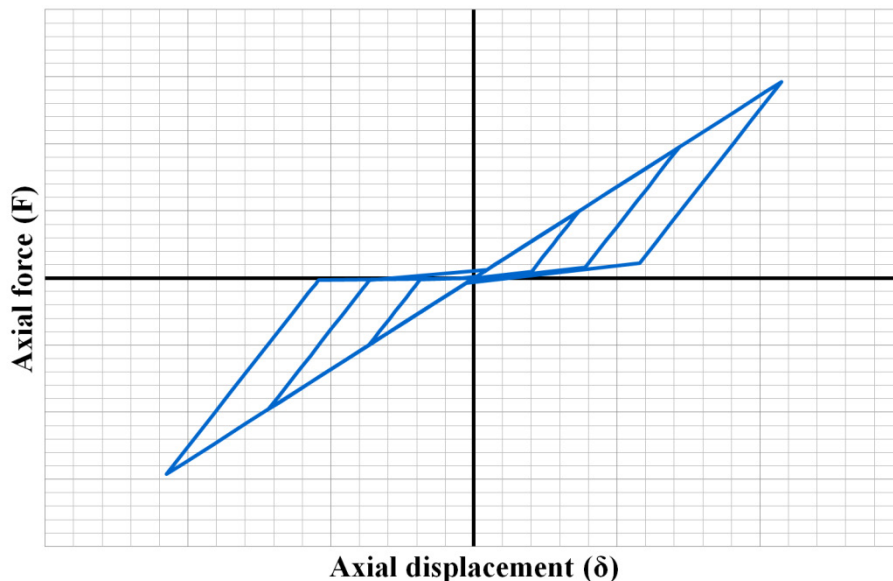
Figure 4.15: Analytical model for loading about the brace joint axial axis.

4.2.4.2 Other degrees of freedom

All degrees of freedom were considered to work in isolation. Therefore, no interaction between degrees of freedom was considered in the analytical model.

The degrees of freedom associated with shear displacements were considered to be linear elastic and to work as rigid (stiffness, k, equal to 1×10^6 N/mm). In the case of the degree of freedom associated with torsion rotations a flexible joint with a linear elastic stiffness given as an input parameter of the analytical model was used and finally the two bending rotations degrees of freedom were considered to be free to rotate. In general, a value equal to 50 kN.m/rad was adopted for the torsional axis.

4.2.5 Modelling of baseplate joints

The modelling of baseplate joints, *i.e.* the joints between the baseplate and the supporting ground, can be performed by explicitly modelling and meshing the baseplate elements and the ground without the need of special joints. However, it would be advantageous in terms of time needed to build the numerical model, runtime and time required to analyse the results if it was possible to develop a sufficiently accurate and flexible special joint.

An example of a model that potentially fulfils the above criteria is the analytical joint model presented in the standard EN 1065 (BSI, 1999) and illustrated in Figure 4.16 to simulate the bending behaviour at the base of a column similar to the ones of bridge falsework systems.
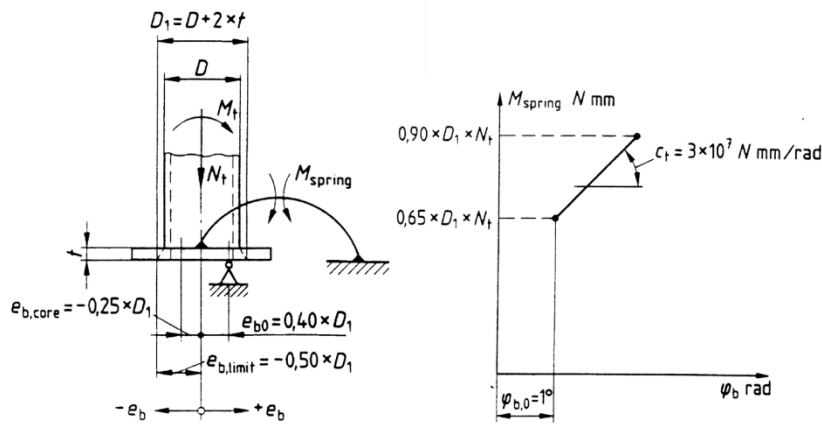
Figure 4.16: Analytical model for baseplate joints presented in EN 1065 (BSI, 1999).

4.2.5.1 Bending axis

For each one of the two bending axis, the model consists in a flexible joint with stiffness given as a function of the baseplate rotation, θ_b (φ_b in Figure 4.16 notation), and of the axial force eccentricity at the joint, M_S / A (M_{spring} / N_t in Figure 4.16 notation). The adopted analytical model differs from the EN 1065 model in that the initial joint rotation limit value, $\theta_{b,0}$ ($\varphi_{b,0}$ in Figure 4.16 notation), used to model base eccentricities is an input parameter that may be different than 1°. In order to avoid numerical problems the stiffness of the segment to be used until the load eccentricity at the base reaches $0.65 \times D_1$ is not taken as infinite but equal to 1×10^9 N.mm/rad. For the same reasons, the stiffness of the initial segment (for $\theta \leq \theta_{b,0}$) and of the segment to be used for load eccentricities larger than $0.90 \times D_1$ is not taken as zero but equal to 1×10^2 N.mm/rad.

The input parameters of the analytical model are the rotation $\theta_{b,0}$, the external diameter of the standard tube (D) and the thickness of the baseplate (t).

As the constitutive model for bending rotations of the baseplate joint depends on the ratio between the axial force and the bending moment, it was necessary to implement the following iteration process:

- Establish four ranges of M/N:

- o number 1, from $|M/N| = 0$ m;
- o number 2, from $0 < |M/N| \leq 0{,}65 \times D_1$;
- o number 3, from $0{,}65 \times D_1 < |M/N| \leq 0{,}90 \times D_1$;
- o number 4, from $0{,}90 \times D_1 < |M/N| < +\infty$.

- Determine the number of N/M range, R^i, based on the last converged bending moment, M^0, and the current axial force value (N). Obtain the updated bending stiffness, k^i, and the corresponding new bending moment, M^i;

- Determine the number of N/M range, R, based on M^i, and the current axial force value (N). Obtain the updated bending stiffness, k, and the corresponding new bending moment, M;

- Determine the number of N/M range, R^j, based on M, and the current axial force value (N). Obtain the updated bending stiffness, k^j, and the corresponding new bending moment, M^j;

- If $R^i = R = R^j$ then the bending moment for the current iteration is M and the current bending stiffness is k;

- If $R^i \neq R = R^j$ but $|R^i - R| \leq 1$ then if $|M - M^i| / M \leq \beta$ the bending moment for the current iteration is M and the current bending stiffness is k. If $|M - M^i| / M > \beta$ then a cutback is enforced;

- If $R^i = R \neq R^j$ but $|R^j - R| \leq 1$ then if $|M - M^j| / M \leq \beta$ the bending moment for the current iteration is M and the current bending stiffness is k. If $|M - M^j| / M > \beta$ then a cutback is enforced;

- If $|R^i - R| > 1$ or $|R^j - R| > 1$ or $|R^j - R^i| > 1$ a cutback is enforced.

The results obtained using $\beta = 0{,}1\%$ and $\beta = 10\%$ were almost coincident but the former value required a greater number of increments for the solver to finish the analysis. Therefore, the value of β was set to 10%.

4.2.5.2 Other degrees of freedom

All degrees of freedom were considered to work in isolation. Therefore, no interaction between degrees of freedom was considered in the analytical model.

The degrees of freedom associated with displacements were considered to be free, as well as in the case of the degree of freedom associated with torsion rotations.

4.2.6 Modelling of jack joints

These joints connect the top and bottom boundary elements (*i.e.* baseplates and headplates) to the jack elements, and the jacks to the main falsework (standard) elements.

The former joint consists of a pin that passes through the existing holes in the walls of the connected elements. Alternatively, the jacks can bear directly onto the baseplates (and headplates) endplates, or both elements can be welded together. The latter joint consists on a collar nut which engages with the outer standard tube. In all joints, there is an overlap length between the jack and the connected elements. These joints are similar to the ones found in prop elements, see (BSI, 1999).

It is assumed that the jacks are welded to the baseplates (and headplates) endplates, and that the collar nut is securely locked. Under these conditions these joints can be modelled as continuous.

4.2.7 Modelling of gap joints

It was necessary to simulate the contact between elements in different locations of bridge falsework systems. Therefore, gap joints were developed that allow free displacements and

rotations if a certain force combination is present at the joint and behave like continuous joints otherwise. These joints were then placed at the following places: (i) interfaces between the baseplate and the supporting ground (at baseplate joints), (ii) interfaces between the falsework system and the formwork system (at forkhead joints) and (iii) at the spigot joints.

As a simplification, it was considered that at the forkhead joints no resistance was available to oppose separation along the vertical axis in the presence of tension forces. If the separation is higher than the height of the wood wedges used to lock the plywood beam to the forkhead, then all restraints are removed and the joint is free to move and rotate.

At the baseplate joint, it was included the optional hypothesis that bolts were used to connect the baseplate to a suitable foundation element: injection bolts for instance on a concrete bedding. If these elements are present, then, only after they fail (in tension, in bending or in shear) is it possible for the joint to separate and move and rotate freely in the presence of tension forces.

At the spigot joint, it was included the hypothesis that a pin was inserted to connect the spigot element to the upper standard tube. If these elements are present, then, only after they fail (in tension, in bending or in shear, see (BSI, 1999)), is it considered that there is no resistance available to oppose separation along the vertical axis in the presence of tension forces. If the separation is higher than the free length of the spigot element, then all restraints are removed and the joint is free to move and rotate.

4.3 Development of numerical models

Numerical models of bridge falsework systems can be developed in various ways and adopting very different modelling options, finite element types, material models, etc. In the following an overview of the numerical models developed to study bridge falsework systems is presented.

4.3.1 Finite element types

4.3.1.1 Bridge falsework main elements

The main elements of bridge falsework systems are standards (including jacks), ledgers and braces. All these elements were modelled using second-order beam elements (*ABAQUS*® B32 element, see (Simulia, 2012a)), suitable for finite strains and large rotations problems, with a maximum mesh size not exceeding 50 mm. The sections of the different parts of the elements were included in the elements definitions.

The 3D mesh allowed to account for: (i) the exact relative positioning of the elements, for example brace joint eccentricities relative to the Cuplok® joint, (ii) nodal eccentricities, for example load eccentricities at the interface between the bridge falsework and the formwork systems, and (iii) geometrical imperfections, either the ones specified in design codes or the ones measured in site surveys.

4.3.1.2 Formwork system

The formwork system was considered made of plywood beams positioned in an orthogonal mesh on top of the bridge falsework system, and of plywood panels to which the construction loads were applied to. All the beam elements were modelled using second-order beam elements (*ABAQUS*® B32 element) with a maximum mesh size not exceeding 50 mm, and the plywood panels were modelled using first order reduced integration shell elements with second-order accuracy and enhanced hourglass modes control (*ABAQUS*® S4R element, see (Simulia, 2012a)), also suitable for finite strains and large rotations problems.

Since the centroids of the plywood beams and panel sections are not at the same height, multi-point constraints (MPC) between the nodes of the plywood beams and a surface defined on the plywood panels plane were activated. The nodes of the plywood beams were considered as slave and

the plywood panels surfaces were considered to be the master of the MPC. This node-to-surface MPC provides a rigid beam between slave nodes and the master surface to constrain the displacement and rotation at the slave nodes to the displacement and rotation at the master surface.

4.3.1.3 Joint elements

From the various types of joints presented in section 4.2 only the gap joints did not need the development of a new finite element. The gap joints were simulated by *ABAQUS®* MPC subroutine which controlled the contact restraints between the two nodes that formed each gap element, *ABAQUS®* GAPUNI element, see (Simulia, 2012d).

For all other joints a spring-like finite user element was developed through *ABAQUS®* UEL subroutine. The spring user element is made of three nodes, labelled *node 1*, *node 2* and *node 3*, respectively, each with six degrees of freedom: three displacements and three rotations. The first two nodes are coincident and were used to control the constitutive behaviour of the user element and each one belonged to a different element (beam element or another user element). The third node of the user element is the second node of one of the beam elements attached to the user element and the distance between the second and third node of the user element is non zero. This third node is used to determine the initial directions of the *x, y* and *z* axis of the local coordinate system of the user element, see Figure 4.17.

Lagrange multipliers were not implemented in the UEL because they are not recommended (Simulia, 2012c ; Shi et al., 2010).
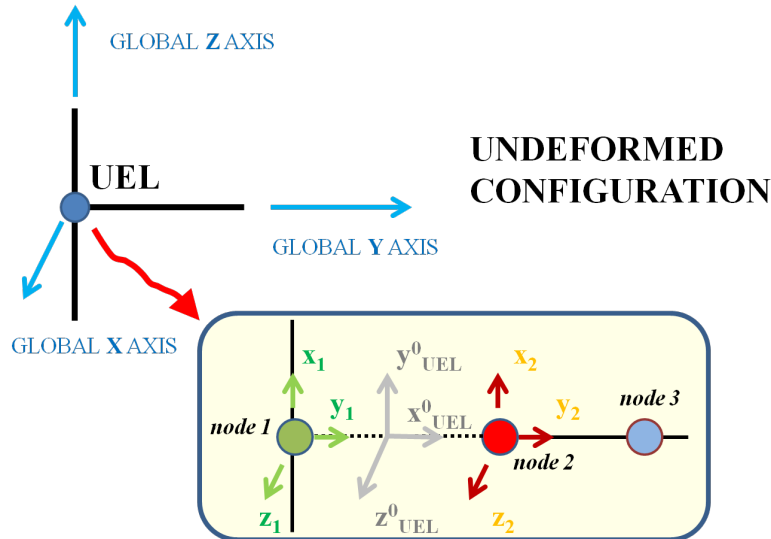
Figure 4.17: Example of the user element nodal definition.

4.3.1.3.1 Notation

E^{ID} is a matrix with additional label *ID*;

q^{ID} is a vector with additional label *ID*;

X_n is a scalar, the *n*th element of the vector *X*.

4.3.1.3.2 Transformation matrix

Let **E** be defined as the transformation matrix that represents the unit vectors of the user element initial local coordinate system (e_x, e_y, e_z) in the global coordinate system (e_X, e_Y, e_Z):

$$\begin{bmatrix} e_x \\ e_y \\ e_z \end{bmatrix} = \begin{bmatrix} \mathbf{E} \end{bmatrix} \begin{bmatrix} e_X \\ e_Y \\ e_Z \end{bmatrix} \qquad (4.1)$$

In the initial undeformed configuration, $\mathbf{E} \equiv \mathbf{E}^0$. The first unit vector of $\mathbf{E}^0$, $E^{0,x}$, is determined from the coordinates of *node 2* and *node 3* of the user element:

$$\left[E^{0,x} \right] = \left[\frac{X_3 - X_2}{\|3 - 2\|}, \frac{Y_3 - Y_2}{\|3 - 2\|}, \frac{Z_3 - Z_2}{\|3 - 2\|} \right] \tag{4.2}$$

$E^{0,z}$ is determined by specifying that it is normal to the plane defined by $E^{0,x}$ and the vector *q*:

$$\left[E^{0,z} \right] = \frac{E^{0,x} \times q}{\|E^{0,x} \times q\|} \text{ with } \left[q \right]^{\mathrm{T}} = \begin{bmatrix} 0 & 0 & 1 \end{bmatrix} \tag{4.3}$$

If $q \mathbin{/\!/} E^{0,x}$ then $E^{0,z} \equiv q$.

Having determined the first and third unit vectors of $\mathbf{E}^0$, the second vector $E^{0,y}$ is obtained by:

$$\left[E^{0,y} \right] = E^{0,z} \times E^{0,x} \tag{4.4}$$

Having defined the initial orthonormal base, the matrix $\mathbf{E}$ in the current *i* (deformed) deformation is given by equation (4.5).

$$^{i}\left[\mathbf{E} \right] = {}^{i}\left[\mathbf{R} \right]^{i-1}\left[\mathbf{E} \right] \tag{4.5}$$

$$\text{for } i = 1 \Rightarrow {}^{1}\left[\mathbf{E} \right] = {}^{1}\left[\mathbf{R} \right]^{0}\left[\mathbf{E} \right] = {}^{1}\left[\mathbf{R} \right]\left[\mathbf{E}^0 \right] \tag{4.6}$$

where $\mathbf{R}$ is a rotation matrix.

4.3.1.3.3 Finite rotations

If arbitrary large rotations occur, relative rotations between *node 1* and *node 2* of the user element cannot be determined by simply subtracting the rotation of *node 1* by the rotation of *node 2*, because finite rotations are not additive. However, if the rotations are small enough the error of using linearised relative rotations may be acceptable.

Finite rotations are expressed by a finite rotation vector, ϕ, consist of a rotation magnitude, $\theta = \|\phi\|$, and a rotation axis or direction in space, P (Simulia, 2012e). Physically, the rotation ϕ is interpreted as a rotation by θ radians around the axis P. To characterise this finite rotation mathematically, the rotation vector is used to define an orthogonal transformation or rotation matrix by the Rodrigues formula (Crisfield, 1997):

$$\left[\mathbf{R} \right] = \left[\mathbf{I} \right] + \frac{\sin\|\phi\|}{\|\phi\|}\left[\hat{\phi} \right] + \frac{1 - \sin\|\phi\|}{\|\phi\|^2}\left[\hat{\phi} \right]^2 \tag{4.7}$$

where $\left[\hat{\phi} \right]$ is the skew-symmetric matrix of ϕ given by:

$$\left[\hat{\phi} \right] = \begin{bmatrix} 0 & -\gamma & \beta \\ \gamma & 0 & -\alpha \\ -\beta & \alpha & 0 \end{bmatrix} \quad , \quad \phi^{\mathrm{T}} = \begin{bmatrix} \alpha & \beta & \gamma \end{bmatrix} \text{ and } \left[\mathbf{I} \right] \text{ is the identity matrix.}$$

4.3.1.3.4 Relative rotations

To calculate the relative rotations, ϕ_i, between *node 1* and *node 2* of the user element it is necessary that both rotation vectors are defined in the same basis. Let this basis be the local coordinate system of *node 1* of the user element. Further, let $\mathbf{R}^{12}$ be the rotation matrix that rotates the local coordinate system of *node 2* into the local coordinate system of *node 1*:

$$\left[\mathbf{R}^{12} \right] = \left[\mathbf{R}^1 \right]\left[\mathbf{R}^2 \right]^{\mathrm{T}} \tag{4.8}$$

Therefore, the rotation vector, ϕ, of the tensor $\mathbf{R}^{12}$ gives the relative rotations between *node 1* and *node 2* of the user element. The Spurrier's algorithm is used to extract ϕ out of $\mathbf{R}^{12}$ (Crisfield, 1997). The vector thus determined is expressed in the global coordinate system. However, the constitutive model requires ϕ expressed in the user element local coordinate system.

First, the user element local coordinate system, $\mathbf{E}$, must be defined, see equation (4.5). It is assumed that the rotation matrix $\mathbf{R}$ in equation (4.5) is the rotation matrix of *node 1* of the user element. Therefore, ϕ expressed in the user element local coordinate system is given by:

$$\left[\phi^L \right] = \left[\mathbf{E} \right]\left[\phi^G \right] = \left[\begin{array}{ccc} \phi_x^L & \phi_y^L & \phi_z^L \end{array} \right]^{\mathrm{T}} \tag{4.9}$$

4.3.1.3.5   Relative displacements

Relative displacements, δ_i, are obtained by:

$$\text{Global coordinate system: } \left[\delta^G \right] = \left[r^{0,2} \right] + \left[u^2 \right] - \left(\left[r^{0,1} \right] + \left[u^1 \right] \right) = \left[r^2 \right] - \left[r^1 \right] \tag{4.10}$$

$$\text{Local coordinate system: } \left[\delta^L \right] = \left[\mathbf{E} \right]\left[\delta^G \right] = \begin{bmatrix} \delta_x^L \\ \delta_y^L \\ \delta_z^L \end{bmatrix} \tag{4.11}$$

where $\left[r^{0,i} \right]$ is the position vector of node i in the undeformed configuration, $i = 1,2$

$\left[r^i \right]$ is the position vector of node i in the current configuration, $i = 1,2$

$\left[u^i \right]$ is the displacement vector of node i in the current configuration, $i = 1,2$

4.3.1.3.6   Stiffness matrix and internal forces

The user element internal force vector expressed in the local coordinate system of the user element for a generic node is determined by:

$$\begin{bmatrix} f^L \\ - \\ m^L \end{bmatrix} = \left[\mathbf{K}^L \right] \begin{bmatrix} \delta^L \\ - \\ \phi^L \end{bmatrix} \tag{4.12}$$

where $\left[f^L \right], \left[m^L \right]$ are the internal forces and moments of the user element:

$$\left[f^L \right] = \begin{bmatrix} F_x^L \\ F_y^L \\ F_z^L \end{bmatrix} \quad , \quad \left[m^L \right] = \begin{bmatrix} M_x^L \\ M_y^L \\ M_z^L \end{bmatrix} \tag{4.13}$$

$\left[\delta^L \right], \left[\phi^L \right]$ are the relative displacements and rotations of the user element

$\left[\mathbf{K}^L \right]$ is the local stiffness matrix of the user element:

$$\left[\mathbf{K}^L \right] = \begin{bmatrix} k_{\delta x}^L & 0 & 0 & 0 & 0 & 0 \\ 0 & k_{\delta y}^L & 0 & 0 & 0 & 0 \\ 0 & 0 & k_{\delta z}^L & 0 & 0 & 0 \\ 0 & 0 & 0 & k_{\theta x}^L & 0 & 0 \\ 0 & 0 & 0 & 0 & k_{\theta y}^L & 0 \\ 0 & 0 & 0 & 0 & 0 & k_{\theta z}^L \end{bmatrix} \tag{4.14}$$

where k_i is the stiffness of the i degree of freedom of the node and is given by the user element constitutive model presented in section 4.2.

These matrices are then discretised between the nodes of the user element. Considering the first two nodes of the user element:

$$
\begin{aligned}
F_i^{L,1} &= -F_i^{L,2} \quad , \quad i = 1,2,3 \\
M_i^{L,1} &= -M_i^{L,2} \quad , \quad i = 1,2,3 \\
k_{ij}^{L,1} &= k_{ij}^{L,2} \quad \text{for} \quad i = j \\
k_{ij}^{L,1} &= -k_{ij}^{L,2} \quad \text{for} \quad i \neq j
\end{aligned}
\tag{4.15}
$$

The user element internal forces vector expressed in the global coordinate system is determined by:

$$
\begin{bmatrix} f^G \\ - \\ m^G \end{bmatrix} = \begin{bmatrix} E \end{bmatrix}^T \begin{bmatrix} f^L \\ - \\ m^L \end{bmatrix}
\tag{4.16}
$$

The user element stiffness matrix expressed in the global coordinate system is determined by:

$$
\begin{bmatrix} \mathbf{K}^G \end{bmatrix} = \begin{bmatrix} \dfrac{df^G}{du^i} & \dfrac{df^G}{d\theta^i} \\ \dfrac{dm^G}{du^i} & \dfrac{dm^G}{d\theta^i} \end{bmatrix}
\tag{4.17}
$$

where $d\theta^i$ is the "linearised" rotation vector of node i of the user element (Simulia, 2012e).

Considering equation (4.16), the derivatives for *node 1* of the user element are expressed by:

$$
\left[\frac{df^{G,1}}{du^i} \right] = \sum_{j=x,y,z} E^j \left[\sum_{k=x,y,z} \left(\frac{dF_k^L}{d\delta_k^L} \frac{d\delta_k^L}{du^i} + \frac{dF_k^L}{d\phi_k^L} \frac{d\phi_k^L}{du^i} \right) \right] + \sum_{j=x,y,z} F_j^L \frac{dE^j}{du^i}
\tag{4.18}
$$

$$
\left[\frac{df^{G,1}}{d\theta^i} \right] = \sum_{j=x,y,z} E^j \left[\sum_{k=x,y,z} \left(\frac{dF_k^L}{d\delta_k^L} \frac{d\delta_k^L}{d\theta^i} + \frac{dF_k^L}{d\phi_k^L} \frac{d\phi_k^L}{d\theta^i} \right) \right] + \sum_{j=x,y,z} F_j^L \frac{dE^j}{d\theta^i}
\tag{4.19}
$$

$$
\left[\frac{dm^{G,1}}{du^i} \right] = \sum_{j=x,y,z} E^j \left[\sum_{k=x,y,z} \left(\frac{dM_k^L}{d\delta_k^L} \frac{d\delta_k^L}{du^i} + \frac{dM_k^L}{d\phi_k^L} \frac{d\phi_k^L}{du^i} \right) \right] + \sum_{j=x,y,z} M_j^L \frac{dE^j}{du^i}
\tag{4.20}
$$

$$
\left[\frac{dm^{G,1}}{d\theta^i} \right] = \sum_{j=x,y,z} E^j \left[\sum_{k=x,y,z} \left(\frac{dM_k^L}{d\delta_k^L} \frac{d\delta_k^L}{d\theta^i} + \frac{dM_k^L}{d\phi_k^L} \frac{d\phi_k^L}{d\theta^i} \right) \right] + \sum_{j=x,y,z} M_j^L \frac{dE^j}{d\theta^i}
\tag{4.21}
$$

The derivatives $\dfrac{dF_k^L}{d\delta_k^L}$, $\dfrac{dF_k^L}{d\phi_k^L}$, $\dfrac{dM_k^L}{d\delta_k^L}$ and $\dfrac{dM_k^L}{d\phi_k^L}$ correspond to the components of the stiffness matrix, see equation (4.14):

$$
\frac{dF_k^L}{d\delta_k^L} = k_{\delta k}^L \quad , \quad \frac{dF_k^L}{d\phi_k^L} = 0 \quad , \quad \frac{dM_k^L}{d\delta_k^L} = 0 \quad , \quad \frac{dM_k^L}{d\phi_k^L} = k_{\phi k}^L
\tag{4.22}
$$

From equations (4.9) and (4.11), the derivatives of the relative rotations and relative displacements with respect to the displacement vectors of *node 1* and *node 2* of the user element are given by:

$$
\frac{d\delta_k^L}{du^1} = -E^k \quad , \quad \frac{d\delta_k^L}{du^2} = E^k \quad , \quad \frac{d\phi_k^L}{du^i} = 0
\tag{4.23}
$$

The derivatives of the relative rotations and relative displacements with respect to the "linearised" rotation vectors of *node 1* and *node 2* of the user element are more complicated. Considering that the rotation matrix, **R**, is expressed in terms of *node 1* rotations, the derivatives of the relative displacements with respect to the "linearised" rotation vectors of *node 1* and *node 2* of the user element are given by:

$$\frac{d\delta_k^L}{d\theta^1} = -\left(\left[r^2\right] - \left[r^1\right]\right)\left[\hat{E}^j\right] \quad , \quad \frac{d\delta_k^L}{d\theta^2} = 0 \tag{4.24}$$

with $\dfrac{dE^j}{d\theta^1} = -\left[\hat{E}^j\right]$ (Crisfield, 1997 ; Simulia, 2012e).

From equation (4.9), the derivatives of the relative rotations with respect to the "linearised" rotation vectors of *node 1* and *node 2* of the user element are given by:

$$\frac{d\phi_k^L}{d\theta^1} = \phi^G \frac{dE^k}{d\theta^1} + E^k \frac{d\phi^G}{d\theta^1} \quad , \quad \frac{d\phi_k^L}{d\theta^2} = \phi^G \frac{dE^k}{d\theta^2} + E^k \frac{d\phi^G}{d\theta^2} \tag{4.25}$$

with:

$$\frac{dE^j}{d\theta^1} = -\left[\hat{E}^j\right] \quad , \quad \frac{dE^j}{d\theta^2} = 0 \quad , \quad \frac{dE^j}{du^i} = 0 \tag{4.26}$$

and:

$$\frac{d\phi^G}{d\theta^i} = \frac{d\phi^G}{d\theta^{12}} \frac{d\theta^{12}}{d\theta^i} \tag{4.27}$$

with (Crisfield, 1997 ; Simulia, 2012e):

$$\theta^{12} = \theta^1 - \mathbf{R}^{12} \theta^2 \tag{4.28}$$

The derivative between the relative rotations vector and the relative "linearised" rotations vector is given by (Crisfield, 1997 ; Simulia, 2012e):

$$\frac{d\phi^G}{d\theta^{12}} = T\left(\phi^{12}\right) \tag{4.29}$$

where:

$$\mathbf{T}\left(\phi^{12}\right) = \frac{1}{\left\|\phi^{12}\right\|^2}\left(\phi^{12}\phi^{12}\right) + \frac{\left\|\phi^{12}\right\|\sin\left\|\phi^{12}\right\|}{2\left(1-\cos\left\|\phi^{12}\right\|\right)}\left[\left[\mathbf{I}\right] - \frac{1}{\left\|\phi^{12}\right\|^2}\left(\phi^{12}\phi^{12}\right)\right] - \frac{1}{2}\left[\hat{\phi}^{12}\right] \tag{4.30}$$

The derivatives between the relative "linearised" rotations vector and the "linearised" rotations vector are given by (Crisfield, 1997 ; Simulia, 2012e):

$$\frac{d\theta^{12}}{d\theta^1} = \left[\mathbf{I}\right] \quad , \quad \frac{d\theta^{12}}{d\theta^2} = -\left[\mathbf{R}^{12}\right] \tag{4.31}$$

Inserting equations (4.26) to (4.31) in equation (4.25):

$$\frac{d\phi_k^L}{d\theta^1} = -\phi^G\left[\hat{E}^k\right] + E^k\left[\mathbf{T}\left(\phi^G\right)\right] \quad , \quad \frac{d\phi_k^L}{d\theta^2} = -E^k\left[\mathbf{T}\left(\phi^G\right)\right]\left[\mathbf{R}^{12}\right] \tag{4.32}$$

For *node 2* of the user element the derivatives are given by enforcing internal equilibrium:

$$\begin{aligned}
\left[\frac{df^{G,2}}{du^i}\right] &= -\left[\frac{df^{G,1}}{du^i}\right] \\[4pt]
\left[\frac{df^{G,2}}{d\theta^i}\right] &= -\left[\frac{df^{G,1}}{d\theta^i}\right] \\[4pt]
\left[\frac{dm^{G,2}}{du^i}\right] &= -\left[\frac{dm^{G,1}}{du^i}\right] \\[4pt]
\left[\frac{dm^{G,2}}{d\theta^i}\right] &= -\left[\frac{dm^{G,1}}{d\theta^i}\right]
\end{aligned} \tag{4.33}$$

For *node 3* the entire internal force vector and the stiffness matrix were considered to be zero.

4.3.2 Materials

Only one type of material was considered for each system: (i) steel for the bridge falsework system and (ii) plywood for the formwork system. Ground was not explicitly modelled.

The steel was modelled by an isotropic elastic material with loading rate independent Young modulus, *E*, and Poisson coefficient, *υ*, with isotropic plasticity and isotropic hardening. A linear damage evolution model was also considered by reducing the internal forces of the element linearly as a function of plastic deformation values larger than the deformation value at tensile strength. When the Ramberg-Osgood relationship parameters were available this model was preferred.

Plywood was modelled as orthotropic elastic material with loading rate independent isotropic plasticity and isotropic hardening. A linear damage evolution model identical to the one used for steel was considered.

4.3.3 Loading

Different loads were considered:

1. Construction loads: By applying pressure loads on the shell elements surface in models where the formwork system was included and by concentrated forces in the models where the formwork system was not included. The concentrated forces were either considered equal or determined based on the influence areas of each vertical element;

2. Wind action: By applying distributed (linear) loads over the length of the vertical elements;

3. Ground settlement: By applying imposed displacements to the model restraints.

4.3.4 Solvers

ABAQUS® offers two types of solvers: (i) implicit solvers which are unconditionally stable, can solve static, quasi-static and dynamic problems, but require the system's stiffness matrix to be inverted at least at every increment, and (ii) explicit solvers which are conditionally stable, are designed for short time events and do not require the system's stiffness matrix to be inverted.

4.3.4.1 Implicit solvers

The most common method to solve nonlinear differential equations is the Newton-Raphson method. *ABAQUS*® also offers for static analyses another method which is based on the Riks arc-length method (Simulia, 2012b).

Dynamic analyses are based on the Hilber-Hughes-Taylor (HHT) time integration method. This method is an extension of the classic Newmark method, introducing the parameter, *α*, which controls the amount of numerical dissipation that is introduced. For *α* = 0 this method reduces to the Newmark method. For quasi-static analysis the backward Euler method is used (Simulia, 2012b). In general, the quasi-static method tends to result in the best convergence behaviour due to high numerical damping dissipation and the Hilber-Hughes-Taylor method tends to have the highest likelihood of convergence difficulty.

If the analysis fails to converge with the classic static solvers it is recommended to try the dynamic solvers, in particular the quasi-static solver.

In the present Thesis, all of the above methods were used. The Hilber-Hughes-Taylor time integration method required additional coding into the user element as follows:

The internal force vector is now given by:

$$^{t+\Delta t}F = -\left[\mathbf{M}\right] \times {}^{t+\Delta t}\ddot{u} + \left(1+\alpha\right) \times {}^{t+\Delta t}G - \alpha \times {}^{t}G \tag{4.34}$$

where **M** is the mass matrix and *G* is the static force residual vector.

It was therefore necessary to store in the UEL subroutine the last converged values of the static force residual, as well as to specify a mass matrix. It was considered that the joint mass was uncoupled, equally distributed by the two first nodes and by each of the six displacements degrees of freedom. The same principle was applied to the rotational inertia for the rotational displacements. It was considered that the joint mass was equal to 10 kg and that the joint rotational inertia was equal to 100 kg.mm^2, both properties equally distributed between the two coincident nodes, *nodes 1* and *2*, of the user element.

The jacobian also changes to:

$$\left[\mathbf{J}\right]=\left[\mathbf{M}\right]\left(\frac{d\ddot{u}}{du}\right)+\left(1+\alpha\right)\left[\mathbf{K}\right] \quad , \quad \frac{d\ddot{u}}{du}=\frac{1}{\beta\left(\Delta t\right)^2} \tag{4.35}$$

where β is beta parameter of the Hilber-Hughes-Taylor time integration method.

4.3.4.2 Explicit solvers

Explicit solvers are a good alternative for pure dynamic problems but require a large number, for some analysis millions, of small time increments to complete the time step.

The equations of motion for the body are integrated using the explicit central-difference integration method which is conditionally stable. The undamped stability limit is given in terms of the highest frequency of the system as (Simulia, 2012b):

$$\Delta t \leq \frac{2}{\omega_{max}} \tag{4.36}$$

The stability limit can be approximately obtained by the smallest time a dilatational wave needs to cross any of the elements in the mesh (Simulia, 2012b):

$$\Delta t \approx \frac{\min(L)}{c_d} \tag{4.37}$$

where min(L) is the smallest element dimension and c_d is the material's dilatational wave speed which for steel can be taken to be equal to 5000 m/s (Simulia, 2012b).

Explicit solvers can also be used in quasi-static analysis but the results should be carefully analysed. It is recommended that the kinetic energy should not exceed 5% of the internal strain energy of the system (Simulia, 2012b).

Since explicit solvers can take a long runtime to complete it is possible to artificially boost the speed of time integration by using mass scaling techniques. By increasing the material density the highest frequency of the system is reduced and thus the maximum value of the stable time increment increases. Special attention should be paid to the results obtained.

It was necessary to develop a new subroutine, ABAQUS® VUEL subroutine which shares the same joint constitutive model of the UEL subroutine but needs additional coding to determine the stable increment:

Let **S, Γ** be two diagonal matrices with the first three diagonal elements equal to the joint rotational stiffnesses and joint rotational inertia, respectively:

$$\left[\mathbf{S}\right]=\begin{bmatrix} k_{\theta x} & & & \\ & k_{\theta y} & & \\ & & k_{\theta z} & \\ & & & 0_{3\times3} \end{bmatrix} \quad \left[\mathbf{\Gamma}\right]=\begin{bmatrix} RI_x & & & \\ & RI_y & & \\ & & RI_z & \\ & & & 0_{3\times3} \end{bmatrix} \tag{4.38}$$

Let λ_S be the maximum eigenvalue of the matrix **S** and λ_{RI} be the minimum eigenvalue of the matrix **Γ**. The trial value of the stable time increment based for rotations is given by:

$$\Delta t_\theta = \sqrt{2\frac{\lambda_{RI}}{\lambda_S}} \tag{4.39}$$

The trial value of the stable time increment based for displacements is given by:

$$\Delta t_\delta = \sqrt{2\frac{m_x}{k_x}} \tag{4.40}$$

where m_x is the joint mass associated with the local x axis.

The undamped stable time increment is given by $\min(\Delta t_\delta, \Delta t_\theta)$.

4.3.5 Overall control procedure

Figure 4.18 illustrates a schematic representation of the overall control process of the numerical models.
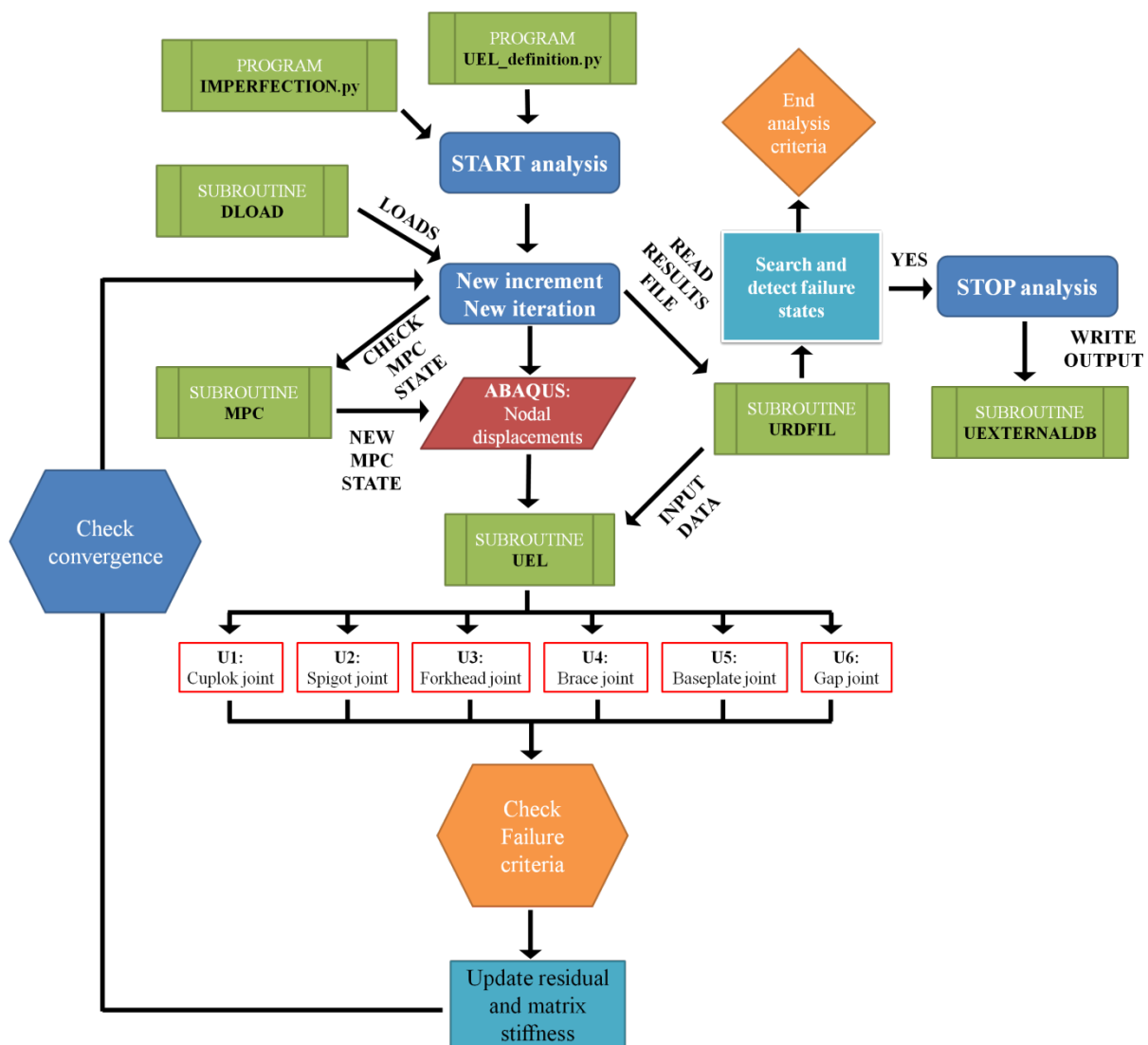
Figure 4.18: Flowchart representation of the overall control process of the numerical models.

At the start of the analysis, python programs generate the mesh imperfection, the user element definitions (nodal connectivity, element definitions, elements constitutive model). At the start of every new increment, or every new iteration, the MPC states are checked and updated and the load distribution and magnitude is updated via *ABAQUS®* DLOAD subroutine. Also at the start of every new increment, output information is written to an output file and read with *ABAQUS®* URDFIL subroutine. Specific information is stored in global variables and made available to *ABAQUS®* UEL subroutine.

Additionally, criteria to stop the analysis are checked and if one criterion is met the analysis is terminated and the specified output is written to a text file by *ABAQUS®* UEXTERNALDB subroutine.

After *ABAQUS®* computes the new nodal displacements and rotations, the UEL subroutine is called to update the residual vector and the stiffness matrix. If the convergence criteria are met the analysis continues to a new increment, if not to a new iteration or cutback.

4.4 Validation of numerical models

In order to validate the numerical models developed to study the behaviour of bridge falsework systems several parameters were analysed.

The model selected consists in a structure used in a series of full-scale tests performed at the University of Sydney in 2006, and published in (Chandrangsu, Rasmussen, 2009a), using the Cuplok® system. The structure displays a grid frame of three-by-three bays with a constant nominal bay width of 1829 mm in both directions, with three lifts with equal nominal lift height of 1,5 m and 600 mm of jack extension height. The bracing configuration used is represented in Figure 4.19.

The standards were made from cold-formed circular steel tube section (CHS) with a nominal yield stress of 450 MPa. The cross-section had a nominal external diameter of 48,3 mm and a wall thickness of 4 mm. Ledgers were made of steel with nominal yield stress of 350 MPa, also of CHS with a nominal external diameter of 48,3 mm and thickness of 3,2 mm. The telescopic brace elements, CHS with outer tube cross-section of 48,3 mm × 4,0 mm and inner tube cross-section of 38,2 mm × 3,2 mm, were connected to the ledgers by hook joints. The nominal yield stress of the brace elements steel was equal to 400 MPa. The adjustable jacks were made of 36 mm diameter threaded steel rods with nominal yield stress equal to 430 MPa. The rectangular baseplates were 180 mm wide and 10 mm thick with nominal yield stress equal 250 MPa (Chandrangsu, Rasmussen, 2009a).

For each test, the initial geometric imperfections of the standard elements were measured and recorded. The load was introduced at the top of the falsework structure by hydraulic jacks pinned on a grid of timber beams which were positioned on top of the forkheads, see Figure 4.19.

In all models considered in the present section, an identical constitutive model was used for the user elements of the same type. The values of the input parameters of each constitutive model were taken as the average values of the results reported in Chapter 3 of this Thesis.

Concentrated vertical loads, of equal magnitude, were applied on the top nodes of the falsework using a ramp function. Initial imperfections equal for all models were also included.

4.4.1 Mesh density

To check the sensitivity of the numerical results to the mesh density, a model with a finer mesh, with a maximum element size equal to 10 mm (compared with the 50 mm of the reference model), was also developed. A generic representation of the models is given in Figure 4.20.

In both the reference model and the model with refined mesh the baseplates were modelled with first-order shell elements with reduced integration and contact was activated between the rigid foundation and the surface of each baseplate. Separation between the master surface (rigid foundation) and the slave surfaces (baseplates) was allowed and a friction coefficient equal to 0,2 was considered for the tangential contact direction using the finite sliding algorithm.

The results obtained from both models are shown in Figure 4.21 expressed in terms of the value of the vertical loads *vs.* the horizontal displacement of the same node. As it can be observed little difference exists between the numerical behaviour obtained by the two models. Therefore, it is considered that the mesh of the reference model is good enough and it will be used in all models hereon.
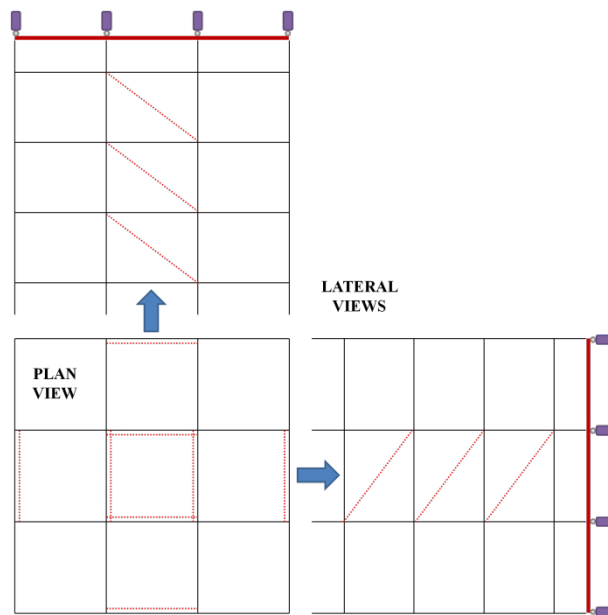
Figure 4.19: Structural layout used in the full-scale tests performed by University of Sydney.
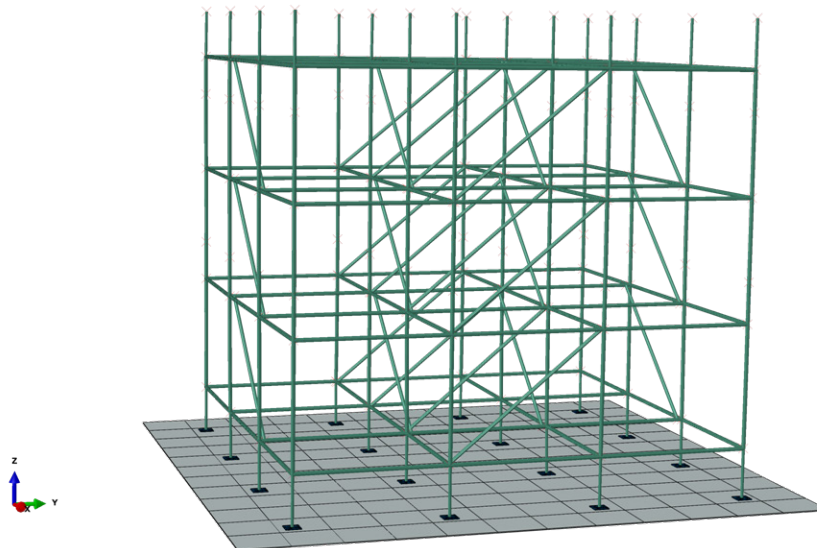
Figure 4.20: Generic representation of the models.

4.4.2 Solvers

Different solvers were used to run the analyses. Static analyses were performed using the classic Newton-Raphson method and the Riks arc-length method. The results are presented in Figure 4.22. It can be seen that the behaviour obtained through both methods match but the Newton-Raphson method is able to continue the analysis for a little higher load value.

Implicit quasi-static and dynamic analyses were also performed. Figure 4.23 compares the results obtained using static solvers and using dynamic solvers. It can be observed that the static solvers are not able to converge until the maximum load is reached and diverge from the correct equilibrium path for increasing load values. This may be justified by the analysis being done with load control and being very unstable. If the analysis is performed with displacement control, convergence improves but the results will be different simply because in hyperstatic structures with nonlinear behaviour the axial force transmitted to a given column depends on the stiffness of that column, which is different of imposing an equal axial force for all columns.
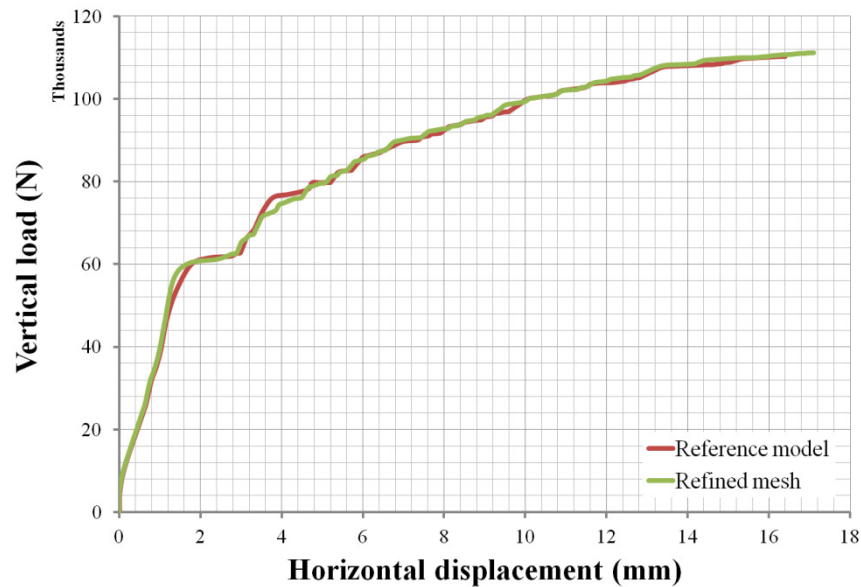
Figure 4.21: Mesh density sensitivity: refined mesh model *vs.* reference mesh model.
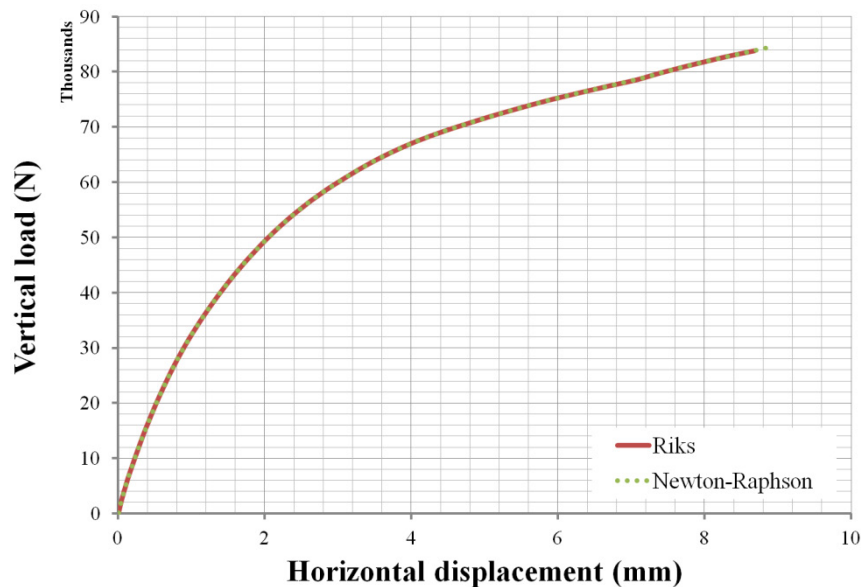
Figure 4.22: Static solvers: Newton-Raphson and Riks methods.

Also, the results obtained using HHT method were very poor (the rate of convergence was very slow and after 2000 increments the maximum load obtained was still order of magnitude lower than the value obtained by other methods). The results using Newmark method match the ones obtained with the Quasi-static method but soon after the failure of the first element occurred, the rate of convergence degraded considerably and it could not reach the same level of deformation as the one provided by the Quasi-static method. Therefore, the Quasi-static method was selected hereon.

The influence of the analysis time period in the results of the dynamic analysis was also studied. From Figure 4.24 it is possible to conclude that this parameter has a slight influence on the behaviour of the structure and on the maximum resistance of the structure. For the models presented in this section a analysis time period of 100 s was selected.

Explicit dynamic analyses were also performed. Figure 4.25 compares the results obtained using explicit solvers and using implicit solvers. It can be observed that the explicit solvers are not able to converge after the first element failure is reached and diverge from the correct equilibrium path for increasing displacement values. This seems to occur because the solution becomes dominated by the inertial effects which are artificially intensified by the mass scaling that was used in order to speed up

the analysis. Even so, the explicit solver required five times more computer runtime to finish the analysis when compared with the implicit solver. Therefore, the implicit solver was preferred hereon.
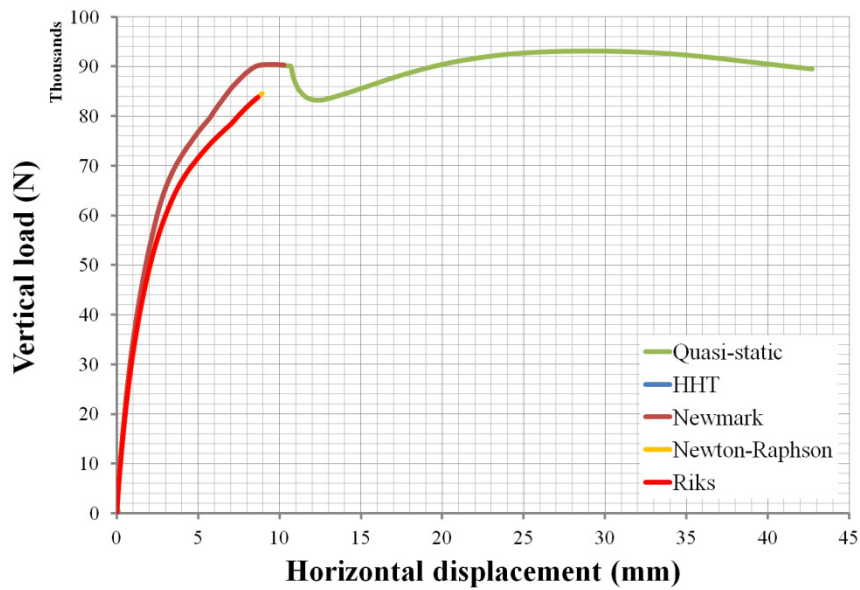
Figure 4.23: Static solvers *vs.* Dynamic solvers.
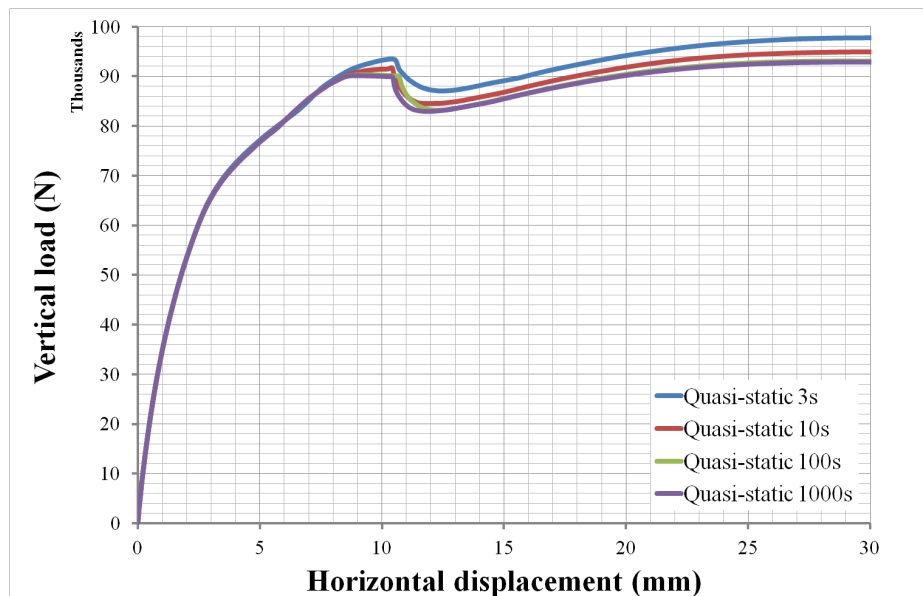
Figure 4.24: Implicit dynamic solvers: Quasi-static methods, influence of analysis time period.

4.4.3 Baseplate joint

To ease the convergence it was convenient not to model the baseplates with shell or solid elements in order to avoid having to use contact algorithms. Therefore, the baseplate joint model presented in section 4.2.4.2 was implemented in the UEL subroutine.

In order to validate the baseplate joint model a comparison was made between the behaviour given by a model in which the baseplates were modelled with shell elements, see Figure 4.26, and the behaviour given by a model using the baseplate joint.

A concentrated vertical load and a horizontal load were applied on the top node of the vertical element. Two loading methods were considered: (i) monotonic and (ii) cyclic with load reversals.
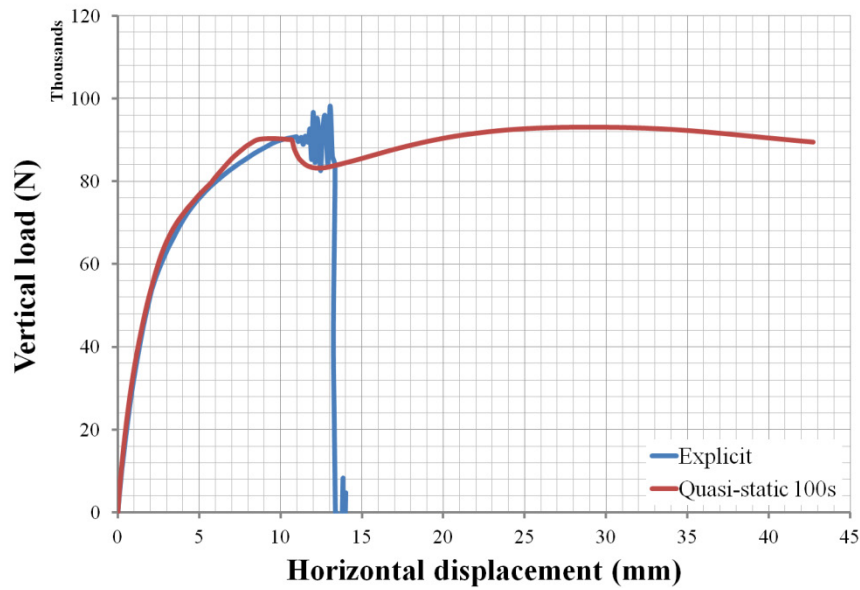
Figure 4.25: Explicit *vs*. implicit dynamic solvers.
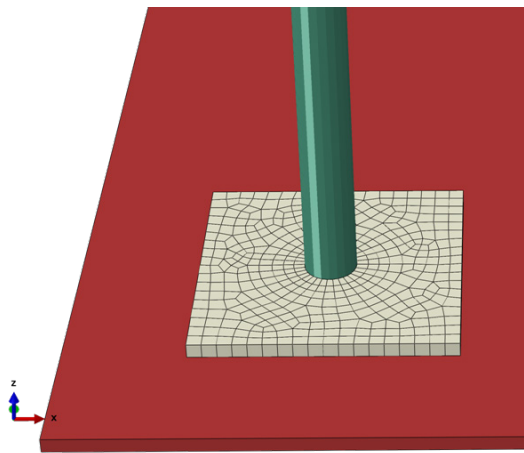
Figure 4.26: Overview of the baseplate shell model.
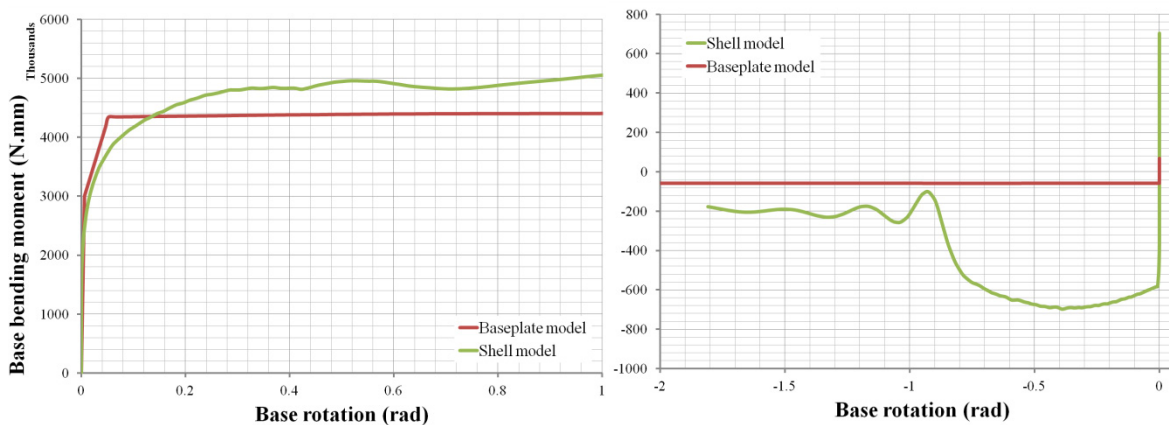
Figure 4.27: *Left*, **results for monotonic loading,** *Right*, **results for cyclic loading.**

In both models, the vertical element was modelled with beam elements. In the shell model, at the interface between the beam elements and the shell elements a beam MPC was established using the beam element node as the master node and, as slave the shell nodes that belong to a partition circle with a diameter equal to the external diameter of the vertical element CHS.

The behaviour obtained for both models and loading methods is presented in Figure 4.27. It can be seen that the baseplate joint model tends to be on the safe side of the predicted behaviour given by the shell model.

Finally, Figure 4.28 shows the results of the numerical model presented in the previous section obtained with the baseplate model and with shell baseplates plus contact. It can be observed that the two curves are very similar. Therefore, the baseplate model was used here on as replacement of the more complex contact modelling with shell elements.
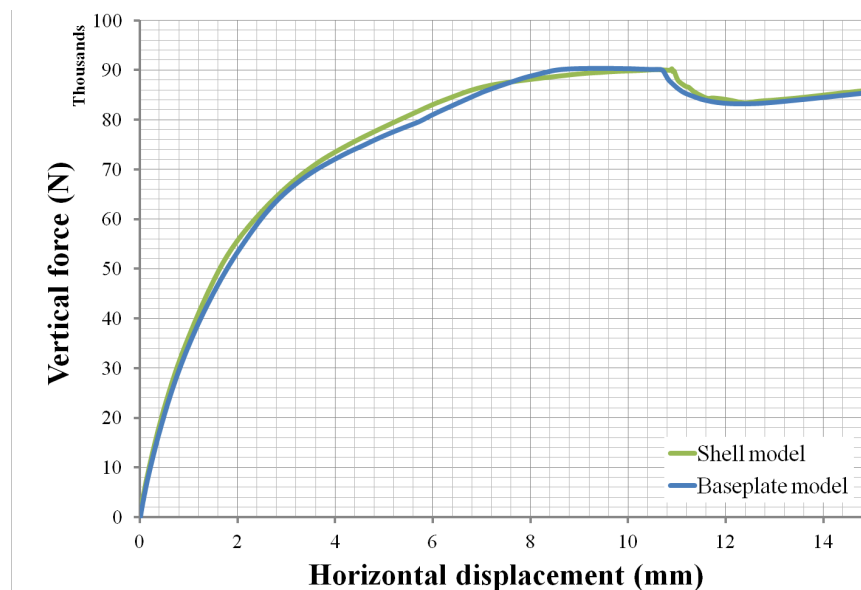
Figure 4.28: Results obtained with the baseplate model and with shell baseplates plus contact.

4.5 Verification of numerical models

After being validated the numerical models were verified by comparing the numerical behaviour with the behaviour measured in the full-scale tests performed at the University of Sydney in 2006, and published in (Chandrangsu, Rasmussen, 2009a). A brief summary of the characteristics of each test will be presented, followed by the results of each test.

A summary of the test configurations which includes test number, lift height, number of lifts, top and bottom jack extension lengths, position of spigot joints, bracing arrangements, type of loading, and loading eccentricity is presented in Table 4.1 (Chandrangsu, 2010).

The bracing arrangements are illustrated in Figure 4.29. Loading and baseplate eccentricities were applied to induce the most unfavourable effect on the structure. In test 14, the load was applied to the top of each column with a distribution that resembles the one obtained using the influence area method to each column. Therefore, the corner columns received a quarter of the load of the centre columns and the other perimeter columns received half the load of the centre columns.

In all numerical models considered in the present section, an identical constitutive model was used for the user elements of the same type. The values of the input parameters of each constitutive model were taken as the average values of the results reported in Chapter 3 of this Thesis.

The material properties of the steel elements (standards, ledgers and braces) were reported in (Chandrangsu, 2010) and included in the numerical models using the Ramberg-Osgood stress-strain relationship.

The grid of timber beams placed on top of the falsework structure was incorporated in the model for an accurate consideration of the stiffness provided by the timber beams. The material properties of the timber was assumed to be orthotropic with the following elastic constants: E_x = 9000 N/mm^2, E_y = 5000 N/mm^2, E_z = 1000 N/mm^2, υ_{xy} = 0,05, υ_{xz} = 0,55, υ_{yz} = 0,45, G_{xy} = 800 N/mm^2, G_{xz} = 400 N/mm^2 and G_{xz} = 200 N/mm^2 (Gerrand, 1987), where E_i is the elastic modulus in the i-direction, υ_{ij} is the Poisson coefficient in the ij plane, G_{ij} is the distortion modulus in the ij plane and

x,y are the mid-plane directions and z the outward direction. The yield stress of timber was considered equal to 25 MPa in tension or compression with an ultimate extension equal to 10%.

Table 4.1: Summary of full-scale tests (Chandrangsu, 2010).

Test ID	Lift height (mm)	Number of lifts	Jack extension (mm)	Location of spigot joints	Type of bracing	Loading distribution	Eccentricities
A1	1500	3	600	2nd and 3rd	full	uniform	25 mm top 15 mm bottom
A2	1500	3	600	2nd and 3rd	full	uniform	25 mm top 15 mm bottom
A3	1500	3	600	2nd and 3rd	full	uniform	25 mm top 15 mm bottom
A4	1500	3	600	2nd and 3rd	**none**	uniform	25 mm top 15 mm bottom
A5	1500	3	600	2nd and 3rd	perimeter	uniform	25 mm top 15 mm bottom
A6	1500	3	600	2nd and 3rd	perimeter	uniform	15 mm bottom
A7	1500	3	300	2nd and 3rd	full	uniform	25 mm top 15 mm bottom
A8	1500	3	300	2nd and 3rd	full	uniform	25 mm top 15 mm bottom
A9	1500	3	300	2nd and 3rd	**none**	uniform	25 mm top 15 mm bottom
A10	1500	3	300	2nd and 3rd	core	uniform	25 mm top 15 mm bottom
A11	1500	3	300	2nd and 3rd	full	uniform	25 mm top 15 mm bottom
A12	1500	3	300	2nd	full	uniform	25 mm top 15 mm bottom
A13	1500	3	300	2nd	N-S only	uniform	25 mm top 15 mm bottom
A14	1500	3	300	2nd	core	1:2:4	25 mm top 15 mm bottom
A15	2000	2	300	2nd	full	uniform	25 mm top 15 mm bottom
A16	1000	3	600	3rd	full	uniform	25 mm top 15 mm bottom
A17	1000	4	300	3rd	full	uniform	25 mm top 15 mm bottom
A18	1000	4	300	3rd	full	uniform	25 mm top 15 mm bottom
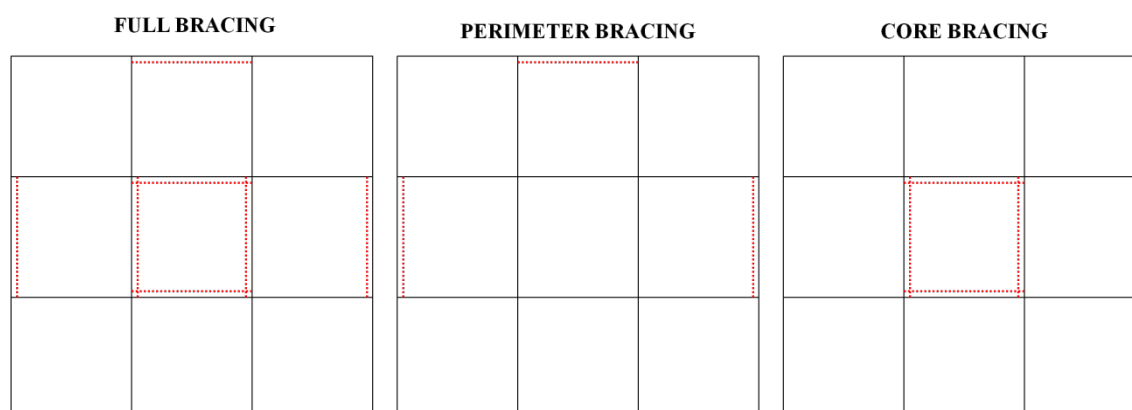
Figure 4.29: Illustration of the different bracing arrangements (Chandrangsu, 2010).

Load was applied to nodes of the timber grid geometrically coincident with each column top node, or with the extreme node of the top eccentricity element where applicable. These points of the timber grid were not allowed to translate horizontally as enforced in the experimental setup (Chandrangsu, Rasmussen, 2009a).

The top and bottom eccentricities were enforced by rigid beam elements with a length equal to the eccentricity to be used. Geometrical imperfections for each test were also available (Chandrangsu, 2010) and included in each numerical model. Figure 4.30 Illustrates an overview of the numerical model used to simulate test A2. North is parallel to global *Y* axis.
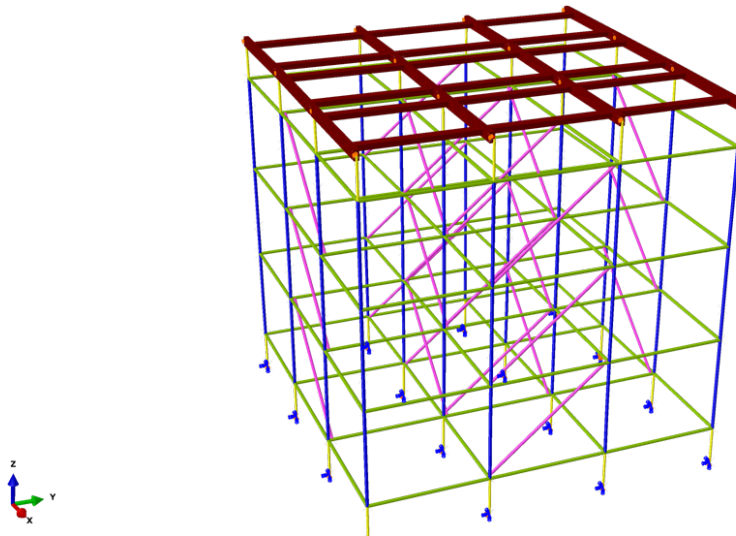
Figure 4.30: Overview of the numerical model used to simulate test A2.

Table 4.2 presents the results obtained with the numerical models and with the experimental tests. Results of tests A1, A7 and A17 are not presented because there were problems either with the test procedure or with data recording. The maximum load obtained in the present work, and reported in Table 4.2, consists in the load value for which the first joint failure occurred. After first failure the load does not increase significantly.

The statistical analysis of the ratio between the recorded maximum load and the numerically predicted value is presented in Table 4.3. It can be observed that the developed numerical models can match the experimental resistance with a better precision and accuracy than the previously developed numerical models.

It is also important to analyse if the numerical models can return as accurate results in terms of the overall structural behaviour. The following Figures illustrate the axial force vs. horizontal displacement of a selected node of the structure obtained in the tests and by both numerical models developed in the present work and presented in (Chandrangsu, 2010).

It can be observed that the developed numerical models are also better in predicting the overall behaviour the falsework systems than the previously developed numerical models.

4.6 Numerical modelling options

In this section the influence of various modelling options will be presented and discussed. In particular, the influence of accounting explicitly for the formwork, but also the influence of assuming continuous or pinned connections to model the various types of joints will be analysed. Finally, the design resistance according to EN 12812 (BSI, 2011, p. 12) design rules will be presented.

4.6.1 Formwork modelling

Formwork modelling was already summarised in section 4.3.1.2. An important parameter that has a significant influence in the behaviour and resistance of the falsework system is the stiffness provided by the formwork system.

The stiffness of the formwork system stems from the material characteristics used but also from the system configuration, namely the plywood panels thickness, the size of the plywood beams and their spacing. Formwork panels are manufactured with an odd number of layers of wood which are glued together with the grain of adjacent layers at right angles. Usually, the strong direction of the plywood (with more layers aligned in parallel) is aligned with the longitudinal axis of the bridge. Below the formwork panels a layer of plywood beams is positioned in the opposite direction to the longitudinal axis of the bridge with a fine spacing. Below this level, a second layer of plywood beams is positioned on top of the falsework forkheads and in alignment with the longitudinal axis of the bridge.

Table 4.2: Summary of results.

Experimental tests (Chandrangsu, 2010)			Previous work (Chandrangsu, 2010)		Present work		
Test number	Max. Load (kN)	Failure mode	Max. Load (kN)	Ratio (Test/Model)	Max. Load (kN)	Ratio (Test/Model)	Failure mode
A2	87	N-S sway, final failure of top and bottom jacks	96	0,906	88	0,989	N-S sway, failure of top jacks and top spigots
A3	91	N-S sway, failure of top and bottom jacks, spigot	91	0,995	90	1,006	N-S sway, failure of top jacks and top spigots
A4	50	N-S sway, final failure of top and bottom jacks	45	1,111	46	1,087	N-S sway, failure of top jacks and bottom spigot
A5	60	N-S sway of centre bay, final failure of top jacks	60	1,000	56	1,071	W-E sway, failure of bottom jacks and spigots
A6	60	N-S sway of centre bay, failure of top jacks and spigot	66	0,909	56	1,071	N-S sway, failure of top spigots and jacks
A8	130	Some N-S sway, failure of standards and spigot at top lift	138	0,942	135	0,963	Mixed sway, failure of top jacks and spigot, top lift
A9	65	N-S sway mode, final failure of top jacks and top standards	50	1,300	60	1,083	N-S sway, failure of top jacks and spigot of corner column
A10	70	N-S sway mode, failure of corner standards and spigots	64	1,094	72	0,972	Some N-S sway, failure of corner standards and spigots, top lift
A11	120	Some N-S sway, final failure of top spigots and standards	127	0,945	130	0,923	Mixed sway, failure top standard
A12	120	Some N-S sway, failure of top spigots and corner standards	129	0,928	133	0,900	Mixed sway, failure of corner standard
A13	70	Some E-W sway, final failure of perimeter spigots in 2nd lift	68	1,029	69	1,014	Some W-E sway, failure of perimeter standard and spigot 2nd lift
A14	160	Some N-S sway, failure of top spigots and centre standards	160	1,000	156	1,026	Some N-S sway, failure of top standards and spigots
A15	105	Failure of corner spigot and top standard	105	1,000	105	1,000	Failure of top standard
A16	100	N-S sway mode, failure of jacks	100	1,000	104	0,962	W-E sway, failure of top jacks
A18	150	Some N-S sway, final failure of corner standard at top lift	147	1,020	153	0,980	Mixed sway, failure of corner standards at bottom lift

Table 4.3: Statistical results.

	Previous work (Chandrangsu, 2010)	Present work
Average ratio	1,012	1,003
Standard deviation of the ratio	0,100	0,057
COV of the ratio	0,098	0,057
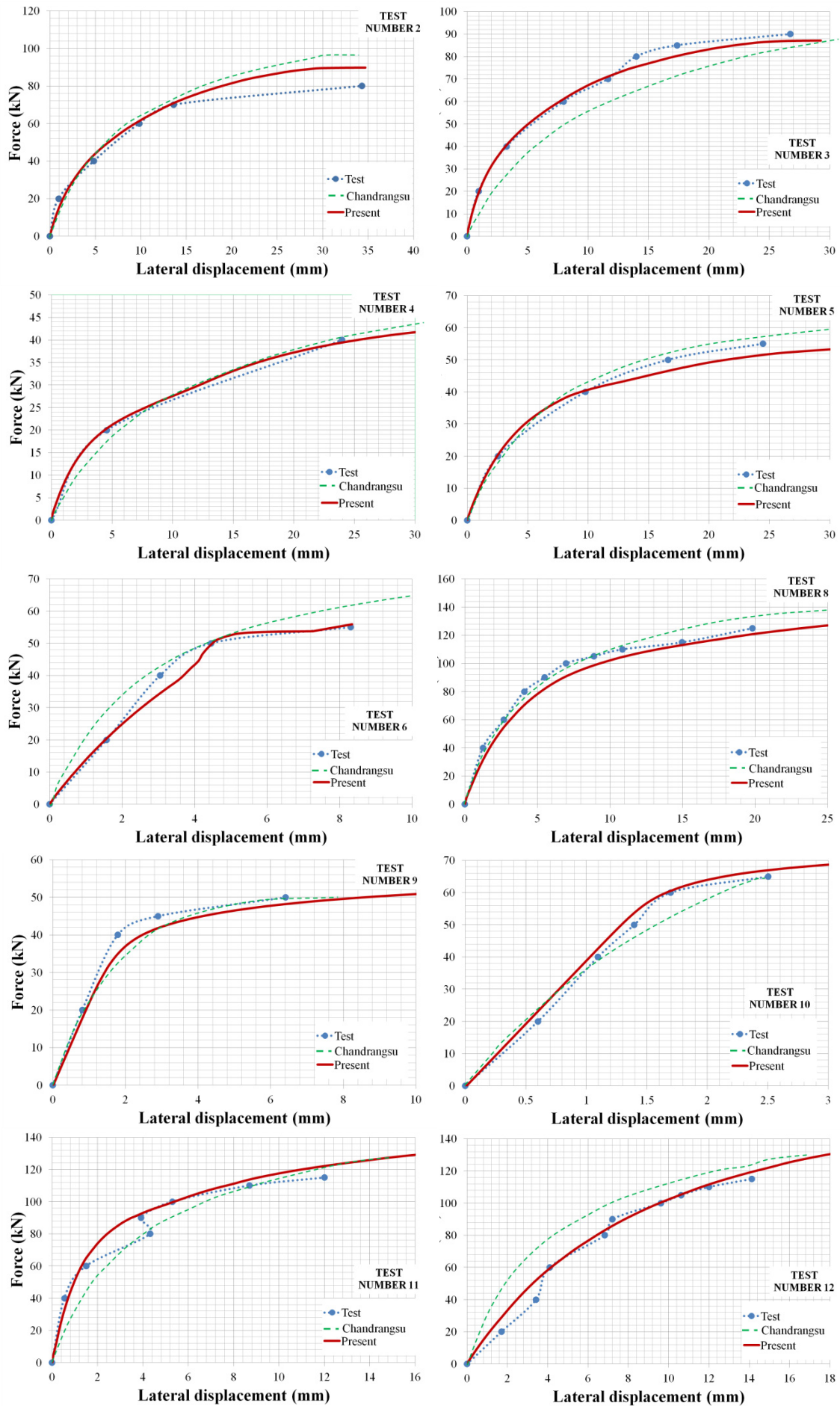
Figure 4.31: Experimental and numerical tests results, tests A2-A12.
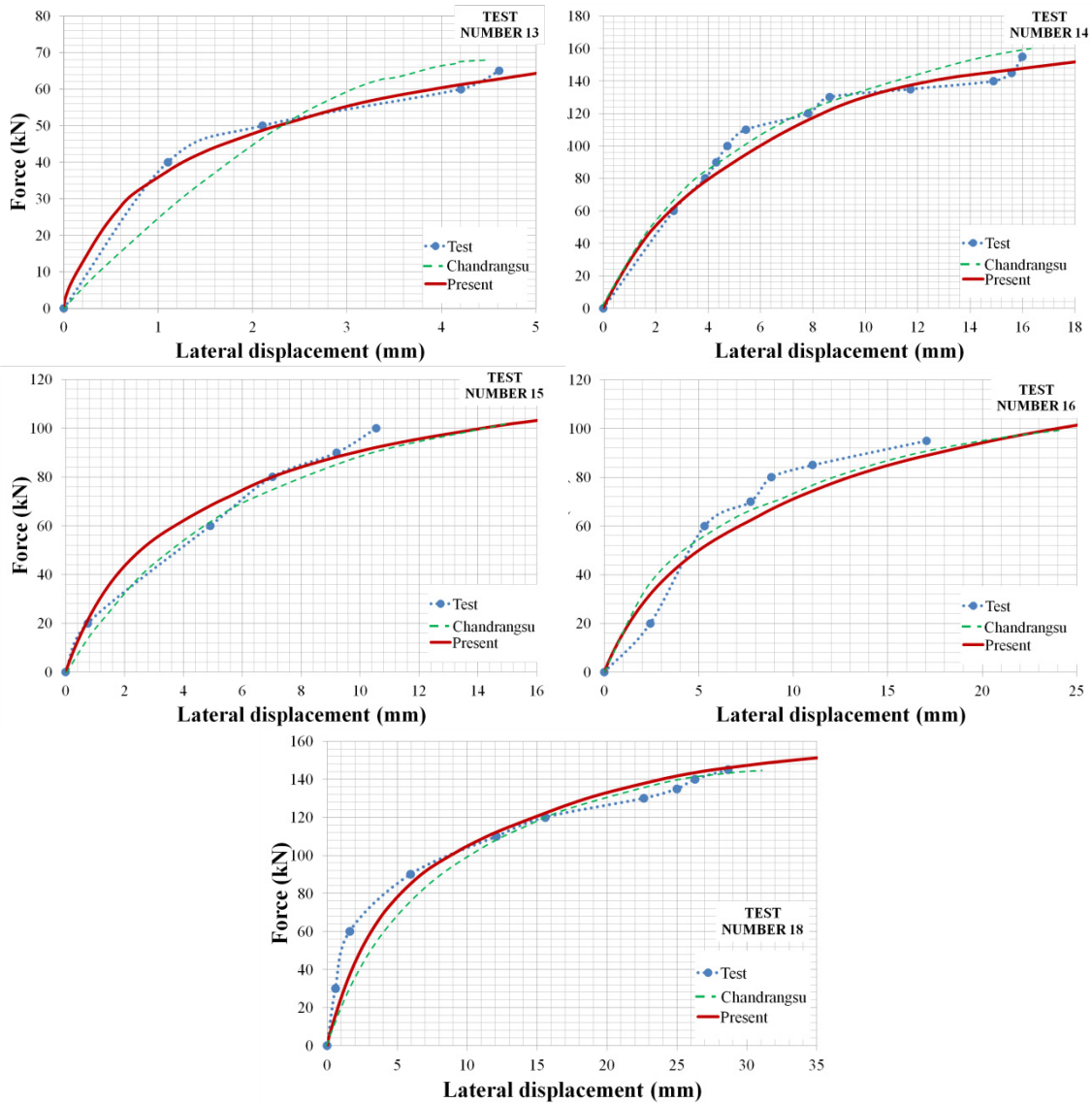
Figure 4.32: Experimental and numerical tests results, tests A13-A18.

With this setting in mind, the modelling of the formwork considered two structures: (i) one that couples the formwork panels with the first level of formwork beams and (ii) a second consisting on the next level of formwork beams.

It was further considered that the former structure could be modelled using shell elements with an equivalent thickness and a material with elastic isotropic characteristics equal to the ones of the plywood grain direction. The equivalent thickness was determined by calculating the thickness of a homogenised panel with uniform thickness with the same moment of inertia as the original section made of the homogenised panel and the plywood beam, see Figure 4.33.
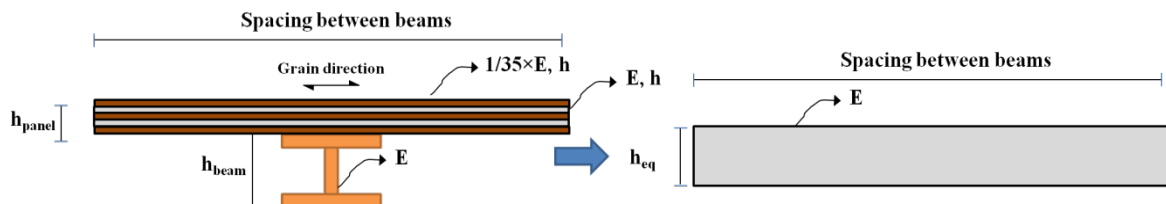
Figure 4.33: Determination of the formwork stiffness.

The numerical models developed to test the influence of the formwork stiffness have been already explained in detail in the previous sections with the difference that none of the nodal degrees of freedom of the formwork and of the top of the falsework were constrained. Therefore,

the formwork system was let free to move and rotate. Also, the load was applied by pressure in the formwork shell surfaces. Models A2 and A4 of Table 4.1 will be used.

Figure 4.34 to Figure 4.36 illustrate the results obtained considering various equivalent formwork thicknesses. It can be observed that for a small formwork thickness (resulting from either a very large beam spacing or from a very small panel thickness) the behaviour of the falsework differs considerably from the one obtained for larger stiffnesses. This difference is due to the high deformation of the soft formwork (h_{eq} = 20 mm) which induces large plastic deformations on the top jacks and consequently results on an early collapse. This compares with the higher resistance for the stiff formwork (h_{eq} = 100 mm) which manages to behave like a rigid diaphragm and prevent excessive rotation on the top jacks. Failure for h_{eq} = 100 mm occurs at the spigot joints.
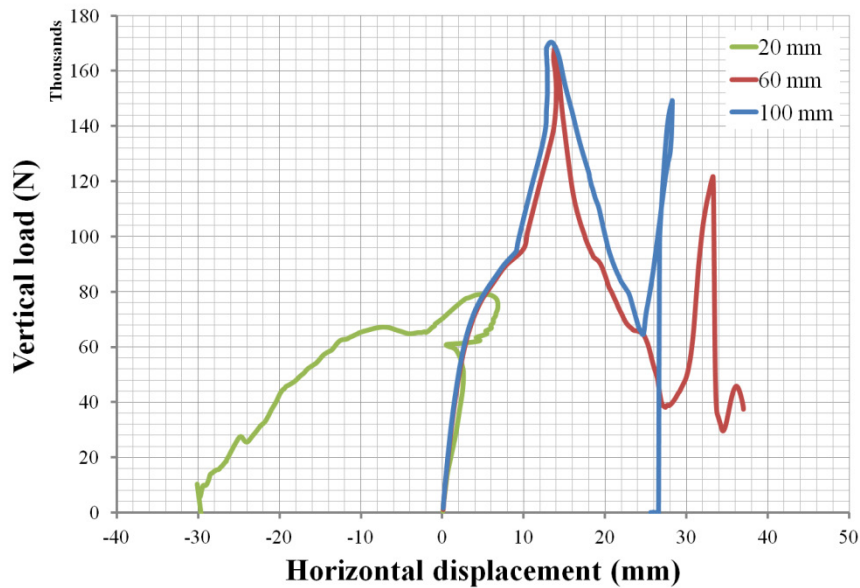
Figure 4.34: Results for different equivalent formwork stiffnesses.
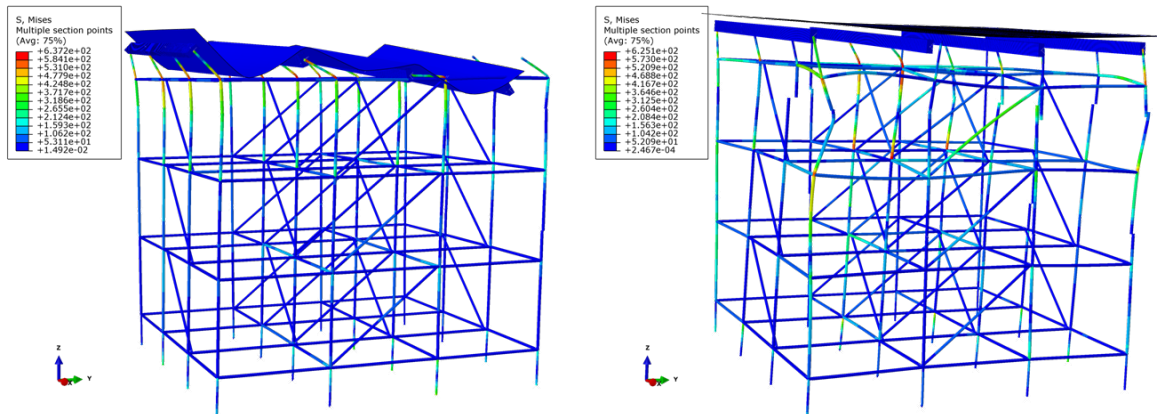
Figure 4.35: Deformed shape and von Mises stresses for different equivalent formwork stiffnesses.

It was also analysed the effect of including the formwork in the numerical model. Figure 4.37 shows the results obtained with and without the formwork. It must be stressed that the loading distribution was not the same between these two models, because in the model without formwork the vertical loads applied on top of the falsework were forced to be equal in magnitude.

Having this difference in mind, it is possible to observe that the results of the model without formwork are completely different from the ones of the model with formwork. The former model overestimates the stiffness of the corner columns and underestimates the stiffness of the perimeter and centre columns, and of course it is not able to capture the load redistributions that take place after each column fails until the total collapse of the falsework happened.
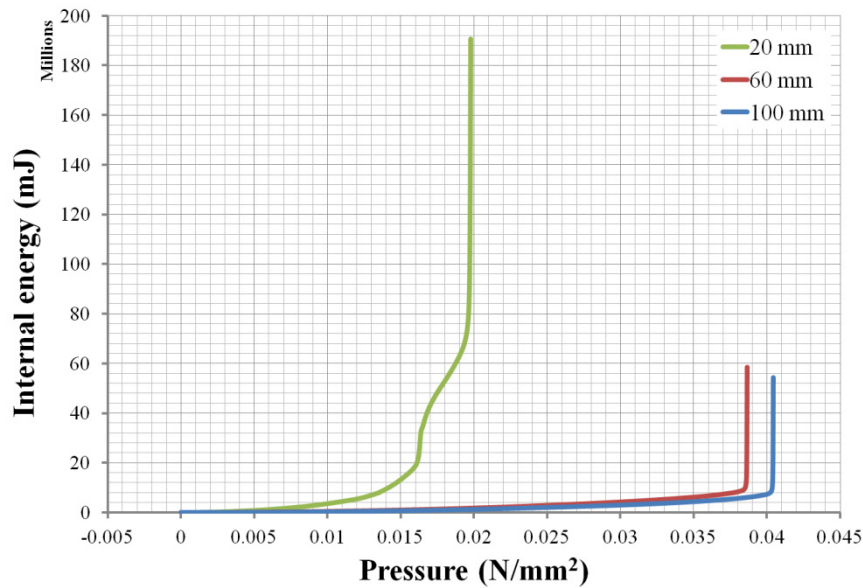
Figure 4.36: Internal dissipated energy for different equivalent formwork stiffnesses.
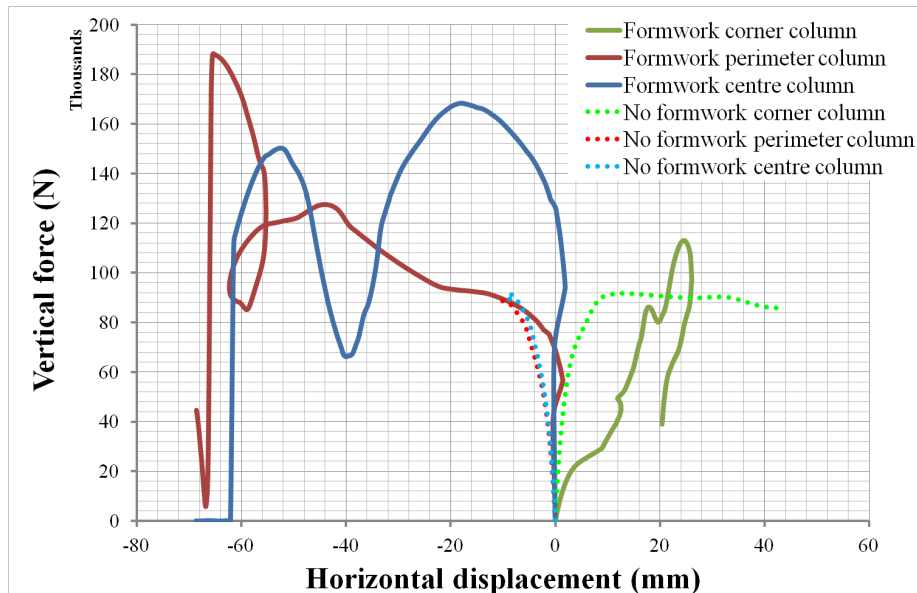
Figure 4.37: Results obtained for models with and without formwork, different loading distribution.

If the loading distribution is made similar by applying vertical loads on top of the falsework with a distribution proportional to the column influence area, the results change to the ones presented in Figure 4.38. The differences between the results obtained using the two models are smaller but still some differences in the load redistribution are noticeable.

The maximum resistance of the model without formwork, in terms of vertical loads, is 124,4 kN in the centre columns. Dividing this load with the influence are of a centre column, 3,345 m^2, the equivalent maximum pressure is equal to 37,14 kN/m^2 which compares with the maximum pressure of 39,17 kN/m^2 obtained in the model with formwork. Performing the same analysis for a numerical model without any brace element, the maximum equivalent pressure obtained in the model with formwork is equal to 19,10 kN/m^2 which compares with the maximum pressure of 14,01 kN/m^2 obtained in the model with formwork.

This apparent paradox of obtaining a smaller resistance with the formwork included in the numerical model, is justified by the fact that the formwork is unrestrained. Therefore, in the braceless model the falsework has no effective lateral restraint (other than the one provided by the ledgers) and it follows the stiff formwork displacements which cause large rotations at the spigot joints which

eventually fail. Thus, it can be concluded that in order to get an accurate estimate of the falsework behaviour and resistance, and prevent obtaining unconservative resistance values, it is necessary to include the formwork system in the numerical model. This recommendation was followed hereon.
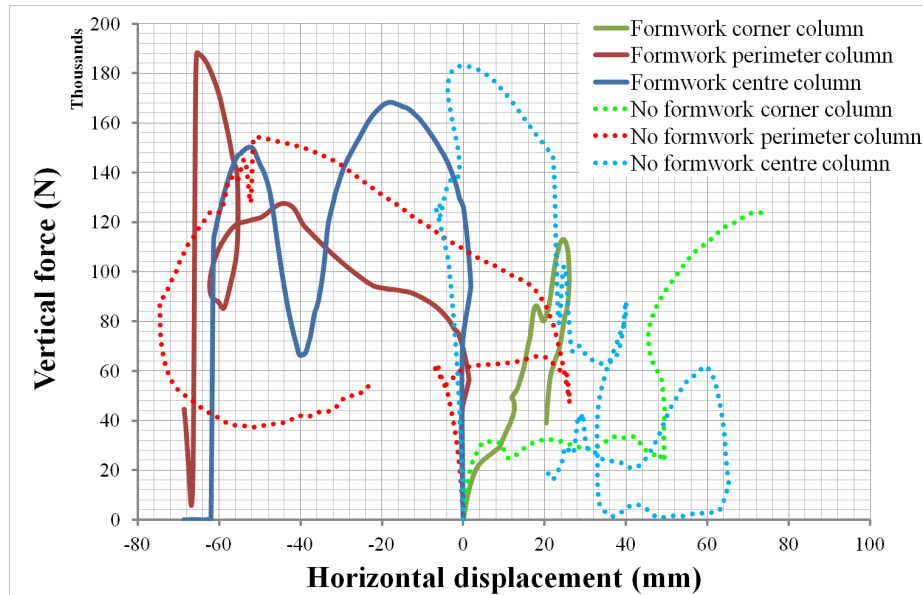
Figure 4.38: Results obtained for models with and without formwork, same loading distribution.

4.6.2   Joint modelling

Various different modelling options can be used to simulate the joint behaviour: from the elastic model to the nonlinear elastoplastic model, and from the pinned joint to the continuous joint. It is therefore important to assess the influence that these modelling options have on the behaviour and resistance of bridge falsework predicted by numerical models.

Two models will be used in this study: Models A2 and A4 of Table 4.1. The following Figures illustrate the results. Joint's failure criteria was activated in the models which results are shown in Figure 4.39 and Figure 4.43, whereas the results presented in Figure 4.42 and Figure 4.43 were obtained without failure criteria being activated.
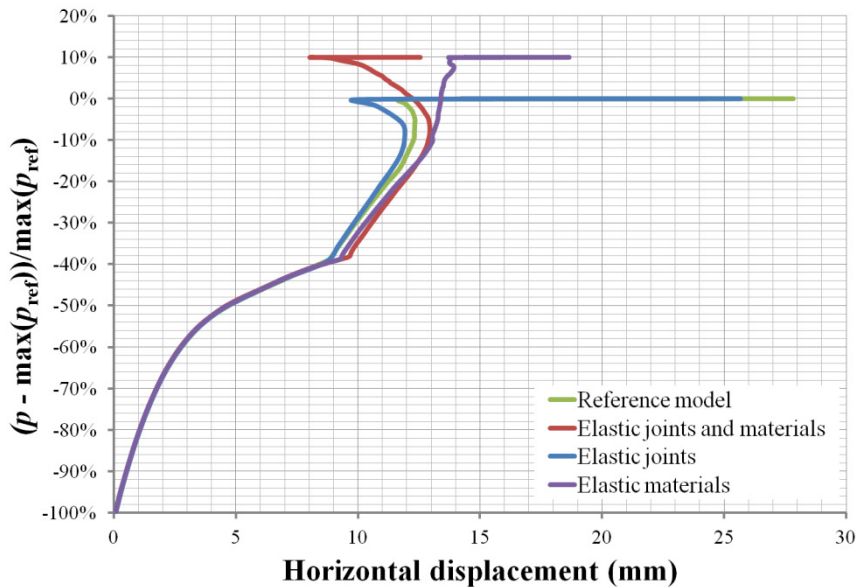
Figure 4.39: Results obtained for Model A2 considering different joint and material constitutive laws.
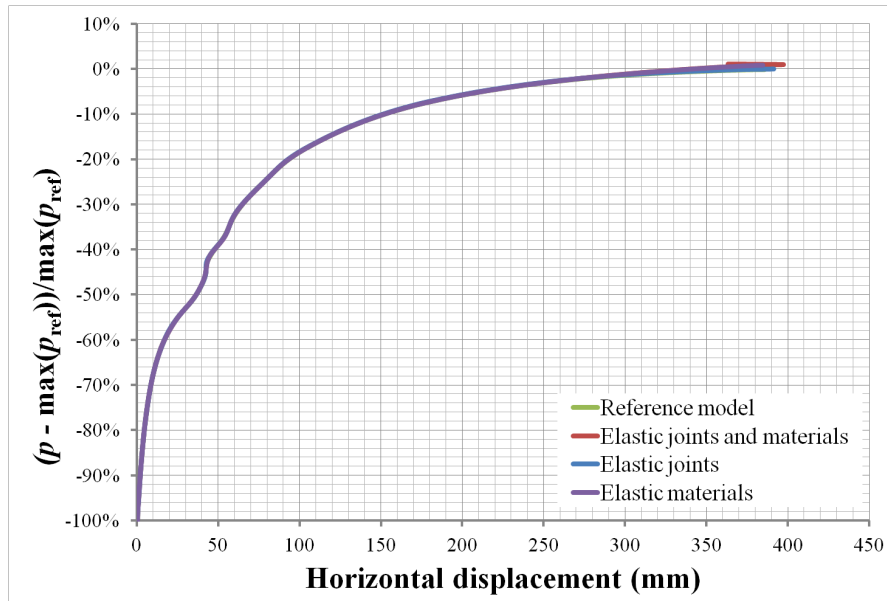
Figure 4.40: Results obtained for Model A4 considering different joint and material constitutive laws.
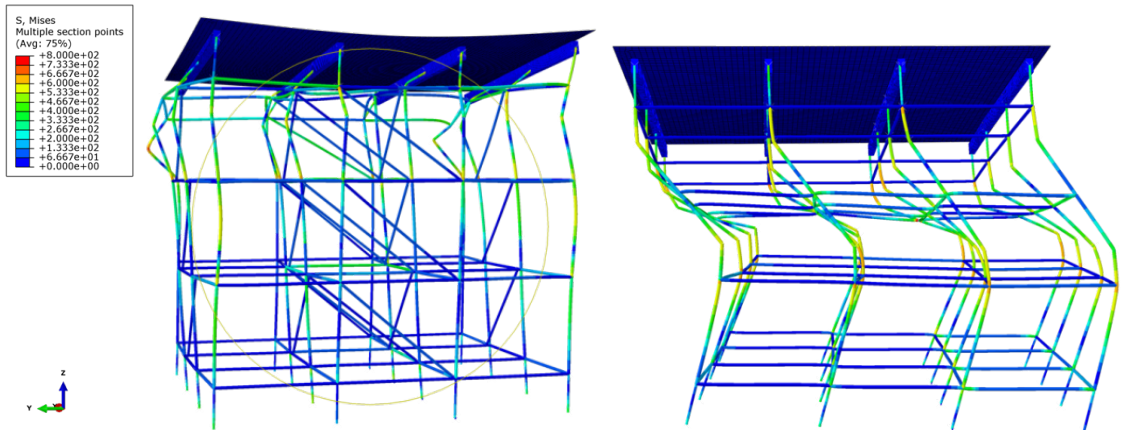
Figure 4.41: Deformed shape and von Mises stresses for reference models 2 and 4.
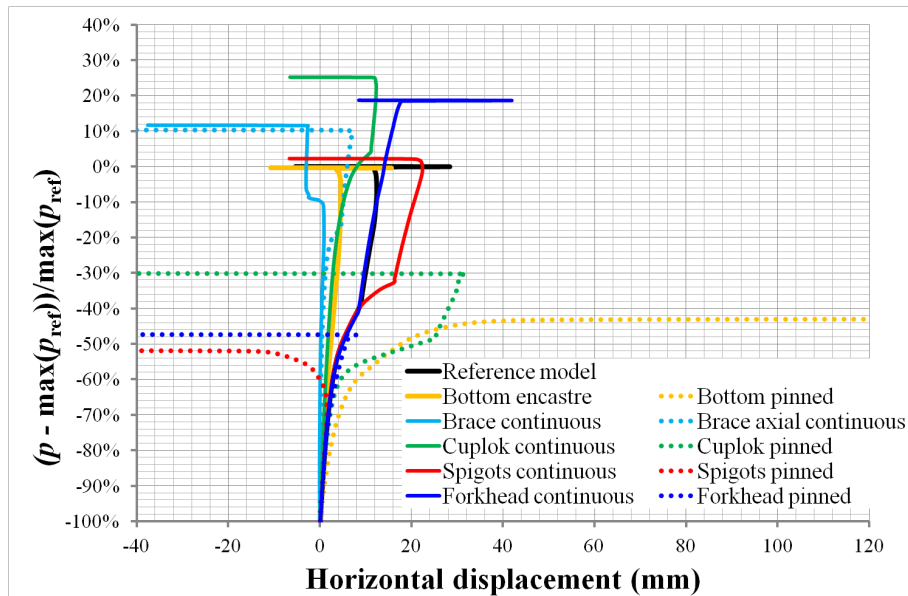
Figure 4.42: Results obtained for Model A2 considering different joint modelling options.
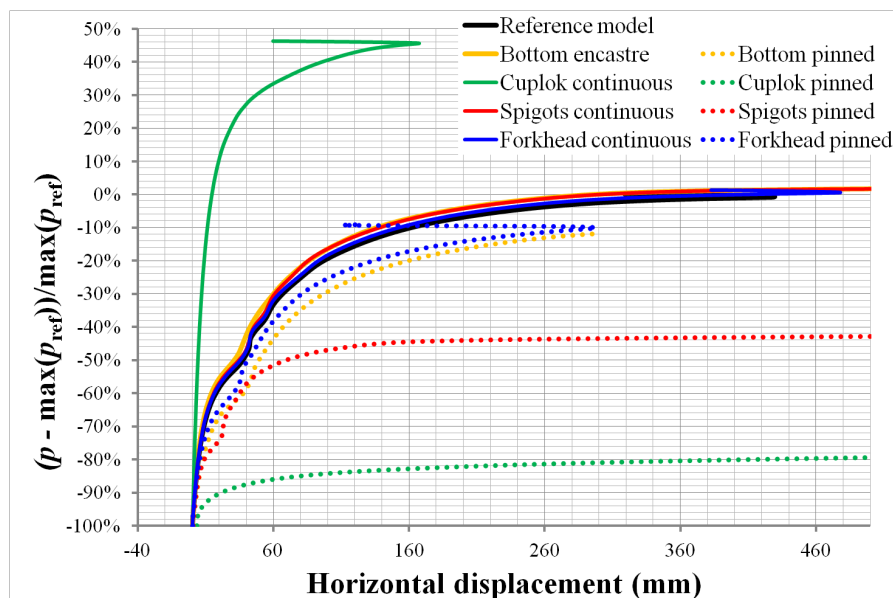
Figure 4.43: Results obtained for Model A4 considering different joint modelling options.

The reference model was considered to be equal to the one described in the previous section.

From Figure 4.39 it can be observed that considering elastic joints has no substantial effect on the maximum resistance of the falsework system when comparing the results of using elastic joints with the ones obtained with the nonlinear model presented in section 4.2. In the other hand, considering elastic materials led to an unconservative value of the maximum resistance of the falsework of approximately 10%, in this case. This fact justifies the need of including material elastoplasticity in the material constitutive model definition.

However, for Model A4 (unbraced version of Model A2) the influence of the material constitutive model definition is not significant, since its behaviour is controlled by the resistance and stiffness of the spigot joints, see Figure 4.41, which without brace elements are submitted to high bending moments resulting in plastic hinges and eventually into a mechanism. Different combinations of spigot joints locations or the use of spigotless standards could increase the influence of the material constitutive model definition on the system's resistance.

From Figure 4.42 and Figure 4.43 it can be seen that for the tested models there is significant influence on how the joints are modelled in the falsework behaviour and resistance. The most important joint seems to be the Cuplok® joint with increases in resistance of about 25% for Model A2 and 45% for Model A4 if it is modelled as continuous (infinite translational and rotational stiffness), and decreases in resistance of approximately 30% for Model A2 and 80% for Model A4 if it is modelled as pinned joint (free rotations). This finding highlights once again the importance of correctly locking the Cuplok® joint and not using damaged elements.

Another important joint is the forkhead joint with increases in resistance of about 20% for Model A2 and 2% for Model A4 if it is modelled as continuous (infinite translational and rotational stiffness), and decreases in resistance of approximately 50% for Model A2 and 10% for Model A4 if it is modelled as pinned joint (free rotations). The result for Model A4 are not as expressive because in the absence of changes in Cuplok® joint the behaviour and resistance of the falsework for this model is controlled by the spigots joints.

The spigot joint is also important, with increases in resistance of about 2% for Model A2 and Model A4 if it is modelled as continuous (infinite translational and rotational stiffness), and decreases in resistance of approximately 50% for Model A2 and 45% for Model A4 if it is modelled as pinned joint (free rotations). From these results it is clearly seen the influence of using improper (damaged or shorter than normal) spigot elements in the behaviour and resistance of the falsework.

Base boundary conditions can decrease the resistance of approximately 43% for Model A2 and 12% for Model A4 if it is modelled as pinned joint (free rotations) with no significant gains if it is considered encastred. This occurs because until the maximum resistance is reached the axial force eccentricity at the base is small and the baseplate joint described in section 4.2.4.2 behaves as an encastre joint. This behaviour is in close agreement with the findings reported in (André, 2008) relative to the behaviour of telescopic steel props.

An interesting finding is that considering the brace elements as rigid for translation displacements (including axial displacements) result in a 10% overestimate of the falsework resistance. This highlights the importance of careful assessment of the behaviour of individual components and of rigorous structural analysis.

Joint eccentricities, *e.g.* between the brace element and the ledger if traditional swivel joint is used (see Figure 4.44), were also analysed. It was found that if its value is kept small by assembling them according to good construction practices they were not relevant and they can be left out of the model.
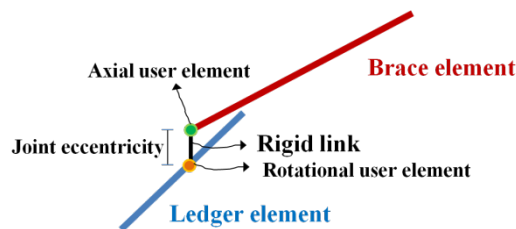
Figure 4.44: Joint eccentricity.

4.6.3 Design by standards

At this last section of this Chapter a study to analyse how numerical modelling of falsework systems typically used in design offices taking into consideration the design rules layout in the European Standard for the design of falsework, BS EN 12812 (BSI, 2011), compares with more accurate modelling techniques.

The materials are introduced as elastic perfect plastic materials with design yield stresses, $f_{y,d}$, determined according to:

$$f_{y,d} = \frac{f_{y,k}}{\gamma_M} \tag{4.41}$$

where $f_{y,k}$ represents the characteristic value of the yield stress and γ_M the partial factor for material properties, which is equal to 1,1.

Steel from all elements were considered to have a characteristic value of the yield stress equal to 355 MPa.

This standard specifies provisions for several types of imperfections:

Looseness at spigot joints, see Figure 4.45:

Angular imperfection $\qquad \tan(\varphi) = 1,25 \times \dfrac{d_i - d_0}{l_0} \times \min\left(\sqrt{0,5 + \dfrac{1}{n_v}};1,0\right)$ $\tag{4.42}$

where d_i, d_0 and l_0 represent the internal diameter of the standards, the external diameter of the spigot and the overlap length, respectively, and n_v represents the number of standards arranged side by side in a row.

Eccentricity $\qquad e = 1,25 \times \dfrac{d_i - d_0}{2}$ $\tag{4.43}$

This imperfection can be applied in two ways, see Figure 4.45: (i) sway-like imperfection or (ii) bow-like imperfection.

Bow imperfections:

Overall bow imperfection
$$e = \frac{l}{250} \times \min\left(\sqrt{0,5 + \frac{1}{n_v}}; 1,0 \right)$$
(4.44)

where l represents the overall length of the standards in each bay and n_v represents the number of standards arranged side by side in a row.

Member bow imperfection
$$e_0 = \frac{l_e}{300} \text{ for elastic analysis and}$$
$$e_0 = \frac{l_e}{250} \text{ for plastic analysis}$$
(4.45)

where l_e represents the member length.

Sway imperfections:

$$\tan(\varphi) = 0,01 \times \sqrt{\frac{10}{h}} \quad \text{but if } h \le 10 \text{ m} \Rightarrow \tan(\varphi) = 0,01$$
(4.46)

The overall sway imperfection and the sway for individual components, see equation (4.43), need not be considered as simultaneous effects.

Load eccentricities:

EN 12812 specifies that load eccentricity at load points shall be taken as a minimum of 5 mm where there is no centring device. Where there is a centring device the eccentricity taken may be reduced to a value consistent with the tolerances of the relevant components.
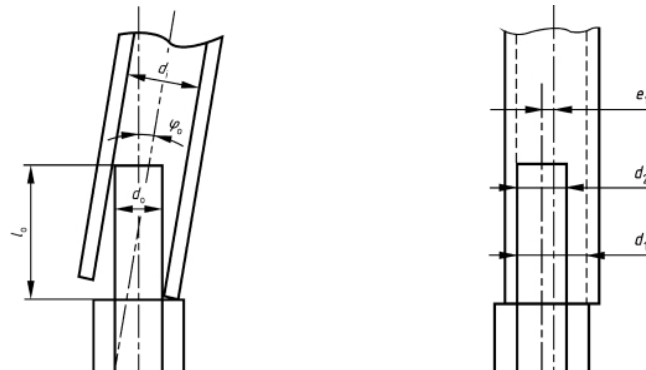
Figure 4.45: *Left,* spigot angular imperfections; *Right,* spigot eccentricities (BSI, 2011).
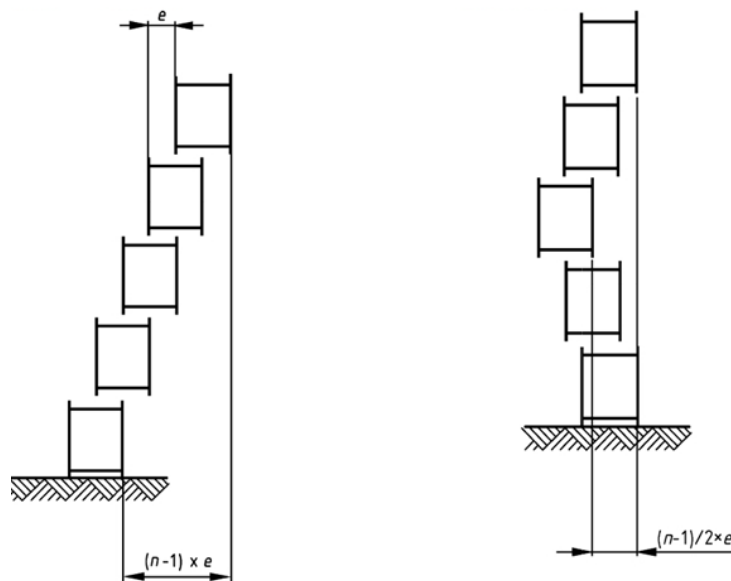
Figure 4.46: *Left,* sway-like imperfections; *Right,* bow-like imperfections (BSI, 2011).

In order to compare the results with the ones presented in the previous sections, the location and value of the baseplate and load eccentricities considered in the design numerical models were the same as in the numerical models previously described, *i.e.* 25 mm load eccentricity at one column alignment and 15 mm baseplate eccentricity in the same column alignment. Model A2 and A4 will be used as examples, without considering the formwork system. Following the same principle, only concentrated vertical loads were applied at the top nodes of the falsework.

Summing up all imperfections terms the resulting imperfection configurations are illustrated in Figure 4.47, see equation (4.47):

$$\delta_{\text{Config. 1}} = \delta_{\text{Eq 4.33}} + \delta_{\text{Eq 4.34}}^{\text{Bow + Sway}} + \delta_{\text{Eq 4.35}} + \delta_{\text{Eq 4.36}}$$
$$\delta_{\text{Config. 2}} = \delta_{\text{Eq 4.33}} + \delta_{\text{Eq 4.34}}^{\text{Bow}} + \delta_{\text{Eq 4.35}} + \delta_{\text{Eq 4.36}} + \delta_{\text{Eq 4.37}}$$

(4.47)
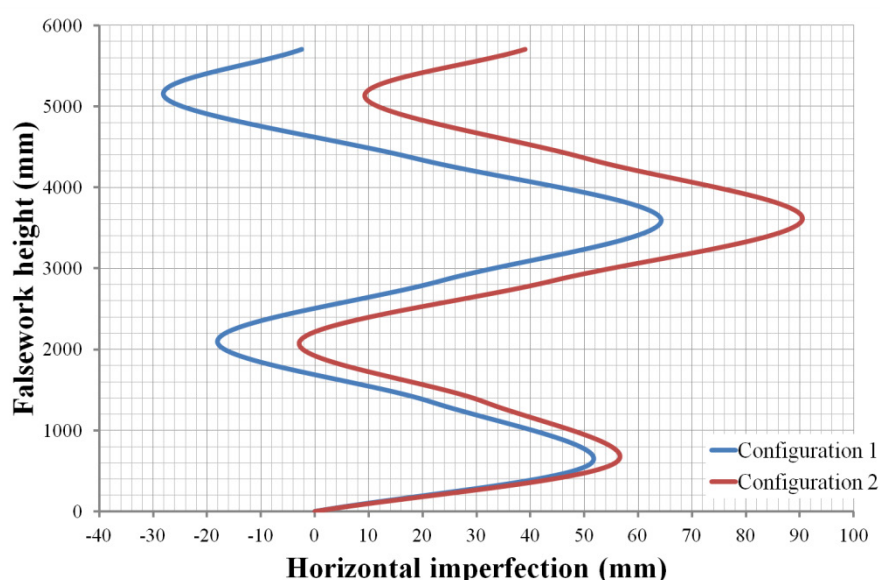
Figure 4.47: Illustration of the geometrical imperfections configurations.

As is usually the case in design, no formwork was modelled and the top falsework nodes were considered to rotate freely (pinned) but were not allowed to move horizontally. Additionally, the base was considered to be pinned and spigot joints to be continuous.

Linear elastic springs were used to model the Cuplok®, spigot and brace joints. The stiffness of each type of joint was determined by considering a joint with the same energy dissipation as the one determined from the bending moment *vs.* joint rotation diagrams obtained experimentally, but with a linear elastic behaviour. The resulting stiffnesses are given in Table 4.4.

The maximum resistance, R_d, is taken equal to the load needed to occur the first yielding in an element. The design resistance is then determined dividing the maximum resistance by a partial factor equal to 1,265 (= 1,1 × 1,15) (BSI, 2011).

Table 4.4: Equivalent joint stiffnesses.

Joint	Equivalent Stiffness
Cuplok® joint, strong rotation axis	$40{,}0 \times 10^6$ N.mm/rad
Cuplok® joint, weak rotation axis	$3{,}5 \times 10^6$ N.mm/rad
Cuplok® joint, axial axis	15000 N/mm
Spigot joint, rotation axis	$65{,}0 \times 10^6$ N.mm/rad
Brace joint, axial axis	1000 N/mm

Only the results for the geometrical imperfections applied in the most unfavourable direction in plan (*x* global axis or *y* global axis) will be shown.

Figure 4.48 and Figure 4.49 show the results obtained. It can be observed that the maximum load varies with the direction (positive or negative) only for the unbraced model (Model A4). The brace elements if properly designed, as in Model A2, effectively redistribute the load between members making the structure not sensitive to the direction of the initial geometrical imperfections.
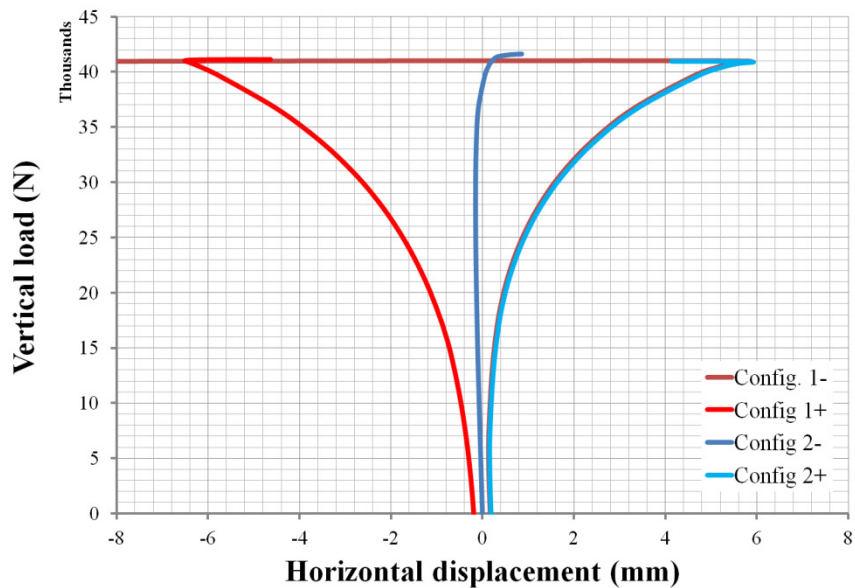
Figure 4.48: Results for Model A2.
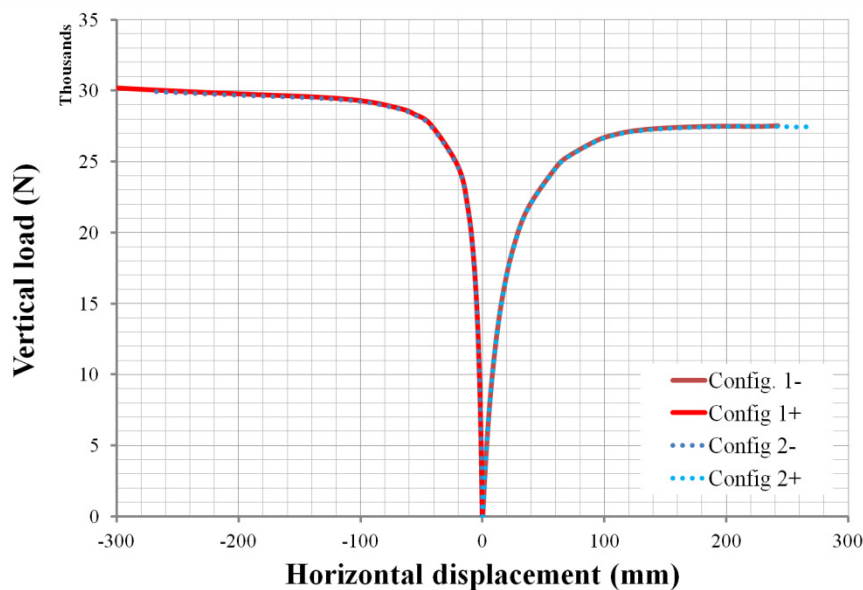
Figure 4.49: Results for Model A4.

Comparing the results obtained with the experimental tests results, the more refined numerical models and the design loads specified in the producer design sheets (SGB, 2009), see Table 4.5, it is possible to conclude that the current design methods by often assuming several simplifying hypothesis, the majority of which are conservative, if correctly used, namely if a proper nonlinear numerical model is developed and is based on reliable data, should return design loads which are smaller (safe) than the actual resistance of the falsework system. Nevertheless, it is recommended that formwork should be explicitly modelled and modelling of spigot joints should follow the model presented in this Chapter.

Falsework systems if properly designed, verified, used and managed on site, using suitable materials and components, and communication between the designer and the contractor is effective, should not collapse, unless hazard scenarios for which risk is considered to be acceptable occur.

However, this observation does not mean that the producer design value should always be greater than the design resistance returned by the standards or even the actual resistance of the falsework system. Multiple and concomitant external actions combined with various internal hazards can reduce the resistance of these structures to values less than the producer design values.

Table 4.5: Comparison of results.

Resistance (kN)	Experimental tests	Refined numerical tests	EN 12812 numerical tests	Producer design value (*)
Model A2	87,0	88,0	32,4	24
Model A4	50,0	46,0	21,7	18
(*) Internal columns.				

4.7 Conclusions

In this Chapter the development, validation and verification of advanced numerical models of bridge falsework numerical models have been presented. The formulation of a new spring-like finite element has been detailed, including consideration of finite rotations. This new finite element presents features that available elements in *ABAQUS®* program do not have, specifically the analytical modelling of the cyclic behaviour of joints with allowance for stiffness and resistance degradation and joint failure.

The numerical simulations included analytical models of the various types of joints present in Cuplok® bridge falsework systems. These models were developed based on the results of the experimental tests presented in Chapter 3. In order to increase the accuracy of the numerical results, the formwork beams and formwork plates were modelled explicitly and an efficient time-integration method was used to solve the transient nonlinear dynamic problem. Using these advanced numerical models it was possible to improve the accuracy and precision to the real behaviour of bridge falsework systems relative to previous numerical studies.

Afterwards, the impact of design simplifications in the joint modelling was analysed. It was concluded that the most important joint type seems to be the Cuplok® joint, followed by the forkhead joint and the spigot joint. For example, it was found that the Cuplok® joint may increase and decrease the system's resistance by more than 25% if it is modelled as a continuous or as a pinned joint, respectively. This finding highlights the importance of correctly locking the Cuplok® joint and not using damaged elements. For the forkhead joint, it was found that modelling it as a continuous or as a pinned joint could lead to a variation of 70% in the system's resistance. This finding stresses the importance of properly designing the falsework/formwork interface and implementing the necessary controls on site.

Finally, it was shown that the current design methods by often assuming several simplifying hypothesis, the majority of which are conservative, if correctly used, namely if a proper nonlinear numerical model is developed and is based on reliable data, should return design loads which are smaller (safe) than the actual resistance of the falsework system. However, this observation does not mean that the values given in the design load tables developed by the system producers are conservative. It is recommended that formwork should be explicitly modelled and modelling of spigot joints should follow the model presented in this Chapter.

5

STRUCTURAL DESIGN IN THE CONTEXT OF RISK INFORMED DECISION-MAKING

5.1 Introduction

The design of engineering structures can essentially be defined as a continuous process of making difficult engineering decisions under severe constraints imposed by society and nature, based on the available knowledge. Any structure can be analysed in an integrated system, made of exposures, hazard events and consequences. However, no matter the time interval, budget size and analysis capacity it is not possible to determine precisely the behaviour of any structure due to uncertainties. The key element is the impact of uncertainties in the available knowledge.

In the traditional approach, engineers resort to structural design codes to make decisions. These documents are developed specifically to address areas where significant past experience exists and where there are not societal critical risks involved. Thereby, codes are established for the purpose of providing a general, simple, safe and economically efficient basis for the design of ordinary structures under normal loading, operational and environmental conditions. Design codes not only greatly facilitate the daily work of structural engineers but also provide the vehicle to ensure a certain standardization within the structural engineering profession which in the end provides an uniformity of reliability of structural performance and enhances an efficient use of the resources of society for the benefit of the individual.

However, problems do exist. The present design codes are based on semi-probabilistic limit states design. In general, the Limit State Design (LSD) methodology was calibrated to provide an appropriate reliability only at the individual element level. Therefore, as resistance safety checks are merely considered at a local level (cross section or structural element) and the global resistance is not directly accounted for, the design efficiency and the global target reliability may not be achieved in practice.

As highlighted by (Starossek, 2006), the safety of the structure depends not only on the safety of all the elements against local failure but also of the system response to local failure. The implied assumption that the adequate resistance of the structure is guaranteed by the resistance of its elements is generally not valid, see (Starossek, Wolff, 2005). An example is a structural system built in series with a critical load path composed of a large number of elements. Each element can be designed to have a very low probability of failure, however the failure probability of such a structure is related to the sum of the failure probabilities of the individual structural elements, which depending on the number of elements can add up to values high enough to be taken seriously

(Starossek, Wolff, 2005). Robustness requirements present in the actual codes are not linked with a quantifiable reliability level of the whole structural system, since target reliabilities specified in codes address only single elements. And as (Ellingwood, 2008) pointed out: *"(...) no attempt was made to rationalise the calibrated reliabilities in explicit risk terms; thus, they are related to social expectations of performance only to the extent that reliability benchmarks obtained from member calibration to historical practice can be related to such expectations"*.

Current code design philosophies continue to be mainly based on prescriptive rules, many of them calibrated only at a local level, from which the final design solution is deemed to satisfy a variety of different goals. Most of the rules were developed for general application, and are expressed by simplified verification formats from which conservative solutions are expected to be obtained. This limits the options made available to the designer to optimise the structure to specific performance objectives. To do so would require the use of different partial factors for each component type, size, structural arrangement, type of loading, type of usage, etc. (CIRIA, 1977).

Therefore, the present basis for design does not assure optimal design in terms of resources allocation and risk acceptance. The traditional standards-based approach is becoming increasingly inadequate to handle allocation of limited resources for structures design, operation, repair or improvement, in a climate of growing public scrutiny.

The prescriptive rules specified in present codes if incorrectly applied or misunderstood can lead to unsafe design. However, this can sometimes be forgotten due to apparent limit-free safety, *i.e.* absence of risk, assured by the use of partial factors together with the fulfilment of a set of more or less standard requirements (CIRIA, 1977). In this approach the engineer tend to forget the phenomenological understanding of structural behaviour and thus the safety or functionality of non-standard or novel structures can become compromised.

When the engineer is confronted with an omission on the structural code about a given problem, generally he/she has no option other than to resort to heuristic methods such as what is considered to represent good practice. The more subtle aspects of this approach are based on intuition, and are often referred to as "engineering judgement". However, examples abound of new issues and new problems, such as bridge falsework related, where the experience of previous work does not provide an adequate guide due to structural or economical aspects. Furthermore, uncertainties can appear in the process of extrapolating past experience to existing problems due to differences in the current and past design methodologies.

It can be concluded that existing codes still have application limitations despite recent advances towards performance-based design and consequence-based design. Therefore, there is still further improvement opportunities to be taken towards a more rational and efficient structural design. This can be particularly important regarding bridge falsework systems where a number of recent accidents demonstrate the need for a more comprehensive approach to design and safety evaluation.

Existing codes certainly introduced improvements but specific important aspects in assessing the safety and structural efficiency of bridge falsework systems are still not adequately addressed. As mentioned previously, existing codes were only calibrated with respect to structures where significant past experience exists. (Sexsmith, 1998) argues that *"Calibration works where the variation of construction cost with safety is not particularly sensitive in the range of acceptable safety, and where there is a very large database of structures upon which to base the calibration. In the case of temporary structures such as bridge falsework, or parts of the permanent bridge that are subjected to temporary erection loads, calibration is unlikely to provide consistent results"*. Furthermore, the safety and performance of bridge falsework structures are by large further affected than permanent structures by uncertainty sources which might be difficult to fully cover in standards, related for instance to QC/QA errors. Therefore, the notional target reliabilities specified in existing temporary structures codes can be insufficient if effective and rigorous quality control procedures are not developed and enforced to achieve adequate structural safety.

As a response to the abovementioned insufficiencies of existing codes' design philosophy a risk informed design methodology as an alternative is advantageous, see (Faber, 2009). In this approach, which will be explored in more detail in the following, the goal is to optimise the structure to achieve minimum risk, not minimum probability of failure which is the goal of reliability-based design.

In this Thesis new robustness and fragility indices will be presented and the latter will form the basis of the risk management framework. This new methodology is applicable, in principle, to all structural analyses not only those concerning bridge falsework systems. It was decided to incorporate it in the present Thesis since it brings significant advantages towards a holistic design approach to civil engineering structures.

This Chapter gives a complete insight to the risk management framework, from the principles of risk and a general layout of the risk management framework, to the methods and procedures to be used to determine robustness, fragility and vulnerability, including guidance on how to address them from an economic cost-benefit point of view in order to achieve rational decisions in civil engineering.

5.2 Notation

Inconsistent notation is a potential source of confusion. In this Chapter, random variable matrices are denoted with capital Roman bold letters and random variable vectors are denoted with italic capital Roman letters. Italic lower case letters denote realisations of random variables. Functions are written as $h(\ )$. The use of $f(\ )$ is reserved for the probability density function, and $F(\ )$ denotes the cumulative distribution function. Roman capital P denotes the probability of an event.

5.3 Concepts and definitions

The structural performance of a structural system, no matter what definition is used, can be analysed considering the framework represented in Figure 5.1.
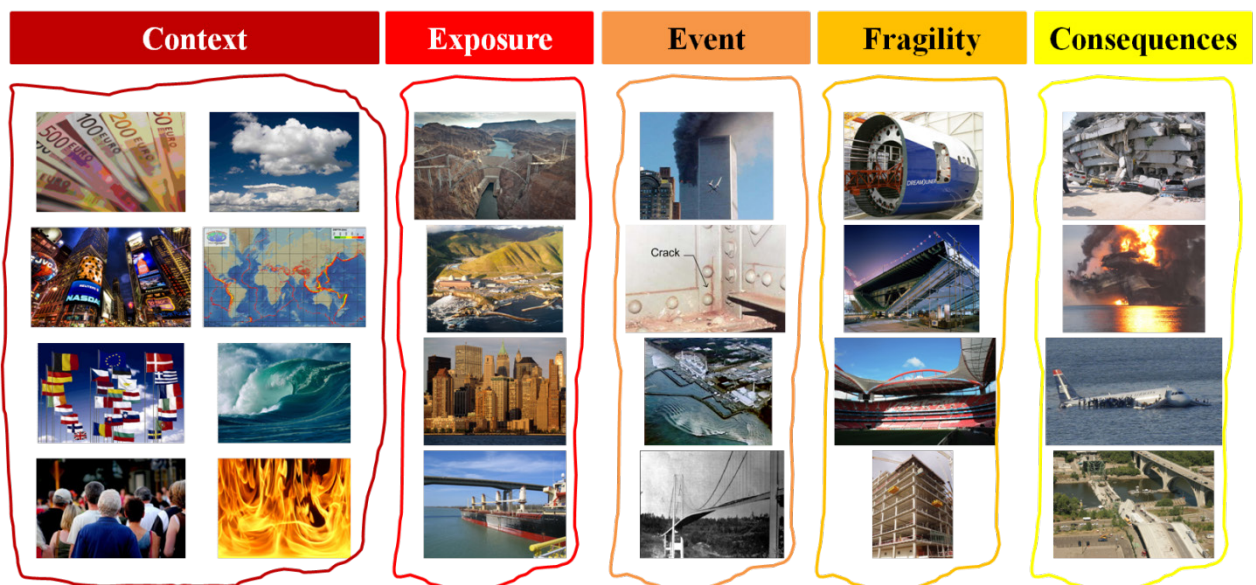
Figure 5.1: Framework for structural design.

5.3.1 System context

"Every organisation functions within an environment which both influences the risks faced and provides a context within which risk has to be managed" (HM Treasury, 2004). The system context is defined by the external and internal variables that together govern the scope, behaviour and objectives of the system. External context can include the cultural, social, political, economic environment whether at

international, national, regional or at local level. Internal context can include the organisational structure, the objectives and the strategies that are in place to achieve them and the capabilities understood in terms of available resources and knowledge (*e.g.* capital, time, people, processes, systems and technologies) (ISO, 2009a).

5.3.2 Exposure and hazard scenarios

The exposure of the system is expressed as the number of different events that could act on the constituents of the system with potential consequences for the considered system. Each event may itself be a hazard scenario or may lead to one or more different hazard scenarios.

Hazard is understood as set of conditions with the potential of leading to undesirable consequences, *i.e.* threat, danger or harm to the resistance and/or function of part or the entire system, arising from a single event or from a combination of multiple events (ANCOLD, 2003 ; HSE, 2001 ; JCSS, 2001). In BS EN 1990 (BSI, 2002a), hazard is defined as *"an unusual and severe event"*. Therefore, a hazard scenario is a critical situation at a particular time consisting of a set of events which can lead to unwanted consequences, if nothing stops it.

It is possible to distinguish between internal and external events. Internal events are those that stem from the structural system, whereas external events are those related to external actions.

Internal events can be related to all phases of the structure life: from design and construction to maintenance and decommissioning. In particular, the influence of human errors is very important. In the design phase internal hazard scenarios can correspond to wrong design assumptions not matching the "real" structural behaviour, whereas in the construction and maintenance phases collapse can happen due to errors in assembly, planning, use of deficient or incorrect elements or components, etc.

External events can correspond to load types not accounted for in the design phase or loads intensity, duration, range or effects (forces, displacements, vibrations, etc.) larger than expected.

5.3.3 Damages, failure events and consequences

Associated with a given hazard scenario are damages to the system. Damages can be defined as unfavourable changes in the condition of a system that can affect the system performance. Damages can be classified as direct damages and indirect damages. Direct damages are related to damages in those elements directly involved in the hazard scenario, which result in the first failures of elements, while indirect damages are the damages that result from the direct damages, due to the incapability of the system to sustain the latter without further damages.

Depending on the characteristics of the damages, failure events can take place when the performance of one, or more, of the structural system elements does not satisfy certain design objectives, regarding safety or serviceability for example.

Damages and failure events lead to consequences. Consequences can range from beneficial to adverse, and may be expressed in qualitatively or quantitatively terms to characterise loss of life, injury, economic loss, environmental harm, disruption of function or/and safety, etc. Both immediate consequences and those that arise after a certain time has elapsed, *i.e. follow-up* consequences, should be considered.

5.3.4 Load paths and failure modes

Load paths can be defined as the integral of all elements of the system affected by internal and external action effects. They are described by element stresses, internal forces, reactions, etc., and can be traced by calculating or measuring those quantities from the point of application of the load to the boundaries of the system (Knoll, Vogel, 2009).

A failure mode describes how element failures can occur resulting in the total or partial collapse of the system. For a given hazard, *e.g.* overload or construction flaw, a structure can exhibit very different failure modes depending on the critical elements and the primary load paths. The most common example is the *weak beam/strong column* concept adopted in most current seismic codes.

5.3.5 Fragility and vulnerability

The fragility of a system is an expression of the system's structural performance, typically in terms of damage extension, for a given hazard event. Traditionally, fragility of a structure or element may be expressed by the conditional probability of failure for a given hazard event. Fragility is a system characteristic, independent of the probability of occurrence of the hazard event.

Vulnerability of a system describes the degree to which it is susceptible to realise a specified degree of loss following the occurrence of an initiating threat event (McGill, Ayyub, 2007). It provides a mapping between a given exposure event and a resulting consequence, typically economic losses or number of fatalities. Therefore, vulnerability links fragility to consequences.

The vulnerability of a system to a given degree of loss with respect to a specific initiating threat event requires all intermediate chains between cause and given consequence to fail. If one chain does not fail the occurrence of the given degree of loss is prevented (McGill, Ayyub, 2007).

In risk terms the vulnerability of a structure to a hazard scenario is defined by the conditional probability of consequence c_i for a given hazard event e_j (McGill, Ayyub, 2007). Faber (Faber, 2009) defines vulnerability of a system as all possible direct consequences (consequences associated with direct damages) integrated (or summed up, depending whether the variables follow discrete or continuous functions) over all possible exposure events. In the present Thesis, however, vulnerability is understood to be associated with all consequences, direct and indirect.

Fragility and vulnerability are both important components that need to be considered for a risk informed decision-making.

5.3.6 A novel definition of robustness

Robustness is defined in ISO 2394 (ISO, 1998) has the *"ability of a structure not to be damaged by events like fire, explosions, impact or consequences of human errors, to an extent disproportionate to the original cause"*. In this definition robustness can be defined as a parameter indicating the sensitivity of a structure to disproportionate collapse, *i.e.* a distinct disproportion between the triggering, spatially limited failure and the resulting widespread collapse, due to a local failure (Starossek, 2009). Or in other words, the robustness of a system is a measure of the ability of a system to restrict the failures to those damaged elements directly involved with a given local hazard scenario.

Structural robustness was only defined and introduced as a design objective, even if only qualitatively, following the partial collapse that occurred at Ronan Point in UK in 1968. As usual, following a peak of inflated focus the research attention given to robustness attenuated, until the Oklahoma City bomb attack on the Alfred P. Murrah Federal Building took place in 1995, and furthermore after the 2001 terrorist attacks to the Twin Towers in New York, turned again the spotlights towards robustness, *e.g.* the study of disproportionate collapse.

According to (Faber, 2009) *"despite many significant theoretical, methodical and technological advances over the recent years, structural robustness is still an issue of controversy and poses difficulties in regard to interpretation as well as regulation"*.

Existing *"design codes have traditionally been developed with the main focus on the structural reliability for individual failure modes or components of structures"*. (Faber, 2009). The satisfactory global behaviour of the structural system and its target reliability are expected to be guaranteed by the individual members' reliability provided by the specified design rules. A general design method for structural integrity, or

structural robustness, is not yet explicitly specified in the existing design codes, although general design guidance is given to assure appropriate strength and ductility of the structural connections between members. An exception to this general observation are the rules that most recent codes provide regarding the structural analysis and structural requirements for accidental load cases, such as failure of a member (typically a column) due to an explosion or vehicle (or ship) collision.

Why is structural robustness important? The answer to this question is given in the Preface of Starossek's book (Starossek, 2009): *"Progressive collapse is arguably the most dramatic and feared form of failure in structural engineering. It usually occurs unexpectedly and causes high losses"*.

In the present Thesis, a broader definition of robustness is introduced: robustness is a measure of the predisposition of a structural system to loss of global equilibrium and global stability, as a result of a failure scenario, *e.g.* a failure of one or more elements of the structure, for a given load case. It is applicable to all design situations and not only those unforeseen, accidental, or concerning local failures (difficult to define and select). Additionally, the influence of uncertainties associated with the manufacturing, the design and assembly, the operating and the maintenance conditions can be directly accounted for in the analysis.

It is the evaluation of the *"what if"* scenario, which is absent from any present code or standard. This omission can lead to unsafe (damage intolerant) structures, since a non-robust structure can crumble in a progressive and disproportionate collapse fashion if submitted to (i) a failure scenario under normal operation conditions, (ii) an accidental load case, with low probability of occurrence, (iii) an unexpected load case, or (iv) a load case unaccounted for.

5.3.7 Uncertainties in civil engineering: a proposal of a different approach

Unlike the deterministic theoretical models considered by Newton and Laplace, the real behaviour of physical systems is uncertain. Chaos Theory, developed by scientists like Poincare, Liapunov, Lorenz and Mandelbrot clearly illustrates the importance of uncertainty.

This theory suggests that one system can behave very differently if the initial conditions vary slightly – the so-called "sensitive dependence on initial conditions". A tiny error or imperfection can have a tremendous influence on the behaviour of the entire system: the "butterfly effect". Therefore, in order to predict accurately the future states of a system it is not only necessary to know the laws of physics that govern the system but also the system's initial conditions. However, it is not always possible to know the initial conditions from observing the present behaviour of a physical system: irreversible systems are a good example. Also, initial conditions are never exactly the same and even small changes in the initial conditions of simple and ordered systems can produce unpredictable and complex behaviour; and the higher the number of random variables involved in a system, the higher is the chance it will become chaotic.

If the uncertainty associated with finite expression of real numbers is not considered, it is possible to postulate that the uncertainty from Chaos Theory derives from imperfect or insufficient information. Therefore, it can be reduced (and even "eliminated") if the necessary resources are made available, and eventually the system becomes "deterministic". The words eliminated and deterministic are written using quotation marks, because there is another type of uncertainty regarding information which is impossible to be known. The basis of this type of uncertainty is the Heisenberg's Uncertainty Principle, which states that *"one cannot assign exact simultaneous values to the position and momentum of a physical system. Rather, these quantities can only be determined with some characteristic 'uncertainties' that cannot become arbitrarily small simultaneously"*.

It is therefore not surprising that despite the recent advances in civil engineering the presence of uncertainties during the design, construction and maintenance of major infrastructures such as bridges can greatly influence their expected performance. In bridge falsework systems, changes in

the initial conditions can lead to very different structural behaviour especially when the structural geometry is complex.

Sources of uncertainty are present everywhere: from our perception of nature, to human errors. In civil engineering this translates to uncertainty in (i) the analysis methods and models used to assess the probabilities of occurrence of an event and of its consequences, and in (ii) the effectiveness of the control measures taken to manage the risk level.

Uncertainties are often classified in two types of uncertainties: aleatory uncertainties and epistemic uncertainties. The former type corresponds to intrinsic variations in time and space of the properties of a given material, element geometry, and inherent variation of environmental loads, for example, that are not easily controlled and reduced. The latter type is related to knowledge-based insufficiencies (scientific and technological) and to human intervention (including human errors) which can be controlled and reduced. See (Ang, Tang, 2007; Ayyub, McCuen, 2011) for more details.

The classification of uncertainties in these two categories is not always obvious, straightforward and beneficial. Humans are not mere observers and should aim to improve their understanding of the world. Equivalent, but clearer definitions, are variability and uncertainty; the first being the result of random processes and the second being the result of approximations made to investigate the behaviour and properties of random processes.

However, the development of a more transparent model to analyse uncertainties is advantageous, such as the one illustrated in Figure 5.2.
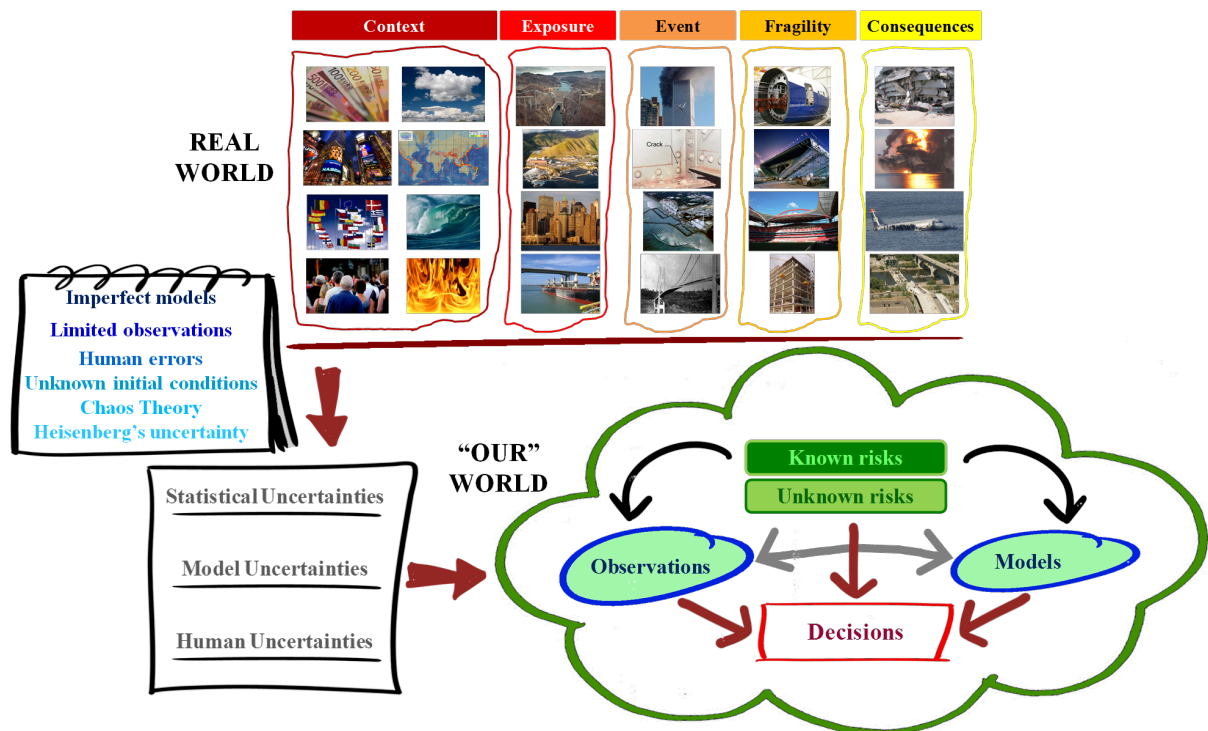
Figure 5.2: Framework for uncertainty analysis.

The level of uncertainties that mankind faces today stems mainly from our insufficient knowledge about natural systems, such as the atmosphere, materials, human mind, etc. Due to our lack of knowledge of the past, present and future, the models developed to interact with or analyse a given system are mere idealisations, often incomplete and inaccurate. This leads to (model) uncertainties. From Heisenberg's Uncertainty Principle and Chaos Theory, random variables exist and can only be expressed in terms of probabilistic models and statistical information, which may use objective and/or subjective information. This uncertain information will then be used in numerical or analytical models, or to test theoretical models in order to predict the behaviour (in time and in space) of the system, sub-system or components being analysed.

For example, model uncertainties can simply *stem* from incorrect measurand definition or from developing an inaccurate model, for example. Statistical uncertainties stem from various different sources. Probabilistic models are only approximations of the true model, since they are determined from samples and not from the entire population. Even the most accurate devices to measure lengths, temperatures or other random variables and random processes introduce uncertainties. All these uncertainties summed with the variability of the measurand add up to form statistical uncertainties. Human interaction with natural systems also introduce uncertainty: when applying a model, measuring a measurand, when analysing the data collected, or when performing other activities such as concrete casting of a bridge slab, erecting a bridge falsework structure, deciding between alternative solutions and implementing the selected measures, for instance. Human uncertainty is transversal since it is always present. The uncertainty of the output obtained from applying a given model is a combined uncertainty of model, statistical and human uncertainties.

Consequently, uncertainties can be classified in three basic categories: (i) model uncertainties, (ii) statistical uncertainties and (iii) human interaction. It is beneficial to keep these different sources separated in the analysis. The so-called aleatory uncertainty is here defined as the uncertainty to predict the future and describing the past, it represents the variability of natural phenomena and cannot be reduced, and is part of the statistical uncertainty. Epistemic uncertainty is present in all the three new uncertainty classifications.

Generally it is very difficult to estimate most of the uncertainties mentioned above. In structural engineering some of them might only be indirectly considered or even be ignored (*e.g.* human errors, phenomenological and decision uncertainties, etc.). This causes the calculated probability of failure to be a notional estimate that does not reflect the actual failure rate of structures.

5.3.8 Probability in civil engineering

According to (Faber, 2009), probability theory forms the basis for the assessment of probabilities of occurrence of uncertain events and thus constitutes a cornerstone in risk and decision analysis. Only when a consistent basis has been established for the analysis of the probability that events with possible adverse, or beneficial, consequences may occur it is possible to assess the risks associated with a given activity and thus to establish a rational basis for decision-making.

There are various possible interpretations of probability: classical, frequentist and subjective (Bedford, Cooke, 2001). In civil engineering probability is best defined by a mathematical expression of the level of uncertainty (Bedford, Cooke, 2001). A more detailed meaning is given by (McDonald et al., 2005) which defines probability as *"a measure of the degree of confidence in a prediction, as dictated by the evidence, concerning the nature of an uncertain quantity or the occurrence of an uncertain future event. It is an estimate of the likelihood of the magnitude of the uncertain quantity, or the likelihood of the occurrence of the uncertain future event. This measure has a value between zero (impossibility) and 1,0 (certainty)"*.

All probabilities are conditional on the background information, including knowledge (Aven, 2004), and the use of the various types of probabilistic models is based on the degree of belief (confidence) that the analyst has on the available information. If the analyst is confident about the available data, then it may be argued that there is no need to propagate the uncertainty of the probabilistic distribution parameters, see (Apeland et al., 2002) for details, which would only be considered if the analyst has vague information about the random variables.

5.3.9 Structural reliability and structural safety

EN 1990 (BSI, 2002a) defines reliability as *"the ability of a structure or a structural member to fulfil the specified requirements, including the design working life, for which it has been designed"*. An alternative definition, commonly used, defines reliability as a stochastic variable given by the complement of probability of failure.

Structural safety is defined in (IStructE, 2007) as referring *"to the strength, stability and integrity of a structure to withstand the conditions that are likely to be encountered during its life-time. Structural safety is achieved through the proper procurement, design, construction, use and maintenance of the structure and the application of best practice"*.

5.3.10 Definition of risk

Risk is defined in (ISO, 2009a) as the effect of uncertainty on objectives, whether positive or negative. Risk depends on the system context and exposure to all relevant types of events, on the system behaviour, on the significance of consequences (beneficial and adverse) of a given event and on the uncertainties in the assessment of these variables over a certain period of time.

In general, considering an activity with only one event with potential consequences, risk is usually expressed as the probability that this event will occur multiplied with the consequences (beneficial or adverse) given the event occurs (Faber, Stewart, 2003). The activity can be the design, construction, use, maintenance or decommissioning of a concrete bridge, for example. However, in civil engineering, risk can also be expressed by the probability of structural failure from all possible causes, usually in terms of the expected annual frequency (Melchers, 1999) or by the expected cost of consequences.

Risk is commonly expressed as an expected value. However, this practice can introduce distortions in the assessment, see (Haimes, 2009 ; Savage, 2009). It is highly recommended to include in the risk model the effect of uncertainties.

Risk can be classified as individual or societal risks, voluntary or involuntary risks; known risks, known unknowns and unknown unknowns (*force-majeure*) risks; recognised or unrecognised risks. See (Blockley, 1992) for an in-depth discussion of risk characteristics.

Individual risk is how individuals see the risk from a particular hazard affecting them and things they value in a given time period. It reflects the individual assessment regarding the expected benefits and the severity of the hazards, but also when (near future or long term?) and for how long is the individual in the proximity of the hazard sources.

Societal risk is the risk experienced in a given time period by a whole group of persons and is related to severe events that if it were to occur would cause widespread or large scale consequences and multiple fatalities. Studies, see (Marsden et al., 2007), have shown that society is risk neutral, *i.e.* society considers that averting 1000 accidents with one fatality each is of nearly equal benefit to averting one accident with 1000 fatalities. However, society does not accept a large number of fatalities even if the risk per individual is small (Kumamoto, 2007).

Voluntary risks are self-willing risks and risks that the individual or society think they can control, while involuntary risks are imposed risks or unknown risks.

5.4 Risk management framework for structural design based on novel robustness and fragility indices

5.4.1 Introduction

Never before have humans lived longer and better. Housing and health care are available to millions of people and equipment, products, and food are quality tested and safer than ever before. Although there is an inherent risk in all human activities, there is an evident downward trend over the years. The common sense tells us that risk in the majority of our daily life activities is low and very well regulated.

As a result of this evolution, individuals and society are risk averse: they are willing to take advantage of advances in science and technology to reach certain objectives but only if the risks are small enough

to be acceptable, or low and clearly controlled to be tolerable. However, not all the risks are known (or recognised) and the ones that are, are not always clearly explained and properly managed.

At the same time, individuals and society are much more risk reactive. The various media sources make information travel the world almost instantaneously and each severe accident is subject to public scrutiny and critics. Although, it is nowadays consensual that safety is not an absolute and infinite condition, but is instead a tolerated situation desirably balanced with low levels of residual risk (McDonald et al., 2005), society demands that proactive rather than reactive measures should be engaged so that risks with the potential to affect the welfare, safety and other interests of the community are kept under review and properly controlled.

In short, individuals and society at large expect that risks are properly managed; they are not willing to accept risk just based on economic factors and do not accept that risks have been hidden behind potential benefits.

Additionally, it is evident that in the last decades there has been an increase of global awareness by society about issues such as sustainable development and conservation of the environment, transparency in political decision-making, political accountability regarding public spending to increase society welfare, health and safety.

It is thus necessary to integrate in the decision-making process the optimal allocation of available natural, economical and technological resources, balanced with the requirement to guarantee and to preserve a proper safety level. In civil engineering applications some gradual shifts are seen to meet these new societal expectations: great advances have been made in using probabilistic methods coupled with simulation analyses rather than pure deterministic ones, and reliability and risk analyses are increasingly gaining importance as decision support tools to ensure that structures' design, operation, maintenance and overall management are both economical and safe (Faber, Stewart, 2003). Therefore, it is not surprising that organizations which cannot demonstrate the rationale supporting its decision-making process, place themselves in a weak position should an adverse event occur.

Risk management is also an important tool of asset management. An asset can be defined as a physical system from which valuable services can be provided. According to (CIRIA, 2009), *"whole-life infrastructure asset management balances maintenance, repair, refurbishment, renewal, replacement, and upgrade activities to optimise the long-term value of an asset"*. Asset management can be defined as *"the systematic and co-ordinated activities and practices through which an organisation optimally and sustainably manages its assets and asset systems, their associated performance, risks and expenditures over their life cycles for the purpose of achieving its organisational strategic plan"* (CIRIA, 2009).

Every bridge is an important infrastructure asset. Therefore each activity that significantly influences the bridge whole-life value needs proper consideration. Bridge falsework fits in this group of activities. Furthermore, bridge falsework is itself an asset which has to be correctly managed. It is thus logical that the structural design of bridge falsework structures must be integrated in a broader scope of asset management to maximise the benefits and minimise the risks.

5.4.2 Risk management

Risk management is the complete process of risk assessment and risk control that aims at achieving a balance between the need to protect against existing and future risks, and the benefits deriving from a given activity. In a framework of a specific context, risk management helps organizations to address risks and make efficient decisions to achieve the desired objectives with a limited and justifiable risk level. Risk management does not dictate decisions but rather contributes to a risk informed decision-making process.

Although one can never remove all uncertainties of a construction project – it is not technologically and economically possible to identify and eliminate all risks – systematic risk management improves

the chances of a given project being completed on time, within budget and accomplishing the required quality, with proper provision for safety and environmental issues (Godfrey, 1996).

Risk management is not new. Traditionally it has been applied instinctively with risks remaining implicit and managed by judgement informed by experience (Godfrey, 1996). The process of risk management is complex and non-linear, based on successive iterations until the correct balance between different inputs and generated outputs is judged to be found. Furthermore, risks cannot be addressed in isolation from each other. Risks are interlinked and the management of one risk may have positive or negative consequences on others. Clear communication, external consultation and constant review are recommended.

The optimal aim of risk management is to reduce as much as possible the risk associated with a given activity or action. Depending on the legal context there are different ways of reaching this central objective. The UK's legal system is the Common Law legal system, where laws are written emphasising goals rather than detailing accepted actions to achieve those goals – the case of the rest of European countries where a Civil Law legal system is used. As a result, in UK, Health and Safety at Work (HSW) regulations are based on risk management principles, namely the ALARP (As Low As Reasonably Practicable) principles (HSE, 2001).

In this legal framework, employers are responsible to ensure, that the risks to health, safety and welfare of their employees and of third persons, are managed to a level which can be justified as being acceptable or tolerable. This can be considered attained if the measures cost increase is not cost-effective or is disproportionate, respectively, in front of the expected risk reduction gains, *e.g.* the decrease of consequence costs of a hazardous event (Bowles, 2003). The amount of risks which are judged to be tolerable is the "risk appetite" (HM Treasury, 2004). These residual risks must be accepted or insured against, always monitored and controlled. Activities with an unacceptable or intolerable risk level should be terminated. Additionally, it is understood that one cannot use ALARP to justify not following good practice; ALARP should rather be used in cases where good practice is unclear, is only partially applicable or where higher levels of quality and safety are aimed.

Risk management should answer three fundamental questions (Kaplan, Garrick, 1981):

- What can go wrong?
- How likely is it to go wrong?
- What are the ensuing consequences?

ISO 31000:2009 (ISO, 2009a) establishes a risk management model, see Figure 5.3. It is presented as having a hierarchical structure with various steps each one with different objectives, but in reality a global strategy must exist to make the process efficient and coherent.

Any activity, or project, is initiated to achieve certain objectives. Their definition and the decision to start the project are influenced by numerous stakeholders. No project can be developed in a self-contained environment since multiple interdependencies and interactions, some of them which cannot be directly controlled, will always exist between the different interested stakeholders: individuals and society, organizations and countries. It is therefore very important to attain at the outset of risk management a detailed understanding of the context in which the activity will be developed: laws and regulations, stakeholders' preferences and expectations, available resources, level of uncertainties, etc. Next, the objectives can be defined along with the analysis scope, requirements and attributes (performance indicators of the objectives) as well as the methodology to be used and the available resources needed (including time and costs). The objectives should be SMART: Specific, Measurable, Achievable, Realistic and Time bounded (HM Treasury, 2003) and attributes should follow rules given in (Goodwin, Wright, 2010).
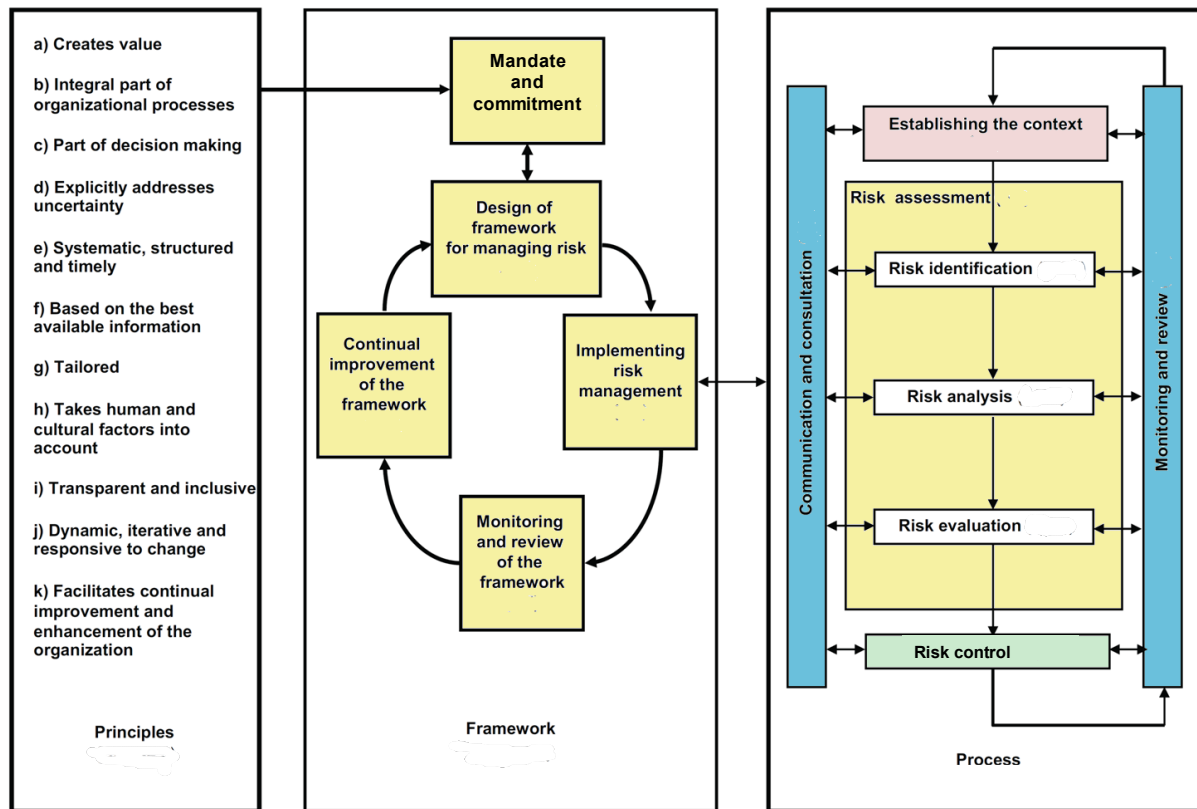
Figure 5.3: Risk management framework, adapted from (ISO, 2009a).

5.4.3 Risk assessment

Risk assessment encompasses risk analysis and risk evaluation. Typically the risk assessment is an iterative process where risk is calculated by a structured, systematic examination of the likelihood of critical events and of the associated potential consequences on the planned objectives should these events occur. Another central characteristic of risk assessment is that it involves making trade-offs (i) between risks to some individuals or groups and risks to the society; and (ii) between costs and benefits of different scenarios. It is also very important to appropriately identify, document and evaluate key types of uncertainty and then to consider them in an explicit and transparent way. At the end of risk assessment, the results must be properly communicated.

5.4.3.1 Risk analysis

Generally, *risk analysis* is the start of risk management. Risk analysis usually begins with a careful description and examination of the system: (i) context, (ii) activity objectives, performance requirements, methods of operation and development, (iii) structural components and their functions, (iv) design concepts, potential hazard events, possible failure modes and (v) consequences over a certain period of time, corresponding to the design working life of the structure (McDonald et al., 2005). Several practical problems can arise at this phase, some of which are described in (Blockley, 1992).

5.4.3.1.1 Risk identification

Risk identification is the compilation, review and use of the available information concerning relevant hazard scenarios, with appropriate consideration of the uncertainties involved, for characterisation of what is known and what is uncertain about the present and future performance of the structure. It generally involves a systematic approach for describing the system context, for identifying and describing the relevant hazard scenarios: what can happen, how, why and who will be involved? At this phase, links are established between hazards, consequences and causes, and their sensitivity to each individual contribution is evaluated.

Civil engineering contains many potential risks, related for instance with: design, construction, testing, maintenance, third party activities, environment, health and safety, finance, legal contracts, management and political organisation (Artamonov et al., 2008 ; Bunni, 2003). If all the relevant hazard scenarios are not identified (some maybe unknown at the start) or correctly characterised then risk analysis will result in biased decision-making, which in general will be cost inefficient and ultimately could lead to unacceptably high risks to people and to the environment (Faber, Stewart, 2003). Thus, it requires a detailed examination and understanding of the system, and a variety of techniques have been developed to assist the engineer in performing this part of the analysis, *e.g.* brainstorming techniques, morphologic boxes, Hazard and Operability analysis [HAZOP], Failure Mode and Effect Analysis [FMEA], Fault Tree Analysis (FTA), Event Tree Analysis (ETA) and Bayesian Probabilistic Networks [BPNs], see (ISO, 2009b).

5.4.3.1.2   Risk estimation

Risk estimation involves the analysis of the probability of occurrence of certain critical hazard events and of their subsequent consequences (sequence of failure events, damages to functionality or other, health and safety). Uncertainty analysis should be part of risk analysis to determine the influence of uncertainties on the likelihood of occurrence of the hazards and of the consequences. Risks must be estimated and expressed in terms of the attributes of the problem in hand.

There are two ways to determine the probability models of hazard scenarios. One uses statistical analysis of empirical data and gives the so called objective probability. The other one uses intuition and relevant experience of the expert engineer and gives the so called subjective probability. Nevertheless, subjectivity is always present in any probabilistic model building process, it is evident that objective probabilities are more effective and it is necessary to use them every time it is possible. However, there are cases where there is insufficient data or large uncertainties. In these cases, probabilities can only be estimated subjectively, quantitatively or the majority of times qualitatively, and the engineer's experience becomes very important. In general, the two approaches are often used in a complementary way.

As a first approach, the probability of occurrence of given hazard scenario and the significance of its expected consequences can be estimated qualitatively, by one of the various available methods, such as FMEA. Doing this for all hazard scenarios one can build a risk matrix, see Table 5.1 – "5×5" matrices are often used, with consequences on a scale of "insignificant / minor/ moderate / major / catastrophic" and likelihood on a scale of "rare / unlikely / possible / likely / almost certain" (HM Treasury, 2004).

Table 5.1: Example of a risk matrix.

Risk		Consequences				
		Insignificant	Minor	Moderate	Major	Catastrophic
Likelihood	Almost certain					
	Likely					
	Possible					
	Unlikely					
	Rare					

Alternatively, or as a subsequent second step, the probability of occurrence of hazard scenarios can be estimated quantitatively by probability analysis. Several methods exist to achieve this goal: First Order Reliability Method (FORM), Second Order Reliability Method (SORM), Monte Carlo methods (MC) or Stochastic Finite Element Methods (SFEM). Probability analysis can also be performed using ETA, FTA or BPN to obtain estimates of the system's reliability. A detailed discussion about these methods is given in (Bedford, Cooke, 2001 ; Hartford, Baecher, 2004 ; Det Norske Veritas, 2002). With this information, the most important (critical) risks can be identified and risks concerning the different attributes can be ranked, possibly with the introduction of weights to allow for multi-criteria.

5.4.4 Risk evaluation

Next follows *risk evaluation*. It is the process of examining and judging the significance of risk (McDonald et al., 2005). First, the risk acceptance criteria are established and the acceptable and the unacceptable risk levels are defined. The UK Health and Safety Executive (HSE, 2001) present three risk criteria, explained in greater detail in (Bowles, 2007):

- *"An equity-based criterion, which starts with the premise that all individuals have unconditional rights to certain levels of protection (…);*

- *A utility-based criterion which applies to the comparison between the incremental benefits of the measures to prevent the risk of injury or detriment, and the cost of the measures (…);*

- *A technology-based criterion which essentially reflects the idea that a satisfactory level of risk prevention is attained when 'state of the art' control measures (technological, managerial, organisational) are employed to control risks whatever the circumstances".*

A fourth criterion, a sustainability criterion, must be also considered. This criterion involves the consideration of problems such as intergenerational equity and allocation of resources in the long-term, for example to maximise the design working life of civil engineering infrastructures at a minimum cost (durability and debt problems) and green engineering (climate change problems), see (Nishijima, 2009) for examples.

Acceptable and unacceptable (*i.e.* limit of tolerability) risk levels must be defined by taking into account the context: nature of risk, type of stakeholders, amount of available resources and magnitude and distribution of consequences to individuals and society. In order to help establishing acceptable and unacceptable risk limits, it is recommended to assess the individual and societal perception and aversion to risks (distinguishing between voluntary or imposed, known or unknown risk scenarios), the Value for Preventing a Fatality (VPF) and the Life Quality Index (LQI), for example.

Risks are classified as acceptable, as unacceptable or as being in the tolerability range by comparing the estimated risks with the risk criteria. It should not be forgotten that it is the total risk that matters in the end. The risk associated with a single hazard scenario can be acceptable but when the risks associated to all identified hazards are summed up the total risk can be higher than the acceptable level.

Furthermore, a list with a range of alternative measures for managing the risks which are higher than the acceptable risk level is developed. Figure 5.4 illustrates a possible framework (the "safety cube") to define the breadth of measures, their application opportunity and the tools involved in their implementation. Measures can also be defined as active or passive, preventive (proactive) or protective (reactive), see (Todinov, 2007) for more details.

5.4.5 Risk control

The last phase of risk management is *risk control*. Here all the information made available in the previous phases is gathered and reviewed. If the estimated risk is greater than the acceptable risk level, and because citing (Fischhoff et al., 1981) *"One accepts options, not risks"*, the risk level must be modified by suitable proportional measures. This process is referred as *risk treatment* and can involve different approaches – see (HSE, 2001) for more detail –, which are summarised below:

- *Risk mitigation*: In essence, risk mitigation is implemented by reducing the probability of the occurrence of the hazard scenario to nominally zero, by for instance restricting the use of the structure (changing the exposure);
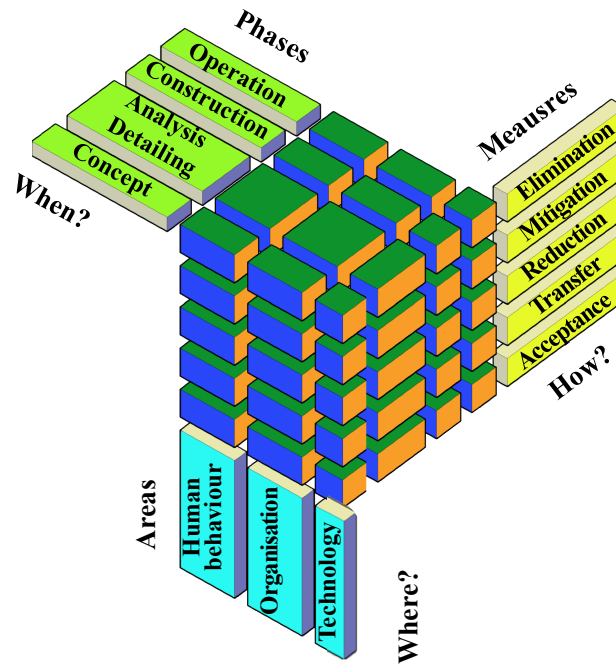
Figure 5.4: Safety cube, adapted from (Schneider, 2006).

- *Risk reduction*: This may be implemented by reducing the probability of the occurrence of the hazard scenario and/or of its consequences. In practice risk reduction can be performed by decreasing the fragility and vulnerability either by changing the exposure of the system, by increasing the reliability and the robustness of the system, and by non-structural measures such as: monitoring, surveillance, and periodic inspections, and planning after-failure measures. Considering the risk of collapse of slender steel frame structures, like bridge falsework systems, due to instability and second-order effects, this might be reduced by bracing critical elements;

- *Risk transfer*: This may be performed by insurance or other financial arrangements where a third party, normally an insurer, takes over the risk. Therefore, risk transfer is normally associated with a premium cost;

- *Risk tolerance and risk acceptance*: Risk can be tolerated if it is ALARP. Risk acceptance may be an option in the case of activities with a low risk profile, close to the acceptable risk level, and for which it can be demonstrated that pursuing with any of the other options would lead to unacceptable economic losses;

- *Risk elimination*: Decision not to start or continue the activity (decommissioning).

Risk control incorporates the selection of the measures most suitable to manage risks and also the definition of the performance objectives and requirements of the implementation methods, as well as the definition of the monitoring, evaluation criteria and review methods of the selected measures (accounting for possible updates when relevant information becomes available).

It must be kept in mind that the greater risk reduction achieved by a single measure the more critical this measure becomes. Therefore, these measures should be very reliable, possibly involving the adoption of safeguard measures and the implementation of a comprehensive and continuous monitoring and review system is recommended. Additionally, it should not be forgotten that in certain circumstances reducing a risk source, by increasing the reliability of a critical element, for example, could create other hazard scenarios which were not accounted for in the initial risk analysis. This is one of the reasons why risk management is an iterative process.

For each one of the selected risk treatment measures, residual risks are estimated and resource allocation is optimised. After consultation with the interested stakeholders, a decision needs now to

be made about whether these reminiscent risks are unacceptable, intolerable, ALARP or acceptable; the concept of "risk appetite".

Risk management should be reviewed on a regular basis throughout the duration of the project: typically at the project development stage, at the contract procurement stage, at the design stage (including a regular review of the temporary works design, for example) and at the construction, operation and maintenance stages (Artamonov et al., 2008).

5.4.6 Structural probabilistic analysis

5.4.6.1 Classical structural probabilistic analysis

Although the origins of classical structural probabilistic analysis, *i.e.* reliability analysis, date back from early 1920s, the basis for its application as an accepted analysis method in civil engineering were mainly developed in the 1970s and 1980s decades, when several fundamental books were published (Ang, Tang, 1975 ; Benjamin, Cornell, 1970 ; Ferry Borges, Castanheta, 1968 ; Thoft-Christensen, Baker, 1982).

The classical reliability (time invariant) problem is defined by a structural system characterised by one resistance random variable, R, and subjected to only one load random variable, S. Both basic random variables, R and S, are considered independent and stationary random processes. Therefore, the probability of failure, P_f, of this system is given by:

$$P_f = P(G = R - S \leq 0) = \int_{-\infty}^{+\infty} \int_{-\infty}^{s \geq r} f_R(r) f_S(s)\, dr\, ds \tag{5.1}$$

Additionally, if R and S are further considered to be normally distributed random variables, then:

$$P_f = P(G \leq 0) = \Phi(-\beta)$$

$$\beta = \frac{\mu_G}{\sigma_G}, \ \mu_G = \mu_R - \mu_S, \ \sigma_G = \sqrt{\sigma_R^2 + \sigma_S^2} \tag{5.2}$$

where $\Phi(\ )$ represents the standard normal distribution function and β the reliability index. For G with probability distributions other than normal, β refers only to a notional failure probability. Target values of β can be found in the most recent structural codes (the Eurocodes, for example) and in the Joint Committee on Structural Safety (JCSS) Probabilistic Model Code (JCSS, 2001) or other guidance documents.

However, it is not always possible to analytical solve the probability of failure integral, see equation (5.3), and closed form solutions of the limit state function, G, often do not exist.

$$P_f = P[G(X) \leq 0] = \int \dots \int_{G(X) \leq 0} f_X(x)\, dx \tag{5.3}$$

Therefore, it may be necessary to use simulation tools, such as the Monte Carlo method. The basic idea behind this method is to generate random simulations of the limit state function and observe the result. The disadvantage of this method is related with the high number of simulations, N, necessary to fulfil the accuracy requirements. In the crude Monte Carlo method, the confidence interval of the estimate of P_f is given by (Melchers, 1999):

$$P(\mu - k \times \sigma < P_f < \mu + k \times \sigma) = CL \tag{5.4}$$

where μ and σ are the estimates of the mean and standard deviation values of P_f and CL is the specified confidence level (95% for instance).

It was proved by (Melchers, 1999), that the value of σ decreases in proportion to $N^{-1/2}$. Additionally, the probability of sampling a point at the failure region is in general very low, since $f_X(x)$ is the sampling function, so to achieve convergence it may be necessary more than 10^6 simulations.

Therefore, several methods were developed to reduce the value of σ by other ways. Methods such as variance reductions techniques (Importance Sampling, Latin Hypercube Sampling or Adaptive techniques) try to reduce the value of σ by using additional information about the limit state function, restricting the sampling to be within the region of interest or adapting the sampling to the shape of the limit state function. The latter can also benefit from estimations of the shape of the limit state function; usually obtained by Response Surface methods and by other Design of Experiments methods (DoE). In certain cases, a description of the problem in the polar coordinate system is convenient; this fact led to the development of Directional Simulation methods.

Alternatively, to simulation methods, it is possible to simplify the limit state function by for example using the first-order or second-order Taylor series expansion about some point x. After, the first and second moments of the simplified equation of $G(X) = 0$ can be obtained and the reliability calculated. It is usual to perform a transformation of coordinates from the original space to a standardised space with zero mean and unit variance. If the distributions of the basic variables X are non-normal then they must be transformed into equivalent normal distributions, using either the Rosenblatt transformation (when the joint probability function $f_X(x)$ is known) or the Nataf transformation (when only the marginal distributions and the correlation matrix are known) (Melchers, 1999). Examples of these methods are the First-Order Reliability Method (FORM) and the Second-Order Reliability Method (SORM) (Melchers, 1999). These simplified methods do not provide a measure of the prediction error and cannot guarantee that the critical design point is found.

It should be noted, that if the probability of failure is determined without accounting for all types of uncertainties, in particular the ones related with human intervention, the value of probability of failure must be considered only as a nominal, or notional, value and not as an estimate of the actual failure frequency. As an indication, a CIRIA report indicates that the actual probability of failure is about one order ($\times 10$) higher than the probability of failure determined using the codes format (CIRIA, 1977). The use of a notional probability of failure for comparison of alternatives purposes must be done very carefully since the influence of ignored uncertainties on the total risk might vary considerably between alternatives. It might only be directly considered when the effect of ignored uncertainties is proportional to all considered alternative solutions.

5.4.6.2 Advanced structural probabilistic analysis

In reality, several limit states exist in every structural system, for instance: bending moment resistance, shear resistance, fatigue resistance or equilibrium related limit states. In general, some of these limit states will not be independent from each other. Additionally, basic variables such as load values and resistance properties can vary over time, for instance: a structure can be subjected to various types of loads which can be applied at different times during the structure lifetime and their values can change over time; material's properties can also change over time by deterioration processes such as corrosion or damages by excessive usage.

Thus, the structural probabilistic analysis of complex structural systems, including geometrical and physical nonlinearities, load-path dependencies and the space-time variation of material and system properties, presents considerable challenges to classical reliability methods, such as FORM. However, the use of finite element methods coupled with advanced numerical algorithms can provide solutions to problems where classical methods fail to return accurate results.

Examples of these numerical algorithms are Adaptive Response Surface methods (ARS), Directional ARS (DARS), Polynomial Chaos Theory and Spectral Methods. Recently, Bayesian Probability Networks (BPN) have started to be used to assess the reliability, and risk, of complex and large systems which cannot be incorporated as a whole in the same analysis model. Application examples of BPN analysis are multiple hazard scenarios such as the ones encountered in the design of ships, tunnels or nuclear power plants. However, in problems with complex inter-dependent variables BPN's can underperform, see (Hayes, 2011).

Time dependent reliability problems are still an open area of research but some background can be found in (Melchers, 1999 ; Sudret, 2007). It is worth noticing that the same action can change in time by changing in space. In these cases it is possible to model the action by different loads, each one considered as stationary variables, which are activated at different times at different spaces. This can be useful when modelling construction loads, for example.

5.4.6.3   Probabilistic modelling in civil engineering

As mentioned previously, our perception and knowledge of the world is limited and uncertain. In order to predict accurately the future behaviour of civil engineering infrastructures, engineers need to work with uncertainties in almost all engineering relevant variables. One way to accomplish this is through probabilistic models and statistical analysis.

The formulation of probabilistic models may be based in existing data alone (*aka* frequentist approach), but most often data is not available to the extent where this is possible. In such cases it is also necessary to base the model building on physical arguments, experience and judgement. (Ouchi, 2004) provides a literature review of how to derive a subjective probabilistic function by combining different expert opinions.

5.4.6.3.1   Model selection

A first aid to model selection is to construct probability plots (*e.g.* Q-Q plots). If more than one model is considered to be acceptable, further analysis can be developed by performing hypothesis testing on the selected distributions. Classical tests are the Kolmogorov-Smirnov test, the chi-square test and the Anderson-Darling test. A drawback of hypothesis testing is that it provides the analyst information regarding if there is significant statistical evidence to reject or not the null hypothesis (*e.g.* that the data follow a specified model), so it may be the case that more than one model cannot be rejected. These methods will not inform about which model is "true", but rather about the relative strength of each model given the information available (strong assumption!).

Other goodness of fit methods include selecting the model with the highest log-likelihood or using information theory methods (Claeskens, Hjort, 2008 ; Ando, 2010). However, these methods do not tell if the models fit the data well, only which one is better considering the hypothesis of each method.

Frequentist and subjective probabilistic models are only approximations of the actual phenomenon being analysed. Therefore, there is statistical uncertainty. To include this uncertainty, Bayesian statistics take into account a set of good models and not only a single "true" model, *e.g.* Bayes factors or other Bayesian model selection methods (Congdon, 2006). Alternative methods are given in the following section.

Point estimates of the model parameters can be obtained by the Method of Moments (MoM) or by the Maximum Likelihood Estimation (MLE) method for example. In Bayesian methods the analyst can assume that the model parameters have unknown distributions which can be updated with observed data.

However, as (Box, Draper, 1987) say: *"all models are wrong, but some are useful"*. The best model may be the wrong model because the data used to validate it, even if there is a large amount of data available, is often still insufficient or unrepresentative to derive with the required accuracy the tails of the frequentist probabilistic distribution. An example is model overfitting: if new data is included the model may no longer be able to return accurate results.

As a mean to circumvent this fact, several standard probabilistic models have been proposed in the literature to model actions, actions effects, resistance variables, and time variant associated problems. Examples of standardised probabilistic models are given in the JCSS Probabilistic Model Code (JCSS, 2001). Another tool to choose the probabilistic model is the Maximum Entropy

principle. In any case, the analyst must use his knowledge and consider the nature of the physical or chemical problems at hand when deciding whether or not the selected distribution function is valid.

5.4.6.3.2 Bayes' theorem

Bayes' Theorem, mentioned above several times, is given by equation (5.5) for continuous random variables:

$$f^*\left(\theta \mid x_1,...,x_n\right) = \frac{f\left(x_1,...,x_n \mid \theta\right) \times f\left(\theta\right)}{\int\left[f\left(x_1,...,x_n \mid \theta\right) \times f\left(\theta\right)\right]d\theta} \tag{5.5}$$

where:

θ is a random variable;

x_j (j = 1 to n) are observations of θ;

$f(\theta)$ is called the prior probability distribution of θ which must be estimated either by expert judgement or by existing databases (which should refer to similar measurands as the one being analysed);

$f(x_1,...,x_n|\theta)$ is called the likelihood of x_j (j = 1 to n) observations given θ, also written as $L(x_1,...,x_n|\theta)$;

$f^*(\theta|x_1,...,x_n)$ is called the posterior probability distribution of θ given x_j (j = 1 to n) observations.

Bayes' Theorem has the advantages over classical probabilistic methods of being able to mix different sources of information, and thus for example providing a mean to update the analysis with new data, as well as of being able to incorporate in the analysis the influence of different types of uncertainties.

It is recommended that the existing dataset should be larger than the new dataset and that the quality of the new information be better than the existing information in order to justify the use of Bayesian Theory. Careful attention should be paid in the cases when there is no information about prior distribution and the posterior distribution is significantly affected by the prior distribution. If the prior distribution and its parameters are uncertain, a weighted fitting method can be used to include several distributions, in particular the approach of Bayes factors, see (van Gelder, 2000).

The evaluation of the posterior distribution can be difficult. In these cases, computational approaches, such as Markov Chain Monte Carlo (MCMC) can be used. Several open source programs are available that use Bayesian statistics such as WinBUGS or OpenBUGS (http://www.openbugs.net/).

5.4.6.4 Uncertainty propagation in civil engineering

Uncertainty propagation is a critical step in risk management. It is a signature of the quality of risk management and it has the power to possible control the decision-making process. Key elements to decision-making process involve knowing how different types and sources of uncertainty propagate in every step of the analysis, which of them contribute more, and what is their significance to the results. A very comprehensive report on different types of uncertainty and on various uncertainty propagation methods is presented in (Hayes, 2011).

Examples of existing methods that allow uncertainty propagation are Bayesian Theory (see (Oakley, O'Hagan, 2004)), Probability Bounds Analysis (PBA) (Zhang et al., 2012, 2010; Muhanna et al., 2013 ; Schweiger, Peschl, 2005 ; Xiao et al., 2011 ; Rao et al., 2011) and second-order Monte Carlo simulations (also named probabilistic sensitivity analysis).

The latter method runs n Monte Carlo simulations each with different input probabilistic distribution model parameters, and for each run a second set of m Monte Carlo simulations are performed to cover the full range of each probabilistic distribution model. In the end, uncertainty from the input models is propagated to the distribution of the output results. In the context of finite element analysis to derive

the relationship between input and output parameters it is possible to use Reponse Surface methods to determine an approximation of that relationship by running a much smaller number of calculations. The error of this approximation can be estimated by Bootstrap methods (Efron, 1979). To limit the number of *n* Monte Carlo runs it is possible to consider only distributions for the inputs that represent the average and two extreme quantiles of the possible distributions.

Probability Bounds Analysis operates in a different way. Instead of approximating the output probability distribution it provides bounds on that distribution. In a pure second-order Monte Carlo the types of probabilistic distributions of the input variables and the distributions parameters must be provided. In many cases the definition of this data is subject to very large uncertainty. On the contrary, in probability bounds analysis the consequences deriving from the need of making strong subjective assumptions about the type of distribution functions or about independence/dependence between input variables are limited since PBA uses conservative bounds to simulate the probabilistic distributions of the input variables. However, applications of PBA to finite element analysis are in its first steps and further work must be done in order to be a real alternative to other methods. In particular, progress is still needed in addressing dependence between input variables to avoid obtaining overly conservative interval bounds for the outputs.

Methods also exist that try to reduce the uncertainty introduced when selecting the probabilistic model for the input parameters. For example, the arbitrary polynomial chaos expansions method (aPC), see (Xie et al., 2014), generalizes chaos expansion techniques towards arbitrary distributions with arbitrary probability measures. The aPC only demands the specification of the distribution moments.

5.4.7 A new framework for fragility and vulnerability analysis

Fragility of a structural system, as it will be demonstrated in this section, is closely related to the system's robustness. Vulnerability of a structure in terms of economical consequences, for example, can be determined from the system's fragility.

5.4.7.1 Robustness analysis

Robustness is a measure of the predisposition of a structural system to progressive and disproportionate collapse. It is an essential tool to design damage tolerant structures because citing (Todinov, 2007) *"maximising the reliability of a system does not necessarily guarantee smaller losses from failures"*.

Robustness can be determined for any given combination of deterministic loads, or loads with a given conditional probability, which causes a failure in the structural system, irrespective of the system context and exposure. As a result of uncertainty on the resistance properties of the structure and consequently on the system's response, robustness is not defined by a single value but by a probabilistic distribution of possible values.

Using this definition it is clear that robustness and reliability are two different concepts, although related. Reliability of a system is associated with the probability of structural failure which depends not only on the resistance properties of the system but also on likelihood of occurrence of the hazard scenario.

In robustness analysis the focus is not in assessing the probability of structural failure but in what happens when there is a failure, measuring the predisposition for failure propagation within the system. Robustness analysis can be considered as a global reliability analysis returning information about the post first failure behaviour. However related these two concepts are different. A system can have a very high reliability but if it is governed by the reliability of very few elements there is always a load scenario for which the system's robustness is very low. The opposite is also true, a system can have a very high robustness but if all the elements have the same resistance there is always a hazard scenario for which the system's reliability is very low.

Problems can arise when comparing reliability and robustness if the former is defined and measured at local level, for instance failure of a beam, and is wrongly used to assess the global reliability of the system. In this case, reliability and robustness are not related since the results of the reliability analysis cannot be interpreted in terms of robustness. This method is often followed in traditional structural codes, although recent improvements have been made. Robustness and reliability are related only if the latter is defined globally.

Robustness is defined to be a structural property, not dependent of possible human or economical risks associated with a failure or collapse. Robustness is a measure of damages and not of consequences, contrary to what is suggested by (Baker et al., 2008), since the latter concept has a broader scope as it encompasses structural consequences (damages) but also social and economical consequences, for example. Therefore, when evaluating the robustness of a structural system it is relevant to assess the direct and indirect damages for a given hazard scenario, and not the direct and indirect consequences. It should be mentioned that the distinction between direct and indirect damages makes the evaluation of robustness very difficult in the majority of the cases. Therefore, in the present Thesis a new robustness index will be proposed where this assessment is not required.

As robustness is understood to be a structural property, it cannot be controlled by external measures such as: (i) reduction of the structure exposure to hazard events or (ii) introduction of external elements to minimise the effects of those hazard scenarios on the structure. However, these types of measures would increase the reliability of the structure and decrease the risk of disproportionate collapse. On the other hand, robustness of existing structures can be maintained or enhanced by adopting appropriate inspection plans, or by rehabilitation and retrofit works.

Like reliability, it is possible to have a system with a very high resistance but with a very low robustness, and vice-versa. Increasing the resistance of all elements of a structure, for instance by choosing materials with higher tensile strength, although a sufficient condition to increase the system's resistance (and reliability for the same exposure), is not a sufficient condition for increasing the robustness of a structure. This is clearly demonstrated by comparing two steel structures, *A* and *B* for example, with the same geometry at global and local levels but where *A* was built with steel of a higher grade than *B*, but the steel used in structure *A* is so brittle, that the increase in resistance does not make up for the loss in deformation capacity. Therefore, the robustness of *A* is smaller than of *B*.

Additionally, increasing material strength, or member resistance, is not always the most cost-effective approach to increase robustness. In some structures it may even be counterproductive. For instance the robustness may decrease by increasing the resistance of joints between different parts of a structure as the collapse might propagate to other initially undamaged (or even unloaded) areas. Finally, the resistance is not a suitable property to measure robustness since it must always have to be expressed in terms of the local behaviour of the structure, which might differ greatly within the structure.

By minimising the extent of failure events, robustness may be linked to safety of use. Through its robustness, the structural system must be able to continue to provide minimum set of functions for which it was created, independent of circumstances. These circumstances include surviving a hazard event without disproportionate damages, but also during a given period of time after the event (defined as the repair period).

The main advantages of this new definition of robustness in relation to the existing definitions are:

- Structural robustness, structural resistance, reliability and risk are four different concepts. The existing robustness definitions mixed these concepts which made the analysis, interpretation and evaluation of the former variables difficult tasks. Furthermore, by coupling in the same definition four different concepts the benefits of determining the robustness was not clear. The present definition makes robustness a property than can be measured independently of the system's resistance, reliability and risk. Structural robustness can for the first time be considered an independent requirement for the structural performance of civil engineering infrastructures. Together

with the structural resistance and reliability they become two powerful tools that can and should be used in the risk management of civil engineering infrastructures;

- The second advantage is that for the first time, progressive and disproportionate collapse analysis is clearly defined as a requirement not only for unforeseen and accidental situations affecting localised areas of a given structure, but also for normal service conditions covering for instance design cases where the permanent load is the dominant action.

Structural robustness is a function of resistance variables, R, of the structural system (Knoll, Vogel, 2009): (i) material strength, (ii) material ductility and strain hardening, (iii) structural integrity and solidarization, (iv) structural redundancy, (v) structural stiffness, (vi) structural continuity and (vii) post-buckling resistance. Additionally, robustness of a structure can be provided by different design strategies such as (Knoll, Vogel, 2009): (i) adopting capacity design philosophies or (ii) introducing special elements to stop the advance of progressive collapse, either by sustaining the additional deformation or by activating suitable failure modes (introducing knock-out elements). See also (Starossek, 2006, 2009 ; Starossek, Haberland, 2008 ; Starossek, Wolff, 2005) for further possible solutions. These strategies will be discussed in greater detail in a following section.

Structural robustness is also a function of the hazard scenario (loads, imposed displacements, etc.), A, and their magnitudes. This is illustrated in Figure 5.5.
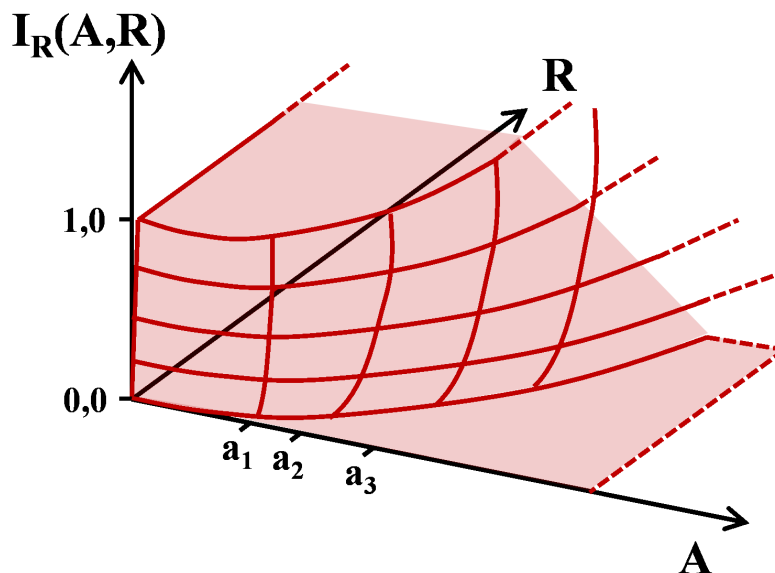
Figure 5.5: Robustness as a function of resistance variables (R) and action (A).

Bridge falsework structures are typically low robust structures since they are an assemblage of similar and slender linear elements prone to instability phenomena, and weak loose connections, where the critical design load is often present at its maximum value, uniformly distributed over the entire, or a significant part, of the structure. This is another differentiating factor between bridge falsework systems and permanent structures. Whereas for the latter robustness is typically evaluated for accidental actions, associated with a live load case, for the former the decisive scenario is frequently associated with the self-weight of the permanent structure. Additionally, since the elements of these systems are linear elements they do not possess alternate resistance models like the slabs of bridge decks, and thus complete failures of elements are more easily reached in bridge falsework systems than complete failures of bridge elements.

Additionally, factors as mentioned before such as lack of competence in design, absence of rigorous quality control supervision, reuse of damaged elements, etc. have a larger impact on the structural behaviour of bridge falsework systems than of permanent structures, which contribute to the existence of high levels of uncertainty associated with these temporary structures.

Therefore, it is extremely important to evaluate the robustness of these temporary structures since (i) their margin of safety given an irreversible failure is usually much lower than the one achieved in permanent structures, (ii) the failure of one element usually leads to the progressive collapse of the entire, or the majority, of the structure, and (iii) their exposure to critical hazard scenarios is also much larger than the one of permanent structures.

Possible solutions to enhance the robustness of these structural systems under the weight of fresh concrete will be discussed in detail in a later section. However, it is possible to observe that three alternatives could be used to increase the robustness of bridge falsework systems:

(i)   Increase the resistance and ductility of the system by over-designing the critical elements.

(ii)   Selective strengthening of the structure by creating a sub-structure capable of resisting by itself the weight of the fresh concrete plus other loads due to equipment and materials stored in the deck while concreting the bridge. Failures could still occur in the remainder of the elements, but would not cause a disproportionate collapse, and could also be used to signal a warning, a sign of distress of the structure. These predictable, controlled and limited failures, *i.e.* safe fails, would work in the same way sprinkler systems or circuit breakers such as fuses, that cut-out when circuits overload, work. After the occurrence of one of these events, construction works should be stopped to evaluate the condition and the safety of the remaining structure and the causes of the partial collapse, followed if necessary by a review of the bridge falsework structural design and/or by changing the construction procedures.

(iii)   Creating divisions within the structure so as to isolate the failure, preventing the propagation to the rest of the system. However, seeking to limit the structural failures to a local area could be insufficient as the consequences of failure could be not much different than the ones of a total collapse.

5.4.7.2   Traditional methods for analysis of robustness of structures

Robustness has been present directly or indirectly in several structural codes throughout the last thirty years. However, to date there is not one document that specifies a general purpose design method for determining robustness in a consistent and effective manner. Until now, such additional considerations have only been made in individual cases, *e.g.* for government buildings, and mostly at the engineer's own discretion; mandatory and specific procedures for general structures do not exist (Starossek, Wolff, 2005).

Moreover, there is an almost complete absence in existing codes and guidance documents regarding rules, design requirements and methods or procedures to evaluate the robustness of temporary structures, and in particular for bridge falsework systems. Only in (ASCE, 2002) there is a rule related to structural integrity in which it is specified the need to consider the stability and the possibility of progressive collapse during its design. However, it is noteworthy to summarise how the most advanced structural codes treat robustness and what are the current design requirements for robustness.

Starting from the first structural codes adopting the limit state design theory, a structural insensitivity requirement was incorporated to avoid progressive collapse scenarios, *i.e.* the structure would not collapse if subjected to a limited damage. Thus robustness was treated indirectly and qualitatively; linked with an undesirable failure mode. No rules for design and verification were specified.

In the CEB/FIP Model Code 90 (Comité Euro-International du Béton, 1993), it is specified that *"Structures should with appropriate degrees of reliability, during their construction and whole intended lifetime, perform adequately and more particularly: (i) withstand all actions and environmental influences, liable to occur, (ii) withstand accidental circumstances without damage disproportionate to the original events (this is called the insensitivity requirement)"*. However, this requirement is treated qualitatively and indirectly by

specifying standard prescriptive detailing rules for members. Additionally, robustness is also associated with the durability of the structure against active deterioration during its service life.

More recently, the EN 1990 (BSI, 2002a) establishes *"robustness (structural integrity)"* as a way to achieve required levels of reliability relating to structural resistance and serviceability. Furthermore, robustness is stated as a basic requirement that:

"A structure shall be designed and executed in such a way that it will not be damaged by events such as (i) explosion, (ii) impact, and (iii) the consequences of human errors, to an extent disproportionate to the original cause".

EN 1990 also specifies three consequence classes, CC1, CC2 and CC3, written in increasing order of analysis complexity, target reliability levels and design requirements.

EN 1991-1-7 (General actions – Accidental actions) (BSI, 2006c) defines robustness as *"the ability of a structure to withstand events like fire, explosions, impact or the consequences of human error, without being damaged to an extent disproportionate to the original cause"*. This part of EN 1991 specifies *"principles and application rules for the assessment of identifiable and unidentifiable accidental actions on buildings and bridges, including: (i) impact forces from vehicles, rail traffic, ships and helicopters, (ii) actions due to internal explosions and (iii) actions due to local failure from an unspecified cause"*.

Depending on the consequence class of the structure, different types of design rules must be followed. For consequence class CC3 a complete risk assessment may be required. Typical structures that fall in this class are grandstands, public buildings where consequences of failure are high (*e.g.* a concert hall). Specific guidance for buildings is given in Annex A of EN 1991-1-7 (BSI, 2006c), similar to the one given in Approved Document A of UK Building Regulations (UK ODPM, 2004).

In EN 1998 (Design of structures for earthquake resistance), parts 1 and 2, buildings (BSI, 2004c) and bridges (BSI, 2005d), respectively, it is specified a no-collapse fundamental requirement which is deemed satisfied if the verification of the ultimate limit state is made according to the rules given in these two documents. Therefore, structures shall retain their structural integrity and a residual load bearing capacity after the seismic events. It is further specified that *"When the design seismic action has a substantial probability of exceedance within the design life of the bridge, the design should aim at a damage tolerant structure"* which can be seen as a robustness requirement. Additional review of robustness related rules present in the structural Eurocodes is given in (Narasimhan, Faber, 2009).

After the occurrence of several disasters involving collapses due to lack of robustness, among which the Ronan Point and the World Trade Centre are the ones more prominent, some national codes (mainly in UK and in USA) for the design of buildings were prepared, defining requirements, rules and verification procedures to achieve collapse-resistant buildings in the event of abnormal loading. Examples of these are the NIST "Best Practices for Reducing the Potential for Progressive Collapse in Buildings" report (Ellingwood et al., 2007) and the US Defence Department United Facilities Criteria (USDOD, 2010).

The first document defines progressive collapse as *"the spread of local damage, from an initiating event, from element to element resulting, eventually, in the collapse of an entire structure or a disproportionately large part of it; also known as disproportionate collapse".*[1]

Therefore, it can be concluded that robustness analysis is yet not fully implemented in the existing structural codes, except for the scenario of an accidental action.

---

[1] *Starossek (Starossek, 2009)* differentiates progressive collapse and disproportionate collapse, saying that the former is more suited for referring to the physical phenomenon and mechanism of collapse while the latter should be used in the context of structural performance and since it is more subjective needs to be defined according to a set of design objectives.

5.4.7.3 Advanced methods for analysis of robustness of structures

There are however, methods available to analyse robustness of structures, some of them developed quite recently. All of these methods are based on different robustness definitions than the one introduced in the present Thesis, and all of them suggest different approaches to measure robustness.

As observed by (Starossek, Haberland, 2008) existing methodologies can either be based on structural behaviour or based on structural attributes. The former ones demand complex structural analysis whereas the latter ones are analytical. Further distinction can be made between methodologies based on the assumption of an initial local damage and those based on the identification of a collapse sequence (Starossek, Haberland, 2008). Finally, it is also possible to distinguish between deterministic approaches and probabilistic approaches.

A common trend in robustness evaluation is to define a robustness measure, often in the form of a robustness index. The first question that needs an answering is why is it useful to measure numerically the robustness of a structural system? One could simply compare resistances or load *vs.* displacement curves associated to different failure scenarios of the same structure. The answer to this question is simple given the definition of robustness presented previously. To assess the robustness of a structure, *i.e.* its global stability reserve, complex non-linear analysis must be performed. It is thus a requisite that the maximum information should be extracted in order to obtain knowledge return for the additional computational and analysis effort. Therefore, the measure should be informative. Additionally, the measure should allow a straightforward comparison between different structures. One can thus conclude that a measure of robustness is an imperative necessity.

The first robustness indexes to be developed were deterministic relating for instance the resistance of the damaged structure to a given load case with the corresponding resistance of the undamaged structure. More recently, probabilistic-based and risk-based indexes were developed. While the former usually compares the probability of failure of the damage structure with the probability of failure of the undamaged structure, the latter is more complex as it weights the indirect risks with the total (direct and indirect) risks.

5.4.7.3.1 Deterministic approaches

A number of different deterministic approaches to analyse robustness of a structural system have been proposed, either based on the load carrying capacity, or on the energy dissipation or on the extent of damages. Let us start by the energy dissipation based approaches.

Smith presented an analytical procedure coupled with simple finite element simulations to analyse the progressive collapse of building structures based on the parallelism of progressive collapse with the theory of unstable fast fracture in fracture mechanics (Smith, 2006). In this method all energy components (potential energy, viscous energy and kinetic energy) are accounted for. The idea behind the method is: *"if the energy released by loss of a damaged member is greater than the energy absorbed by the destroyed member and other damaged members, then progressive collapse will occur"* (Smith, 2006).

Smith determined the energy required to destroy sufficient structural members to develop an unstable mechanism (which he named damage energy) and using a minimisation process, consisting basically in continuously deleting damaged elements from the mesh, coupled with a sorting procedure, he identified the sequence of damage events that required the least amount of damage energy. Smith then used this minimum damage energy as a measure of the structural system robustness.

However, this measure has some limitations. Besides being based on an absolute value which is inconvenient when comparing different structures, it assumes that higher damage energy necessarily translates to higher structural robustness. This is not always the case. For example, it is possible to have two similar structures, A and B, subject to the same loading conditions but with different yield loads, $p_{y,A} < p_{y,B}$, where A is more resistant than B ($p_{u,A} > p_{u,B}$) and B has more damage

energy than A ($W_{d,B} > W_{d,A}$), because the materials of B have a larger deformation capacity, for instance, see Figure 5.6.

The damage energy dissipated by structure B is larger than the one dissipated by structure A, but the relative energy reserve after yield load of structure A is larger than of structure B. Therefore A must be more robust than B, which contradicts Smith definition. Increasing the damage energy is not a sufficient condition to achieve higher structural robustness. Smith approach lacks a comparative term. Nevertheless, the energy approach suggested by Smith is very interesting and will be explored in greater detail in a future section of the present Thesis.
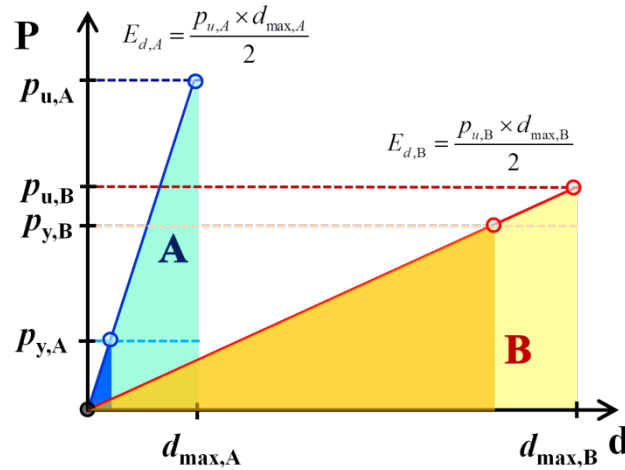
Figure 5.6: Example of the limitations of Smith's definition of robustness.

An alternative energy-based measure of robustness was suggested by (Starossek, Haberland, 2009). These authors compare the energy released by an initial failure with the energy required for a collapse progression, see equation (5.6).

$$R_e = \max_j \frac{E_{r,j}}{E_{s,k}} \tag{5.6}$$

where:

R_e represents the energy-based robustness measure;

$E_{r,j}$ represents the energy released by the initial failure of a structural element j and available for the damage of the next structural element k;

$E_{s,k}$ represents the energy required for the failure of the next structural element k.

As the authors recognise this measure has some important drawbacks, the most important being:

- It assumes that the structure will collapse with the failure of the second element. This can only occur when there are a small number of critical elements or when their number is large but they are overloaded or close to it;

- It assumes that the energy of triggering event is completely absorbed by the damage of the initially failing component.

In 2009, (Starossek, Haberland, 2009) also suggested a damage-based measure of robustness given by the ratio of the maximum extent of additional damage caused by the assumed initial damage with the acceptable damage progression. It requires complex numerical analysis and its evaluation introduces risk related decision options, *i.e.* acceptable damage progression, within the robustness definition.

Still focusing on energy-based robustness indexes, (Fang, 2007) suggests the following:

$$I_{rob} = \frac{E_u}{E_d} \tag{5.7}$$

where E_u is the amount of energy the structure absorbs before it reaches the ultimate failure state and E_d is the amount of energy the structure absorbs before reaching the limit state of its design load-bearing capacity.

Therefore, using the proposed index, the robustness of the same structure depends on the structural code used, which is a limitation.

Another robustness formulation was also presented in (Starossek, Haberland, 2009) based on the ratio between the determinant of the stiffness matrix of the damaged structural system and that of the undamaged structural state. According to the authors the values returned by this method still do not exhibit a high correlation with the reduction in load capacity after the loss of structural elements. Additionally, a local failure has to be assumed initially.

Another possible deterministic robustness index could relate the resistance of the damaged structure with the resistance of the undamaged structure. However, this index has evident weaknesses and will not be discussed further.

5.4.7.3.2 Probabilistic-based approaches

In terms of probabilistic-based approaches two different methodologies exist: one focusing in the probability of failure and the other on the risk of the structure.

The first measures based on the former methodology were the redundancy indexes proposed by Frangopol *et al* (Frangopol, Curley, 1987; Fu, Frangopol, 1990):

$$RI = \frac{P_f\left(\text{damaged}\right) - P_f\left(\text{intact}\right)}{P_f\left(\text{intact}\right)} \tag{5.8}$$

$$\beta_R = \frac{\beta_{\text{intact}}}{\beta_{\text{intact}} - \beta_{\text{damaged}}} \tag{5.9}$$

where P_f represents the probability of failure and β represents the reliability index.

(Lind, 1995) proposed an index based on the ratio between the probability of failure of a damaged structure with the probability of failure of an undamaged structure.

Finally, in 2008 (Baker et al., 2008) presented a novel robustness index based on a complete risk analysis where the consequences are divided in direct and indirect risks and the measure is given by the ratio between the direct risks with the total risk (sum of the direct and indirect risks).

In this methodology, it is useful to use the event tree illustrated in Figure 5.7, where:

EX_{BD} represents the exposure event before damage;

D represents damage ($\bar{D}$ refers to no damage);

F represents system failure ($\bar{F}$ refers to no failure);

C_{Dir} represents the direct consequences, *i.e.* those associated with the initial damage;

C_{Ind} represents the indirect consequences, *i.e.* those associated with the subsequent system failure.
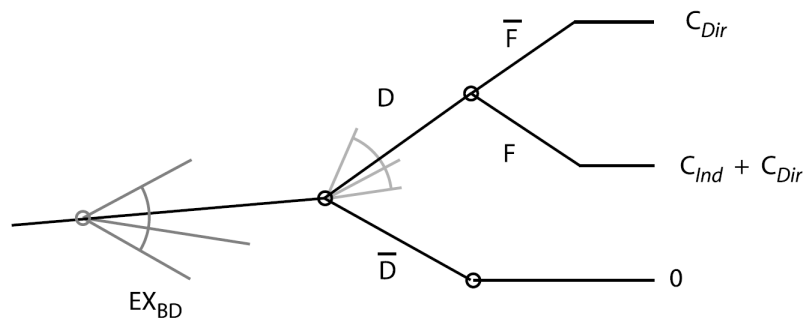
Figure 5.7: Event tree for robustness evaluation (Baker et al., 2008).

In the majority of cases the direct consequences are relatively small in comparison with the indirect consequences, therefore risk (direct, R_{Dir}, and indirect, R_{Ind}) can be evaluated by:

$$R_{Dir} = \sum_x \sum_y C_{Dir} \times P\left(\bar{F} \mid D = y\right) \times P\left(D = y \mid EX_{BD} = x\right) \times P\left(EX_{BD} = x\right) \tag{5.10}$$

$$R_{Ind} = \sum_x \sum_y C_{Ind} P\left(F \mid D = y\right) \times P\left(D = y \mid EX_{BD} = x\right) \times P\left(EX_{BD} = x\right) \tag{5.11}$$

Based on these definitions the following robustness index can be developed, I_{Rob}:

$$I_{Rob} = \frac{R_{Dir}}{R_{Dir} + R_{Ind}} \tag{5.12}$$

This formula can be simplified if robustness is defined conditionally to the occurrence of a specified exposure event followed by a specified damage event:

$$I_{Rob} \mid D = y, EX_{BD} = \frac{C_{Dir}}{C_{Dir} + P\left(F \mid D = y, EX_{BD}\right) \times C_{Ind}} \tag{5.13}$$

A list of a number of relevant advantages of the abovementioned index is presented in (Baker et al., 2008).

5.4.7.4   A new measure of structural robustness

From the analysis of the existing deterministic and probabilistic measures it can be seen that two types of analysis are used: (i) one where the failure modes of the structure are analysed explicitly and in a rigorous way, see (Smith, 2006) and the other (ii) where it is assumed a particular fictitious damage in the structure. Using this latter methodology one can only get an indication of the sensitivity of the structure to a local failure, although a possible unconservative estimate since in reality when an element fails several other elements could have suffered severe deformations (close to failure) and the configuration of the global system could have changed also. Therefore, important second-order effects are neglected and possible secondary load paths and resistance models are not taken into account which can introduce a significant bias to the proposed simplified measures of robustness.

From the information presented previously, it can be concluded that some of the mentioned robustness evaluation strategies do not fully comply with the robustness definition used in the present Thesis. In some indexes, mainly in the newly developed risk-based index, it is considered that robustness of a structural system depends not only on the structural characteristics of the structure but also on the variation of the loads and the exposure of the structure (probability of occurrence of the loads). In the risk-based index, robustness is also linked with the consequences (economic, social, etc.) of the collapse. Therefore, an alternative robustness measure will be proposed.

The idea behind developing a new robustness index stems from analysing the strengths and weaknesses of the existing indexes. Most of them require the separate evaluation of direct and indirect damages (or consequences). This step is often very difficult and depends on the validity of the adopted assumptions, which are frequently subjective. Damages are a continuum and it is very difficult to break apart direct and indirect damages. The proposed robustness index relates to structural damages rather than to risk or reliability, making robustness, risk and reliability three different variables that can be evaluated independently. Together, these three variables can be used to support and improve rational decision-making in civil engineering. Additionally, the index concerns only one hazard scenario and not all the range of hazard scenarios. In this way, it is more clearly identifiable which are the more relevant hazard events and allow for a direct comparison of different systems.

According to (Starossek, Haberland, 2008) robustness indexes should possess the following properties:

- **"Expressiveness:** *The measure should express all aspects of robustness and collapse resistance but no other aspects. It should allow for a clear differentiation between robust and non-robust or collapse-resistant and collapse-susceptible structures. For this, compliance with given design objectives is to be checked.*

- **Objectivity:** *The measure should be independent of user's decisions. The result for the measure should be reproducible under the same conditions.*

- **Simplicity:** *In the interest of objectivity and generality as well as for promoting acceptance, the definition of the measure should be as simple as possible.*

- **Calculability:** *It should be possible to derive the measure from the attributes or the behaviour of the structure. All necessary input parameters must be quantifiable. The numerical calculation of the measure should not require excessive effort and should be sufficiently accurate.*

- **Generality:** *The measure should be applicable to arbitrary structures".*

The basis for the development of the new robustness index is the analysis of the structural behaviour in terms of energy balance. There are plenty of advantages of energy-based measures over resistance-based or reliability-based robustness measures. Energy-based measures concern the global behaviour of the structure which removes the need, in multi-hazard scenarios, for subjective selection of the degree of freedom to monitor with all the possible loss of objectivity, expressiveness and generality that comes with it.

In a closed system, the principle of conservation of energy defines that the change in the total energy (E_{Total}) between a system and its surroundings is constant, *i.e.* energy is not created or destroyed but can be transformed:

$$\Delta E_{Total} = \Delta P + \Delta K = \Delta E + \Delta W + \Delta K = \text{constant} \qquad (5.14)$$

where:

ΔP represents the variation of the potential energy of the system;

ΔK represents the variation of the kinetic energy of the system;

ΔE represents the variation of the internal energy of the system: internal strain energy of the system plus the variation of the other sources of energy such as electrical energy, chemical energy and energy dissipated by friction, creep, etc.;

ΔW represents the variation of the work done by external actions on the system.

The internal strain energy, E_S, is the total potential energy contained in the system. In structural mechanics, the internal potential energy may be expressed by:

$$E_S = E_{El} + E_{Pl} \qquad (5.15)$$

where:

E_{El} represents the elastic (recoverable) strain (potential) energy of the structure;

E_{Pl} represents the plastic (dissipated) strain (potential) energy of the structure.

By using an energy based robustness criterion it is possible to get a deeper insight about the behaviour of the structure. For example, analysing energies it is possible to distinguish between recoverable (*e.g.* elastic strain energy) and unrecoverable energies (*e.g.* viscous energy and plastic strain energy). The presence of unrecoverable energy makes the system non-conservative because some of the energy is dissipated and after unloading the system does not recover the initial state (path dependent problem). This type of energies can be used as an evidence of existence of damages in specific dissipative elements of the system.

Several robustness indexes were developed and tested. Below is a short-list of some of the tested indexes, highlighting their relative disadvantages and merits.

A possible robustness index, I_R, is expressed by:

$$I_R = \frac{E_{max} - E_{1st\ failure}}{E_{max}} \tag{5.16}$$

where:

$E_{1st\ failure}$ represents the internal energy of the structure when the first failure takes place for the hazard scenario considered;

E_{max} represents the maximum internal energy of the structure when subjected to the load case being considered;

The advantage of this index is that it expresses the reserve of energy of the system after the first failure has occurred. However, this index has a problem.

Consider first two building structures, A and B, subjected to the same value of the action P: p. The design strategy used to give robustness to structure A is the knock-out element, where the critical sections are contained in a selected area of the structure which is connected to the rest of the structure by very fragile connections, the idea being to stop the collapse from propagating beyond this selected area. Structure B was designed with the objective of maximizing the energy dissipated by the structure in a stable fashion by using ductile materials and ductile connections. These two structures will be further subjected to the same localised failure of the same magnitude due to an explosion or impact of a vehicle for instance. Additionally, let us consider that this accidental action is applied in the weak zone of structure A. Figure 5.8 illustrates the possible strain energy curve for both structures.
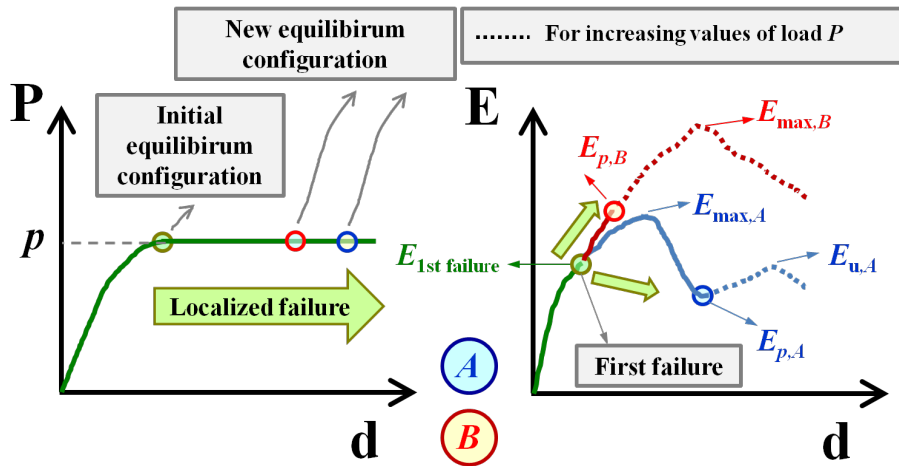
Figure 5.8: Load and strain energy curves of buildings *A* and *B*.

It can be observed that in the way this example is formulated it is not possible to compare the robustness of structure A with the robustness of structure B using the index of equation (5.16). This happens because it assumes that the maximum system energy, E_{max}, matches the system energy at collapse, E_u, which does not occur for structure A.

However, even if E_{max} is replaced by the total sum of the positive energy variations, this index might not give correct results: Equation (5.16) considers in the denominator the energy starting from zero energy and not from a given "failure" state. Most importantly, this index considers in the numerator E_{max}, or the total sum of the positive energy variations, but collapse may be unavoidable for a much lower value of the internal energy. Therefore, it is not capable of including the disproportionality between the source and the consequence.

Therefore, an index which is capable of overcoming these limitations was finally developed as the mathematical expression of:

$$I_R\left(A_L \mid H\right) = \frac{\text{Damages up to unavoidable collapse state for hazard } h}{\text{Damages up to collapse state for hazard } h} \qquad (5.17)$$

The general expression is given by:

$$I_R\left(A_L \mid H\right) = \frac{D_{uc} - D_{\text{1st failure}}}{D_c - D_{\text{1st failure}}} \text{ with } \begin{cases} 0 \le I_R \le 1 \\ D_c - D_{\text{1st failure}} = 0 \Rightarrow I_R = 1 \end{cases} \qquad (5.18)$$

where (see Figure 5.9):

A_L represents the leading action;

$H = \{h_1, h_2, ..., h, ..., h_n\}$ is a set of hazard scenarios: {base conditions} + {impact on column 1, impact on column 2, ..., impact on column n}, a set of different actions or a combination of different actions, for example;

$D_{\text{1st failure}}$ represents the damage energy of the structure when the "first failure" state takes place for the hazard scenario considered;

D_{uc} represents the damage energy corresponding to the state where collapse is unavoidable for the hazard scenario considered;

D_c represents the damage energy corresponding to the collapse state for the hazard scenario considered.
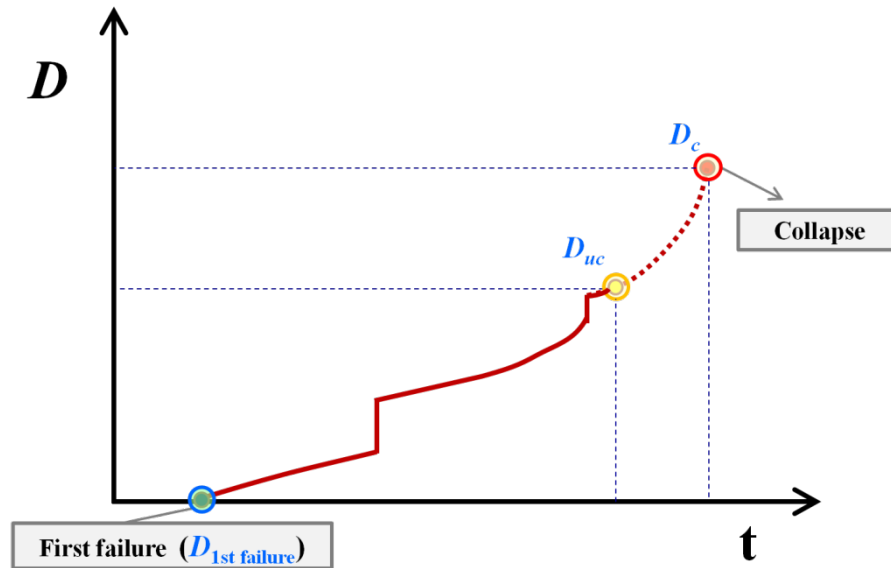
Figure 5.9: Illustration of the robustness index notation.

The selected criteria for monitoring the damages and the collapse of a structure is the system's damage energy (D) evolution, because it gives a good estimate of the capability of the system to redistribute forces by alternative load paths and resistance mechanisms.

The damage energy is given by the sum of the plastic strain energy (non-decreasing function) with the energy released in each failure (stepped function). Therefore the damage energy is a non-decreasing function. Failure is any state where there is a release of energy: it can be the formation of a crack, failure of a joint, failure of a cross-section, for example. Care should be paid not to consider the plastic strain energy of a failed element twice: in the plastic strain energy and in the energy released in the failure.

It is assumed that the damage energy is zero if there no plastic strains and no failures occurred. As a result, a system that behaves elastically up to failure may have a robustness index equal to one.

Also, robustness evaluation is assumed here to be only relevant for resistance limit states and not for serviceability limit states.

The above expression is slightly different than the one presented in an earlier work (André et al., 2013), in that the strain energy was replaced by the damaged energy. This is due to the fact that a structure or a structural element in their elastic regime should retain a value of the robustness index equal to one.

Also, robustness is no longer a function of the system's energy for a given action value, *p*. This is needed to disassociate robustness from the applied action value. As stated earlier, robustness and reliability are two different parameters. Robustness is only a function of the damage initiation mechanism and of its structural consequences.

In order to calculate this robustness index a three step procedure must be followed, see Figure 5.10.
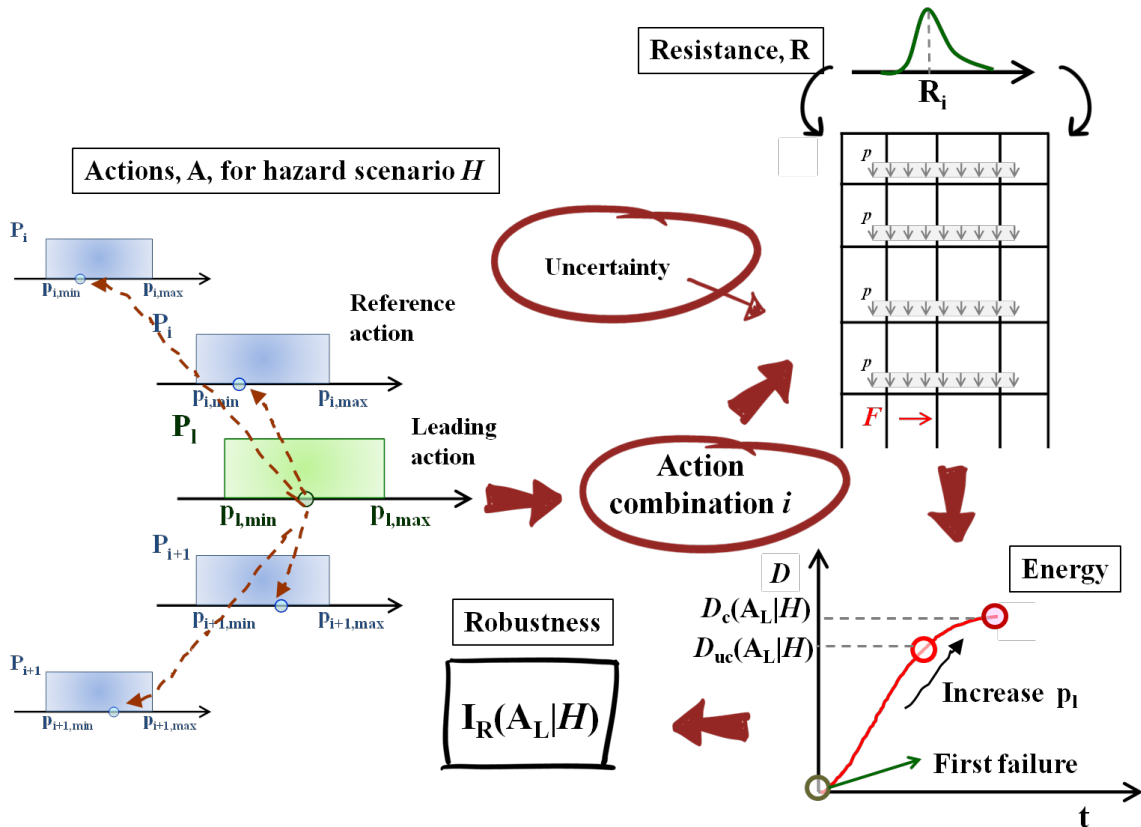
Figure 5.10: Procedure to determine the robustness index.

First step: define the *nominal* loading conditions (hazard scenario), *i.e.* the sequence of action (loads) application is rationally chosen and the initial values of the several loads, material properties, system imperfections, etc. are generated, corresponding to values obtained from the corresponding probability density functions (loads are modelled with uniform probability density distributions and resistance variables can also be modelled with uniform probability density distributions but preferably with more informative distributions). Correlations could be considered, for example: complete or incomplete correlation between load values – incomplete correlation means that values of different loads can be correlated for only a range of values of one of the loads; for example seismic loads and traffic loads. The value of D_c is determined.

Second step: while holding everything constant ("*ceteris paribus*"), a leading action that can cause the structure to collapse (if it has not already occurred during the first step) is selected and increased until the collapse is attained. However, several actions can be increased simultaneously if it is considered appropriate (if correlated for example). The aim should be to obtain a realistic safety assessment of the structure and therefore of the most likely damage propagation within the structure. In the example illustrated in Figure 5.11 *(Left)* it may be necessary to evaluate the

robustness index for increasing values of the action p and not of F, while in Figure 5.11 *(Right)* it may be possible to select either actions. The value of D_{uc} is determined.

Third step: the robustness index is determined from equation (5.18) based on the adopted limit state which defines the first failure state (the value of $D_{1st\ failure}$ is determined).
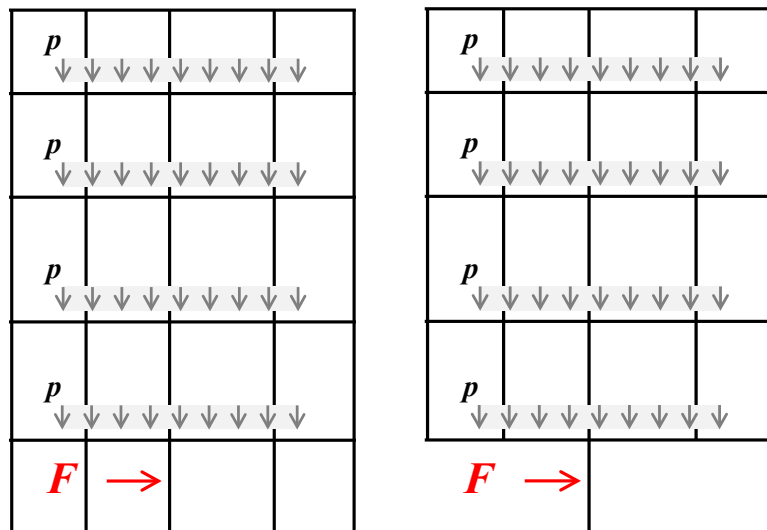
Figure 5.11: Possible different selections of leading actions to evaluate robustness.

The index is also flexible since the inputs can change, for example: the "first failure" state can be replaced by another criterion, possibly related to a particular element failure, and the "unavoidable collapse" and "collapse" states can also be changed to represent a maximum limit of acceptable damage, D_{max}, for instance. In the latter case $D_{max} \leq D_{uc}$.

The value of the robustness index is a function of the hazard scenario (*i.e.* action values) because in general D_{uc} and $D_{1st\ failure}$ depend on the loading conditions.

A value of the robustness index equal to one means that the structure is completely optimised in terms of robustness, for the hazard scenario considered. In the contrary, a value of the robustness index equal to zero may indicate that the structure completely lacks optimisation in terms of robustness, for the hazard scenario considered.

The value of D_{uc} can be estimated from the theory detailed in (Dusenberry, Hamburger, 2006). As explained in that paper, following a structural failure the system's energy balance can be expressed *"through comparison of the release of potential energy that occurs as the structure falls, the strain energy that accumulates as the structure deforms, and the kinetic energy associated with the moving mass"."For all conditions when the kinetic energy is positive, portions of the structure are in motion, and collapse has not been arrested. When kinetic energy attains a value of zero strain energy accumulated by the structure equals the change in potential energy the moving portion of the structure is at rest, and collapse potentially has been averted. If strain energy never equals the change in potential energy, the mass remains in motion and collapse is inevitable."* (Dusenberry, Hamburger, 2006).

Applying this theory to a framed structural system, see Figure 5.12 for example, such as a bridge falsework, the collapse of a lower level of elements due to the failure of an upper level of elements can only be arrested if and if only (Bažant, Verdure, 2007):

$$W(t) < E_S(t) \tag{5.19}$$

where:

$W(t)$ represents the value of the work done at time t by external actions on the lower level elements, including the potential energy associated with the kinetic energy of the moving mass of the upper level elements.

$E_S(t)$ represents the value of the internal strain energy of the lower level elements at time t.
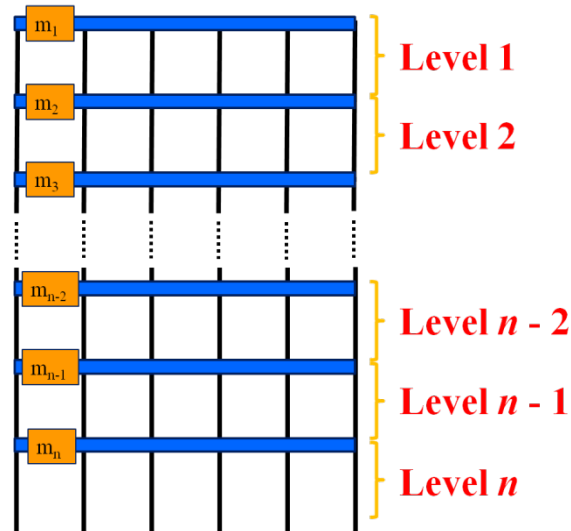
Figure 5.12: Example of a framed structural system.

For such a system, the progressive collapse criterion given by equation (5.19) can be expressed by:

$$W(t) < E_{S,\max} \tag{5.20}$$

where $E_{S,max}$, represents the maximum internal strain energy dissipated by all the non-failed columns of the lower level. $E_{S,max}$ can be estimated numerically, analytically or experimentally for each element and summed over all the elements of the level, see (Smith, 2006), (Bažant et al., 2008 ; Bažant, Zhou, 2002) and (Korol, Sivakumaran, 2014), respectively.

For a steel frame and assuming a three plastic hinge dissipative mechanism for the columns of each level, $E_{S,max}$ of level j can be estimated by (Bažant et al., 2008):

$$E_{S,\max}^{j} = \sum_{i=1}^{N_{columns}^{j}} \left[2 \times \int_{0}^{\theta_{e,pl}} M_{e,i}^{j}(\theta)\, d\theta + \int_{0}^{\theta_{m,pl}} M_{m,i}^{j}(\theta)\, d\theta \right] \tag{5.21}$$

where:

θ represent the rotation at the column i extremities and middle of column i, respectively;

$\theta_{e,pl}$ and $\theta_{m,pl}$ represent the maximum rotation capacity at the column i extremities and middle of column i, respectively, with $\theta_m = 2 \times \theta_e$;

$M_{e,i}$ and $M_{m,i}$ represent the bending moments at the extremities and middle of column i;

$N_{columns}^{j}$ represents the number of columns of level j that have not failed.

It is assumed that outside the plastic hinges length, the elements behave elastically. (Bažant et al., 2008) argue that the value of $E_{S,max}$ returned by equation (5.21) should be reduced by a factor, β, to account for: "*1) multi-story buckling of some columns, 2) softening due to local plastic flange buckling, and 3) fracture of steel in inelastic hinges*". For elements with circular hollow cross-sections, point *2)* does not apply.

However, this plastic hinge model neglects any contribution of the axial deformation energy capacity to the internal energy and therefore it may underestimate the actual dissipated energy (Korol, Sivakumaran, 2014). Nevertheless, (Bažant et al., 2008) suggest that β is "*reasonably expected to lie within the range (0,5; 0,8) for normal structural steel (yield limit 250 MPa), but in the range (0,1; 0,3) for the high-strength steel (yield limit 690 MPa)*".

In order to improve the accuracy of the $E_{S,max}$ value, the values of the maximum bending moments at the plastic hinges, $M_{e,i}$ and $M_{m,i}$ in equation (5.21), can be obtained using exact analytical expressions, taking into account the interaction between the bending moment and axial forces, the elastoplastic model type and the maximum deformation capacity of the element's material. For steel CHS (circular hollow sections), see (Baptista, Muzeau, 2001). If local buckling

occurs, the maximum deformation and bending moment capacities are lower than their maximum plastic values and can be estimated by the method developed by (Gardner, 2008), with some restrictions. Additionally, the maximum rotations at the plastic hinges, $\theta_{m,pl}$ and $\theta_{e,pl}$ in equation (5.21), can be determined by the following procedure:

Under the Bernoulli hypothesis, the extensions, e, and deformations, ε, at any cross-section of a linear element are given by:

$$\text{Extension: } e(z) = e_N - \theta \times z \quad , \quad e_N = e(z=0) \tag{5.22}$$

$$\text{Deformation: } \varepsilon(z) = \varepsilon_N - \chi \times z \quad , \quad \varepsilon_N = \varepsilon(z=0) \tag{5.23}$$

where:

z represents the coordinate along an axis perpendicular to the longitudinal axis of the element with origin at the cross-section geometric centre;

ε_N and e_N represent the deformation and extension due to the axial force, respectively;

χ and θ represent the curvature and rotation at a given cross-section, respectively.

Considering a linear function for the deformations, ε, along the longitudinal development (x coordinate) of the element:

Functions of ε over the plastic hinge length:

$$\text{Hinge at column middle: } \varepsilon(z=z_{\max}, x)_m \approx \begin{cases} \varepsilon_y + \dfrac{2 \times (\varepsilon_u - \varepsilon_y)}{l_{pl,m}} x & \text{for} \quad \dfrac{L}{2} - \dfrac{1}{2} \times l_{pl,m} \leq x \leq \dfrac{L}{2} \\[4mm] \varepsilon_u - \dfrac{2 \times (\varepsilon_u - \varepsilon_y)}{l_{pl,m}} x & \text{for} \quad \dfrac{L}{2} \leq x \leq \dfrac{L}{2} + \dfrac{1}{2} \times l_{pl,m} \end{cases} \tag{5.24}$$

$$\text{Hinge at column extremities: } \varepsilon(z=z_{\max}, x)_e \approx \begin{cases} \text{Column top: } \varepsilon_y + \dfrac{(\varepsilon_e - \varepsilon_y)}{l_{pl,e}} x & \text{for} \quad L - l_{pl,e} \leq x \leq L \\[4mm] \text{Column bottom: } \varepsilon_e - \dfrac{(\varepsilon_e - \varepsilon_y)}{l_{pl,e}} x & \text{for} \quad 0 \leq x \leq l_{pl,e} \end{cases} \tag{5.25}$$

where:

ε_u and ε_y represent the ultimate and yield deformations of the element's material, respectively;

ε_e represents the maximum deformation of the element's material at column extremities hinges;

L represent the column length;

l_{pl} represent the plastic hinge length. For steel CHS a conservative estimate of l_{pl} was determined, based on the results of numerical simulations, equal to:

$$l_{pl} \approx d_{ext} \rightarrow \begin{cases} \text{Hinge at column middle: } l_{pl,m} = d_{ext} \\ \text{Hinge at column extrimities: } l_{pl,e} = l_{pl,m} \end{cases} \tag{5.26}$$

where d_{ext} is the external diameter of the cross-section.

Knowing that the extensions are a function of the deformations:

$$e(z,x) = \int_l \varepsilon(z,x) \, dx \tag{5.27}$$

Introducing equations (5.23) to (5.27) in equation (5.22) gives: detect

$$\theta_{m,pl} = \left[\frac{(\varepsilon_u + \varepsilon_y)}{2} \times l_{pl} - e_N \right] \Big/ \left(\frac{d_{ext}}{2} \right) \tag{5.28}$$

with:

$$\theta_{e,pl} = \frac{\theta_{m,pl}}{2} \tag{5.29}$$

The value of ε_e can be obtained by using equations (5.22) to (5.29).

Having determined an estimate of $E_{S,max}$, D_{uc} can be estimated by the following procedure:

Energy demand at level h, E_D^h:

$$E_D^h(t) = K_D^h(t) + E_S^h(t) \tag{5.30}$$

where K_D^h represents the kinetic energy at level h transferred by the levels above level h.

Considering levels as rigid blocks, K_D^j is determined by:

$$\text{If: } E_D^{j-1}(t) < E_{S,max}^{j-1} \Rightarrow K_D^j(t) = \sum_{i=1}^{j-1} K^i(t) \text{ Else: } K_D^j(t) \equiv \sum_{i=1}^{j-1} m_i \times g \times h^{ij} \tag{5.31}$$

where:
m_i represents the moving mass of level i
g gravitational acceleration
h^{ij} vertical distance between levels i and j

Finally, an estimate of D_{uc} is obtained by:

$$E_D^{n_{level}}\left(t^{n_{level}}\right) = E_{S,max}^{n_{level}} \Rightarrow \begin{cases} t_{uc} = t^{n_{level}} \\ D_{uc} = D(t_{uc}) \end{cases} , \quad n_{level} \text{ represents the bottom level index} \tag{5.32}$$

In order to further improve the accuracy of the procedure, multi-story column buckling can be approximately accounted for by summing the energy demand of the buckled columns. Also, to capture local effects due to gravity action, the values of the leading action should only be increased when a static equilibrium between the applied loads and the internal forces has been reached. A suitable failure search and detection algorithm should also be developed in order to update the values of E_D and E_S of each level.

It is assumed that the upper level of elements will fall onto a lower level of elements. If not, the upper level of elements will free fall until reaching the ground. In this case, the kinetic energy of the upper level of elements should not be considered when evaluating the resistance capacity of the lower level of elements. Also, care should be paid in choosing the leading action, since the entire mass where the selected leading action is applied may be in free fall and thus might not cause the complete collapse of the system.

The denominator of equation (5.18) is also a difficult value to be determined since it involves the calculation of the potential sum of damage energy and an iterative search for the maximum potential sum of damage energy, D_c. However, this value can be estimated in a numerical analysis by the sum of damage energy up to collapse. Nevertheless, this method still poses considerably difficult numerical challenges. An alternative method, simpler but also approximated, is to numerically or analytically estimate its value for each element and sum over all the elements of the system. For a system similar to the one depicted in Figure 5.12, D_c can be estimated by:

$$D_c = \sum_{i=1}^{N_{levels}} E_{S,max}^i \tag{5.33}$$

The ratio presented in equation (5.18) may have a potential limitation in the cases when the robustness value is controlled by just a very few elements. For example, for a structure which resistance is controlled by very few elements (only one element in the extreme case), in general in this case $I_R \approx 0$ ($D_c \gg D_{uc}$) but when $D_c \approx D_{uc}$, which could happen when the available damage energy of the remaining elements is exceptionally low when compared with the available damage energy of the controlling elements, then $I_R \approx 1$ which may not be the expected result. In these cases, equation (5.18) could be modified by introducing a parameter, α, that accounts for the relation

between the total number of failed elements needed to attain the "unavoidable collapse" state and the total number of elements present in the system, see equation (5.34).

$$I_R\left(A_L \mid H\right) = \alpha \times \frac{D_{uc} - D_{1st\ failure}}{D_c - D_{1st\ failure}} \quad \text{with} \quad \begin{cases} \alpha = \dfrac{n_{uc}}{n_{total}} \\ 0 \le I_R \le 1 \\ D_c - D_{1st\ failure} = 0 \Rightarrow I_R = 1 \end{cases} \tag{5.34}$$

where:

n_{uc} represents the number of failed elements for the "unavoidable collapse" state, *i.e.* when $D = D_{uc}$;

n_{total} represents the total number of elements present in the system.

In a framed system, as a plausible simplification, n_{uc} can be given by the number of element failures (including joints) and n_{total} can be given by the total number of elements present in the system.

By using advanced finite element analysis programs it is also possible to follow the damage (failure) path throughout the system as the loading increases, for instance by using flag variables in the numerical model which are activated if a given damage criterion is met. This information can be used to modify the value of the robustness index by giving more emphasis to the existence of damages in selected critical areas or critical elements of the system. This can be easily done by introducing penalty weight factors ($\zeta < 1$) into the calculation of D_{uc}, specifically applied to the damage energy of those critical areas or critical elements, see equation (5.35).

$$I_R\left(A_L \mid H\right) = \frac{\sum_i^j \left(\zeta_i \times D_{uc,i}\right) - D_{1st\ failure}}{D_c - D_{1st\ failure}} \quad \text{with} \quad \begin{cases} 0 \le I_R \le 1 \\ D_c - D_{1st\ failure} = 0 \Rightarrow I_R = 1 \end{cases} \tag{5.35}$$

However, this type of differentiation should be preferably done only in the vulnerability analysis where the costs associated to damages are calculated, see section 5.4.7.6, to avoid introducing risk related parameters or subjectivity into the determination of structural robustness.

The proposed index can also be used to calculate the residual robustness of a system against follow-up hazards after a selected hazard event has taken place. This type of analysis comes with the cost of having to run multiple dynamic numerical analyses. For example considering an earthquake: for each analysis, the analyst has to select the seismic action value (typically the peak ground acceleration), apply the seismic action plus the permanent actions and accompanying variable actions, and if a stable static equilibrium state can be achieved after finishing applying and removing the seismic action, he/she has to introduce the follow-up hazard into the model and calculate the robustness of this system. This procedure may be cumbersome but it is necessary since the residual structural robustness strongly depends on the previous damaged state. To ease the calculation, only a finite number of seismic action values can be considered, for example.

The index presented in equation (5.34) does not exhibit the same limitations has the other indices previously discussed. Thus, it is thought that the index given by equation (5.34) fulfils all conditions listed by (Starossek, Haberland, 2008) and will be used here on as a measure of the robustness of a structural system.

Let us get back to the example of structures *A* and *B*. Figure 5.8 presents the possible strain energy diagrams for both structures. The robustness index of structures *A* and *B* are given by:

$$I_{R,A}\left(A_L \mid H\right) = \alpha_A \times \frac{D_{uc,A} - D_{1st\ failure}}{D_{c,A} - D_{1st\ failure}} \quad , \quad I_{R,B}\left(A_L \mid H\right) = \alpha_B \times \frac{D_{uc,B} - D_{1st\ failure}}{D_{c,B} - D_{1st\ failure}} \tag{5.36}$$

and $I_{R,A} < I_{R,B}$ considering $\alpha_A = \alpha_B$, see Figure 5.8.

For this academic example, it may seem that there is no use of adopting the knock-out element strategy, see section 5.4.7.8 for details. However, if structure *A* had not been designed using any robustness strategy, structure *Am* see Figure 5.13, its robustness index, $I_{R,Am}$, could be smaller than $I_{R,A}$:

$$I_{R,Am}\left(A_L \mid H\right) = \alpha_{Am} \times \frac{D_{uc,Am} - D_{1\text{st failure}}}{D_{c,Am} - D_{1\text{st failure}}} < I_{R,A}\left(A_L \mid H\right) \quad \text{and} \quad D_{c,Am} \approx D_{c,A} \quad \text{and} \quad \alpha_{Am} = \alpha_A \quad (5.37)$$

Thus, the knock-out element strategy may be useful when the entire structure is very fragile and prone to progressive and disproportionate collapse.

Figure 5.14 presents further examples where the new robustness index can be applied with benefits over the existing indexes.
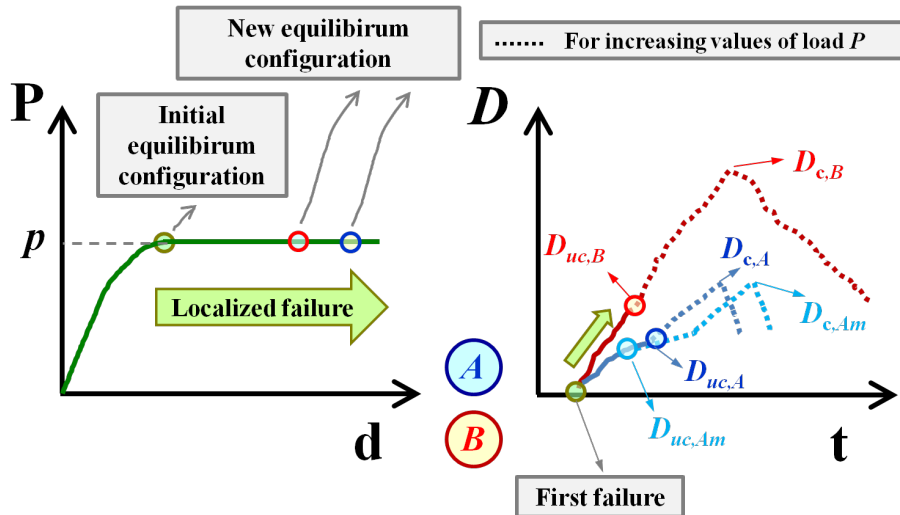
Figure 5.13: Loads and strain energy curves of buildings *A*, *Am* and *B*.
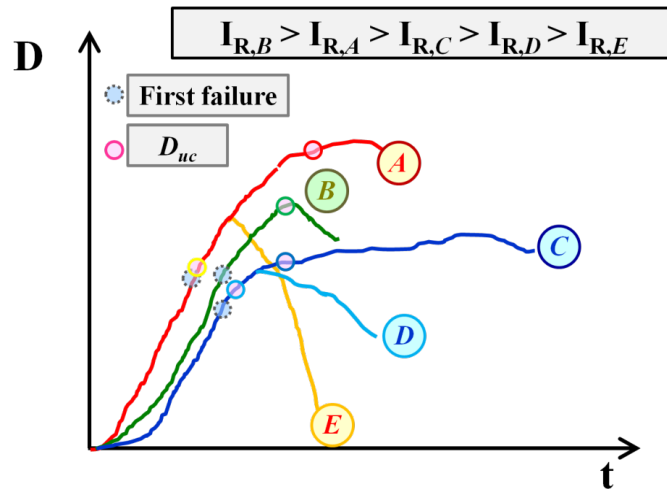
Figure 5.14: Example of the application of the robustness index for different systems.

As an additional demonstrative example, the Model A2 tested in the Sydney University, see Chapter 4 and (Chandrangsu, Rasmussen, 2009a), will be considered. The cross-section geometrical characteristics as well as the material properties of the various elements which are part of the falsework system are identical to the ones used in the structures tested in the Sydney University, see Chapter 4 and (Chandrangsu, Rasmussen, 2009a). Additionally, the finite element mesh properties are the same as detailed in Chapter 4 for Model A2. The formwork was explicitly modelled, with an equivalent thickness equal to 100 mm, and the joint characteristics considered were taken as the average values of the tests results reported in Chapter 3. The value of the top and bottom jacks' extension lengths was considered equal to 600 mm. The initial geometrical imperfections were taken as the values measured *in situ* during the full scale tests performed at Sydney University, see Chapter 4 and (Chandrangsu, Rasmussen, 2009a). Figure 5.15 illustrates the numerical representation of Model A2.
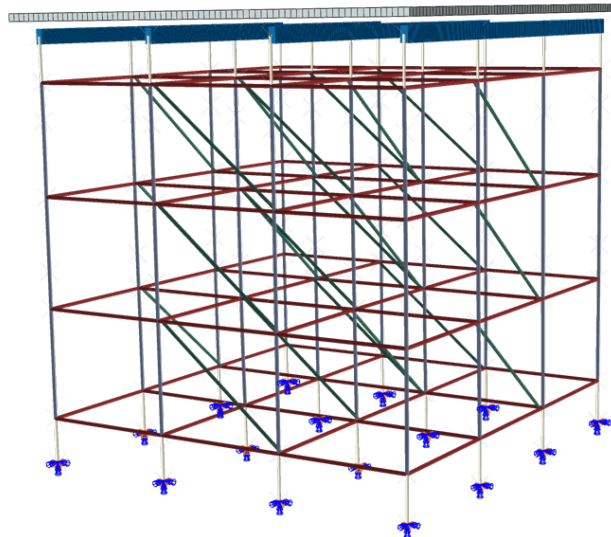
Figure 5.15: Overview of Model A2.

Additionally to Model A2, two variations of this model will also be used: (i) Model A4, which is the braceless version of Model A2, and Model A2m which is equal to Model A2 except the value of the top and bottom jacks extension lengths is equal to 300 mm. Figure 5.16 and Figure 5.17 illustrate the numerical representation of models A4 and A2m, respectively.
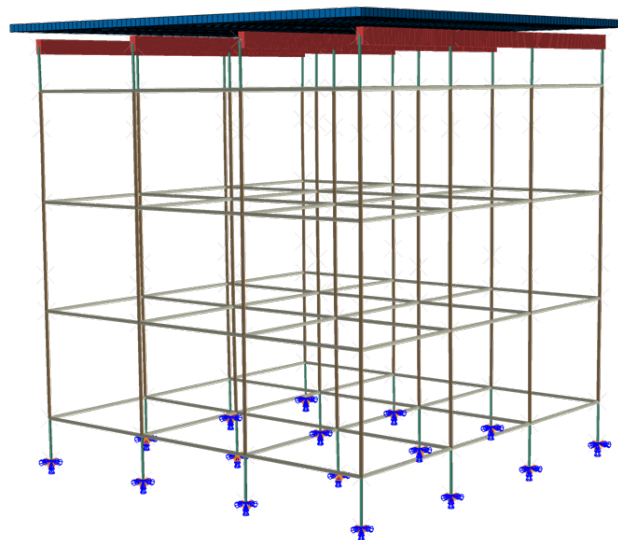
Figure 5.16: Overview of Model A4.
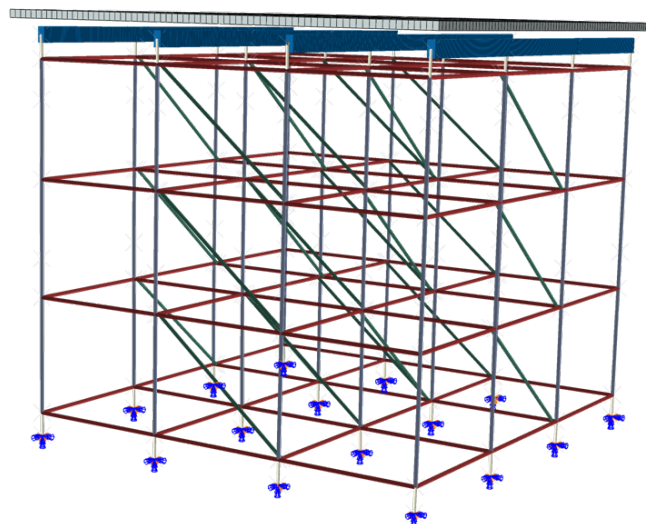
Figure 5.17: Overview of Model A2m.

The only action considered in this example, besides the materials' self-weight, was the weight of the concrete slab. This action was selected as the leading action and applied uniformly to the formwork elements and increased monotonically.

Taking Model A2 as the reference model, Figure 5.18 shows how the procedure developed to detect the "unavoidable collapse" state is applied. For each one of the five levels of Model A2, the values of the energy deformation demand and energy deformation capacity were determined for increasing values of the leading action. As the load value increased, so the internal forces and material strains in the various elements of the structure. Eventually, an element(s) breaks or looses substantially its stiffness. Table 5.2 presents the various element failures of Model A2. It took a total of 13 element failures for the collapse of Model A2 to become unavoidable, the majority of which located at level 1, more specifically due to excessive rotation of the forkhead plates making them loose their rigidity and resistance capacity, and consequently of the attached jack elements.
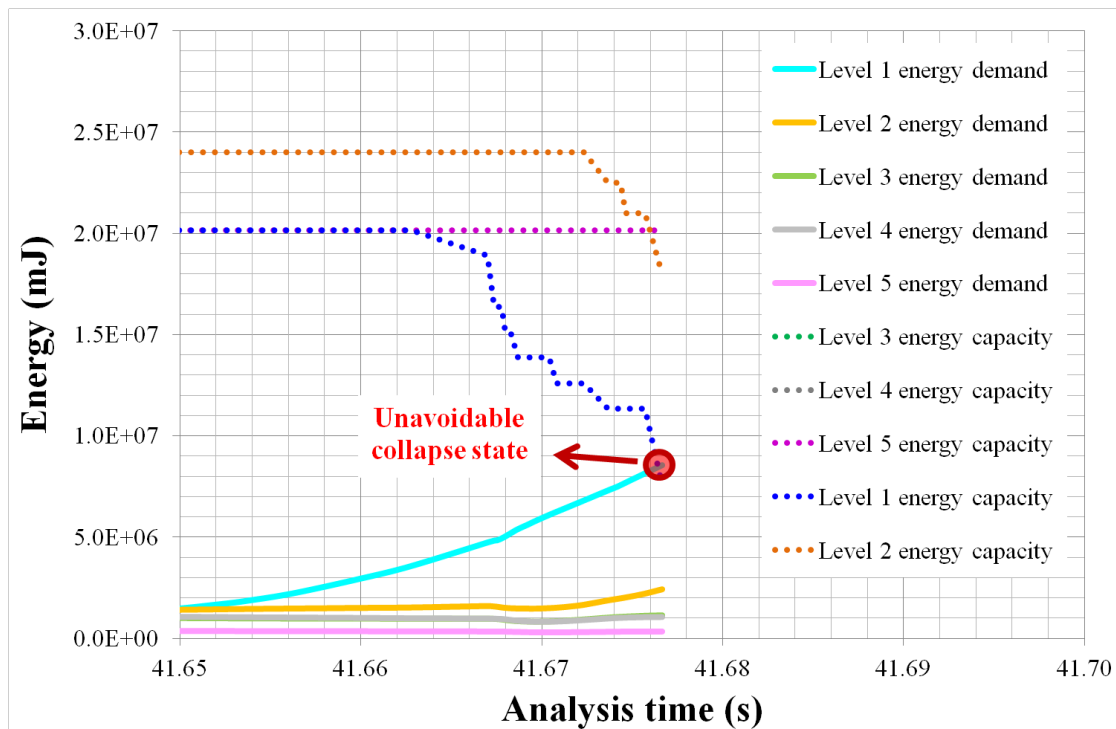
Figure 5.18: Application of the procedure used to detect the "unavoidable collapse" state of Model A2.

Table 5.2: Element failures of Model A2.

Element type	Time (s)	Level
Forkhead joint	42,6670	1
Forkhead joint	42,6674	1
Forkhead joint	42,6674	1
Column	42,6680	1
Forkhead joint	42,6687	1
Column	42,6708	1
Column	42,6737	2
Column	42,6746	2
Column	42,6767	1
Column	42,6767	1
Column	42,6767	1
Column	42,6767	2
Column	42,6767	2

Failure of the spigot joint occurred by excessive bending rotation. Column failure was considered when three plastic hinges (plastic deformations) formed at sections of the column spaced by at least 15% of the column length from each other.

Each element failure means that there are fewer elements available to contribute to the resistance of the structure and consequently the energy deformation capacity decreases. On the other hand, energy deformation demand increases. When the energy deformation demand at one level equals the energy deformation capacity of that level, collapse of that level is unavoidable. The collapse of one level implies that the potential energy stored at the levels above will be converted, mainly, into kinetic energy. The motion of this moving mass will only be stopped if and if only the energy deformation capacity of the levels below is greater than the kinetic energy of the moving mass.

Considering Model A2, the collapse of level 1 means that the weight of the formwork and of the poured concrete will move at least from their respective height at time of collapse of level 1 to the height of level 2. Therefore, a mass equal to the applied pressure times the formwork area is put in motion by gravity as it drops from height of level 1 to the height of level 2. The kinetic energy associated with this movement equals $8,42 \times 10^8$ mJ. The estimated maximum energy deformation capacity of level 2, determined according to equation (5.21), is $2,40 \times 10^7$ mJ (neglecting existing damages in level 2 at the time of collapse of level 1). Therefore, level 2 will also collapse, and the same happens for levels 3, 4 and 5. In conclusion, the collapse of level 1 induces the global collapse of the entire structure, and therefore it corresponds to the "unavoidable collapse" state of Model A2.

If the formwork was connected to other elements, other than the columns of level 1, then collapse may have occurred for higher values of the leading action.

Robustness index of Model A2 is given by equation (5.34). The value of D_c is equal to $1,12 \times 10^8$ mJ. The value of D_{uc} is equal to $9,15 \times 10^6$ mJ. The number of elements in the model was considered equal to the number of columns at each level, plus the number of beam-to-column joints, plus the number of brace-to-beam(column) joints (if applicable), plus the number of forkhead and baseplate joints. For Model A2, the number of elements is 200 (the number of columns represents 40% of this number). Therefore, a robustness index equal to 0,006 is obtained, or equal to 0,082 if equation (5.18) is used instead.

Applying the same procedure to models A4 and A2m, the following robustness indices were obtained: 0,012 (0,129) and 0,013 (0,164), respectively. The values in brackets were obtained using equation (5.18).

The maximum resistance to concrete pressures applied to the formwork of Model A2, A4 and A2m is equal to $0,03909$ N/mm^2, $0,01401$ N/mm^2 and $0,04776$ N/mm^2, respectively.

It can be observed that Model A2 has the smallest robustness index value of the three models considered. This is justified because the critical elements to the collapse resistance of this model were the forkhead plates and top jacks. The jacks have an energy deformation capacity lower than the standard elements since their cross-section dimensions are smaller. Therefore, damage concentrated in few elements which have a lower energy deformation capacity than the rest of the elements of the structure.

Decreasing the jacks extension length allowed damages to concentrate at the columns (of levels 2 and 3), which can dissipate more energy and thus can endure more damages. It also provided extra resistance to Model A2m.

Removing the brace elements makes the structure to exhibit large sway displacements and concentrates damages at the columns of level 3. However, because the spigot joints, which do not have a large energy deformation capacity, are also severely deformed, they end up limiting the collapse resistance of A4 model, in terms of robustness and resistance.

Using equation (5.18) or (5.34) results in different robustness index values. The latter equation includes the ratio between the number of element failures and the total number of joints present in the system. Therefore, it can be seen that Model A2m dissipates more energy than Model A4, but in less number of elements.

No matter what equation is used to calculate robustness, equation (5.18) or (5.34), all values are low, meaning that the systems have a small robustness against uniformly applied actions to the formwork. Also, damages up to "unavoidable collapse" state are concentrated in a very small number of elements.
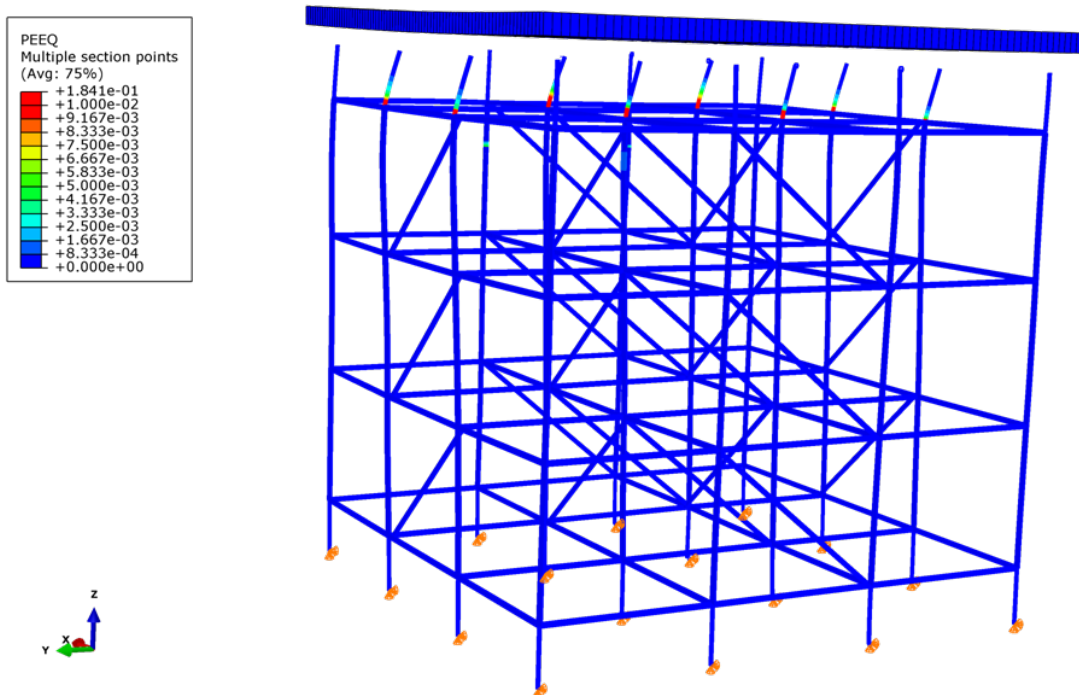
Figure 5.19: Deformed shape and plastic extensions distribution at unavoidable collapse state: Model A2.
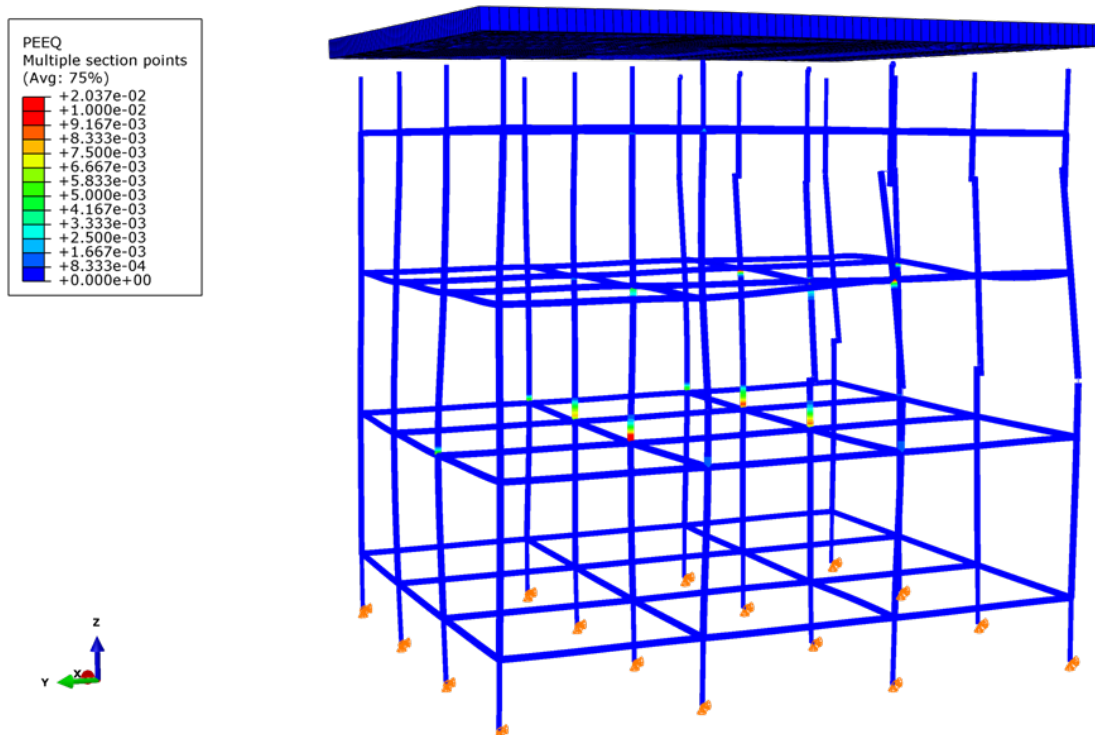
Figure 5.20: Deformed shape and plastic extensions distribution at unavoidable collapse state: Model A4.

As a closing remark to this application example, it must be pointed out that the applied procedure thus provide an accurate (numerical wise) value of the system's maximum resistance and of the robustness index. If the value of the leading action was set to just a fraction lower than the maximum action value that the structure is capable of resist, collapse would not have occurred.

Figure 5.22 shows the energy demand and energy capacity evolution of the five levels of Model A2 loaded with concrete pressures applied to the formwork up to 0,03908 N/mm^2, *i.e.* 99,97% of the maximum action value. As it can be seen, for this action value the damages that occur are not sufficient to bring the structure to the ground. This occurs because the kinetic energy of the mass of the Model A2 is very small in this case, but becomes very large when loaded up to the maximum action value, see Figure 5.23 and Figure 5.24.
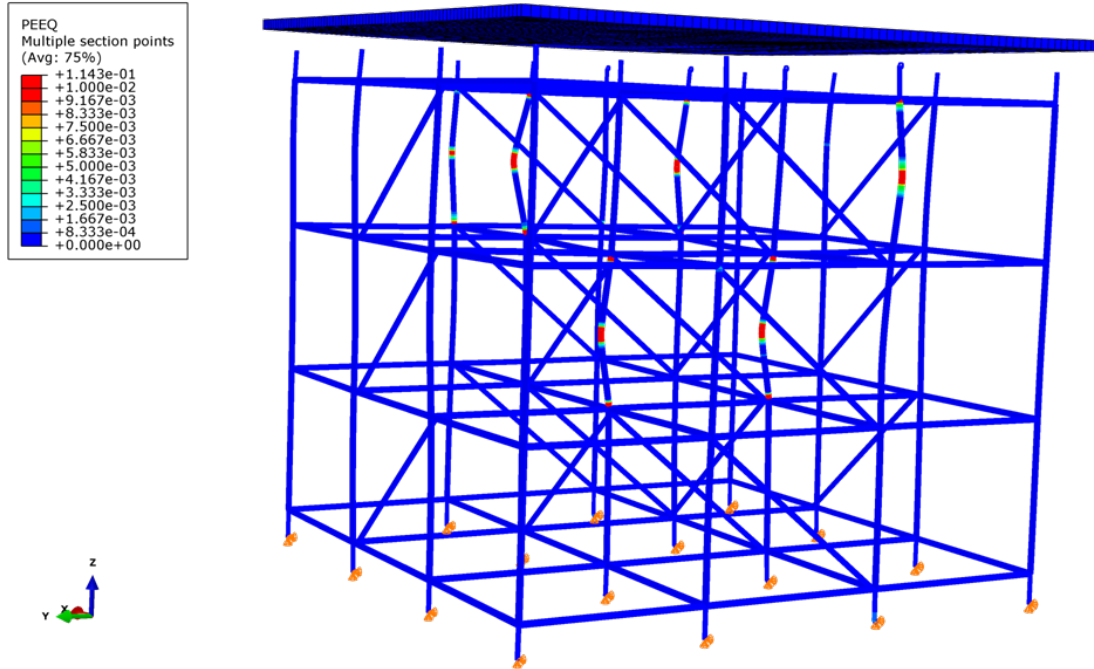
Figure 5.21: Deformed shape and plastic extensions distribution at unavoidable collapse state: Model A2m.
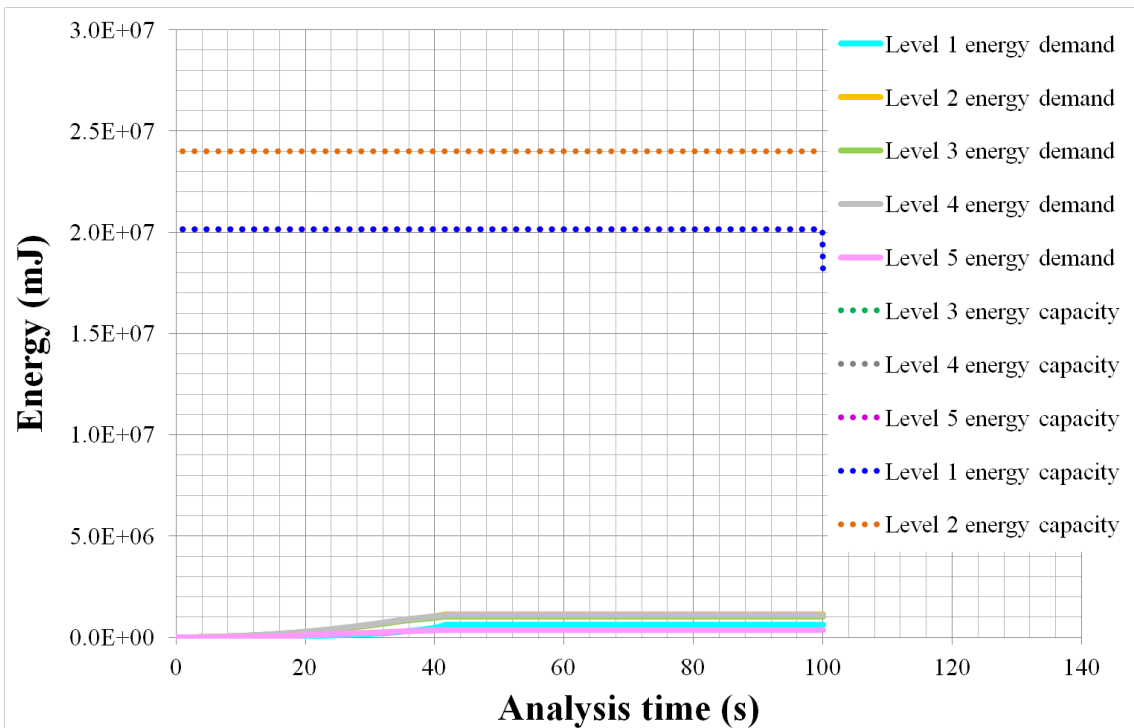
Figure 5.22: Energy demand and energy capacity for Model A2 loaded just a fraction less than the maximum load, *i.e.* the "unavoidable collapse" state.
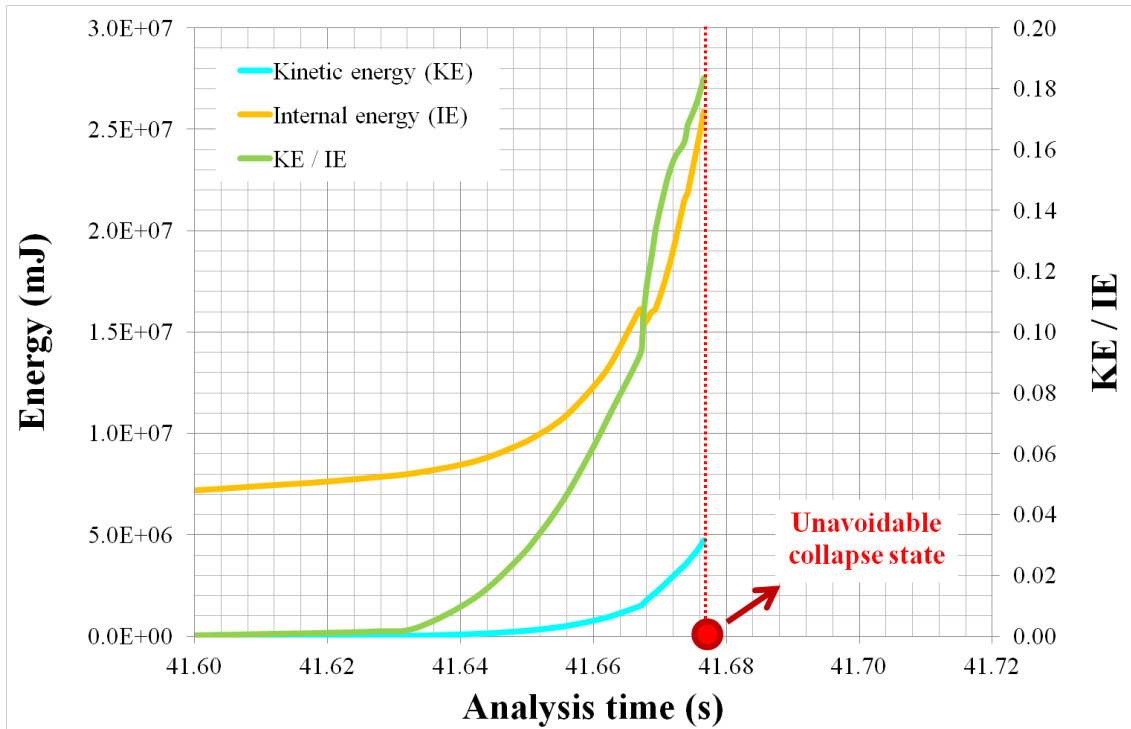
Figure 5.23: Kinetic energy and internal energy for Model A2 loaded until "unavoidable collapse" state.
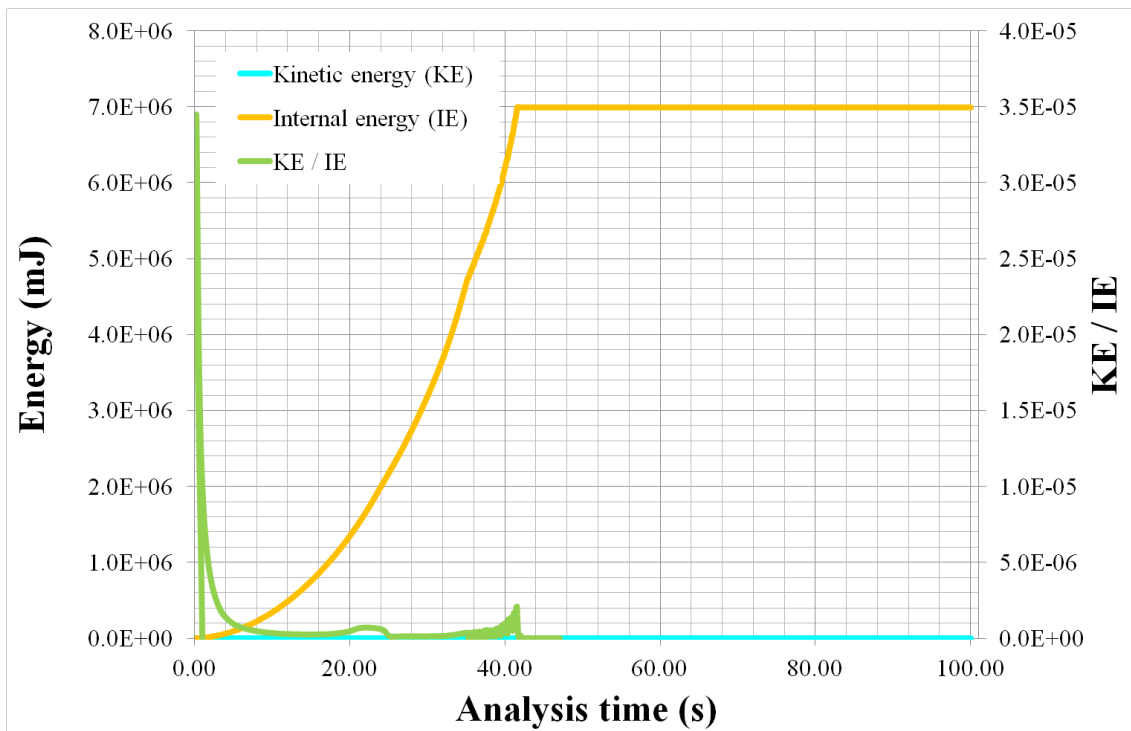
Figure 5.24: Kinetic energy and internal energy for Model A2 loaded just a fraction less than the maximum load, *i.e.* the "unavoidable collapse" state.

In the analyses, the kinetic energy value was controlled and if it increased between consecutive increments, using a minimum reference time increment, the leading action value was not increased in order to obtain near static solutions, if possible.

However, the detection of "unavoidable collapse" state is subject to uncertainties and despite the developed procedure captures the most important features that govern the dynamic behaviour of a structure, it has some limitations.

Among the most important ones is the definition of the maximum energy deformation capacity. Equation (5.21) is a simplification since it does not account for axial and shear deformations. Also, the plastic hinge length at maximum extension contributes for uncertainties. Lower values of this parameter lead to lower estimated energy deformation capacity. In the developed procedure a conservative value for the plastic hinge length for steel CHS was considered.

However, these two limitations have conservative implications in the results obtained from the developed procedure. It is considered that the developed procedure is sufficiently accurate and that for each structural system the errors with respect to the actual values are proportional, allowing the direct comparison of the resistance and robustness values of different structural systems.

Robustness is a function of the hazard scenario, H, in particular of the actions values, A, which have an impact on the initial damage mechanism (*e.g.*, an explosion of magnitude *a*) and damage propagation, and of the resistance variables of the structural system, R. Resistance variables are random variables and robustness directly depends on the resistance variables of the system. Therefore robustness is a random variable, function of resistance variables and action variables.

In certain cases, for example, geotechnical problems or when self-weight loads are very important, values of resistance variables are not independent of action values. However, in general the assumption of complete independence between actions and resistance variables is commonly used (Haldar, Mahadevan, 2000 ; Melchers, 1999). Let us consider the simple case of deterministic resistance. If g is an invertible function and $I_R = g(H)$, then the cumulative distribution function (cdf) of robustness would be obtained by:

$$F_{I_R}\left(I_R\right) = \int_{-\infty}^{g^{-1}(I_R)} f_H\left(H\right) dH \qquad (5.38)$$

where and $f_H(H)$ is the joint probability density function (pdf) of actions considered in the hazard scenario H, each action considered to have an uniform distribution.

In the general case:
1. Considering dependence between resistance and action

$$F_{I_R}\left(I_R\right) = \int_{-\infty}^{+\infty} \int_{-\infty}^{h^{-1}(I_R,R)} f_{H,R}\left(H,R\right) dHdR \qquad (5.39)$$

2. Considering independence between resistance and action

$$F_{I_R}\left(I_R\right) = \int_{-\infty}^{+\infty} \int_{-\infty}^{h^{-1}(I_R,R)} f_H\left(H\right) f_R\left(R\right) dHdR \qquad (5.40)$$

where $I_R = h(H,R)$ and $f_{H,R}(H,R)$ is the joint pdf of actions in hazard scenario H and resistance R, respectively.

Determining analytical expressions for the functions $g(H)$ and $h(H,R)$ is quite difficult and solving the above integrals is quite complex. Therefore, simulation schemes, like Monte Carlo or others, are a viable alternative solution to determine the robustness cdf and pdf (see Figure 5.25 for illustrative examples).
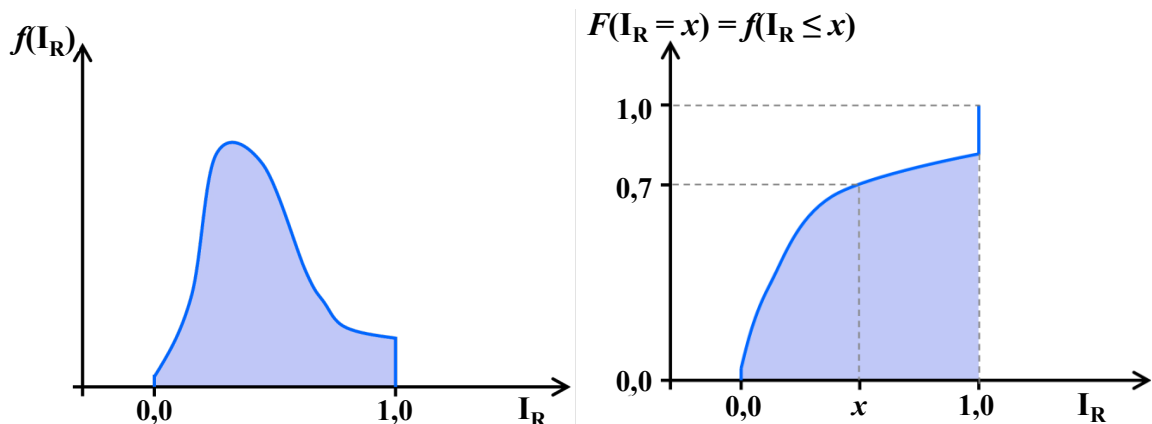
Figure 5.25: Illustrative example of robustness index probability density function *(Left)* and cumulative distribution function *(Right)*.

The probability distribution of the robustness index has some particular properties: it is a truncated distribution and the probability contents of the extremes, *i.e.* $I_R = 0$ and $I_R = 1$, are not equal to zero. Therefore the distribution of robustness index is a mixture distribution with the cdf given by:

$$\begin{cases} F_{I_R}\left(I_R \leq 0\right) = f\left(I_R = 0\right) = \dfrac{\text{number of simulations where } I_R = 0}{\text{total number of simulations}} \\[2mm] F_{I_R}\left(0 < I_R < 1\right) \times \left[1 - F_{I_R}\left(I_R \leq 0\right) - F_{I_R}\left(I_R \geq 1\right)\right] + F_{I_R}\left(I_R \leq 0\right) \\[2mm] F_{I_R}\left(I_R \geq 1\right) = f\left(I_R = 1\right) = \dfrac{\text{number of simulations where } I_R = 1}{\text{total number of simulations}} \end{cases} \tag{5.41}$$

From the cdf of robustness a graphic representation of robustness curves can be obtained, which could express simply robustness as a function of action values, namely the leading action *nominal* values defined in the first step of the procedure to calculate the robustness index, or the probability of non-exceedance of robustness values as a function of the actions values, see Figure 5.26, for example.

As a remark, there are cases where combinations of action and resistance variables lead to robustness values always higher than zero and lower than one, *i.e.* $I_R \subset [a,b], (a > 0, b < 1)$.
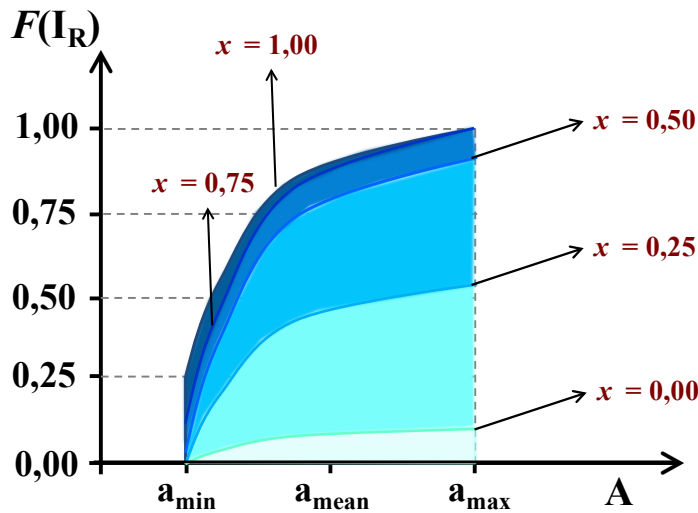
Figure 5.26: Example of a representation of robustness curves.

Finally, as discussed previously, uncertainties will always exist and it is important to assess their impact on the results. Uncertainty propagation can be considered in robustness analysis by using methods presented in section 5.4.6.4 to the resistance variables (actions are modelled with uniform probability density functions). Therefore, different robustness probability functions are obtained.

5.4.7.5 Fragility analysis

Robustness is a measure of the predisposition of a structural system to progressive and disproportionate collapse. Therefore, it is not the best parameter to evaluate when the objective is to assess the system's resistance against the applied actions. The development of such a measure is of great benefit, and even more, if this measure could relate directly to the damage extension within the system for a given action combination.

A fragility index, F_R, which is capable of addressing adequately these objectives, was developed as the mathematical expression of:

$$F_R\left(A_R, A_L \mid H\right) = \frac{\text{Damages up to equilibrium state for action } A_R \text{ for hazard } h}{\text{Damages up to collapse state for hazard } h} \tag{5.42}$$

The general expression is given by:

$$F_R\left(A_R, A_L \mid H\right) = \frac{D_p - D_{1st\ failure}}{D_c - D_{1st\ failure}} \quad \text{with} \quad \begin{cases} 0 \leq F_R \leq 1 \\ D_c - D_{1st\ failure} = 0 \Rightarrow F_R = 1 \\ A_L \geq A_{L,uc} \Rightarrow F_R = 1 \end{cases} \tag{5.43}$$

where (see Figure 5.27):

A_R represents the reference action;

A_L represents the leading action, which can be different from the reference action. $A_{L,uc}$ represents the value associated with D_{uc};

$H = \{h_1, h_2, ..., h, ..., h_n\}$ is a set of hazard scenarios: {base conditions} + {impact on column 1, impact on column 2, ..., impact on column n}, a set of different actions or a combination of different actions, for example;

D_p represents the value of the damage energy of the structure when the new static equilibrium state is reached for value p of the reference action within the considered hazard scenario;

$D_{1st\ failure}$ represents the damage energy of the structure when the "first failure" state takes place for the hazard scenario considered;

D_{uc} represents the damage energy corresponding to the state where collapse is unavoidable for the hazard scenario considered;

D_c represents the damage energy corresponding to the collapse state for the hazard scenario considered.
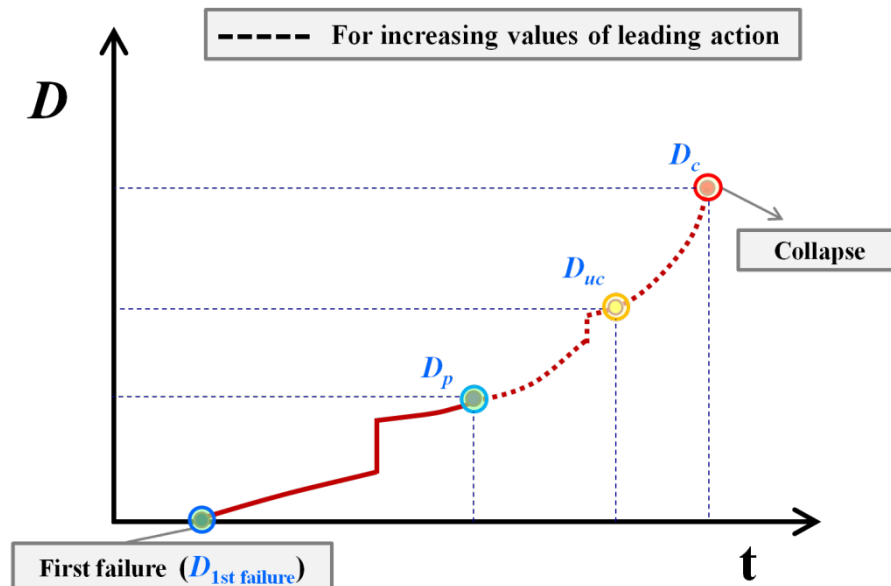
Figure 5.27: Illustration of the fragility index notation.

The above expression is slightly different than equation (5.18) used to calculate the robustness index. Since fragility relates to system's damage energy reserve capacity under the applied actions, in particular value p of the reference action, in the numerator D_{uc} – $D_{1st\ failure}$ is replaced by D_p – $D_{1st\ failure}$. In the denominator, D_c is kept to obtain the actual damage relative to the maximum damage possible. Therefore, robustness and fragility are two closely related structural parameters.

In order to calculate this fragility index a three step procedure must be followed, see Figure 5.28.

First step: defined the *nominal* loading conditions (hazard scenario), *i.e.* the sequence of action (loads) application is rationally chosen and the initial values of the several loads, material properties, system imperfections, etc. are generated, corresponding to values obtained from the corresponding probability density functions (loads are modelled with uniform probability density distributions and resistance variables can also be modelled with uniform probability density distributions but preferably with more informative distributions). Correlations could be considered, for example: complete or

incomplete correlation between load values – incomplete correlation means that values of different loads can be correlated for only a range of values of one of the loads; for example seismic loads and traffic loads. The reference action is chosen and the value of D_p is determined. The system performance should be sensitive to the selected reference action values. The value of D_c is also determined.

Second step: while holding everything constant ("*ceteris paribus*"), a leading action that can cause the structure to collapse (if it has not already occurred during step 1) is selected and increased until the collapse is attained. However, several actions can be increased simultaneously if it is considered appropriate (if correlated for example). The aim should be to obtain a realistic safety assessment of the structure and therefore of the most likely damage propagation within the structure. In the example illustrated in Figure 5.29 *(Left)* it may be necessary to evaluate the fragility index for increasing values of the action *p* and not of *F*, while in Figure 5.29 *(Right)* it may be possible to select either actions. The value of D_{uc} is determined.

Third step: the fragility index is determined from equation (5.43) based on the adopted limit state which defines the first failure state (the value of $D_{1st\ failure}$ is determined).
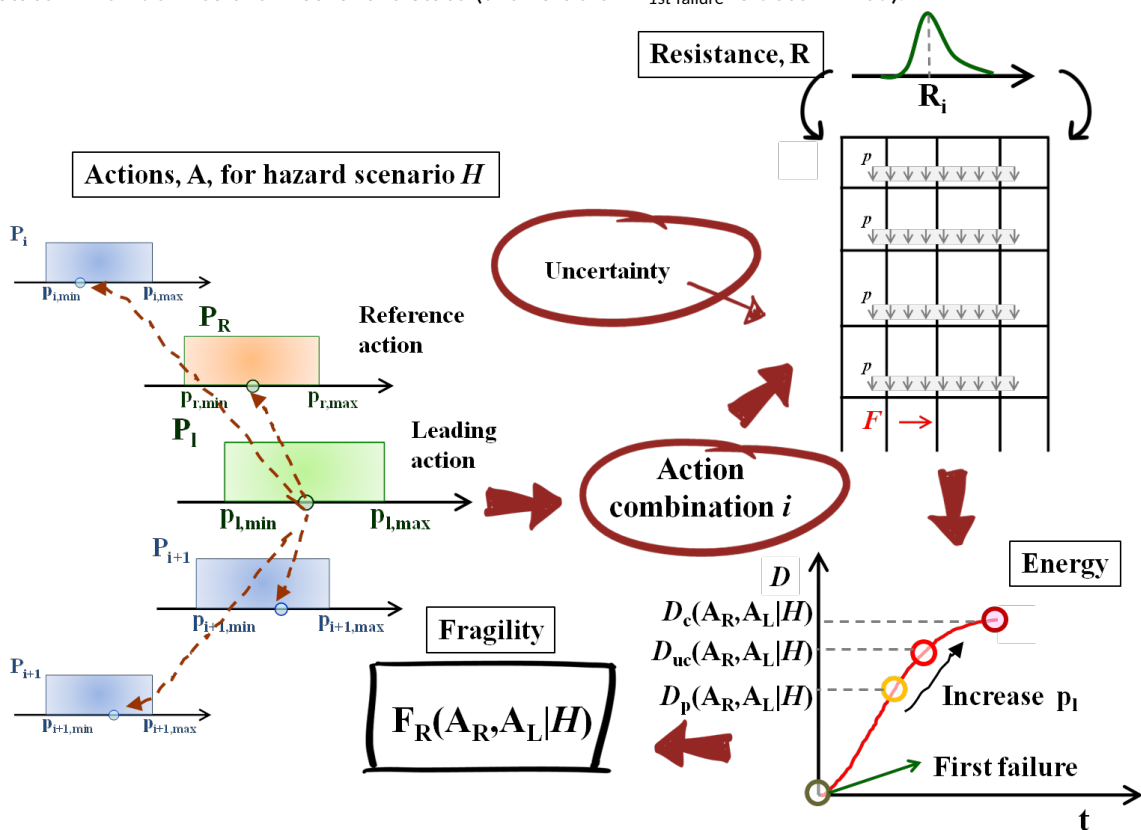
Figure 5.28: Procedure to determine the fragility index.

For damage energy values higher than D_{uc}, the fragility index is equal to one; for values below $D_{1st\ failure}$, the fragility index is equal to zero.

The index is also flexible since the inputs can change, for example: the "first failure" state can be replaced by another criterion, possibly related to a particular element failure, and the "unavoidable collapse" state can also be changed to represent a maximum limit of acceptable damage, for instance.

This flexibility is important. For example, in structural systems where there is a large discrepancy between the damage energy of great part of the elements (*e.g.* they are very brittle and weak and thus have a very low damage energy) and the remaining few (*e.g.* they are very resistant and ductile and thus have a very high damage energy), a hazard scenario may occur where only the majority of these weak elements fail. Since the sum of their damage energy is only a fraction of the sum of the damage energy of the strong elements, the fragility index will still be close to zero despite the bulk of the elements have failed. In these cases it is possible to define a maximum limit of acceptable damage,

namely the sum of the damage energy of the weak elements, and assign it to D_{uc}. An alternative, is to include in equation (5.42) the parameter α used in the robustness calculation, see equation (5.34).
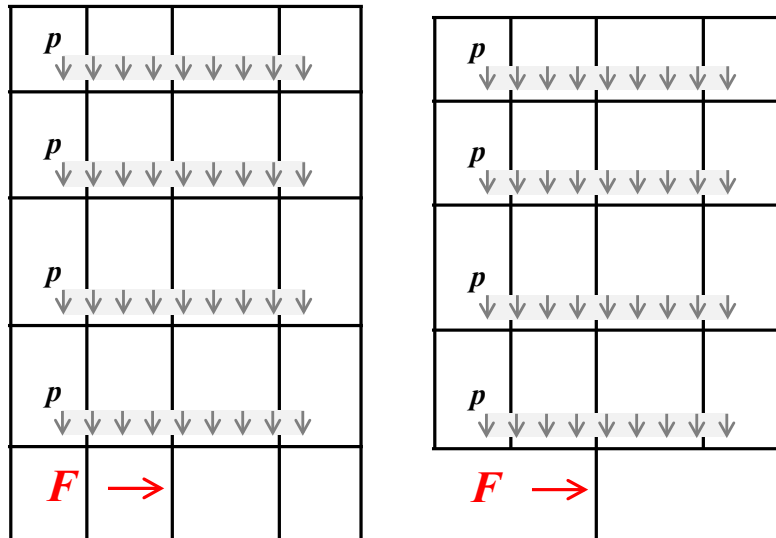
Figure 5.29: Possible different selections of leading actions to evaluate fragility.

Another extreme case is where there are very few controlling elements. In these cases there is no need to adapt the parameters of the fragility index since D_{uc} is almost only defined by the damage energy of these controlling elements.

As with the robustness index, by using advanced finite element analysis programs it is also possible to follow the damage (failure) path throughout the system as the loading increases, for instance by using flag variables in the numerical model which are activated if a given damage criterion is met. This information can be used to modify the value of the fragility index by giving more emphasis to the existence of damages in selected critical areas or critical elements of the system. This can be easily done by introducing weight factors ($\omega > 1$) into the calculation of D_p, specifically applied to the damage energy variations of those critical areas or critical elements, see equation (5.35).

$$F_R\left(A_R, A_L \mid H\right) = \frac{\sum_i^j \left(\omega_i \times D_{p,i}\right) - D_{1\text{st failure}}}{D_c - D_{1\text{st failure}}} \text{ with } \begin{cases} 0 \leq F_R \leq 1 \\ D_c - D_{1\text{st failure}} = 0 \Rightarrow F_R = 1 \\ A_L \geq A_{L,uc} \Rightarrow F_R = 1 \end{cases} \quad (5.44)$$

However, this type of differentiation should be preferably done only in the vulnerability analysis where the costs associated to damages are calculated to avoid introducing risk related parameters or subjectivity into the determination of structural fragility.

The proposed index can also be used to calculate the residual fragility of a system against follow-up hazards after a selected hazard event has taken place, in the same manner as for the robustness index.

An additional remark should be made about the analysis of fragility using the proposed index. Looking at Figure 5.30, it is possible to observe that structures A and B despite having the same yield and ultimate energy values, the same increment of the action value (A: load, displacement, rotation, temperature, etc.) causes different increments in the system's fragility.

This translates to structural fragility (damage accumulation) sensitivity to action values, which may be important when performing risk analysis. For example, two structures A and B with the same geometry and similar maximum damage energy (or robustness index) might have the same fragility index value for load $P = p_1$ but for $P = p_2$, with $p_2 > p_1$, the fragility index value of structure A might be very small when compared with structure B. This may be justified because structure A might have more critical elements or critical joints than structure B, for example, which limits its load redistribution capacity. Thus, it is important to analyse fragility as a function of the action values.
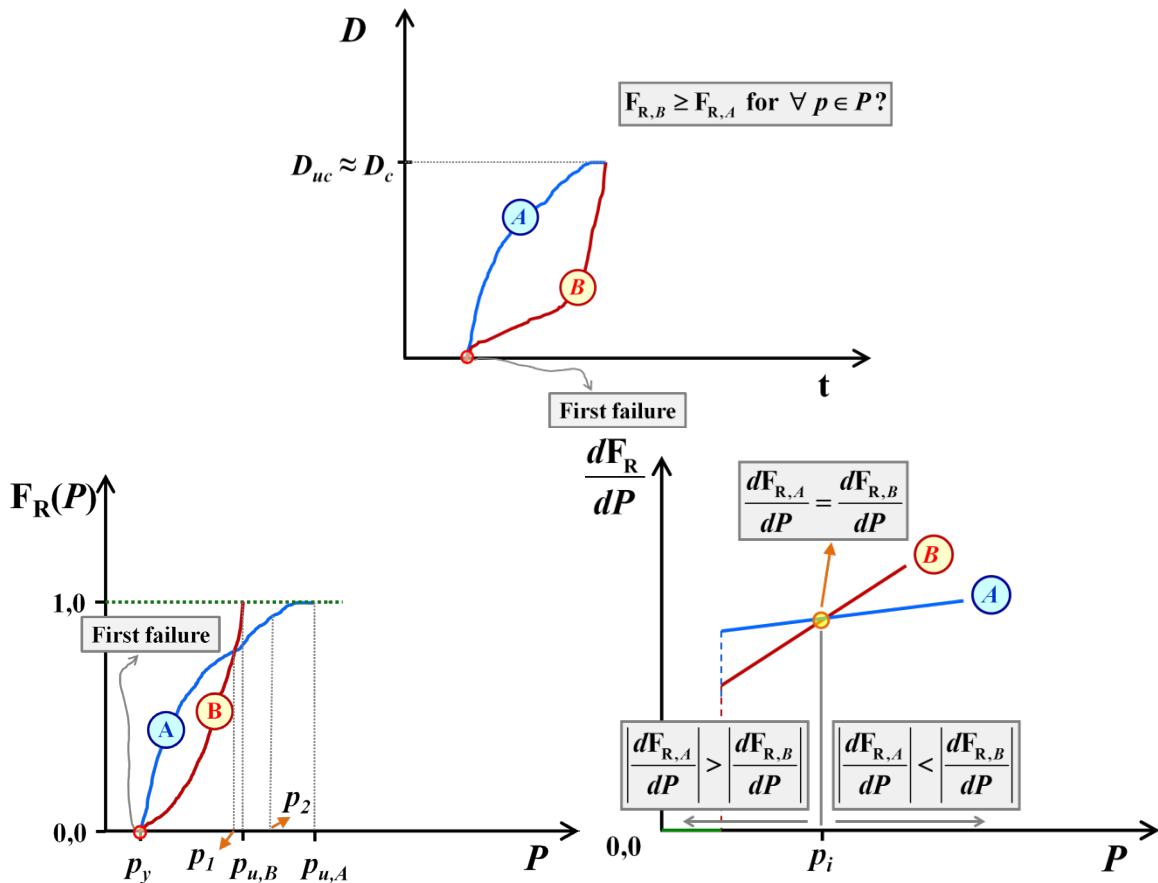
Figure 5.30: Damage energy and fragility index sensitivity to action values.

The same models presented at the previous section will be used as an example to evaluate fragility. Figure 5.31 and Figure 5.32 illustrate the damage energy and fragility index sensitivity to action values, respectively, for all three models (A2, A4 and A2m). It is possible to observe that damage progression (after first failure) in Model A2m is slower than in Model A2 (where collapse occurs almost after first failure) and than in Model A4, but damage increases exponentially in both A2 and A2m models after a certain load value, whereas in Model A4 damage increases gradually for increasing action values. This means that in Model A4 it may be easier to identify a potential collapse than in models A2 and A2m.

It may be concluded that adopting small values for the jacks' extension length is one strategy to increase both the resistance and robustness of the bridge falsework Model A2, and to decrease its structural fragility which has beneficial implications in terms of structural risks and economic risks.

The values of the fragility index just before "unavoidable collapse" state is attained are not equal to the robustness values given by equation (5.18) because D_{uc} is the energy needed to bring to collapse the entire structure which requires the collapse of at least one level of the structure. Hence, when the damage energy equals D_{uc}, fragility index is equal to one (meaning that the entire structure will collapse and maximum damage will occur). Robustness is calculated based on the value of D_{uc}, and not on the value of the damage energy corresponding to the state just before "unavoidable collapse" state, D^*, because is the former value that characterises correctly the collapse resistance of a given structure. Note that the difference between D^* and D_{uc} can be large.

Fragility is also a random variable, function of resistance variables and action variables. The probabilistic description of fragility follows closely the one described for robustness. From the cdf of fragility, see Figure 5.33 for an illustrative example, a graphic representation of fragility curves can be obtained, which could express simply fragility as a function of action values, or the probability of non-exceedance of fragility values as a function of the actions values, see Figure 5.34, for example.
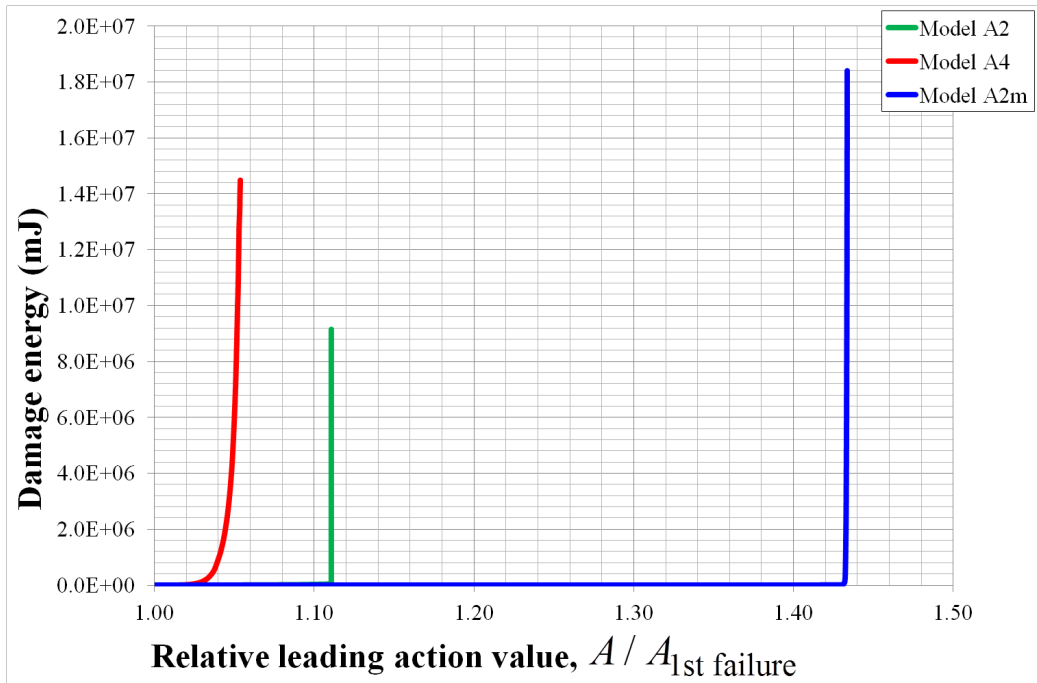
Figure 5.31: Damage energy sensitivity to action values for models A2, A4 and A2m.
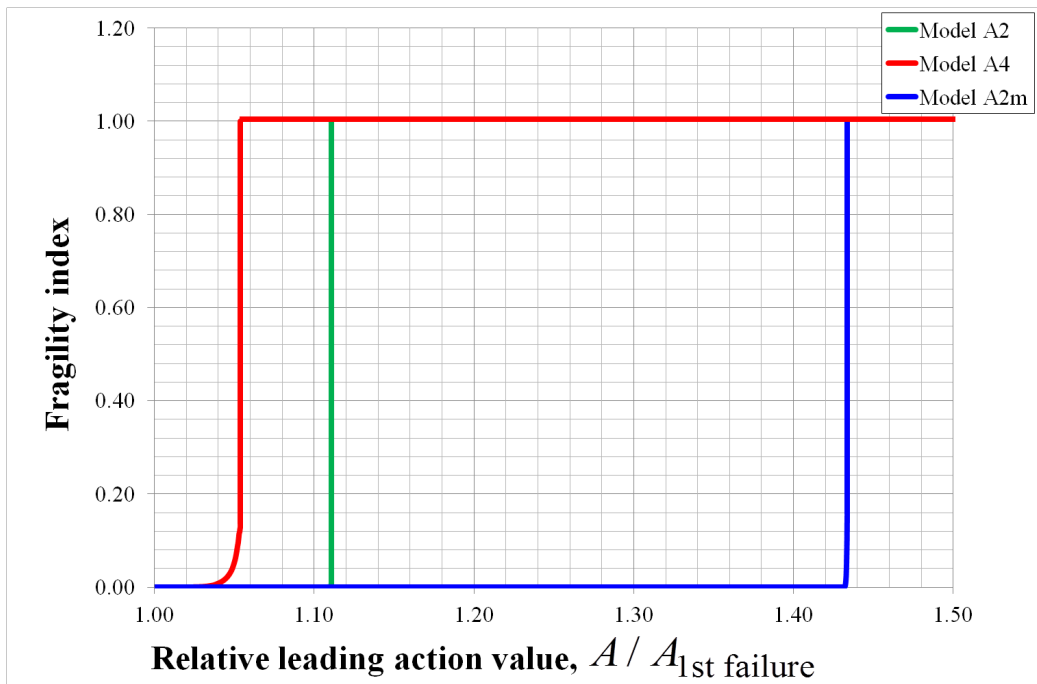
Figure 5.32: Fragility index sensitivity to action values for models A2, A4 and A2m.
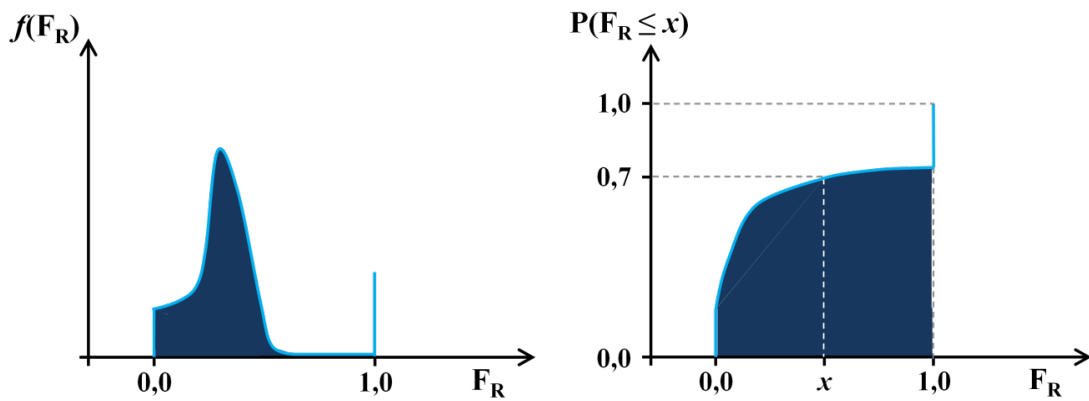
Figure 5.33: Illustrative example of fragility index probability density function *(Left)* and cumulative distribution function *(Right)*.
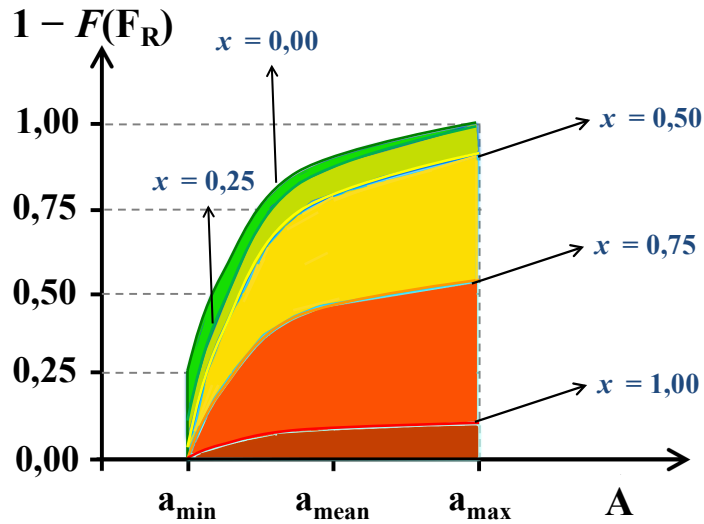
Figure 5.34: Example of a representation of fragility curves.

5.4.7.6 Vulnerability analysis

Vulnerability, in terms of costs of consequences, is related with fragility by a cost function κ(C), which translates levels of structural damages to costs of consequences. The cost function will be introduced later.

5.4.7.7 Risk measures

Risk is generally expressed in terms of the probability of structural collapse times the cost of the consequences given the collapse. Additionally, in the classical approach, risk can also be expressed by a probability of failure.

However, these definitions are quite limited since they do not account for the various damage states that might occur (damage is a continuous function) but that do not directly imply the global collapse of the structure. Therefore, valuable information is lost that could be used during the risk informed decision-making process. For instance, two structural systems *A* and *B* can have the same probability of failure but the damage evolution in *A* can be quite different than in *B*.

In the suggested framework, if actions and resistance variables are simulated by their real probability distributions and not by uniform probability distributions, fragility becomes an expression of the damage extension (D) of the structural system, a measure of the system's structural risk and damage tolerance, and vulnerability becomes a measure of risk that can be used in a Cost-Benefit analysis (CBA). In the present Thesis, these two risk measures are presented, see Figure 5.35 for conceptual representations. With this approach it is possible to analyse how risk changes with robustness or with other risk control measures thus contributing to a better decision-making process.
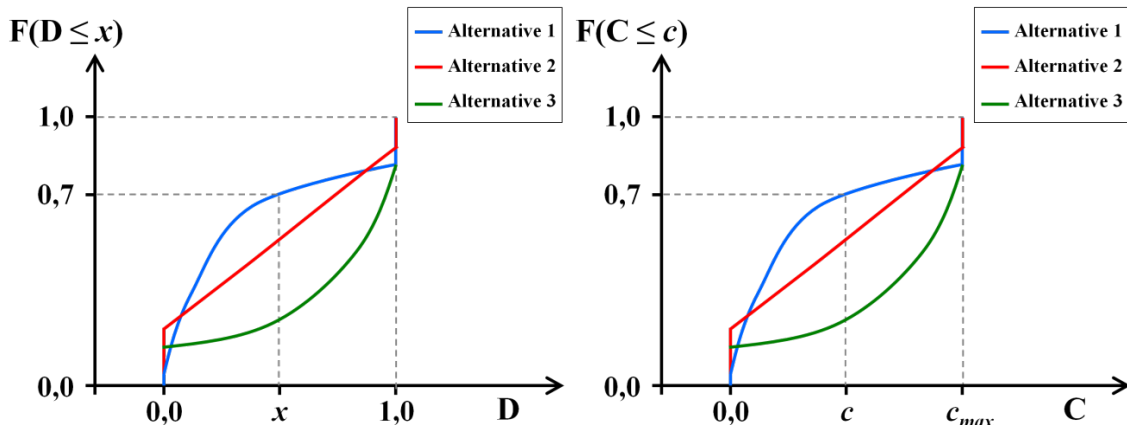
Figure 5.35: New risk measures, (*Left*) structural damages and (*Right*) costs of consequences.

If the consequences are only assessed in terms of structural damages, then risk is expressed by:

$$RISK = f(D) \tag{5.45}$$

and its expected value is given by:

$$\overline{RISK} = \int_D \left[f(D) \times D \right] dD \tag{5.46}$$

where D represents the structural damages and f(D) is the pdf of the structural damages.

Structural vulnerability may be analysed if the consequences are assessed in terms of costs of all consequences:

$$RISK = f(C) \tag{5.47}$$

and its expected value is given by:

$$\overline{RISK} = \int_C \left[f(C) \times C \right] dC \tag{5.48}$$

where C represents the costs related to the consequences and f(C) is the pdf of the costs.

For example, suppose the cdf of the fragility of a certain bridge falsework structure under permanent actions (self-weight and construction dead loads) is illustrated in Figure 5.36, and that the costs (C) are a function of the fragility (F_R) as follows:

$$0 \le F_R \le 0,2 \rightarrow C = 0,$$
$$0,2 < F_R \rightarrow \overline{C} = \frac{C}{C_{Total}} = \frac{F_r - 0,2}{0,8} \tag{5.49}$$

Then it is possible to determine the cdf of the costs based on the cdf of the fragility. The result is shown in Figure 5.37.

The potential benefits of using the suggested fragility index over the traditional risk measures, *i.e.* probability of failure × total cost, can be readily observed. In the traditional risk framework only one damage state is usually analysed, typically structural collapse. This corresponds to a single value of cost of consequences. With the new proposed methodology several damage states are already included in the fragility index calculation and therefore it is possible to obtain with no added effort additional and important information for a wide range of probable damage states that if not accounted for in the decision-making process could lead to inefficient solutions.
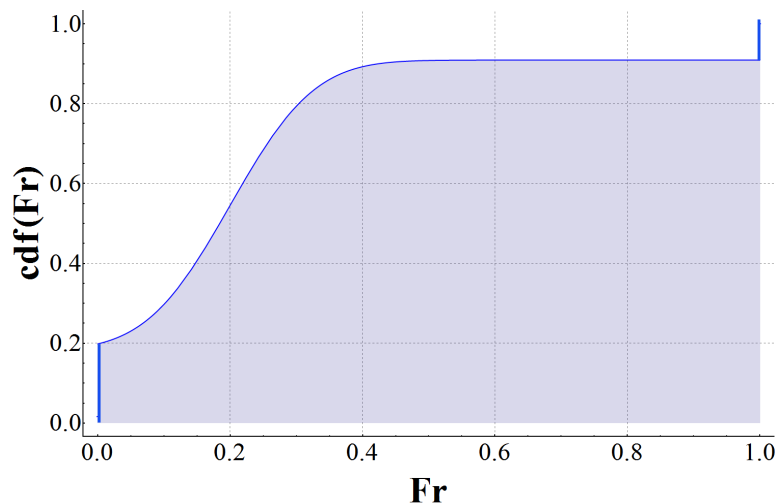
Figure 5.36: Example of fragility cdf.
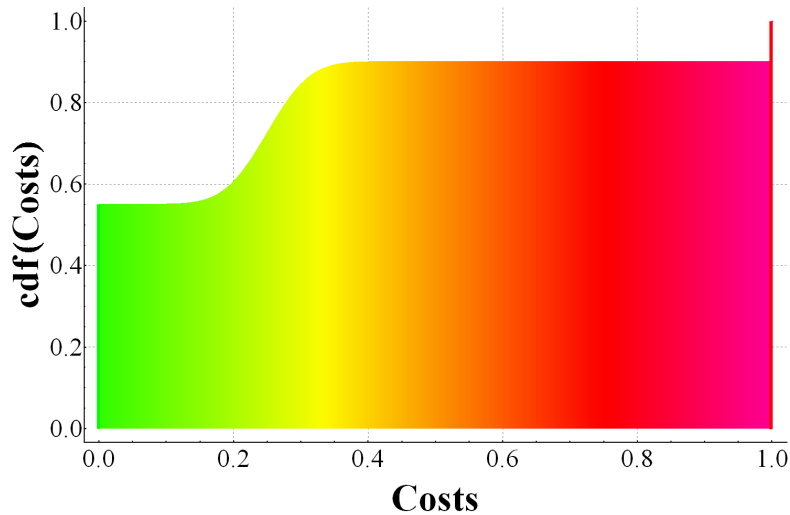
Figure 5.37: Example of damage costs cdf.

Of course, more intricate, complex cost functions can be used depending on the problem. For instance, flag variables can be included in the numerical model so to indicate that a given criterion (structural, *e.g.* nature of damage, or other such as type of operation, *e.g.* number of persons in the affected area) in a certain critical location of the system has been met. Different cost functions can be attributed to each criteria and location, and the overall cost is determined by the sum of all these particular functions. In the limit, a different cost function can be used for each element.

Multiple failure criteria can be used simultaneously, *e.g.* failure is attained when the first criterion is met. As in general, there is not a univocal (single) relationship (function) between the damage costs and the damages intensity (fragility) for every failure criterion a slight change must be considered in deriving the probabilistic models for vulnerability. Instead of determining the probabilistic models for vulnerability based on the probabilistic model for fragility, the vulnerability must be determined for each combination of input values, for which the function between the damage costs and the fragility is known. Having a sample of vulnerability values, or a surrogate model, it is possible to estimate the probabilistic model for vulnerability.

Also, with the new definition of fragility, different possible definitions for failure can be used. If the objective is to analyse a structural system until a damage state other than the complete collapse, for instance to control the rotation of a particular joint, then, as was already mentioned, it is just necessary to assign a fragility index equal to one to that target damage state.

Furthermore, in the existing probability of failure based stochastic design methods it is not straightforward to analyse the sensitivity of the system's probability of failure to a change in the input variables, as well as to perform uncertainty propagation analysis. Consider a structural system to which an acceptable probability of failure was determined using certain input probabilistic models and model parameters. What would happen to the system's probability of failure if these initial hypotheses change? Also, uncertainty may be unevenly distributed across all possible damage states.

In the majority of cases it is not possible to know with appropriate confidence the types of probabilistic models of the input variables and of the distributions parameters, or the degree of dependence/independence between input variables. Knowing that many engineering problems are governed by the extreme values of the input variables, the analyst choices play a crucial role in the follow-up assessment of the results and in the decision-making process. Therefore, uncertainty propagation needs to be considered in the analysis.

The new fragility index gives a direct insight to the consequences of changing the initial hypotheses and if coupled with other tools such as Probability Bounds Analysis (Hayes, 2011) and simulation methods it can also easily incorporate directly the influences of different uncertainties sources.

However, the benefit of using the suggested fragility index reduces in cases where fragility variability is low or in cases where the difference between the values of the reference action corresponding to D_{uc} and to $D_{1st\ failure}$ is low. The former happens when the variability of the reference action values is low (since by definition the system performance must be sensitive to the reference action values). The latter happens for example in systems made of nominal equal elements loaded by a uniformly distributed (reference) action, typically systems with low robustness. An example of such a system are bridge falsework structures when the reference action is considered to be the weight of the concrete: the value of the reference action needed to produce the first element (joint) failure is close to the value of the reference action needed to promote the collapse of the entire structure. In this case, fragility values would be either equal to 0 or equal to 1, with a very small probability of being between 0 and 1.

It is important to emphasise that, in principle, risk in structural engineering can be controlled without structural robustness. This can be readily seen by analysing how risk of consequence X is determined:

$$RISK(X) = P(X|PC) \times P(PC|F \cap H) \times P(F|H) \times P(H) \qquad (5.50)$$

where:

H represents the hazard event;

$P(H)$ represents the probability of occurrence of the hazard event;

$P(F|H)$ represents the conditional probability of occurrence of a local failure given H;

$P(PC|F \cap H)$ represents the conditional probability of occurrence of a progressive collapse (PC) given H and F.

Risk can be controlled:

- At the source, *i.e.* the hazard event, by diminishing its probability of occurrence, P*(H)*, by eliminating the hazard source or by reducing the hazard source, *e.g.* by better control of the application of concrete casting loads, reducing the dynamic load effects and their variability, or by specifying maximum working wind velocities for the assembly and operation phases;

- By diminishing the severity of the hazard, P*(F|H)*: externally by reducing the magnitude of the loads effects, adopting protective barriers outside the structure for example, or internally (structurally) by increasing the structure's resistance and/or reducing the resistance variability of each element of the system (especially in the lower-tail region of the probabilistic distributions). It is also possible to use passive isolation techniques such as base isolation of the structure;

- By managing the consequences of the hazard applying protective (reactive) measures: (i) structurally by increasing the resistance (reliability) and/or the robustness of the structure, *i.e.* by modifying P*(PC|F∩H)*, or (ii) by changing the context (*e.g.* by moving valuable goods, people to safer areas or by installing alarm systems and defining efficient exit routes), *i.e.* by modifying P*(X|PC)*.

The first two measures are preventive (proactive) measures and will increase the system's structural reliability. It is possible to choose a combination of both measures.

It is also necessary to recognise that material properties, geometrical characteristics and actions values vary with time. This fact implies that the behaviour, resistance, reliability, robustness and risk of a structural system changes with time. Therefore, it is important that risk management includes prediction of the risk measures over time: time variant problem. Here, it is beneficial to refine and to update the models with information, new and more accurate, acquired over time.

5.4.7.8 Strategies to enhance structural robustness

Below, some selected examples of strategies to enhance robustness are presented. Robustness is especially important in structures where it is economically unfeasible to adopt measures to (i) reduce the probability of occurrence of the critical events, or to (ii) minimise the structural damages by adopting a higher target reliability level for the critical elements. In such cases damages can be limited instead, by activating secondary load paths and structure redundancy, or using knock-out elements for example. Additionally, it should always be acknowledged that absolute safety against local failure cannot be achieved, and thus in face of unknown future actions, strategies such as increasing resistance of key elements can underperform as the expected safety may not be as high as hoped for.

5.4.7.8.1 Resistance

One way to enhance the robustness of an element or structure is to selectively increase the resistance of some elements, either by increasing the elements strength, or the elements stiffness. The former can be achieved by choosing materials with higher mechanical properties (strength and deformation capacity), while the latter can be attained by adding local or global reinforcements.

In the absence of elastic instability, mechanical properties control the structural resistance of elements and the failure mode of the structural system.

Stiffness is an important property since it provides structural stability. In comparison with a more flexible structure, the structure with a higher stiffness could exhibit a more direct load path if the structural form is properly chosen. Also, second-order effects would be smaller meaning that elements could be subjected to less stresses. Another aspect is the stiffness distribution within the structure. It is well known that structures with abrupt changes in stiffness and irregular structures in general are more vulnerable to hazards.

A usual misconception is to assume that increasing the mechanical properties of all elements will always lead to an increase of the system's robustness. As shown previously this may not be the case. This is also applicable to measures targeting increasing the strength of components upon which the structure's stability depends (*key elements*). More efficient alternative options are available. Examples are the reinforcement of brittle elements in critical load paths, and the strengthening of the beam-column joints.

5.4.7.8.2 Structural integrity

This strategy concerns primarily elements continuity. This can be assured by specifying appropriate levels of tying strength between structural elements to avoid physical separation between elements of the structure. Additionally, integrity relates to soil stability, to avoid collapse due to insufficient resistance of the foundation. Care should be taken to ensure that structural integrity is not dependent on only one (or few) element(s).

5.4.7.8.3 Redundancy

Redundancy means multiple load paths. If an element fails the stresses are transferred to neighbouring elements, the goal being to maintain the overall stability of the structure. However, in order for this strategy to be effective the elements and connections which will be overloaded must possess appropriate strength reserves and ductility. If not, for instance if the elements are brittle then the failure of one element can lead to the progressive collapse of adjacent elements in a domino fashion. Another important thing to bear in consideration is the distribution of redundancy within the structure: critical regions may lack redundancy whereas non-critical regions can be over-redundant.

5.4.7.8.4 Second line of defence

Another strategy is to introduce elements with *second line of defences* (Knoll, Vogel, 2009) on the system, *i.e.* elements with secondary load paths. For example, a slab can resist to vertical loads by bending, but when a central column is removed it behaves as a membrane (catenary action). One should be aware that to activate secondary load paths, the elements, including supporting elements, and their connections must undergo significant deformations, which mean that they need to be ductile enough.

5.4.7.8.5 Ductility

Ductility can be defined as the capacity of one material to continue to resist after yielding by absorbing energy and thus allowing energy to be dissipated in a stable fashion and stresses to be redistributed without significant deterioration of the structure's performance. Material ductility can be achieved by material strain-hardening and/or by material deformation capacity.

Ductility have a relevant rule when designing for robustness, since ductility allows the structure (element) to absorb and dissipate energy in a controlled way, avoiding brittle failures and giving a early warning to users of the structure about the distress of the structure. Additionally, strain-hardening represents a resistance reserve after yielding until the fracture of the material. Ductility is a key material property to enable structural redundancy and second line of defence resistance models.

5.4.7.8.6 Capacity design principles

The principle of capacity design is to avoid energy dissipation mainly by brittle elements. Material ductility, well defined redundancy and wise choice of energy dissipating regions are key aspects to reach this goal. For example: it may be preferable to avoid concentrating maximum stresses on the connection zones where these are made by several components with brittle behaviour.

5.4.7.8.7 Knock-out element

Robustness can also be achieved by limiting the damage to restricted areas. In some structures structural continuity can produce opposite results than the ones expected and contribute to a disproportionate collapse of the system. An example of this behaviour is a structure which was not designed to resist the additional forces redistributed by continuity after an element failure.

Therefore, a possible solution could be to limit the extent of the tolerable collapse progression. To achieve this goal, forces transmitted between elements are eliminated or minimised, by reducing the possible load paths *i.e.* reducing the redundancy of parts of the structure, or by disrupting elements continuity (Starossek, Wolff, 2005). The structure would be made of a series of low robust parts, or with a limited number of low robust parts being the others high robust parts.

In this structural concept, a particular area of the structure would collapse in case of a failure event without damaging the nearby structure. However, the remaining structure must remain in place and operational, possibly under higher loads *e.g.* it could be subjected to impact loads. If not, a domino like progressive collapse of the entire structure could take place.

However appealing, the application of this strategy to bridge falsework structures may be inadequate. Bridge falsework collapses are characterised by a high cost of failure, with or without the, partial or total, collapse of the permanent structure. Restricting damage to a particular location may still however introduce significant deformations to the permanent and temporary structure which could lead to significant repair costs and direct and indirect costs due to delay of the construction. This should be considered in the decision-making process.

5.4.8 Acceptable, tolerable and unacceptable risks

Acceptable risk is defined by the Health and Safety Executive (HSE, 1995) as *"a risk, which for the purposes of life or work, everyone who might be impacted is prepared to accept assuming no changes in*

risk control mechanisms". In turn tolerable risk *"refers to a willingness to live with a risk so as to secure certain benefits and in the confidence that it is being properly controlled. It is a range of risk that we do not regard as negligible or as something we might ignore, but rather as something we need to keep under review and reduce it still further if and as we can".*

The acceptability of risk is affected by many factors such as the nature of the hazard, the exposure level to the risk (voluntary or involuntary risk, short or long periods), the importance of the possible benefits and the scale of the associated consequences (individual and societal risks: who is affected?), the state of knowledge about the risk (known and unknown risks), the individual and societal awareness, degree of control and fear about the hazard, individual and societal moral and ethical values (Sommer et al., 1999 ; Das, 1997).

In general, except for large scale hazards, individual acceptable risks are smaller than societal acceptable risks, especially regarding contained hazard scenarios affecting very few people. Consider the example of a construction worker of a bridge critical to link two villages on each side of a river. The risk of death during the construction of the bridge acceptable to the worker (individual) may be estimated to be smaller than the risk society considers to be acceptable for a death of an individual during the construction of the bridge. This latter risk must be viewed as an average acceptable risk and unevenly distributed: society accepts that risk can be larger for some few people if it is smaller for the majority of people, even if the benefits are not profited at all by that small group of people more exposed, as could be the case of the workers at a bridge under construction. This is in part justified by the completely different ways society and individuals tend to consider the scale of benefits and its redistribution over time periods. While individuals are likely to make their decisions mainly based on short term self-centred benefits, society is more focused on global benefits, is more aware to large scale risks and aims to reach a balance between short and long term benefits.

It is therefore very difficult to assign values to individual acceptable risks or to individual unconditionally unacceptable risks. However, guidance can be found in specialised textbooks concerning dam, nuclear or bridge engineering, or in regulatory reports produced by public institutions. Based on these documents, the value commonly assigned to individual acceptable risk (*i.e.* the broadly acceptable risk limit) ranges from 1 in 10^6 to 10 in 10^6 deaths per year, and to individual unconditionally unacceptable risk (*i.e.* the limit of tolerability) ranges from 100 in 10^6 to 1000 in 10^6 deaths per year, see (ANCOLD, 2003 ; Das, 1997 ; HSE, 1988, 2001 ; UK DfT, 1999).

It is also a very difficult task to define acceptable risks for society. A commonly used approach are *F-N* curves, being *F* the annual probability of exceedance of *N* or more fatalities, see Figure 5.38 for an example. (Vrijling et al., 2004) present a methodology to evaluate societal risks based on *F-N* curves. However, *F-N* curves have some inconsistencies when different risk scenarios are combined, see (Bedford, Cooke, 2001).
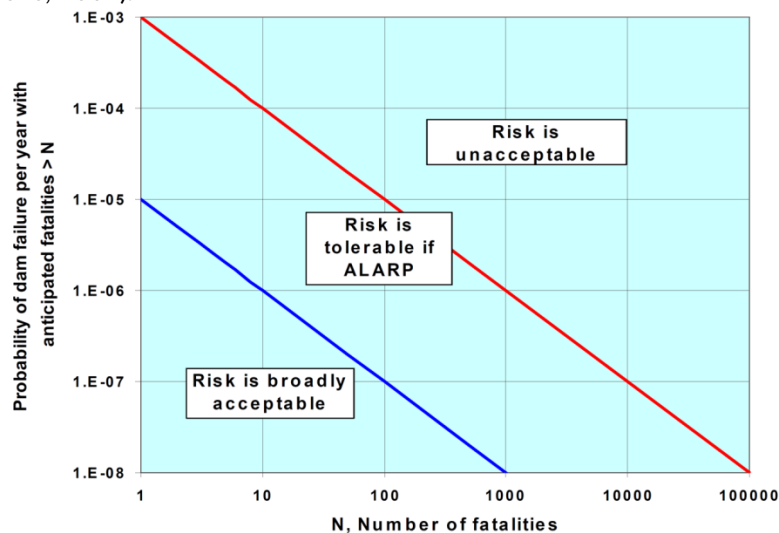
Figure 5.38: Societal risk criteria based on *F-N* curves, taken from (Zielinski, 2008).

Some documents specify formulae to derive the acceptable risk level values. According to ISO 2394 (ISO, 1998) the maximum accepted annual individual risk of death caused by a structural failure, $P(d|f)$, is equal to 1 in 10^4/year. The maximum allowable annual probability of structural failure depends on the conditional probability of a person being killed, given the failure of the structure, and is obtained by equation (5.51).

$$P_f \leq \frac{10^{-6}}{P(d|f)} \qquad (5.51)$$

For societal risks, the criterion is expressed by:

$$P_f \leq A \times N^{-\alpha} \qquad (5.52)$$

where:

N is the expected number of fatalities per year;

A and α are constants: A ranges between 0,01 to 0,1 and α ranges between 1 to 2.

According to EN 1990 (BSI, 2002a, 2004a) a typical bridge is likely to fall into reliability class 2 and therefore an annual probability of failure of 10^{-6} per year is acceptable. Here it should be noted, that Eurocodes do not give recommendations for the target reliability level in accidental design situations. An earlier version of BS EN 1991-1-6 suggested that in absence of quantification of consequences and economical optimisation, a failure probability of 100×10^{-6} per year seems to be appropriate for accidental actions (Gifford, 2004). In an AASHTO Guide for vessel collision design of highway bridges a 100×10^{-6} per year frequency of collapse is indicated for critical bridges and a 1000×10^{-6} per year frequency of collapse is indicated for regular bridges.

In an excellent report published by CIRIA (CIRIA, 1977) it is suggested a method to determine a rational target of probability of failure of civil engineering structures:

$$P_f = \frac{10^{-4}}{n_r} \times K_s \times n_d \qquad (5.53)$$

where P_f is the acceptable probability of failure due to any cause during the design working life (n_d years), n_r is the number of people at risk in the event of failure and K_s is equal to:

- Places of public assembly, dams: K_s = 0,005;
- Domestic, office or trade and industry: K_s = 0,05;
- Bridges: K_s = 0,5;
- Towers, masts offshore structures: K_s = 5.

Another method presented in (McDonald et al., 2005) is expressed by the following formula:

$$P_f = \frac{\beta_i}{P_{d|fi}} \times 10^{-4} \qquad (5.54)$$

where P_f is the acceptable probability of failure due to any cause during the design working life, $P_{d|fi}$ denotes the probability of being killed in the event of an accident and β_i is a policy factor which varies with the degree of voluntariness with which an activity i is undertaken and with the manner the benefit is perceived. It ranges from 100 in the case of complete freedom of choice, to 0,01 in case of an imposed risk without any perceived direct benefits. (Vrijling et al., 1998) proposes the values for β_i given in Table 5.3.

The concepts of acceptable, tolerable, intolerable and unacceptable risks (written in ascending risk order) are used to assess the trade-offs between the importance of expected benefits and the significance of the expected adverse consequences, not forgetting the resources involved.

As (HSE, 2001) emphasises *"tolerable does not mean acceptable"*. Acceptable risk is typically associated with residual risk to life, property or other fundamental values, either because the probabilities of occurrence of the hazards are so small or whose consequences are so slight, whereas tolerable risk is associated with greater risk levels which can be tolerated if certain conditions are met in order to achieve a given set of relevant benefits. In the latter case, the focus is set more on the analysis of the consequences rather than on the computation of the likelihood of the hazards.

When the risks are acceptable, structural reliability can be optimised solely based on economical constraints. However, when the risks are higher than the broadly acceptable risk limit, societal concerns come into play. For the risk to be tolerable the amount of resources used to reach certain desired benefits must guarantee that the level of risk to life and property is not unacceptable and moreover is reduced as reasonably as practicable, what is usually called the "ALARP" principle, see next section. Otherwise risk is classified as intolerable or unacceptable.

Table 5.3: Values for policy factor β_i (Vrijling et al., 1998).

β_i	Voluntariness	Benefit	Example
100	voluntary	direct benefit	mountaineering
10	voluntary	direct benefit	motor biking
1,0	neutral	direct benefit	car driving
0,1	involuntary	some benefit	factory
0,01	involuntary	no benefit	LPG-station

5.4.9 Risk informed decision-making framework

Decision-making is the process of committing resources available today to reach results in the future. Therefore, decision-making involves uncertainties; and risk management is a way of analysing and judging these uncertainties. In order to achieve a rational, correct, efficient and transparent decision-making under uncertainty that maximises the benefits and minimises the losses, several decision support tools can be used. These include the Cost-Benefit Analysis (CBA), the Cost-Effectiveness Analysis (CEA), Utility and Prospect Theories and the Life Quality Index (LQI). Examples of these models can be found in (Bedford, Cooke, 2001 ; McDonald et al., 2005) and in (Nathwani et al., 1997). Additionally, as mentioned earlier, in the UK the ALARP principles need to be taken into account in risk management. It is important to emphasise again that these decision support tools are just that, tools, they do not force a decision. An aid to set up the decision-making criteria is given in (UKOOA, 1999), see Figure 5.39.
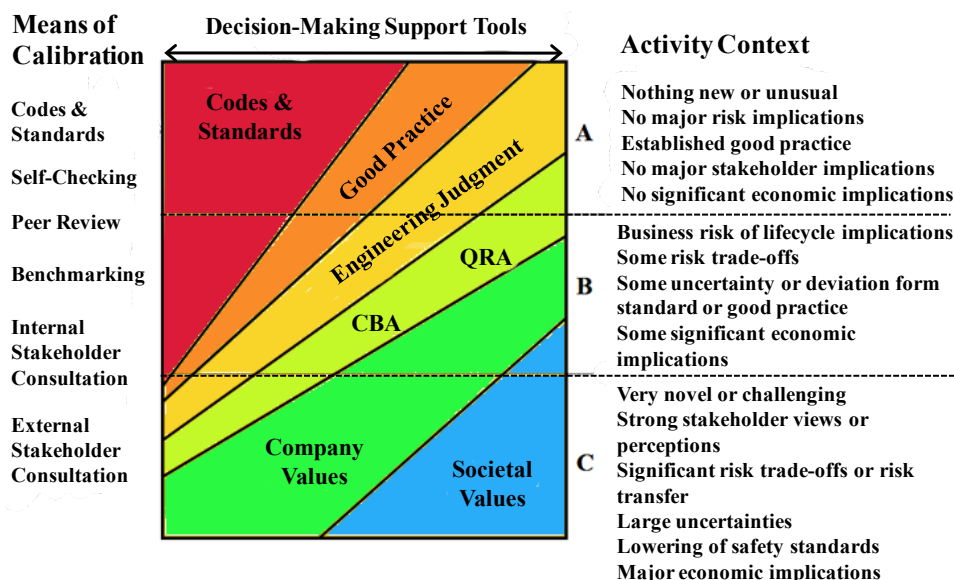
Figure 5.39: Decision-making aid (UKOOA, 1999).

Decision-making should allocate resources efficiently within the context of a given activity, but also in the broader context of society priorities and preferences: how much benefit does it buy, and could the same resource, if directed elsewhere, result in better gain for society as a whole? This is a challenging question with a very difficult answer (if it is possible to give an answer). A way society found to efficiently distribute resources was the development of a general regulatory and normative environment that manages most of human related activities. In this context, acceptable minimum standards of operation are specified. It is, therefore, a requirement that activities, such as bridge construction, follow specific rules and codes of practice to ensure that the benefits for society are greater or equal to the total losses that society may bear.

However, more often than not, risk governance is complicated, see (Berry et al., 2006). Despite the abovementioned society risk neutrality, often public decision-makers assign priorities to activities with a potential for large loss of life in a single event and to activities with the potential for saving a large number of lives. However, it may be argued that this form of decision-making lacks fundamentals. The growing use of CBA, CEA and other methods may be seen as a step forward in this regard. Nevertheless, because decisions are dictated by multiple stakeholders' preferences defined in a specific context it is clear that decisions cannot be determined by solving a more or less complex equation. It is clear that decision-making must move toward a broader consultation with society in order to achieve optimal allocation of resources with ample consensus across society. The lack of active participation of society in the decision-making process is the main reason why some projects did not return the expected benefits and society confidence in the engineering community abilities may be degraded.

A commonly used approach for decision appraisal where different alternatives are compared is to define a baseline scenario. The basic approach is to consider a future scenario without incurring additional costs, the "business as usual" forecast also known as "do-nothing" scenario. If it is considered that the activity must comply with regulatory requirements at all times, then certain future costs such as maintenance costs or upgrade costs should be included: this scenario is often termed "do-minimum".

The potential benefits that come from risk informed decision-making are multiple and wide-ranging (Goodwin, Wright, 2010). For example, the analysis can provide guidance on what new information is worth to gather before a decision is made. For example: is it worth performing more advanced reliability analysis, further testing or measurements? If the cost of obtaining a given additional information is more than the expected benefits (savings, safety, time or other tangible or intangible objectives) which arise from this additional information, then it may not be worth obtaining it. The process of determining whether it is worth obtaining new information is referred to as preposterior analysis or as *value of information* analysis (Goodwin, Wright, 2010).

5.4.9.1 Cost-benefit analysis

According to (Jones-Lee et al., 2008) cost-benefit analysis (CBA) is the welfare economic model that currently provides the normative basis for much of UK public policy. CBA *"seeks to quantify in monetary terms as many of the costs and benefits of a proposal as feasible, including items for which the market does not provide a satisfactory measure of economic value"* (HM Treasury, 2003). In CBA, a proposal should only be implemented if all of its benefits are equal to or greater than all of its costs (Eales et al., 2003). Therefore, among a set of competing alternatives, the preferred option should be the alternative with the highest positive risk adjusted Net Present Value (NPV), including the effect of uncertainties.

In CBA it is necessary to assign a value to costs and benefits. This can be done on the basis of individuals' preferences, namely by using the concepts of willingness to pay (WTP) to obtain a benefit or willingness to accept (WTA) the loss of that benefit. Values of WTP and WTA are usually obtained by examining people's attitudes towards risk, either by observing people's revealed preferences or by

testing their stated preferences, respectively. The latter approach is by and large the preferred in Europe (Spackman et al., 2011). As these values are generally given in market prices, costs must contain indirect taxes (Spackman, Holder, 2007).

As (Bedford, Cooke, 2001) note, there is a significant difference between WTP and WTA. The choice between these two concepts, depends on the weights (preferences) given to innovation and to risk aversion. If the former is preferred then WTP might be used, whereas if the latter is favoured WTA might be used instead.

It should be mentioned that CBA by using WTP, or WTA, as relevant measures of strength of preference, incorporates elements of Utility Theory and of Prospect Theory (see next section). In fact, the *"individual's maximum willingness to pay for a good or service is a clear reflection of what that good or service is worth to the individual relative to other potential objects of expenditure, taking account of the individual's ability to pay – which is, of course, ultimately a reflection of society's overall resource constraint. Obtaining data concerning individuals' maximum willingness to pay for safety is therefore a natural way in which to feed information concerning individual preferences – and, more particularly, strength of preference – into the allocative decision making process"* (Jones-Lee et al., 2008).

Critics of CBA refer that valuing monetarily human, environmental and cultural matters raises ethical issues. Additionally, the methods used in CBA to express losses or benefits to these matters are subject to high uncertainties. There are plenty of past examples where CBA has not been used properly, but it also true that there are many past examples where CBA suggestions have been refused based on environmental and cultural matters but for which today there is a general consensus that the opportunity costs of not having started the suggested activities are very large and are not compensated by the resulting benefits.

In CBA, the concepts of Pareto efficiency and/or Kaldor-Hicks efficiency could be used. An outcome of a given measure is considered Pareto efficient if at least one individual is made better off with no individual being made worse off. A less strict principle is the Kaldor-Hicks efficiency in which an outcome is more efficient if those that are made better off could in principle compensate those that are made worse off (Bellinger, 2007).

The analysis of the optimum level of risk can be formulated as an economic optimisation problem. The investment costs (construction costs, insurance costs, debt payment costs, etc.) are compared with the expected costs of damages, including, maintenance costs, repair/retrofit costs, reconstruction costs, penalties and compensation costs, user costs, etc. Other costs sources such as operation costs (including inspection costs and costs of decommissioning activities) should be considered. The function that relates consequences to costs is termed the cost function. Finally, the benefits from the activity may also be included in the economic optimisation equation, including the infrastructure residual value.

Insurance costs depend on the insurance coverage: (i) Construction All Risks (CAR) policy or (ii) Erection All Risks (EAR) policy. Insurance coverage can also include Delay in Start Up (DSU), Advanced Loss of Profit (ALOP) and Third Party Liability (TPL) policies.

User costs comprise losses related with deferred benefits in terms of travel time, vehicle operating costs and the number of accidents, see (Daniels et al., 1999 ; Imhof, 2004 ; UK DfT, 2011b) but also fatalities/injuries during construction phases. Reconstruction and repair/retrofit costs include material, equipment and labour costs, see (Imhof, 2004). Reconstruction costs also include the demolition costs and supervision and traffic management costs. The latter costs can also be applicable to bridge falsework collapses over an existing road.

The cost function $\kappa(C)$ is given by:

$$\kappa\left(C\right) = C_I + C_{DU} + C_O \tag{5.55}$$

where:

C_I represents the investment costs;

C_{DU} represents the damage and user costs;

C_O represents the operation costs.

In order to compare costs at different times, all values must be adjusted to a reference year prices, multiplying the costs by:

$$\frac{1}{\left(1+r\right)^{\Delta T}} \tag{5.56}$$

where:

r represents the discount rate;

ΔT is given by T_i - T_r, where T_i represents the year of cost i and T_i represents the reference year.

(HM Treasury, 2003) recommends to consider a mean discount rate equal to 3,5% to future costs and cost savings for the first 30 years, and lower values for longer periods, for instance 3,0% up to 75 years and 2,5% up to 125 years. Different values are recommended in (Florio, Maffii, 2008). Careful consideration should be paid when choosing the discount rate value.

Assuming a constant net discount rate, the investment costs are given by:

$$C_I\left(T_r\right) = \frac{1}{\left(1+r\right)^{\Delta T_C}} \times C_C + \sum_{i=0}^{n} \frac{1}{\left(1+r\right)^{\Delta T_{IS,i}}} \times C_{IS,i} + \sum_{j=0}^{m} \frac{1}{\left(1+r\right)^{\Delta T_{DB,j}}} \times C_{DB,j} \tag{5.57}$$

where:

C_C represents the construction costs, including material, equipment, labour costs and possible penalties costs;

$C_{IS,i}$ represents the insurance costs at year i;

$C_{DB,j}$ represents the debt payment costs at year j, which is given by the interest rate paid at year j times the initial borrowed capital.

The damage costs are given by:

$$C_{DU}\left(T_r\right) = \sum_{i=0}^{n} \frac{1}{\left(1+r\right)^{\Delta T_{D,i}}} \times \left[C_{SD,i} + C_{P+C,i} + C_{U,i}\right] \tag{5.58}$$

where:

$C_{SD,i}$ represents the costs associated with structural damages at year i. The structural damages at each year are derived from the probabilistic distribution of the structural fragility. Maintenance costs are associated with low levels of damage whereas repair/retrofit costs are associated with medium levels of damage and reconstruction costs are associated with high levels of damage;

$C_{P+C,i}$ represents the penalties and compensations costs at year i. These penalties costs will occur if the construction deadlines are not met due to damages or when the level of service provided is less than required under the contract, for example, whereas compensation costs include payment of fees for injuries and fatalities or for environmental damages;

$C_{U,i}$ represents the user costs at year i, which is given by equation (5.59) (Imhof, 2004):

$$\begin{aligned}
C_U &= \left(VOC + TTC + AC\right) \times t \\
VOC &= AADT \times VOC_u \times L_d \\
TTC &= \frac{g_{day} \times L_d \times n_p \times AADT}{V} \\
AC &= \left(AR \times L_d + N_W\right) \times VPF
\end{aligned} \tag{5.59}$$

where:

VOC represents the vehicle operating costs;

TTC represents the travel time costs;

AC represents the accidents costs;

AADT represents the annual average daily traffic on original route, given in (UK DfT, 2011b) for example;

VOCu represents the Unit vehicle operating costs, given in (UK DfT, 2011b) for example;

L_d represents the additional length of the detour route;

g_{day} represents the GDP per capita per day;

n_p represents the average number of people per vehicle, given in (UK DfT, 2011b) for example;

V represents the average velocity of vehicles;

AR represents the accident rate on original route (fatalities per kilometre per day);

N_W represents the number of workers and users injured or dead in the course of construction works (fatalities per day).

The operation costs are given by:

$$C_O\left(T_r\right) = \sum_{i=0}^{n} \frac{1}{\left(1+r\right)^{\Delta T_{I,i}}} \times C_{I,i} + \sum_{j=0}^{m} \frac{1}{\left(1+r\right)^{\Delta T_{OO,j}}} \times C_{OO,j} \tag{5.60}$$

where:

$C_{I,i}$ represents the inspection costs at year *i*;

$C_{OO,j}$ represents other operational costs at year *j*.

The benefits, B, are given by:

$$B\left(T_r\right) = \sum_{i=0}^{n} \frac{1}{\left(1+r\right)^{\Delta T_{HL,i}}} \times B_{HL,i} + \sum_{j=0}^{m} \frac{1}{\left(1+r\right)^{\Delta T_{OB,j}}} \times C_{OB,j} \tag{5.61}$$

where:

$B_{HL,i}$ represents the benefits due to human lives saved at year *i*.;

$B_{OB,j}$ represents other benefits at year *j*.

These values should be updated with the growth of the GDP per capita per year.

The optimisation problem can now be defined as:

$$\arg\ \max\ f\left(T\right) = B\left(T\right) - \kappa\left(T\right) \tag{5.62}$$

Several constraints will need to be included such as those specified in the previous section. Solving this optimisation problem is complex since it requires running a time variant problem or multiple time invariant problems. A simple comparison of the average values of the benefits and costs may not be sufficient and considerable intolerable risks may eventually end up being tolerated where otherwise an analysis taking full account of the probabilistic distributions could produce very different outcomes. Uncertainty propagation should also be considered.

A simplification is to consider the benefits as constant in all alternatives. The validity of this hypothesis must be checked before being used. When it holds acceptable, the decision problem is made easier (see next section for details).

5.4.9.2 Other methods

In contrast to CBA, in Cost-Effectiveness Analysis (CEA), the benefits do not have to be expressed in monetary terms. Limitations of CEA are given in (House of Lords, 2006 ; Spackman et al., 2011).

When not all decision variables are expressed in the same units, such as in CEA, a useful tool to compare several efficient choices in a multi-criteria decision-making framework is to develop Pareto sets or to use Utility Theory. Utility (von Neumann, Morgenstern, 1944) is a measure of stakeholder satisfaction. A utility function should incorporate all relevant decision criteria, including the various constraints (rationality requirements), express the hierarchy of objectives and preference ordering, and finally the trade-offs between different criteria and uncertainties. For example: for an investor the utility function could have only two variables, the expected return of the portfolio and the associated risk. Thus, the decision-making problem is to maximise the expected return of the portfolio and minimise the corresponding risk. Utility Theory is appealing but it may be difficult to determine consistent utility functions and also utility theory has its own limitations as clearly evidenced by the Allais's paradox (Goodwin, Wright, 2010), see also (Kahneman, Tversky, 1979). As a final remark, if the utility function is linear, meaning a risk neutral attitude as for example society attitude towards fatalities, then Utility Theory will return the same results obtained by a cost-benefit analysis.

As an answer to the limitations of Utility Theory, the Cumulative Prospect Theory (CPT) was developed, see (Tversky, Kahneman, 1992). This theory suggests that people make decisions based on a reference context and value gains and losses from this reference point rather than absolute wealth considerations. Also, it is postulated that people are risk seeking towards high probability losses and towards low probability gains but risk averse towards high probability gains and towards low probability losses. Nevertheless, several questions have also been raised regarding the adequacy of CPT to decision-making problems, see (Birnbaum, 2008 ; Goda, Hong, 2008 ; Nwogugu, 2006).

Classical decision support tools are the maxmini, minimax criteria, however they have a number of limitations see (Goodwin, Wright, 2010 ; Levy, 2006). Other methods include the first and second-degree stochastic dominance to compare cdfs of different alternatives (Goodwin, Wright, 2010 ; Levy, 2006).

Another tool was presented by (Schneider, 2006), where alternative risk measures are ordered by the so-called "rescue cost" (RC_M) which is given by the ratio between the safety costs of the measure and the variation of risk achieved determined in relation to a reference state. The smaller the value of RC_M the more efficient is the measure.

As a final example, (Nathwani et al., 1997) developed the LQI method. They consider that the maximisation of healthful life for all is the proper basis for managing risk in the public interest, and this criterion is considered *"achieved when the net contribution to the total saving of life from the wealth produced is balanced against the loss of life from the risk of operation"*. The LQI method is expressed by:

$$LQI = g^w \times e^{(1-w)} \tag{5.63}$$

where g represents the personal income (GDP per capita), e is the national life expectancy and w is the national average working time. See (Nathwani et al., 1997) for details.

Developments of the LQI to decision-making are given in (Ditlevsen, Friis-Hansen, 2005 ; Rackwitz, 2004 ; Vrijling et al., 2004). Limitations of LQI method, similar to CEA, are given in (House of Lords, 2006 ; Jones-Lee et al., 2008 ; Spackman et al., 2011 ; Spackman, 2009). Namely, it is argued that *"the method is too simplistic to be a competitor to the methods now established in the UK and elsewhere for the valuation of fatality risks"* (Spackman, 2009). For example, the LQI method is based on historic economic data, but society expectations and preferences regarding the future can be quite different from past situations. Other doubts relate to philosophical issues of conditioning human preferences mainly to economic data which society cannot control completely and therefore may not represent true human preferences.

5.4.9.3 The ALARP principle

The ALARP principle, see Figure 5.40, reject the simplistic and non-dynamic idea that there can only be two possibilities in the end of risk assessment: the risk is either (i) acceptable or (ii) unacceptable. It enforces the consideration of an intermediate region in which risks could be tolerated in order to gain benefits (Rimington et al., 2003).
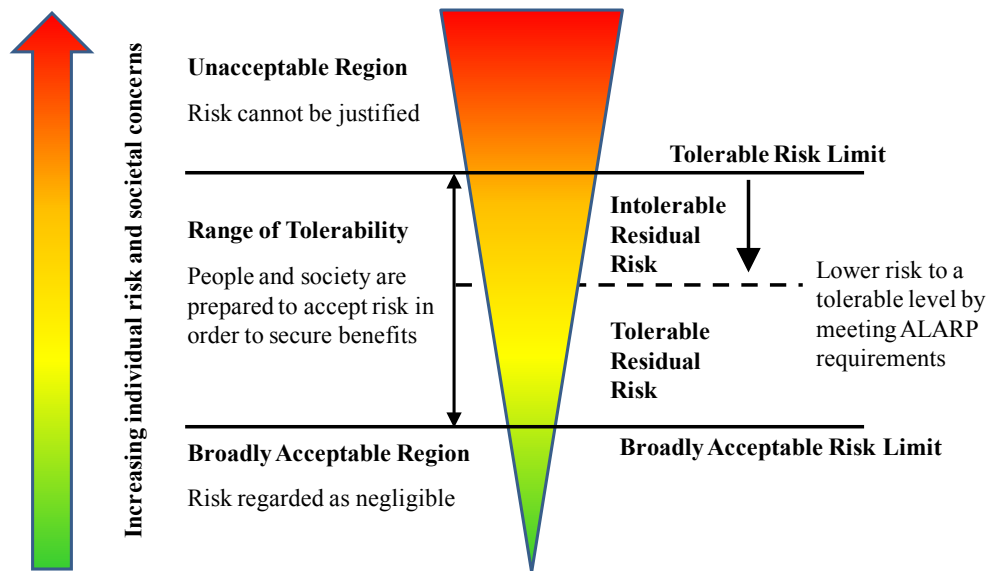
Figure 5.40: ALARP principle, adapted from (ANCOLD, 2003).

In general, the application of the ALARP principle involves three essential requirements. The first relates to the cost effectiveness of a solution and can be determined by a Cost-Benefit Analysis (CBA), comparing for example the Cost of Preventing a Fatality (CPF) with the accepted Value of Preventing a Fatality (VPF). The second corresponds to the assessment of the disproportionality of a solution and can be evaluated by comparing the CPF with the VPF multiplied by a proportion factor. The third requirement is related with the quality of the analysis and the competence of the analysts, the level of uncertainty attached to the options, the effectiveness of the risk treatment measures and also the time feasibility, *i.e.* the time available and the time necessary to implement alternative options.

As seen in a previous section, these three requirements are necessary but not necessarily sufficient to make a risk informed decision, for instance to consider a risk level tolerable. During the decision-making process they will weight, but also the significance of the benefits *vs.* the significance of the adverse consequences, the consideration of state-of-the-art technology and of existing good practice, as well as sustainability, political, societal, equity, moral, ethical and other intangible matters will be considered. See (HSE, 2001) for an in-depth analysis.

For less risky activities, *i.e.* corresponding to a risk level near the acceptable risk level, one may not reduce the risk further if it is demonstrated that it is not cost effective. Nonetheless, the implementation of monitoring and control measures is enforced, especially when the nature, scale and the likelihood of the hazards are extremely uncertain. For activities with a higher risk level, just below the limit of tolerability, as the consequences are so severe, or so uncertain, the precautionary principle stipulates the need to reduce the risk level, even if it is by a very small amount. If not the risk should be classified has intolerable unless it can be demonstrated (i) that the costs of the additional risk reduction solutions are in gross disproportion with the amount of risk averted, but also (ii) that the expected benefits to society are of such fundamental importance so to justify the increase of risk exposure and the associated expected adverse consequences, (iii) that the risks are distributed equitatively and (iv) that relevant good practice is followed; or it must be demonstrated that ALARP principle is not applicable or it is overly conservative. In short, the higher the risk the more biased is the decision-making methodology towards health and safety, and more stringent measures to reduce the risks are required.

The value of CPF is determined by dividing the total final cost with the total number of fatalities prevented. The cost of a solution is disproportionate to its benefits if the following criterion is not met:

$$\frac{CPF}{VPF} \geq F \tag{5.64}$$

where F is a proportion factor which increases proportionally with the increase of the risk level, to provide a higher margin of safety, and is in the range of two (one) to ten (HSE, 2009a) for typical problems where ALARP principles must be used.

(ANCOLD, 2003) presents tentative monetary values for which the justification of the ALARP principle varies from strong to poor. It is the opinion of some economists, see (Viscusi, Gayer, 2002), that demanding safety improvements corresponding to CPF values higher than a certain amount will result in a net harm to society by drawing resources away from more cost-effective improvements to health and safety.

VPF values can be related with Willingness to Pay (WTP) values by equation (5.65). However, other relations have been published see (Spackman et al., 2011). An alternative approach to obtain the value of VPF is the Life Quality Index (LQI) approach (Nathwani et al., 1997).

$$VPF = \frac{WTP}{\text{risk reduction}} \tag{5.65}$$

VPF is often misunderstood to mean that a value is being placed on a life. This is not the case. It is simply another way of saying what people are prepared to pay to secure a certain averaged risk reduction. For example, a VPF of £1 million corresponds to a reduction in risk of one in 100 000 being worth about £10 to an average individual (HSE, 2001).

Several methods have been presented in the literature to determine the value of VPF. The values recommended by the various experts are widely different: from less than 1 million € to over 10 million €, see (Chilton et al., 1998 ; Cropper, Sussman, 1990 ; Le Guen, 2008 ; U.S. DOT, 2009 ; Viscusi, Aldy, 2003 ; Viscusi, 1993) and Figure 5.41. In the UK, the Department for Transport (DfT) publishes the value of VPF. The latest value is equal to £1 585 510, at 2009 prices. Figure 5.42 shows the evolution of the value of VPF in the UK over the years. According to (UK DfT, 2011a), future values of VPF can be obtained by multiplying the present values by a factor equal to:

$$1 + \frac{\text{\% increase in nominal GDP per capita}}{100} \tag{5.66}$$

	VPF (PPP adjusted) 2008\$	GDP per head (PPP) 2008\$	VPF/GDP per head	(VPF/GDP per head)/ UK value
Austria	3.17	36,617	87	1.20
Belgium*	6.31	33,997	186	2.61
Canada	3.95	39,950	99	1.39
Denmark	1.4	36,362	38	0.54
France	1.26	29,936	42	0.59
Germany	1.36	31,310	43	0.61
Netherlands	2.84	34,760	82	1.15
New Zealand	2.11	26,651	79	1.11
Norway	3.62	57,524	63	0.88
Singapore	1.26	33,767	37	0.52
Sweden	2.41	36,618	66	0.92
U.K.	2.59	36,362	71	1
U.S.A.	5.8	47,186	123	1.73

*The value for Belgium is not an official value

Figure 5.41: Comparison of international values of VPF divided by GDP per head (Spackman et al., 2011).
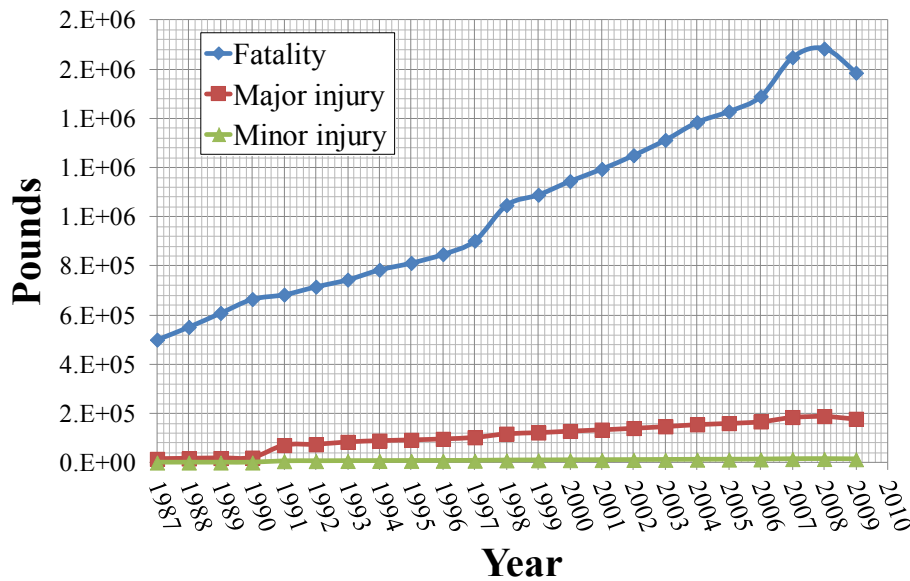
Figure 5.42: UK's official values of preventing a road fatality, major injury and minor injury: 1987-2009, £ at 2011 prices (Spackman et al., 2011).

A question can also be raised concerning the treatment of injuries (major and minor). Documents from UK public institutions such as HSE, DETR, DfT, Highways Agency and the Railways Inspectorate indicate the following weights: VPF ≅ 10 major Injuries ≅ 200 minor Injuries, see Table 5.4. In comparison, (Viscusi, Aldy, 2003) showed that the majority of the existing research considered one injury in the range of $20,000–$70,000. Other interesting data is reported by (Steven, 2010). In this study approximately 2 million accidents in the USA were analysed. This research showed that for every major injury there can be as many as 10 causing minor injury, 30 causing property damage and 600 near misses that resulted in neither injury nor damage.

Table 5.4: Injury classification, weights and values (UK DfT, 2011a).

Injury	Description	Weight	Average value, £ June 09
Fatality	Fatality within one year of the causal accident	1,0	1 585 510
Major injury	An injury as defined in schedule 1 of RIDDOR 1995, or where the injury resulted in hospital attendance for more than 24 hours	0,1	158 551
Reportable minor injury	For workforce, any injury resulting in more than 3 days off work, which is not a major injury. For passengers and members of the public, any injury that leads to a person being taken from the site of the accident to hospital for treatment, which is not a major injury	0,005	7 928
Non-reportable minor injury	Any other physical injury that is not a fatality, major or reportable minor injury	0,001	1 586
Class 1 shock/trauma injury	Shock/trauma injuries due to witnessing all fatal incidents, attempted suicides, passengers struck by trains, train accidents (except "Collision of train with object on line (not resulting in derailment)")	0,005	7 928
Class 2 shock/trauma injury	Shock/trauma injuries due to physical and verbal assaults, witnessing non-fatal incidents of near misses, assaults, trespasser and workers struck by train, and all other miscellaneous events	0,001	1 586

5.5 Conclusions

In this Chapter, new robustness and fragility indices were presented and formed the basis of a risk management framework. This new methodology is applicable, in principle, to all structural analyses not only those concerning bridge falsework systems. This Chapter gave a complete insight to the risk management framework, from the principles of risk and a general layout of the risk management framework, to the methods and procedures to be used to determine robustness, fragility and

vulnerability, including guidance on how to address them from an economic cost-benefit point of view in order to achieve rational decisions in civil engineering.

The main advantages of this new definition of robustness in relation to the existing definitions are:

- Structural robustness, structural resistance, reliability and risk are four different concepts. The existing robustness definitions mixed these concepts which made the analysis, interpretation and evaluation of the former variables difficult tasks. Furthermore, by coupling in the same definition four different concepts the benefits of determining the robustness was not clear. The present definition makes robustness a property than can be measured independently of the system's resistance, reliability and risk. Structural robustness can for the first time be considered an independent requirement for the structural performance of civil engineering infrastructures. Together with the structural resistance and reliability they become two powerful tools that can and should be used in the risk management of civil engineering infrastructures;

- The second advantage is that for the first time, progressive and disproportionate collapse analysis is clearly defined as a requirement not only for unforeseen and accidental situations affecting localised areas of a given structure, but also for normal service conditions covering for instance design cases where the permanent load is the dominant action.

An explicit expression to determine the robustness index was given based on the concept of damage energy and representative illustration examples were presented.

The fragility index was developed as a tool to assess the system's structural damages for a given action combination. Using this measure it is possible to perform progressive collapse analysis and also evaluate the sensitivity of damage accumulation to action values, which may be important when performing risk analysis.

In general, traditional structural risk analyses focus on probability of failure. These analyses are quite limited since they do not account for the various damage states that might occur (damage is a continuous function) but that do not directly imply the global collapse of the structure. Therefore, valuable information is lost that could be used during the risk informed decision-making process potentially leading to inefficient solutions. For instance, two structural systems *A* and *B* can have the same probability of failure but the damage evolution in *A* can be quite different than in *B*.

As a conclusion, the newly developed robustness index can be used as a design option to reduce the structural risk and the newly developed fragility index is an analysis tool that should be used to assess the structural risk.

Finally, the risk framework presents several advantages over traditional engineering methods which make it a useful tool to properly consider the effects of uncertainties in the safety of future and in-service infrastructures, such as bridge falsework systems:

- Risk management allows increased confidence in achieving the desired outcomes;

- Risk management is applicable to existing and new structures, standard and innovative structures, low risk and high risk activities;

- In risk management the idea of being possible to completely avoid risk by following code rules and good practice is abandoned: estimated risks are evaluated against established risk criteria, from which risks are classified as acceptable, as tolerable, as intolerable or as unacceptable;

- Risk management encompasses a holistic assessment of the system's structural performance and reliability: starting with the definition of the system context and exposure conditions, followed by the identification of the relevant hazard scenarios (environmental and human made) and their subsequent qualitative and/or quantitative risk analysis evaluating their probability of occurrence and considering not only the structural damages but also the associated economical, social and environmental consequences;

- Risk management includes whole-life cycle considerations and encourages continuous improvements: throughout the entire lifetime of the structure, risks must be kept under control, reviewed, and reduced as soon as reasonably possible. Therefore inspection, monitoring, control and maintenance requirements are included in the analysis;

- Explicit and transparent consideration of uncertainties in the risk analysis process, with the chance of including newly gained information;

- Risk informed decision-making focus on relating performance levels to consequences: the most cost-efficient solutions to reduce risks and increase benefits are selected, which could demand the adoption of solutions which use state-of-the art technology, thus representing improvements regarding established good practice benchmarks. Existing good practice is considered as a baseline requirement; the aim is to promote best practice benchmarks (Rimington et al., 2003);

- Decisions are made based on a rational multivariable optimal decision-making process: individual and societal, economy and safety issues.

However, it is also necessary to acknowledge that risk informed decision-making has limitations at the present time. The key limitations are:

- Nonexistent, or incomplete, statistical databases needed to define probabilistic models of hazard scenarios;

- Absence of a common framework for the definition of acceptable and tolerable risk levels;

- Risk informed decision-making does not guarantee the achievement of an optimal solution because it is based on the preferences and judgments made during the course of the analysis.

Research to reduce or overcome these limitations is an important requirement to justify, and promote, the use of risk informed decision-making methods for structures. In Chapter 6, the first two problems will be addressed in detail for the particular case of bridge falsework systems.

6

APPLICATION OF THE PROPOSED STRUCTURAL DESIGN METHODOLOGY TO BRIDGE FALSEWORK SYSTEMS

6.1 Introduction

The context of the use of bridge falsework is based on a decision to build a bridge included in the national, or local, transport infrastructure network: road, highway or railway, see Figure 6.1. This decision, of building the infrastructure, is based on the potential benefits for the society in the near future and in the long-term, for example economic benefits and user benefits. As in every project the construction of a bridge is bounded by several constraints of various sources: (i) societal and cultural, (ii) financial and economical, (iii) political and (iv) environmental for example.
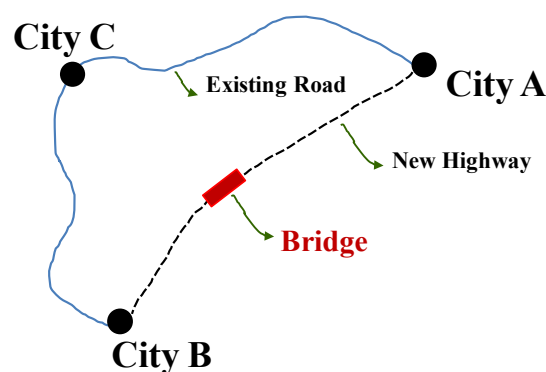
Figure 6.1: Context of a bridge construction.

Every bridge falsework project should therefore be developed considering a risk framework illustrated, such as the one presented in Figure 6.2. The efficient, safe and durable use of a particular bridge falsework depends on the specific requirements and features of each transport infrastructure project, and of course of each bridge project. The requirements placed upon a given bridge falsework solution can lead to a structural system 30 m high, with complex 3-D geometry, an assembly of thousands of slender steel elements over soft soils, requiring multiple assembly/dismantling cycles and being exposed to several hazards, natural and man-made, for six months or more. In general, bridge falsework elements have a design working life much larger than

the duration of one single bridge project. Typically these elements with good quality control and maintenance procedures can be continuously used for 15 or more years.
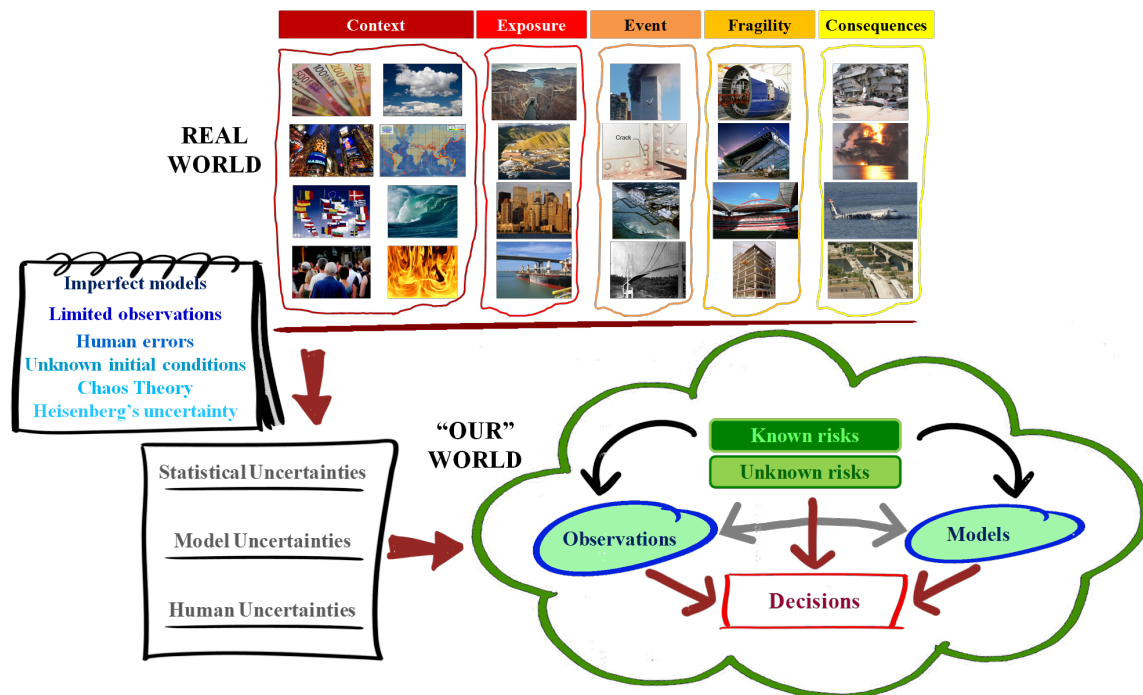
Figure 6.2: Framework for the design of bridge falsework.

In Chapter 2 of the present Thesis, bridge falsework was discussed and a comprehensive overview of the most important hazards and of their initiating events was also given. In the present Chapter, the risk management methodology presented in Chapter 5 will be applied to bridge falsework systems. First, formal risk identification methods will be employed, followed by the use of rigorous methods for the estimation of suitable risk measures. After, these risks will be evaluated against proper risk criteria and alternatives for risk control will be analysed and discussed in a risk informed decision-making framework. Two scenarios will be defined: a "do-nothing" scenario and a "do-something" scenario. The objectives of this investigation are to reduce the existing risks to as low as reasonably practicable by broadly accepted, rational and efficient risk treatment measures. Figure 6.3 presents the selected risk informed decision-making framework.

This investigation will include identification of the relevant risks for the safety of the structure and the critical failure modes during assembly, operation and QC/QA (quality control/quality assurance) phases of a bridge falsework project. The risks to workers and users not deriving from structural damages will not be included in the analysis. Therefore, risks to workers from falling at height or risks to workers or users from falling objects will not be considered. Risks related exclusively with the formwork system and with the superstructure (bridge) will also not be considered.

This investigation will focus on Cuplok® bridge falsework. The information presented in the previous Chapters, namely (i) the data presented in Chapter 3 obtained from tests on several types of joints will be used during the analysis, (ii) the numerical procedures outlined in Chapters 3 and 5, as well as (iii) relevant bibliographic information regarding loads during bridge construction. Where information is not available, for instance concerning the number of workers and the user costs due to a bridge falsework collapse, general hypothesis and expert judgement will be used. It is believed that the effects of the expert judgements limitations, in the development and on the conclusions of the investigation are uniform and therefore will not invalidate the results.
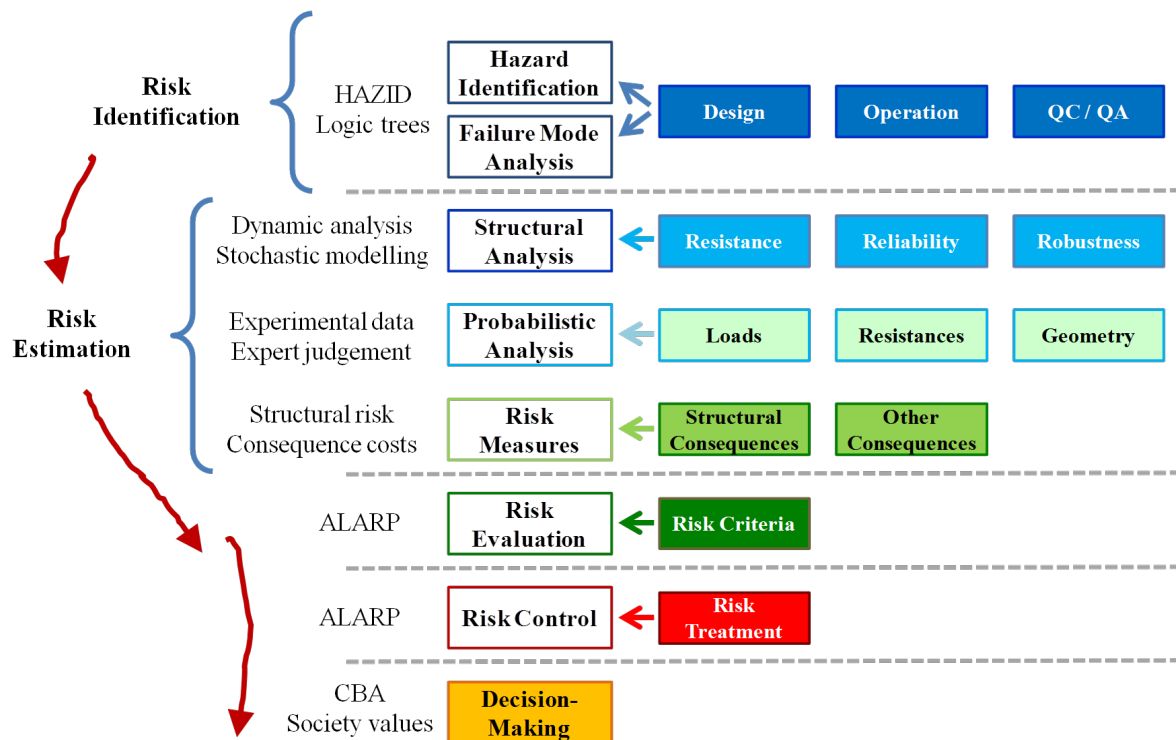
Figure 6.3: Selected risk informed decision-making framework.

6.2 Justification

Why is it necessary to apply risk management to bridge falsework systems? It was already shown in Chapter 2 that almost 20% of the total number of bridge collapses, total or partial, are due to the failure of the bridge falsework solution. Furthermore, the total costs of the consequences of a bridge falsework collapse can outweigh the direct costs of reconstruction of the bridge, namely because of the costs associated with loss of human lives, the user costs together and with the sustainability costs. In addition, the potential benefits of a risk informed decision-making methodology were already listed, where the advantages over the traditional design methods have been clearly highlighted. Yet, are these factors enough to justify undertaking a complex risk management methodology? Are the existing risks acceptable?

In order to answer these important questions, estimates of risks to individuals, and of structural risks, are presented, respectively the Individual Risk Per Annum (IRPA), *i.e.* the annual probability of a fatal accident during the construction of a bridge using bridge falsework systems and the annual probability of structural failure of bridge falsework systems. See also (André et al., 2012b).

These variables are calculated based on the survey presented in Chapter 2 about bridge falsework collapses since 1970 in 19 countries. Note that the two collapses recorded in the survey for the UAE occurred in the Emirate of Dubai. The values presented below correspond to notional estimates since they are based on a necessarily limited sample, and therefore are subject to uncertainties. The methodology adopted can only provide an estimate of the average of individual and structural risk, since it is determined from a sample of heterogeneous data in terms of: (i) design standards used (*e.g.* target reliability levels), (ii) context and exposure characteristics, (iii) modes of failure and procedural, enabling and triggering events and (iv) types of bridge falsework systems. Therefore, they should only be interpreted in a comparative sense and not taken as the actual values.

In the absence of information, the risk measures were obtained considering the following assumptions (assumed conservative):

- 60% of the concrete bridges and viaducts were built using bridge falsework systems;

- 80% (in the case of developed countries) and 90% (in the case of developing countries) of the existing concrete bridges were built after 1970;

- The average number of persons exposed to the risk of collapse of the bridge falsework structure was determined based on the number of reported fatalities and injuries, considering a minimum number of 40 persons (in the case of developed countries) and a maximum number of 100 persons (in the case of developing countries) at risk in each falsework structure.

Using these assumptions and the data presented in Table 6.1, the value of IRPA is obtained by:

$$IRPA = \frac{\text{Number of fatalities}}{\text{Number of persons at risk}}$$ (6.1)

**Table 6.1: Summary of data used to calculate
risk estimates for bridge falsework systems in 19 countries since 1970.**

Country	Accidents	Fatalities	Injuries	Number of bridges (a)	Reference (accessed on 15-02-13)	Persons at risk (b)
Andorra	1	5	6	200 (c)		40
Australia	1	0	15	20368	(Court et al., 2005)	50
Austria	1	2	0	12942	http://cost345.zag.si/ and http://www.sustainablebridges.net/	40
Brazil	2	32	40	2700	(Mendes, 2009)	100
Canada	3	7	16	17280	(Hammad et al., 2007)	40
Czech Republic	1	7	67	6633	http://cost345.zag.si/ and http://www.sustainablebridges.net/	60
China	8	98	118	43200	(Wang et al., 2011)	100
Denmark	2	1	5	6152	http://cost345.zag.si/ and http://www.sustainablebridges.net/	40
Germany	19	19	42	31762	http://cost345.zag.si/ and http://www.sustainablebridges.net/	40
India	3	53	24	10044	http://www.pib.nic.in/	100
Indonesia	1	4	19	2000 (c)		80
Japan	1	4	14	27938	(Nishikawa, 2009)	60
New Zealand	1	0	0	7376	http://www.kiwirail.co.nz and http://www.nzta.govt.nz	40
Portugal	7	10	38	2352	www.refer.pt and http://www.estradasdeportugal.pt/	40
South Africa	1	2	20	3840	http://www.nra.co.za	80
UAE	2	7	29	1021	www.rta.ae/	100
UK	1	3	10	21833	http://cost345.zag.si/ and http://www.sustainablebridges.net/	40
USA	17	24	72	113400	(Balafas, Burgoyne, 2004)	60
Vietnam	1	60	80	500 (c)		100
Total	**73**	**338**	**615**			

(a) Number of concrete bridges built after 1970 using the bridge falsework construction method
(b) Average number of workers exposed to the risk of collapse of the bridge falsework structure.
(c) Estimated

The data presented in Table 6.1 corresponds to the complete information collected in each country since 1970 (until 2012). Since data relative to the number of bridges built each year in each country analysed is not available, an average value of IRPA in the last 42 years was determined for

each country considering the total number of reported fatalities and the total number of persons exposed to the risk of collapse of a bridge falsework structure. The latter is given by the product of the total number of concrete bridges built using these systems with the average number of persons exposed to the risk of collapse of the bridge falsework structure.

Figure 6.4 illustrates the IRPA values for 19 countries. It can be observed that in four countries (Andorra, Brazil, Portugal and Vietnam), there is an estimated chance of at least 100 in 10^6 of a fatal accident per year for this bridge construction method, which is much higher than the one registered in UK for the construction sector which is 24 in 10^6, 2008/2009 figures (HSE, 2009b) – which represents a significant improvement following the high rate of 59 in 10^6 registered in 2000/2001 (HSE, 2001). On the other hand, the fatal accident rate for bridge falsework systems is similar to the one observed in the construction sector in Portugal and in the US (CPWR, 2008 ; Eurostat, 2012).
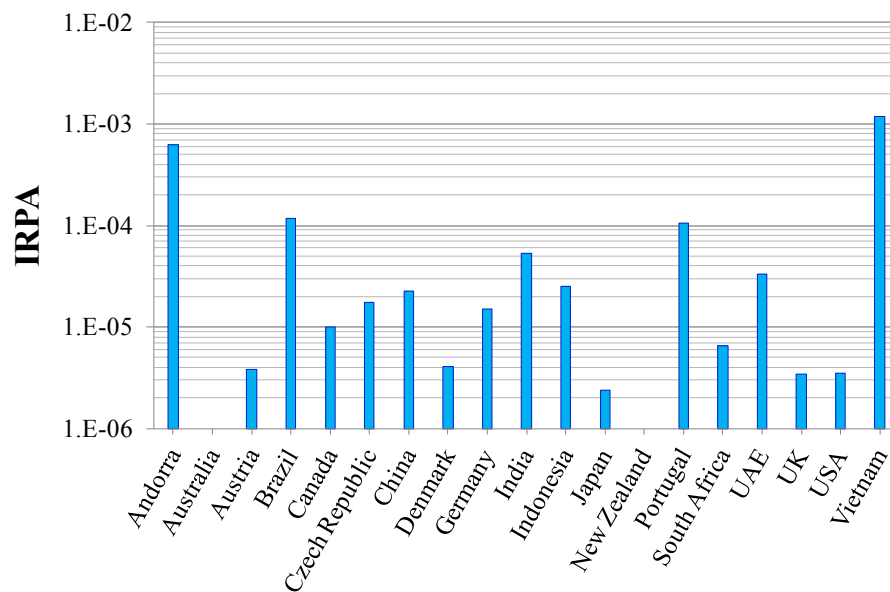
Figure 6.4: IRPA values for the 19 countries considered in the survey.

The results obtained from the survey carried out can be considered conservative because it is very likely that there are a number of unreported accidents with bridge falsework systems. This fact makes the recorded number of collapses and, possibly, the number of fatalities, a lower boundary.

It can be considered, with confidence, that the relative effect, in the IRPA values, of the uncertainties associated with the assumptions used to determine the total number of workers at risk (involving the number of bridges built each year and the number of workers involved in the casting operations), is lower than the relative effect of the uncertainties associated with the total number of accidents that happened in each of the 19 countries for the time period considered in the analysis.

Comparing the value for the individual risk obtained for bridge falsework systems with the limits presented in Chapter 5 for the acceptable and unacceptable annual risk levels, it can be concluded that in all countries included in the analysis, except Australia and New Zealand where no fatal injury was reported, the individual risk is higher than the broadly acceptable risk level (taken as 1 in 10^6 fatalities per year) and that in all countries, except Vietnam, the individual risk is lower than the unacceptable risk level (taken as 1000 in 10^6 fatalities per year). Therefore, the individual risk for bridge falsework systems is in general within the risk tolerability zone and must be ALARP.

The data presented in Table 6.1 can also be used to estimate the annual probability of failure, $P_{f,1}$, of a bridge falsework system, which can be obtained by equation (6.2). The results are presented in Figure 6.5. As for the IRPA, the annual probability of failure was determined considering the total number of failures and the total number of concrete bridges built using bridge falsework systems in each country since 1970.

$$P_{f,1} = \frac{\text{Number of failures}}{\text{Number of concrete bridges}} \qquad (6.2)$$

Using the method presented in the CIRIA report (CIRIA, 1977), see Chapter 5, a value for the acceptable annual probability of failure of the bridge falsework equal to 1×10^{-6} is obtained, considering $K_s = 0,5$ and $n_r = 50$, or $2,5\times10^{-6}$, considering $K_s = 0,5$ and $n_r = 20$. Observing Figure 6.5 it can also be concluded that this criterion is not satisfied. Additionally, using the method presented in (McDonald et al., 2005) the acceptable annual probability of failure is equal to 18×10^{-6} (considering $\beta_i = 0,1$), which is also not satisfied.
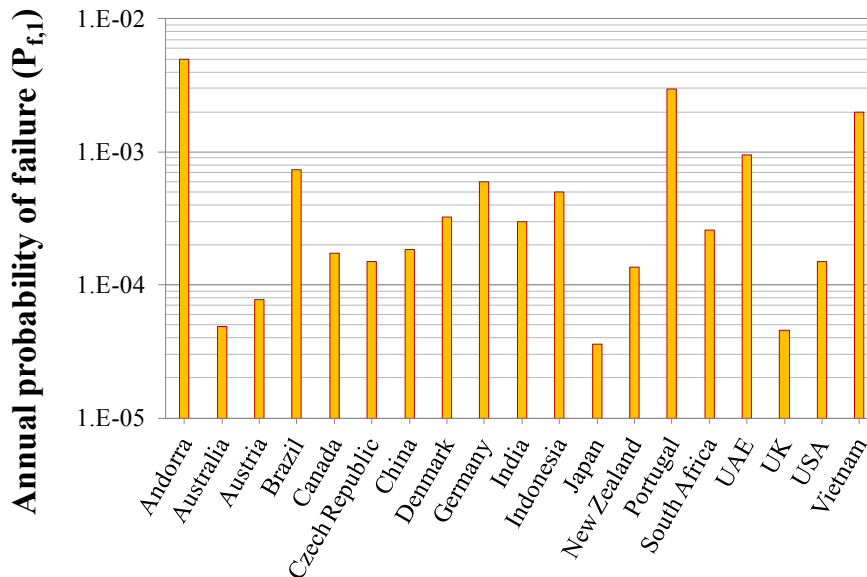
Figure 6.5: $P_{f,1}$ values for the 19 countries considered in the survey.

Comparing the $P_{f,1}$ values presented in Figure 6.5 with the structural risk of other temporary structures, the UK Health and Safety Executive (HSE) investigated 471 reported scaffold collapses during the period between 1986-1993, see (Beale, Godley, 2003). Considering an estimated 7,5 million scaffold erections it gives a failure rate of 63 collapses per 10^6 erections (*i.e.* 63×10^{-6} per year), which in the UK compares with an estimated probability of 46 collapses per 10^6 bridge projects for bridge falsework systems, a value close to the one observed for scaffold systems.

Finally, it is also possible to calculate the annual conditional probability of a person being killed given the failure of the bridge falsework system, which is obtained by equation (6.3). The results are presented in Figure 6.6.

$$P(d \cap f) = \frac{\text{Number of failures with fatalities}}{\text{Number of bridges}} \qquad (6.3)$$

It can be observed that the criterion specified in ISO 2394 for accepting the annual probability of a person being killed in a structural accident, equal to 1 in 10^6 fatalities, is not satisfied in all countries, except Australia and New Zealand.

Time analysis of risks to individuals and of structural risks are not presented due to the difficulty in collecting required data, in particular regarding the number of bridges built each year in each country analysed.

In conclusion, the calculated estimated annual probabilities of a fatality and of a failure of a bridge falsework system are higher than the acceptable risk levels and, therefore, the development of a risk informed decision-making framework for bridge falsework systems is fully justified.
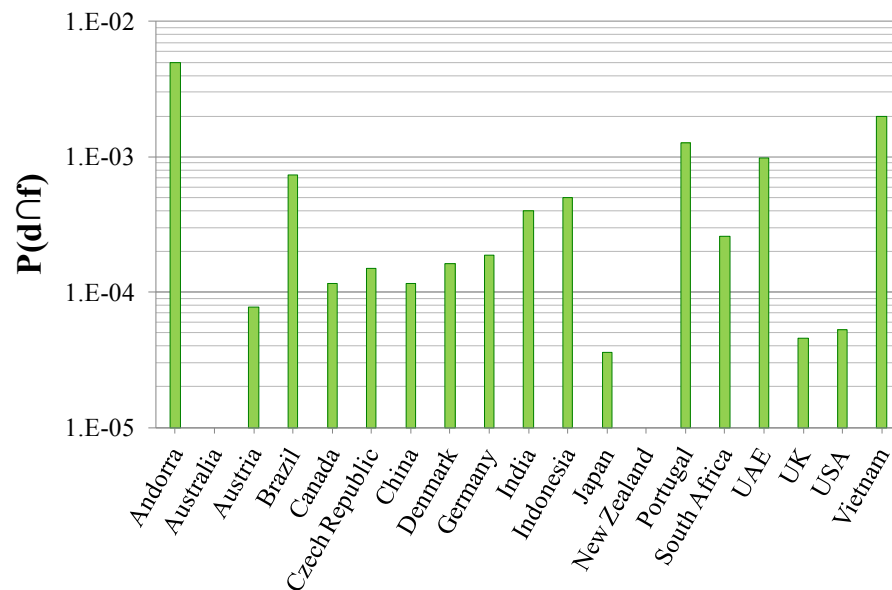
Figure 6.6: P(d∩f) values for the 19 countries considered in the survey.

6.3 Risk identification

Hazards exist everywhere, in particular at the interfaces of system activities. The basis for the hazard identification, already described qualitatively in Chapter 5, is primarily based on reported information concerning accidents but also on expert judgement. In this section the failure modes, failure effects and failure consequences will be presented in graphic terms using logic trees and hazard tables, see Figure 6.7 and Table 6.2. In Chapter 2 some of the listed hazards have already been discussed.

Furthermore, from the information given in Figure 6.7 it is possible to identify opportunities to include suitable barriers to manage the failure modes and the failure effects. This is illustrated in Figure 6.8.

It is also important to study in detail the risks stemming from the reusage cycles of bridge falsework elements in each bridge project and on the various bridge projects throughout their entire design working life, namely the possible detriment effects of lack of maintenance on the probability of failure as well as the possible effects of changing the exposure conditions of the bridge falsework system. The new exposure conditions might lead to a higher, lower or equal value of initial probability of failure than the one obtained in the first bridge falsework project.

6.4 Risk estimation

As detailed in Chapter 2, risk can be expressed by different measures and using various numerical tools. In the present section, risks associated with bridge falsework will be analysed for the most relevant hazard scenarios:

A. Actions: (i) concrete casting loads, including dynamic effects and local overloads; (ii) wind loads, with varying values according to the construction phases of the bridge relevant to the falsework system, *i.e.* assembling of the falsework, casting of the concrete and curing of the concrete; (iii) ground settlements; (iv) combined effect of actions of different nature;

B. System configuration: (i) bracing configurations; (ii) joint characteristics; (iii) falsework system using steel beam girders; (iv) gross initial geometrical imperfections; (v) use of special elements such as spigots, anchor bolts or pins.

For each considered hazard scenario, the resistance, robustness and fragility of the system will be first calculated and analysed based on deterministic analyses.

After, the data collected from the experimental campaign of joint tests presented in Chapter 3 will be used together with other appropriate data to build probabilistic models for the most important stochastic variables. These variables will be selected based on the results of a sensitivity analysis of the stochastic response of a chosen reference bridge falsework system. In the end, stochastic models for the resistance, reliability, robustness and fragility for selected case studies will be determined, based on which the structural risk will be estimated.
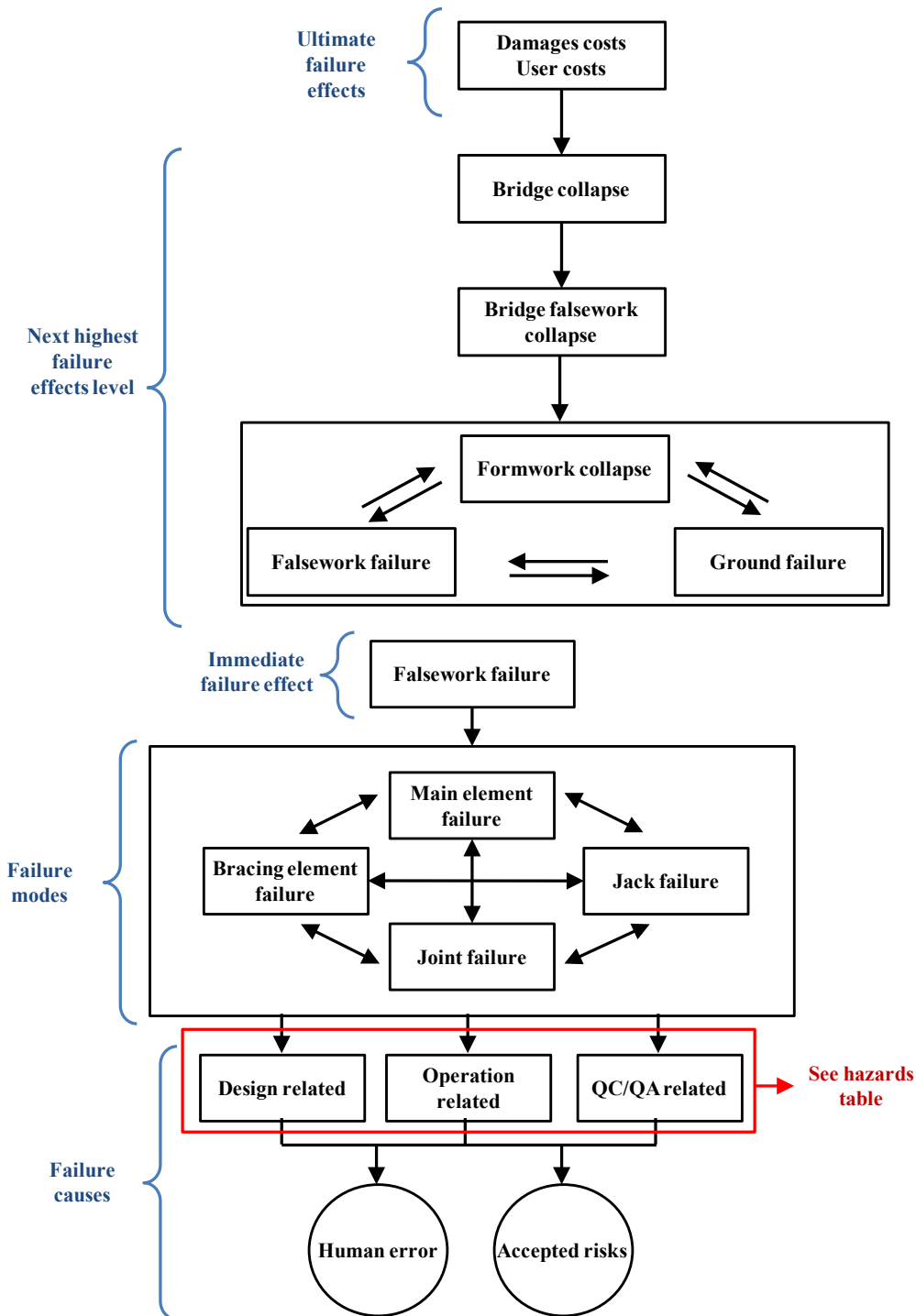
Figure 6.7: Decomposition of failure effects, failure modes and failure effects.

Table 6.2: List of primary hazard events.

(A) Design	
1. Actions	
Activities	**Primary hazard events (Enabling events)**
1.1. Action cases selection	• Forgetting to consider action cases
Dead Loads: • Self-weight	
Construction Loads: • Concrete weight • Reinforcing steel weight • Precast units weight • Dynamic effects (concrete casting, bridge launching, etc.) • Storage of materials and equipment • Personnel • Prestress	
Settlements: • Ground • Foundation elements	
Wind	
Rain	
Temperature	
Snow	
Ice	
Earthquake	
Impact Loads	
1.2. Estimation of actions values Directly specified in design standards. However, some loads values are project specific.	• Underestimation of the action values: • Dynamic effects • Storage loads • Wind loads (use of reduction factors) • Incorrect assessment of the ground conditions • Underestimation of the period of exposure • Unaccounted changes in the design of the bridge project and/or of the method of construction
1.3. Load combinations	• Forgetting to consider concomitant action cases • Underestimation of concomitant action values
During assembly	
During operation	
During dismantling	
2. Resistances	
Activities	**Primary hazard events (Enabling events)**
Determination of mechanical properties of materials, ground characteristics: • Testing • Design standards • Expert judgment	• Deficient estimation or overestimation of resistance values determined by testing or obtained from theoretical or empirical models • Forgetting to consider actions cases
Determination of behaviour and resistance of elements and joints under static and dynamic actions • Testing • Design standards • Expert judgment	
3. Modelling	
Activities	**Primary hazard events (Enabling events)**
Determination of actions effects: • Loads • Displacements • Rotations • Vibrations • Static/dynamic loads	• Forgetting to consider actions cases • Underestimation of actions effects • Not accounting for all actions effects • Forgetting to consider resistances models • Inadequate modelling of resistances models • Inadequate modelling of geometry • Forgetting to consider imperfections, damages, deterioration mechanisms • Underestimation of effect of imperfections, damages, deterioration mechanisms
Resistance modelling: • Ground • Materials • Elements • Joints • Deterioration mechanisms	
Geometry modelling: • Elements • Joints • Ground • Imperfections • Damages	

(continues)

Table 6.2: List of primary hazard events.

(A) Design	
4. Structural Analysis	
Activities	**Primary hazard events (Enabling events)**
Selection of analysis type: • Design tables • Analytical methods • Numerical methods • Linear or non-linear analysis • Static or dynamic analysis	• Inaccuracy of analysis results • Incomplete analysis • Inadequate analysis
5. Structural Design	
Activities	**Primary hazard events (Enabling events)**
Serviceability and safety verification: • Sections • Main elements, brace elements and foundations • Joints • System • Ground	• Incorrect use of serviceability and safety design procedures • Incomplete serviceability and safety design checks • Under-designed element, joint, foundation, structure • Incomplete or wrong documentation

Documentation:
• Drawings
• Design justification
• Method statement:
  o Assembly procedure
  o Ground investigation
  o Minimum ground characteristics
  o Maximum loads for various stages
  o Loading sequence
  o Monitoring requirements
  o Inspection and testing requirements
  o Imperfections considered
  o Dismantling procedure	

(B) Operation	
1. Assembly	
Activities	**Primary hazard events (Enabling events)**
Carry out ground investigation	• Inadequate or incomplete ground investigation • Incorrect analysis of the results of ground investigation • System assembled over ground with weaker characteristics than the ones considered in the design • Errors in the execution of the foundation elements • Assembly procedure different from the one considered in the design • System's configuration different from the one specified in the design (overextended jacks, spacing of lacing members, bracing configuration, deficient joints between formwork and falsework) • Assembly with weather conditions not in accordance with the specified in the design • System's imperfections larger than the design tolerances • Use of incorrect or damaged elements, joints
Execute foundations (sole plates, concrete pads, piles, ground improvement)	
Assembly baseplate, jack, vertical, lacing and bracing elements, jacks and forkheads, bolts and tie rods, formwork Lock joints between members	
Check extension lengths of jacks, tightness of joints, correct execution of joints between falsework and formwork, spacing of lacing and configuration of bracing	
Check member and system imperfections, element defects	
2. Operation	
Activities	**Primary hazard events (Triggering events)**
Check loading sequence and allowed weather conditions	• Loading sequence not as considered in the design • Operation under weather conditions outside the maximum design limits • Loading method not as specified in the design (by bucket or by pump, *e.g.*: casting concrete from large heights
Concrete casting of bridge deck or placement of precast units from cranes	• Impact of the crane with the falsework system • Falling precast units from crane into falsework • Impact of a vehicle with the falsework • Overload falsework by applying more prestress than considered in the design
Apply partial prestress	• Overload falsework with equipment and storage materials more than considered in the design • Occurrence of actions with intensities larger than the ones considered in the design • Occurrence of actions not considered in the design

(continues)

Table 6.2: List of primary hazard events.

(B) Operation	
3. Dismantling	
Activities	**Primary hazard events (Triggering events)**
Check if the superstructure is already self-supporting	• Superstructure is still not self-supporting
Follow dismantling procedure	• Early dismantling or improper dismantling procedure
(C) QC/QA	
Activities	**Primary hazard events (Procedural causes)**
Selection of skilled staff and workers	• Insufficient communication and cooperation between stakeholders (*e.g.* unreported changes in the bridge design)
Training programmes	• Deficient assignment of responsibilities of supervision
Appointment of a health and safety team	• Selection of unskilled, untrained staff and workers
Appointment of a temporary works supervision team	• Undetected, uncorrected errors, damages, imperfections
Cooperation and communication between stakeholders	• Improperly corrected errors, damages, imperfections
Self-checking	• Selection of inadequate methods of inspection and maintenance
Internal and external reviews of the project procedures and documents	• Under-designed structure
Preparation of inspection plans	
Preparation of maintenance plans	
Definition of damages and imperfections limits	
Definition of criteria for the selection of methods, methods of appraisal and review procedures	
Approval requirements to start assembly, operation and dismantling	

(ends)
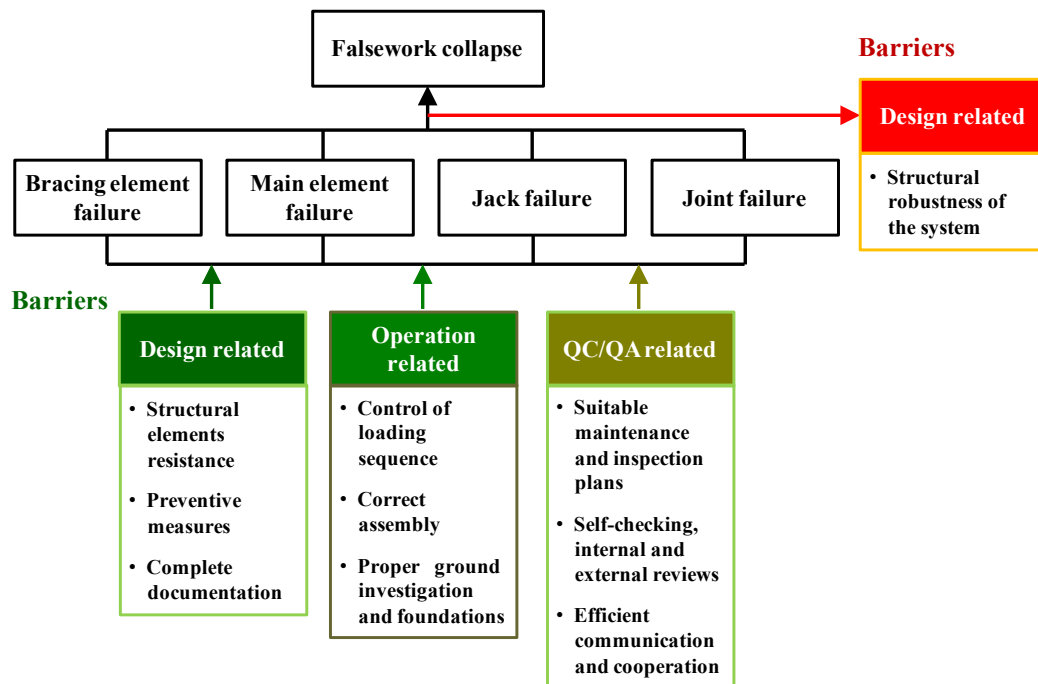
Figure 6.8: Possible barriers to manage the failure modes and the failure effects.

6.4.1   Deterministic investigation

Different models were considered in this section. Unless noted otherwise, the models considered resemble the structures A2 and A4 tested in the Sydney University (referenced in this Chapter as Models A2 and A4, respectively), see Chapter 4 and (Chandrangsu, Rasmussen, 2009a). These systems were chosen because the effect of localised internal and external actions on their safety and performance is more significant than the effect due to the same localised actions on more complex (larger) systems. As a consequence, the results presented in the following were obtained for severe scenarios and serve as a point of reference for other cases. In spite of constituting severe scenarios, it is possible that the analysis may not have encompassed all the potential failure modes. This is important when extrapolating the results obtained for less severe cases, for example in the definition of the bracing requirements.

In all cases, the cross-section geometrical characteristics as well as the material properties of the various elements which make the falsework system are identical to the ones used in the structures tested in the Sydney University, see Chapter 4 and (Chandrangsu, Rasmussen, 2009a). Additionally, the finite element mesh properties are the same as detailed in Chapter 4. The formwork was explicitly modelled in all models, with an equivalent thickness equal to 100 mm, and the joint characteristics considered in all models, unless otherwise noted, were taken as the average values of the results reported in Chapter 3. The same applies to the top and bottom jacks' extension lengths, where 600 mm was considered as the default extension length value and to the default initial geometrical imperfections whose values were measured *in situ* during the full scale tests performed at Sydney University.

6.4.1.1 Actions related hazards

6.4.1.1.1 Concrete casting action

For single span concrete bridges, the bridge decks when casted in situ can be concreted in a single operation, starting from one end or from the middle of the span. For continuous span concrete bridges, alternative casting methods can be used involving construction joints at one fifth of the span length, see for example (fib, 2000).

Concrete can be placed either by skips or by pumps. The latter is nowadays the most used method for placing concrete on bridge decks. Concrete casting loads consist in a combination of dead loads and variable loads. The former consists on the weight of the fresh concrete plus the weight of the reinforcing steel. The latter consists in weight of the workers, tools and equipment, plus allowance for heaping of the concrete and dynamic effects.

The self-weight of the fresh concrete and of the reinforcing steel can be considered equal to 26 kN/m^3 see (BSI, 2002c). Figure 6.9 illustrates the possible local heaping of the concrete during concrete placing (*Left*) and the unfactored load values to account for this variable load suggested in (BSI, 2011, 2005b) (*Right*). The loads specified in codes (BSI, 2011, 2005b) allow for concrete to be dropped by no more than 1 m height and the heap height must not be greater than three times the depth of the slab, subject to a maximum area equal to 1 m^2 as shown in Figure 6.9 (*Left*), (The Concrete Society, 2012).

The dynamic effects of concrete placing are complex. (Ikäheimonen, 1997) suggested an approximate method. The maximum dynamic load, *P*, can be approximately calculated by:

$$P = Q \times \sqrt{2 \times g \times h} \tag{6.4}$$

where *Q* is the rate of flow of concrete in kg/s, *h* is the drop of concrete in m, and *g* is the gravitational constant in m/s^2.

Based on the values also published in (Ikäheimonen, 1997), for skips this would translate in a dynamic load in the range of 0,8 to 1,6 kN. For pumps, as the rates of flow of concrete are much lower than the ones of using skips, the dynamic load is estimated not to be greater than 0,5 kN.
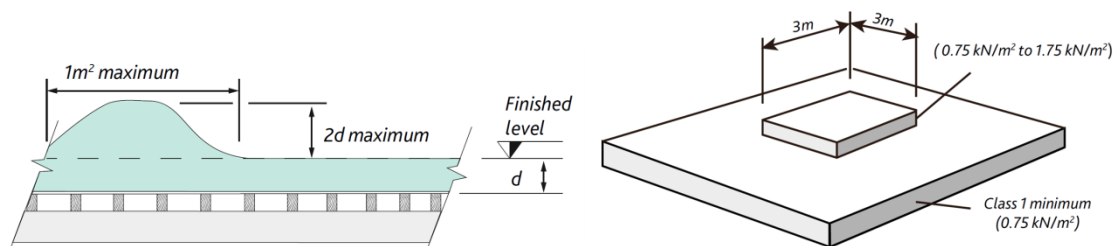
Figure 6.9: Local heaping of the concrete (The Concrete Society, 2012).

Several numerical models were developed to test if under a number of different scenarios the concrete casting could be a critical hazard to the safety and performance of bridge falsework structures. Therefore, two different concrete placing methods were analysed combined with various

local concrete heaping values, see Table 6.3 for model labels and characteristics and Figure 6.10 for other details. Models A2 and A4 were used in this study. In all models, a 0,5 kN dynamic load was considered, associated to concrete blocks representing a 1 m^2 formwork area.

The only loads considered were the ones associated with the concrete casting action itself: (i) weight of the fresh concrete, (ii) local concrete heaping and (iii) dynamic effects. Both the local concrete heaping and the dynamic effects were applied in 50% of the time considered for the full application of the concrete layer thickness in each concrete block and then removed. The application of the concrete casting action was applied over the entire formwork area considering an analysis time period equal to 100 s. Afterwards, if collapse of the falsework system had not been already attained, the thickness of the slab was increased until collapse state was reached. Therefore, in terms of robustness index calculation the leading action was the weight of the concrete slab.

Table 6.3: Summary of different model characteristics used to analyse concrete casting actions.

Model-ID	Structure (s)	Concrete placing method (c)	Local heaping height (h)	Slab thickness (t)	Number of concrete layers (l)
s-c-h-t-l	A2, A4	1, 2	h = 1: None h = 2: 1×slab thickness h = 3: 2×slab thickness	0,25 m, 0,5 m, 1,0 m, 1,5 m	1, 2, 5, 10

Example of Model A2-1-1-0,25-1: Model A2 with concrete placing method #1, with no local heaping height, a slab thickness equal to 0,25 m and the number of concrete layers is equal to one.

36	35	34	33	32	31
30	29	28	27	26	25
24	23	22	21	20	19
18	17	16	15	14	13
12	11	10	9	8	7
6	5	4	3	2	1

Concrete placing method	Concrete casting blocks order
1	1st layer: 1 → 36 2nd layer: 1 → 36 nth layer: 1 → 36
2	odd layer #: 18 → 1, 19 → 36 even layer #: 1 → 18, 36 → 19
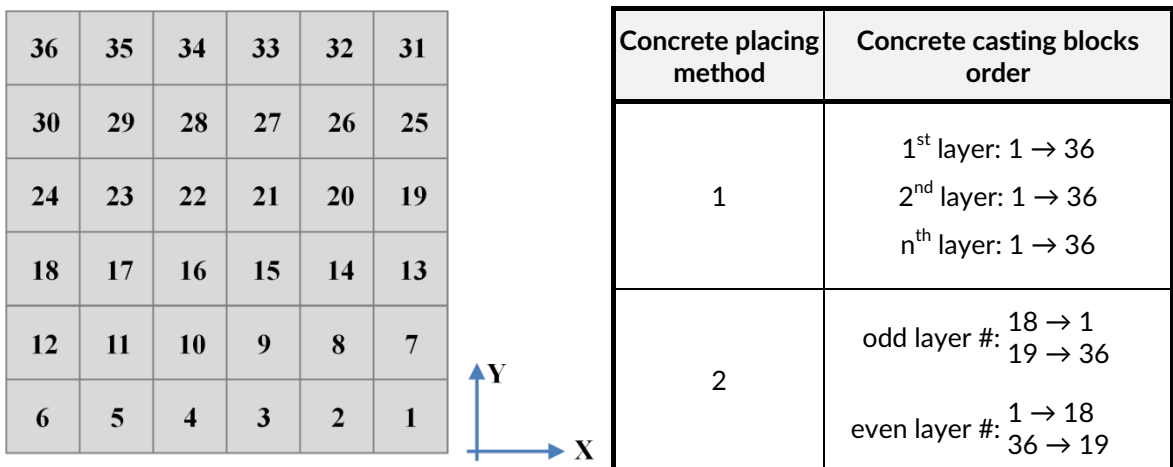
Figure 6.10: Numbering of the concrete casting blocks on formwork surface.

Comparing the results obtained in Model A2-1-1-0,5-1 with the ones registered *in situ* for a real bridge during casting of concrete, see Figure 6.11, it is possible to observe that the numerical models can satisfactorily predict the behaviour of a falsework system during this construction phase of the bridge.
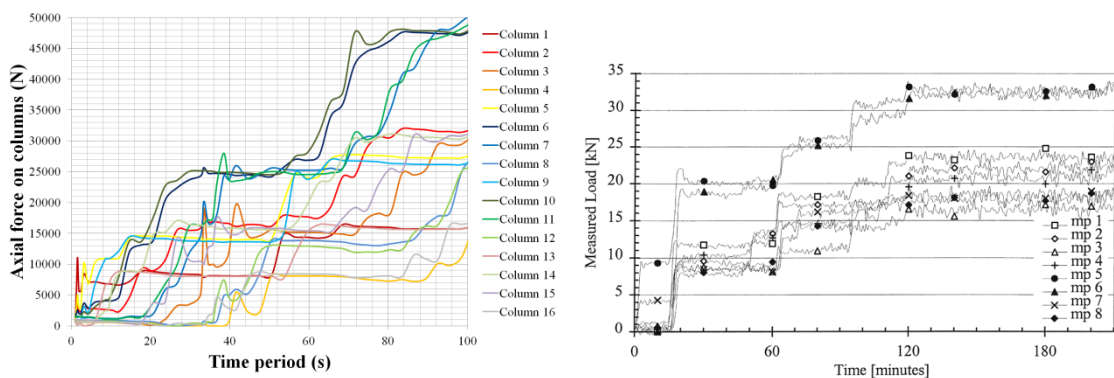
Figure 6.11: Comparison between column axial force numerical results (*Left*) and *in situ* results (*Right*) (Ikäheimonen, 1997) during concrete casting.

The results in terms of maximum pressure applied to the formwork and robustness index values for 15 different models are presented in Table 6.4. Figure 6.12 and Figure 6.13 show the undeformed and deformed configurations for models A2-1-1-1,0-1 and A4-2-1-0,5-2, respectively.
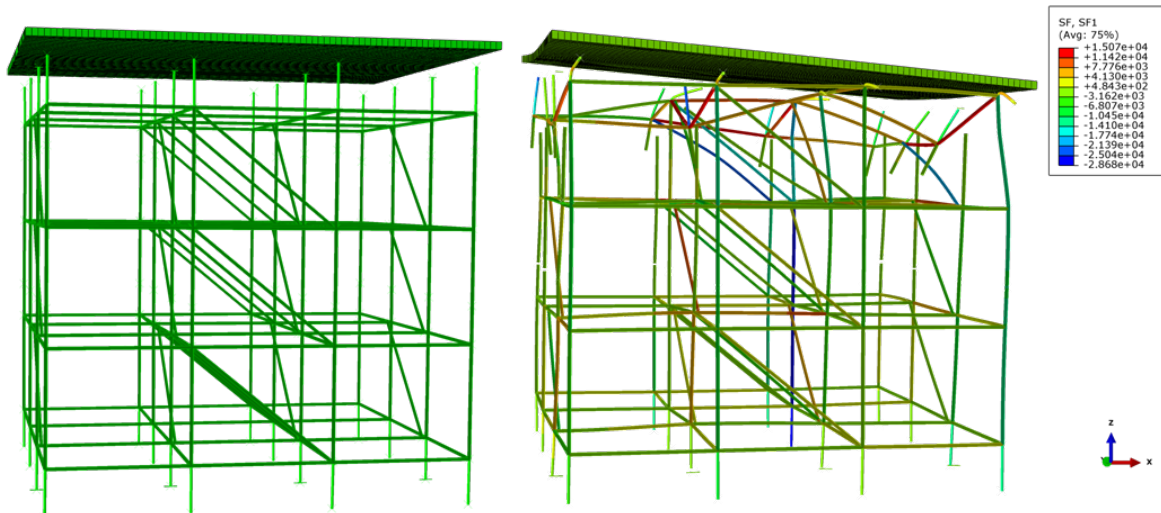
Figure 6.12: Undeformed configuration and deformed configuration with elements axial force distribution (N) for Model A2-1-1-1,0-1.
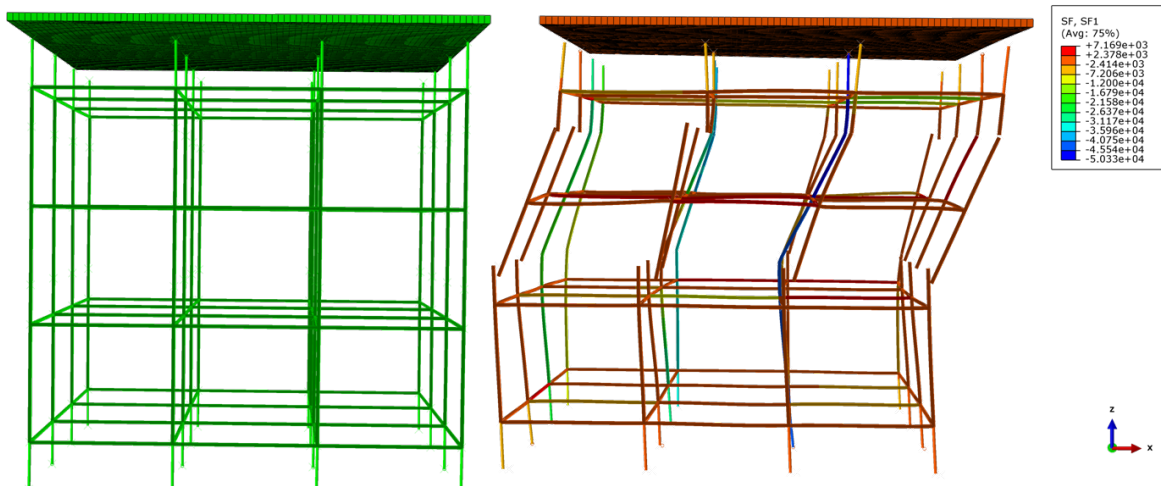
Figure 6.13: Undeformed configuration and deformed configuration with elements axial force distribution (N) for Model A4-2-3-0,5-2.

Analysing Table 6.4 results, it is possible to observe that the most influencing factor related with the concrete casting action is the local concrete heaping height. However, only considerable unrealistically high values lead to an important degradation of the maximum pressure value that the system can resist, see results for Model A2 and 1,0 m slab thickness for example. The number of concrete layers seems to also have a negative influence on the resistance of the structure, but only when coupled with large concrete heaping heights. All other variables, *i.e.* concrete placing method, slab thickness and dynamic effects, seem to have a very small influence on the resistance of the falsework system. In conclusion, local concrete heaping height should be controlled and its value should be limited, in particular for falsework systems which are subject to loads close to their resistance capacity, especially for thin slabs.

In terms of collapse mode, it was possible to observe that it was enabled by the large jack extension lengths which suffered severe plastic deformations, as well as by the resistance of the spigot joints. The A2 models, which included brace elements, exhibited small global sway displacements with an S-shaped column buckling collapse mode whereas the A4 models, which did not include any brace elements, exhibited a pronounced global sway collapse mode.

Table 6.4: Results of the models developed to analyse concrete casting actions.

Model	Maximum pressure (N/mm²)	Robustness index Eq. 5.34 / Eq. 5.18
A2 reference	**0,03909 (0,0%)**	**0,006 (0,0%)/0,082 (0,0%)**
A2-1-1-0,5-1	0,03906 (-0,1%)	0,003 (-44,6%)/0,057 (-29,5%)
A2-1-3-0,5-2	0,03800 (-2,8%)	0,004 (-38,1%)/0,059 (-27,8%)
A2-2-3-0,5-2	0,03795 (-2,9%)	0,003 (-50,1%)/0,044 (-46,2%)
A2-2-3-0,5-5	0,03788 (-3,1%)	0,004 (-32,7%)/0,048 (-41,1%)
A2-1-1-1,0-1	0,03900 (-0,2%)	0,003 (-43,7%)/0,054 (-34,3%)
A2-2-2-1,0-2	0,03793 (-3,0%)	0,005 (-15,7%)/0,057 (-30,6%)
A2-2-3-1,0-2	Collapse was reached for t=51,2s	0,010 (+68,2%)/0,160 (+96,3%)
A2-2-3-1,0-5	Collapse was reached for t=67,8s	0,015 (+168,2%)/0,219 (+168,2%)
A2-1-1-1,5-2	Collapse was reached for t=98,8s	0,006 (+4,0%)/0,108 (+32,4%)
A2-2-1-1,5-2	0,03900 (-0,2%)	0,005 (-6,6%)/0,089 (+8,9%)
A2-2-1-1,5-10	0,03900 (-0,2%)	0,006 (-2,5%)/0,101 (+24,0%)
A4 reference	**0,01401 (0,0%)**	**0,012 (0,0%)/0,129 (0,0%)**
A4-2-3-0,25-2	0,01391 (-0,7%)	0,010 (-13,0%)/0,120 (-7,2%)
A4-2-3-0,5-1	0,01395 (-0,5%)	0,010 (-11,7%)/0,130 (+1,0%)
A4-2-3-0,5-2	0,01382 (-1,3%)	0,010 (-12,8%)/0,164 (+26,8%)
A4-2-3-0,5-10	0,01354 (-3,4%)	0,007 (-37,0%)/0,145 (+12,0%)

In A2-2-3-1,0-2 and A2-2-3-1,0-5 models, an early collapse was attained due to the sliding of the central baseplates (under severe loading) which then failed in bending, see Figure 6.14.

In terms of robustness, the most influential variable is the extension length of the jack elements and the existence of bracing elements. In the considered braced systems, the weak link turns out to be the jack elements, as already detailed in the examples presented in Chapter 5. This fact leads to a lower robustness of the system. In the unbraced systems, the weak links are the spigot joints which limit both the resistance and the robustness of the structure. However, in the braceless structures, when compared with the braced structures, more elements dissipate energy, and elements which have a larger maximum deformation energy than the jack elements.
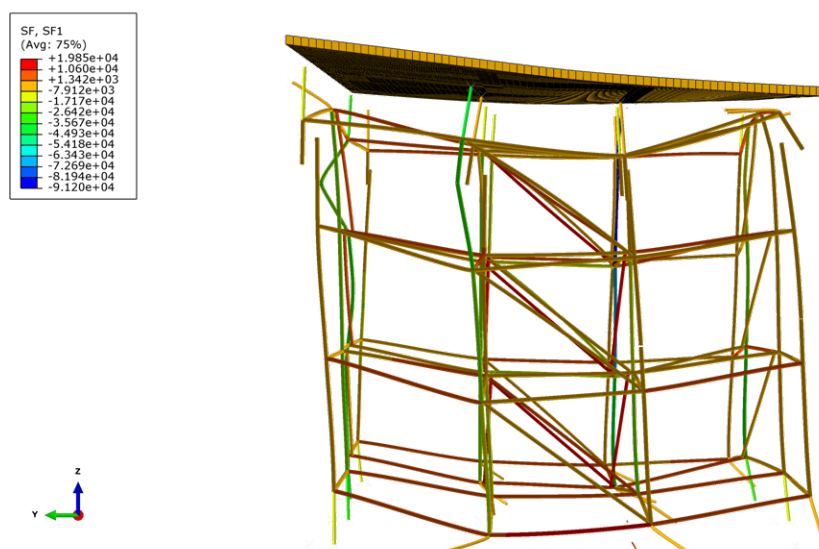
Figure 6.14: Deformed configuration with element's axial force distribution (N) for Model A2-2-3-1,0-2.

Nevertheless, all the robustness values are low (less than 0,20) and damages are concentrated in a small number of elements. This is in line with the prior knowledge concerning falsework structures. It is also possible to observe that the robustness index values for models A2-2-3-1,0-2 and A2-2-3-1,0-5 are higher than the rest of the values even though the resistance capacity of these models is lower than the rest of A2 models. This apparent paradox is justified due to the different collapse modes observed in these models which involved not only the top jacks but also

the bottom jacks; therefore, there was a participation of a larger number of elements to the energy dissipation capacity of the system.

Figure 6.15 presents additional results, related with structural fragility. It was already shown that for the structural configurations and external actions considered, robustness index values were small which means that collapse is disproportionate. The fragility curves further show that the structural resistance after first damage occurs is also small (15% is the maximum value of the ratio between maximum and first damage action value), so collapse is abrupt after first damage. In the braced systems, structural damages propagate slowly until the "unavoidable collapse" state is attained. For unbraced systems, damages propagate more gradually, despite having a lower structural resistance after first damage than the braced systems. Therefore, costs that stem from structural damages propagate differently depending on the structural configuration and external actions considered. For all models, the damages just before collapse do not represent more than 15% of the potential damage capacity of the entire structure in the case of unbraced systems and 5% in the case of braced systems, so if a damage detection system is used it should be developed having this in mind.

Fragility values of bridge falsework systems are found to be extremely sensitive to concrete casting action values. If these structures are underdesigned there is a high probability that complete structural damages take place.
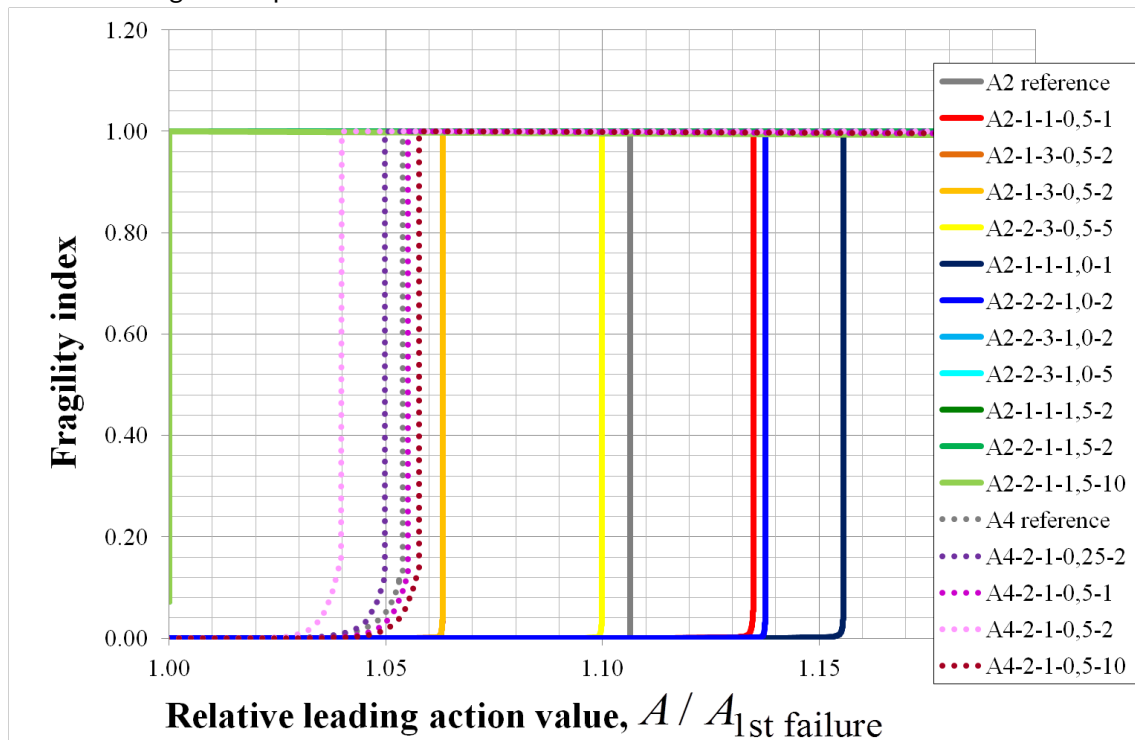
Figure 6.15: Fragility curves of the models developed to analyse concrete casting actions.

6.4.1.1.2 Wind action

The wind is another important action to be considered in the design of bridge falsework structures. Wind action is always present in any given instant of time with a certain direction and intensity which are both complex to characterise and to predict and subjected to a large uncertainty. During the operation of bridge falsework structures wind may play a critical role in any one of the three most important phases: (i) during assembly of the system, (ii) during the casting of the concrete and (iii) after concrete has been placed but before the concrete has hardened to a degree where it can resist the applied actions by itself, including the wind action.

Traditionally, wind action is specified in the design standards. For bridge falsework, EN 12812 (BSI, 2011) specifies the following requirements:

(i)　　Assembly phase: Maximum wind velocity;

(ii)   Concrete casting phase: Working wind velocity;

(iii)   Phase before concrete has hardened: Maximum wind velocity.

Wind velocity can be determined from EN 1991-1-4 (BSI, 2005c) or from BS 5975 (BSI, 2008a). In this Chapter the specifications included in the former documents are followed. Having determined the wind velocity, the wind action on an element of the bridge falsework can be calculated and applied as a pressure distribution or through the resultant loads. The overall procedure is lengthy and will only be summarised below.

Based on some prior information, namely location, altitude and orography of the site and geometrical dimensions of the system and of its constituents, the wind velocity is determined by a mean wind velocity and a fluctuating component of the wind velocity. The former component is given by the basic wind velocity, v_b (BSI, 2005c):

$$v_b = c_{dir} \times c_{season} \times v_{b,0}$$
(6.5)

where (BSI, 2005c):

$v_{b,0}$ is the fundamental value of the basic wind velocity, at 10 m above ground of terrain category I;

c_{dir} is the directional factor, with a recommended value equal to 1,0;

c_{season} is the season factor.

The fundamental value of the basic wind velocity is the 10 minutes mean wind velocity having a given probability P for an annual exceedence. In general, a 50 years return period is chosen. For temporary structures it is allowed to increase p and thus diminish the basic wind velocity. By default this procedure is highly unrecommended based on evidence provided from the results presented in Chapter 2. What can certainly be applied is the season factor which could reduce or increase the basic wind velocity depending on the climate characteristics of the site during a specific timeframe.

The distribution of wind velocity with height needs also to be accounted for. This depends on the structure height but also on the site orography and terrain roughness. As a safe simplification, the wind velocity distribution can be modelled as constant along the height of the element (structure) with a value equal to the wind velocity at maximum height of the element (structure).

The fluctuating component of the wind velocity is simulated by a turbulence intensity parameter. The two components of the wind, mean and fluctuating, are then combined and the resulting wind action is expressed in terms of a peak velocity pressure parameter.

To account for action-structure interaction the peak velocity pressure is multiplied by a structural factor, which practice has shown that it can be considered to be equal to one for bridge falsework systems. Finally, the wind action resultant load (or equivalent distributed load) in each structural element is determined by multiplying the peak velocity pressure with the force coefficient and with the reference area of each element.

As BS 5975 (BSI, 2008a) points out *"unclad falsework presents a skeletal arrangement that allows the wind to pass through"*. In Annex M of BS 5975 (BSI, 2008a) a method is specified to determine the internal shielding effect. However, in general, for such systems little internal shielding effect is obtained.

Formwork is also subjected to wind action. No specific guidance is given in EN 1991-1-4 (BSI, 2005c) but BS 5975 (BSI, 2008a) gives a possible procedure to determine the wind effects on the formwork (formwork beams and formwork edge panels), including a possible shielding effect of the leeward edge panels of the formwork before casting of the concrete.

In this Chapter, the following initial assumptions have been considered to calculate the wind action on the falsework elements of Models A2 and A4: (i) altitude less than 600 m, (ii) $c_{dir} = c_{season} = 1,0$, (iii) terrain category II, (iv) $v_{b,0} = 27$ m/s and (v) orography coefficient equal to one. Taking into account these assumptions, the following distributed loads (distributed along the element's length) were calculated for the maximum wind action on the various falsework elements

of Models A2 and A4, see Table 6.5. The corresponding values for the working wind velocity are calculated by considering a wind pressure equal to 200 N/m^2 (BSI, 2005c), see Table 6.6.

The design values are obtained by multiplying the values of Table 6.5 and Table 6.6 by a partial factor equal to 1,5. As the internal shielding effect, determined according to the method specified in Annex M of BS 5975 (BSI, 2008a), does not exist, the wind action was applied in all elements of the falsework displayed in directions normal to the direction of the wind. Nevertheless, the total wind force on all falsework elements is still lower than the one that would be obtained if the falsework was claded in the faces normal to the wind direction.

Table 6.5: Distributed loads for the maximum wind action on the various falsework elements.

Element	Distributed load (N/mm)
Tubes (standards, ledgers, jacks, braces)	0,047
Formwork beams	0,746
Formwork windward edge panel	0,859
Formwork leeward edge panel	0,403

Table 6.6: Distributed loads for the working wind action on the various falsework elements.

Element	Distributed load (N/mm)
Falsework (standards, ledgers, jacks, braces)	0,009
Formwork beams	0,080
Formwork windward edge panel	0,100
Formwork leeward edge panel	0,047

Several numerical models were developed to test if under a number of different scenarios the wind action could be a critical hazard to the safety and performance of bridge falsework structures, see Table 6.7 for model labels and characteristics. Wind action was only considered in one direction: the direction of the collapse mode of Models A2 and A4 under vertical loads.

Table 6.7: Summary of different model characteristics used to analyse concrete casting actions.

Model-ID	Structure (s)	Wind action during assembly phase (*p1*)	Wind action during concrete casting phase (*p2*)	Wind action after concrete casting is finished (*p3*)	Spigot pins present? (sp)	Baseplate anchor bolts present? (ab)
s-p1-p2-p3-sp-ab	A2, A4	*p1* = 1: Maximum wind *p1* = 2: Working wind	*p2* = 1: Working wind + reference slab	*p3* = 1: Upper limit wind + reference slab *p3* = 2: Working wind+ upper limit slab	sp = 1: No sp = 2: Yes	ab = 1: No ab = 2: Yes
Example of Model A2-1-1-1-1: Model A2 with maximum wind during phase *p1*, working wind during phase *p2*, and wind as leading action during phase *p3*, with no spigots and no anchor bolts.						

Wind action was combined with concrete casting loads in phases *p2* and *p3* (see Table 6.7). As a simplification, during phase *p2* the concrete casting loads were modelled as a uniform load distributed over the entire formwork surface which value increased until the weight of a reference slab thickness was attained. For Model A2 a 0,5 m reference slab thickness was considered whereas for Model A4 a 0,25 m reference slab thickness was considered.

In phase *p3*, either the weight of the slab was increased until collapse was reached (leading action) maintaining the wind action equal to the working wind, or the wind action was increased until collapse was reached (leading action) maintaining the thickness of the slab equal to the reference thickness.

It was also analysed the effects of incorporating anchor bolts in the baseplates and pins at the spigot joints to add resistance against uplift loads. The anchor bolts considered were made of steel, had 10 mm nominal external diameter and the steel had an ultimate tensile strength equal to 600 MPa. One anchor bolt was positioned at each corner of every baseplate, separated 100 mm from each other, making a total of four anchor bolts per baseplate. It is assumed that the anchor bolts resistance is equal to the tensile resistance of the anchor bolts. Therefore, the anchor bolts should have an appropriate anchorage length and an adequate resistance should be given to the ground,

either by adding a special mortar mixture or concrete, see (CEN, 2009) for details. It is also considered that the thickness and material properties of the baseplate are such that it will not fail before the anchor bolts. The pins were also made of steel, had 8 mm nominal external diameter and the steel had a yield strength and an ultimate tensile strength equal to 400 MPa and 500 MPa, respectively.

The results in terms of maximum load applied to the system by the leading action and robustness index values for 13 different models are presented in Table 6.8. It is possible to observe that the most influential factor related with the wind action is the occurrence of the maximum design wind during phase $p1$ or phase $p3$. High values of wind action lead to a significant degradation not only of the resistance of the system but also of the system robustness. This is particularly true for braceless falsework systems. However, even the occurrence of working wind velocities has an impact on the system resistance and robustness, in particular in the latter parameter and for braced falsework systems, see Model A2-2-1-2-1-1 for example. This is justified because wind action subjects spigot joints to larger rotations, thus larger bending moments, and spigot joints are a weak link of bridge falsework structures, see Chapter 4. Therefore, collapse occurs for lower concrete pressures than the ones obtained when wind action is not considered, and robustness is smaller since structural damage is concentrated at the spigot joints which trigger the collapse of the system.

Table 6.8: Results of the models developed to analyse wind actions.

Model	Maximum wind pressure on falsework (N/mm^2)	Maximum concrete pressure on formwork (N/mm^2)	Robustness index Eq. 5.34 / Eq. 5.18
A2 reference		**0,03909 (0,0%)**	**0,006 (0,0%)/0,082 (0,0%)**
A2-1-1-1-1-1 (*)	0,03749 (*)		0,000 (-99,7%)/0,000 (-99,8%) (*)
A2-2-1-1-1-1	0,17658		0,003 (-39,1%)/0,063 (-22,5%)
A2-2-1-2-1-1		0,03659 (-6,4%)	0,003 (-54,4%)/0,052 (-36,2%)
A2-1-1-1-2-2	0,14598		0,002 (-68,2%)/0,026 (-68,2%)
A2-1-1-2-2-2		0,01558 (-60,2%)	0,016 (+172,3%)/0,222 (+172,3%)
A2-1-1-1-1-2	0,08281		0,003 (-49,1%)/0,024 (-70,3%)
A2-1-1-1-2-1 (*)	0,03787 (*)		0,000 (-99,9%)/0,000 (-99,9%) (*)
A4 reference		**0,01401 (0,0%)**	**0,012 (0,0%)/0,129 (0,0%)**
A4-1-1-1-1-1	0,03408 (*)		0,000 (-100,0%)/0,000 (-100,0%) (*)
A4-2-1-1-1-1	0,07930		0,011 (-7,4%)/0,074 (-43,0%)
A4-2-1-2-1-1		0,01345 (-4,0%)	0,004 (-66,5%)/0,058 (-55,3%)
A4-1-1-1-2-2 (**)	0,07105 (**)	0,00344 (-75,5%) (**)	0,000 (-100,0%)/0,000 (-100,0%) (**)
A4-1-1-1-1-2 (*)	0,06215 (*)		0,000 (-100,0%)/0,000 (-100,0%) (*)
A4-1-1-1-2-1 (*)	0,03726 (*)		0,000 (-100,0%)/0,000 (-99,9%) (*)
(*) Collapse occurred during phase $p1$. (**) Collapse occurred during phase $p2$.			

It is also possible to observe that in braced systems, including pins at the spigot joints and anchor bolts at the baseplates has a significant beneficial effect to the system's resistance and robustness when compared with the option of not using these components, see models A2-1-1-1-1-1 and A2-1-1-1-2-2 for example and Figure 6.16. The use of anchor bolts in isolation is found to be a better solution than only using pins at the spigot joints. This is to be expected since anchor bolts confer uplift resistance to the system and the spigot joints by having an overlap length continue to ensure structural integrity even when sliding occurs at these joints, although with limited resistance. Therefore, if high wind velocities are forecasted one option to increase structural resistance and structural robustness is to use brace elements and anchor bolts at the baseplates.

In terms of collapse mode, when it occurred during phase $p1$, it was possible to observe that the uplift forces due to the maximum wind were enough to overturn the falsework system. When collapse occurred during phase $p2$, the combined action of wind action and weight of the concrete slab led to the premature bending failure of the spigot joints. In all other A2 models, failure occurred by excessive damage at the bottom jack elements, and in all other A4 models, failure occurred by failure of spigot joints, see Figure 6.16 (Left) and Figure 6.17, respectively.
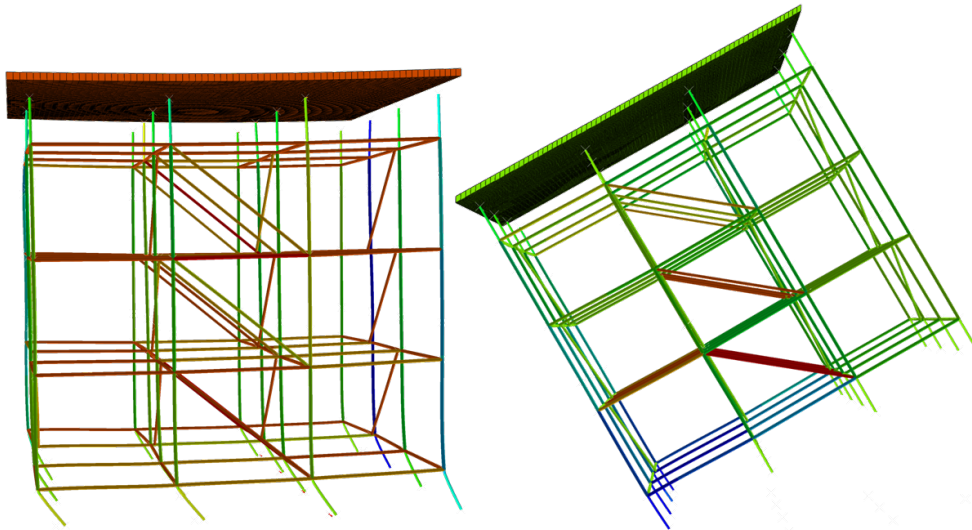
Figure 6.16: Deformed configuration with element's axial force distribution (N) for models A2-1-1-1-2-2 (Left) and A2-1-1-1-1-1 (Right).
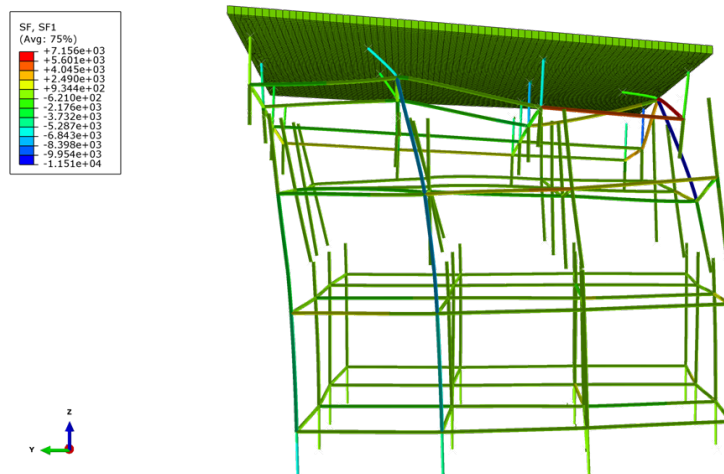
Figure 6.17: Deformed configuration with element's axial force distribution (N) for Model A4-2-1-2-1-1.

Figure 6.18 presents additional results, related with structural fragility. It was already shown that for the structural configurations and external actions considered, robustness index values were low (less than 0,10) meaning that collapse is disproportionate, and damages concentrate in a small number of elements. For systems that collapsed before phase *p3* starts, fragility is equal to one for the entire range of the leading action values. In these cases, fragility could be analysed as a function of the reference action values, for example the concrete pressure on formwork during the concrete casting phase. Nevertheless, in the following only the results obtained for the leading action will be analysed.

The fragility curves further show that the structural resistance after first damage occurs is in general also small (in the majority of the scenarios 20% is the maximum value of the ratio between maximum and first damage action value), so collapse is abrupt after first damage.

However, for some configurations and specific hazard scenarios, there is a substantial resistance capacity reserve after first damage occurs, namely when the wind is the leading action, anchor bolts are used at the baseplates and collapse does not occur during the application of the reference actions. In these cases, collapse may be avoided if early damages are detected in time as damage accumulation with increasing action values is slow, until collapse occurs.

For unbraced systems, damages propagate more gradually, despite having a lower structural resistance after first damage than the braced systems. For the great majority of models, the damages just before collapse do not represent more than 10% of the potential damage capacity of the entire structure but for Model A2-1-1-2-2-2 this value reaches 20%. Therefore, costs that stem

from structural damages increase differently depending on the structural configuration and external actions considered. If a damage detection system is used it should be developed having this in mind.

Fragility values of bridge falsework systems are found to be extremely sensitive to system configurations and to wind action values. If these structures are not properly designed, accounting in particular for the various construction phases, and are overloaded there is a high probability of complete structural damages take place. On the other hand, if they are properly designed there is a resistance capacity reserve that can be used if they are overloaded, but a monitoring system with an early damage detection capability must be used since structural collapse is abrupt and disproportionate.

(*) Collapse occurred during phase *p1*.
(**) Collapse occurred during phase *p2*.
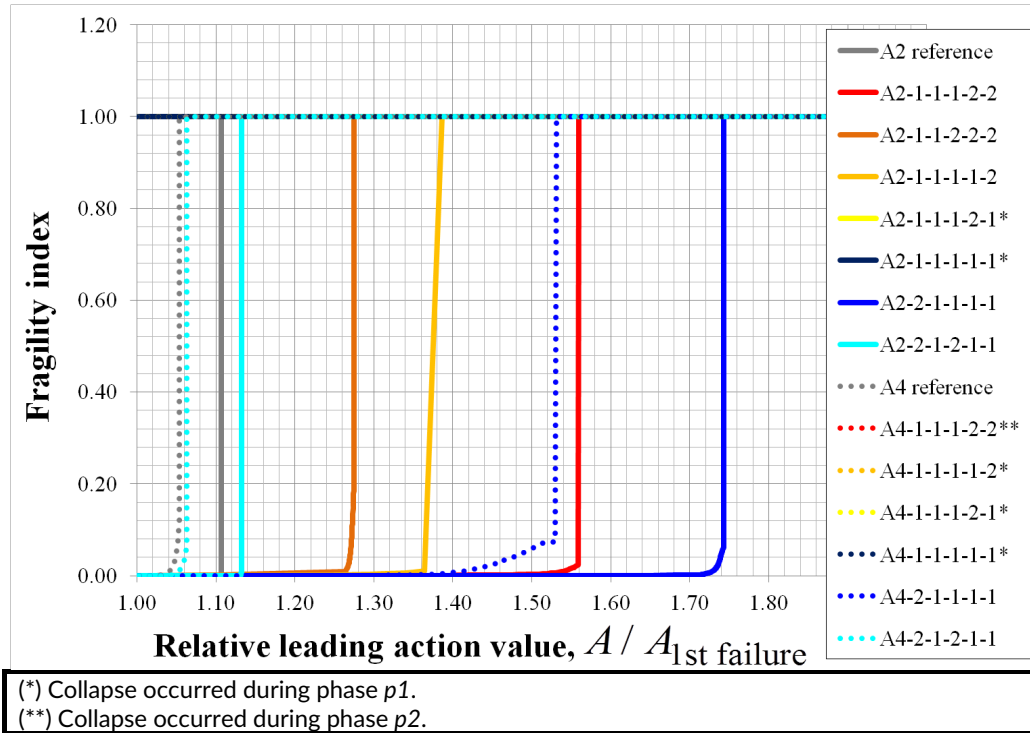
Figure 6.18: Fragility curves of the models developed to analyse wind actions.

6.4.1.1.3 Ground settlement

Ground settlements are also another potential critical hazard which deserves an in-depth analysis. Due to the low robustness of bridge falsework systems any imposed load redistribution may not find the required force redistribution capacity driving the system to collapse. Chapter 2 and Table 6.2 already covered the procedural, enabling and triggering events related with ground settlements.

Ground settlements are a function of the ground characteristics and applied actions. The ground where falsework structures foundations are laid upon typically exhibits poor resistance and rigidity characteristics since they consist of top ground layers, *e.g.* soft and loose soils. Without proper care, large ground settlements can result from the applied loads transmitted to the falsework system and from this to the ground via the foundation elements. Differences between displacements of the foundation ground can originate differential settlements at the foundation level of the falsework system with potential negative structural consequences.

In this section, various hazard scenarios were studied based on the already presented Models A2 and A4. In all scenarios, the differential ground settlement action was combined with concrete casting loads as follows: during concrete casting phase, differential ground settlements were increased until reaching a target reference value which coincided with the end of the concrete placement. In all models, the concrete casting loads were modelled as a uniform load distributed over the entire formwork surface which value increased until the weight of a reference slab thickness was attained. For Model A2 a 0,5 m reference slab thickness was considered whereas for

Model A4 a 0,25 m reference slab thickness was considered. Afterwards, concrete pressure was increased until collapse was attained.

Several numerical models were developed to test if under a number of different scenarios the differential ground settlement action could be a critical hazard to the safety and performance of bridge falsework structures, see Table 6.9 for model labels and characteristics.

The default Cuplok® joint characteristics (j = 1, see Table 6.9) were taken as the average values of the tests results reported in Chapter 3: the strong bending axis exhibits 0,0055 rad (≈0,31°) looseness, *i.e.* first linear segment rotation increment, $\Delta\theta1$, is equal to 0,0055 rad, and the first linear segment stiffness, *k1*, is equal to 19,3 kN.m/rad. An alternative scenario (j = 2, see Table 6.9) considered the Cuplok® joint with large looseness and small initial stiffness, to analyse how the structure can accommodate the ground settlements with small strains. In this scenario, the strong bending axis exhibits 0,03 rad (≈1,72°) looseness, *i.e.* first linear segment rotation increment, $\Delta\theta1$, is equal to 0,03 rad, and the first linear segment stiffness, *k1*, is equal to 1 kN.m/rad.

Table 6.9: Summary of different model characteristics used to analyse ground settlement actions.

Model-ID	Structure (s)	Differential ground settlements configuration (c)	Differential ground settlements value (v)	Cuplok® joint characteristics (j)
s-c-v-j	A2, A4	See Figure 6.19.	v = 1: 10 mm v = 2: 100 mm v = 3: 0 mm	j = 1: default j = 2: large looseness
Example of Model A2-1-1-1: Model A2 with differential ground settlement applied at position 1, equal to 10 mm, and default joint characteristics.				

The results in terms of maximum load applied to the system by the leading action and robustness index values for 32 different models are presented in Table 6.10.

Table 6.10: Results of the models developed to ground settlement actions.

Model	Maximum concrete pressure on formwork (N/mm^2)	Robustness index Eq. 5.34 / Eq. 5.18
A2 reference	**0,03909 (0,0%)**	**0,006 (0,0%) / 0,082 (0,0%)**
A2-1-1-1	0,03565 (-8,8%)	0,005 (-4,3%) / 0,078 (-4,3%)
A2-2-1-1	0,03587 (-8,2%)	0,012 (+104,7%) / 0,195 (+138,8%)
A2-3-1-1	0,03409 (-12,8%)	0,011 (+99,6%) / 0,207 (+154,1%)
A2-4-1-1	0,03039 (-22,3%)	0,007 (+16,1%) / 0,166 (+103,2%)
A2-5-1-1	0,03513 (-10,1%)	0,006 (+2,5%) / 0,098 (+19,6%)
A2-6-1-1	0,03532 (-9,6%)	0,010 (+73,0%) / 0,164 (+101,8%)
A2-7-1-1	0,03571 (-8,7%)	0,014 (+139,3%) / 0,161 (+97,1%)
A2-1-2-1	0,03538 (-9,5%)	0,007 (+14,5%) / 0,093 (+14,5%)
A2-2-2-1	0,02974 (-23,9%)	0,015 (+161,1%) / 0,199 (+143,7%)
A2-4-2-1	0,02051 (-47,5%)	0,010 (+78,5%) / 0,157 (+92,3%)
A2-6-2-1	0,02082 (-46,7%)	0,014 (+151,3%) / 0,179 (+119,9%)
A2-7-2-1	0,01630 (-58,3%)	0,010 (+79,3%) / 0,136 (+67,3%)
A2-8-3-2	0,02873 (-26,5% / 0,0%)	0,008 (38,0% / 0,0%) / 0,098 (20,7% / 0,0%)
A2-7-1-2	0,02757 (-29,5% / -4,0%)	0,007 (28,2% / -7,1%) / 0,098 (19,6% / -0,9%)
A2-7-2-2	0,01525 (-61,0% / -46,9%)	0,005 (-15,6% / -38,8%) / 0,074 (-9,1% / -24,7%)
A4 reference	**0,01401 (0,0%)**	**0,012 (0,0%) / 0,129 (0,0%)**
A4-1-1-1	0,01386 (-1,1%)	0,006 (-49,9%) / 0,074 (-42,7%)
A4-2-1-1	0,01366 (-2,5%)	0,009 (-23,3%) / 0,093 (-27,8%)
A4-3-1-1	0,01355 (-3,3%)	0,006 (-52,8%) / 0,061 (-52,8%)
A4-4-1-1	0,01243 (-11,3%)	0,006 (-48,0%) / 0,054 (-58,4%)
A4-5-1-1	0,01372 (-2,1%)	0,004 (-63,5%) / 0,075 (-41,6%)
A4-6-1-1	0,01369 (-2,3%)	0,005 (-53,6%) / 0,068 (-47,0%)
A4-7-1-1	0,01386 (-1,1%)	0,009 (-21,5%) / 0,125 (-3,4%)
A4-1-2-1	0,01383 (-1,3%)	0,006 (-51,5%) / 0,077 (-40,3%)
A4-2-2-1	0,01348 (-3,8%)	0,009 (-25,4%) / 0,128 (-0,5%)
A4-4-2-1	0,01185 (-15,4%)	0,005 (-58,6%) / 0,086 (-33,8%)
A4-6-2-1	0,01121 (-20,0%)	0,008 (-29,5%) / 0,112 (-13,3%)
A4-7-2-1	0,01092 (-22,1%)	0,007 (-37,9%) / 0,128 (-0,6%)
A4-8-3-2	0,01027 (-26,7% / 0,0%)	0,006 (-44,6% / 0,0%) / 0,082 (-36,7% / 0,0%)
A4-7-1-2	0,01024 (-27,0% / -0,3%)	0,006 (-49,1% / -8,1%) / 0,081 (-37,4% / -1,0%)
A4-7-2-2	0,00791 (-43,6% / -23,0%)	0,006 (-51,1% / -11,7%) / 0,072 (-44,2% / -11,7%)
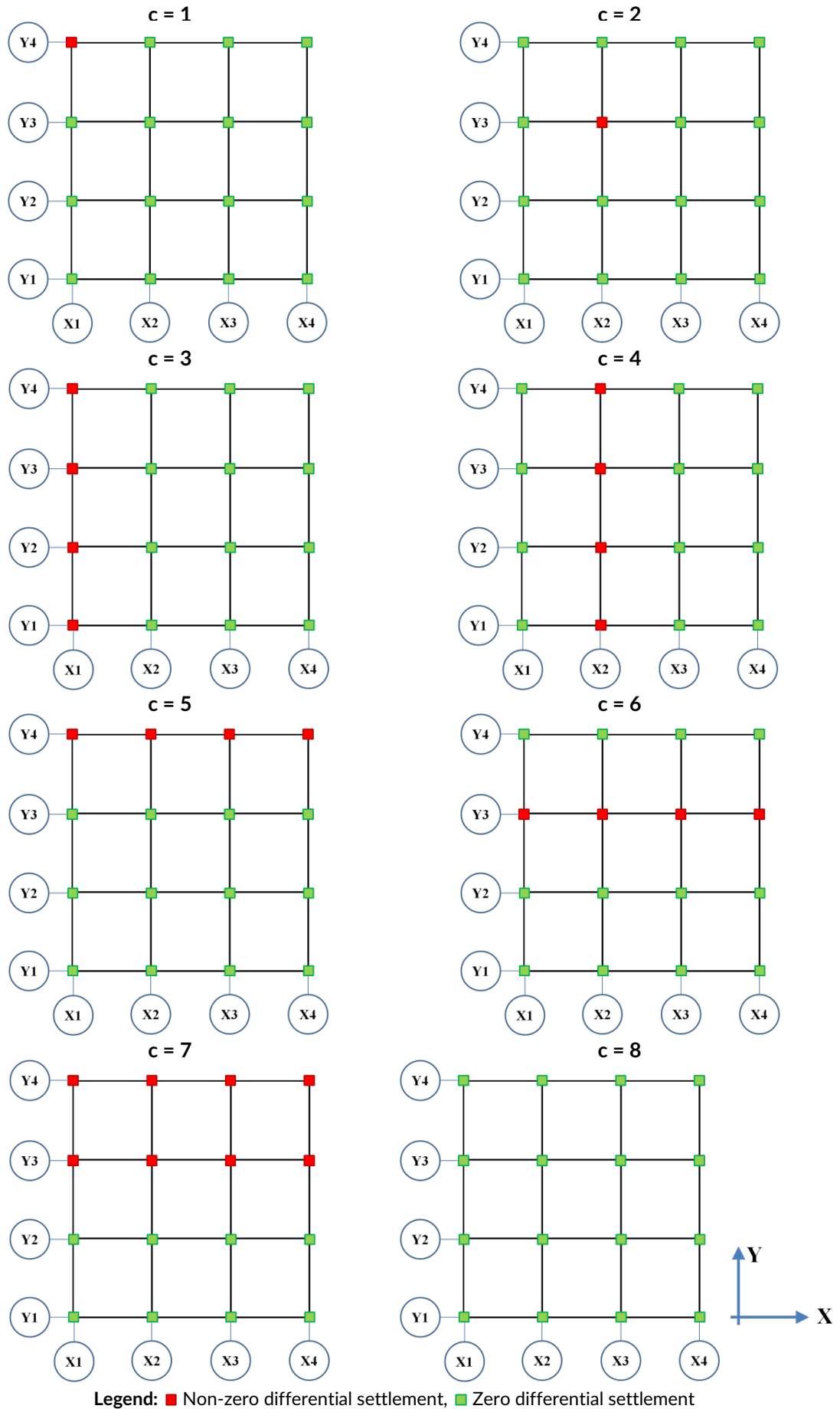
Figure 6.19: Differential ground settlements configurations.

It is possible to observe that there is a noticeable (negative) sensitivity of the considered bridge falsework structures resistance, and of its variability, to the possibility of differential ground settlements. Even for residual differential ground settlements (*e.g.* 10 mm) it was found that there is a critical scenario where a localised residual differential ground settlement can generate a significant reduction of the resistance capacity of the tested falsework structures, see result of Model A2-4-1-1 (*i.e.* larger than 20% of the resistance of the reference system). For higher settlement values, the critical scenario changes from a localised occurrence to a more widespread occurrence, see models A2-7-2-1 and A4-7-2-1 for example, with an increase of the negative impact on the system's resistance, which could represent less than 50% of the resistance of the reference system.

It is also possible to conclude that the resistance of stiffer falsework systems seems to be more sensitive to differential ground settlements. When comparing the results from models A2 (braced systems) with the results from models A4 (unbraced systems), the reduction of the resistance in the former models can reach values up to 50% whereas in the latter models the maximum reduction is approximately half of this value, against the resistance of the reference system.

In addition, the influence of the presence of large looseness at the Cuplok® joints was also analysed. This can occur due to application of a deficient lock procedure of these joints. The result is a large drop on the system's resistance, see results of models A2-8-3-2 and A4-8-3-2. However, these systems, with increased looseness at the Cuplok® joints, are relatively less sensitive to differential ground settlements than the original systems with residual looseness; compare the differences between the results of model "A2 reference" with models A2-7-1-1 and A2-7-2-1 against the differences between the results of Model A2-8-3-2 with models A2-7-1-2 and A2-7-2-2. This can be justified because the presence of significant looseness at the Cuplok® joints helps the system to accommodate differential ground settlements with less induced strains than the ones that occur in a system with smaller looseness at the Cuplok® joints.

Not only the resistance of stiffer falsework systems seems to be more sensitive to differential ground settlements, but also their robustness. However, in contrary to what happened with resistance, differential ground settlements can actually increase (up to 150% more) the robustness of these more stiff systems. This apparent paradox is justified because differential ground settlements submit these structures to higher deformations and in a larger scale in terms of number of elements than if no differential ground settlements were imposed, compare Figure 6.20 with Figure 6.21.
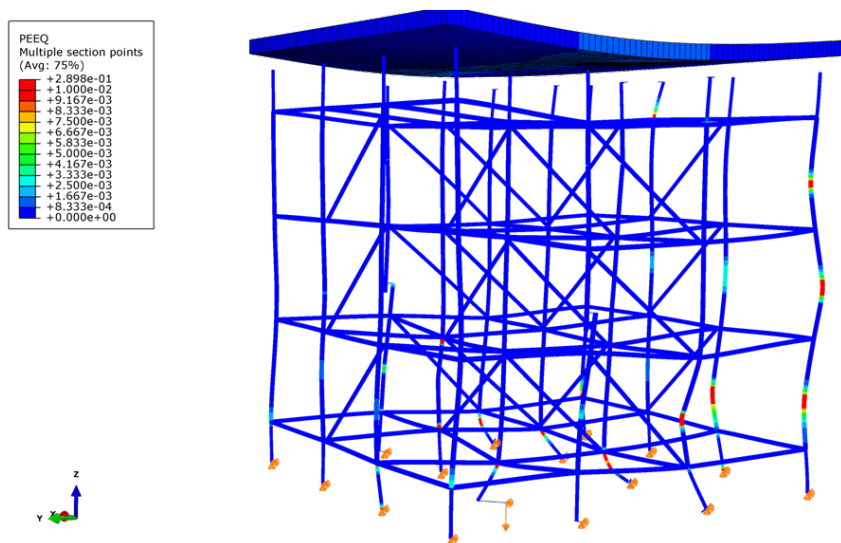
**Figure 6.20: Deformed shape and plastic strains distribution
at "unavoidable collapse" state: Model A2-2-2-1.**
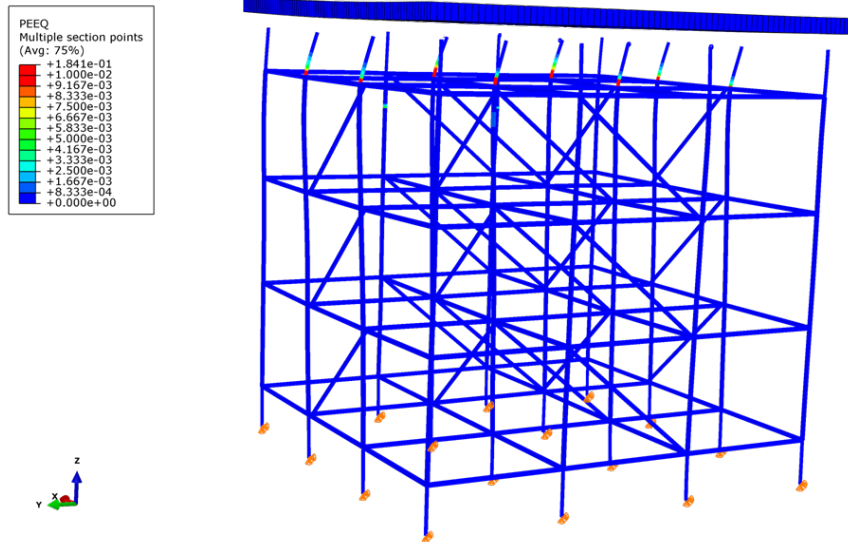
Figure 6.21: Deformed shape and plastic strains distribution at "unavoidable collapse" state: Model A2 reference.
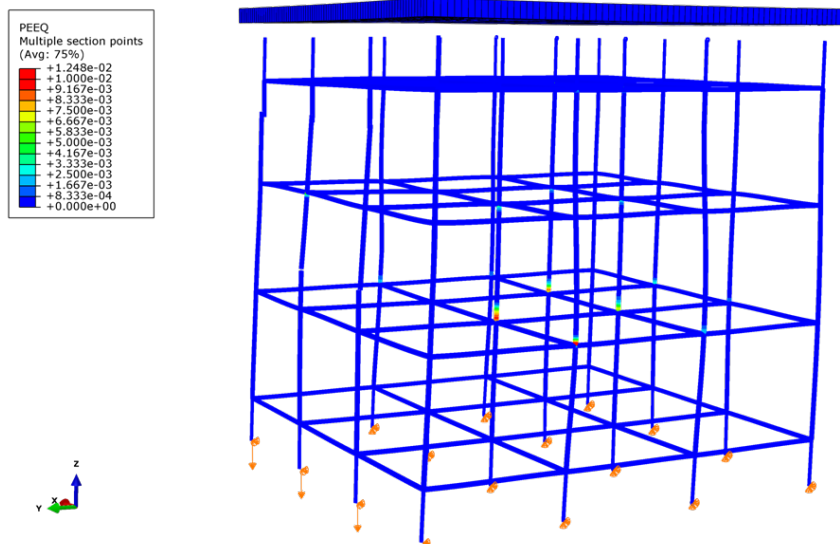
Figure 6.22: Deformed shape and plastic strains distribution at "unavoidable collapse" state: Model A4-5-1-1.
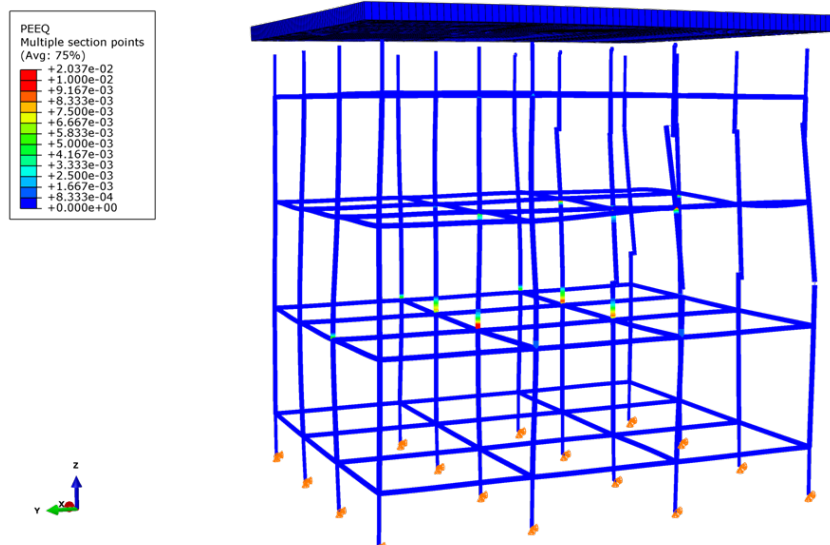
Figure 6.23: Deformed shape and plastic strains distribution at "unavoidable collapse" state: Model A4 reference.

On the other hand, the same does not occur for the braceless models, since there is less resistance to imposed deformations and so the structure deforms without major damages, compare Figure 6.22 with Figure 6.23. The reduction of the robustness index values in the A4 models can reach values up to 60%. Finally, the presence of high values of looseness in the Cuplok® joints reduces further the system robustness.

Figure 6.24 and Figure 6.25 present additional results, related with structural fragility for models of type A2 and A4, respectively. It was already shown that for the structural configurations and external actions considered, robustness index values were low (less than 0,20) meaning that collapse is disproportionate, and damages concentrate in a small number of elements.
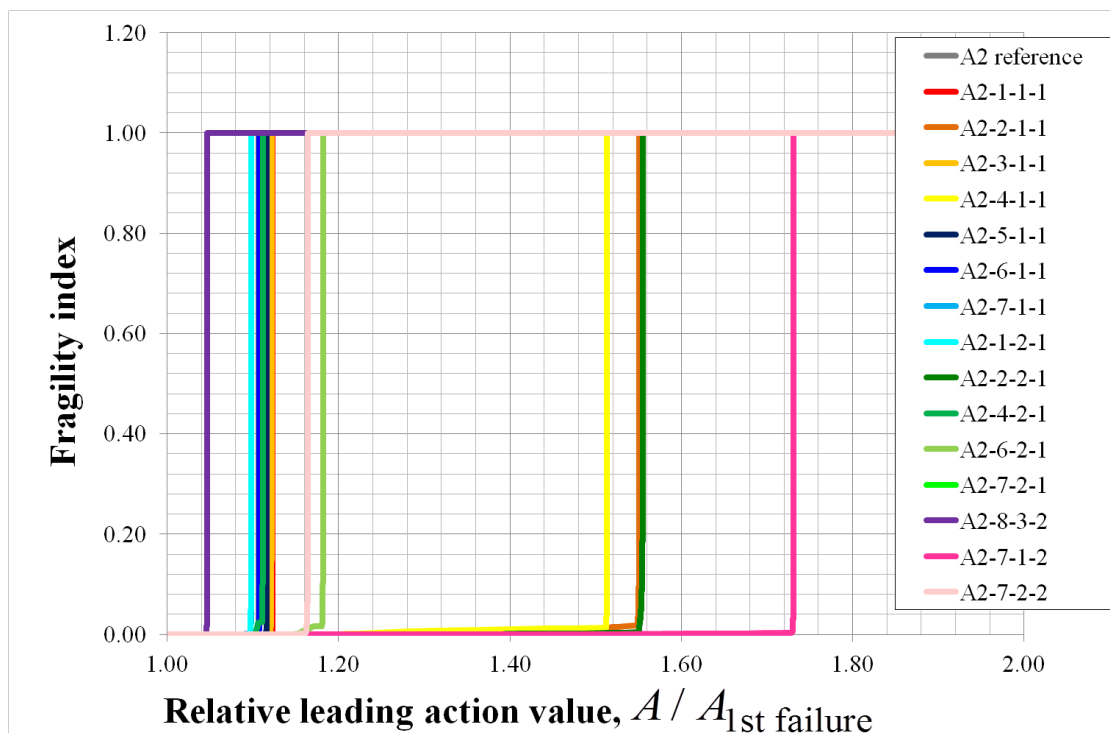
Figure 6.24: Fragility curves of the models developed to analyse ground settlement actions: A2 models.
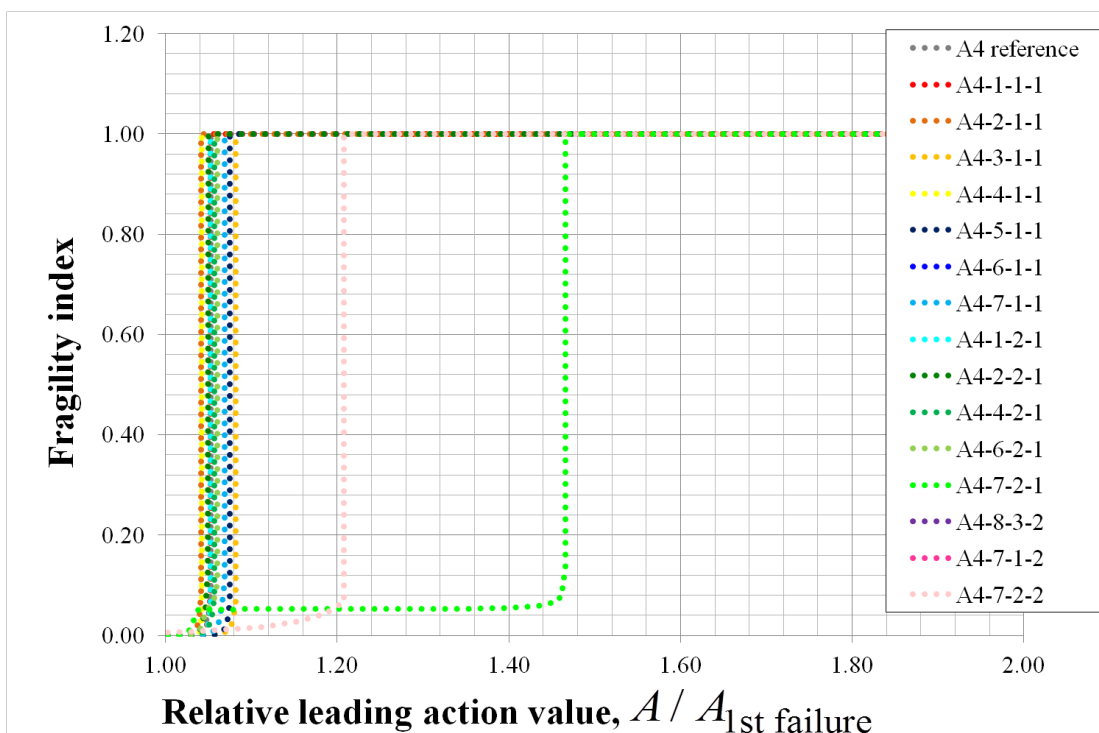
Figure 6.25: Fragility curves of the models developed to analyse ground settlement actions: A4 models.

The fragility curves further show that the structural resistance after first damage occurs is in general also small (in the majority of the scenarios 20% is the maximum value of the ratio between maximum and first damage action value), particularly in the A4 type models, so collapse is abrupt after first damage.

However, for some configurations and specific application scenarios of ground settlements, there is a substantial resistance capacity reserve after first damage occurs, namely when the settlement is widespread in the structure and high values of looseness exist in the Cuplok® joints. In these cases, collapse may be avoided if early damages are detected in time as damage accumulation with increasing action values is slow, until collapse is imminent where they increase exponentially. For the great majority models, the damages just before collapse do not represent more than 10% of the potential damage capacity of the entire structure, so if a damage detection system is used it should be developed considering this information. In some braced models, this value can reach 20%.

As for the previous actions, fragility values of bridge falsework systems are also found to be extremely sensitive to ground settlement action values, since for the majority of the action values fragility is either approximately equal to zero or equal to one.

6.4.1.1.4 Actions combination

The previous sections concentrated in studying the potential impact of the application of external actions of three different natures, *i.e.* concrete pressures, wind and ground settlements, in the safety and performance of bridge falsework structures, taking as application examples cases of simple structural systems. It could be concluded that in general the robustness of this type of structures is very small, with only a small number of elements significantly damaged and less than 20% of the total damage energy of the system being needed to attain complete collapse. Also, the resistance capacity reserve after first damage is also in general not large. Thus, collapse was found to be disproportionate and abrupt. Structural fragility values are almost dual, either equal to zero or equal to one because of the previous considerations.

However, up until now the combined effect of these three different actions was not considered.

Several numerical models were developed to determine how much penalising combining the three different actions would be to the safety and performance of bridge falsework structures with respect to the results of each action applied in isolation. A total of eight models were developed. Table 6.11 presents the model labels and characteristics.

Regarding wind action, only the working wind velocity was considered to analyse the most frequent hazard scenario. Also, two scenarios were considered for the differential ground settlements: (i) a localised and (ii) a widespread differential ground settlement.

Table 6.11: Summary of different model characteristics used to analyse combined effect of external actions.

Model-ID	Structure (s)	Actions during assembly phase (p1)	Actions during concrete casting phase (p2)			Actions after concrete casting is finished (p3)
s-p2	A2, A4	Working wind	Working wind + differential ground settlement + reference slab			Working wind+ upper limit slab
			Label	Differential ground settlement		
				Value	Location (see Figure 6.19.)	
			p2 = 2-10	10 mm	c = 2	
			p2 = 2-100	100 mm		
			p2 = 7-10	10 mm	c = 7	
			p2 = 7-100	100 mm		

During phase *p1* only the wind action was applied. All actions were combined in phase *p2*. As a simplification, during this phase, the concrete casting loads were modelled as a uniform load distributed over the entire formwork surface which value increased until the weight of a reference

slab thickness was attained. For Model A2 a 0,5 m reference slab thickness was considered whereas for Model A4 a 0,25 m reference slab thickness was considered.

In phase *p3*, the weight of the slab was increased until collapse was reached (leading action) maintaining the wind action equal to the working wind.

The results in terms of maximum load applied to the system by the leading action and robustness index values for eight different models are presented in Table 6.12.

Table 6.12: Results of the models developed to analyse combined effect of external actions.

Model	Maximum concrete pressure on formwork (N/mm^2)	Robustness index Eq. 5.34 / Eq. 5.18
A2 reference	**0,03909 (0,0%)**	**0,006 (0,0%) / 0,082 (0,0%)**
A2-2-10	0,03493 (-10,7%)	0,017 (+196,8%) / 0,188 (+130,8%)
A2-2-100	0,02901 (-25,8%)	0,024 (+328,9%) / 0,350 (+328,9%)
A2-7-10	0,03072 (-21,4%)	0,030 (+425,9%) / 0,375 (+360,2%)
A2-7-100 (**)	0,01208 (-69,1%)	0,002 (-56,5%) / 0,062 (-23,8%)
A4 reference	**0,01401 (0,0%)**	**0,012 (0,0%) / 0,129 (0,0%)**
A4-2-10	0,01336 (-4,6%)	0,005 (-55,6%) / 0,092 (-28,9%)
A4-2-100	0,01290 (-8,0%)	0,006 (-52,7%) / 0,098 (-24,3%)
A4-7-10	0,01337 (-4,6%)	0,006 (-52,8%) / 0,097 (-24,5%)
A4-7-100	0,01063 (-24,2%)	0,006 (-52,1%) / 0,099 (-23,3%)
(**) Collapse occurred during phase *p2*.		

Comparing the results of Table 6.12 with the corresponding results presented in Table 6.4, Table 6.8 and Table 6.10, *i.e.* considering only the models in which the wind action matched the working wind velocity, it can be observed that the combined effect of external actions is more severe than the effect of each action in isolation. For example, the resistance values of Model A4-2-1-2-1-1 (see Table 6.8) and Model A2-2-1-1 (see Table 6.10) are noticeably larger than the corresponding result of Model A2-2-10. The same applies for all the other models.

Therefore, bridge falsework systems must be designed accounting for all foreseeable actions and their concomitant values. As Table 6.13 shows, the safety value that is obtained if during the design only vertical loads are considered, relative to the producer design value, is almost eaten up entirely by just considering the combined effect of multiple external actions. It is not difficult to think of cases where this smaller partial factor would be reduced even further and possibly exhausted, for example: if larger initial geometrical imperfections and/or lower stiffness values of some of the various joints occurred, or the design was not done properly (including adopting wrong values from design load tables published by producers). Details on these risks, and others, have already been given in this Chapter and previous Chapters of the present Thesis.

Table 6.13: Comparison of results.

Resistance (N/mm^2)	Reference models (R)	Table 6.12 results (C)	Producer design value (P) (*)	R/P	C/P
Model A2	0,03909	0,01208 (a)	0,0072	5,43	1,68
Model A4	0,01401	0,00750 (b)	0,0054	2,59	1,39
(a) Model A2-7-100					
(b) Model A4-7-100					
(*) Based on internal columns design value (namely over-extended internal jack elements)					

Conversely, robustness index values increase due to the effects of the differential ground settlements for braced models and decrease further in the unbraced models. This means that there are more elements participating to the deformation energy dissipated by the system in the former models and less elements and with smaller damage energy capacity in the latter models (namely the spigot joints), as can be seen in Figure 6.26 and Figure 6.27.

Figure 6.28 present additional results, related with structural fragility for models of type A2 and A4, respectively. It was already shown that for the structural configurations and external actions

considered, robustness index values were in general low (less than 0,10) meaning that collapse is in general disproportionate. However, for some braced models subject to large values of isolated differential ground settlements (Model A2-2-100) or small values of widespread differential ground settlements (Model A2-7-10), robustness index can reach values up to 0,35 meaning that the structure dissipates a third of its maximum energy dissipation capacity before collapse is attained.

The fragility curves further show that the structural resistance after first damage occurs is in general also small (in the majority of the scenarios 20% is the maximum value of the ratio between maximum and first damage action value), particularly in the A4 type models, so collapse is abrupt after first damage.
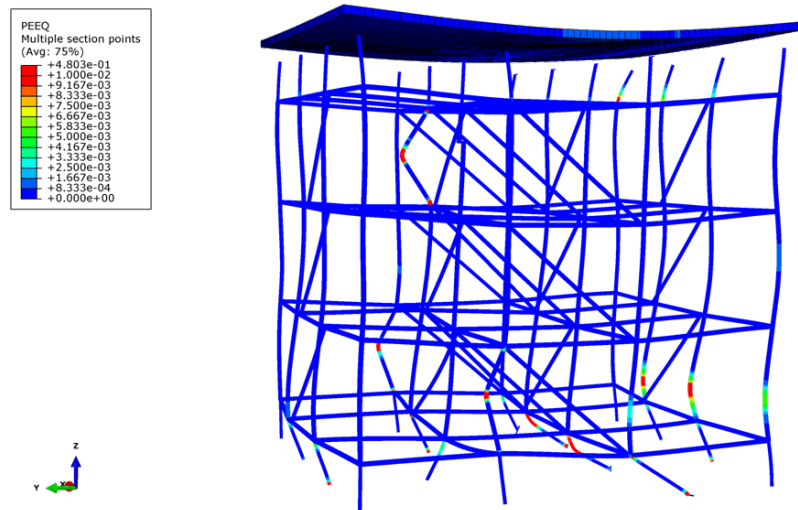
**Figure 6.26: Deformed shape and plastic strains distribution
at "unavoidable collapse" state: Model A2-2-100.**
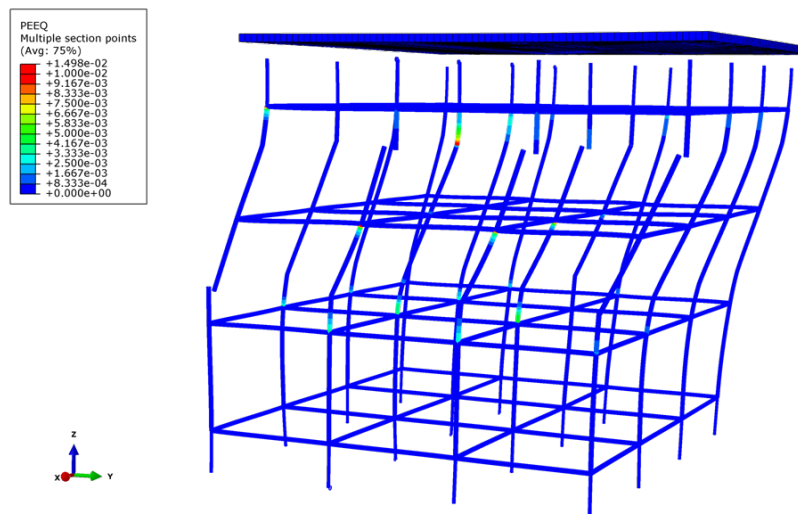
**Figure 6.27: Deformed shape and plastic strains distribution
at "unavoidable collapse" state: Model A4-2-100.**

However, for some configurations, namely A2 type models, there is a substantial resistance capacity reserve after first damage occurs. In these cases, collapse may be avoided if early damages are detected in time as damage accumulation with increasing action values is slow, until collapse is imminent where they increase exponentially. For braced models (A2 type models), the damages just before collapse could represent 30% of the potential damage capacity of the entire structure, but for unbraced models (A4 type models) this value is smaller (about 10%). Therefore, if a damage detection system is used it should be developed considering this information.

As for the previous actions, fragility values of bridge falsework systems are also found to be extremely sensitive to ground settlement action values, since for the majority of the action values fragility is either approximately equal to zero or equal to one.
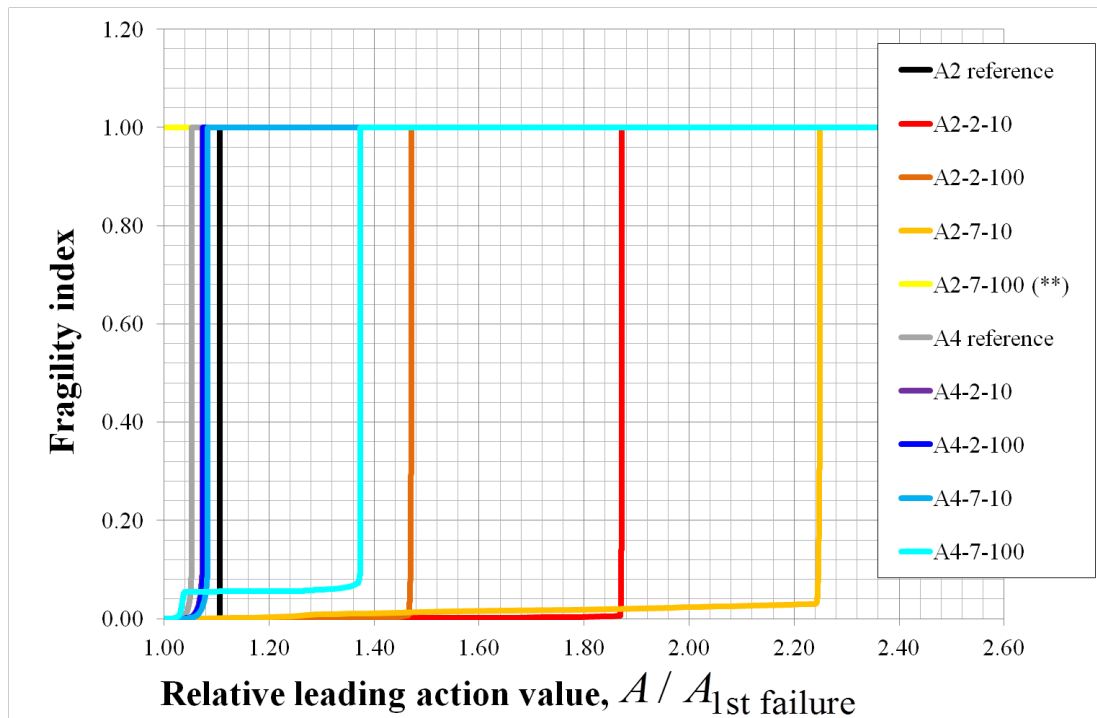
Figure 6.28: Fragility curves of the models developed to analyse combined effect of external actions.

6.4.1.2   System configuration related hazards

In the previous section the critical external hazards were analysed. In this section the internal hazards will be studied. In particular (i) bracing configurations; (ii) joint characteristics; (iii) falsework system with steel beam girders; (iv) gross initial geometrical imperfections; (v) positioning of spigot joints and ledger elements.

6.4.1.2.1   Bracing elements configuration

Bracing is an essential part of any bridge falsework since it increases the system's lateral stability. As was already seen, not including bracing elements has a severe impact on the falsework resistance and can also decrease the system's robustness. However, there are many possible bracing configurations and it is of interest to analyse which of these are more beneficial in terms of safety and performance of bridge falsework structures.

Producer documents recommend not placing brace elements more than 50 mm apart of the ledger-to-standard joints (SGB, 2006). Nevertheless, values much higher are often found in practice. Also, brace elements can be connected to a ledger element or to a standard element. Additionally to the bracing eccentricity, another variable was considered which is the positioning of internal braces when connected to ledgers, see Figure 6.29.

To analyse how these variables influence the system's resistance and robustness various models were developed and summarised in Table 6.14. The geometry, material and joint properties of the reference models are identical to the ones presented in the previous sections, where the brace elements are internally connected to the ledgers with an eccentricity equal to 60 mm.

The only action considered was the one due to the concrete weight placed on top of the formwork. This load was increased until collapse was attained. The results are presented in Table 6.15.
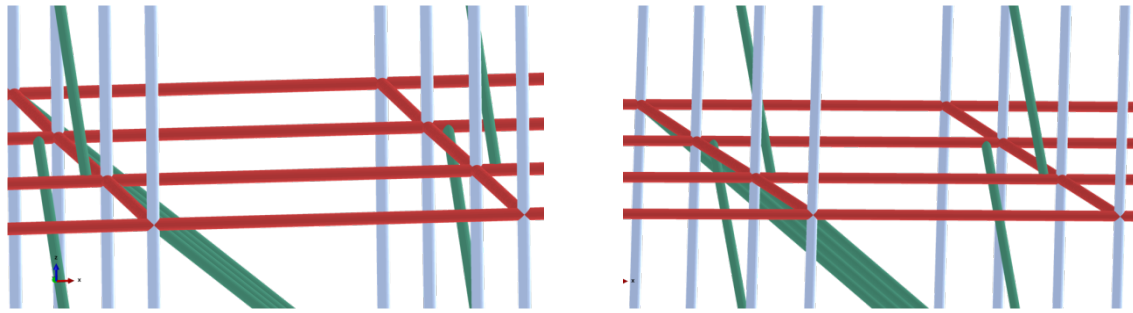
Figure 6.29: Outside (*Left*) and inside (*Right*) positioning of the brace elements.

Table 6.14: Summary of different model characteristics used to analyse bracing eccentricities.

Model-ID	Structure (s)	Connected elements (c) see Figure 6.29	Eccentricity (e)
s-c-e-p	A2, A4	c = 1O: Brace-to-ledger (outside) c = 1I: Brace-to-ledger (inside) c = 2: Brace-to-standard	e = 1: 0 mm e = 2: 50 mm e = 3: 100 mm e = 4: 200 mm e = 5: 400 mm

Table 6.15: Results of the models developed to analyse bracing eccentricities.

Model	Maximum concrete pressure on formwork (N/mm^2)	Robustness index Eq. 5.34 / Eq. 5.18
A2 reference	**0,03909 (0,0%)**	**0,006 (0,0%) / 0,082 (0,0%)**
A2-X-1	0,03971 (1,6%)	0,008 (+33,2%) / 0,101 (+24,3%)
A2-1O-3	0,03797 (-2,9%)	0,005 (-3,9%) / 0,078 (-3,9%)
A2-1I-3	0,03842 (-1,7%)	0,005 (-9,8%) / 0,064 (-21,1%)
A2-1O-4	0,03459 (-11,5%)	0,005 (-18,4%) / 0,072 (-12,1%)
A2-1I-4	0,03555 (-9,1%)	0,004 (-21,7%) / 0,069 (-15,7%)
A2-1O-5	0,02463 (-37,0%)	0,004 (-23,8%) / 0,072 (-11,1%)
A2-1I-5	0,02724 (-30,3%)	0,004 (-34,2%) / 0,063 (-23,2%)
A2-2-2	0,03897 (-0,3%)	0,005 (-18,9%) / 0,062 (-24,3%)
A2-2-3	0,03856 (-1,4%)	0,006 (-0,9%) / 0,075 (-7,5%)
A2-2-4	0,03634 (-7,1%)	0,006 (+5,6%) / 0,093 (+13,7%)
A2-2-5	0,02679 (-31,5%)	0,008 (+35,9%) / 0,119 (+46,4%)
A4 reference	0,01401 (-64,2%)	0,012 (+105,7%) / 0,129 (+58,4%)

It can be observed that resistance and robustness decrease with the increase of the brace eccentricity when brace elements are connected with ledger elements. Also, the inside positioning of the bracing is found to be beneficial when compared to the outside positioning. This happens because the bracing when the former positioning is adopted is more effective in providing lateral stiffness to the core columns (more stressed).

When bracing is connected to standard elements, resistance also decreases with the increase of the brace eccentricity, but robustness increases and tends to the robustness of the braceless system. This did not occur when brace elements are connected with ledger elements because the brace elements introduce large forces on the ledgers, mainly in the direction of the weak bending axis of the Cuplok® joints. Thus brace and ledger elements exhibit large displacements which diminish the stiffness of Cuplok® joints about the weak bending axis, see Figure 6.30. Therefore both lacing and bracing effectiveness is reduced and lateral stability of the system is rapidly lost.

Combined with loss of resistance and robustness, large bracing eccentricities also reduce the resistance capacity reserve after first damage, see Figure 6.31.

The fragility curves further show that the structural resistance after first damage occurs is in general also small (15% is the maximum value of the ratio between maximum and first damage action value), so collapse is abrupt after first damage.

Figure 6.30: Overview of deformed shape and bending moment distribution (about weak bending axis of Cuplok® joints) in Model A2-1I-5. Columns have been removed for clarity.
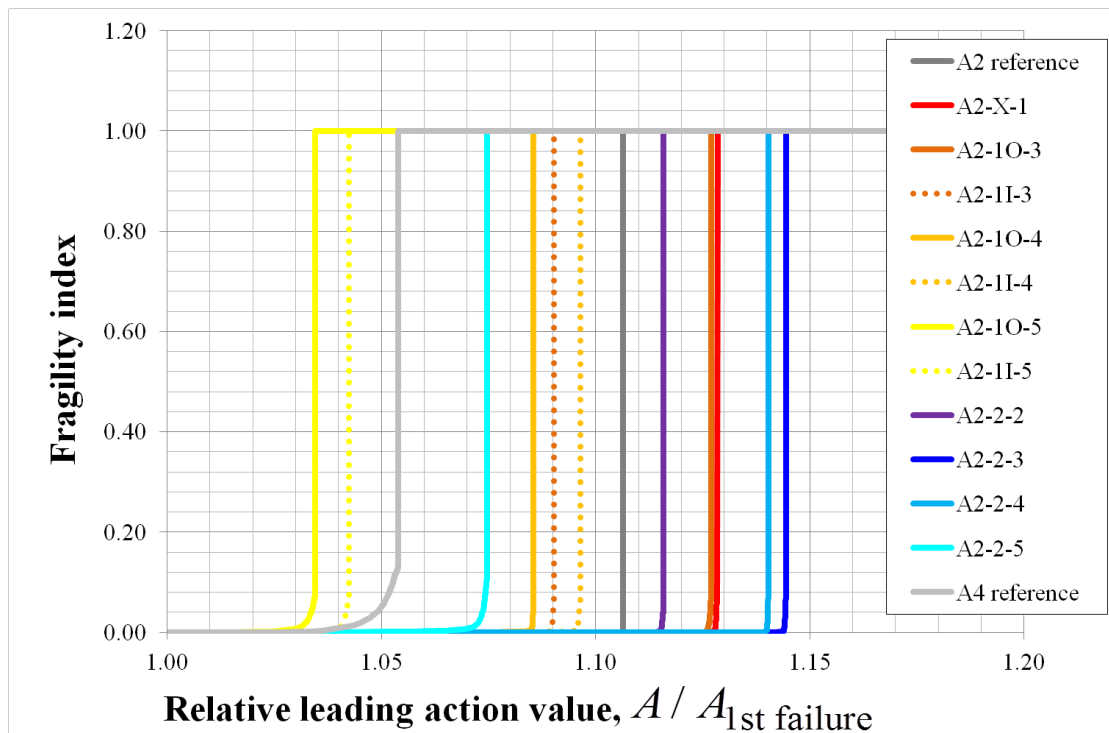
Figure 6.31: Fragility curves of the models developed to analyse bracing eccentricities.

The damages just before collapse only represent 10% of the potential damage capacity of the entire structure. Therefore, if a damage detection system is used it should be developed considering this information.

As for the previous cases, fragility values of bridge falsework systems are also found to be extremely sensitive to bracing eccentricities, since for the majority of the action values fragility is either approximately equal to zero or equal to one.

Also, there are many possible bracing arrangements. As a minimum amount of bracing it is recommended that "*one complete brace from the top to the bottom ledger level in a continuous diagonal line, on each row of standards, one in seven bays in each direction*" (SGB, 2009), see Figure 6.32. "*This is preferable to the zig-zag or parallel bracing in one bay (...) as it reduces the additional load in a leg due to the horizontal loading. It is preferable that braces in adjacent panels should also be alternated in direction, as*

shown by the dashed lines" in Figure 6.32 (SGB, 2009). It is however common to find bridge falsework structures with bracing only at the extreme faces, in both directions. Also, jack bracing is usually avoided but often it is necessary.

In order to assess the outcome of different bracing arrangements on the safety and performance of bridge falsework structures several models were developed. Table 6.16 summarises the various models and their characteristics. The bracing shown in Figure 6.33 (b = 12 and b = 13) alternates the direction in adjacent bays. The geometry, material and joint properties of the reference models are identical to the ones presented in the previous sections. The only action considered was the one due to the concrete weight placed on top of the formwork. This load was increased until collapse was attained. The results are presented in Table 6.17.


Figure 6.32: Recommended bracing layout (©HARSCO, www.harsco-i.co.uk).

Table 6.16: Summary of different model characteristics used to analyse bracing arrangements.

Model-ID	Structure (s)	Bracing arrangements (b)
s-b	A2, A4	See Figure 6.33.

Table 6.17: Results of the models developed to analyse bracing arrangements.

Model	Maximum concrete pressure on formwork (N/mm^2)	Robustness index Eq. 5.34 / Eq. 5.18
A2 reference (A2-1)	**0,03909 (0,0%)**	**0,006 (0,0%) / 0,082 (0,0%)**
A2-2	0,04673 (+19,5%)	0,041 (+617,2%) / 0,527 (+547,1%)
A2-3	0,04225 (+8,1%)	0,007 (+18,6%) / 0,100 (+22,9%)
A2-4	0,04629 (+18,4%)	0,027 (+374,0%) / 0,445 (+445,6%)
A2-5	0,04951 (+26,6%)	0,022 (+289,0%) / 0,458 (+461,8%)
A2-6	0,03576 (-8,5%)	0,027 (+374,2%) / 0,285 (+249,4%)
A2-7	0,01909 (-51,2%)	0,001 (-81,9%) / 0,023 (-71,9%)
A2-8	0,04736 (+21,1%)	0,033 (+473,1%) / 0,451 (452,8%)
A2-9	0,02027 (-48,1%)	0,021 (+267,8%) / 0,262 (+221,8%)
A2-10	0,01424 (-63,6%)	0,009 (+62,7%) / 0,116 (+42,4%)
A2-11	0,01405 (-64,1%)	0,009 (+58,5%) / 0,113 (+38,7%)
A2-12	0,04764 (+21,9%)	0,054 (+848,2%) / 0,610 (+648,2%)
A2-13	0,04848 (+24,0%)	0,053 (+832,8%) / 0,508 (+522,8%)
A2-1 (jack length = 300 mm)	0,04776 (+22,2%)	0,013 (+129,8%) / 0,164 (+101,1%)
A4 reference (A4-1)	0,01401 (-64,2%)	0,012 (+105,7%) / 0,129 (+58,4%)

A2 reference model, b = 1

A2 reference model + central jacks braced, b = 2

All braced, except jacks, b = 3

A2 reference model + all jacks braced, b = 4

All braced, b = 5

1 diagonal per face, b = 6

1 diagonal per face,
tied only at extreme nodes, b = 7

2 diagonals per face, b = 8
2 diagonals per face, only external faces braced, b = 9
2 diagonals per face, only *x* direction braced, b = 10
2 diagonals per face, only *y* direction braced, b = 11

2 diagonals per face, alternate, b = 12

2 diagonals per face, alternate, b = 13

Figure 6.33: Different bracing arrangements.

It can be observed that adding bracing to over-extended jack elements can increase the resistance and increase substantially the robustness of the structure, see models A2-2, A2-4 and A2-5. Introducing these additional brace elements is comparable to reducing considerably (by at least half in the case studied) the jacks extension length, compare Model A2-2 with Model A2-1-300. Also, it can be concluded that adding additional brace elements but not in the over-extended jack elements is not an efficient design strategy, compare Model A2-2 with Model A2-3.

Reducing the number of connections between the brace elements and other elements of the falsework reduces the resistance of the system, see models A2-6 and A2-7. The same conclusion can be drawn in the cases where bracing is only placed at external faces or just in one direction, see models A2-9, A2-10 and A2-11.

As given in the producer recommendations, it is preferable to have one complete brace from the top to the bottom falsework levels in a continuous diagonal line, alternated in direction in adjacent faces, than parallel bracing in one bay (compare models A2-1 and A2-13), or than having multiple diagonal brace lines that are discontinuous (compare models A2-8, A2-12 and A2-13).

In fact, when bracing is placed from the top to the bottom falsework levels in every bay, connected in every level to other falsework elements, it is possible to increase considerably the robustness of the system when compared with other bracing arrangements. For the system configuration investigated in this section robustness index increased from less than 0,10 to up to 0,50. This means that the structure dissipates half of its maximum energy dissipation capacity before collapse is attained. Therefore, collapse is no longer disproportionate in these cases for the external actions considered (concrete weight applied on top of the formwork).

The fragility curves, see Figure 6.34, further show that the structural resistance after first damage occurs is in general also small (15% is the maximum value of the ratio between maximum and first damage action value), so collapse is abrupt after first damage.
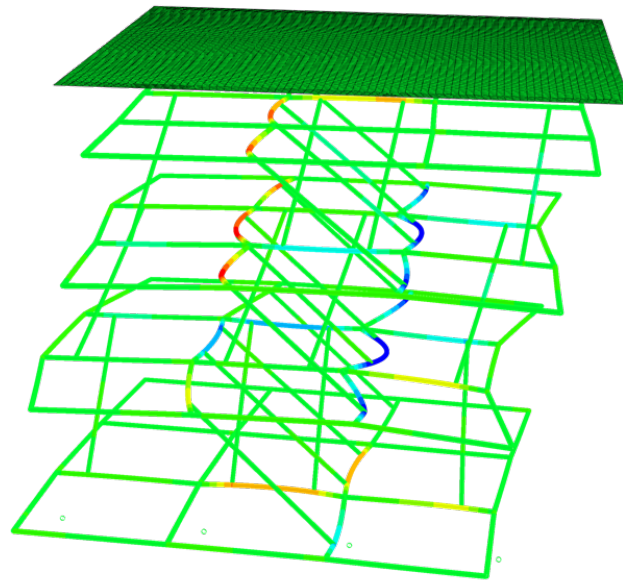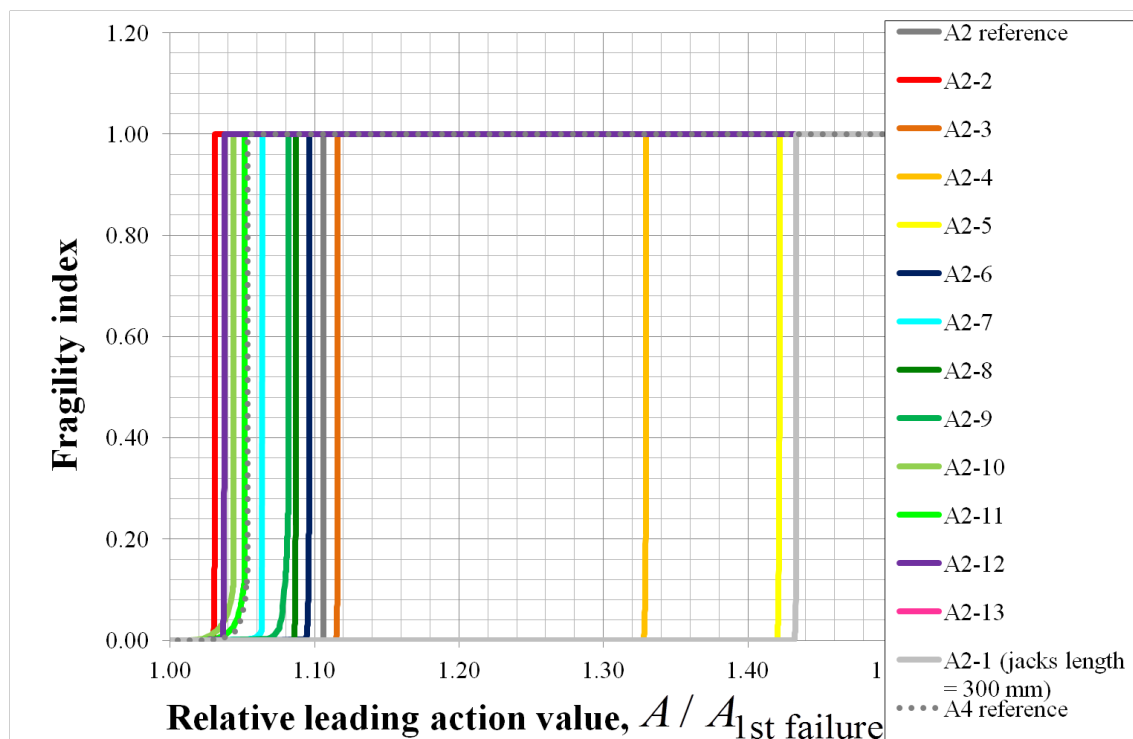

Figure 6.34: Fragility curves of the models developed to analyse bracing arrangements.

Only when the over-extended jacks are fully braced or the extension length is reduced in half, there is a substantial resistance capacity reserve after first damage occurs. In these cases, collapse may be avoided if early damages are detected in time as damage accumulation with increasing action values is slow, until collapse is imminent where they increase exponentially.

An open question that cannot be answered by the simple models that have been used thus far is to assess the last part of this sentence regarding bracing requirements "*one complete brace from the top to the bottom ledger level in a continuous diagonal line, on each row of standards, one in seven bays in each direction*" (SGB, 2009). To assess how sensitive is the resistance and robustness of bridge falsework to spacing between bracing, several models were prepared, see Table 6.18. The falsework of models M1-M3 is 4,4 m high whereas the falsework of models M4-M6 is 12,7 m high. In all models, the bays are spaced 1,8 m apart.

Table 6.18: Summary of different model characteristics used to analyse spacing between bracing.

Model-ID	Bracing arrangements (b)
M-b	See Figure 6.35.

The geometry of the elements, material and joint properties of the models are identical to the ones presented in the previous sections. Bracing was placed in every bay in both directions in plan, alternating its orientation in adjacent bays. The only action considered was the one due to the concrete weight placed on top of the formwork. This load was increased until collapse was attained. The results are presented in Table 6.19.
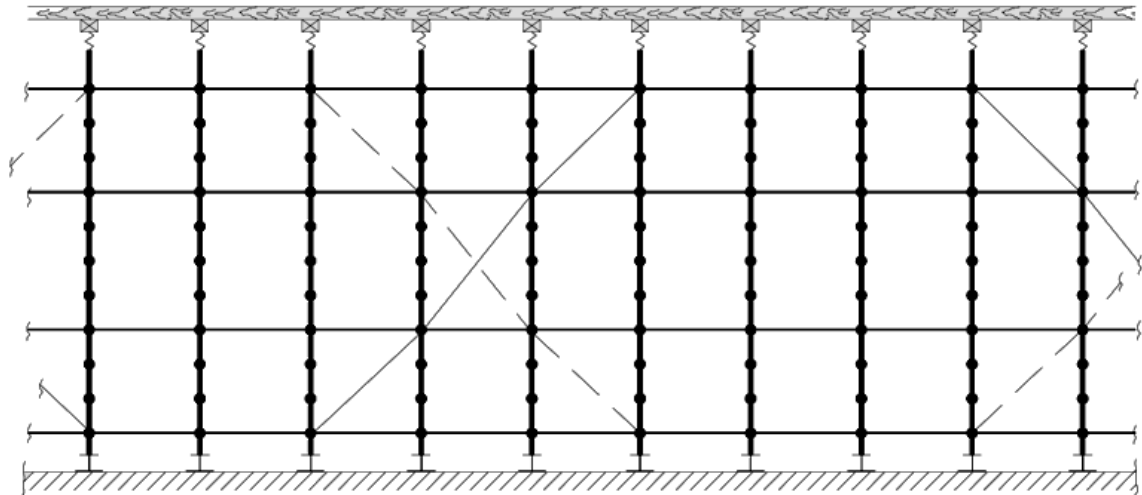
Table 6.19: Results of the models developed to analyse bracing spacing.

Model	Maximum concrete pressure on formwork (N/mm^2)	Robustness index Eq. 5.34 / Eq. 5.18
M-1	**0,04434 (0,0%)**	**0,016 (0,0%) / 0,308 (0,0%)**
M-2	0,04007 (-9,6%)	0,009 (-42,5%) / 0,196 (-36,2%)
M-3	0,03662 (-17,4%)	0,002 (-86,6%) / 0,162 (-47,5%)
M-4	**0,03479 (0,0%)**	**0,001 (0,0%) / 0,041 (0,0%)**
M-5	0,03400 (-2,3%)	0,001 (-45,0%) / 0,028 (-31,6%)
M-6	0,02375 (-31,7%)	0,001 (-58,9%) / 0,026 (-36,0%)

It can be observed that increasing bracing spacing longitudinally decreases both the resistance and robustness of the system, see models M-1 to M-3. In fact spacing each diagonal seven bays apart leads in this case to a reduction of resistance of about 10% when compared with the case where each diagonal starts where the other ends. If spacing is further increased to nine bays the reduction of resistance almost doubles. Regarding robustness, the drop is more pronounced with almost 50% decrease for a nine bays spacing.

However, it is not only the longitudinal spacing that matters. In terms of effectiveness of the bracing its free length is also important (by free length it is meant the length where bracing has the same slope direction). A continuous diagonal line from top to bottom levels of the falsework loses its effectiveness in providing lateral stability if its free length is large when compared with a bracing arrangement with the same total length but where the slope direction is not continuous. This is what can be concluded from models M4 to M6. Therefore, it is important to explicitly model the bridge falsework since design recommendations given in documents released by system producers only contain minimum requirements that may not be sufficient for a specific use. This is especially true for bracing arrangements as was demonstrated.

It can also be observed that structural robustness seem to decrease as the height of the falsework increases. This can be attributed to the fact that bracing loses its effectiveness in providing adequate lateral stability to every column of every bay, at least in the bracing arrangements considered (see models M4 to M6). Thus as one standard buckles others soon follow and the system collapses shortly after.

The fragility curves, see Figure 6.36, confirm that the structural resistance after first damage is very small (2% is the maximum value of the ratio between maximum and first damage action value), so collapse is abrupt after first damage. As for the previous cases, fragility values of bridge falsework systems are also found to be extremely sensitive to bracing eccentricities, since for the majority of the action values fragility is either approximately equal to zero or equal to one.

M-1

M-2

M-3

M-4

M-5

M-6
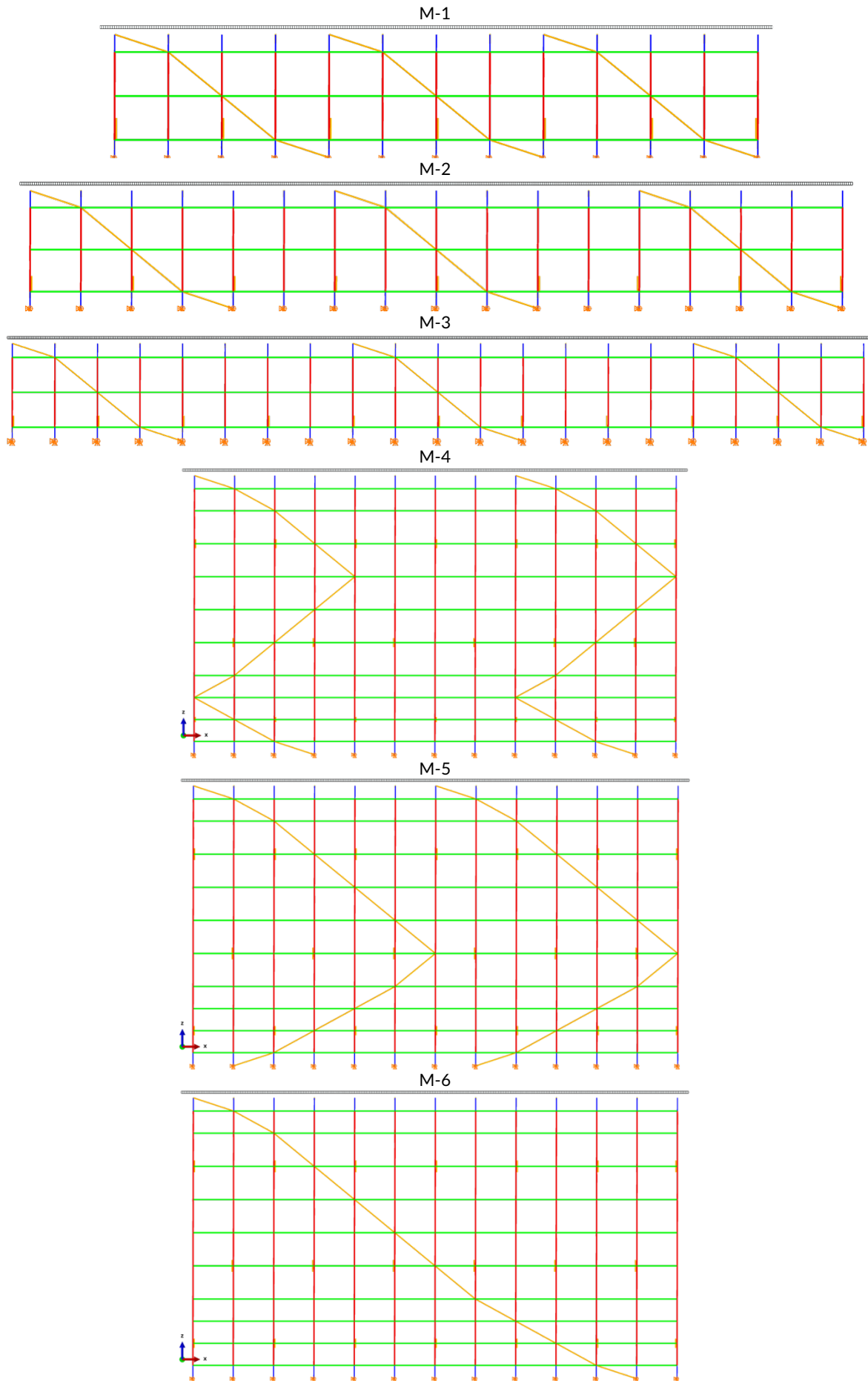
Figure 6.35: Different bracing spacing.
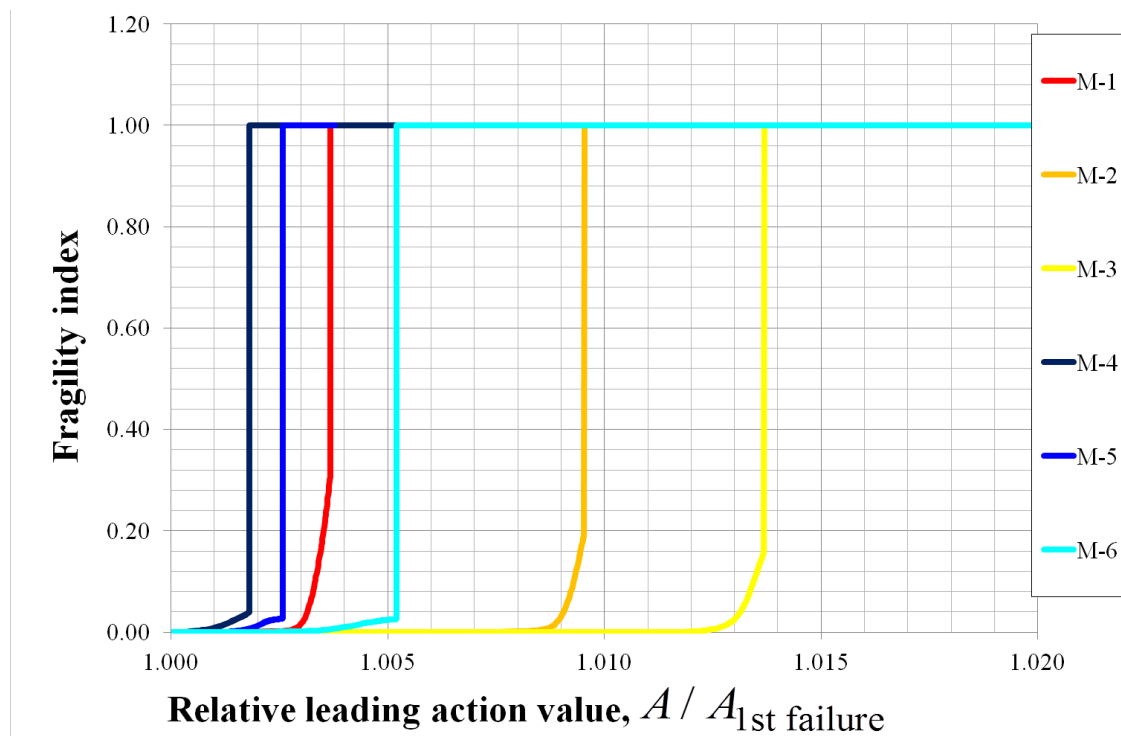
Figure 6.36: Fragility curves of the models developed to analyse bracing arrangements.

6.4.1.2.2 Spigot joints configuration

Having studied the bracing configuration, in this section the focus is on the spigot joints. As was seen in Chapter 4, spigot joints are a weak link of any bridge falsework structure. Depending on the spigot joint stiffness the resistance of the system can vary substantially.

In Cuplok® systems, spigot joints can only be positioned at discrete locations along the vertical element between two consecutive storeys, but they can be near the bottom, the middle or the top of the storey, depending on the length of the storey.

The behaviour of spigots joints depends not only of its characteristics but also on the bending-moment distribution at the column elements. In elastic regime the bending-moment distribution at the column elements depends mainly on (i) the stiffness provided by the ledger-to-standard joints, (ii) the initial imperfections magnitude and shape of the column and (iii) the applied actions. In general, the stiffness of the Cuplok® joints is not large and the ledger-to-standard joints behave as semi-rigid joints. Thus, under distributed horizontal loads (due to wind action for example) the maximum bending-moments are located around mid-height of the column. For vertical loads, the location of maximum bending-moments can either be near the column ends or around mid-height of the column. The deciding factor is the relative weight of the second-order bending-moments distribution due to the combination of local and global initial imperfections of the column against the first-order bending-moments distribution. As the actual initial imperfection configurations are unknown variables during design, the actual effect of the spigot joints positioning is uncertain. Nevertheless, it is of interest to investigate what is the influence on the resistance and robustness of bridge falsework of the positioning of the spigot joints, for the same initial conditions.

Table 6.20 summarises the various models and their characteristics. The same initial imperfections were considered in all models of the same type (A2 and A4). Their values were the ones registered along the columns height during the full-scale tests of models A2 and A4 performed at Sydney University, see Chapter 4 and (Chandrangsu, Rasmussen, 2009a) for details. Under these initial conditions, in some columns bow imperfections were larger than the sway imperfections while in others the opposite case occurred.

Table 6.20: Summary of different model characteristics used to analyse spigot positioning.

Model-ID	Structure (s)	Spigot positioning (p)
s-p	A2, A4	p = 1: near bottom column end p = 2: 1/3 column height p = 3: mid-height of column p = 4: 2/3 column height p = 5: no spigot joints

The geometry, material and joint properties of the reference models are identical to the ones presented in the previous sections. The spigot joints were located at the second and third storeys above bottom jacks (at 1/3 storey height and 2/3 storey height, respectively).

The only action considered was the one due to the concrete weight placed on top of the formwork. This load was increased until collapse was attained. The results are presented in Table 6.21.

Table 6.21: Results of the models developed to analyse spigot positioning.

Model	Maximum concrete pressure on formwork (N/mm^2)	Robustness index Eq. 5.34 / Eq. 5.18
A2 reference	**0,03909 (0,0%)**	**0,006 (0,0%) / 0,082 (0,0%)**
A2-1	0,03984 (+1,9%)	0,006 (+6,8%) / 0,122 (+49,5%)
A2-2	0,03930 (+0,5%)	0,007 (+26,8%) / 0,096 (+18,3%)
A2-3	0,03881 (-0,7%)	0,005 (-19,6%) / 0,066 (-19,6%)
A2-4	0,03901 (-0,2%)	0,006 (+11,1%) / 0,079 (-2,8%)
A2-5	0,04076 (+4,3%)	0,028 (+387,2%) / 0,347 (+326,3%)
A4 reference	**0,01401 (0,0%)**	**0,012 (0,0%) / 0,129 (0,0%)**
A4-1	0,01314 (-6,2%)	0,002 (-79,8%) / 0,035 (-73,1%)
A4-2	0,01424 (+1,6%)	0,010 (-16,7%) / 0,115 (-11,2%)
A4-3	0,01433 (+2,3%)	0,012 (+5,6%) / 0,136 (+5,6%)
A4-4	0,01404 (+0,2%)	0,010 (-11,3%) / 0,122 (-5,4%)
A4-5	0,01470 (+4,9%)	0,018 (+56,7%) / 0,180 (+39,3%)

It can be observed that the influence on the resistance and robustness of bridge falsework of the positioning of the spigot joints differs from each model type (A2 and A4). In the unbraced models (A4) the collapse mode involves large sway displacements which favour the location of maximum bending-moments near the column ends. On the contrary, in braced models the collapse mode is dominated by column buckling which favours the location of maximum bending-moments near the column mid-height. As spigot joints are a weak link, positioning them near the maximum bending-moments leads to a reduction of the resistance and robustness of the system. The inverse case is also true.

If spigot joints can be avoided the robustness of the system increases considerably as full plastic hinges can be formed along the columns. This conclusion must be read having practical considerations in mind.

6.4.1.2.3 Ledger elements configuration

The configuration of ledger elements is also an important part of any bridge falsework solution, since besides bracing they constitute the only internal element that contributes to increase falsework's lateral stability. The recommended layout is to display ledger elements in a continuous uninterrupted line across all vertical elements. Often this recommendation is not followed by not being feasible, by a conscious design option or as a result of bad procedural practices.

In this section, the influence of different ledger layouts on the resistance and robustness of bridge falsework will be investigated. Based on the reference Model A2, previously detailed, three models with alternative ledger configurations were prepared and analysed. Table 6.22 summarises the various models and their characteristics.

The only action considered was the one due to the concrete weight placed on top of the formwork. This load was increased until collapse was attained. The results are presented in Table 6.23 and Figure 6.38.

It can be observed that increasing the column length by adopting an inefficient ledger layout, such as the one of models A2-3 and A2-4, leads to a reduction in the system's resistance when compared with the resistance of a system where the recommended ledger configuration was used. However, by virtue of favouring column buckling instead of failure of jack elements (as in Model A2-1) the robustness of models A2-3 and A2-4 is larger than the one of the reference model.

Also, Model A2-2 shows that missing to understand the behaviour of a bridge falsework solution may lead to ineffective designs. Model A2-2 contains more ledger elements than Model A2-1 but returns almost identical results. This happens because resistance and robustness in both models are controlled by the over-extended jack elements.

Table 6.22: Summary of different model characteristics used to analyse ledgers configuration.

Model-ID	Ledgers configuration (l)
A2-l	See Figure 6.37.

A2 reference model, l = 1   l = 2

l = 3   l = 4

All braced, b = 5   1 diagonal per face, b = 6
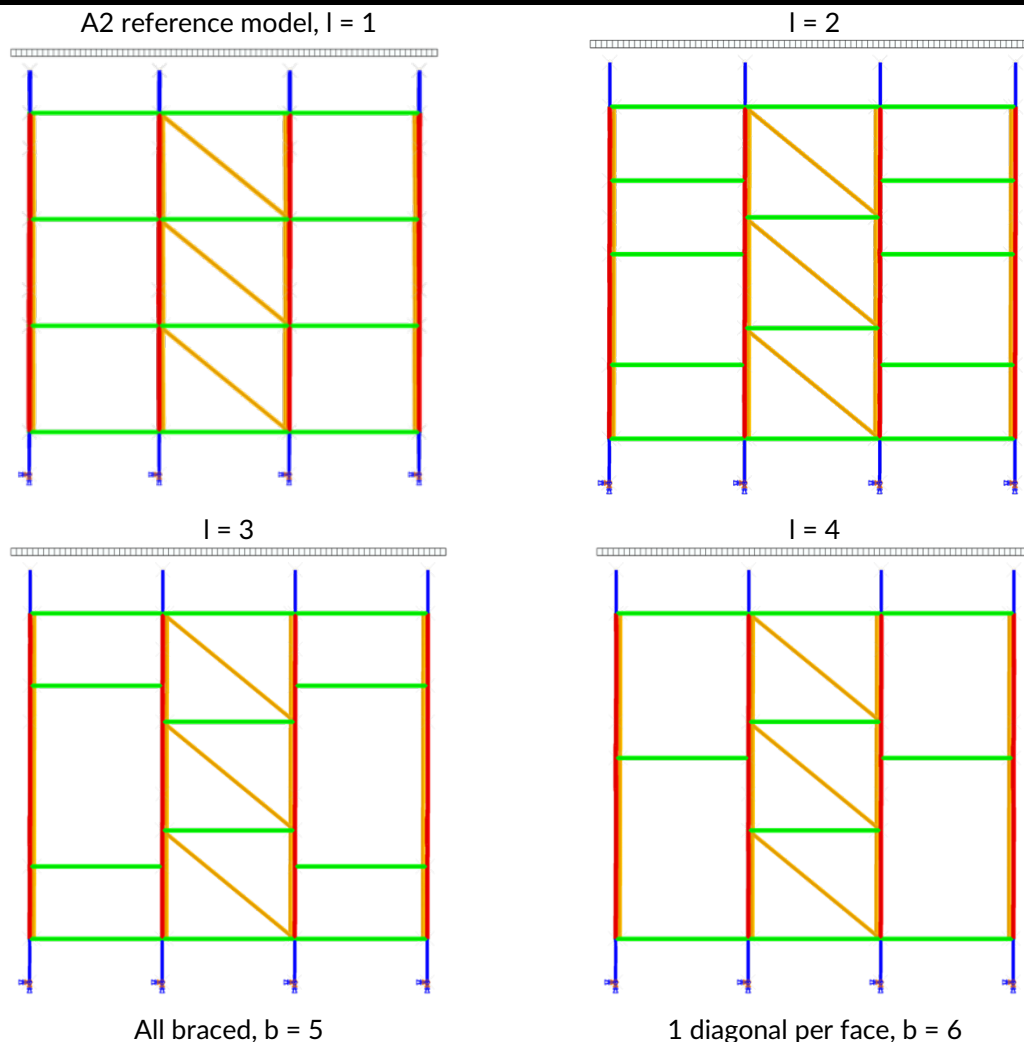
Figure 6.37: Different ledger configurations.

Table 6.23: Results of the models developed to analyse ledgers configuration.

Model	Maximum concrete pressure on formwork (N/mm^2)	Robustness index Eq. 5.34 / Eq. 5.18
A2 reference	**0,03909 (0,0%)**	**0,006 (0,0%) / 0,082 (0,0%)**
A2-2	0,03906 (-0,1%)	0,004 (-25,3%) / 0,077 (-5,9%)
A2-3	0,03698 (-5,4%)	0,021 (+272,6%) / 0,304 (+272,6%)
A2-4	0,03673 (-6,0%)	0,013 (+128,5%) / 0,200 (+145,2%)
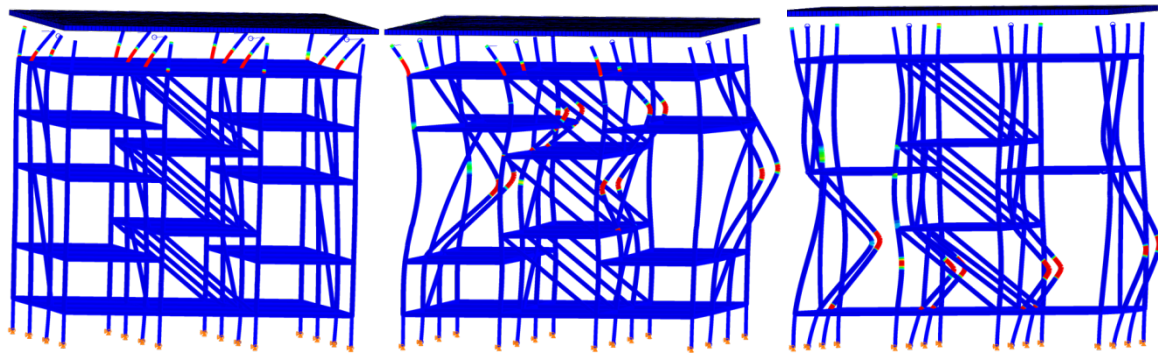
Figure 6.38: Deformed shape and plastic strains distribution of models A2-2 (*Left*), A2-3 (*Centre*) and A2-4 (*Right*) at "unavoidable collapse" state.

6.4.1.2.4 Steel girders configuration

Where the bridge crosses waterways or roads, or the soil properties are weak, steel trusses or steel girders can be used to sustain the formwork, transmitting the loads to falsework towers placed at the ends of the span in order to avoid the obstacles. This system can also be used if the height of the bridge piers is high.

If a simple bridge falsework structure can be a complex design problem, designing bridge falsework with steel girders sustaining a part of the falsework presents some further challenges.

One challenge is to quantify the influence that using steel girders has on the forces distribution on all falsework elements. The vertical elements resting on top of the steel girders will behave as if they were placed over a soft soil with the centre elements experiencing larger "ground" settlements due to the deformation of the steel girder.

Another challenge is to design properly the falsework towers that support the steel girders. These towers bear very large concentrated forces which are transmitted by the steel girders. Therefore, bracing as to be explicitly designed and properly assembled.

There can be also problems related with eccentricities of the falsework vertical elements resting on top of the steel girders with respect to the steel girder shear centre introducing torsion into the beams which in turn can lead to failure of the bottom jack elements of the vertical elements. Also, the steel girders have to be properly designed to resist large concentrated forces and not to lateral buckle. Problems can also appear because gaps might exist between the top jack elements of the falsework towers and the steel girders leading to unbalanced force distributions between tower elements.

To investigate some of these problems various numerical models were developed based on a reference example of a bridge falsework structure using steel girders (model M-1), see Figure 6.39.

The girders structure is made of a central set of seven steel beams spanning 11,6 m. The girders have a square hollow section (SHS) with 500 mm side and 19 mm thickness. The girders rest on each end on top of continuous steel beam with a length equal to the width of the falsework. These beams have a HEB240 section. Lastly, the HEB240 beams transmit the loads to SHS160 steel beams that are simply supported at the extremities by the forkhead plates of the falsework towers.

The width of the falsework is equal to 10,8 m. All ledgers have 1,8 m length, except the ones of the falsework towers which are 1,0 m long. The maximum height of the falsework is 12,65 m and the maximum height of the falsework towers is 5,90 m. The extension lengths of the jacks are as follows: 600 mm for the top and bottom jacks, except the top jacks of the towers which are 300 mm. The minimum storey height of the falsework is 1,0 m and the maximum is 1,5 m.

The bracing shown in Figure 6.39 and Figure 6.40 alternates the direction in adjacent bays.

As the length of the ledger elements of the falsework towers is not the same as the one used for the rest of the falsework, the longitudinal axis of some of the SHS500 girders are on the same vertical

plane than one alignment of vertical elements of the falsework tower, see Figure 6.40. This is not a favourable design solution since these vertical elements will be subjected to very large forces.
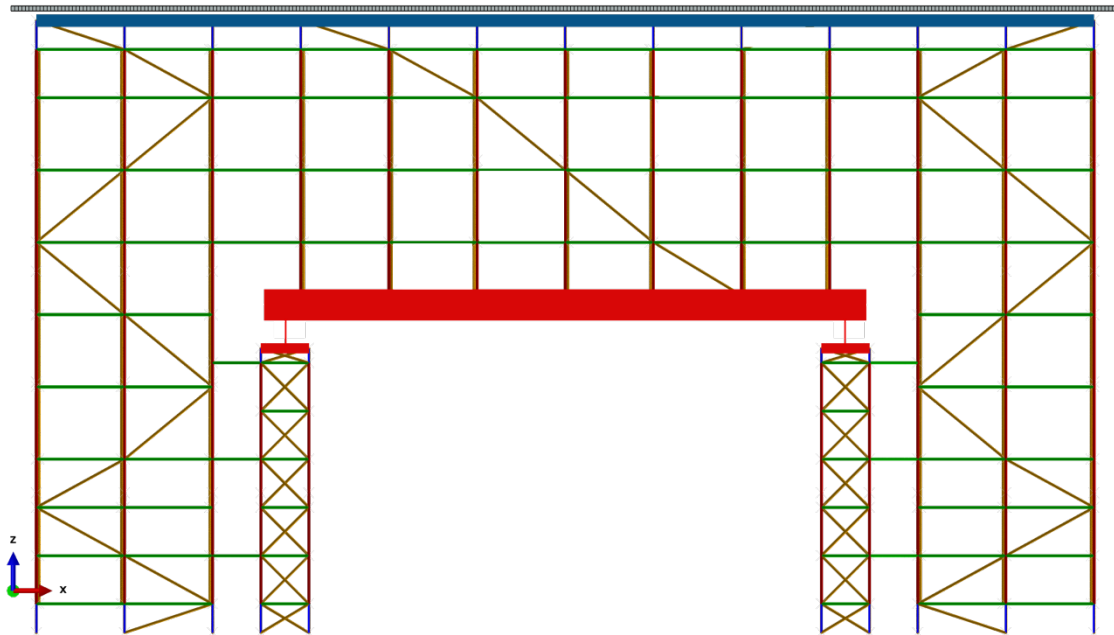
Figure 6.39: Reference example of a bridge falsework structure using steel girders (model M1).
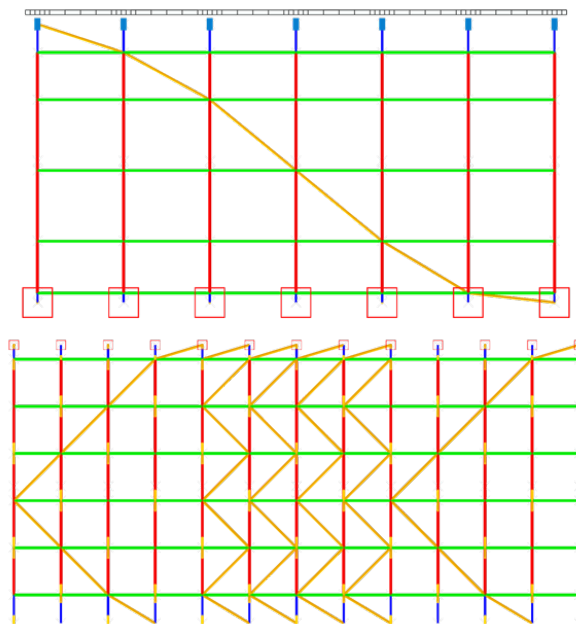
Figure 6.40: Bracing arrangement along the width of the falsework towers (reference model).

A more suitable, but less seen, design option is to use ledger elements of the same length in the falsework towers and in the falsework that is supported by the steel girders. If so, the falsework towers should be moved to one side along their width so that each steel girder meets the falsework towers halfway from two adjacent alignments of vertical elements. Also, instead of using a continuous steel beam to support the girders, it is preferable to use multiple simply supported beams so that the load redistribution is more evenly distributed to the falsework towers. If this method is followed and if no more than eight vertical elements rest on top of steel girders, it is possible to use a storey height in the falsework towers similar to the one used in the falsework elements supported by the steel girders. As always, appropriate bracing should be determined.

The geometry, material and joint properties of the falsework elements and joints are identical to the ones presented in the previous sections. The beams are made of S355 steel.

Additionally, to the reference example, two other models were developed for comparison. One, model M-2, in which bracing of the falsework towers was reduced and another, model M-3, which is a solution without using steel girders, see Figure 6.41 and Figure 6.42. In model M-2 the girders cross-section were also modified to HEB500 which are susceptible to flexural-torsional buckling.

The bracing shown in Figure 6.41 and Figure 6.42 alternates the direction in adjacent bays.
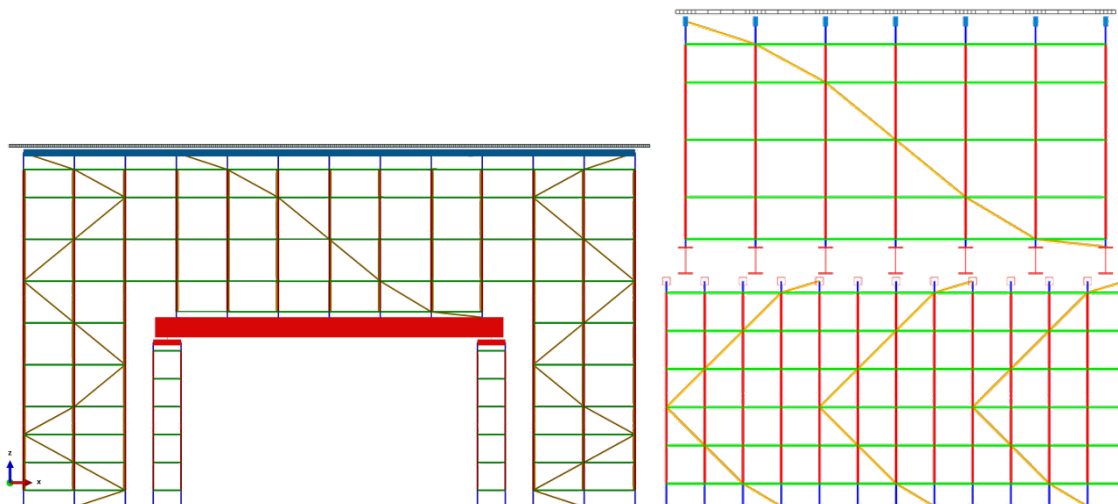
Figure 6.41: Overview of model M-2 and bracing arrangement along the width of the falsework towers.
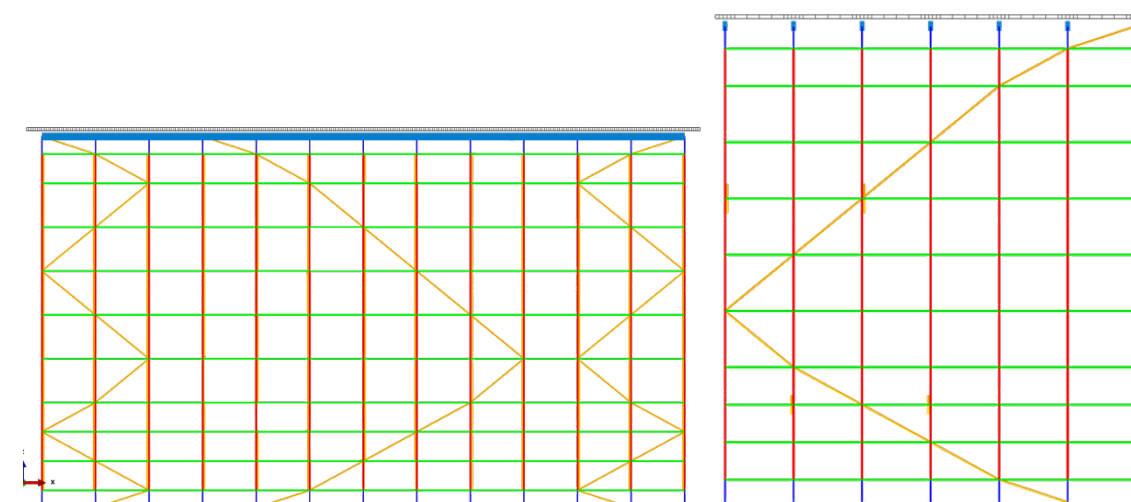
Figure 6.42: Overview of model M-3 and bracing arrangement along the width of the falsework.

The only action considered was the one due to the concrete weight placed on top of the formwork. This load was increased until collapse was attained. The results are presented in Table 6.24.

It can be observed that not designing correctly the bracing of the falsework towers and its connection to the surrounding elements can reduce considerably (to half in the case studied) the resistance obtained if otherwise bracing was properly calculated and assembled on site. Figure 6.43 illustrates the deformed shape of both models during collapse. It can be seen that collapse in model M-2 occurs by failure of the spigot joints of the falsework tower under excessive bending-moments due to large lateral sway displacements, whereas collapse in model M-1 involves failure of different parts of the falsework.

Table 6.24: Results of the models developed to analyse falsework using steel girders.

Model	Maximum concrete pressure on formwork (N/mm^2)	Robustness index Eq. 5.34 / Eq. 5.18
M-1	**0,02676 (0,0%)**	**0,003 (0,0%) / 0,061 (0,0%)**
M-2	0,01436 (-46,4%)	0,000 (-87,1%) / 0,017 (-71,7%)
M-3	0,02507 (-6,3%)	0,000 (-92,3%) / 0,004 (-92,7%)
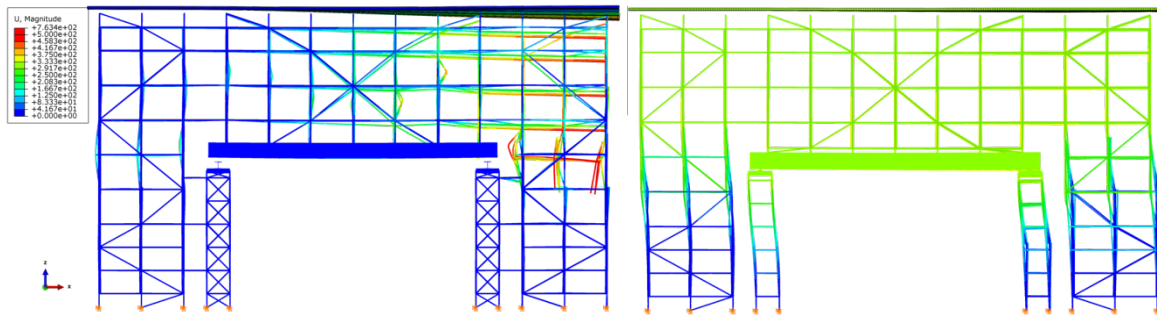
Figure 6.43: Deformed shape of model M-1 (*Left*) and M-2 (*Right*).

From Table 6.24 it can also be observed that the model with steel girders returns a higher value of resistance than the considered traditional-like model with no steel girders.

These findings bring again to consideration an already discussed issue. As can be seen in Figure 6.39 to Figure 6.42 the bracing adopted spans in general a large number of bays. As it was shown previously, bracing loses its effectiveness in cases like these and as a result the resistance and robustness of the system are negatively affected.

Regarding forces distribution within the elements of the falsework that are supported by the steel girders, Figure 6.44 illustrates the elastic second-order axial force distribution.

It can be observed that the axial force distribution is not uniform across the vertical elements of the falsework for a given steel girder alignment. In fact, the maximum axial force value occurs at the vertical elements which are directly above the supports of the steel girders (*i.e.* falsework towers). This physically makes sense since the falsework towers act as a restraint to the displacements of the steel girders. Thus, the falsework vertical elements located near them have a rigid support in contrast with the flexible support of the falsework vertical elements located near mid-span of the girders. As a result, the falsework vertical elements located near the falsework towers attract more forces than the rest of the vertical elements supported over the steel girders.
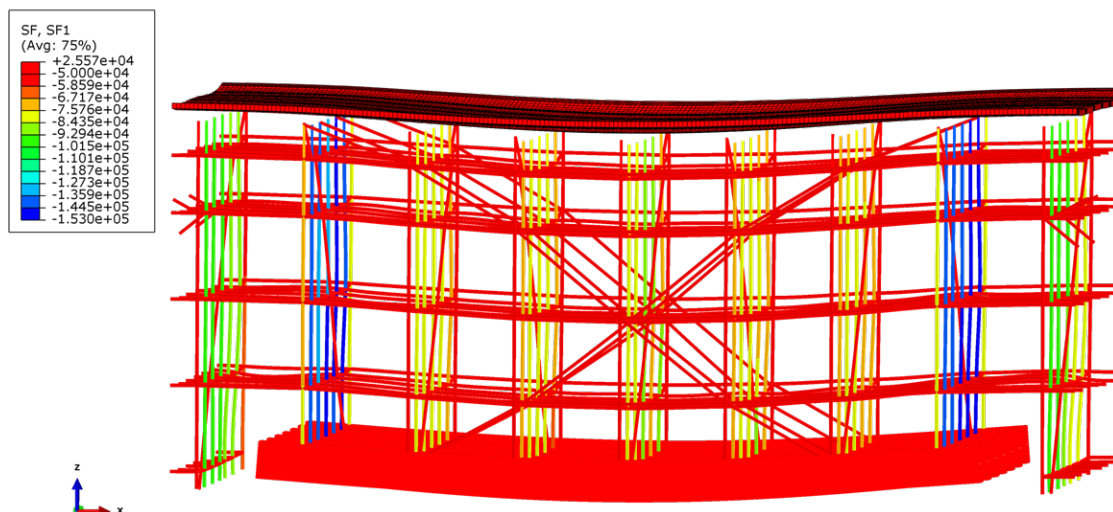
Figure 6.44: Axial force distribution within the falsework elements supported by the steel girders.

Consequently, if the falsework design is carried out based on the traditional and simple influence area method, where the forces transmitted from the formwork to the falsework vertical elements are determined based on the influence (formwork) area of each vertical element, a gross error is made with possibly catastrophic consequences. In the example under evaluation, based on the influence area method the axial forces of the vertical elements in the central girders alignments equals 90 kN, whereas the actual values range between 80 kN for the central vertical elements and 140 kN for the exterior vertical elements. For this level of forces, design using producer safe load values is not possible and an explicit model must be developed.

The fragility curves, see Figure 6.45, show that the structural resistance after first damage is very small (the ratio between maximum and first damage action value is less than 7%), so collapse is disproportionate and abrupt after first damage. As for the previous cases, for the majority of the action values fragility is either approximately equal to zero or equal to one.
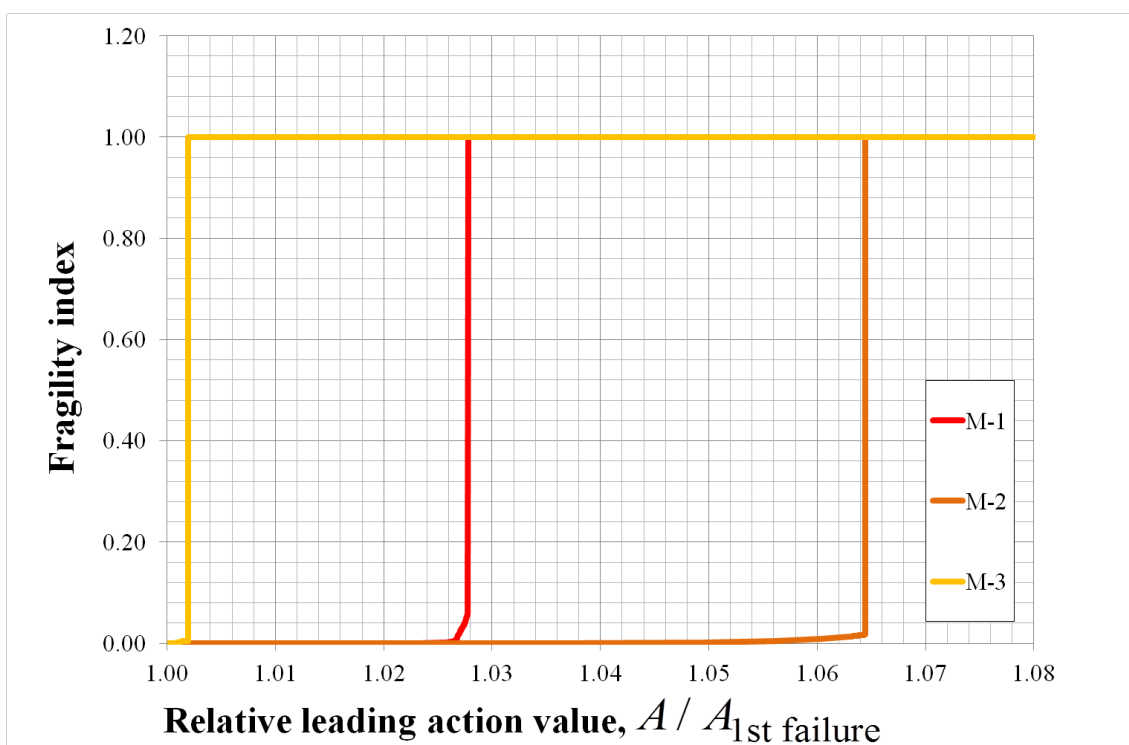
Figure 6.45: Fragility curves of the models developed to analyse falsework using steel girders.

6.4.1.2.5 Gross initial imperfections

As a last variable to be investigated, gross initial imperfections occur more often than not in bridge falsework. Bow imperfections of amplitude equal to $L/400$, where L represents the length of the standard, have been measured *in-situ* (Xie, Wang, 2009), but higher values are not uncommon.

Based on the reference Model A2 and on the initial imperfections measured along the columns height during the full-scale tests of Model A2 performed at Sydney University, see Chapter 4 and (Chandrangsu, Rasmussen, 2009a) for details, three numerical models were prepared with increasing initial imperfections magnitude. Model M-1 has two times the magnitude of the initial imperfections of reference Model A2; Model M-2 has four times the magnitude of the initial imperfections of reference Model A2 and Model M-3 has six times the magnitude of the initial imperfections of reference Model A2. Model M-3 contains an average member bow imperfection value equal to $L/500$. Also, different shapes of the initial geometrical imperfections were analysed: Models M-Ua and M-Sa, where U and S are the deformed shape configurations and a is the local and global imperfection factor, *i.e.* $a = H/\Delta$ and $a = L/\delta$ with H, L, Δ and δ representing the total system height, column length, maximum system sway imperfection and maximum element bow imperfection, respectively.

Table 6.25: Results of the models developed to analyse gross imperfections.

Model	Maximum concrete pressure on formwork (N/mm²)	Robustness index Eq. 5.34 / Eq. 5.18
A2 reference	0,03909 (0,0%)	0,006 (0,0%) / 0,082 (0,0%)
M-1	0,03868 (-1,1%)	0,004 (-31,2%) / 0,056 (-31,2%)
M-2	0,02891 (-26,1%)	0,002 (-59,4%) / 0,039 (-52,6%)
M-3	0,02436 (-37,7%)	0,002 (-62,2%) / 0,036 (-55,9%)
M-U750	0,03842 (-1,7%)	0,002 (-65,8%) / 0,030 (-63,2%)
M-S750	0,03728 (-4,6%)	0,003 (-49,8%) / 0,038 (-53,2%)
M-U20	0,01617 (-58,6%)	0,010 (+83,2%) / 0,105 (+28,3%)
M-S20	0,01271 (-67,5%)	0,0010 (-78,0%) / 0,015 (-81,8%)

The only action considered was the one due to the concrete weight placed on top of the formwork. This load was increased until collapse was attained. The results are presented in Table 6.25.

It can be observed how important it is to measure, control and adjust the initial imperfections of the falsework members and of the falsework system to predefined appropriate levels. In particular, S shaped configurations should be avoided as well as large deformed overextended jacks.
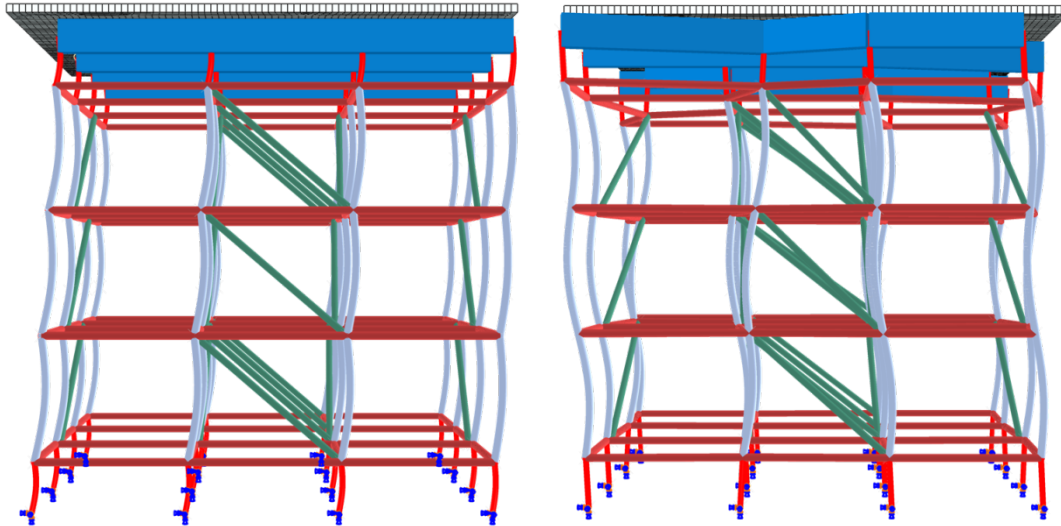
Figure 6.46: Different shapes of the initial geometrical imperfections: U shape (*Left*) and S shape (*Right*).

6.4.2 Stochastic investigation

Up until now the analyses have been performed assuming that both the actions and the resistance variables have been considered deterministic. However, in order to have a complete assessment of the performance of any structure a stochastic investigation must be carried out.

6.4.2.1 Choice of stochastic variables

As a first step of the stochastic investigation it is relevant to carry out a stochastic sensitivity analysis in order to understand the variance of the results and to determine which random variables are the most important to explain the stochastic structural behaviour.

As explained in Chapter 5 there are many procedures available to perform stochastic analyses. Here, Design of Experiments (DoE) followed by surrogate modelling and Monte Carlo analyses will be used, see Figure 6.47. The procedure will be explained in detail in the following section.
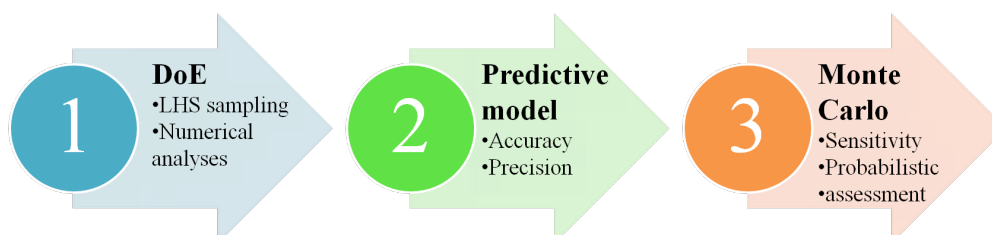
Figure 6.47: Stochastic procedure.

It is important to state that as any other investigation several constraints were present. In particular, the available time and computational resources were limited. Therefore, the case studies considered needed to be adjusted to these constraints. As a result, the structural layout of Model A2, with variants, was adopted. One complete numerical analysis of this model took approximately 20 minutes to finish on a high end PC.

In the DoE, several random variables were considered, representing the various types of joints present in Cuplok® systems but also the geometrical and material properties of the system. In total, 34 random variables corresponding to structural properties were selected, see Table 6.26 for details.

The DoE assumed uniform distributions for each random variable. Table 6.26 also presents the minimum and maximum values considered for each variable. These values were based on results presented in Chapter 3 and on relevant bibliographic references (Vila Real et al., 2004 ; JCSS, 2001 ; Chandrangsu, 2010 ; Voelkel, 1990). The rationale was to use DoE to get an envelope of the stochastic behaviour of the structure.

Table 6.26: Random variables considered in the DoE analysis.

Random variables		
Initial imperfections	**Minimum value**	**Maximum value**
Local bow imperfection factor (limpf)	50	2000
Global sway imperfection factor (gimpf)	50	2000
Material properties	**Minimum value**	**Maximum value**
Yield stress (fy), MPa	300	500
Tensile resistance (fu), MPa	450	650
Maximum strain (εu)	0,1	0,3
Young modulus (E), GPa	180	220
Joints	**Minimum value**	**Maximum value**
Ledger-to-standard joint (Cuplok® joint), Strong bending axis		
Looseness (θ1c), rad	0	0,04
Initial stiffness (k1c), kN.m/rad	1	20
Stiffness after looseness, 2 ledgers (k22Lc), kN.m/rad	30	100
Stiffness after looseness, 3 ledgers (k23Lc), kN.m/rad	30	130
Stiffness after looseness, 4 ledgers (k24Lc), kN.m/rad	30	150
Maximum bending moment (Muc), kN.m	1,5	5
Deformation capacity factor (dfc)	0,5	3
Ledger-to-standard joint (Cuplok® joint), Axial axis	**Minimum value**	**Maximum value**
Maximum axial force (Pmaxc), kN	30	130
Standard-to-standard joint (Spigot joint)	**Minimum value**	**Maximum value**
Looseness (θ1s), rad	0	0,04
Initial stiffness (k1s), kN.m/rad	1	20
Stiffness after looseness, ratio 1 (k21s), kN.m/rad	150	300
Stiffness after looseness, ratio 2 (k22s), kN.m/rad	100	250
Stiffness after looseness, ratio 3 (k23s), kN.m/rad	20	50
Maximum bending moment, ratio 1 and 2 (Mu12s), kN.m	2	5
Maximum bending moment, ratio 3 (Mu3s), kN.m	1	3
N/M Ratio 12 (r12s)	30	70
N/M Ratio 23 (r23s)	10	30
Deformation capacity factor (dfs)	0,5	3
Forkhead joint	**Minimum value**	**Maximum value**
Looseness (θ1f), rad	0	0,04
Initial stiffness (k1f), kN.m/rad	1	20
Stiffness after looseness (k2f), kN.m/rad	20	100
Maximum bending moment (Muf), kN.m	1	4
Deformation capacity factor (dff)	0,5	3
Brace joint	**Minimum value**	**Maximum value**
Stiffness after looseness (k2b), kN/m	1000	2000
Maximum axial force (Pmaxb), kN	10	50
Deformation capacity factor (dfb)	0,5	3
Baseplate joint	**Minimum value**	**Maximum value**
Looseness (θ1bp), rad°	0	20
Maximum rotation capacity (θubp), rad	0,1	0,5
Legend: Deformation capacity factor represents the ratio between the maximum joint deformation and the sum of deformations of each linear segment of the joint's constitutive model. N/M ratio specified in the spigot joint was defined in Chapters 3 and 4 and is used to establish different values for the spigot joint constitutive model		

Over than 700 numerical analyses were performed using Latin Hypercube (LHS) sampling of each variable. The only action considered was the one due to the pressure applied on top of the formwork. This action was also considered as a random variable. The joint finite element presented in Chapter 4 was included in all analyses, as well as the eccentricities at the forkheads and at the baseplates which were already detailed in previous sections, see Chapter 4 also.

After, a predictive model was determined for the resistance, robustness and fragility results from the DoE results and a sensitivity analysis was performed to identify the most relevant random variables which were then selected for the case studies presented in the following section. Subsequently, for each predictive model, a Monte Carlo analysis was carried out with one million LHS samples taken from the assumed probabilistic distributions and respective parameters for each random variable. Details are given in Table 6.27 for structural properties. As it can be observed, the uncertainty in estimating the distribution parameters was accounted for by assigning a bounded Normal probabilistic distribution for each distribution parameter. The range values were based on results presented in Chapter 3 and on relevant bibliographic references (Vila Real et al., 2004 ; JCSS, 2001 ; Chandrangsu, 2010 ; Voelkel, 1990).

Table 6.27: Random variables considered in the Monte Carlo analysis.

Random variables	Probabilistic distribution	Distribution parameters		Minimum value	Maximum value
Initial imperfections					
limpf	Lognormal	mean = N(750;100;650;850)	sd = N(1000;250;500;1500)	50	2000
gimpf	Normal	mean = N(625;100;500;700)	sd = N(1800;250;1000;2500)	50	2000
Material properties					
fy, MPa	Lognormal	mean = N(419;10;400;440)	sd = N(20;5;15;25)	355	500
fu, MPa	Lognormal	mean = N(533;10;500;550)	sd = N(16;5;10;25)	470	630
εu	Lognormal	mean = N(0,26;0,1;0,2;0,3)	sd = N(0,06;0,02;0,1;0,3)	0,1	0,3
E, GPa	Lognormal	mean = N(209;10;205;215)	sd = N(12;5;5;20)	180	220
Joints					
Ledger-to-standard joint (Cuplok® joint)					
Strong bending axis[a)]					
θ1c, rad	Normal	mean = N(-0,008;0,005;-0,03;0,01)	sd = N(0,012;0,007;0,006;0,019)	0	0,04
k1c, kN.m/rad	Normal	mean = N(-13; 20;-98;71)	sd = N(27;10;5;57)	1	20
k22Lc, kN.m/rad	Weibull	shape = N(8;2;6;10)	scale = N(75;5;71;78)	30	90
k23Lc, kN.m/rad	Weibull	shape = N(4,8;1,5;3,2;6,5)	scale = N(90;10;80;99)	30	120
k24Lc, kN.m/rad	Weibull	shape = N(6,2;2,5;3,7;8,6)	scale = N(92;7;84;100)	30	140
Muc, kN.m	Weibull	shape = N(14,8;2,5;12;17)	scale = N(3,99;0,05;3,92;4,05)	1,5	5
dfc	Normal	mean = N(1;0,2; 0,75; 1,25)	sd = N(0,25; 0,1; 0,1; 0,5)	0,5	2
Axial axis					
Pmaxc, kN	Weibull	shape = N(7,35; 2; 5,0; 9,6)	scale = N(76;5;71;81)	30	110
Standard-to-standard joint (Spigot joint)					
θ1s, rad	Normal	mean = N(0,005;0,005;0,001;0,01)	sd = N(0,007; 0,002; 0,005; 0,01)	0	0,04
k1s, kN.m/rad	Normal	mean = N(-13; 20;-98;71)	sd = N(27;10;5;57)	1	20
k21s, kN.m/rad	Normal	mean = N(162;10;150;170)	sd = N(41;10;20;60)	150	200
k22s, kN.m/rad	Normal	mean = N(128;10;110;140)	sd = N(35;15;20;50)	100	150
k23s, kN.m/rad	Normal	mean = N(28;10;20;40)	sd = N(7;4;2;10)	20	50
Mu12s, kN.m	Normal	mean = N(3,5;1;3;4)	sd = N(0,3;0,2;0,2;0,5)	2,5	4
Mu3s, kN.m	Normal	mean = N(1,8;0,5;1,5;2)	sd = N(0,4;0,4;0,2;0,8)	1	2,5
r12s	Normal	mean = N(50;10;40;60)	sd = N(10;5;5;20)	30	70
r23s	Normal	mean = N(20;10;15;25)	sd = N(10;5;5;20)	10	30
dfs	Normal	mean = N(1;0,2;0,75;1,25)	sd = N(0,25;0,1;0,1;0,5)	0,5	2
Forkhead joint					
θ1f, rad	Normal	mean = N(0,005;0, 005;0,001;0,01)	sd = N(0,007; 0,002; 0,005; 0,01)	0	0,04
k1f, kN.m/rad	Normal	mean = N(-13; 20;-98;71)	sd = N(27;10;5;57)	1	20
k2f, kN.m/rad	Normal	mean = N(29;10;20;40)	sd = N(5;5;5;2;15)	20	50
Muf, kN.m	Normal	mean = N(3;1;2,5;3,5)	sd = N(1;1;0,5;2)	2	4
dff	Normal	mean = N(1;0,2;0,75;1,25)	sd = N(0,25;0,1;0,1;0,5)	0,5	2
Brace joint					
k2b, kN/m	Normal	mean = N(1360;250;1000;1500)	sd = N(322;150;100;500)	1000	2000
Pmaxb, kN	Normal	mean = N(23;5;20;25)	sd = N(16,6;5;10;40)	10	40
dfb	Normal	mean = N(1;0,2;0,75;1,25)	sd = N(0,25;0,1;0,1;0,5)	0,5	2
Baseplate joint					
θ1bp, °	Normal	mean = N(5;1;3;4)	sd = N(2;1;1;3)	0	20
θubp, rad	Normal	mean = N(0,2;0,1;0,15;0,25)	sd = N(0,1;0,1;0,05;0,2)	0,1	0,5

a) See also Table 6.28 for correlation matrix.

Legend: *N(a,b,c,d)* represents a bounded Normal distribution with mean equal to *a*, standard deviation (sd) equal to *b*, minimum value equal to *c* and maximum valued equal to *d*.

Table 6.28: Correlation coefficients (Cuplok® joint, strong bending axis).

Correlation matrix	fy	fu	eu	k22Lc	k23Lc	k24Lc	Muc	dfc
fy	1	0,75	-0,45					
fu	0,75	1	-0,6					
eu	-0,45	-0,6	1					
k22Lc				1	0,41	0,41	0,29	
k23Lc				0,41	1	0,41	0,29	
k24Lc				0,41	0,41	1	0,29	
Muc				0,29	0,29	0,29	1	0,35
dfc							0,35	1

The results of the sensitivity analysis resulting from the 700 numerical results and the one million Monte Carlo analyses are presented in Figure 6.48 for the maximum resistance (R), robustness index (I_R), yield pressure (R_y), damage energy corresponding to the collapse state (D_c) and two other variables that were used to calculate the fragility index: R_1 and D_{uc1}, see Figure 6.49. They correspond to the values of the leading action and damage energy, respectively, at the discrete numerical increment just before the "unavoidable collapse" state is attained.
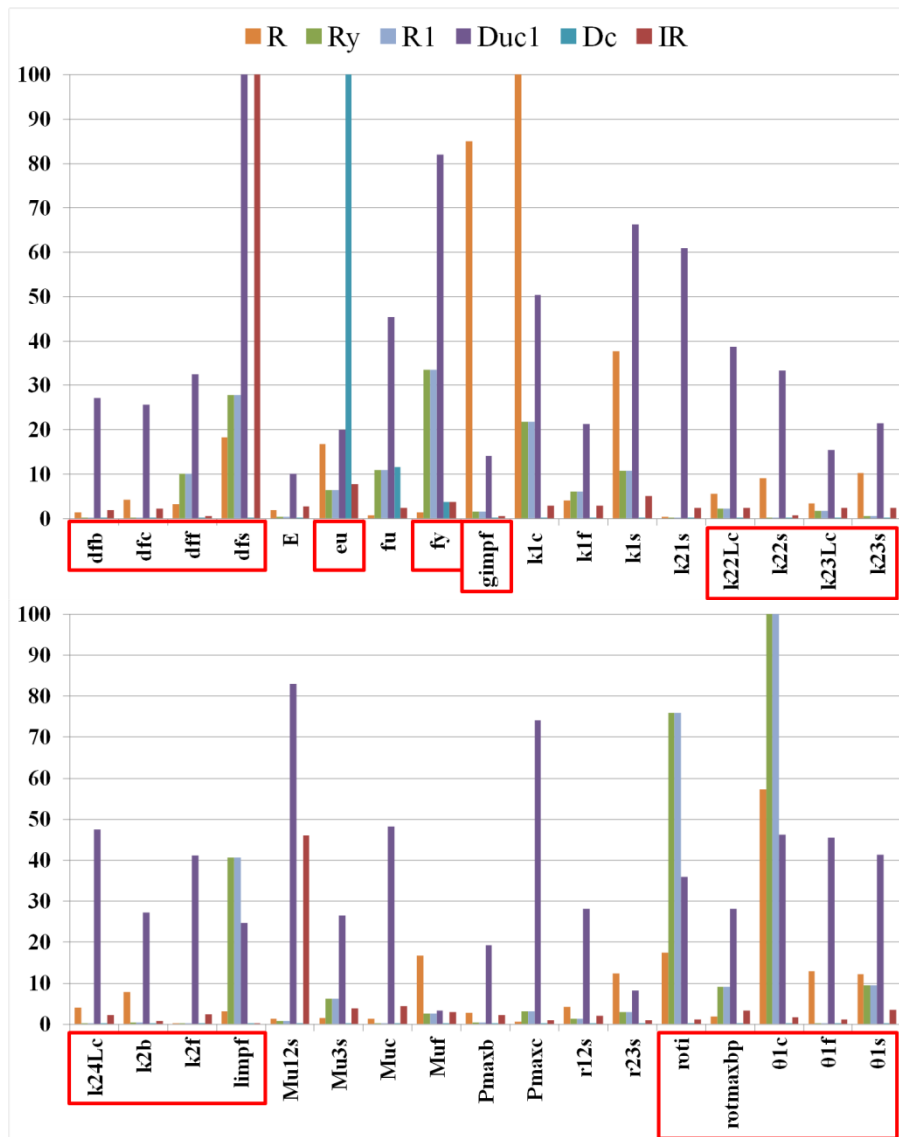
Figure 6.48: Stochastic sensitivity coefficients (scaled to 100).
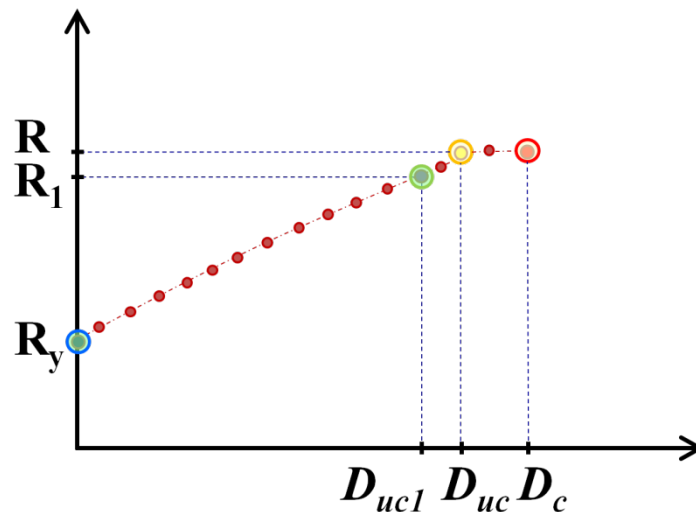
Figure 6.49: Representation of R_1 and D_{uc1} variables.

The results exhibit a large variability across the five target variables considered. Nevertheless, the most important random variables could be identified from the total 34. These involved the initial rotation (looseness) of the joints, the stiffness after looseness (slope of the second linear segment of the joints analytical constitutive model presented in Chapters 3 and 4), the deformation capacity factor and the initial imperfections. The stiffness associated with looseness was also identified as an important variable to the stochastic response of bridge falsework systems, but due to its large variability it was decided to adopt a safe simplification of assuming a very small deterministic value (equal to 1 kN.m/rad). It could also be observed that the Young's modulus and the limit ratios between bending moment and axial force used in the spigot joint constitutive models almost do not contribute to the stochastic behaviour of the system.

The most important joints are the Cuplok® and the spigot joints. Therefore, gains of efficiency can be achieved by reducing the variability of the parameters that control the behaviour and resistance of these joints. In the limit, if it was possible to consider these values as deterministic it would result in a significant decrease of the variance of the stochastic behaviour of the system which in terms of the system's reliability and fragility can be extremely beneficial.

As such, 20 random variables were selected from the total 34, a significant decrease which will alleviate the numerical analysis demand and ease the analysis of the results since it is not always favourable to take into account the entire set of variables; for example: some variables may only introduce noise to the results making their analysis much more limited in scope and objectivity terms.

As a final remark, different results are to be expected for structural layouts other than the one considered, for different actions and even for different random variables variability. Notwithstanding, the overall trend described above should not be significantly altered and therefore it is assumed that there is no loss of generalisation in the results of future analyses.

6.4.2.1.1 Reliability

The maximum action value in terms of the pressure applied on top of the formwork can be obtained from the producer's design tables. For Model A2, with 1,5 m spacing between storeys, 1,8 m spacing between bays, braced but with unbraced jacks with 600 mm extension length and elements made of S355 steel, a safe resistance approximately equal to 7,0 kN/m^2 is obtained (limited by the unbraced jacks resistance) (SGB, 2009). In the scenario where the user of the design tables applied them incorrectly taking the safe load of the internal columns as the resistance of the system, *i.e.* ignoring the lower resistance of the jacks, a value approximately equal to 16,5 kN/m^2 is obtained (SGB, 2009). As these values implicitly contain a high partial factor, the reliability of the system was compared against a vertical pressure action with a mean value equal to 24,0 kN/m^2 (roughly 1,5 times 16,5 kN/m^2).

The pressure action was modelled as a dead load, ignoring the dynamic effects of concrete casting, because the material's self weight (mainly concrete) constitute the critical vertical action when compared with the construction live loads due to equipment, personnel, etc. Therefore, the variance considered for the pressure action was small: a standard deviation equal to 7,5% of the mean value was adopted (Zhang et al., 2011). The action values were assumed to follow a bounded Normal probabilistic distribution with minimum value equal to 20 kN/m^2 and a maximum value equal to 26 kN/m^2 (Zhang et al., 2011). Since the action was applied directly on the formwork there was no need to account for the uncertainty of the action redistribution within the columns of the bridge falsework system. However, the uncertainty of estimating the parameters of the Normal distribution was propagated. It was considered that the parameters also followed the same type of distribution: mean ~ N(24;5;23;25) and coefficient of variation (COV) ~ N(0,075; 0,025; 0,06; 0,09).

Under these conditions the histograms of the action and resistance were determined aggregating the results from one million Monte Carlo runs. These are shown in Figure 6.50 along with the respective Normal probabilistic density function and the kernel density estimation. The latter was obtained using system functions from the R program (R Core Team, 2012). As it can be seen both the action and resistance values follow closely a Normal distribution.

Repeating multiple times (100 in this case) a procedure involving randomly selecting one value of the action and running one million Monte Carlo runs, it was possible to obtain the distribution of the values of the probability of failure. This is illustrated in Figure 6.51. It can be seen that under the considered conditions the mean value of the probability of failure is prohibitively high (almost 1%).

From the probability of failure, an equivalent reliability index was determined and illustrated in Figure 6.52. It can be observed that the mean value (about 2,4) is significantly lower than the minimum recommended value for the less important consequence class specified in EN 1990 (BSI, 2002a) which is 4,2 for a one year reference period.

Therefore, it can be concluded that the structure under consideration for the hypothesis assumed, namely in terms of the value and variability of the resistance and action variables, does not meet the minimum safety levels required by the relevant standards. The risk of failure of any underdesigned structure is extremely high. This shows how dangerous it is to make wrong use of the producer's design tables.

To further stress this last observation, if the mean value of the applied action was fixed at the correct specified safe load, *i.e.* 7,0 kN/m^2, instead of 24,0 kN/m^2, then the probability of collapse would be virtually equal to zero (< 1 ×10^{-8}), again for the considered load and system specificities.
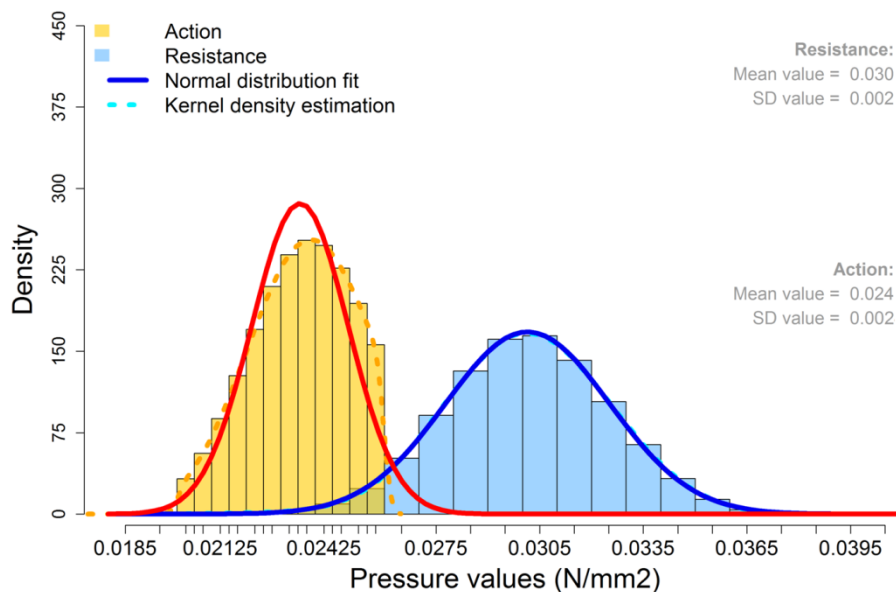
Figure 6.50: Histograms of action and resistance (Model A2).
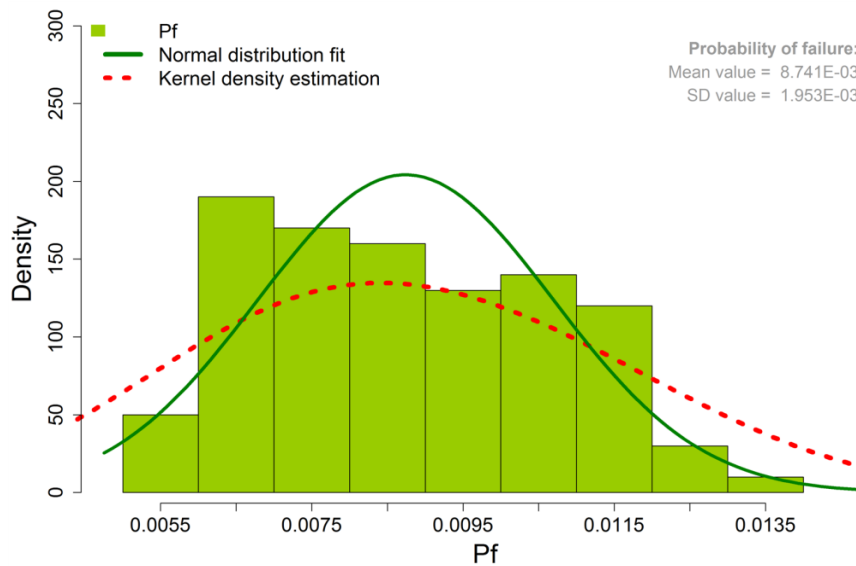
Figure 6.51: Histograms of probability of failure (Model A2).
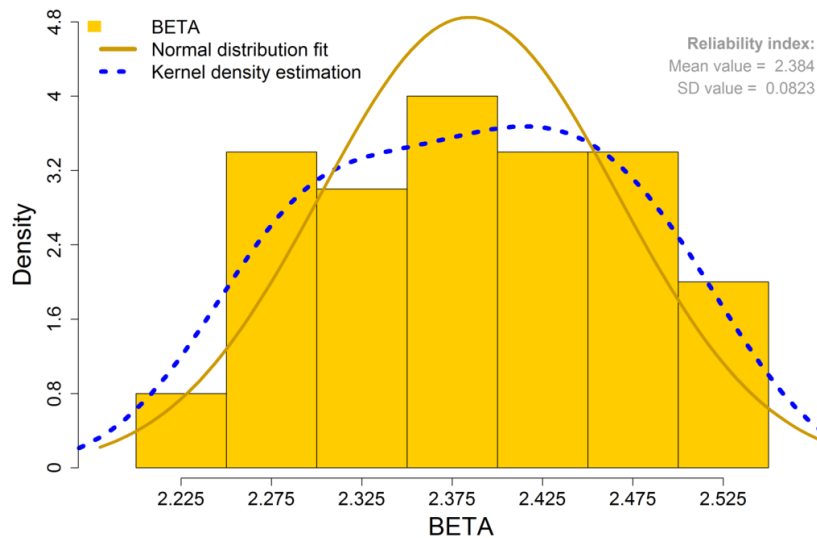
Figure 6.52: Histograms of the reliability index (Model A2).

6.4.2.1.2   Robustness

In terms of robustness, Figure 6.53 illustrates the histogram of the possible values of the robustness index given by equation 5.18 (Chapter 5). The only action considered was the pressure applied on top of the formwork. The action values were assumed to follow a uniform probabilistic distribution with minimum value equal to 20 kN/m^2 and a maximum value equal to 26 kN/m^2. If collapse did not occur during step 1 of the robustness procedure, the action value was increased until collapse was attained.

It is possible to observe that the values of the robustness index for this particular structural system show a bimodal distribution (with two different modes). This occurs due to the large variability of the system resistance related random variables. The values are small which indicates that the collapse is disproportionate.

6.4.2.1.3   Fragility

Finally, in terms of fragility, Figure 6.54 and Figure 6.55 present the histogram and the empirical cumulative density function (cdf) of the fragility index, respectively. As before, the only action considered was the pressure applied on top of the formwork. The action values were assumed to follow a uniform probabilistic distribution with minimum value equal to 20 kN/m^2 and a maximum value equal to 26 kN/m^2. If collapse did not occur during step 1 of the fragility procedure, the action value was increased until collapse was attained.
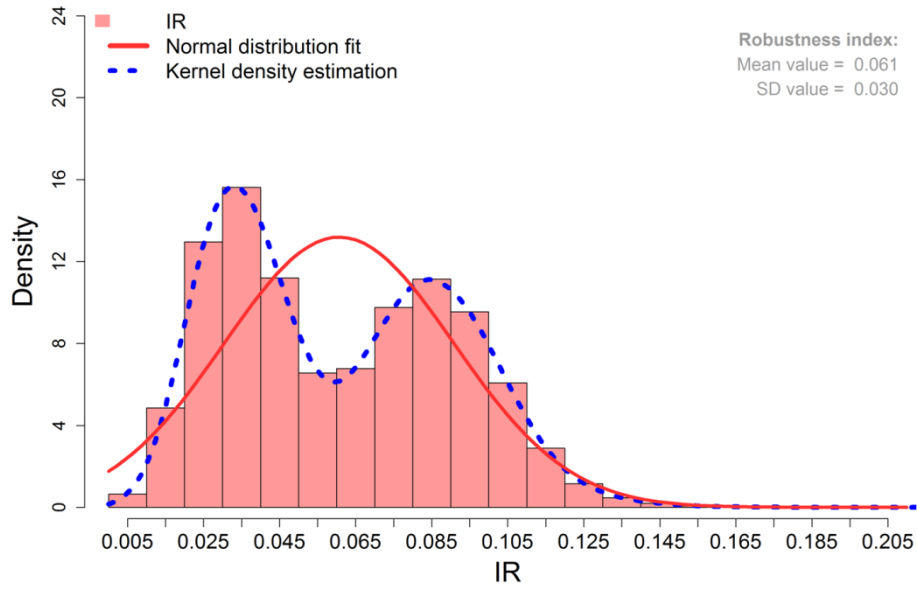
Figure 6.53: Histograms of the robustness index (Model A2).
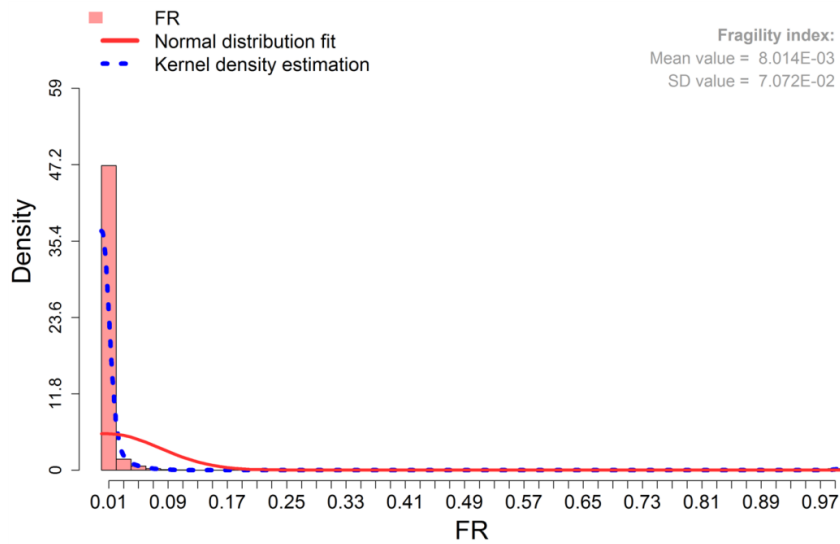
Figure 6.54: Histograms of the fragility index (Model A2).
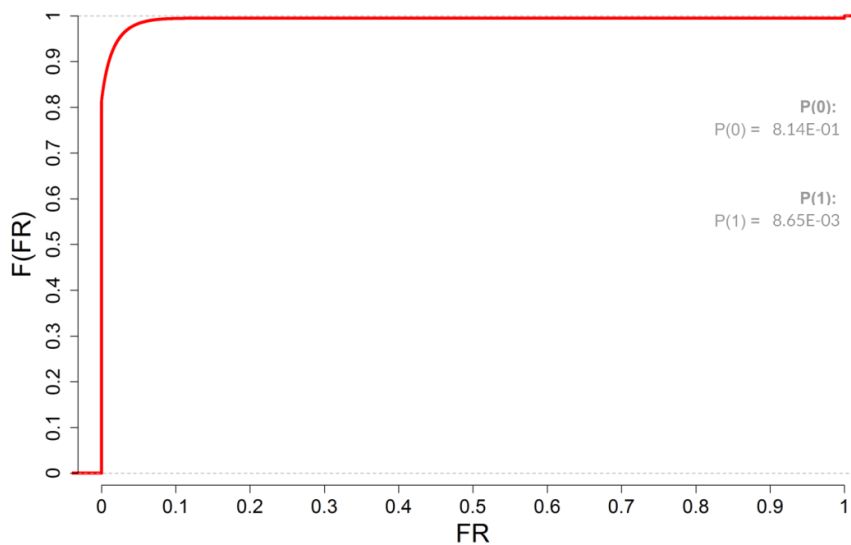
Figure 6.55: Empirical cumulative density function (cdf) of the fragility index (Model A2).

It can be seen that most of the values (around 80%) of the fragility index are equal to zero, representing non-damaged states. Nevertheless, the risk of total collapse is about one percent which is extremely high. In between zero and one, fragility index takes values up to 0,15 which is in line with the findings already presented when discussing robustness index results.

Other interesting results are the fragility curves which relate fragility with the applied leading action, see Figure 6.56. Figure 6.57 illustrates the complementary fragility curves. As it can be seen, the isolines corresponding to fragility index values between 0,01 and 0,75 are very close to each other, meaning that fragility (damage) is extremely sensitive to the applied action values, *i.e.* a small positive variation of the action can lead to a large positive variation of fragility. This finding indicates that the collapse is also prone to be abrupt, which is confirmed by the results shown in Figure 6.58 that support this idea by demonstrating that after first damage the resistance capacity reserve is small, in general less than 15% of the value of yield load.
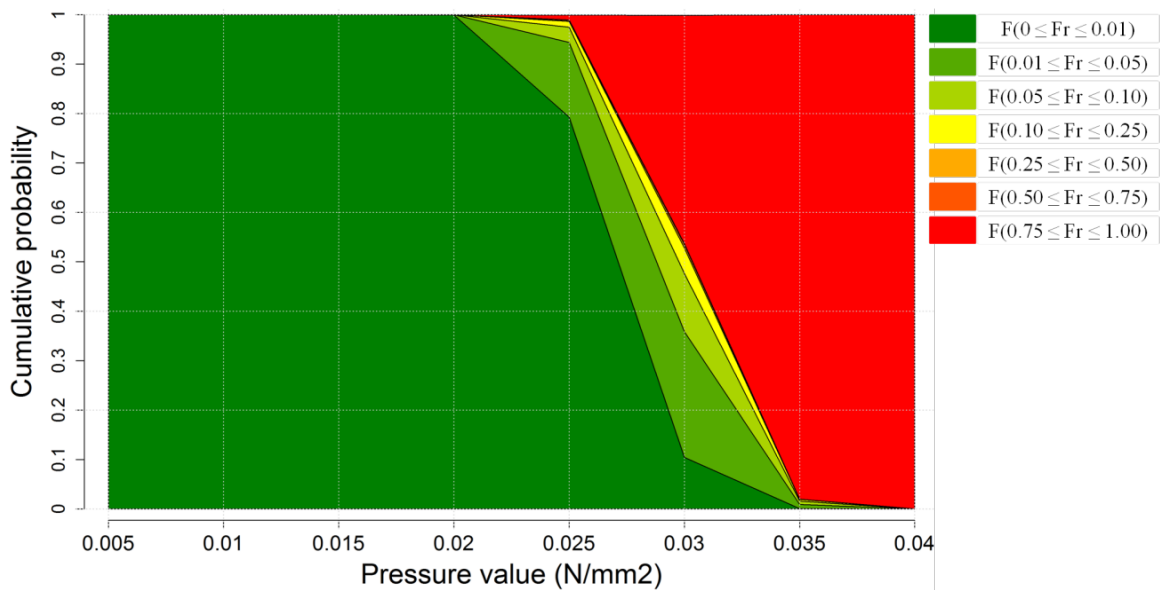
Figure 6.56: Fragility curves (Model A2).
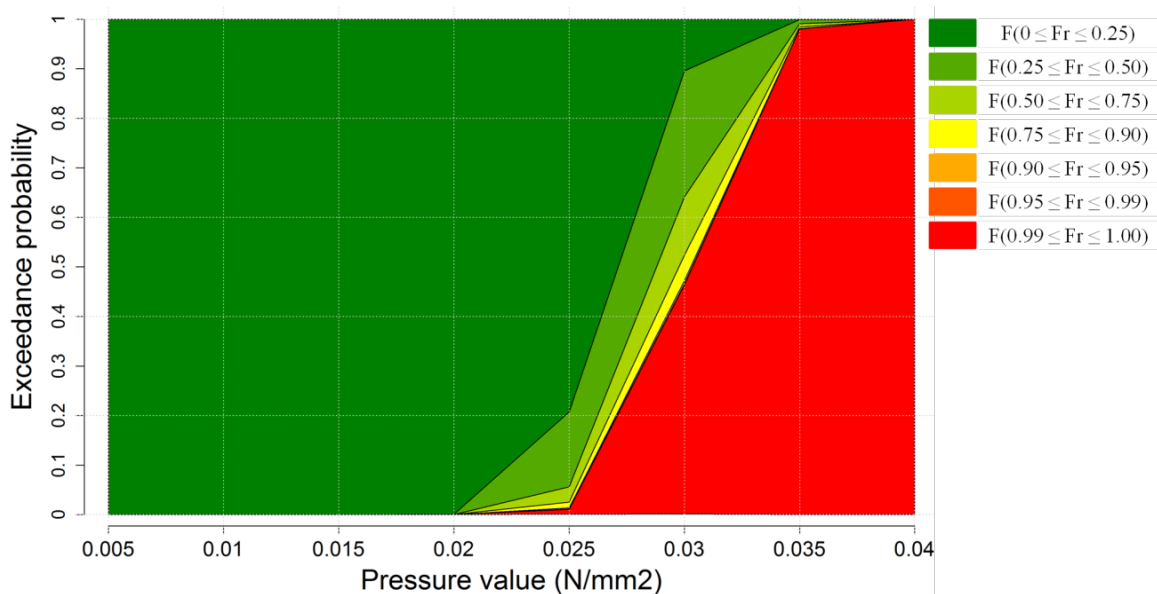
Figure 6.57: Complementary fragility curves (Model A2).
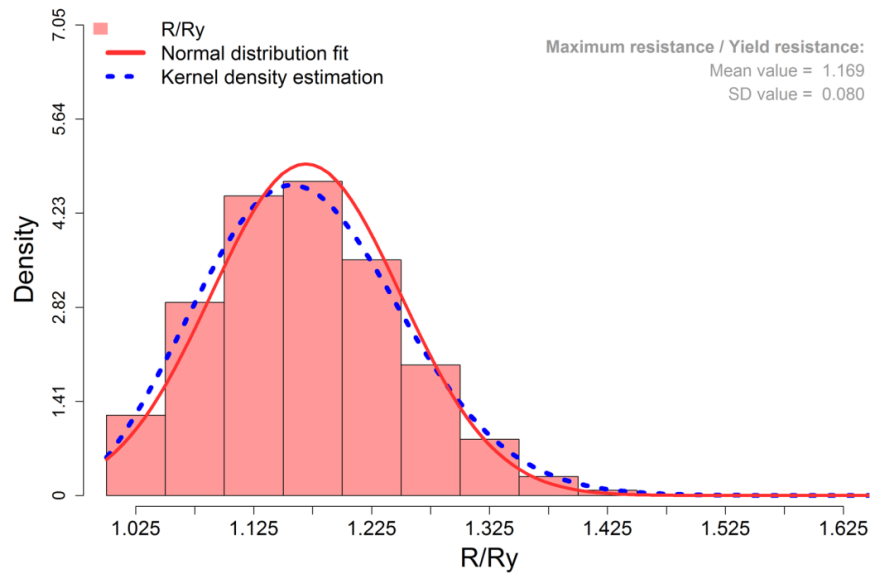
Figure 6.58: Relative leading action value (Model A2).

6.4.2.2   Case studies

Two case studies, named CS1 and CS2, were selected and studied in detail. The results are presented in this section.

Both case studies share the same structural layout, depicted in Figure 6.59, which consists in a variation of the bracing configuration from Model A2. In this new layout, the top and bottom jacks are braced by a continuous brace element placed in every bay, alternating its direction in consecutive bays, along two orthogonal directions.

The only thing that distinguishes the two case studies is the nature and number of applied actions. In CS1 only vertical pressure was applied at the top of the formwork, whereas in CS2 additionally to the vertical pressure, the wind pressure corresponding to the working wind velocity and a localised differential ground settlement were also considered. The differential ground settlement was applied under a central column, identified as position $c = 2$ in Figure 6.19, with a value equal to 100 mm.
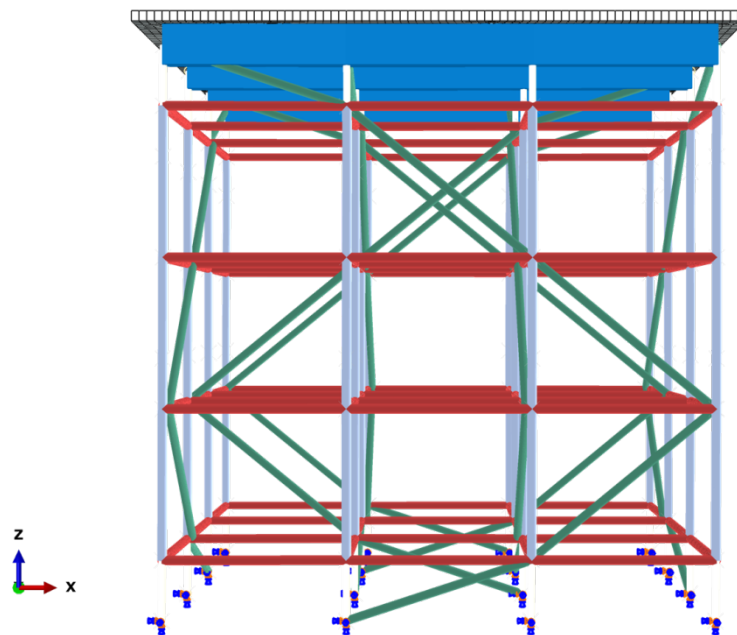
Figure 6.59: Case studies structural layout.

In the hazard scenario considered for CS2 the loads were applied sequentially: first the unloaded bridge falsework structure was submitted to the wind action which was thereafter kept constant. The differential ground settlement was applied as soon as the wind action reached its maximum value, which also coincided with the start of the application of the uniform pressure action onto the formwork surface. The settlement reached its maximum value when the uniform pressure action was equal to the random value defined in step 1 of the robustness procedure (or the weight of a 0,5 m concrete slab (normal density concrete) for the deterministic analyses). After, the uniform pressure action value (leading action) was increased until structural collapse occurred.

As mentioned in the previous section, 20 resistance related variables were modelled as random variables. These variables were already identified as well as their corresponding probabilistic models.

To start, the deterministic results of each case study will be presented, after which the procedure to validate, verify and select the predictive models will be detailed. Finally, the results of the stochastic analysis of the two case studies will be presented.

6.4.2.2.1 Deterministic results

In both cases, the cross-section geometrical characteristics as well as the material properties of the various elements which make the falsework system are identical to the ones used in the structures tested in the Sydney University, see Chapter 4 and (Chandrangsu, Rasmussen, 2009a). Additionally, the finite element mesh properties are the same as detailed in Chapter 4. The formwork was explicitly modelled in all models, with an equivalent thickness equal to 100 mm, and the joint characteristics considered in all models, unless otherwise noted, were taken as the average values of the results reported in Chapter 3. The same applies to the top and bottom jacks' extension lengths, where 600 mm was considered as the default extension length value and to the default initial geometrical imperfections whose values were measured *in situ* during the full scale tests performed at Sydney University.

Figure 6.60 presents the evolution of the load *vs.* lateral displacements measured at the same node. It can be seen that applying the combination of actions gradually decreases the stiffness of the system. Also, in CS2 due to the severe differential settlement applied at a central column the surrounding columns endured larger plastic strains for the same load value than the elements of the CS1, see Figure 6.61. In fact, due to the stiffness provided essentially by the bracing, the central column in CS2 under which the differential settlement was applied remains ineffective at least until the "unavoidable collapse" state is attained. Therefore, CS2 collapses for a lower load value than CS1, but in the damage accumulation and damage evolution process more energy is dissipated than in CS1. As a result, CS2 exhibits a higher robustness value than CS1 despite having a lower resistance.
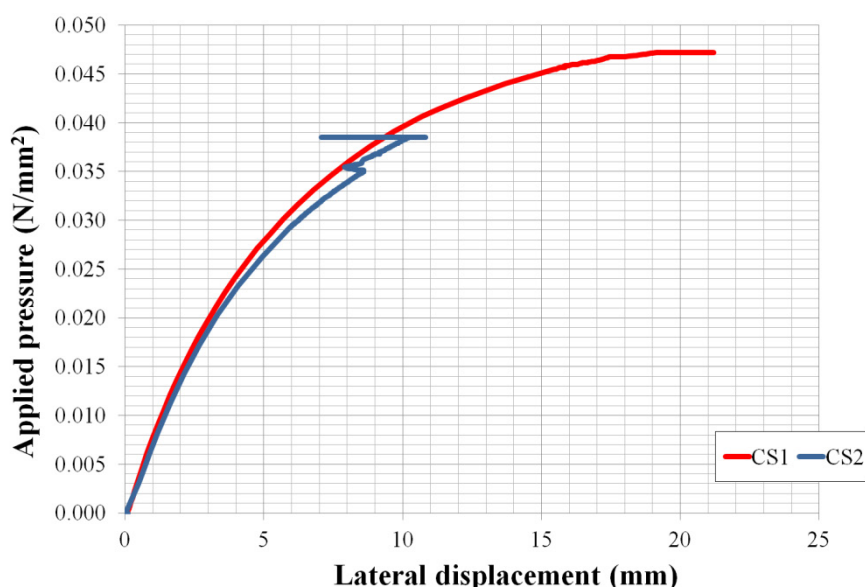
Figure 6.60: Load *vs.* lateral displacement diagrams for the two case studies.
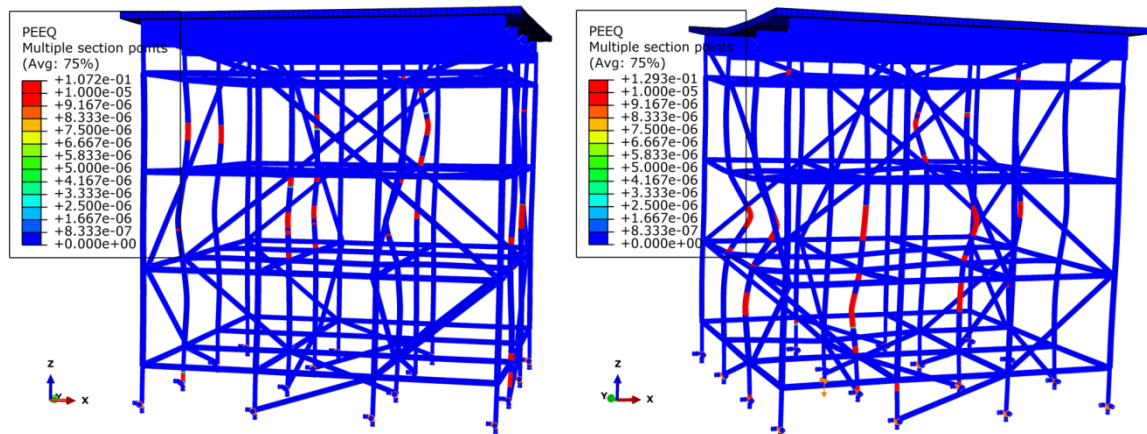
**Figure 6.61: Deformed shape and plastic strains distribution of models
CS1 (*Left*) and CS2 (*Right*) at "unavoidable collapse" state.**

Not only CS2 has a higher robustness index but also a higher resistance capacity reserve than CS1, see Figure 6.62.

When compared to Model A2, the structural layout selected to form the basis of the case studies constitutes an improved structural solution. From the information presented in Table 6.29 it is possible to observe that the results of CS2 and Model A2 are comparable despite the former being submitted to a combination of actions, whereas in the latter only vertical pressures are considered.
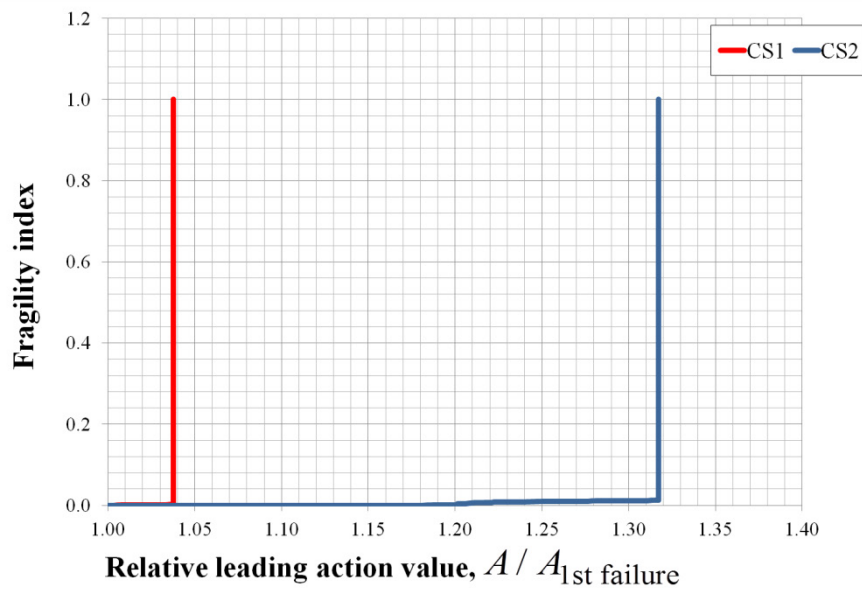
Figure 6.62: Fragility curves of the case study models.

Table 6.29: Summary of results of the case study models.

Model	Maximum concrete pressure on formwork (N/mm^2)	Robustness index Eq. 5.18
A2 reference (A2-1)	0,03909 (0,0%)	0,082 (0,0%)
CS1	0,04722 (+20,8%)	0,117 (+43,2%)
CS2	0,03853 (-1,4%)	0,152 (+86,6%)

6.4.2.2.2 Predictive models

The need and the usefulness of good predictive models are invaluable, in particular in regression problems such as the one at hand. Indeed, without machine learning models it would be much more difficult and less productive the task of analysing complex systems and phenomena.

In this section it is given a brief but sufficiently complete overview about the procedure used in the present Chapter to validate, verify and select the predictive models for the maximum resistance

(R), robustness index (I_R), yield pressure (R_y), damage energy corresponding to the collapse state (D_c) and two other variables that were used to calculate the fragility index: R_1 and D_{uc1}, see Figure 6.49.

Ample bibliographic references are available, from which it is worth mentioning (Kuhn, Johnson, 2013 ; Hastie et al., 2009).

In order to obtain a good predictive model it is critical that an appropriate data set is available. By appropriate it is meant that it encompasses all the processes involved in building up the data and it is representative. An example of achieving this goal is Design of Experiments (DoE). After, it is important to have an understanding concerning the fundamentals behind the data values. This is imperative as the predictive models can return information that is not suitable to use and therefore it is essential that the analyst has sufficient knowledge to ascertain about the goodness of fit of the predictive models.

From the several types of models available (Boosting models, Generalized additive models, Model trees, Regression Splines models, Support Vector Machines and Random Forests just to name a few) three to five candidates are selected for validation.

Nowadays validation and verification is usually performed in the same step. But prior, the data set needs to be partitioned in validation (including verification) and independent testing data sets. In the present, this splitting of the data is considered essential to attest the accuracy of the model on a testing data set that remained untouched and unseen during validation (and verification). However, if the data sets are very small there is just no escape of using the entire data set to perform validation and verification (Kuhn, Johnson, 2013 ; Hawkins et al., 2003).

If an independent test set is available there is also the question on how to split the data. If the data set is the result of a DoE then it may be assumed that the data is sufficiently stratified and representative. In this case it may be relevant to place the majority of the extreme points to the validation data set. This can be done by creating sub–samples using a maximum dissimilarity approach that can be used to maximize the minimum and total differences (Martin et al., 2012 ; Kuhn, Johnson, 2013). As an initial seed the median or the mean of the cloud of points can be used. In the present Thesis the size of the independent test set varied from 20% to 10% of the size of the original data set.

Whether a test set is or is not available, there are currently two state-of-the-art methods to perform the validation and verification of the models: (i) cross-validation and (ii) bootstrap. In particular repeated K-fold cross validation is quite popular. It was shown that this method has some interesting properties that prevent overfitting and at the same time limit the maximum bias (Molinaro et al., 2005 ; Kohavi, 1995 ; Martin, Hirschberg, 1996 ; Arlot, Celisse, 2010). However, bootstrap algorithm, in particular newer versions, yields, in general, models with lower variance. In the present Thesis a 100 × 10-fold CV and 1000 resamples using 632 bootstrap algorithm were employed.

During training (validation plus verification), tuning of the model hyperparameters is done in an inner loop and in an outer loop the model is verified. After model validation and verification has finished, models are tested using the independent test set. In general, the best model during testing (more accurate) and validation (higher precision) phases is selected, unless there is enough data to be able to perform hypothesis testing to do statistically meaningful model comparisons, which was not the case in this Thesis.

To illustrate the procedure used in Thesis, the selection of the model to predict the maximum resistance (R) of the CS1 model will be detailed. Figure 6.63 presents the scatterplot of random variables against maximum resistance (R) for this model obtained in the DoE analysis. For all random variables a uniform probabilistic distribution was considered with parameters given in Table 6.26. In the model CS2, the leading action value applied during step 1 of robustness (and fragility) procedure was also considered in the determination of the predictive models, assumed to follow a uniform probabilistic distribution with minimum value equal to 20 kN/m^2 and a maximum value equal to 26 kN/m^2.

The total data set comprised 250 values for each variable. A 80%/20% data split was used, *i.e.* 200 samples of each variable for training and 50 samples of each variable for testing.
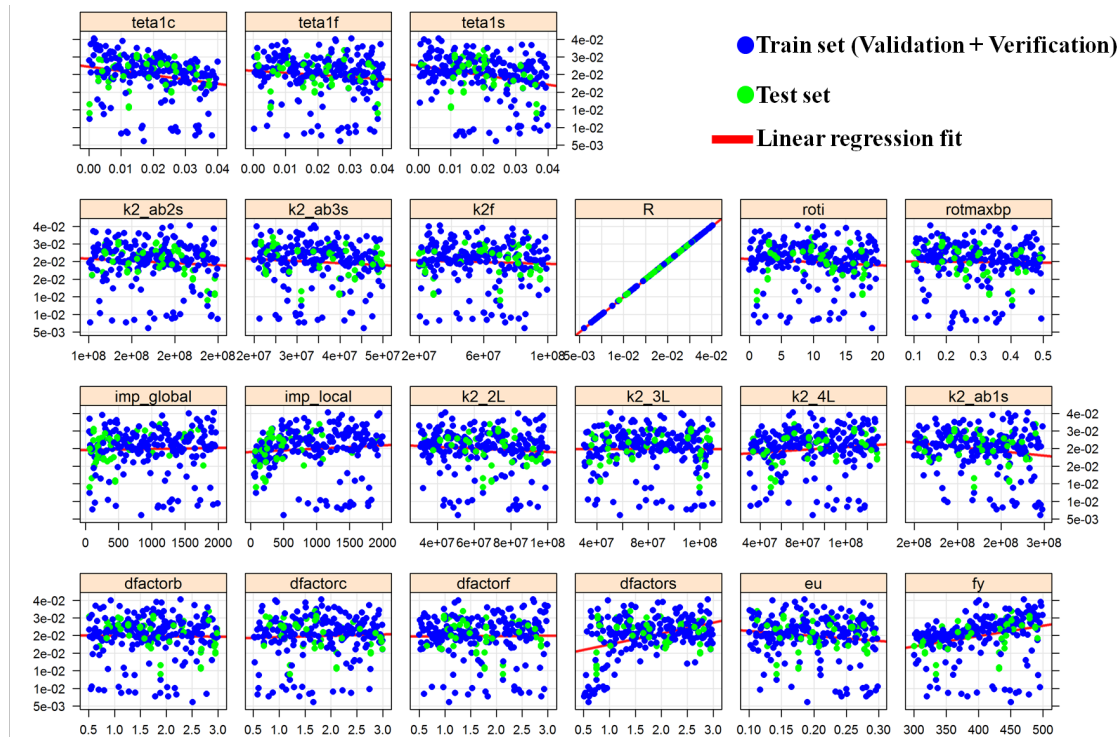
Figure 6.63: Scatterplot of random variables against maximum resistance (R) (CS1), units expressed in N and mm.

Several different models were considered. Among these, the models belonging to the boosted trees family returned the best results. In particular, the Stochastic Gradient Boosting model and the Cubist model were selected for analysis. In all models the R package *caret* was used (Kuhn, 2008).

Table 6.30 presents the results obtained. It can be seen that the Stochastic Gradient Boosting model outscores the Cubist model in every performance metric considered and it is therefore selected. The results shown were obtained using 1000 repetitions of the Bootstrap resampling method.

Table 6.30: Summary of results of training and testing of predictive models.

Model	Train data set	Results								
		Performance metrics		Relative differences						
	Model parameters	RMSE	R^2	Max	3rd quartile	Mean	Median	1st quartile	Min	
Cubist	# committees = 32 # neighbours = 9	mean = 0,0030 sd = 0,00073	mean = 0,726 sd = 0,119	49,9%	1,0%	0,8%	-2,0%	-3,8%	-17,6%	
Stochastic Gradient Boosting	# trees = 2100 Interaction depth = 43 Shrinkage = 0,01	mean = 0,0026 sd = 0,00059	mean = 0,782 sd = 0,094	13,3%	3,1%	0,7%	0,5%	-1,8%	-9,4%	
Model	Test data set	Results								
		Performance metrics		Relative differences						
	Model parameters	RMSE	R^2	Max	3rd quartile	Mean	Median	1st quartile	Min	
Cubist	# committees = 32 # neighbours = 9	0,00145	0,939	30,3%	0,3%	-1,1%	-2,3%	-3,2%	-17,6%	
Stochastic Gradient Boosting	# trees = 2100 Interaction depth = 43 Shrinkage = 0,01	0,00110	0,960	10,9%	1,8%	-0,2%	-0,1%	-2,2%	-12,7%	

Legend:
RMSE represents the relative mean square error;
R^2 represents the coefficient of determination;
Relative differences are given by: $\left(X_{pred} - X_{obs}\right)/X_{obs} \times 100$

Figure 6.64 illustrates more results concerning the accuracy of the Stochastic Gradient Boosting model. The figure on the left shows that the residuals (*i.e.* observed minus predicted values) are approximately evenly distributed around zero over the entire range of predicted values which is a good indicator of the predictive power (capacity to generalise the results) of the selected model.
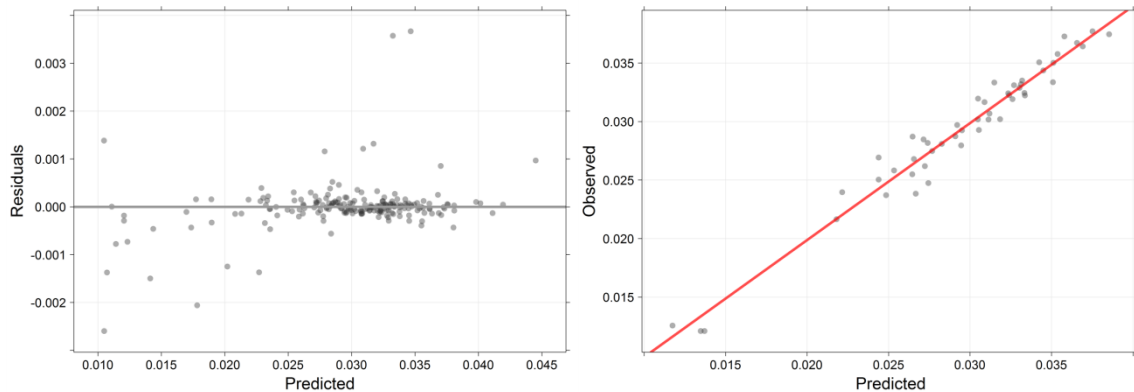
Figure 6.64: Residuals plot for resistance (*Left*) and Observed resistance vs. Predicted resistance plot (*Right*) for Stochastic Gradient Boosting model (CS1), in N/mm^2.

Figure 6.65 just shows another possible view of the results, in this case the relative model differences between predicted and observed data. It is possible to observe that a Normal distribution fits quite well the model differences values distribution.
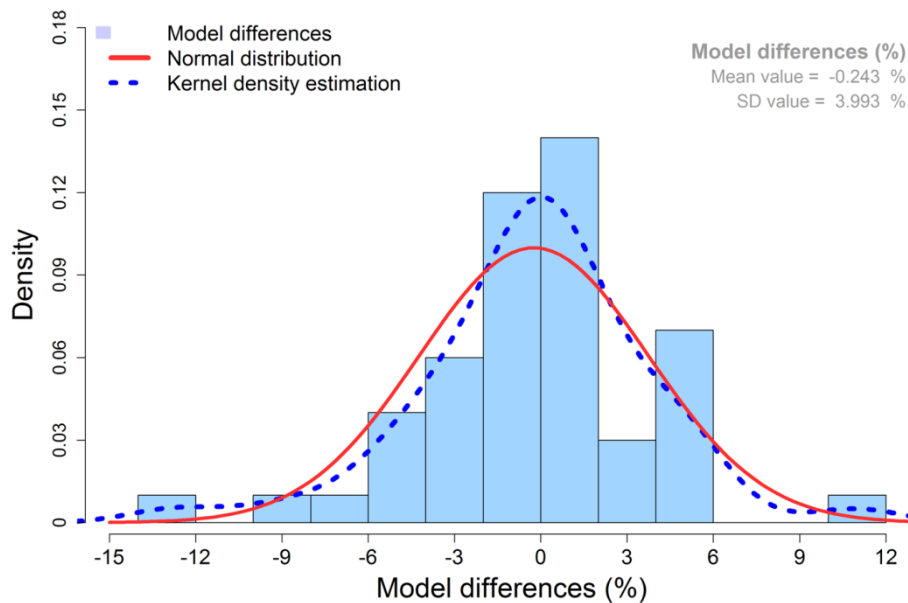
Figure 6.65: Model differences histogram for Stochastic Gradient Boosting model (CS1).

Using a surrogate model to foresee the actual behaviour under unknown and uncertain conditions introduces another component to the model uncertainty, besides the uncertainty of the numerical results. Nevertheless, this uncertainty is relatively small for the Stochastic Gradient Boosting model and CS1, see Figure 6.66. The abscissa represents the ratio between the observed data and the predicted data. This type of uncertainty was modelled using a Normal distribution with the parameters given in Figure 6.66. This is a conservative decision.

Regarding the numerical uncertainty, from the results presented in Chapter 4 it is possible to estimate it. The histogram of the ratio between the observed resistance and the numerically predicted resistance is given in Figure 6.67. This type of uncertainty was modelled also using a Normal distribution with the parameters given in Figure 6.67.
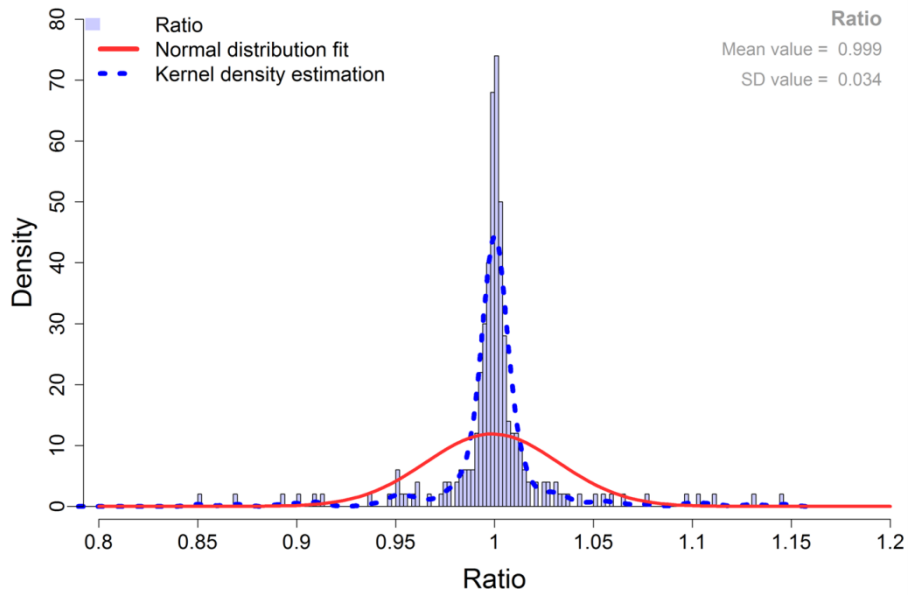
Figure 6.66: Predictive model uncertainty (CS1).
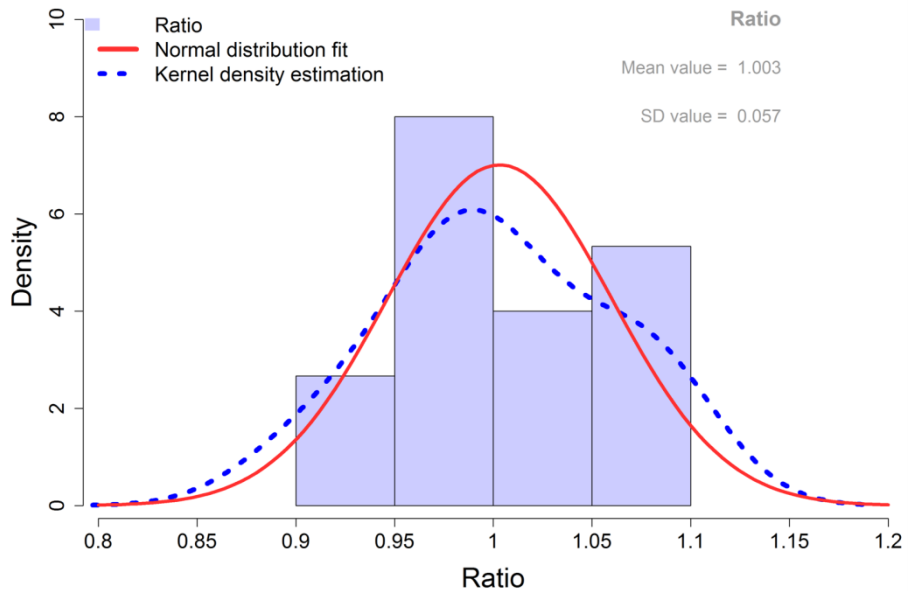
Figure 6.67: Numerical uncertainty.

Both types of uncertainty were applied to the maximum resistance (R), yield resistance (R_y) and R_1 resistance. For the damage energy only the predictive model uncertainty was considered since it was assumed that numerical uncertainty will only introduce translations to the damage energy, so the relative differences between damage energy values will not be significantly affected.

For the other variables, similar analyses to the one shown above were performed. In all cases the boosted trees family provided the best models, either by the Stochastic Gradient Boosting or by the Cubist model, achieving a coefficient of determination always higher than 90% for the test data set and relative differences not exceeding 25%.

6.4.2.2.3 Stochastic results

Twenty variables associated with the system's resistance, selected and detailed previously, were modelled as random with distributions given in Table 6.27, while the rest of the variables were considered deterministic with values equal to the mean values indicated in Table 6.27, with the exception of the stiffness (k1) associated with joint looseness which was considered equal to 1 kNm.rad.

Regarding actions, only the value of the pressure load applied on top of the formwork surface was considered random. For the reliability analyses, the performance of the system was compared against a

vertical pressure action modelled by a Normal distribution with mean value equal to 24,0 kN/m^2 and a COV equal to 0,075, taking also into account the uncertainty in estimating these parameters as previously explained. On the contrary, the distribution was considered uniform with a minimum value equal to 20 kN/m^2 and a maximum value equal to 26 kN/m^2 for the robustness and fragility analyses. For the latter analyses, the vertical pressure action was subsequently increased until collapse was reached.

The value of the wind action was made equal to the working wind velocity and the application direction was fixed along the y-y axis, see Figure 6.59. The application point of the differential ground settlement was also considered fixed and the same as the one described in the deterministic results section. The evolution of these actions was also considered the same as the one described in the latter section.

6.4.2.2.3.1   Case study #1

The results obtained in terms of reliability, robustness index (from Eq. 5.18, see Chapter 5) and fragility index are shown below. It may be concluded that for the rather large range (variability) of input random variables the probability of failure is exceedingly high, the robustness is low and fragility before the "unavoidable collapse" state is also small. These means that collapse was triggered by a small amount of damages and its probability of occurrence is extremely high when compared to the maximum recommended values given in specialised literature (BSI, 2002a ; JCSS, 2001).
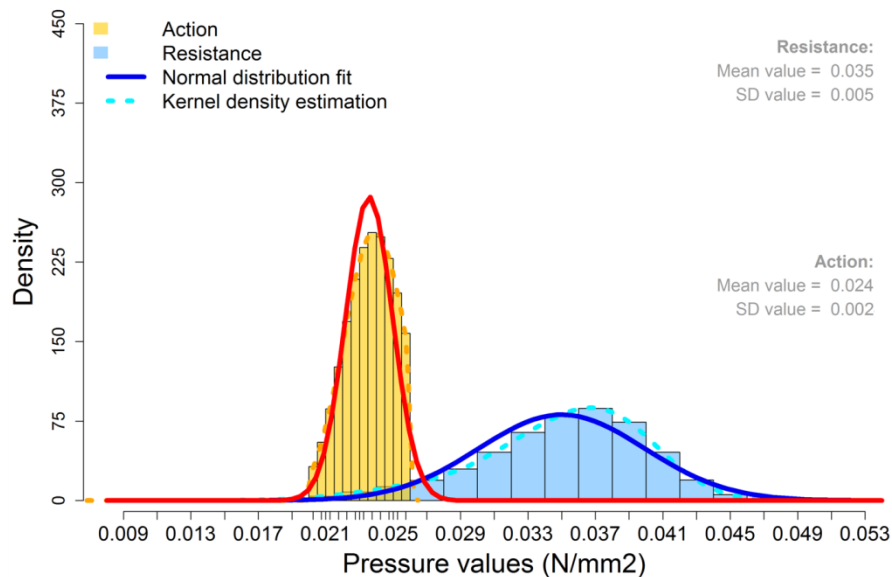
Figure 6.68: Histograms of action and resistance (CS1).
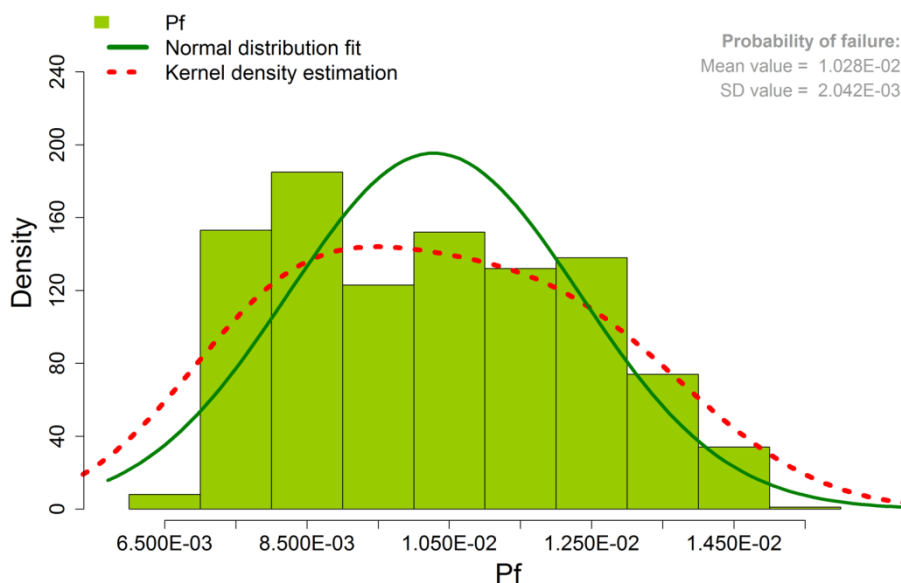
Figure 6.69: Histograms of probability of failure (CS1).
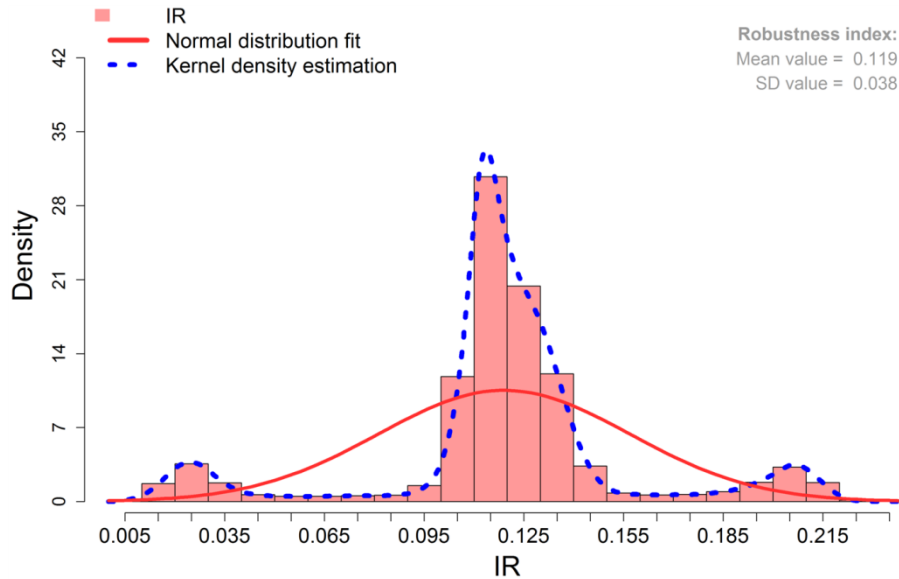
Figure 6.70: Histograms of robustness index (CS1).

Figure 6.71: Cdf's of fragility, with the dispersion due to uncertainty propagation and highlighting the average curve (CS1).
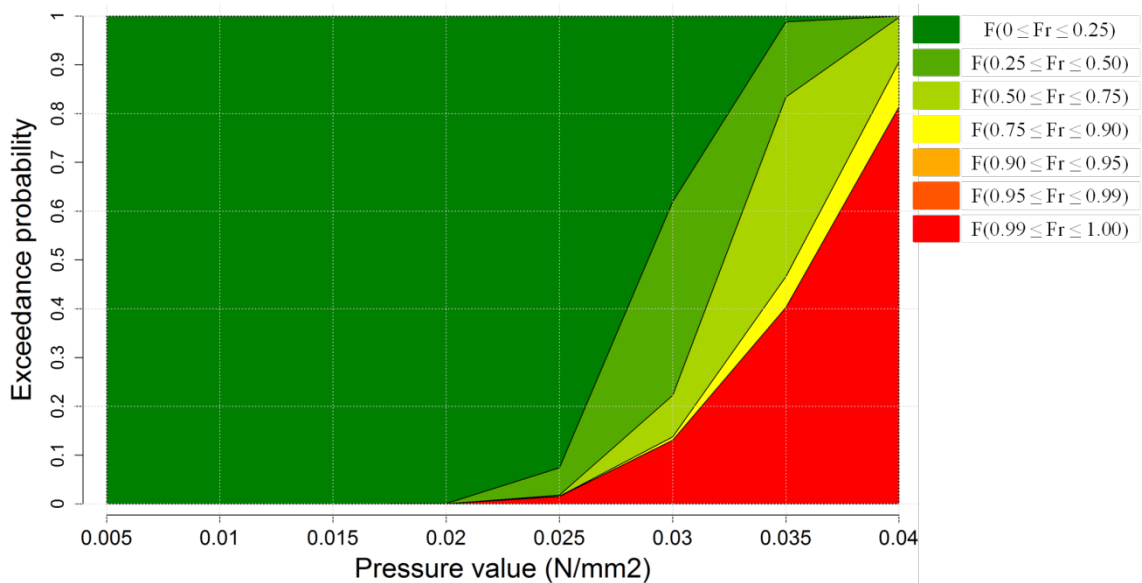
Figure 6.72: Complementary fragility curves (CS1).

6.4.2.2.3.2   Case study #2

The results for case study #2 are more severe than for case study #1 since additional actions were considered for the former case study. This is indeed confirmed by the results in terms of reliability, robustness index (from Eq. 5.18, see Chapter 5) and fragility index shown below. This reconfirms the dangers of underdesigning a bridge falsework system.

The mean value of the resistance drops significantly (18%) and this fact penalises reliability (8 times higher probability of failure) and fragility index since it is now even more likely that significant damages will occur. Robustness index increases but it may not be enough to avoid collapse without warning, depending also on the values of the actions applied.

The effect of propagating uncertainty is also more pronounced in absolute terms, see Figure 6.74 and Figure 6.76.

Fragility curves are shifted towards lower values of action but the gap between levels of damage increases due to the higher robustness.
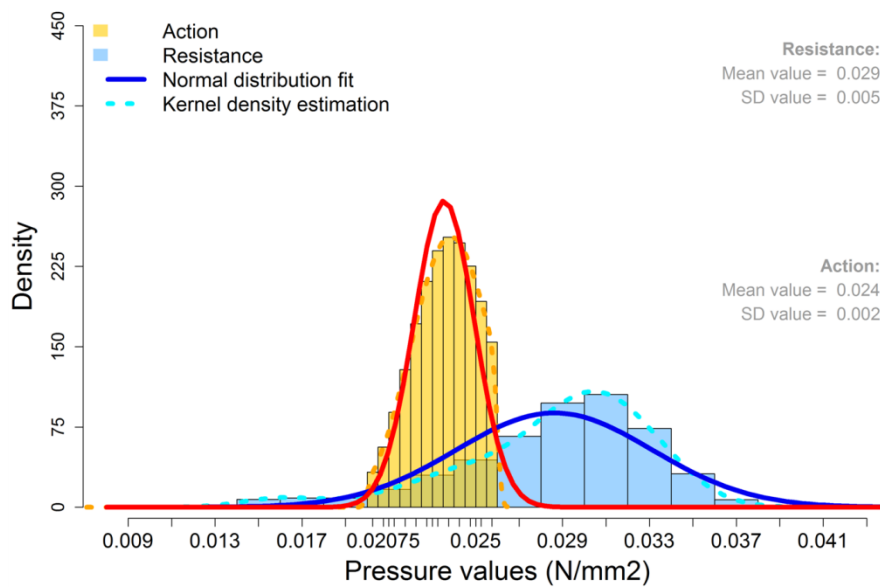
Figure 6.73: Histograms of action and resistance (CS2).
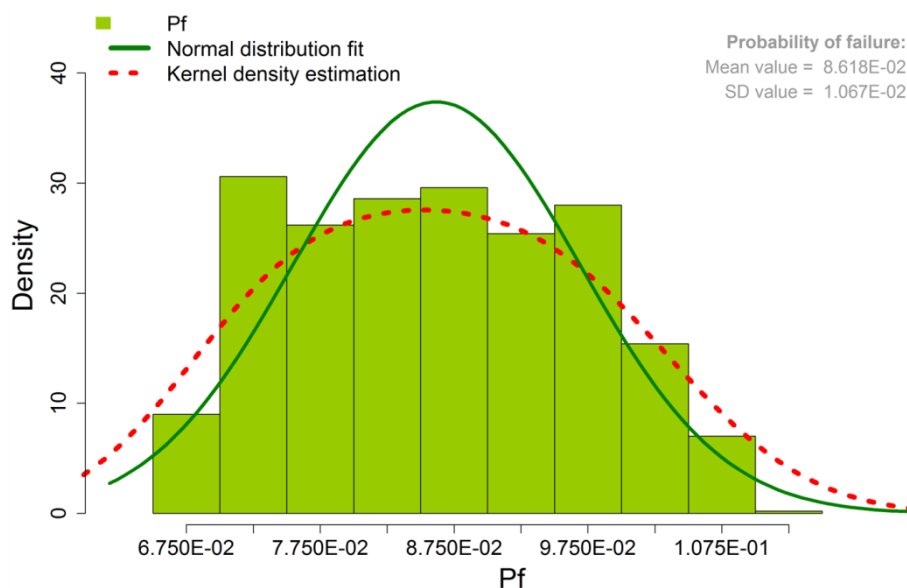
Figure 6.74: Histograms of probability of failure (CS2).
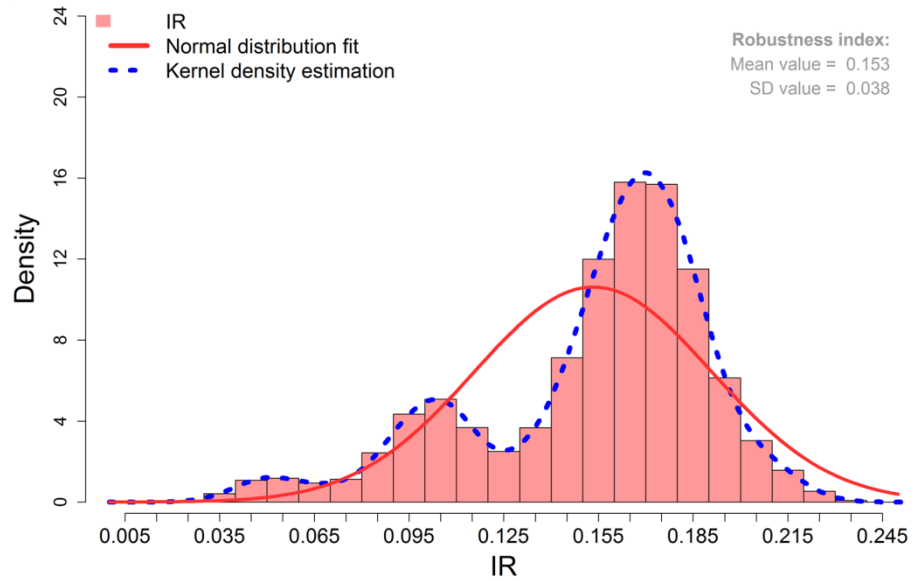
Figure 6.75: Histograms of robustness index (CS2).

Figure 6.76: Cdf's of fragility, with the dispersion due to uncertainty propagation and highlighting the average curve (CS2).

Figure 6.77: Complementary fragility curves (CS2).

6.4.2.2.4   Further stochastic results

Based on the results presented in the previous section it is the time to discuss alternative strategies to increase the robustness and decrease the fragility of bridge falsework systems, using the same case studies as application examples.

As detailed in Chapter 5, there are many possible strategies to increase the robustness of a structure. Nevertheless, some of these will be more or less efficient depending on the type of structure. For bridge falsework systems the following strategies seem more appropriate: (i) increase resistance, (ii) structural integrity and (iii) ductility.

One way to enhance the robustness of these structures is to selectively increase the resistance of critical elements, either by increasing the elements strength, or the elements stiffness. The former can be achieved by choosing materials with higher mechanical properties (strength and deformation capacity), while the latter can be attained by adding bracing elements, pins at the spigot joints or placing anchor bolts at the baseplates for example. Also, adding translational restraints to the formwork system is another way of increasing the falsework resistance.

These solutions improve the system's behaviour. However, it is also of interest to be able to control and possibly reduce the system's response variability. For example, considering CS1 and CS2, the stochastic sensitivity coefficients presented in Figure 6.78 indicate that initial imperfections, spigot and Cuplok® joint properties are the most important stochastic variables. Therefore, the potential contribution of these variables to reduce fragility and increase the reliability and robustness of the system is two-fold: increasing the mean value and reducing the variance.
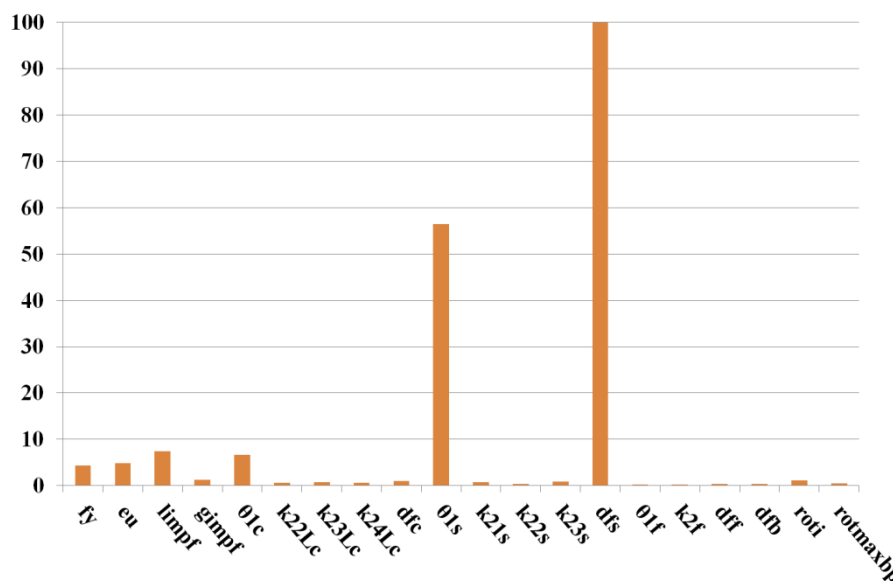
Figure 6.78: Overall (averaged) stochastic sensitivity coefficients, considering CS1 and CS2.

Structural integrity is also an effective strategy since it relates to proper bracing and lacing of the system but also possibly tying it to another, stiffer, structure. As was seen previously, efficient bracing arrangements are extremely beneficial in terms of resistance, robustness and fragility. However, finding the best bracing arrangements involve using design practices other than simply following the minimum recommended bracing requirements given in most of the system's producers design guides.

Additionally, structural integrity relates to soil stability, to avoid collapse due to insufficient resistance of the foundation. To properly address this problem, it is, in general, not sufficient to look only from the point of view of the bridge falsework structural solution. In fact, as was demonstrated, increasing the system's stiffness may amplify the system's sensitivity to differential ground settlements. Therefore, measures to correctly characterise the foundation ground and make sure it has the necessary resistance and stiffness, *i.e.* compatible with the falsework system performance, should also be considered.

Finally, ductility is also a valid strategy by increasing capacity of the materials to continue to resist after yielding by absorbing energy and thus allowing energy to be dissipated in a stable fashion and stresses to be redistributed without significant deterioration of the structure's performance. Material ductility can be achieved by material strain-hardening and/or by material deformation capacity.

Applying the above concepts and guidance to the case studies at hand, the values of the following random variables were modified: (i) decreasing initial geometrical imperfections, (ii) decreasing looseness rotation, (iii) increasing the k2 stiffness of the Cuplok® joints and (iv) increasing the deformation capacity of the joints. The changes are given in Table 6.31 and form an alternative (improved) scenario to the reference case studies (CS1 and CS2) discussed previously.

In practice, these changes reflect simple controls related to better quality checks, inspection and maintenance plans. The results of these changes are given in the following Figures.

Table 6.31: Improved random variables values (changes highlighted in bold).

Random variables	Probabilistic distribution	Distribution parameters		Minimum value	Maximum value
Initial imperfections					
limpf	Lognormal	mean = N(**1200**;100;**1100**;**1300**)	sd = N(1000;250;500;1500)	**1000**	2000
gimpf	Normal	mean = N(**1200**;100;**1100**;**1300**)	sd = N(1000;250;500;1500)	**1000**	2000
Ledger-to-standard joint (Cuplok joint)					
Strong axis					
θ1c, rad	Normal	mean = N(-0,008;0,005;-0,03;0,01)	sd = N(0,012;0,007;0,006;0,019)	0	**0,01**
k22Lc, kN.m/rad	Weibull	shape = N(8;2;6;10)	scale = N(75;5;71;78)	**60**	90
k23Lc, kN.m/rad	Weibull	shape = N(4,8;1,5;3,2;6,5)	scale = N(90;10;80;99)	**60**	120
k24Lc, kN.m/rad	Weibull	shape = N(6,2;2,5;3,7;8,6)	scale = N(92;7;84;100)	**60**	140
dfc	Normal	mean = N(1;0,2; 0,75; 1,25)	sd = N(0,25; 0,1; 0,1; 0,5)	**1**	2
Standard-to-standard joint (Spigot joint)					
θ1s, rad	Normal	mean = N(0,005;0,005;0,001;0,01)	sd = N(0,007; 0,002; 0,005; 0,01)	0	**0,01**
dfs	Normal	mean = N(1;0,2;0,75;1,25)	sd = N(0,25;0,1;0,1;0,5)	**1**	2
Forkhead joint					
θ1f, rad	Normal	mean = N(0,005;0, 005;0,001;0,01)	sd = N(0,007; 0,002; 0,005; 0,01)	0	**0,01**
dff	Normal	mean = N(1;0,2;0,75;1,25)	sd = N(0,25;0,1;0,1;0,5)	**1**	2
Brace joint					
dfb	Normal	mean = N(1;0,2;0,75;1,25)	sd = N(0,25;0,1;0,1;0,5)	**1**	2
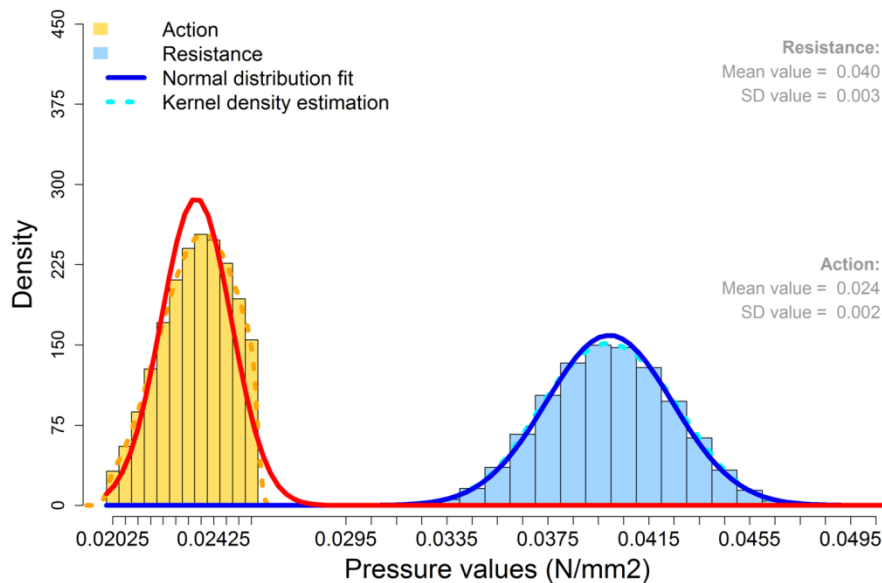
Figure 6.79: Histograms of action and resistance (CS1 alternative, CS1a).
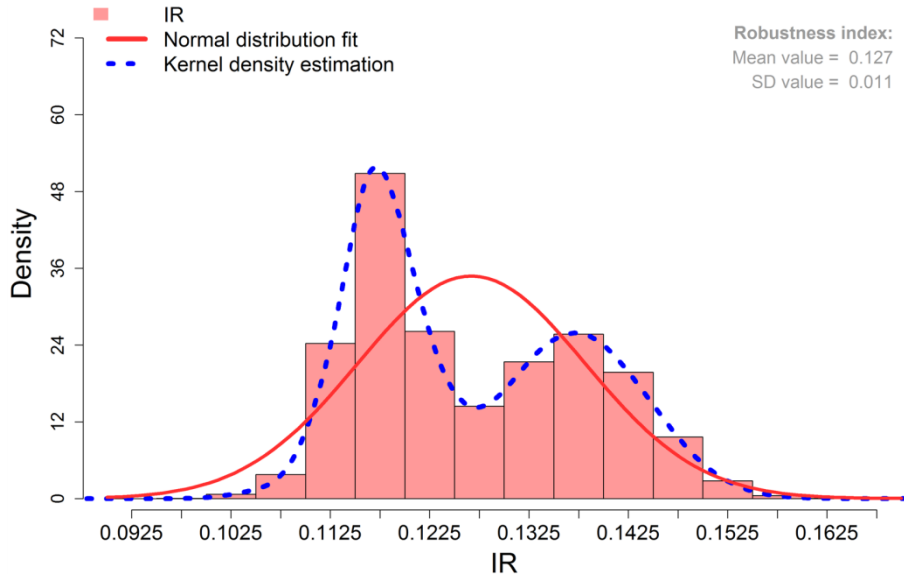
Figure 6.80: Histograms of robustness index (CS1 alternative, CS1a).
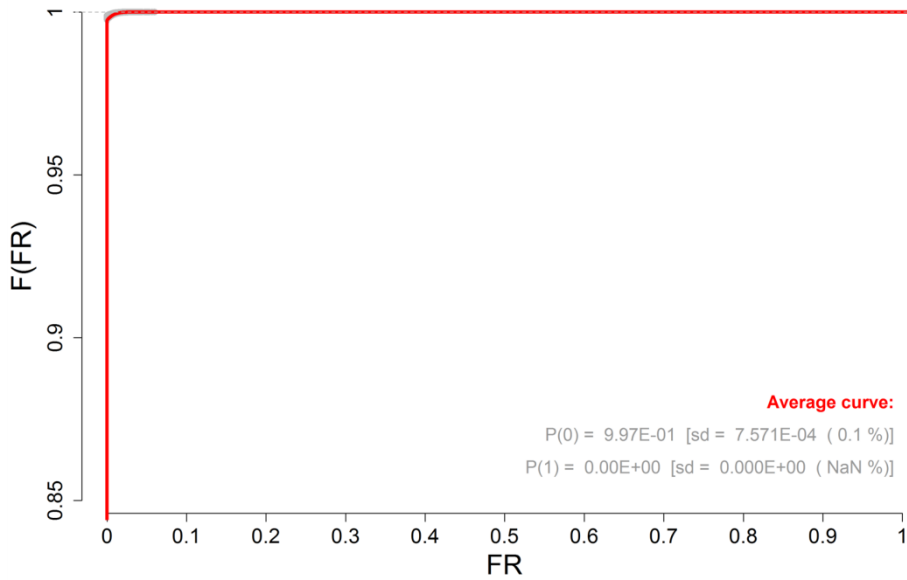
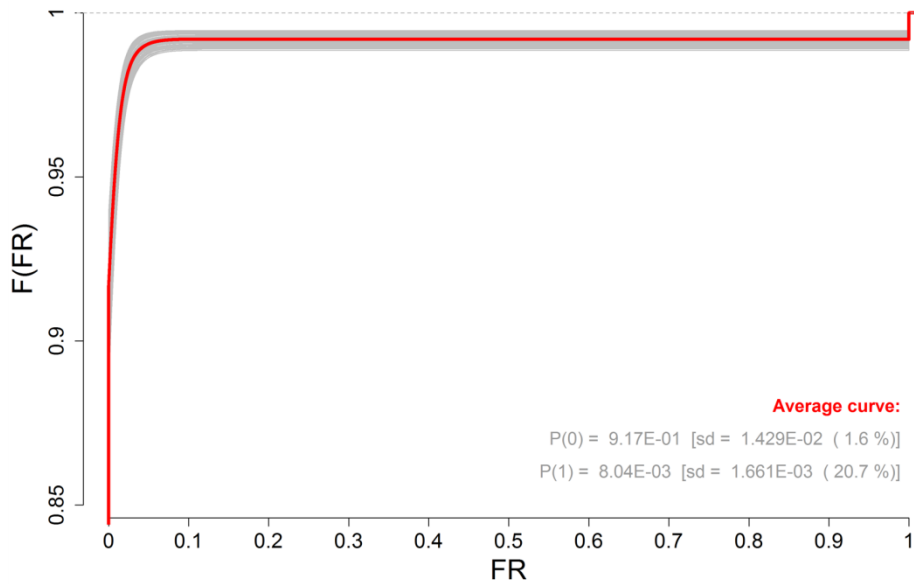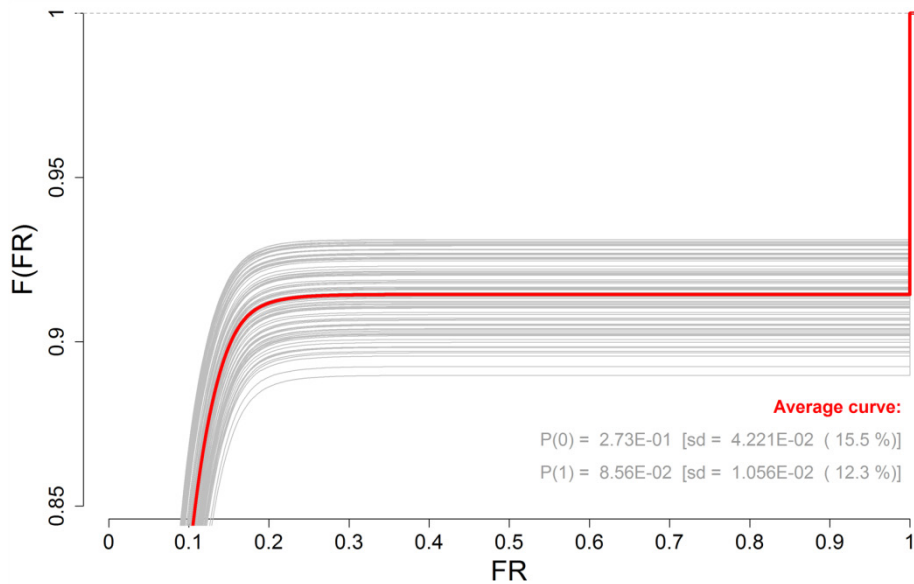**Figure 6.81: Cdf's of fragility, with the dispersion due to uncertainty propagation and highlighting the average curve (CS1 alternative, CS1a).**
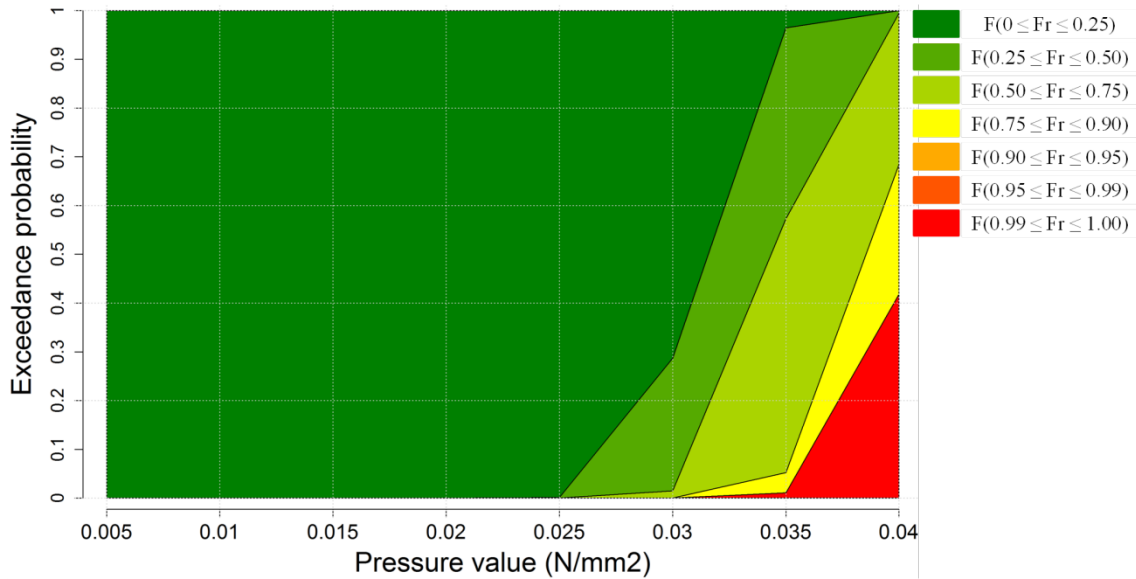
Figure 6.82: Complementary fragility curves (CS1 alternative, CS1a).
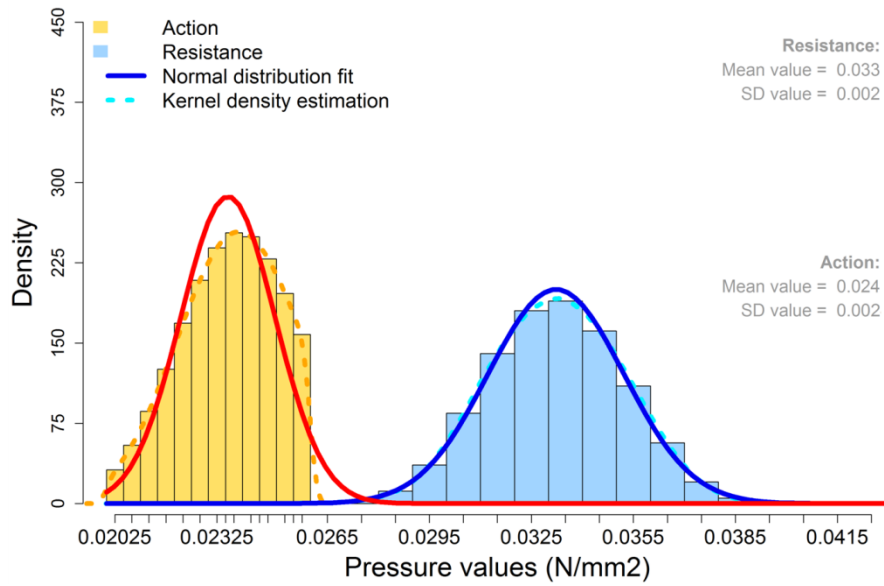
Figure 6.83: Histograms of action and resistance (CS2 alternative, CS2a).
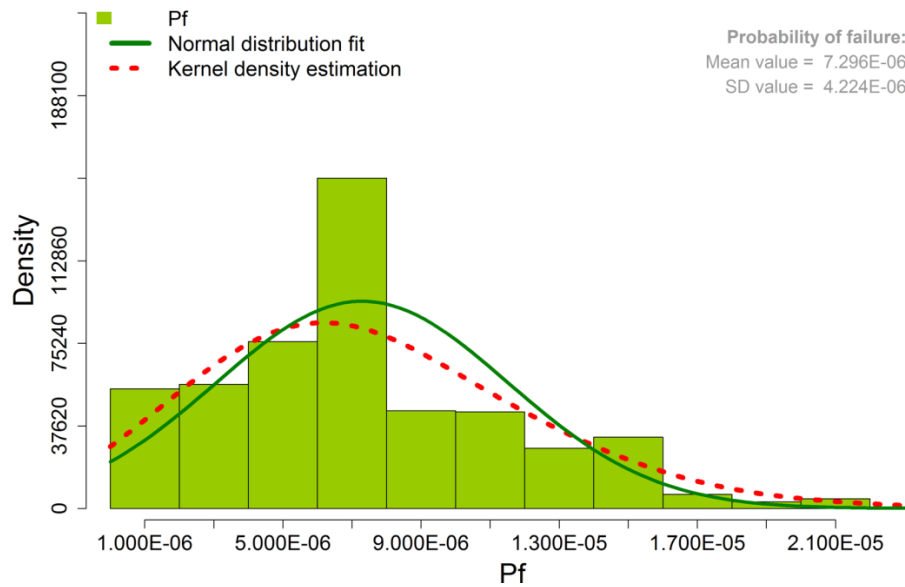
Figure 6.84: Histograms of probability of failure (CS2 alternative, CS2a).
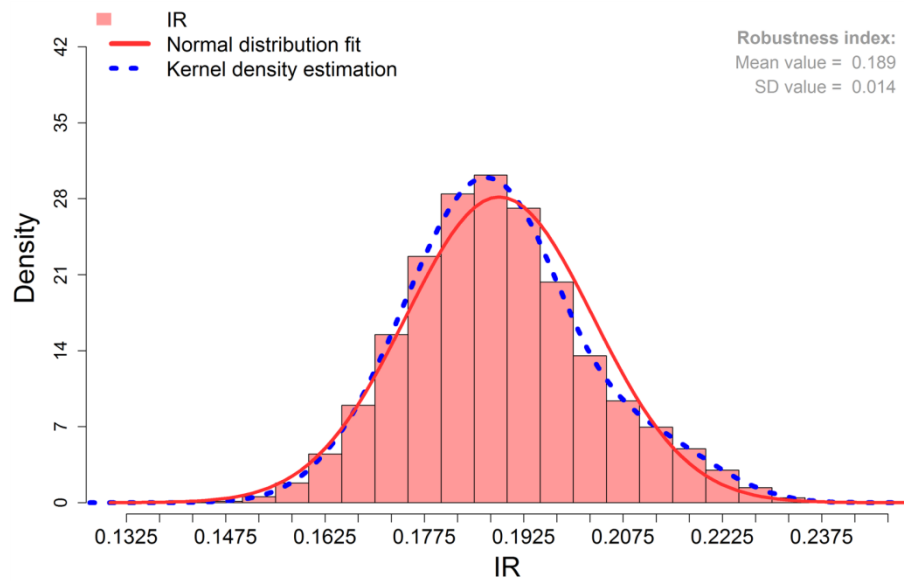
Figure 6.85: Histograms of robustness index (CS2 alternative, CS2a).
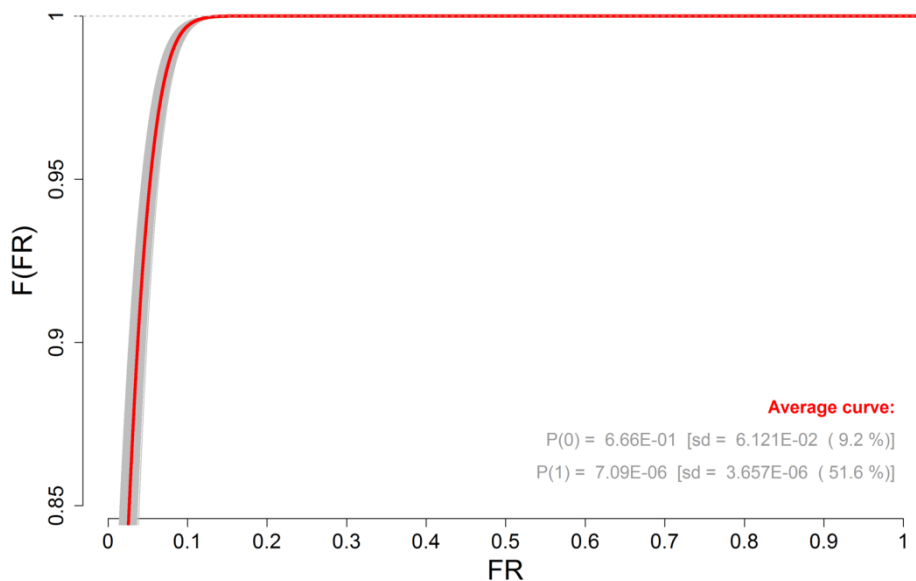
Figure 6.86: Cdf's of fragility, with the dispersion due to uncertainty propagation and highlighting the average curve (CS2 alternative, CS2a).
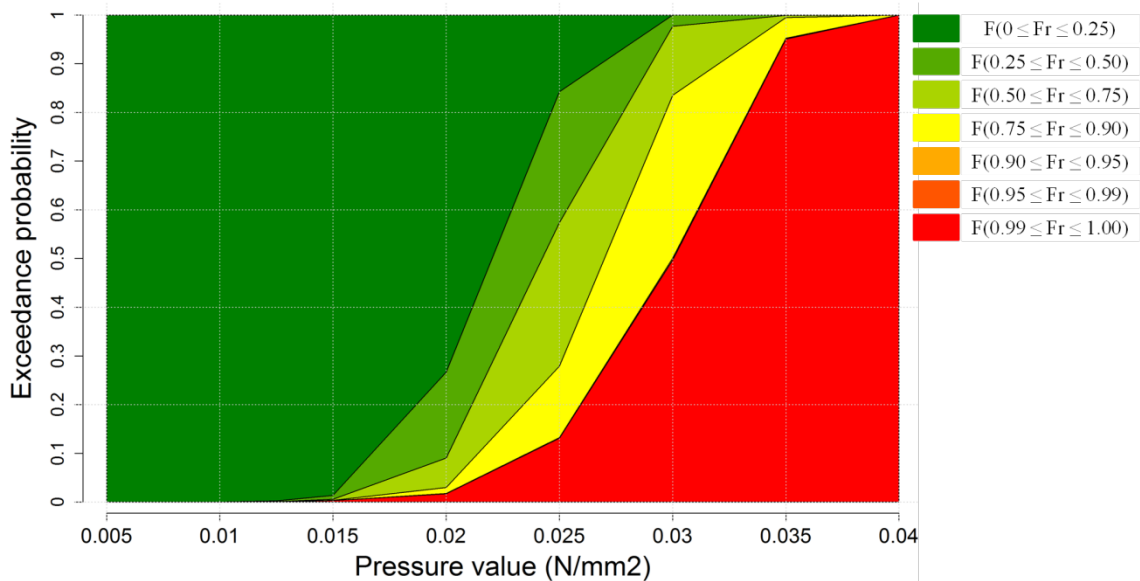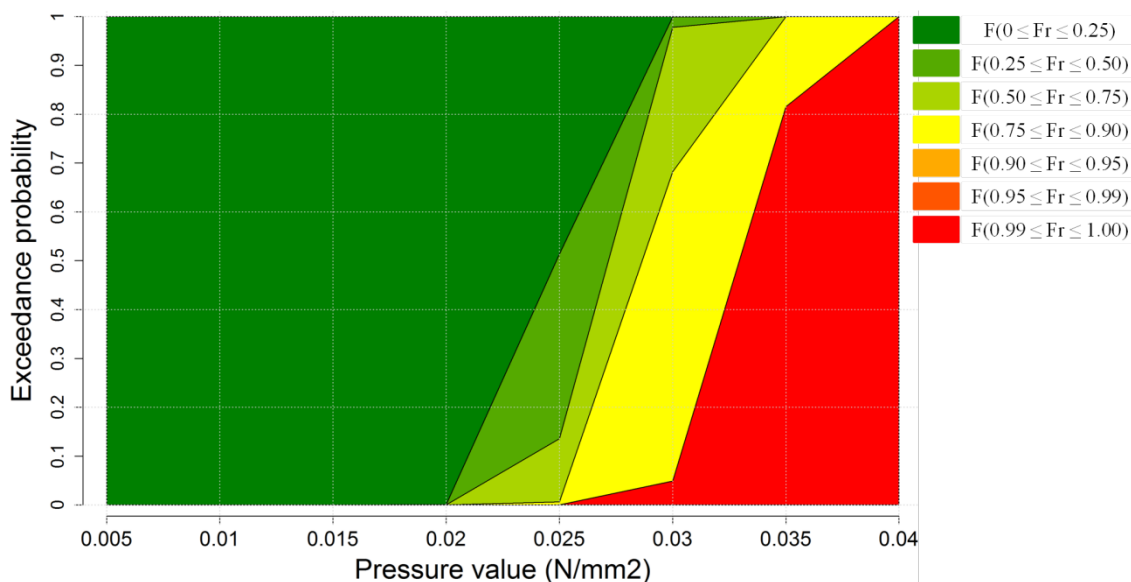

Figure 6.87: Complementary fragility curves (CS2 alternative, CS2a).

6.4.2.2.4.1   Case study #1, alternative scenario

The impact of the outlined small changes is significant. Not only the mean value of resistance and robustness has increased over 10% but also the variability of resistance, robustness and fragility decreased considerably. In fact, failure probability is residual (less than 1×10^{-8}) and therefore small values of fragility mean low structural damages with extremely low risks of collapse. This can be confirmed by observing the fragility curves.

6.4.2.2.4.2   Case study #2, alternative scenario

Results are also expressive in the case of CS2a. The mean value of resistance and robustness increased also over 10% and the variability of resistance, robustness and fragility also decreased considerably. In fact, the mean value of the failure probability decreased four orders of magnitude (from 80000×10^{-6} to 7×10^{-6}). Also, for this order of values, small values of fragility imply low structural damages with extremely low risks of collapse. This can be confirmed by observing the fragility curves.

6.5   Risk evaluation

Risk evaluation is the task of defining risk criteria and comparing it with the risk levels obtained during risk analysis. Risk criteria were introduced in Chapter 5 and have already been applied at the beginning of the present Chapter. Based on the findings presented in Chapter 5, the value commonly assigned to individual acceptable risk (*i.e.* the broadly acceptable risk limit) ranges from 1 in 10^6 to 10 in 10^6 deaths per year, and to individual unconditionally unacceptable risk (*i.e.* the limit of tolerability) ranges from 100 in 10^6 to 1000 in 10^6 deaths per year, see (ANCOLD, 2003 ; Das, 1997 ; HSE, 1988, 2001 ; UK DfT, 1999 ; ISO, 1998). For structural risk, the acceptable annual probability of failure due to any cause range from 1 in 10^6 to 10 in 10^6 failures per year (BSI, 2002a, 2004a ; CIRIA, 1977 ; McDonald et al., 2005).

Therefore, the probability of failure determined in the previous sections can be evaluated. Comparing the acceptable probability of failure levels with the results presented in Table 6.32 and assuming that the considered system is only used once per year (the annual probability of failure can be expressed as the sum of all conditional failure probabilities for one year return period), it is possible to conclude that in the original (reference) scenario the risk is exceedingly high and cannot be accepted or tolerated. Therefore, corrective measures need to be implemented to lower the risk level to acceptable, or tolerable, levels. By applying an example of the strategies outlined in this section to improve the performance of the falsework systems, materialised in the alternative scenarios, it can be seen that it was possible to decrease considerably the failure probability to a level within the range of acceptability.

Table 6.32: Probability of failure for the case studies considered.

Probability of failure (P_f)	CS1		CS2	
	Original	Modified	Original	Modified
Mean value	10×10^{-3}	1×10^{-8}	$8,5\times10^{-2}$	7×10^{-6}
Standard deviation	2×10^{-3}	0	1×10^{-2}	4×10^{-6}
Maximum value	12×10^{-3}	1×10^{-8}	11×10^{-2}	20×10^{-6}

In terms of annual individual risk, assuming a value for the conditional probability of a fatality given a bridge falsework collapse equal to 0,5 (based on the collapse survey results presented at the start of the present Chapter), the individual risks for the alternative scenario are also within the broadly acceptable risk limit. Of course, if the system is used multiple times the annual failure probability increases, not only because of the higher number of uses but also of the damage accumulation which might decrease the value of the resistance and possibly increase its variability.

6.6   Risk control and risk informed decision-making

In this section an economical justification for adopting the alternative (improved) scenario, instead of the reference (baseline) scenario, will be analysed. In order to perform this analysis a cost function must be derived, such as the one suggested in Chapter 5. Since it is a comparison exercise between two alternatives, *i.e.* reference scenario and an alternative (improved) scenario, only the relative cost differences are of interest. Therefore, as fixed costs are equal in both cases they do not need to be considered. As a simplification, only the costs associated with structural damages and operation of the structure were not considered as fixed costs. Costs due to individual injuries were also not considered.

It was assumed that the sum of the cost of the structure supported by the bridge falsework and the cost of the bridge falsework, C_{max}, was equal to £200.000,00. Additionally, the function between fragility index and damage costs was considered to be linear, *i.e.* when fragility index is equal to zero, structural damages are equal to zero, whereas when fragility index is equal to one, structural damages are maximum.

The operational costs stem mainly from labour and operation costs, *e.g.* expenditures on bridge falsework maintenance related activities. Since the alternative scenario does not require any

reinforcement of the system, as a simplification, it was assumed that implementing the improved quality standards represents a fraction, *e.g.* 20%, of the total cost of a new bridge falsework system, per use. Fixing this latter value at £20.000,00 (based on material's cost and labour cost), the extra costs associated with the alternative scenario are estimated to be equal to £4.000,00 (2014 prices), per use.

The benefits are calculated using the Value of Preventing a Fatality (VPF) concept, which is fixed annually in the UK by the Department for Transport (DfT). The latest number (2014 prices) is equal to £1.700.000,00. The benefits depend on the damage types and levels, their probability of occurrence, on the conditional probability of an injury level given a damage and on the number of persons at risk. The probability of a given damage level also depends on the damage accumulation throughout the uses and on the effectiveness of the measures employed to minimise the effects of these damages.

Benefits are calculated by the improvements relative to the worst case scenario: the collapse of the structure, *i.e.* when fragility equals one. As a simplification it was considered that benefits decrease linearly with the fragility index, *i.e.* when fragility index is equal to zero, benefits are equal to its maximum value, whereas when fragility index is equal to one, benefits are equal to zero. The maximum benefits value (B_{max}) was considered equal to 50% of the VPF. This value was established also taking into account the differences between the probabilities of various injury levels when fragility is equal to zero and equal to one.

Considering CS2 and CS2a as two independent bridge falsework structures subject to uncertain actions, a single use per year of each structures and that only one person is at risk per use, the cdf of the relative Net Value (Net Value of CS2a - Net Value of CS2) between choosing the alternative scenario (CS2a) and the reference scenario (CS2) is presented in Figure 6.88 (red curve). In this analysis, fragility was calculated considering a vertical pressure action modelled by a Normal distribution with mean value equal to 24,0 kN/m^2 and a COV equal to 0,075, taking also into account the uncertainty in estimating these parameters as previously explained.

Despite the fragility cdf of the reference system alternative system exhibits a second-order stochastic dominance over the fragility cdf of the alternative system, it is possible to observe that this alone does not guarantee that a positive net value is always obtained. This happens because it was considered that CS2 and CS2a are two independent bridge falsework structures. Nevertheless, there is approximately 64% probability that a positive relative Net Value is obtained, with a mean relative Net Value of more than £100.000,00. It can be concluded that it is justified the choice of selecting the alternative scenario, CS2a, over the reference scenario, CS2, since the additional costs are outweighed by the dramatic reduction in individual and structural risks. This conclusion remains valid if the uncertainty in fragility values is propagated to the relative Net Value.
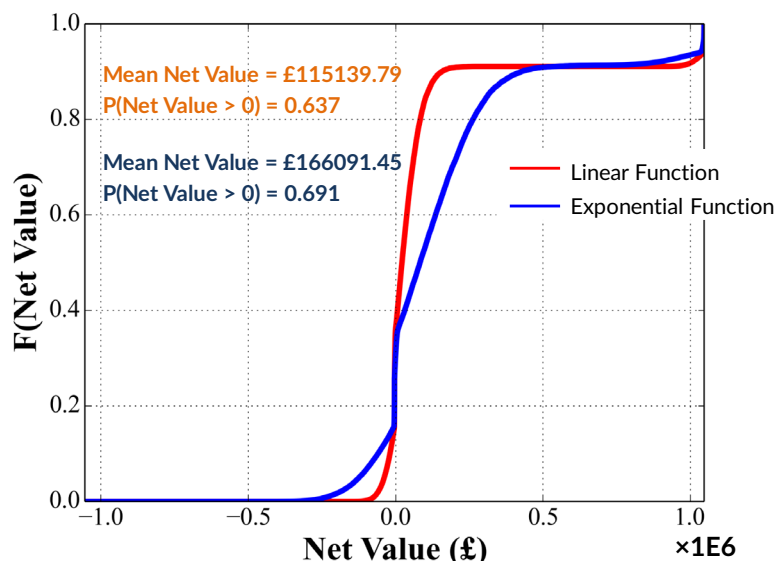
Figure 6.88: Cdf of relative Net Value (for CS2 model), linear and exponential functions.

It is of interest to study how the relative Net Value varies for instance with the function between costs and fragility, and between benefits and fragility. Choosing an exponential law instead of a linear law, see Figure 6.89, results in the curve shown also in Figure 6.88 (blue curve). It can be observed that the maximum possible value of relative Net Value is slightly reduced but the mean relative Net Value increases significantly and the probability that a positive relative Net Value is obtained also increases. This apparent paradox occurs because of the different configuration of the fragility curves of the reference and alternative scenarios.
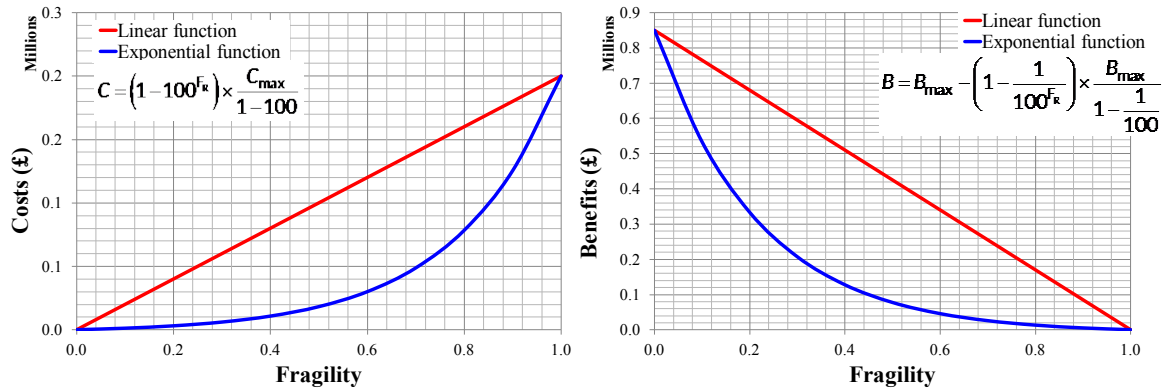
Figure 6.89: Illustration of different possible functions between Costs and Fragility (*Left*, for CS2 reference model) and Benefits and Fragility (*Right*).

It is also important to assess how the relative Net Value changes with the maximum value of the benefits (MBV). Considering a MBV value equal to 0,1%, instead of 50%, of the VPF the results presented in Figure 6.90 are obtained.
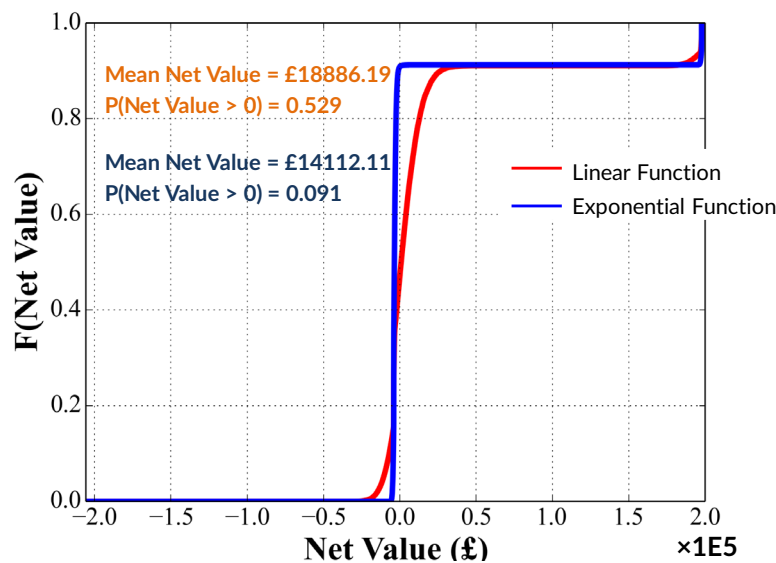
Figure 6.90: Cdf of relative Net Value (for CS2 model), linear and exponential functions, MBV = 0,1%.

For low MBV values the relative Net Value depends mainly on potential cost savings due to structural damages, since the benefits due to reduction of individual risks are now much smaller. It can be observed that this fact makes the relative Net Value cdf extremely sensitive to the type of function between costs and fragility. If for a linear function the probability that a positive relative Net Value is obtained is close to 53%, for an exponential function this probability decreases to 9%. The mean relative Net Value also decreases considerably in both cases, but still remains positive.

Further, if the ratio between the cost of the permanent structure and the cost of the temporary structure (PTR) was considered lower than the initial considered, for example 0,001 (residual) instead of 9, but the extra costs associated with the alternative scenario remained equal to £4.000,00, the results would change, see Figure 6.91. It can be observed that the relative Net Value further deteriorates and now the mean value for both types of functions is negative, with a probability close

to 9% that a positive relative Net Value is obtained in both cases. These results do not necessarily mean that the alternative model should be disregarded, but it is an indicator that under the considered conditions the cost-benefit of choosing the alternative model can be questioned in particular if other competitor models exist with a more favourable relative Net Value.
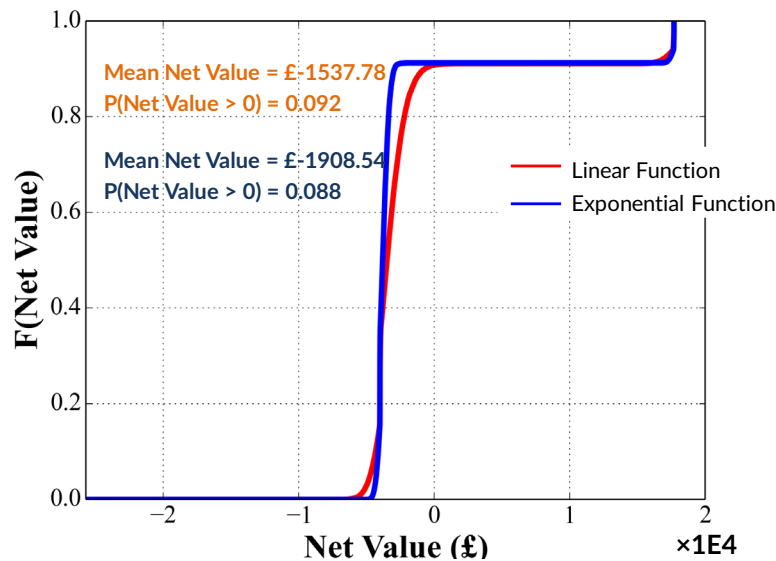
**Figure 6.91: Cdf of relative Net Value (for CS2),
linear and exponential functions, MBV = 0,1% and PTR = 0,001.**

The above set of results clearly illustrates the advantages of the methodology proposed in Chapter 5, and the sensitivity of the decision-making process to input parameters.

It can be concluded that if the cost of the permanent structure significantly exceeds (about one order higher) the cost of the temporary structure, the extent of improvements in terms of structural and economical risks completely justified the small extra costs incurred with selecting the alternative scenario.

By performing optimisation analysis using the methodology detailed above for various structural solutions it is possible to determine the optimal cost-benefit alternative scenario. It is also possible to optimise inspection and maintenance plans considering different damage evolution and accumulation scenarios. However, the uncertainty owing to not knowing with appropriate accuracy the functions relating costs and fragility, benefits and fragility, and other variables, is such that it is not possible to present any meaningful results.

Nevertheless, the procedure outlined in Chapter 5 and exemplified in the previous sections forms a rational method to evaluate the risk of bridge falsework systems taking into account the whole life cycle of these structures.

6.7 Conclusions

In the present Chapter the risk informed methodology to structural design presented in Chapter 5 was applied to bridge falsework. The Chapter started by giving a historic justification to perform such a complex procedure to design bridge falsework. Based on an extensive survey of bridge falsework systems over the last 40 years it was possible to obtain notional values of different risk measures, all of them fully justifying the purpose and interest of the risk informed methodology.

After, a thorough risk and hazard scenarios identification was carried out both qualitatively and quantitatively. Regarding the latter, both actions related and system related hazards were investigated using deterministic models.

It was found that:

1. Concrete casting loads, including dynamic effects and local overloads can be considered only important for thin slabs supported by falsework structures which do not offer a large safety margin;

2. Wind loads, on the other hand were found to be critical loads since they reduce, in some cases drastically, the resistance of the falsework. In particular, when the falsework is still unloaded during the assembly phase and before concrete casting has begun, when strong winds can overturn the bridge falsework structure. Various solutions were analysed and it was found that including anchor bolts at the falsework baseplates was the most efficient solution and could even prevent early collapses. Of course, assuming that the foundation is properly designed;

3. Differential ground settlements were also analysed. It was demonstrated that even a small value of isolated differential ground settlements could reduce by more than 10% the resistance of the system. It was also found that stiffer systems are more sensitive to differential ground settlements than more flexible solutions because the latter can accommodate with significant strains the imposed deformation. However, excessive looseness at the joints can reduce considerably the resistance of the system;

4. The combined effect of actions should, unless demonstrated that it is not the case, always be considered during the design of bridge falsework systems. Reductions of more than 50% on the resistance value were observed when compared with the limited action application of only vertical pressures to model construction loads;

5. The bracing configuration is the most important parameter regarding system configurations. It was demonstrated that usual bracing layouts can be inefficient when compared with other simple layouts. Including bracing elements from the top to bottom falsework levels is recommended, but care should be taken to limit the bracing free length (*i.e.* brace element length with the same slope direction) and also the spacing between the end and the start of consecutive bracing diagonals at the same bay since bracing can lose efficiency for large values of free length and spacing;

6. The optimal spigot positioning depends on the relative measure between the type of applied actions (in particular lateral loads), initial geometrical imperfections, bracing arrangements and joint characteristics;

7. Falsework solutions adopting steel girder to span highways or rivers raise further complex problems. Therefore, their design should deserve special care and rigorous modelling. From the examples considered it was demonstrated the importance of correctly bracing the falsework towers that support the steel girders. Failure to do so can lead to a 50% reduction of resistance and possibly to a uncontrolled failure;

8. Gross initial geometrical imperfections were also analysed and they are also another parameter that has a considerable influence on the resistance of falsework systems. In particular, the shape of the initial geometrical imperfections is important. Deformed configurations which are associated with low internal energy tensors are particularly critical, for example S shaped initial geometrical imperfections or large deformed overextended jacks;

9. It is important to explicitly model the bridge falsework since design recommendations given in documents released by system producers only contain minimum requirements that may not be sufficient for a specific use. This is especially true for bracing arrangements as was demonstrated.

After, the data collected from the experimental campaign of joint tests presented in Chapter 3 was used together with other appropriate data to build probabilistic models for the most important stochastic variables. These variables were selected based on the results of a sensitivity analysis of

the stochastic response of a chosen reference bridge falsework system. In the end, stochastic models for the resistance, reliability, robustness and fragility for two case studies were determined, presented and discussed. The advantages of the proposed methodology were highlighted. As an example, resistance, reliability, robustness and fragility could be analysed independently and important conclusions could be drawn out namely in terms of characterising the collapse as progressive or abrupt, proportionate or disproportionate. Also, the sensitivity of these parameters to the action values could be easily analysed including the effect of propagating model and statistical uncertainties.

Finally, strategies to enhance robustness and minimise risk were discussed and one possible solution was used as an application example. This solution profited from the results of previous stochastic analyses which highlighted the major random variables, namely initial geometric imperfections and parameters of the Cuplok® and spigot joints. The approach was to target those variables and reduce their impact. In practice, this translated on more rigorous inspection plans and tighter quality controls.

Risks were determined for the reference (baseline) scenario and the alternative (improved) scenario and later evaluated against valid risk criteria. It could be concluded that if the cost of the permanent structure significantly exceeds the cost of the temporary structure the extent of improvements in terms of structural and economical risks completely justified the small extra costs incurred with using the alternative scenario rather than the reference scenario.

7

FINDINGS AND CONCLUSION

7.1 Research objectives

The present research programme concerns bridge falsework systems made of slender (prone to buckling) vertical and horizontal steel tubes connected by special couplers. Failures involving these structures are one of the most common types of accidents in civil engineering leading to disproportionate consequences. This reality calls for a paradigm change regarding the design and use of bridge falsework systems.

Researchers and designers must realise that uncertainty is always present despite the significant evolution in structural engineering knowledge brought (i) by the use of ever-increasing computational capacity and (ii) by advances in experimental investigation. The natural consequence of uncertainty is risk. A risk free structure is a naive, uneconomical objective: risk cannot be eliminated; rather it must be managed rationally through a risk informed decision-making process. It is therefore essential that those who research or design structures realise the importance of considering the design working life risks to structural safety and the benefits that will come by doing so. These design principles are even more important in the field of temporary structures, and in particular bridge falsework systems.

In practice the design of bridge falsework is usually an oversimplified process, based on a comparison of the design forces with reference resistance values given by falsework system producers, without knowing their fundamentals, which may lead to their misuse.

Various factors that have a decisive influence on the behaviour, resistance and performance of falsework are not usually directly accounted for in the design. They are often expected to be covered by the safety margins adopted by the falsework system producers, but these may be insufficient.

The severe consequences of all the accidents involving bridge falsework clearly justify the research needs for a holistic approach of bridge falsework systems risk management. The present research contributes for a better understanding of the structural behaviour, robustness and risk of these structures, so that adequate margins against failure may be maintained throughout the whole design/construction/operation process. In particular, the objectives of this Thesis are:

- Identify relevant hazard scenarios and their procedural causes, enabling and triggering events.

- Increase the available database of results regarding the behaviour of different types of joints of a selected structural solution, some of which have not yet been studied. Also, the existing disagreements between past researches are analysed.

- Perform advanced deterministic and stochastic analysis of selected structural systems to (i) identify critical components to the system's structural behaviour, reliability, robustness and risk, and (ii) evaluate its sensitivity to factors, such as: geometrical imperfections of the members (vertical, horizontal and top and base jacks), as a result of less than effective inspection, and actions of different nature.

- Suggest solutions to enhance the reliability, the robustness and reduce risk of these structures. Select one simple solution and analyse it under a risk informed decision-making process. This involves the development of a new risk methodology based on novel robustness and fragility measures.

The tasks developed in the frame of this Thesis are divided in three work packages. Its execution required a link with a leading industry partner, Harsco Corporation (www.harsco.com), which shared their practical experience and initial guidance on research focus, and finally cooperated in the supply of experimental test materials.

Work package one is dedicated to a bibliographic review, namely about (i) characterizing existing structural solutions of bridge falsework systems, (ii) identifying of the main causes for their collapses, (iii) the state-of-the-art of experimental and numerical investigations about the behaviour of bridge falsework systems.

Work package two defines experimental procedures and characterises experimentally several types of joints between members of bridge falsework Cuplok® systems. This package also contains the development, validation and verification of the numerical modelling of bridge falsework systems. More specifically, a new joint finite element will be presented. Additionally, the influence of several numerical modelling hypotheses is discussed.

In Work package three, a methodology of structural design in the context of risk informed decision-making is presented using the definition and advantages of new robustness and fragility measures. This methodology is then applied to studies intended to:

- Identify critical scenarios to the system's structural behaviour, reliability, robustness and risk;
- Evaluate its sensitivity to factors, such as: (i) material properties, (ii) geometrical imperfections of the members, (iii) bracing configurations, (iv) actions of different nature (construction loads, wind, differential ground settlements) (vi) efficiency of the inspection and quality assurance plans (vii) structural system configurations (namely using steel girder beams to span over roads or other obstacles).

Finally, a possible simple solution for the reduction of risks involving bridge falsework systems is also presented, analysed and discussed. During the development of the Thesis several papers were published in International Journals and in Conferences, see Annex A for a list of publications.

7.2 Findings

The findings and conclusions of each Chapter are as follows:

7.2.1 Chapter 2

From the background review presented in Chapter 2 it was possible to conclude that the choice of the appropriate reduction factors to determine the design wind velocities for short return periods is influenced by many uncertainties: from the validity of the assumptions regarding the stationarity and the temporal independence of the measured data, to the methods used to fit probabilistic

distributions to the wind velocity data records and to obtain the distribution parameters and moments, ending in considerations about the design working life of bridge falsework systems. Furthermore, it was demonstrated that if load values are derived from return periods less than the design working life of bridge falsework structures than in order to achieve an acceptable risk at the end of this period it is necessary to use larger partial factors applied to the loads, which is often not the case. It is therefore recommended not to use any reduction factor and adopt return periods equal to the design working life when designing bridge falsework systems. At least, for cases where meteorological data and site specific information is not available that can be used to reduce the uncertainty levels, in particular for short term usage periods of bridge falsework systems.

Also, an extensive research over the available literature and media information has been performed concerning the numbers and causes of bridge falsework incidents and accidents. It was found that since 1970, up to 2012, 73 major accidents have occurred involving the collapse of bridge falsework structures in 19 countries.

The results show that no reported collapse happened because of accepted risks related to deficiencies in structural codes, or related to extraordinary severe external hazards like earthquakes, floods, landslides and hurricanes or tornados. All the collapses resulted from human errors, and the main cause of failure were design errors (28%).

It was found that the main contributors to procedural causes are inadequate and/or insufficient (i) review of falsework design/assembly/operation methods, including falsework dismantling, (58%), (ii) QC/QA practices, including design and site procedures, (26%), (iii) and four more specific procedural causes which occurred in more than 15% of the collapses. However, in 49% of the accidents the procedural causes were still unknown. It can also be concluded that in general several procedural causes coincide in a given accident, meaning that accidents are caused by the occurrence of multiple errors in the various phases of the project.

It was found that the most important ones are (i) inadequate falsework bracing (19%), (ii) inadequate falsework main element (15%) and (iii) inadequate falsework foundation (11%). The survey showed that the primary enabling event associated with bridge falsework collapses is insufficient or missing bracing elements. The second most important enabling event was found to be under-designed components such as jacks, couplers, standards or ledgers, but also support steel girders used to span open traffic areas.

Three triggering events emerged as the most critical ones: (i) construction material loads (55%), (ii) unknown events (21%) and (iii) effects of improper/premature falsework or formwork assembly/removal (12%). It can be seen that expected loads during design of the falsework are responsible for 55% of collapses by triggering a local failure which then generally develops as a progressive and disproportionate collapse of part of the bridge falsework structure. These loads are mainly due to concreting operations.

After, a thorough description of the key types of procedural causes, enabling and triggering events involved in bridge falsework failures was presented.

Finally, several research needs have been identified regarding bridge falsework systems:

- One of the identified research needs is to develop a rational method to take into account the multiple usage cycles of bridge falsework systems during their lifetime.

- It is clear that a consistent methodology focused on risk informed decision-making in bridge falsework is necessary, minimizing the risks and maximizing the benefits in a cost effective way.

- In terms of design it was evident that particular aspects which can have a significant effect on the structural performance of bridge falsework systems are not explicitly considered in existing design codes. Therefore, research is needed.

7.2.2 Chapter 3

Five types of tests were performed to characterise the mechanical properties of three different types of joint: (i) Cuplok® joint between a standard element and one or more ledger elements, (ii) Spigot joint between two standard elements, and (iii) Forkhead joint between the falsework system and the formwork system. A total of 192 tests were performed. Regarding the latter two types of tests, it should be highlighted that prior to this study no results have been reported and the available models lacked verification.

From the extensive experimental campaign detailed in Chapter 3 the following findings could be determined:

Cuplok® joint

Strong bending axis

- Averaging all results the effect of the application of the initial cycles may not be perceptible. However, for each particular test, the application of the initial cycles could lead to an important increase in the looseness or to a significant decrease of the initial stiffness; and the opposite cases can also occur. For example, it was observed that after the last initial cycle looseness can increase by 0,006 rad or decrease by 0,009 rad, whilst the stiffness can more than double or can decrease to just a fraction of the initial value. This effect could be important in the serviceability limit states range and justifies the need for carrying out cyclic tests. The average value of the joint looseness is equal to 0,007 rad (≈0,40°). Therefore, testing monotonically to failure could lead to artificially high initial stiffness values. This effect could be important in the serviceability limit states range and justifies the need for carrying out cyclic tests.

- In the present study the bending moment vs. joint rotation (M vs. θ) diagrams, in each loading quadrant, were fitted with three (for tests without looseness) or four (for tests showing looseness) linear segments. The stiffness value of each linear segment was determined by a best fit method. It can be observed that in average the various stiffness values obtained for upward and downward displacements are comparable;

- For joints correctly locked with a hammer, no evidence was found to support the hypothesis that looseness significantly affects the stiffness after looseness of the joint. However, tightening the joint by hand doubles the joint looseness values. This increased looseness contributes to an average 30% decrease in the stiffness of the joint;

- It could be observed that the joint stiffness tends to be lower (20% less) in reloading segments when compared to loading segments. This can be justified by the fact that the unloading (end of loading phase) was performed when the bending moment vs. displacement diagrams started to deviate from linearity (around 2/3 of the ultimate bending moment resistance) which meant that plastic deformations occurred at the joint;

- Regarding modes of failure, gathering all the available information it was possible to distinguish between modes of failure of joints loaded upwards and downwards. In the former tests, failure was characterised by significant plastic deformations at the wall of the bottom cup, ledger lower blade and bottom cup weld, for both "as new" and used elements; while in the latter, failure was characterised by cracks at the top cup for "as new" elements and by cracks at the upper blade for used elements;

- It is possible to observe that the joints could not endure more than two load/reload cycles. Also, it was possible to observe a degradation of the stiffness and of the resistance with the cyclic loading.

Weak bending axis

- Different stiffnesses were obtained for upward and downward rotations, the latter being larger, due to higher friction resistance. However, the stiffness in this axis was considerably smaller (approximately five times) than that in the strong axis;

- Furthermore, if the joint was locked by hand then the joint stiffness in this direction was negligible and the joint could be considered to be pinned. This finding highlights again the importance of a correct locking of the joints.

Axial axis

- It was possible to observe that the average values of the axial stiffness of the ledger-to-standard joints are three orders of magnitude (×1000) higher than the bending stiffness.

Spigot joint

- It was possible to observe that the joint behaviour depended on the ratio between the axial force and the bending moment at the joint. The higher this ratio is, the stiffer the joint becomes;

- With the results obtained it was also possible to validate, or not, the analytical model proposed by (Enright, Harris, Hancock 2000). It was possible to observe that the effect of the axial load on the stiffness and resistance of the spigot joint cannot be captured by the analytical model, returning unsafe values bending stiffness for low lateral to axial load ratios and possibly conservative values for high ratios.

Forkhead joint

- The test results showed, that it is possible to mobilise an important bending stiffness at the interface between the falsework and the formwork if it is correctly designed, assembled and these conditions remain throughout the operation.

Finally, as an example, the results for the ledger-to-standard joint were analysed statistically. The selection of the probabilistic distribution for each parameter was based on classic goodness of fit tests but also on more advanced analysis. The results show that in some parameters the most suited distributions deviate greatly from normality.

7.2.3 Chapter 4

In Chapter 4 the development, validation and verification of advanced numerical models of bridge falsework numerical models have been presented. The formulation of a new spring-like finite element has been detailed, including consideration of finite rotations. This new finite element presents features that available elements in ABAQUS® program do not have, specifically the analytical modelling of the cyclic behaviour of joints with allowance for stiffness and resistance degradation and joint failure.

The numerical simulations included analytical models of the various types of joints present in Cuplok® bridge falsework systems. These models were developed based on the results of the experimental tests presented in Chapter 3. In order to increase the accuracy of the numerical results, the formwork beams and formwork plates were modelled explicitly and an efficient time-integration method was used to solve the transient nonlinear dynamic problem. Using these advanced numerical models it was possible to improve the accuracy and precision to the real behaviour of bridge falsework systems relative to previous numerical studies.

Afterwards, the impact of design simplifications in the joint modelling was analysed. It was concluded that the most important joint type seems to be the Cuplok® joint, followed by the forkhead joint and the spigot joint. For example, it was found that the Cuplok® joint may increase and decrease the system's resistance by more than 25% if it is modelled as a continuous or as a pinned joint, respectively. This finding highlights the importance of correctly locking the Cuplok® joint and not using

damaged elements. For the forkhead joint, it was found that modelling it as a continuous or as a pinned joint could lead to a variation of 70% in the system's resistance. This finding stresses the importance of properly designing the falsework/formwork interface and implementing the necessary controls on site.

Finally, it was shown that the current design methods by often assuming several simplifying hypothesis, the majority of which are conservative, if correctly used, namely if a proper nonlinear numerical model is developed and is based on reliable data, should return design loads which are smaller (safe) than the actual resistance of the falsework system. However, this observation does not mean that the values given in the design load tables developed by the system producers are conservative. It is recommended that formwork should be explicitly modelled and modelling of spigot joints should follow the model presented in this Chapter.

7.2.4 Chapter 5

In this Chapter, new robustness and fragility indices were presented and formed the basis of a risk management framework. This new methodology is applicable, in principle, to all structural analyses not only those concerning bridge falsework systems. This Chapter gave a complete insight to the risk management framework, from the principles of risk and a general layout of the risk management framework, to the methods and procedures to be used to determine robustness, fragility and vulnerability, including guidance on how to address them from an economic cost-benefit point of view in order to achieve rational decisions in civil engineering.

The main advantages of this new definition of robustness in relation to the existing definitions are:

- Structural robustness, structural resistance, reliability and risk are four different concepts. The existing robustness definitions mixed these concepts which made the analysis, interpretation and evaluation of the former variables difficult tasks. Furthermore, by coupling in the same definition four different concepts the benefits of determining the robustness was not clear. The present definition makes robustness a property than can be measured independently of the system's resistance, reliability and risk. Structural robustness can for the first time be considered an independent requirement for the structural performance of civil engineering infrastructures. Together with the structural resistance and reliability they become two powerful tools that can and should be used in the risk management of civil engineering infrastructures;

- The second advantage is that for the first time, progressive and disproportionate collapse analysis is clearly defined as a requirement not only for unforeseen and accidental situations affecting localised areas of a given structure, but also for normal service conditions covering for instance design cases where the permanent load is the dominant action.

An explicit expression to determine the robustness index was given based on the concept of damage energy and representative illustration examples were presented.

The fragility index was developed as a tool to assess the system's structural damages for a given action combination. Using this measure it is possible to perform progressive collapse analysis and also evaluate the sensitivity of damage accumulation to action values, which may be important when performing risk analysis.

In general, traditional structural risk analyses focus on probability of failure. These analyses are quite limited since they do not account for the various damage states that might occur (damage is a continuous function) but that do not directly imply the global collapse of the structure. Therefore, valuable information is lost that could be used during the risk informed decision-making process potentially leading to inefficient solutions. For instance, two structural systems *A* and *B* can have the same probability of failure but the damage evolution in *A* can be quite different than in *B*.

As a conclusion, the newly developed robustness index can be used as a design option to reduce the structural risk and the newly developed fragility index is a analysis tool that should be used to assess the structural risk.

7.2.5   Chapter 6

In this Chapter, the risk informed methodology to design bridge falsework presented in Chapter 5 was applied to bridge falsework. The Chapter started by giving a historic justification to perform such a complex procedure to design bridge falsework. Based on an extensive survey of bridge falsework systems over the last 40 years it was possible to obtain notional values of different risk measures, all of them fully justifying the purpose and interest of the risk informed methodology.

After, a thorough risk and hazard scenarios identification was carried out both qualitatively and quantitatively. Regarding the latter, both actions related and system related hazards were investigated using deterministic models. It was found that:

1. Concrete casting loads, including dynamic effects and local overloads can be considered only important for thin slabs supported by falsework structures which do not offer a large safety margin;

2. Wind loads, on the other hand were found to be critical loads since they reduce, in some cases drastically, the resistance of the falsework. In particular, when the falsework is still unloaded during the assembly phase and before concrete casting has begun, when strong winds can overturn the bridge falsework structure. Various solutions were analysed and it was found that including anchor bolts at the falsework baseplates was the most efficient solution and could even prevent early collapses. Of course, assuming that the foundation is properly designed;

3. Differential ground settlements were also analysed. It was demonstrated that even a small value of isolated differential ground settlements could reduce by more than 10% the resistance of the system. It was also found that stiffer systems are more sensitive to differential ground settlements than more flexible solutions because the latter can accommodate with significant strains the imposed deformation. However, excessive looseness at the joints can reduce considerably the resistance of the system;

4. The combined effect of actions should, unless demonstrated that it is not the case, always be considered during the design of bridge falsework systems. Reductions of more than 50% on the resistance value were observed when compared with the limited action application of only vertical pressures to model construction loads;

5. The bracing configuration is the most important parameter regarding system configurations. It was demonstrated that usual bracing layouts can be inefficient when compared with other simple layouts. Including bracing elements from the top to bottom falsework levels is recommended, but care should be taken to limit the bracing free length (*i.e.* brace element length with the same slope direction) and also the spacing between the end and the start of consecutive bracing diagonals at the same bay since bracing can lose efficiency for large values of free length and spacing;

6. The optimal spigot positioning depends on the relative measure between the type of applied actions (in particular lateral loads), initial geometrical imperfections, bracing arrangements and joint characteristics;

7. Falsework solutions adopting steel girder to span highways or rivers raise further complex problems. Therefore, their design should deserve special care and rigorous modelling. From the examples considered it was demonstrated the importance of correctly bracing the falsework towers that support the steel girders. Failure to do so can lead to a 50% reduction of resistance and possibly to a uncontrolled failure;

8. Gross initial geometrical imperfections were also analysed and they are also another parameter that has a considerable influence on the resistance of falsework systems. In particular, the shape of the initial geometrical imperfections is important. Deformed configurations which are associated with low internal energy tensors are particularly critical, for example S shaped initial geometrical imperfections or large deformed overextended jacks;

9. It is important to explicitly model the bridge falsework since design recommendations given in documents released by system producers only contain minimum requirements that may not be sufficient for a specific use. This is especially true for bracing arrangements as was demonstrated.

After, the data collected from the experimental campaign of joint tests presented in Chapter 3 was used together with other appropriate data to build probabilistic models for the most important stochastic variables. These variables were selected based on the results of a sensitivity analysis of the stochastic response of a chosen reference bridge falsework system. In the end, stochastic models for the resistance, reliability, robustness and fragility for two case studies were determined, presented and discussed. The advantages of the proposed methodology were highlighted. As an example, resistance, reliability, robustness and fragility could be analysed independently and important conclusions could be drawn out namely in terms of characterising the collapse as progressive or abrupt, proportionate or disproportionate. Also, the sensitivity of these parameters to the action values could be easily analysed including the effect of propagating model and statistical uncertainties.

Finally, strategies to enhance robustness and minimise risk were discussed and one possible solution was used as an application example. This solution profited from the results of previous stochastic analyses which highlighted the major random variables, namely initial geometric imperfections and parameters of the Cuplok® and spigot joints. The approach was to target those variables and reduce their impact. In practice, this translated on more rigorous inspection plans and tighter quality controls.

Risks were determined for the reference (baseline) scenario and the alternative (improved) scenario and later evaluated against valid risk criteria. It could be concluded that if the cost of the permanent structure significantly exceeds (one order higher) the cost of the temporary structure the extent of improvements in terms of structural and economical risks completely justified the small extra costs incurred with using the alternative scenario rather than the reference scenario.

The results clearly illustrate the advantages of the methodology proposed in Chapter 5, and the sensitivity of the decision-making process to input parameters.

The procedure outlined in Chapter 5 and exemplified in Chapter 6 forms a rational method to evaluate the risk of bridge falsework systems taking into account the whole life cycle of these structures.

7.3 Future works

As in any research there are always matters that could not be addressed and thus constitute potential subject areas for future investigations. Examples are:

- Rational definition of action values, taking into account the action nature and the exposure time of bridge falsework systems;
- Development of a design procedure to obtain solutions for bridge falsework systems adapted to the specific requirements of each use, namely regarding bracing;
- Development of optimised inspection and quality assurance plans for bridge falsework systems;
- Application of the risk informed decision-making process presented to other types of structures.

REFERENCES

AASHTO, 2008, AASHTO GSBTW-1-M - Guide Design Specifications for Bridge Temporary Works, with 2008 Interim Revisions. 1st. USA: American Association of State Highway and Transportation Officials (AASHTO).

AASHTO, 2010, AASHTO LRFDUS-5 - LRFD Bridge Design Specifications, with 2010 Interim Revisions. 5th Edition. USA: American Association of State Highway and Transportation Officials (AASHTO).

ABDEL-JABER, M., BEALE, R., GODLEY, M. and ABDEL-JABER, M., 2009, Rotational strength and stiffness of tubular scaffold connectors. Proceedings of the ICE - Structures and Buildings. 2009. Vol. 162, no. 6, pp. 391–403.

ACI, 2004, ACI 347-04 - Guide to Formwork for Concrete. USA: American Concrete Institute (ACI).

ANCOLD, 2003, Guidelines on Risk Assessment. Australia: The Australian National Committee on Large Dams (ANCOLD).

ANDO, T., 2010, Bayesian Model Selection and Statistical Modeling. Boca Raton, USA: Chapman & Hall/CRC.

ANDRÉ, J., 2008, Behaviour and Quality of Steel Telescopic Props. Analytical, Numerical and Experimental Investigation. M.Sc. Thesis. Lisbon, Portugal: Instituto Superior Técnico, Technical University of Lisbon.

ANDRÉ, J., BEALE, R. and BAPTISTA, A., 2012a, Bridge Construction Equipment: An overview of the existing design guidance. Structural Engineering International. 2012. Vol. 22, no. 3, pp. 365-379.

ANDRÉ, J., BEALE, R. and BAPTISTA, A., 2012b, A survey of bridge falsework systems since 1970. Proceedings of the ICE - Forensic Engineering. 2012. Vol. 65, Issue FE4, pp. 161-172.

ANDRÉ, J., BEALE, R. and BAPTISTA, A., 2013, Recent advances and existing challenges in the design of bridge falsework systems. Civil Engineering and Environmental Systems. 2013. Vol. 30, Issue 2, pp. 130-145.

ANG, A. and TANG, W., 1975, Probability Concepts in Engineering Planning and Design: Basic Principles. 1st. USA: Wiley.

ANG, A. and TANG, W., 2007, Probability Concepts in Engineering: Emphasis on Applications in Civil and Environmental Engineering. 2nd Edition. Wiley.

APELAND, S., AVEN, T. and NILSEN, T., 2002, Quantifying uncertainty under a predictive, epistemic approach to risk analysis. Reliability Engineering & System Safety. 2002. Vol. 75, no. 1, pp. 93–102.

ARLOT, S. and CELISSE, A., 2010, A survey of cross-validation procedures for model selection. Statistics Surveys. 2010. Vol. 4, pp. 40–79.

ARTAMONOV, A., BENDEL, C., BLUECKERT, C., LANDRIN, H., SPENCER, M., WALLACE, P., WASSMER, L. and WANNICK, H., 2008, Bridges – Construction, insurance and risk management. In: Proceedings of the 41st annual Conference of The International Association of Engineering Insurers (IMIA). Gleneagles, Scotland: The International Association of Engineering Insurers (IMIA). 2008.

ASCE, 2002, ASCE/SEI 37-02 - Design Loads on Structures during Construction. USA: American Society of Civil Engineers (ASCE).

ASCE, 2010, ASCE 7-10 - Minimum Design Loads for Buildings and Other Structures. USA: American Society of Civil Engineers (ASCE).

AVEN, T., 2004, On how to approach risk and uncertainty to support decision-making. Risk Management. 2004. Vol. 6, no. 4, pp. 27–39.

AYAHO, M., HIDEYUKI, K. and HIDEAKI, N., 1997, Development of a knowledge-based expert system for selection of steel bridge erection method. In: Proceedings of NEW TECH Lisbon 97: New Technologies in Structural Engineering. Lisbon, Portugal. 1997. pp. 203–211.

AYYUB, B. and MCCUEN, R., 2011, Probability, Statistics, and Reliability for Engineers and Scientists. Taylor and Francis.

BAKER, J., SCHUBERT, M. and FABER, M., 2008, On the assessment of robustness. Structural Safety. 2008. Vol. 30, no. 3, pp. 253–267.

BALAFAS, I. and BURGOYNE, C., 2004, Economic viability of structures with FRP reinforcement and prestress. In: Proceedings of the 4th International Conference on Advanced Composite Materials in Bridges and Structures. Calgary, Canada: Canadian Society for Civil Engineering. 2004.

BAPTISTA, A. and MUZEAU, J., 2001, Analytical formulation of the design of circular hollow sections in the elastoplastic regime (in Portuguese). In: Proceedings of III Portuguese National Conference of Steel and Composite Construction. Aveiro, Portugal: The Portuguese Steelwork Association (cmm). 2001. pp. 513–522.

BAPTISTA, A. and SILVA, S., 2002, Promotion of quality in the management of construction temporary structures (in Portuguese). In: Proceedings of Portuguese National Conference of Structural Engineering. Lisbon, Portugal: Portuguese National Laboratory for Civil Engineering (LNEC). 2002. pp. 583–594.

BASHOR, R. and KAREEM, A., 2009, Comparative study of major international standards. In: Proceedings of the 7th Asia-Pacific Conference on Wind Engineering (APCWE-VII). Taipei, Taiwan. 2009.

BAŽANT, Z. and VERDURE, M., 2007, Mechanics of progressive collapse: Learning from World Trade Center and building demolitions. Journal of Engineering Mechanics. 2007. Vol. 133, no. 3, pp. 308–319.

BAŽANT, Z. and ZHOU, Y., 2002, Why did the World Trade Center collapse? - Simple analysis. Journal of Engineering Mechanics. 2002. Vol. 128, no. 1, pp. 2–6.

BAŽANT, Z., LE, J., GREENING, F. and BENSON, D., 2008, What did and did not cause collapse of World Trade Center Twin Towers in New York? Journal of Engineering Mechanics. 2008. Vol. 134, no. 10, pp. 892–906.

BEALE, R. and GODLEY, M., 2003, Common causes of failure of metal scaffolds in the UK and stability checks on scaffolds. In: Proceedings of the Technical Seminar on Metal Scaffolding (Falsework) – Design, Construction and Safety. Hong Kong: Hong Kong Institute of Steel Construction. 2003. pp. 62–79.

BEALE, R. and GODLEY, M., 2006, Numerical modelling of tube and fitting access scaffold systems. Advanced Steel Construction. 2006. Vol. 2, no. 3, pp. 199–223.

BEALE, R. and GODLEY, M., 2009, Numerical modelling of full-scale tube and fitting scaffold tests. In: Proceedings of the 7th EUROMECH Solid Mechanics Conference. Lisbon. 7 September 2009. pp. 1–12.

BEALE, R., 2014, Scaffold research — A review. Journal of Constructional Steel Research. 2014. Vol. 98, pp. 188–200.

BEALE, R., GODLEY, M. and MILOJKOVIC, B., 1996, The Influence of the Quality of Design and Site Control on Safety Factors for Tube and Fitting Façade Scaffold. UK: Oxford Brookes University, Report 294.

BEDFORD, T. and COOKE, R., 2001, Probabilistic Risk Analysis: Foundations and Methods. Cambridge, UK: Cambridge University Press.

BELLINGER, W., 2007, The Economic Analysis of Public Policy. Routledge.

BENJAMIN, J. and CORNELL, C., 1970, Probability, Statistics, and Decision-Making for Civil Engineers. 3rd Edition. USA: McGraw-Hill.

BENNETT, L., 2004, Peer Review of Analysis of Specialist Group Reports on Causes of Construction Accidents. UK: Habilis Ltd., Health and Safety Executive, Report 218.

BERRY, L., LINDSAY, J., SALOMON, E. and VEALE, S., 2006, Risk, Responsibility and Regulation – Whose Risk is it Anyway?. UK: UK's Better Regulation Commission.

BILLINGS, I. and ROUTLEY, R., 1978, Falsework load measurement at Newton No. 1 bridge. New Zealand Engineering. 1978. Vol. 33, no. 6, pp. 127–134.

BIRNBAUM, M., 2008, New paradoxes of risky decision making. Psychological Review. 2008. Vol. 115, no. 2, pp. 463–501.

BLOCKLEY, D., 1992, Engineering Safety. UK: McGraw-Hill Book Company.

BLOCKLEY, D., 2011, Engineering safety. Proceedings of the ICE - Forensic Engineering. 2011. Vol. 164, no. 1, pp. 7–13.

BOGGS, D. and PETERKA, J., 1992, Wind speeds for design of temporary structures. In: Proceedings of the 10th ASCE Structures Congress. San Antonio, USA: American Society of Civil Engineers (ASCE). 1992.

BOWLES, D., 2003, ALARP evaluation: Using cost effectiveness and disproportionality to justify risk reduction. In: Proceedings of ANCOLD 2003 Conference on Dams. Hobart, Australia: The Australian National Committee on Large Dams (ANCOLD). 2003.

BOWLES, D., 2007, Tolerable risk for dams: How safe is safe enough? In: Proceedings of the US Society on Dams Annual Conference. Philadelphia, USA: United States Society on Dams (USSD). 2007.

BOX, G. and DRAPER, N., 1987, Empirical Model-building and Response Surfaces. Wiley.

BRAGG, S., 1975, Final Report of the Advisory Committee on Falsework. UK: Her Majesty's Stationery Office (HMSO).

BSI, 1982, BS 5975:1982 - Code of Practice for Falsework. UK: British Standards Institution (BSI).

BSI, 1990, BS 4360:1990 - Specification for Weldable Structural Steels. UK: British Standards Institution (BSI).

BSI, 1999, BS EN 1065:1999 - Adjustable Telescopic Steel Props - Product Specifications, Design and Assessment by Calculation and Tests. UK: British Standards Institution (BSI).

BSI, 2001, BS EN 39:2001 - Loose Steel Tubes for Tube and Coupler Scaffolds - Technical Delivery Conditions. UK: British Standards Institution (BSI).

BSI, 2002a, BS EN 1990:2002+A1:2005 - Eurocode 0: Basis of Structural Design. UK: British Standards Institution (BSI).

BSI, 2002b, BS EN 12811-3:2002 - Temporary Works Equipment - Part 3: Load Testing. UK: British Standards Institution (BSI).

BSI, 2002c, BS EN 1991-1-1:2002 - Eurocode 1: Actions on Structures - Part 1-1: General Actions - Densities, Self-Weight, Imposed Loads for Buildings. UK: British Standards Institution (BSI).

BSI, 2003, BS EN 12811-1:2003 - Temporary Works Equipment - Part 1: Scaffolds - Performance Requirements and General Design. UK: British Standards Institution (BSI).

BSI, 2004a, BS EN 1990:2002+A1:2005 - UK National Annex. UK: British Standards Institution (BSI).

BSI, 2004b, BS EN 12811-2:2004 - Temporary Works Equipment - Part 2: Information on Materials. UK: British Standards Institution (BSI).

BSI, 2004c, BS EN 1998-1:2004 - Eurocode 8: Design of Structures for Earthquake Resistance - Part 1: General Rules, Seismic Actions and Rules for Buildings. UK: British Standards Institution (BSI).

BSI, 2005a, BS EN 74-1:2005 - Couplers, Spigot Pins and Baseplates for Use in Falsework and Scaffolds - Part 1: Couplers for Tubes - Requirements and Test Procedures. UK: British Standards Institution (BSI).

BSI, 2005b, BS EN 1991-1-6:2005 - Eurocode 1: Actions on Structures - Part 1-6: General Actions - Actions during Execution. UK: British Standards Institution (BSI).

BSI, 2005c, BS EN 1991-1-4:2005 - Eurocode 1: Actions on Structures - General Actions - Part 1-4: Wind Actions. UK: British Standards Institution (BSI).

BSI, 2005d, BS EN 1998-2:2005+A1:2009 - Eurocode 8: Design of Structures for Earthquake Resistance - Part 2: Bridges. UK: British Standards Institution (BSI).

BSI, 2005e, BS EN 1993-1-1:2005 - Eurocode 3: Design of steel structures - Part 1-1: General rules and rules for buildings. UK: British Standards Institution (BSI).

BSI, 2005f, BS EN 1993-1-8:2005 - Eurocode 3: Design of Steel Structures - Part 1-8: Design of Joints. UK: British Standards Institution (BSI).

BSI, 2006a, BS EN 10210-1:2006 - Hot Finished Structural Hollow Sections of Non-Alloy and Fine Grain Steels - Part 1: Technical Delivery Conditions. UK: British Standards Institution (BSI).

BSI, 2006b, BS EN 10219-1:2006 - Cold Formed Welded Structural Hollow Sections of Non-Alloy and Fine Grain Steels - Part 1 : Technical Delivery Requirements. UK: British Standards Institution (BSI).

BSI, 2006c, BS EN 1991-1-7:2006 - Eurocode 1: Actions on Structures - Part 1-7: General Actions - Accidental Actions. UK: British Standards Institution (BSI).

BSI, 2008a, BS 5975:2008 - Code of Practice for Temporary Works Procedures and the Permissible Stress Design of Falsework. UK: British Standards Institution (BSI).

BSI, 2008b, BS EN 1991-1-6:2005 - UK National Annex. UK: British Standards Institution (BSI).

BSI, 2008c, BS EN 1991-1-4:2005+A1:2010 - UK National Annex. UK: British Standards Institution (BSI).

BSI, 2009a, BS EN 15512:2009 - Steel Static Storage Systems - Adjustable Pallet Racking Systems - Principles for Structural Design. UK: British Standards Institution (BSI).

BSI, 2009b, BS 1139-2.2-2009 - Metal Scaffolding - Part 2: Couplers - Section 2.2: Aluminium Couplers and Special Couplers in Steel. UK: British Standards Institution (BSI).

BSI, 2009c, PD 6698:2009 - Recommendations for the Design of Structures for Earthquake Resistance to BS EN 1998. UK: British Standards Institution (BSI).

BSI, 2010a, BS EN 74-3:2007 - Couplers, Spigot Pins and Baseplates for Use in Falsework and Scaffolds - Part 3: Plain Base Plates and Spigot Pins - Requirements and Test Procedures. UK: British Standards Institution (BSI).

BSI, 2010b, BS EN 74-2:2008 - Couplers, Spigot Pins and Baseplates for Use in Falsework and Scaffolds - Part 2: Special Couplers - Requirements and Test Procedures. UK: British Standards Institution (BSI).

BSI, 2011, BS EN 12812:2008 - Falsework. Performance Requirements and General Design. UK: British Standards Institution (BSI).

BSI, BS EN 1991 - Eurocode 1: Actions on Structures - Parts 1 to 4. UK: British Standards Institution (BSI).

BSI, BS EN 1993 - Eurocode 3: Design of Steel Structures - Parts 1 to 6. UK: British Standards Institution (BSI).

BULLER, P., 1993, Gales of January and February 1990: Damage to Buildings and Structures. UK: Building and Research Establishment (BRE), Report BR 248.

BUNNI, N., 2003, Risk and Insurance in Construction. 2nd Edition. London, UK: Taylor & Francis.

BURROWS, B., 1989, Organisation and Quality of Falsework Construction. PhD. UK: Warwick University.

CARDWELL, S., 2010, Bridge deck types and construction methods. In: IABSE WG 6 Seminar: State-of-the-art Bridge Deck Erection; Safe and Efficient use of Special Equipment. Singapore: International Association for Bridge and Structural Engineering (IABSE). November 2010. pp. 28.

CARVALHO, A., PEREIRA, C. and MARTINS, R., 2004, Problems with falsework foundations (in Portuguese). In: Proceedings of the 9th Portuguese National Congress of Geotecnics. Aveiro: Universidade de Aveiro. 20 April 2004.

CASTILLO, E, HADI, A., BALAKRISHNAN, N. and SARABIA, J., 2004, Extreme Value and Related Models with Applications in Engineering and Science. Wiley.

CEN, 2006, EN 14509:2006 - Self-supporting double skin metal faced insulating panels. Factory made products. Specifications. Brussels, Belgium: European Committee for Standardization (CEN).

CEN, 2009, CEN/TS 1992-4:2009 - Design of Fastenings for Use in Concrete - . Parts 1 to 5. Brussels, Belgium: European Committee for Standardization (CEN).

CHANDRANGSU, T. and RASMUSSEN, K., 2008, Scaffold Cuplok Joint Tests. Centre for Advanced Structural Engineering: The University of Sydney, Report R893.

CHANDRANGSU, T. and RASMUSSEN, K., 2009a, Full-scale tests and advanced structural analysis of formwork subassemblies. In: Proceedings of the Sixth International Conference on Advances in Steel Structures. Hong Kong: The Hong Kong Institute of Steel Construction. 16 December 2009. pp. 1083–1090.

CHANDRANGSU, T. and RASMUSSEN, K., 2009b, Geometric imperfection measurements and joint stiffness of support scaffold systems. In: Proceedings of the Sixth International Conference on Advances in Steel Structures. Hong Kong: The Hong Kong Institute of Steel Construction. 16 December 2009. pp. 1075–1082.

CHANDRANGSU, T. and RASMUSSEN, K., 2009c, Structural Modelling of Support Scaffold Systems. Centre for Advanced Structural Engineering: The University of Sydney, Report R896.

CHANDRANGSU, T. and RASMUSSEN, K., 2011, Investigation of geometric imperfections and joint stiffness of support scaffold systems. Journal of Constructional Steel Research. 2011. Vol. 67, no. 4, pp. 576–584.

CHANDRANGSU, T., 2010, Advanced Analysis and Probabilistic-Based Design of Support Scaffold Systems. PhD Thesis. Australia: University of Sydney.

CHILTON, S., JONES-LEE, M., LOOMES, G., ROBINSON, A., HOPKINS, L., COOKSON, R., COVEY, J., SPENCER, A. and BEATTIE, J., 1998, Valuing Health and Safety Controls. A Literature Review. UK: Health and Safety Executive (HSE), Report CRR 171.

CHU, A., ZHOU, Z., KOON, C., CHAN, S., PENG, J. and PAN, A., 1996, Design of steel scaffolding using an integrated design and analysis approach. In: Proceedings of International Conference on Advances in Steel Structures. Hong Kong: S.L. Chan and J.G. Teng, Pergamon. 11 December 1996. pp. 245–250.

CIP, 2011, Temporary Works and Falsework. In: Construction Health and Safety Manual. UK: Construction Industry Publications Ltd. pp. 16.

CIRIA, 1977, Rationalization of Safety and Serviceability Factors in Structural Codes. UK: Construction Industry Research and Information Association (CIRIA), Report 63.

CIRIA, 2007, CDM2007 – Construction Work Sector Guidance for Designers. UK: Construction Industry Research and Information Association (CIRIA), Report C662.

CIRIA, 2009, Whole-Life Infrastructure Asset Management: Good Practice Guide for Civil Infrastructure. UK: Construction Industry Research and Information Association (CIRIA), Report C677.

CIRIA, 2011, Guidance on Catastrophic Events in Construction. UK: Construction Industry Research and Information Association (CIRIA), Report C699.

CLAESKENS, G. and HJORT, N., 2008, Model Selection and Model Averaging. Cambridge, UK: Cambridge University Press.

COLES, S., 2001, An Introduction to Statistical Modeling of Extreme Values. London, UK: Springer-Verlag.

COMITÉ EURO-INTERNATIONAL DU BÉTON, 1993, CEB-FIP Model Code 90. UK: Thomas Telford.

CONGDON, P., 2006, Bayesian Statistical Modelling. 2nd Edition. Chichester, UK: John Wiley & Sons.

COURT, R., FRANCIS, D., GROGAN-JONES, A., HUMPHREY, J., KIDNEI, M., METCALFE, J., O'CONNOR, B., SORBIE, J. and TIGHE, D., 2005, RoadFacts 2005. Sydney, Australia: Austroads Inc.

CPWR, 2008, The Construction Chart Book. The U.S. Construction Industry and its Workers. 4th Edition. Maryland, US: The Center for Construction Research and Training (CPWR).

CRÉMER, J., 2003, Conception des Ponts. Liège, Belgium: Liège University.

CRISFIELD, M. A, 1997, Nonlinear Finite Element Analysis of Solids and Structures. New York, USA: Wiley.

CROPPER, M. and SUSSMAN, F., 1990, Valuing future risks to life. Journal of Environmental Economics and Management. 1990. Vol. 19, no. 2, pp. 160–174.

CSA, 1975, S269.1-1975 R2003 - Falsework for Construction Purposes - Part 1: Design. Canada: Canadian Standards Association (CSA).

CSA, 2006, CSA-S6-06 + S6S1-10: Canadian highway bridge design code. Canada: Canadian Standards Association (CSA).

DANIELS, G., ELLIS, D. and STOCKTON, W., 1999, Techniques for Manually Estimating Road User Costs Associated with Construction Projects. USA: Texas Transportation Institute.

DAS, P., 1997, Safety of Bridges. Thomas Telford.

DELIGNETTE-MULLER, M., POUILLOT, R., DENIS, J. and DUTANG, C., 2012, fitdistrplus: help to fit of a parametric distribution to non-censored or censored data.

DEPARTMENT OF TRANSPORTATION, DIVISION OF STRUCTURES, 2001, California Falsework Manual. 32nd Edition. USA: State of California.

DET NORSKE VERITAS, 2002, Marine Risk Asessment. UK: The Health and Safety Executive (HSE).

DITLEVSEN, O. and FRIIS-HANSEN, P., 2005, Life quality time allocation index – an equilibrium economy consistent version of the current life quality index. Structural Safety. 2005. Vol. 27, no. 3, pp. 262–275.

DUSENBERRY, D. and HAMBURGER, R., 2006, Practical means for energy-based analyses of disproportionate collapse potential. Journal of Performance of Constructed Facilities. 2006. Vol. 20, no. 4, pp. 336–348.

EALES, R., SMITH, S., TWIGGER-ROSS, C., SHEATE, W., ÖZDEMIROGLU, E., FRY, C. and TOMLINSON, P., 2003: Integrated Appraisal Methods. Bristol, UK: UK Environment Agency, Report E2-044/TR.

EFRON, B., 1979, Bootstrap methods: Another look at the jackknife. The Annals of Statistics. 1979. Vol. 7, no. 1, pp. 1–26.

ELDUKAIR, Z. and AYYUB, B., 1991, Analysis of recent U.S. structural and construction failures. Journal of Performance of Constructed Facilities. 1991. Vol. 5, no. 1, pp. 57–73.

ELLINGWOOD, B., 2008, Reliability based codes in the United States. Challenges to professional engineering practice. In: Proceedings of the 4th International ASRANet Colloquium on Integrating for Structural Analysis, Risk & Reliability. Athens, Greece. 2008.

ELLINGWOOD, B., SMILOWITZ, R., DUSENBERRY, D., DUTHINH, D., LEW, H. and CARINO, N., 2007, Best Practices for Reducing the Potential for Progressive Collapse in Buildings. USA: National Institute of Standards and Technology (NIST), Report NISTIR 7396.

ENRIGHT, J., HARRIS, R. and HANCOCK, G., 2000, Structural stability of braced scaffolding and formwork with spigot joints. In: Proceedings of 15th International Specialty Conference in Cold-Formed Steel Design and Construction. Missouri, USA. 2000. pp. 357–376.

EUROSTAT, 2012, ec.europa.eu/eurostat/. 2012.

FABER, M. and STEWART, M., 2003, Risk assessment for civil engineering facilities: critical overview and discussion. Reliability Engineering and System Safety. 2003. Vol. 80, pp. 173–184.

FABER, M., 2009, Risk and Safety in Engineering Course Lecture Notes. Switzerland: Swiss Federal Institute of Technology Zurich (ETHZ).

FANG, Z., 2007, Energy-Based Approach to Structural Robustness. Journal of Southwest Jiaotong University. 2007. Vol. 15, no. 4, pp. 319–234.

FAWCETT, L., 2005, Statistical Methodology for the Estimation of Environmental Extremes. PhD Thesis. Newcastle upon Tyne: University of Newcastle.

FERRY BORGES, J. and CASTANHETA, M., 1968, Structural Safety. 1st. Lisbon, Portugal: Laboratorio National de Engenharia Civil (LNEC). Course 101.

FIB, 2000, Guidance for Good Bridge Design. Switzerland: International Federation for Structural Concrete (fib), Bulletin No. 9.

FIB, 2009, Formwork and Falsework for Heavy Construction. Guide to Good Practice. Switzerland: International Federation for Structural Concrete (fib), Bulletin No. 48.

FISCHHOFF, B., LICHTENSTEIN, S., SLOVIC, P., DERBY, S. and KEENEY, R., 1981, Acceptable Risk. Cambridge University Press.

FISHER, R., 1921, On the `probable error' of a coefficient of correlation deduced from a small sample. Metron. 1921. Vol. 1, no. 4, pp. 3–32.

FLORIO, M. and MAFFII, S., 2008, Guide to Cost-Benefit Analysis of Investment Projects. Brussels, Belgium: European Commission.

FRANGOPOL, D. and CURLEY, J., 1987, Effects of Damage and Redundancy on Structural Reliability. Journal of Structural Engineering. July 1987. Vol. 113, no. 7, pp. 1533–1549.

FU, G. and FRANGOPOL, D., 1990, Balancing weight, system reliability and redundancy in a multiobjective optimization framework. Structural Safety. March 1990. Vol. 7, no. 2-4, pp. 165–175.

GARDNER, L., 2008, The continuous strength method. Proceedings of the ICE - Structures and Buildings. 2008. Vol. 161, no. 3, pp. 127–133.

GERRAND, C., 1987, The equivalent orthotropic elastic properties of plywood. Wood Science and Technology. 1 December 1987. Vol. 21, no. 4, pp. 335–348.

GIFFORD, W., 2004, Risk analysis and the acceptable probability of failure. In: Proceedings of 2004 Henderson Colloquium: Designing for the consequences of hazards. IABSE British Groupp. 2004. pp. 5.

GODA, K. and HONG, H., 2008, Application of cumulative prospect theory: Implied seismic design preference. Structural Safety. 2008. Vol. 30, no. 6, pp. 506–516.

GODFREY, P., 1996, Control of Risk: A Guide to the Systematic Management of Risk from Construction. London: Construction Industry Research and Information Association (CIRIA).

GODLEY, M. and BEALE, R., 1997, Sway stiffness of scaffold structures. The Structural Engineer. 1997. Vol. 75, no. 1, pp. 4–12.

GODLEY, M. and BEALE, R., 2001, Analysis of large proprietary access scaffold structures. Proceedings of the ICE - Structures and Buildings. 2001. Vol. 146, no. 1, pp. 31–39.

GODLEY, M., BEALE, R. and FENG, X., 1998, Rotational stiffness of semi-rigid baseplates. In: Proceedings of the 14th Specialty Conference on Cold-Formed Steel Structures. St. Louis, USA: Wei-Wen Yu Center for Cold-Formed Steel Structures. 1998. pp. 323–335.

GOODWIN, P. and WRIGHT, G., 2010, Decision Analysis for Management Judgment. 4th Edition. Wiley.

GORLIN, W., 2009, Wind loads for temporary structures: Making the case for industrywide standards. Journal of Architectural Engineering. 2009. Vol. 15, no. 2, pp. 35–36.

GORST, N., WILLIAMSON, S., PALLETT, P. and CLARK, L., 2003, Friction in Temporary Works. School of Civil Engineering: The University of Birmingham, Report rr071.

GRAUBNER, C. and PROSKE, T., 2005, Formwork pressure - A new concept for the calculation. In: Proceedings of the Second North American Conference on the Design and Use of Self-Consolidating Concrete and the Fourth RILEM International Symposium on Self-Compacting Concrete. Chicago. 2005. pp. 605–612.

GRAUBNER, C. and PROSKE, T., 2010, Formwork pressure of highly workable concretes–Experiments focused on setting and vibration and design approach. In: Proceedings of the 6th RILEM Conference on Self-Compacting Concrete. Montreal: Springer Verlag. 2010.

GULVANESSIAN, H., CALGARO, J. and HOLICKÝ, M., 2002, Designer's Guide to EN 1990 Eurocode: Basis of Structural Design. UK: Thomas Telford.

HADIPRIONO, F. and WANG, H., 1987, Causes of falsework collapses during construction. Structural Safety. 1987. Vol. 4, no. 3, pp. 179–195.

HADIPRIONO, F., LIM, C. and WONG, K., 1986, Event tree analysis to prevent failures in temporary structures. Journal of Construction Engineering and Management. 1986. Vol. 112, no. 4, pp. 500–513.

HAIMES, Y., 2009, Risk Modeling, Assessment and Management. 3rd Edition. USA: John Wiley & Sons.

HALDAR, A. and MAHADEVAN, S., 2000, Probability, Reliability, and Statistical Methods in Engineering Design. John Wiley & Sons.

HAMMAD, A., YAN, J. and MOSTOFI, B., 2007, Recent development of bridge management systems in Canada. In: 2007 Annual Conference of the Transportation Association of Canada. Saskatchewan, Canada: Transportation Association of Canada. 2007.

HARTFORD, D. and BAECHER, G., 2004, Risk and Uncertainty in Dam Safety. London, UK: Thomas Telford.

HARUNG, H., LIGHTFOOT, E. and DUGGAN, D., 1975, The strength of scaffold towers under vertical loading. The Structural Engineer. 1975. Vol. 53, no. 1, pp. 23–30.

HASTIE, T., TIBSHIRANI, R. and FRIEDMAN, J., 2009, The Elements of Statistical Learning - Data Mining, Inference, and Prediction. 2nd Edition. New York, USA: Springer.

HAWKINS, D., BASAK, S. and MILLS, D., 2003, Assessing model fit by cross-validation. Journal of Chemical Information and Modeling. 2003. Vol. 43, no. 2, pp. 579–586.

HAYES, K., 2011, Uncertainty and Uncertainty Analysis Methods. Australia: CSIRO Mathematics, Informatics and Statistics, Report EP102467.

HILL, H., 2004, Rational and irrational design loads for "temporary"' structures. Practice Periodical on Structural Design and Construction. 2004. Vol. 9, no. 3, pp. 125–129.

HM TREASURY, 2003, Appraisal and Evaluation in Central Government (The Green Book). UK: Controller of Her Majesty's Stationery Office.

HM TREASURY, 2004, Management of Risk - Principles and Concepts (The Orange Book). UK: Controller of Her Majesty's Stationery Office.

HOLMES, J., 2007, Wind Loading of Structures. 2nd Edition. Oxford: Taylor & Francis.

HOUSE OF LORDS, 2006, 5th Report of Session 2005–06: Government Policy on the Management of Risk. London, UK: The Stationery Office Limited.

HSE, 1988, The Tolerability of Risk from Nuclear Power Stations. UK: The Health and Safety Executive (HSE).

HSE, 1995, Generic Terms and Concepts in the Assessment and Regulation of Industrial Risks. UK: The Health and Safety Executive (HSE).

HSE, 2001, Reducing Risks, Protecting People: HSE's Decision Making Process. UK: The Health and Safety Executive (HSE), Report R2P2.

HSE, 2007a, The Construction (Design and Management) Regulations 2007 (CDM2007). UK: The Health and Safety Executive (HSE).

HSE, 2007b, Managing Health and Safety in Construction. Construction (Design and Management) Regulations 2007. Approved Code of Practice. UK: The Health and Safety Executive (HSE).

REFERENCES

HSE, 2009a, ND guidance on the demonstration of ALARP (as low as reasonably practicable). UK: The Health and Safety Executive (HSE), T/AST/005 - Issue 4 - Rev 1.

HSE, 2009b, Construction Intelligence Report: Analysis of Construction Injury and Ill Health Intelligence 1997/98 - 2008/09. UK: The Health and Safety Executive (HSE).

HSE, 2010, The Management of Temporary Works in the Construction Industry. UK: The Health and Safety Executive (HSE), Report SIM 02/2010/04.

HSE, 2011, Preventing Catastrophic Events in Construction. Prepared by CIRIA and Loughborough University. UK: The Health and Safety Executive (HSE), Report RR834.

IKÄHEIMONEN, J., 1997, Construction Loads on Shores and Stability of Horizontal Formworks. PhD Thesis. Stockholm, Sweden: Royal Institute of Technology (KTH).

IMHOF, D., 2004, Risk Assessment of Existing Bridge Structures. PhD Thesis. Cambridge, UK: University of Cambridge.

ISO, 1998, ISO 2394 - General Principles on Reliability for Structures. Geneva, Switzerland: International Organization for Standardization (ISO).

ISO, 2009a, ISO 31000 - Risk Management - Principles and Guidelines. Geneva, Switzerland: International Organization for Standardization (ISO).

ISO, 2009b, ISO 31010 - Risk Management - Risk Assessment Techniques. Geneva, Switzerland: International Organization for Standardization (ISO).

ISTRUCTE, 2007, Temporary Demountable Structures: Guidance on Procurement, Design and Use. 3rd Edition. UK: The Institution of Structural Engineers.

JCSS, 2001, JCSS Probabilistic Model Code. Joint Committee on Structural Safety.

JONES-LEE, M., LOOMES, G., YATES, D., MITCHELL, E., SPACKMAN, M., MCQUAID, J. and THOMSON, T., 2008, T440: Fatalities and Weighted Injuries. London, UK: Rail Safety and Standards Board (RSSB).

KAHNEMAN, D. and TVERSKY, A., 1979, Prospect theory: An analysis of decision under risk. Econometrica. 1979. Vol. 47, no. 2, pp. 263–291.

KAPLAN, S. and GARRICK, B., 1981, On the quantitative definition of risk. Risk Analysis. 1981. Vol. 1, no. 1, pp. 11–27.

KNOLL, F. and VOGEL, T., 2009, Design for Robustness. Zurich: International Association for Bridge and Structural Engineering (IABSE). Structural Engineering Documents (SED), 11.

KOHAVI, R., 1995, Wrappers For Performance Enhancement And Oblivious Decision Graphs. PhD Thesis. USA: Stanford University.

KOROL, R. and SIVAKUMARAN, K., 2014, Reassessing the plastic hinge model for energy dissipation of axially loaded columns. Journal of Structures. 2014. Vol. 2014, no. 1.

KUHN, M. and JOHNSON, K., 2013, Applied Predictive Modeling. New York, USA: Springer.

KUHN, M., 2008, Building predictive models in R using the caret package. Journal of Statistical Software. 2008. Vol. 5, no. 28.

KUMAMOTO, H., 2007, Satisfying Safety Goals by Probabilistic Risk Assessment. London, UK: Springer-Verlag.

LAU, H., BEALE, R. and GODLEY, M., 2005, The influence of column base connections on the stability of slender multi-bay frame structures. In: Proceedings of the 4th International Conference on Advances in Steel Structures. Shanghai, China: Elsevier. 2005. pp. 1421–1426.

LE GUEN, J., 2008, Tolerability of risk: UK principles & practice for controlling work activities. In: Workshop on Tolerable Risk Evaluation sponsored by US Army Corps of Engineers. Virginia, USA: U.S. Department of the Interior: Bureau of Reclamation. March 2008.

LEADBETTER, M., BAILEY, G. and ROOTZÉN, H., 1983, Extremes and Related Properties of Random Sequences and Processes. New York, USA: Springer-Verlag.

LEE, M. and DAEBRITZ, M., 2010, Moveable scaffolding systems - MSS. In: IABSE WG 6 Seminar: State-of-the-art Bridge Deck Erection; Safe and Efficient use of Special Equipment. Singapore: International Association for Bridge and Structural Engineering (IABSE). November 2010.

LEVY, H., 2006, Stochastic Dominance: Investment Decision Making under Uncertainty. 2nd Edition. New York, USA: Springer.

LIND, N., 1995, A measure of vulnerability and damage tolerance. Reliability Engineering & System Safety. 1995. Vol. 48, no. 1, pp. 1–6.

LIU, H., ZHAO, Q., WANG, X., ZHOU, T., WANG, D., LIU, J. and CHEN, Z., 2010, Experimental and analytical studies on the stability of structural steel tube and coupler scaffolds without X-bracing. Engineering Structures. 2010. Vol. 32, no. 4, pp. 1003–1015.

MARSDEN, J., MCDONALD, L., BOWLES, D., DAVIDSON, R. and NATHAN, R., 2007, Dam safety, economic regulation and society's need to prioritise health and safety expenditures. In: Proceedings of the NZSOLD/ANCOLD Workshop on "Promoting and Ensuring the Culture of Dam Safety." Queenstown, New Zealand. 2007.

MARTIN, J. and HIRSCHBERG, D., 1996, Small sample statistics for classication error rates. I: Error rate measurements. USA: University of California, Report No. 96-21.

MARTIN, T., HARTEN, P., YOUNG, D., MURATOV, E., GOLBRAIKH, A., ZHU, H. and TROPSHA, A., 2012, Does rational selection of training and test sets improve the outcome of QSAR modeling? Journal of Chemical Information and Modeling. 2012. Vol. 52, no. 10, pp. 2570–2578.

MASUMOTO, H., HARA, K. and YAMASHITA, M., 1994, Design plan of super multi-span continuous Menshin bridge with deck length of 725m. In: Proceedings of the Third U.S.- Japan Workshop on Earthquake Protective Systems for Bridges. California, USA: U.S. National Center for Earthquake Engineering Research. 1994. pp. 69–84.

MATOUSEK, M. and SCHNEIDER, J., 1976, Untersuchungen zur Struktur des Sicherheitsproblems bei Bauwerken (in German). Swiss Federal Institute of Technology Zurich (ETHZ), Institut für Baustatik und Konstruktion, Report 59.

MCDONALD, L., BOWLES, D., HARTFORD, D., VAN DER MEER, J. and VRIJLING, J., 2005, Risk Assessment in Dam Safety Management. France: International Commission of Large Dams (ICOLD), Bulletin 130.

MCGILL, W. and AYYUB, B., 2007, The Meaning of Vulnerability in the Context of Critical Infrastructure Protection. In: Critical infrastructure protection: Elements of risk. George Mason University School of Law. pp. 25–48.

MCGRAW-HILL, 2007, McGraw Hill Encyclopedia of Science & Technology.

MELCHERS, R., 1999, Structural Reliability Analysis and Prediction. 2nd Edition. Wiley.

MELCHERS, R., BAKER, M. and MOSES, F., 1983, Evaluation of experience. In: Proceedings of IABSE Workshop on Quality Assurance within the Building Process. Rigi, Switzerland: International Association for Bridge and Structural Engineering (IABSE). 1983. pp. 9–30.

MENDES, P., 2009, Contributions for the Development of a Concrete Bridges Management Model Applied to Brazil Roadways (in Portuguese). PhD Thesis. Brazil: Escola Politécnica da Universidade de São Paulo.

MINITAB INC, 2010, Minitab 16 Statistical Software (www.minitab.com). Pennsylvania, USA.

MOHAMMADI, J. and HEYDARI, A., 2008, Seismic and wind load considerations for temporary structures. Practice Periodical on Structural Design and Construction. 2008. Vol. 13, no. 3, pp. 128–134.

MOLINARO, A., SIMON, R. and PFEIFFER, R., 2005, Prediction error estimation: A comparison of resampling methods. USA: Yale University, Report No. 96-21.

MUHANNA, R., RAO, M. and MULLEN, R., 2013, Advances in interval finite element modelling of structures. Life Cycle Reliability and Safety Engineering. 2013. Vol. 2, no. 3, pp. 15–22.

NARASIMHAN, H. and FABER, M., 2009, Categorisation and assessment of robustness related provisions in European standards. In: Proceedings of the Joint Workshop of COST Actions TU0601 and E55. Ljubljana, Slovenia. 2009. pp. 147–164.

NATHWANI, J., LIND, N. and PANDEY, M., 1997, Affordable Safety by Choice: The Life Quality Method. Waterloo, Canada: Institute of Risk Research, University of Waterloo.

NEWMAN, J. and CHOO, B., 2003, Advanced Concrete Technology: Processes. USA: Butterworth-Heinemann.

NIETO, F., HERNÁNDEZ, S., JURADO, J. and ROMERA, L., 2010, Code provisions for wind Loads on short road bridges: Spanish IAP code, UNE-EN 1991-1-4 & 2007 AASHTO LRFD bridge design specifications. In: Proceedings of the 2010 Structures Congress. Florida, USA: American Society of Civil Engineers (ASCE). 2010. pp. 2122–2133.

NISHIJIMA, K., 2009, Issues of Sustainability in Engineering Decision Analysis. PhD Thesis. Switzerland: ETH Zurich.

NISHIKAWA, K., 2009, Road planning and design in Japan. Past decisions and current challenges. National Institute for Land and Infrastructure Management (NILIM). Japan. 2009.

NITSCHKE, J., 2010, Form-traveller systems. In: IABSE WG 6 Seminar: State-of-the-art Bridge Deck Erection; Safe and Efficient use of Special Equipment. Singapore: International Association for Bridge and Structural Engineering (IABSE). November 2010.

NWOGUGU, M., 2006, A further critique of cumulative prospect theory and related approaches. Applied Mathematics and Computation. 2006. Vol. 179, no. 2, pp. 451–465.

OAKLEY, J. and O'HAGAN, A., 2004, Probabilistic sensitivity analysis of complex models: a Bayesian approach. Journal of the Royal Statistical Society: Series B (Statistical Methodology). 2004. Vol. 66, no. 3, pp. 751–769.

OUCHI, F., 2004, A literature review on the use of expert opinion in probabilistic risk analysis. Washington, USA: The World Bank.

PALLETT, P., BURROW, M., CLARK, L. and WARD, R., 2001, Investigation into aspects of falsework. School of Civil Engineering: The University of Birmingham, Report crr01394.

PENG, J., 1994, Analysis Models and Design Guidelines for High-Clearance Scaffold Systems. Ph.D. Dissertation. West Lafayette: Purdue University.

PENG, J., 2002, Stability analyses and design recommendations for practical shoring systems during construction. Journal of Construction Engineering and Management. 2002. Vol. 128, no. 6, pp. 536–544.

PENG, J., YEN, T., KUO, C. and CHAN, S., 2009, Structural analysis and modeling of system scaffolds used in construction. In: Proceedings of the Sixth International Conference on Advances in Steel Structures. Hong Kong: The Hong Kong Institute of Steel Construction. 2009. pp. 1099–1108.

PENG, J., YEN, T., LIN, Y. and WU, K., 1997, Performance of scaffold frame shoring under pattern loads and load paths. Journal of Construction Engineering and Management. 1997. Vol. 123, no. 2, pp. 138–145.

PENG, J., YEN, T., PAN, A., CHEN, W. and CHAN, S., 1996, Structural modeling and analysis of scaffold systems. In: Proceedings of International Conference on Advances in Steel Structures. Hong Kong: S.L. Chan and J.G. Teng, Pergamon. 1996. pp. 251–256.

PIERRE, L., KOPP, G., SURRY, D. and HO, T., 2005, The UWO contribution to the NIST aerodynamic database for wind loads on low buildings: Part 2. Comparison of data with wind load provisions. Journal of Wind Engineering and Industrial Aerodynamics. 2005. Vol. 93, no. 1, pp. 31–59.

PROSKE, T. and GRAUBNER, C., 2008, Formwork pressure asserted by highly workable concretes. Darmstadt Concrete - Annual Journal on Concrete and Concrete Structures. 2008. Vol. 23.

QUINION, D., 1984, Load variations in bridge falsework. In: Proceedings of IABSE 12th Congress. Vancouver, Canada: International Association for Bridge and Structural Engineering (IABSE). 1984.

R CORE TEAM, 2012, R: A language and environment for statistical computing. http://www.R-project.org/. Vienna, Austria: R Foundation for Statistical Computing.

RACKWITZ, R., 2004, Discounting for optimal and acceptable technical facilities involving risks. HERON. 2004. Vol. 49, no. 2, pp. 139–170.

RAO, M., MULLEN, R. and MUHANNA, R., 2011, A new interval finite element formulation with the same accuracy in primary and derived variables. International Journal of Reliability and Safety. 2011. Vol. 5, no. 3/4, pp. 336 - 357.

RATAY, R., 1996, Handbook of Temporary Structures in Construction. 2nd Edition. USA: McGraw-Hill Professional.

RATAY, R., 2009, Forensic Structural Engineering Handbook. USA: McGraw Hill Professional.

REASON, J., 1990, Human Error. UK: Cambridge University Press.

RIMINGTON, J., MCQUAID, J. and TRBOJEVIC, V., 2003, Application of Risk-Based Strategies to Workers' Health and Safety Protection: UK Experience. The Netherlands: Ministry of Social Affairs and Employment.

RODRIGUES, A., 2010, Simulations du Comportement Structurel Non-Linéaire de Tours d'Étaiement (in French). Thesis for graduation in Civil Engineering. Clermont-Ferrand: University Blaise Pascal (UBP).

ROSIGNOLI, M. and DAEBRITZ, M., 2010, Special equipment. In: IABSE WG 6 Seminar: State-of-the-art Bridge Deck Erection; Safe and Efficient use of Special Equipment. Singapore: International Association for Bridge and Structural Engineering (IABSE). November 2010.

ROSIGNOLI, M., 2002, Bridge Launching. UK: Thomas Telford.

ROSIGNOLI, M., 2007, Robustness and stability of launching gantries and movable shuttering systems - Lessons learned. Structural Engineering International (SEI). 2007. Vol. 17, no. 2, pp. 133–140.

ROSIGNOLI, M., 2010, Incremental lauching. In: IABSE WG 6 Seminar: State-of-the-art Bridge Deck Erection; Safe and Efficient use of Special Equipment. Singapore: International Association for Bridge and Structural Engineering (IABSE). November 2010.

ROSOWSKY, D., 1995, Estimation of design loads for reduced reference periods. Structural Safety. March 1995. Vol. 17, no. 1, pp. 17–32.

ROSOWSKY, D., HUSTON, D., FUHR, P. and CHEN, W., 1994, Measuring formwork loads during construction. Concrete International. 1994. Vol. 16, no. 11, pp. 21–25.

SAA, 1995, AS 3610:1995 - Formwork for Concrete. Australia: Standards Association of Australia (SAA).

SAA, 2002a, AS 1170.0:2002 - Structural Design Actions - Part 0: General Principles. Australia: Standards Association of Australia (SAA).

SAA, 2002b, AS 1170.2:2002 - Structural Design Actions - Part 2: Wind Actions. Australia: Standards Association of Australia (SAA).

SAA, 2007, AS 5100. Parts 1-7: Bridge design. Australia: Standards Association of Australia.

SAVAGE, S., 2009, The Flaw of Averages: Why We Underestimate Risk in the Face of Uncertainty. New Jersey, US: John Wiley & Sons.

SCHEER, J., 2010, Failed Bridges: Case Studies, Causes and Consequences. UK: Wiley VCH.

SCHNEIDER, J., 2006, Introduction to Safety and Reliability of Structures. 2nd Edition. Switzerland: IABSE. Structural Engineering Documents (SED), 5.

SCHWEIGER, H. and PESCHL, G., 2005, Reliability analysis in geotechnics with the random set finite element method. Computers and Geotechnics. 2005. Vol. 32, no. 6, pp. 422–435.

SCOSS, 2002, Falsework: Full Circle?. UK: Standing Committee on Structural Safety (SCOSS), Topic Paper SC/T/02/01.

SCOSS, 2005, 15th Biennial Report from SCOSS. UK: Standing Committee on Structural Safety (SCOSS).

SEXSMITH, R. and REID, S., 2003, Safety factors for bridge falsework by risk management. Structural Safety. 2003. Vol. 25, no. 2, pp. 227–243.

SEXSMITH, R., 1998, Reliability during temporary erection phases. Engineering Structures. November 1998. Vol. 20, no. 11, pp. 999–1003.

SGB, 2001, Safety Guide: Cuplok Falsework Erection Procedure. UK: SGB Group (now HARSCO).

SGB, 2006, Cuplok: User's Manual. UK: SGB Group (now HARSCO).

SGB, 2009, Cuplok: Datasheet. UK: SGB Group (now HARSCO).

SHI, J., CHOPP, D., LUA, J., SUKUMAR, N. and BELYTSCHKO, T., 2010, Abaqus implementation of extended finite element method using a level set representation for three-dimensional fatigue crack growth and life predictions. Engineering Fracture Mechanics. 2010. Vol. 77, no. 14, pp. 2840–2863.

SIA, 2003, SIA 260 - Bases pour L'élaboration des Projets de Structures Porteuses. Switzerland: Société Suisse des Ingénieurs et des Architectes.

SIKKEL, R., 1982, Health and safety in construction. In: Proceedings of IABSE Workshop on Health and Safety in Construction. Tokyo, Japan: International Association for Bridge and Structural Engineering (IABSE). 1982. pp. 37–56.

SIMULIA, 2012a, Abaqus Analysis User's Manual. Part VI: Elements. Simulia.

SIMULIA, 2012b, Abaqus Analysis User's Manual. Section 40: Contact elements in Abaqus/Standard. Simulia.

SIMULIA, 2012c, Abaqus Analysis User's Manual. Section 32.15.1 User-defined elements. Simulia.

SIMULIA, 2012d, Abaqus Theory Manual. Section 1.3.1 Rotation variables. Simulia.

SIMULIA, 2012e, Abaqus Analysis User's Manual. Section 6: Analysis procedures. Simulia.

SMITH, J., 2006, Structural robustness analysis and the fast fracture analogy. Structural Engineering International (SEI). 2006. Vol. 16, no. 2, pp. 118–123.

SOMMER, H., SEETHALER, R., CHANEL, O., HERRY, M., MASSON, S. and VERGNAUD, J., 1999, Health Costs due to Road Traffic-Related Air Pollution. An Impact Assessment Project of Austria, France and Switzerland. Economic Evaluation. Bern, Switzerland: World Health Organization (WHO).

SORENSEN, J., RIZZUTO, E. and FABER, M., 2009, Robustness - theoretical framework. In: Proceedings of the Joint Workshop of COST Actions TU0601 and E55. Ljubljana, Slovenia. September 2009.

SPACKMAN, M. and HOLDER, S., 2007, Discount Rates for Rail Safety Scheme Appraisals. Final Report for the Office of Rail Regulation. UK: NERA Economic Consulting.

SPACKMAN, M., 2009, Review of the J-value Literature – Final Report. UK: The Health and Safety Executive (HSE).

SPACKMAN, M., EVANS, A., JONES-LEE, M., LOOMES, G., HOLDER, S. and WEBB, H., 2011, Updating the VPF and VPIs: Phase 1: Final Report. UK: UK Department for Transport, Local Government and the Regions.

STAROSSEK, U. and HABERLAND, M., 2008, Measures of structural robustness — Requirements & applications. In: Proceedings of the ASCE SEI 2008 Structures Congress – Crossing Borders. Vancouver, Canada. 2008.

STAROSSEK, U. and HABERLAND, M., 2009, Evaluating measures of structural robustness. In: Proceedings of the Structures Congress 2009: Don't Mess with Structural Engineers - Expanding Our Role. Austin, Texas. 2009. pp. 1758–1765.

STAROSSEK, U. and WOLFF, M., 2005, Progressive collapse: design strategies. In: CD-ROM Proceedings of IABSE Symposium, Structures and Extreme Events. Lisbon, Portugal: International Association for Bridge and Structural Engineering (IABSE). 2005.

STAROSSEK, U., 2006, Progressive collapse of structures: Nomenclature and procedures. Structural Engineering International (SEI). 2006. Vol. 16, no. 2, pp. 113–117.

STAROSSEK, U., 2009, Progressive Collapse of Structures. UK: Thomas Telford.

STEVEN, S., 2010, Chapter 5: The different phases in construction – design in health and safety to the project life cycle. In: ICE Manual of Health and Safety in Construction. London: Thomas Telford Ltd. pp. 51–69.

SUDRET, B., 2007, Uncertainty Propagation and Sensitivity Analysis in Mechanical Models. Contributions to Structural Reliability and Stochastic Spectral Methods. Paris, France: Ecole Nationale des Ponts et Chaussees.

SURDAHL, R., MILLER, D. and GLENN, V., 2010, The positive legacy of a bridge collapse. Public Roads, Federal Highway Administration, US Department of Transportation. 2010. Vol. 73, no. 5.

THE CONCRETE CENTRE, 2008, Concrete Bridges: The Benefits of Concrete in Bridge Design and Construction. UK: The Concrete Centre.

THE CONCRETE SOCIETY, 2012, Formwork: A Guide to Good Practice. 3rd Edition. UK: The Concrete Society, Report CS30.

THOFT-CHRISTENSEN, P. and BAKER, M., 1982, Structural Reliability Theory and Its Applications. UK: Springer.

TODINOV, M., 2007, Risk-Based Reliability Analysis and Generic Principles for Risk Reduction. Amsterdam: Elsevier.

TURKSTRA, C. and MADSEN, H., [no date], Load combinations in codified structural design. Journal of the Structural Division. Vol. 106, no. 12, pp. 2527–2543.

TVERSKY, A. and KAHNEMAN, D., 1992, Advances in prospect theory: Cumulative representation of uncertainty. Journal of Risk and Uncertainty. 1992. Vol. 5, no. 4, pp. 297–323.

U.S. DOT, 2009, Treatment of the Economic Value of a Statistical Life in Departmental Analyses – 2009 Annual Revision. USA: U.S. Department of Transportation.

UK DFT, 1999, Guidance on Robustness and Provision Against Accidental Actions. The Current Application of Requirements A3 of the Building Regulations 1991. Final Report Including Background Documentation. UK: UK Department for Transport, Local Government and the Regions.

UK DFT, 2011a, Guidance Documents - Expert. TAG Unit 3.5: The Economy Objective. UK: UK Department for Transport.

UK DFT, 2011b, Guidance Documents - Expert. TAG Unit 3.4: The Safety Objective. UK: UK Department for Transport.

UK ODPM, 2004, Building Regulations 2004, Approved Document A - Structure. UK: Office of the Deputy Prime Minister.

UKOOA, 1999, Industry Guidelines on a Framework for Risk Related Decision Support. UK: UK Offshore Operators Association (UKOOA), Report HS006.

USDOD, 2010, Unified Facilities Criteria (UFC), Design of Buildings to Resist Progressive Collapse. United States of America Defence Department, Report UFC 4-023-03.

VAN GELDER, P., 2000, Statistical Methods for the Risk-Based Design of Civil Structures. PhD Thesis. Delft, The Netherlands: Delft University of Technology.

VILA REAL, P. M. M., LOPES, N., SIMÕES DA SILVA, L. and FRANSSEN, J. -M., 2004, Lateral-torsional buckling of unrestrained steel beams under fire conditions: improvement of EC3 proposal. Computers & Structures. August 2004. Vol. 82, no. 20-21, pp. 1737–1744.

VISCUSI, W. and ALDY, J., 2003, The value of a statistical life: A critical review of market estimates throughout the world. Journal of Risk and Uncertainty. 2003. Vol. 27, no. 1, pp. 5–76.

VISCUSI, W. and GAYER, T., 2002, Safety at any price? Regulation. 2002. Vol. 25, no. 3, pp. 54–63.

VISCUSI, W., 1993, The value of risks to life and health. Journal of Economic Literature. 1993. Vol. 31, no. 4, pp. 1912–1946.

VOELKEL, W., 1990, German Assessment for the Cuplok Scaffold System Within the Framework of the Comparison of the Procedures in Different European Countries - Part 1: Test Report. Berlin: Institut fur Bautechnik (IfB), Report T 2381/1.

VON NEUMANN, J. and MORGENSTERN, O., 1944, Theory of Games and Economic Behavior. USA: Princeton University Press.

VRIJLING, J., VAN GELDER, P., GOOSSENS, L., VOORTMAN, H. and MANDEY, P., 2004, A framework for risk criteria for critical infrastructures: fundamentals and case studies in the Netherlands. Journal of Risk Research. 2004. Vol. 7, no. 6, pp. 569–579.

VRIJLING, J., VAN HENGEL, W. and HOUBEN, R., 1998, Acceptable risk as a basis for design. Reliability Engineering and System Safety. 1998. Vol. 59, no. 1, pp. 141–150.

WANG, H., YANG, X., REN, Q. and DONG, P., 2011, Research progress basalt fiber in civil engineering. Applied Mechanics and Materials. 2011. Vol. 71-78, pp. 1484–1487.

WARDHANA, K. and HADIPRIONO, F., 2003, Analysis of recent bridge failures in the United States. Journal of Performance of Constructed Facilities. 2003. Vol. 17, no. 3, pp. 144–150.

WILLFORD, M. and ALLSOP, A., 1990, Design Guide for Wind Loads on Unclad Framed Building Structures During Construction. Building and Research Establishment (BRE), Report BR 173.

WONG, S., ONOF, C. and HOBBS, R., 2005, Models for evaluating the costs of bridge failure. Proceedings of the ICE - Bridge Engineering. 2005. Vol. 158, no. 3, pp. 117–128.

XIAO, N., HUANG, H., WANG, Z., PANG, Y. and HE, L., 2011, Reliability sensitivity analysis for structural systems in interval probability form. Structural and Multidisciplinary Optimization. 2011. Vol. 44, no. 5, pp. 691–705.

XIE, N. and WANG, G., 2009, Test analysis on hidden defect in high falsework and its effect on structural reliability. In: Proceedings of the 8th International Conference on Reliability, Maintainability and Safety, ICRMS 2009. Chengdu, China: Institute of Electrical and Electronics Engineers (IEEE). 2009. pp. 1077–1080.

XIE, Q., LU, S., CÓSTOLA, D. and HENSEN, J., 2014, An arbitrary polynomial chaos-based approach to analyzing the impacts of design parameters on evacuation time under uncertainty. Fire Safety Science. 2014. Vol. 11.

YEN, T., HUANG, Y., CHEN, W. and LIN, Y., 1995, Design of Scaffold Systems for Concrete Buildings During Construction. Lafayette: School of Civil Engineering, Purdue University, Report CE-STR-95-4.

ZENG, F. and HU, C., 2010, Determination of effect factors scoring weights of bridge falsework based on the uncertain analytic hierarchy process. In: Proceedings of the International Conference on E-Product E-Service and E-Entertainment (ICEEE). Henan, China. 2010. pp. 1–4.

ZHANG, H., CHANDRANGSU, T. and RASMUSSEN, K., 2009, System reliability of steel scaffold systems. In: Proceedings of the Sixth International Conference on Advances in Steel Structures. Hong Kong: The Hong Kong Institute of Steel Construction. 16 December 2009. pp. 1065–1074.

ZHANG, H., MULLEN, R. and MUHANNA, R., 2010, Finite element structural analysis using imprecise probabilities based on p-box representation. In: Proceedings of the 4th International Workshop on Reliable Engineering Computing (REC 2010). University of Singapore: Research Publishing Services. 2010. pp. 211–225.

ZHANG, H., MULLEN, R. and MUHANNA, R., 2012, Structural analysis with probability boxes. International Journal of Reliability and Safety. 2012. Vol. 6, no. 1, pp. 110–129.

ZHANG, H., RASMUSSEN, K. and ELLINGWOOD, B., 2011, Reliability analysis of steel scaffold shoring structures. In: Applications of Statistics and Probability in Civil Engineering. London: Taylor & Francis Groupp. pp. 2898–2906.

ZIELINSKI, P., 2008, Risk in dam safety Canadian perspective. In: Workshop on Tolerable Risk Evaluation sponsored by US Army Corps of Engineers. Virginia, USA: U.S. Department of the Interior: Bureau of Reclamation. March 2008.

A

PUBLICATIONS

Journal articles

ANDRÉ, J., BEALE, R. and BAPTISTA, A., 2013, Recent advances and existing challenges in the design of bridge falsework systems. *Civil Engineering and Environmental Systems*. 2013. Vol. 30, Issue 2, pp. 130-145.

ANDRÉ, J., BEALE, R. and BAPTISTA, A., 2012, Bridge Construction Equipment: An overview of the existing design guidance. *Structural Engineering International*. 2012. Vol. 22, no. 3, pp. 365-379.

ANDRÉ, J., BEALE, R. and BAPTISTA, A., 2012, A survey of bridge falsework systems since 1970. *Proceedings of the ICE - Forensic Engineering*. 2012. Vol. 65, Issue FE4, pp. 161-172.

Conference papers

ANDRÉ, J., BEALE, R. and BAPTISTA, A., 2014, Robustness and risk evaluation of bridge falsework structures. In: *JPEE2014,5^{as} Jornadas Portuguesas de Engenharia de Estruturas Encontro Nacianal Betão Estrutural 2014, 9º Congresso Nacional de Sismologia e Engenharia Sísmica (5th Portuguese Conference on Structural Engineering/9th Portuguese National Congress on Seismology and Seismic Engineering)*, Lisbon, Portugal: Portuguese National Laboratory for Civil Engineering. 2014. Paper No 62, 15p.

ANDRÉ, J., BEALE, R. and BAPTISTA, A., 2014, Numerical investigation of bridge falsework structures. In: *JPEE2014,5^{as} Jornadas Portuguesas de Engenharia de Estruturas Encontro Nacianal Betão Estrutural 2014, 9º Congresso Nacional de Sismologia e Engenharia Sísmica (5th Portuguese Conference on Structural Engineering/9th Portuguese National Congress on Seismology and Seismic Engineering)*, Lisbon, Portugal: Portuguese National Laboratory for Civil Engineering. 2014. Paper No 63, 15p.

ANDRÉ, J., BEALE, R. and BAPTISTA, A., 2013, Experimental investigation of bridge falsework joints. In: *X Congresso de Construção Metálica e Mista e I Congresso Luso-Brasileiro de Construção Metálica Sustentável (10th Portuguese Congress on Steel and Concrete Construction and 1st Brazilian Conference on Sustainable Steel Construction)*, Porto, Portugal. 2013. pp. 655-664.

ANDRÉ, J., BEALE, R. and BAPTISTA, A., 2012, Advances and challenges in the design of bridge falsework systems, In: *6th International Forum on Engineering Decision Making (IFED)*, Lake Louis, Canada. 2012. 32p.

ANDRÉ, J., BEALE, R. and BAPTISTA, A., 2011, Experimental investigation of bridge falsework Cuplok joints. In: *VIII Congresso de Construção Metálica e Mista (8th Portuguese Congress on Steel and Concrete Construction)*, Guimarães, Portugal. 2011. pp. 795-804.

B

MECHANICAL PROPERTIES
OF THE ELEMENTS TESTED IN CHAPTER 3 GIVEN IN
FACTORY PRODUCTION CONTROL CERTIFICATES

3400 samples	Yield strength (MPa)	Tensile strength (MPa)	Elongation after fracture (%)
Mean value	449,74	524,22	24,98
Required value	>355	470-630	>20

C

GEOMETRICAL CHARACTERISTICS
OF THE ELEMENTS TESTED IN CHAPTER 3

Standard elements

Thickness (mm)		External diameter (mm)	
3,4	3,4	48,5	48,8
3,5	3,5	48,7	48,8
3,3	3,5	48,4	49
3,5	3,4	48,7	48,8
3,3	3,3	48,4	49
3,5	3,3	48,6	48,8
3,3	3,4	48,5	48,9
3,3	3,4	48,6	48,9
3,6	3,4	48,6	49
3,6	3,4	48,7	48,7
3,5	3,5	48,7	48,6
3,5	3,3	49	49
3,5	3,6	48,6	48,5
3,5	3,6	48,7	48,7
3,5	3,7	48,9	48,4
3,6	3,4	48,9	48,4
3,6	3,4	48,7	48,7
3,6	3,4	48,3	49,1
3,4	3,5	48,4	48,8
3,4	3,5	48,7	48,7
3,3	3,5	48,6	48,7
3,5	3,4	48,6	48,7
3,3	3,4	48,7	48,4
3,7	3,2	48,9	48,6
3,6	3,3	48,6	48,5
3,4	3,4	48,6	48,6
Average (mm)	3,5	48,7	
Standard deviation (mm)	0,1	0,2	
Nominal value (mm)	3,2	48,3	

Ledger elements

	Thickness (mm)	External diameter (mm)
	3,3	48,5
	3,5	48,7
	3,7	48,4
	3,2	48,7
	3,6	48,4
	3,5	48,7
	3,6	48,7
	3,3	48,5
	3,4	48,5
	3,3	48,7
Average (mm)	3,4	48,6
Standard deviation (mm)	0,2	0,1
Nominal value (mm)	3,2	48,3

Brace elements

	Thickness (mm)	External diameter (mm)
	3,2	48,1
	3,6	48,6
	3,5	48,5
	3,2	48,5
	3,4	48,4
	3,5	48,6
	3,4	48,2
	3,7	48,6
	3,3	48,4
	3,5	48,6
Average (mm)	3,4	48,5
Standard deviation (mm)	0,2	0,2
Nominal value (mm)	3,2	48,3

Forkhead elements

	External diameter tube segment (mm)	Thickness of tube segment (mm)	Length tube segment (mm)	Side lengths forkhead plate (mm)		Thickness of forkhead plate (mm)
				Length	Width	
	48	3,1	75	179	150	8,1
	49	3,2	76	182	149	8,2
	49	3,2	75	179	150	8
	49	3,2	76	179	150	8
	48	3,1	76	182	150	8,1
	49	3,1	76	180	150	8,1
		3,2				
		3,2				
		3,2				
		3,1				
		3,5				
		3,4				
		3,2				
		3,1				
		3,3				
		3,3				
Average (mm)	48,7	3,2	75,7	180,2	149,8	8,1
Standard deviation (mm)	0,5	0,1	0,5	1,5	0,4	0,1
Nominal value (mm)	48,3	3,2	76	178	150	8

Baseplate elements

	External diameter tube segment (mm)	Thickness of tube segment (mm)	Length tube segment (mm)	Side lengths baseplate plate (mm)	Thickness of baseplate plate (mm)
	48	3,8	95	150	9,6
	48	4,2	95	152	10
	49	4,1	95	152	9,9
	48	3,9	95	152	9,9
	48	4,1	96	151	9,9
	49	4,1	95	150	9,8
Average (mm)	48,3	4,0	95,2	151,2	9,9
Standard deviation (mm)	0,5	0,2	0,4	1,0	0,1
Nominal value (mm)	48,3	4	95	150	10

Spigot elements

	External diameter tube segment (mm)	Thickness of tube segment (mm)	Free length (mm)
	32,5	3,5	150
	32,5	3,7	155
	32,5	3,45	155
	32,7	3,7	155
	32,8	3,6	160
	33,0	3,7	135
	31,3	3,6	150
	35,0	3,6	150
	32,2	3,2	150
	32,6	3,3	170
	33,3	3,2	140
	33,5	3,4	160
	35,0	3,5	155
	35,0	3,6	
	34,0	3,3	
	34,0	3,4	
	31,7	3,2	
	31,9	3,7	
Average (mm)	33,1	3,5	152,7
Standard deviation (mm)	1,1	0,2	8,8
Nominal value (mm)	32	3,2	150

Jack elements

	Non threaded part			Total length (mm)
Thickness (mm)	External diameter (mm)	Length (mm)		
4,6	38,1	190		850
4,9	38,2	200		870
5,0	38,6	195		870
5,0	38,6	195		870
5,0	38,6	195		870
5,0	38,4	190		860
4,9	38,4	195		860
4,9	38,7	190		870
4,9	38,3	190		870
4,8	38,7	190		850
5,1	38,3	200		850
4,9	38,6	200		850
Average (mm)	4,9	38,5	194,2	861,7
Standard deviation (mm)	0,1	0,2	4,2	9,4
Nominal value (mm)	5	38	195	860